
**Characterising and evaluating the efficacy
of metabolic therapies for the treatment of
Duchenne Muscular Dystrophy**

By

Cara A Timpani

BSc (Hons)

College of Health and Biomedicine

Victoria University

Thesis submitted in fulfilment of the requirements for the degree of Doctor of
Philosophy

ABSTRACT

Duchenne Muscular Dystrophy (DMD) is a fatal skeletal muscle wasting disease underpinned by extensive metabolic dysfunction. This culminates in reduced energy production which is detrimental to dystrophic muscle since buffering damage and stimulating repair are energy dependent processes. Current treatment options for DMD are limited and do not address this metabolic dysfunction despite the extensive role it plays in DMD pathogenesis and disease progression. Therefore, this thesis investigated the efficacy of two metabolic therapies, sodium nitrate and adenylosuccinic acid (ASA), to improve skeletal muscle metabolism and architecture in the well-established *mdx* mouse model of DMD, and in immortalised myoblasts derived from DMD patients.

Despite nitrate supplementation being previously demonstrated to exert beneficial metabolic adaptations in the skeletal muscle of healthy individuals, eight weeks of supplementation in the *mdx* mouse failed to improve glucose uptake and mitochondrial function but did reduce oxidative stress (also observed in DMD myoblasts). Unexpectedly, nitrate induced significant, concomitant increases in peroxynitrite which escalated the histopathology in *mdx* muscle. This suggests that chronic enhancement of NO through nitrate supplementation may not be a viable therapeutic option for the treatment of DMD.

In contrast to nitrate, eight weeks of ASA supplementation in the *mdx* mouse was therapeutically beneficial. While ASA did not modulate glucose uptake, downstream mitochondrial respiration or the phosphorylation potential of the skeletal muscle as expected, it did increase mitochondrial content and

viability and reduce oxidative stress (also evidenced in DMD myoblasts). Most significantly and clinically relevant, however, was the reduction in various indices of histopathology. Calcium accumulation, muscle damage, and fat and connective tissue infiltration were all attenuated by ASA therapy. These data highlights an exciting and promising potential clinical application for ASA as a therapeutic candidate for the treatment of DMD, albeit via unknown mechanisms.

DECLARATION

I, Cara Timpani, declare that the PhD thesis entitled “Characterising and evaluating the efficacy of metabolic therapies for the treatment of Duchenne Muscular Dystrophy” is no more than 100,000 words in length including quotes and exclusive of tables, figures, appendices, bibliography, references and footnotes. This thesis contains no material that has been submitted previously, in whole or in part, for the award of any other academic degree or diploma. Except as indicated below, this thesis is my own work.

Chapter Four

- Mr Adam Trewin performed the respirometry experiments
- Dr. Craig Goodman assisted with performing the western blot analysis
- Ms Vanesa Stojanovska & Ms Ainsley Robinson assisted with performing immunohistochemical experiments

Chapter Six

- Dr. Craig Goodman performed the western blot analysis
- Dr. Christos Stathis performed the metabolite analysis
- Ms Vanesa Stojanovska performed the immunohistochemical experiments



Cara Timpani

31st August 2016

ACKNOWLEDGEMENTS

First and foremost, I would like to express my deepest gratitude and appreciation to my supervisors Dr. Emma Rybalka and Associate Professor Alan Hayes for their unwavering support and guidance, not only throughout my PhD, but since my undergraduate and honours degrees. The last eight years have been a fantastic learning experience and you have only ever pushed me to strive for excellence; for this, I am extremely grateful and I hope I have made you both proud. I would like to make a special mention to Emma, my fearless (and sometimes crazy) supervisor who has been an important role model and mentor that has helped shape me into the person I am today. Without your perseverance and belief in me, I do not know if I would have been able to accomplish what I have today. Most importantly, I would like to express my sincerest appreciation for your friendship – thank you for willingly listening to my whining and complaining and for always talking me off of the proverbial cliff. I really cannot express to you how grateful I am for your friendship during these very challenging PhD years.

Secondly, I would like to thank all of the other Honours and PhD students I have had the pleasure and privilege of meeting and working with along the way. Without your friendship and support, and random outbursts of singing and dancing, it would have been difficult to drag myself into the lab in the very early hours of the morning. Thank you for helping to brighten my days!

Thirdly, I would like to acknowledge the assistance of Dr. Jason White (Murdoch Children's Research Institute, Melbourne, Australia) for his assistance in setting up the collaboration with Drs. Vincent Mouly and Gillian Butler-Browne

(Institut de Myologie, Paris, France). Without this partnership, and the kind donation of immortalised human cells, this thesis would not have been completed. Additionally, thank you to Professor Glenn McConell and Dr. Andrew Betik for their expertise in perfecting the glucose uptake method and Dr. Kulmira Nurgali for donation of antibodies for immunohistochemical analysis.

Lastly, and most importantly, thank you to my family – thank you for your love, patience and support throughout the last four years and throughout my entire education. To my mother Mary and my father Phil – I cannot express to you both how thankful I am for your unwavering love and support and for all the sacrifices you have ever made for me. All I have achieved is a reflection of you both and I hope that I have, and will continue to, make you both proud. To my sister Adriana - thank you for always knowing how to make me laugh and for embracing how nerdy I am. I hope that you are proud of what I have achieved and know that I will be creating more PowerPoint presentations for you to enjoy in the future. Finally, to my dearest husband Andrei – I truly do not know where to begin thanking you since the list is endless and there is not enough space in this thesis to write it all down. When I started at Victoria University I did not think in my wildest dreams that I would meet the love of my life but I am thankful every day that our paths crossed. You have been nothing but my pillar of strength, my voice of reason and my greatest supporter – without you, and your understanding that sometimes you need to start work at 5 in the morning and get back at 2 in the morning, I do not know if I would have been able to reach this milestone. Thank you for being the constant in my life when it felt like life

was nothing but chaos and for always having that hug ready when I needed it most.

I would like to dedicate this thesis to my grandparents Frank, Lina and Rocco – you always taught me the importance of a good education and encouraged me to never stop learning. I hope this thesis, and all the hard work that has gone into it, makes you proud of what I have achieved.

LIST OF COMMUNICATIONS & AWARDS

Conference Presentations

1. Timpani, C.A., Hayes, A. & Rybalka, E. (2016). Metabolic therapy as a superhero treatment for Duchenne Muscular Dystrophy. Melbourne, Victoria, Australia. **3 Minute Thesis** presentation at The Australian Society for Medical Research Victorian Student Symposium.
2. Sorensen, J.C., Timpani, C.A., Stojanovska, V., Stewart, M., Hayes, A, Petersen, A. & Rybalka, E. (2016). Platinum-based chemotherapy induces skeletal muscle wasting and mitochondrial dysfunction in mice. Melbourne, Victoria, Australia. **Poster** presentation at The Australian Society for Medical Research Victorian Student Symposium.
3. Viverette, R.J., Koceja, M.D., Dua, S.A., Williams, B., Betik, A.C, Timpani, C.A., Hayes, A. & Hanson, E.D. (2016). Role of testosterone on load-mediated hypertrophy in rats. Greenville, South Carolina, USA. **Poster** presentation at the South Eastern American College Sports Medicine conference.
4. Timpani, C.A., Clark, J., Mier, J., Hayes, A. & Rybalka, E. (2015). Adenylosuccinic acid therapy attenuates skeletal muscle histopathology in the dystrophin-deficient *mdx* mouse. In *Proceedings of the Australian Physiological Society* Vol. 46 (pp. 77P). Hobart, Tasmania, Australia. **Poster** presentation at the Australian Physiological Society Conference.
5. Timpani, C.A., Trewin, Robinson, A., Nurgali, K., A., Betik, A., Stepto, N., Hayes, A., McConell, G.K. & Rybalka, E. (2015). Glucose uptake & mitochondrial function following 8 weeks of dietary nitrate supplementation in the dystrophin-deficient *mdx* mouse. Melbourne, Victoria, Australia. **Poster** presentation at The Australian Society for Medical Research Victorian Student Symposium.
6. Stojanovska, V., McQuade, R.M., Stewart, M., Timpani, C.A., Sorensen, J., Orbell, J., Rybalka, E. & Nurgali, K. (2015). Platinum accumulation and changes in mitochondrial function of the longitudinal muscle and myenteric plexus following oxaliplatin administration. In *Proceedings of the Australian Physiological Society* Vol. 46 (pp. 91P). Hobart, Tasmania, Australia. **Poster** presentation at the Australian Physiological Society Conference.
7. McQuade, R.M., Sorensen, J., Timpani, C.A., Nurgali, K. & Rybalka, E. (2015). Idebenone therapy protects against oxaliplatin-induced gastrointestinal dysfunction. In *Proceedings of the Australian Physiological Society* Vol. 46 (pp. 90P). Hobart, Tasmania, Australia. **Poster** presentation at the Australian Physiological Society Conference.
8. Hayes, A., Andreacchio, N., Timpani, C.A., Hanson, E.D. & Rybalka, E. (2015). Effects of vitamin D supplementation on dystrophic (*mdx*) muscles during damage and repair. In *Proceedings of the Australian Physiological Society* Vol. 46 (pp. 9P). Hobart, Tasmania, Australia. **Oral** presentation at the Australian Physiological Society Conference.

9. Blazev, R., **Timpani, C.A.**, McConell, G.K, Hayes, A. & Rybalka, E. (2015). The effect of nitrate supplementation on sarcoplasmic reticulum Ca²⁺ handling in dystrophic skeletal muscle fibres. In *Proceedings of the Australian Physiological Society* Vol. 46 (pp. 106P). Hobart, Tasmania, Australia. **Oral** presentation at the Australian Physiological Society Conference.
10. Sorensen, J., **Timpani, C.A.**, Campelj, D., Petersen, A.C., Hayes, A. & Rybalka, E. (2015). Idebenone protects against chemotherapy-induced skeletal muscle wasting and mitochondrial dysfunction in mice. In *Proceedings of the Australian Physiological Society* Vol. 46 (pp. 142P). Hobart, Tasmania, Australia. **Oral** presentation at the Australian Physiological Society Conference.
11. **Timpani, C.A.**, Trewin, A., Betik, A., Stepto, N., Hayes, A., McConell, G.M. & Rybalka, E. (2015). Glucose uptake & mitochondrial function following 8 weeks of dietary nitrate supplementation in the dystrophin-deficient *mdx* mouse. Brighton, England. **Poster** presentation at the 20th World Muscle Society Conference.
12. Cheregi, B., **Timpani, C.A.**, Hayes, A., Nurgali, K. & Rybalka, E. (2015). Chemotherapy-induced mitochondrial respiratory dysfunction, oxidant production and death in healthy skeletal muscle C2C12 myoblast and myotube models. Brighton, England. **Poster** presentation at the 20th World Muscle Society Conference.
13. Stojanovska, V., Stewart, M., McQuade, R., Rahman, A., **Timpani, C.A.**, Orbell, J., Rybalka, E. & Nurgali, K. (2015). Platinum-based chemotherapy: drug accumulation in neurons controlling gastrointestinal functions. **Oral** presentation at The Australian Society for Medical Research: Bugs, Bowels and Beyond Symposium, Adelaide, South Australia, Australia.
14. Stojanovska, V., Stewart, M., McQuade, R., Rahman, A., **Timpani, C.A.**, Orbell, J., Rybalka, E. & Nurgali, K. (2015). Effects of colorectal cancer and anti-cancer chemotherapy on the enteric nervous system. **Invited oral** presentation, Enteric Nervous System Meetings, University of Melbourne, Melbourne, Victoria, Australia.
15. Stojanovska, V., McQuade, R., Stewart, M., Rahman, A., **Timpani, C.A.**, Rybalka, E., Orbell, J. & Nurgali, K. (2015). Oxaliplatin-induced neurotoxicity: platinum accumulation in the medulla oblongata and enteric neurons. Melbourne, Victoria, Australia. **Oral** presentation at The Australian Society for Medical Research Victorian Student Symposium
16. **Timpani, C.A.**, Hayes, A., & Rybalka, E. (2013). The effects of increasing extramitochondrial calcium concentration on mitochondrial function in dystrophic muscle. In *Proceedings of the Australian Physiological Society* Vol. 44 (pp. 71P). Melbourne, Victoria, Australia: **Oral** presentation at the Australian Physiological Society Conference.
17. Andreacchio, N., **Timpani, C.A.**, Hanson, E. D., Sanders, K. M. & Hayes, A. (2013). The effect of a yearly dose of vitamin D on skeletal muscle function. In *Proceedings of the Australian Physiological Society* Vol. 44 (pp. 55P). Melbourne, Victoria, Australia. **Poster** presentation at the Australian Physiological Society Conference.

Publications

Peer-reviewed Papers

1. Sorensen, J.C., Cheregi, B.D., **Timpani, C.A.**, Nurgali, K., Hayes, A. & Rybalka, E. (2016). Mitochondria: Inadvertent targets in chemotherapy-induced skeletal muscle toxicity and wasting?. *Cancer, Chemotherapy and Pharmacology*. doi: [10.1007/s00280-016-3045-3](https://doi.org/10.1007/s00280-016-3045-3). **IF=2.824**, SciMago **Q1**. **Contribution to published work:** Editing manuscript and figure illustrations
2. Rybalka, E., **Timpani, C.A.**, Stathis, C.G, Hayes, A. & Cooke, M.B (2015). Metabogenic and nutraceutical approaches to address energy dysregulation and skeletal muscle wasting in Duchenne Muscular Dystrophy. *Nutrients*, 7(12). doi: [10.3390/nu7125498](https://doi.org/10.3390/nu7125498). **IF=3.3**, SciMago **Q1**. **Contribution to published work:** Authoring a section, editing manuscript and figure illustrations.
3. **Timpani, C.A.**, Hayes, A. & Rybalka, E (2015). Revisiting the dystrophin-ATP connection: How half a century of research still implicates mitochondrial dysfunction in Duchenne Muscular Dystrophy aetiology. *Medical Hypotheses*, 85(6). doi: [10.1016/j.mehy.2015.08.015](https://doi.org/10.1016/j.mehy.2015.08.015). **IF=1.1**, SciMago **Q2**. **Contribution to published work:** Authoring manuscript and figure illustrations.
4. Rybalka, E., **Timpani, C.A.**, Cooke, M.B., Williams, A.D., & Hayes, A. (2014). Defects in mitochondrial ATP synthesis in dystrophin-deficient *mdx* skeletal muscles may be caused by complex I insufficiency. *PLoS ONE*, 9(12). doi: [10.1371/journal.pone.0115763](https://doi.org/10.1371/journal.pone.0115763). **IF=3.2**, SciMago **Q1**. **Contribution to published work:** Performed mitochondrial swelling experiments, manuscript preparation and figure illustrations.

Papers Under Review

1. **Timpani, C.A.**, Trewin, A., Stojanovsja, V., Robinson, A., Goodman, C.A., Nurgali, K., Betik, A.C., Stepto, N., Hayes, A., McConell, G.K. & Rybalka, E. (2016). Attempting to compensate for reduced nNOS protein with nitrate supplementation cannot overcome metabolic dysfunction but rather has detrimental effects in dystrophin-deficient *mdx* muscle. *Neurotherapeutics*.
2. **Timpani, C.A.**, Hayes, A. & Rybalka, E (2016). Therapeutic strategies to address neuronal Nitric Oxide Synthase deficiency and the loss of nitric oxide bioavailability in Duchenne Muscular Dystrophy. *Neuromuscular Disorders*.

Peer-reviewed Published Abstracts

1. **Timpani, C.A.**, Trewin, A., Betik, A., Stepto, N., Hayes, A., McConell, G.M., Rybalka, E. (2015) Glucose uptake & mitochondrial function following 8 weeks of dietary nitrate supplementation in the dystrophin-deficient *mdx* mouse. *Neuromuscular Disorders Supplement: World Muscle Society Proceedings*, 25(2). **IF=2.7**, SciMago **Q1**. **Contribution to published work:** Performed data collection and analysis; authoring and presentation of abstract.
2. Cheregi, B., **Timpani, C.A.**, Hayes, A., Nurgali, K. & Rybalka, E. (2015) Chemotherapy-induced mitochondrial respiratory dysfunction, oxidant production and death in healthy skeletal muscle C2C12 myoblast and myotube models. *Neuromuscular Disorders Supplement: World Muscle Society Proceedings*, 25(2). **IF=2.7**, SciMago **Q1**. **Contribution to published work:** Assisted with data collection and analysis.

Commissioned Reports

1. Rybalka, E., & **Timpani, C. A.** (2015). Duchenne Muscular Dystrophy as a mitochondrial myopathy: Why therapeutically targeting the mitochondria is a plausible treatment avenue. For: Santhera Pharmaceuticals Liestal, Switzerland.

Awards

2016	Victoria University 3 Minute Thesis Finals Runner-Up (\$500)
2016	Victoria University 3 Minute Thesis Heats Winner (\$200)
2016	Victoria University 3 Minute Thesis College of Health & Biomedicine Winner (\$200)
2016	Australian Society for Medical Research People's Choice (3 Minute Thesis)
2015	Australian Physiological Society Young Investigator Award - Best Poster Presentation (\$AUD250)
2015	World Muscle Society Fellowship (\$EUR500)
2015	Australian Society for Medical Research Young Investigator High Commendation Award
2012	Vice-Chancellor's Outstanding Student Leader
2012	Vice-Chancellor's PhD Scholarship (incorporating an Australian Postgraduate Award) (4 years)
2011	University Medal
2011	Executive Deans Scholar Award
2011	Outstanding Honours Student in Bachelor of Science (Honours) in Biomedical Sciences
2010	Outstanding Final Year Student in Bachelor of Science in Biomedical Sciences
2010	Victoria University Summer Scholarship (\$3000)
2009	Victoria University Summer Scholarship (\$3000)
2008	Invited Golden Key International Honour Society Member
2008	Victoria University Promising Student Entry Scholarship (entire undergraduate degree)

TABLE OF CONTENTS

ABSTRACT	ii
DECLARATION	iv
ACKNOWLEDGEMENTS	v
LIST OF COMMUNICATIONS & AWARDS	viii
TABLE OF CONTENTS	xiii
LIST OF FIGURES	xx
LIST OF TABLES	xxiv
LIST OF ABBREVIATIONS	xxv
CHAPTER ONE: LITERATURE REVIEW	1
1.1 Introduction	2
1.2 Duchenne Muscular Dystrophy	7
1.2.1 Disease Background	7
1.2.1.1 The C57BL/10 <i>mdx</i> mouse	9
1.2.2 DMD as a metabolic myopathy	11
1.3 Metabolic System Deficits in DMD	13
1.3.1 Macronutrient Uptake	15
1.3.2 Glycolysis	18
1.3.2.1 Glycogen Storage and Utilisation	21
1.3.3 Fat Oxidation	24
1.3.4 Mitochondria	25
1.3.4.1 The Tricarboxylic Acid Cycle & Electron Transport Chain	27
1.3.4.2 Mitochondrial Morphology & Density	34
1.3.5 The Creatine Phosphagen System	36
1.3.6 Purine Nucleotide Salvage & <i>De Novo</i> Synthesis	38
1.4 Dystrophic muscle does not respond normally to master energy signals	41
1.5 The Dystrophin-ATP Connection: Is a mitochondrial disease at the heart of DMD?	47
1.6 Clinical Case Studies	51
1.7 Could metabogenic therapy be a future DMD treatment direction?	54

1.7.1	Creatine supplementation	55
1.7.2	Allopurinol	57
1.7.3	Idebenone	61
1.7.4	New metabogenic therapies for the treatment of DMD	63
1.7.4.1	The dystrophin-metabolism connection – <i>nNOS</i>	63
1.7.4.1.1	Increasing NO bioavailability	65
1.7.4.1.2	Restoring <i>nNOS</i> protein expression	66
1.7.4.1.3	Inhibition of phosphodiesterase activity	68
1.7.4.1.4	NO donors	70
1.7.4.1.5	Could nitrate therapy be beneficial?	73
1.7.4.2	ASA supplementation	75
1.8	Concluding comments	83
CHAPTER TWO: AIMS & HYPOTHESES		84
2.1	Principal aim and hypothesis	85
2.1.1	Part one aims and hypotheses	85
2.1.2	Part two aims and hypotheses	86
CHAPTER THREE: METHODS		88
3.1	<i>mdx</i> mouse model experiments	89
3.1.1	Animals	89
3.1.1.1	Dietary supplementation	89
3.1.1.2	Surgeries	91
3.1.2	Glucose uptake (GU)	93
3.1.2.1	Muscle dissection and contraction protocol	93
3.1.2.2	Radioactive determination of GU	94
3.1.3	Mitochondrial respirometry/metabolism	98
3.1.3.1	Measurement of mitochondrial respiration	98
3.1.3.2	Mitochondrial content, viability and metabolites	109
3.1.4	Immunolabelling and histology	122
3.1.4.1	Immunolabelling of dystrophin-associated proteins	122
3.1.4.2	Histology	125

3.2	Cell experiments	131
3.2.1	Cell culture maintenance	132
3.2.2	Determination of ASA and nitrite dosages	132
3.2.2.1	Crystal violet assay	132
3.2.2.2	Cell proliferation assay	133
3.2.3	Determination of mitochondrial viability	134
3.2.4	Determination of O ₂ ⁻ production	134
3.2.5	Mitochondrial & glycolytic metabolism using the Extracellular Flux Analyser	134
3.3	Statistical analysis	136
PART ONE: NITRATE/NITRITE SUPPLEMENTATION		137
CHAPTER FOUR: EVALUATION OF NITRATE THERAPY IN THE <i>MDX</i> MOUSE		138
4.1	Introduction	139
4.2	Methods	143
4.2.1	Ethical approval	143
4.2.2	Animals and supplementation	143
4.2.3	Muscle dissection and contraction protocol	143
4.2.4	Glucose uptake (GU)	144
4.2.5	Mitochondrial respiration and hydrogen peroxide (H ₂ O ₂) emission measurements	144
4.2.6	Western blot analysis of mitochondrial respiratory chain proteins	144
4.2.7	Citrate Synthase (CS) activity	145
4.2.8	Histological analysis	145
4.2.8.1	Dystrophin, nNOS and nitrotyrosine immunolabelling	145
4.2.8.2	Haematoxylin & Eosin staining	145
4.2.9	Statistics	146
4.3	Results	147
4.3.1	Effect of NITR supplementation on body weight, food and water consumption and muscle weights	147
4.3.2	Immunolabelling of dystrophin and nNOS	147

4.3.3	Effect of NITR supplementation on GU	153
4.3.4	Effect of NITR supplementation on mitochondrial function	155
4.3.4.1	Respirometry	155
4.3.4.2	Electron transport chain complex expression	159
4.3.4.3	Citrate synthase activity	162
4.3.5	Effect of NITR supplementation on ROS production in red and white gastrocnemius	162
4.3.6	Effect of NITR supplementation on peroxynitrite production	165
4.3.7	Effect of NITR supplementation on muscle architecture	165
4.4	Discussion	170
4.5	Conclusion	180
CHAPTER FIVE: EVALUATION OF NITRITE THERAPY IN HUMAN DMD MYOBLASTS		181
5.1	Introduction	182
5.2	Methods	185
5.2.1	Cell culture maintenance	185
5.2.2	Determination of nitrite dosage	185
5.2.2.1	Crystal violet assay	185
5.2.2.2	Cell proliferation assay	186
5.2.3	Determination of mitochondrial viability	186
5.2.4	Determination of mitochondrial superoxide (O_2^-) production	186
5.2.5	Measurement of mitochondrial & glycolytic metabolism using the Extracellular Flux Analyser	187
5.2.6	Statistics	187
5.3	Results	188
5.3.1	Effect of acute nitrite supplementation on cell viability	188
5.3.2	The effect of acute nitrite supplementation on mitochondrial viability	192
5.3.3	The effect of acute nitrite supplementation on mitochondrial superoxide (O_2^-) production	193
5.3.4	The effect of acute nitrite supplementation on oxidative and glycolytic Metabolism	197
5.4	Discussion	208

5.5	Conclusion	216
PART TWO: ASA THERAPY		217
CHAPTER SIX: EVALUATION OF ASA THERAPY IN THE <i>MDX</i> MOUSE		218
6.1	Introduction	219
6.2	Methods	222
6.2.1	Ethical approval	222
6.2.2	Animals and supplementation	222
6.2.3	Muscle dissection and contraction protocol to induce GU	222
6.2.4	Mitochondrial respiration measurements	223
6.2.5	Mitochondrial viability and superoxide production	223
6.2.6	Western blot analysis of metabolic stress (AMPK), and mitochondrial biogenesis (PGC-1 α/β) and respiratory chain proteins (CI-V)	224
6.2.7	Citrate synthase (CS) activity	224
6.2.8	Metabolites	225
6.2.9	Histopathology analysis	225
6.2.9.1	Haematoxylin & Eosin (H&E) staining	225
6.2.9.2	Oil Red O (ORO) staining	225
6.2.9.3	Gomori trichrome staining	226
6.2.9.4	Alizarin Red staining	226
6.2.9.5	Succinate dehydrogenase (SDH) staining	226
6.2.9.6	Dystrophin and utrophin immunolabelling	227
6.2.10	Nrf2 quantification	227
6.2.11	Statistics	227
6.3	Results	229
6.3.1	Effect of ASA supplementation on body weight, food and water consumption and muscle and organ weights	229
6.3.2	Effect of ASA supplementation on GU	232
6.3.3	Effect of ASA supplementation on metabolism	237
6.3.3.1	Respirometry	237
6.3.3.2	Mitochondrial viability and superoxide (O ₂ ⁻) production	242

6.3.3.3	Electron transport chain (ETC) complex expression	244
6.3.3.4	Metabolites	244
6.3.3.5	Metabolic stress signalling	247
6.3.4	Effect of ASA supplementation on histopathology	250
6.3.4.1	Haematoxylin and Eosin (H&E)	250
6.3.4.2	Oil Red O (ORO)	253
6.3.4.3	Gomori Trichrome	253
6.3.4.4	Alizarin Red	256
6.3.4.5	Succinate Dehydrogenase (SDH)	256
6.3.4.6	Dystrophin and utrophin expression	259
6.3.5	Effect of ASA supplementation on Nrf2	259
6.4	Discussion	263
6.5	Conclusion	272
CHAPTER SEVEN: EVALUATION OF ASA THERAPY IN HUMAN DMD MYOBLASTS		273
7.1	Introduction	274
7.2	Methods	277
7.2.1	Cell culture maintenance	277
7.2.2	Determination of ASA dosage	277
7.2.2.1	Crystal violet assay	277
7.2.2.2	Cell proliferation assay	278
7.2.3	Determination of mitochondrial viability	278
7.2.4	Determination of mitochondrial superoxide (O ₂ ⁻) production	278
7.2.5	Mitochondrial & glycolytic metabolism using the Extracellular Flux Analyser	279
7.2.6	Statistics	279
7.3	Results	280
7.3.1	Effect of acute ASA supplementation on cell viability	280
7.3.2	The effect of acute ASA supplementation on mitochondrial viability	281
7.3.3	The effect of acute ASA on mitochondrial superoxide (O ₂ ⁻) production	287
7.3.4	The effect of acute ASA supplementation on oxidative and glycolytic metabolism	287

7.4	Discussion	298
7.5	Conclusion	306
CHAPTER EIGHT: CONCLUSIONS, LIMITATIONS & FUTURE DIRECTIONS		307
8.1	Conclusions	308
8.2	Limitations	313
8.3	Future Directions	319
CHAPTER NINE: REFERENCES		323

LIST OF FIGURES

FIGURE 1.1. The location and role of the dystrophin protein in skeletal muscle	6
FIGURE 1.2. Accumulation of intramyofibrillar lipids is a feature of dystrophin-deficient muscle	14
FIGURE 1.3. Glycolytic impairment in dystrophin-deficient skeletal muscle	23
FIGURE 1.4. Widespread mitochondrial dysfunction in dystrophin-deficient skeletal muscle	30
FIGURE 1.5. Challenging the accepted paradigm of DMD aetiology: the potential for metabolic therapy to anaplerotically “correct” dystrophin-deficiency-mediated pathology	31
FIGURE 1.6. Creatine phosphagen (Cr/PCr) system function in skeletal muscle	39
FIGURE 1.7. Adenylate kinase (AK) dysregulation in dystrophin-deficient skeletal muscle	43
FIGURE 1.8. The consequences of dysfunctional Purine Nucleotide Cycle (PNC) activity in dystrophin-deficient skeletal muscle	44
FIGURE 1.9. Schematic of methods utilised to increase NO bioavailability in dystrophic skeletal muscle and the downstream effects	76
FIGURE 1.10. Proposed effects of ASA supplementation	81
FIGURE 3.1. Muscle dissection and contractile bath setup	92
FIGURE 3.2. Muscle dissection and contractile bath setup	95
FIGURE 3.3. Timeline of contraction protocol to determine glucose uptake (GU)	96
FIGURE 3.4. Examples traces obtained during glucose uptake (GU) experimentation	97
FIGURE 3.5. Representative traces of mitochondrial respiration (A) and hydrogen peroxide (H ₂ O ₂) emission (B) from the Oxygraph respirometer.	100
FIGURE 3.6. Indication of the position of FDB in the sole of the foot	101
FIGURE 3.7. Representative traces of oxygen consumption rate (OCR, A) and extracellular acidification rate (ECAR, B) in isolated FDB fibres	107
FIGURE 3.8. Representative images of immunohistochemical analysis of TA	124
FIGURE 3.9. Representative images of histological analysis	130
FIGURE 4.1. Body weight of unsupplemented and NITR-supplemented mice over the supplementation period	148

FIGURE 4.2. Average food and water consumption of unsupplemented and NITR supplemented mice over the supplementation period	149
FIGURE 4.3. Proportion of dystrophin and nNOS immunoreactivity in unsupplemented and supplemented CON and <i>mdx</i> TA	152
FIGURE 4.4. GU in isolated EDL and SOL from unsupplemented and NITR supplemented CON and <i>mdx</i> mice	154
FIGURE 4.5. Mitochondrial function in intact, permeabilised muscle fibres from the white portion of gastrocnemius from unsupplemented and NITR-supplemented CON and <i>mdx</i> mice	157
FIGURE 4.6. Mitochondrial function in intact, permeabilised muscle fibres from the red portion of gastrocnemius from unsupplemented and NITR supplemented CON and <i>mdx</i> mice	158
FIGURE 4.7. Mitochondrial respiratory chain complex proteins, and citrate synthase activity, from the white portion of gastrocnemius from unsupplemented and NITR-supplemented CON and <i>mdx</i> mice	160
FIGURE 4.8. Mitochondrial respiratory chain complex proteins, and citrate synthase activity, from the red portion of gastrocnemius from unsupplemented and NITR supplemented CON and <i>mdx</i> mice	161
FIGURE 4.9. H ₂ O ₂ emission in intact fibres from the white (A) and red (B) portions of gastrocnemius from unsupplemented and NITR-supplemented CON and <i>mdx</i> mice	164
FIGURE 4.10. Immunohistological analysis of TA from unsupplemented and NITR supplemented CON and <i>mdx</i> mice	168
FIGURE 4.11. Histological analysis of TA from unsupplemented and NITR supplemented CON and <i>mdx</i> mice	169
FIGURE 5.1. Cell viability, as determined by crystal violet staining, in unsupplemented and nitrite supplemented CON myoblasts	190
FIGURE 5.2. Cell Index (viability), as determined by real-time monitoring, in unsupplemented and nitrite supplemented CON myoblasts	191
FIGURE 5.3. Mitochondrial viability of unsupplemented and nitrite supplemented CON and DMD myoblasts	194
FIGURE 5.4. Total mitochondrial pool of unsupplemented and nitrite supplemented CON and DMD myoblasts	195
FIGURE 5.5. Mitochondrial superoxide (O ₂ ⁻) production of unsupplemented and nitrite supplemented CON and DMD myoblasts	196
FIGURE 5.6. OCR of unsupplemented and nitrite supplemented CON and DMD myoblasts	199
FIGURE 5.7. ECAR of unsupplemented and nitrite supplemented CON and DMD myoblasts	200
FIGURE 5.8. Mitochondrial function of unsupplemented and nitrite supplemented CON and DMD myoblasts	204

FIGURE 5.9. Metabolic potential of unsupplemented and nitrite supplemented CON and DMD myoblasts	205
FIGURE 5.10. Metabolic phenograms of unsupplemented and nitrite supplemented CON and DMD myoblasts	206
FIGURE 6.1. Weight gain of unsupplemented and ASA supplemented mice over the supplementation period	231
FIGURE 6.2. Final body weight, heart weight and heart weight to body weight ratio of unsupplemented and ASA supplemented mice	232
FIGURE 6.3. Average food and water consumption of unsupplemented and ASA supplemented mice during the supplementation period	234
FIGURE 6.4. GU in isolated EDL and SOL from unsupplemented and ASA supplemented CON and <i>mdx</i> mice	236
FIGURE 6.5. Mitochondrial function in isolated FDB fibres from unsupplemented and ASA supplemented CON and <i>mdx</i> mice	240
FIGURE 6.6. Metabolic phenograms of isolated FDB fibres from unsupplemented and ASA supplemented CON and <i>mdx</i> mice	241
FIGURE 6.7. Mitochondrial viability, pool and superoxide (O ₂ ⁻) production of isolated FDB fibres from unsupplemented and ASA supplemented CON and <i>mdx</i> mice	243
FIGURE 6.8. Mitochondrial respiratory chain complex proteins of the quadriceps from unsupplemented and ASA-supplemented CON and <i>mdx</i> mice	245
FIGURE 6.9. Intramuscular Cr, PCr, TCr, ATP, lactate and glycogen content of unsupplemented and ASA supplemented CON and <i>mdx</i> mice	246
FIGURE 6.10. AMPK protein content of quadriceps from unsupplemented and ASA-supplemented CON and <i>mdx</i> mice	248
FIGURE 6.11. PGC-1 α and -1 β protein content of quadriceps from unsupplemented and ASA-supplemented CON and <i>mdx</i> mice	249
FIGURE 6.12. Histological analysis of TA from unsupplemented and ASA supplemented CON and <i>mdx</i> mice	251
FIGURE 6.13. Histogram of TA fibre size distribution from unsupplemented and ASA	252
FIGURE 6.14. Assessment of lipid accumulation in TA from unsupplemented and ASA supplemented CON and <i>mdx</i> mice	254
FIGURE 6.15. Assessment of fibrotic tissue in TA from unsupplemented and ASA supplemented CON and <i>mdx</i> mice	255
FIGURE 6.16. Assessment of Ca ²⁺ content in TA from unsupplemented and ASA supplemented CON and <i>mdx</i> mice	257
FIGURE 6.17. Assessment of succinate dehydrogenase (SDH) in TA from unsupplemented and ASA supplemented CON and <i>mdx</i> mice	258
FIGURE 6.18. Proportion of dystrophin and utrophin immunoreactivity in unsupplemented and supplemented CON and <i>mdx</i> TA	261

FIGURE 6.19. Nrf2 protein content of quadriceps from unsupplemented and ASA-supplemented CON and <i>mdx</i> mice	262
FIGURE 7.1. Cell viability, as determined by crystal violet staining, in unsupplemented and ASA supplemented CON myoblasts	283
FIGURE 7.2. Cell Index (viability), as determined by real-time monitoring, in unsupplemented and ASA supplemented CON myoblasts	284
FIGURE 7.3. Mitochondrial viability of unsupplemented and ASA supplemented CON and DMD myoblasts	285
FIGURE 7.4. Total mitochondrial pool of unsupplemented and ASA supplemented CON and DMD myoblasts	286
FIGURE 7.5. Mitochondrial superoxide (O_2^-) production of unsupplemented and ASA supplemented CON and DMD myoblasts	289
FIGURE 7.6. OCR of unsupplemented and ASA supplemented CON and DMD myoblasts	293
FIGURE 7.7. ECAR of unsupplemented and ASA supplemented CON and DMD myoblasts	294
FIGURE 7.8. Mitochondrial function of unsupplemented and ASA supplemented CON and DMD myoblasts	295
FIGURE 7.9. Metabolic potential of unsupplemented and ASA supplemented CON and DMD myoblasts	296
FIGURE 7.10. Metabolic phenograms of unsupplemented and ASA supplemented CON and DMD myoblasts	297

LIST OF TABLES

TABLE 1.1. Summary of the metabolic deficits in the metabolic pathways of dystrophic skeletal muscle	17
TABLE 1.2. Summary of methods utilised to increase NO production dystrophic muscle	77
TABLE 3.1. Protocol utilized to measure OCR and ECAR in the XF24 Analyser	106
TABLE 3.2. Metabolic parameters employed to assess the metabolic/mitochondrial effects of the supplementation periods	108
TABLE 3.3. Reagent cocktail for ATP-CP metabolite analysis	116
TABLE 3.4. Reagent cocktail for Cr metabolite analysis	117
TABLE 3.5. Reagent cocktail for lactate metabolite analysis	118
TABLE 3.6. Reagent cocktail for glycogen metabolite analysis	118
TABLE 3.7. Antibody details for immunolabelling	123
TABLE 3.8. Protocol utilised for Haematoxylin & Eosin staining of TA	126
TABLE 3.9. Protocol utilised for Oil Red O staining of TA	127
TABLE 3.10. Protocol utilised for Alizarin Red staining of TA	127
TABLE 3.11. Protocol utilised for SDH staining of TA	128
TABLE 3.12. Protocol utilised for Gomori Trichrome staining of TA	129
TABLE 4.1. Weights of muscles and organs from unsupplemented and NITR supplemented mice over the supplementation period	150
TABLE 6.1. Post-treatment muscle and organ weight from unsupplemented and ASA supplemented mice	233

LIST OF ABBREVIATIONS

[]	Concentration
$\Delta\Psi$	Mitochondrial membrane potential
ADP	Adenosine diphosphate
AICAR	5'-aminoimidazole-4-carboxamide-1- β -D-ribofuranoside
AK	Adenylate kinase
AMP	Adenosine monophosphate
AMPK	Adenosine monophosphate-activated protein kinase
ASA	Adenylosuccinic acid
ATP	Adenosine triphosphate
BHI	Bioenergetical health index
BMD	Becker Muscular Dystrophy
BSA	Bovine serum albumin
Ca ²⁺	Calcium
cGMP	Cyclic guanosine monophosphate
CI	Complex I
CII	Complex II
CIII	Complex III
CIV	Complex IV
CK	Creatine kinase
CON	Control
CoQ10	Coenzyme Q10
Cr	Creatine
CS	Citrate synthase
CSA	Cross sectional area
DAP	Dystrophin-associated proteins

DAPI	4',6-diamidino-2-phenylindole
DMD	Duchenne Muscular Dystrophy
DPC	Dystrophin protein complex
DTNB	5,5'-dithiobis-2-nitrobenzoic acid
EBD	Evans Blue Dye
ECAR	Extracellular acidification rate
EDL	Extensor digitorum longus
EDTA	Ethylediniaminetetra-acetic acid
ETC	Electron transport chain
ETS	Electron transport system
FADH ₂	Flavin adenine dinucleotide
FBS	Foetal bovine serum
FCCP	Carbonyl cyanide- <i>p</i> -trifluoromethoxyphenylhydrazone
FDB	Flexor digitorum brevis
G-6-P	Glucose-6-phosphate
GLUT4	Glucose transporter 4
GTP	Guanosine triphosphate
GU	Glucose uptake
H&E	Haematoxylin and eosin
H ⁺	Proton
H ₂ O ₂	Hydrogen peroxide
IDH	Isocitrate dehydrogenase
IMP	Inosine monophosphate
iNOS	Inducible nitric oxide synthase
LDH	Lactate dehydrogenase
LHON	Leber's hereditary optic neuropathy
L _o	Optimal length
<i>mdx</i>	Muscular dystrophy x-linked on c57BL/10 background (mouse)

MELAS	Mitochondrial encephalomyopathy, lactic acidosis and stroke-like episodes
Mi-CK	Mitochondrial creatine kinase
MQ	Milli Q ultrapure water
MT	Metabolic therapy
mtDNA	Mitochondrial DNA
NAD	Nicotinamide adenine dinucleotide
NADH	Nicotinamide adenine dinucleotide
NADPH	Nicotinamide adenine dinucleotide phosphate
NIT	Nitrite
NITR	Nitrate
nNOS	Neuronal nitric oxide synthase
NO	Nitric oxide
Nrf2	Nuclear factor (erythroid-derived 2)-like 2
NSAID	Non-steroidal anti-inflammatory drug
O ₂	Oxygen
O ₂ ⁻	Superoxide
OCR	Oxygen consumption rate
OCT	Optimal cutting temperature
ONOO ⁻	Peroxynitrite
ORO	Oil red O
OXPPOS	Oxidative phosphorylation
P-AMPK	Phosphorylated adenosine monophosphate-activated protein kinase
PCA	Perchloric acid
PCr	Phosphocreatine
PDE	Phosphodiesterase
PDH	Pyruvate dehydrogenase
PFK	Phosphofructokinase

PGC1- α/β	PPAR γ -coactivator 1 α/β
P _i	Inorganic phosphate
PK	Pyruvate kinase
PKG	cGMP-regulated protein kinase
PNC	Purine nucleotide cycle
PPAR	Peroxisome proliferator-activated receptor
PTP	Permeability transition pore
RCR	Respiratory control ratio
RG	Red gastrocnemius
RNS	Reactive nitrogen species
ROS	Reactive oxygen species
RTCA	Real time cell analysis
sCG	Soluble guanylyl cyclase
SDH	Succinate dehydrogenase
SOL	Soleus
sPO	Specific force
SUIT	Substrate, uncoupler, inhibitor titration
TA	Tibialis anterior
TCA	Tricarboxylic acid cycle
TCr	Total intramuscular creatine
TMPD	N,N,N',N'-tetramethyl-p-phenylenediamine
TNB	5-thio-2-nitrobenzoic acid
TNF α	Tumour necrosis factor- α
UNSUPP	Unsupplemented
WG	White gastrocnemius

Chapter One

Literature Review

Publications from this chapter:

1. **Timpani et al.** Revisiting the dystrophin-ATP connection: How half a century of research still implicates mitochondrial dysfunction in Duchenne muscular dystrophy aetiology, *Medical Hypotheses*, Volume 85, Issue 6, 2015
2. Rybalka, **Timpani et al.** Metabogenic and nutraceutical approaches to address energy dysregulation and skeletal muscle wasting in Duchenne Muscular Dystrophy, *Nutrients*, Volume 7, Issue 12, 2015
3. **Timpani et al.** Therapeutic strategies to address nNOS deficiency and the loss of nitric oxide bioavailability in Duchenne Muscular Dystrophy, Under Review, *Neuromuscular Disorders*

1.1 Introduction

Duchenne Muscular Dystrophy (DMD) is the most prevalent muscular dystrophy afflicting ~1 in 3,500 live born males (Emery, 1991). Regarded as a debilitating and fatal skeletal muscle disease, it is characterised by muscular weakness, exercise intolerance and progressive deterioration of skeletal muscle. Sufferers are generally confined to a wheelchair by 12 years of age with cardiorespiratory failure ultimately ensuing by the third decade of life (Brooke *et al.*, 1981, Brooke *et al.*, 1989).

Some 125 years after DMD was first described (Duchenne, 1868), the cause was identified as a mutation on the short arm of the X-chromosome (Hoffman *et al.*, 1987). The product of this mutation is the ablation of dystrophin, a 427kDa rod-shaped protein (Koenig *et al.*, 1988) usually associated with the sarcolemma of muscle fibres via a complex of glycoproteins (Figure 1.1A). The presence of dystrophin and its associated glycoproteins provides integrity and rigidity to the fibre, however dystrophin-deficiency and the secondary reduction of these glycoproteins (Ohlendieck and Campbell, 1991) renders the fibres more susceptible to damage as they become structurally unstable and exceedingly porous to the extracellular environment (Figure 1.1B). As a result, excessive calcium (Ca^{2+}) influx (Bodensteiner and Engel, 1978, Jackson *et al.*, 1985, Turner *et al.*, 1991, Alderton and Steinhardt, 2000, Vandebrouck *et al.*, 2002), poor Ca^{2+} handling (Imbert *et al.* 1996, William *et al.* 2007, Robert *et al.* 2001), activation of proteases/lipases (Haycock *et al.*, 1996, Disatnik *et al.*, 1998, Dudley *et al.*, 2006a, Messina *et al.*, 2006) and mitochondrial Ca^{2+} overload (Wrogeman *et al.* 1973, Glesby *et al.* 1988, Lucas-Heron *et al.* 1989, Viola *et al.* 2013), precede muscle degeneration. Over time, and as

regeneration fails, fatty and connective tissue replacement culminates in non-functional muscle with the later involvement of the diaphragm leading to respiratory impairment.

In a bid to cure this progressive and fatal muscle wasting, the majority of research since 1987 has focused on genetically manipulating the disease by reintroducing the dystrophin gene (or a miniature version) back into the genome (Wells *et al.*, 1995, Clemens *et al.*, 1996, Sakamoto *et al.*, 2002) and pharmacological intervention (Willmann *et al.*, 2009, Matsumura *et al.*, 2009). While some success has been observed with exon skipping and termination codon read-through trials (as reviewed in (Fairclough *et al.*, 2013)), many complications with genetic therapy, including immunological reaction to delivery vectors, affordability and suitability (Cossu and Sampaolesi, 2007), have been reported. As yet, there is no cure. Currently, corticosteroid treatment is used to delay muscular weakness and prolong function but has a multitude of side effects including cardiomyopathy, weight gain, cataracts, hypertension, cushingoid features and osteoporosis (Moxley *et al.* 2005).

Prior to the discovery of dystrophin (and by several research groups afterwards), DMD was considered to be a disease of metabolic origin, with a strong body of literature demonstrating deficiency of key metabolic systems and regulators, including the mitochondria. As mitochondria constitute the ubiquitous adenosine triphosphate (ATP)-producing machinery of the cell and consequently play a crucial role in signalling cell death, their dysfunction seemingly induces a myriad of physiological events that underscore, or at least exacerbate, dystrophinopathy. Deficits encompassing the cytosolic enzymes of glycolysis (Dreyfus, 1954, Di Mauro, 1967, Hess, 1965, Chi *et al.*, 1987, Chinet

et al., 1994) and the Purine Nucleotide Cycle (PNC) (Sanada and Yamaguchi, 1979, Fitt and Parliament, 1982, van Bennekom *et al.*, 1984), and the mitochondrial enzymes of the Tricarboxylic Acid (TCA) cycle (Bonsett and Rudman, 1984, Chinet *et al.*, 1994) and Electron Transport Chain (ETC) (Glesby *et al.*, 1988, Kuznetsov *et al.*, 1998, Rybalka *et al.*, 2014) have been consistently reported in DMD sufferers, female carriers and animal models of the disease. Severely reduced ATP content (Ronzoni, 1958, Vignos Jr and Warner, 1963, Shuttlewood and Griffiths, 1982, Tamari *et al.*, 1982, Cole *et al.*, 2002) is the downstream consequence of these deficits and has been observed in skeletal muscle from both DMD patients and animal models.

Dysregulation of cellular energy homeostasis has a variety of consequences for muscle including (1) impaired contractile apparatus function leading to reduced strength, ambulatory capacity and exercise tolerance (Fitts 1994); (2) impaired intracellular Ca^{2+} buffering leading to loss of homeostasis and Ca^{2+} -induced degeneration (Halachmi & Eilam, 1993); (3) reduced protein synthesis (Pasiakos *et al.*, 2010); and (4) reduced satellite cell activation, replication, migration and differentiation leading to a markedly decreased capacity for regeneration of damaged muscle fibres (Ryten *et al.*, 2002). The mitochondria are also explicitly involved in maintaining, and are strongly regulated by, cytosolic Ca^{2+} concentration ($[\text{Ca}^{2+}]$). Heightened mitochondrial $[\text{Ca}^{2+}]$ increases ATP synthesis until overload induces permeability transition, collapses the mitochondrial membrane potential and signals apoptotic cellular death pathways. Thus an important question that could be asked is: What comes first, the chicken (Ca^{2+} -induced pathophysiology) or the egg (mitochondrial dysfunction)? That impaired metabolism has been observed in

mdx myoblasts independent of dystrophin-deficiency (dystrophin is not phenotypically expressed until myoblastic fusion into myotubes) (Onopiuk *et al.*, 2009), indeed suggests an intrinsic metabolic deficiency. Metabolic impairment is also evident in a variety of tissues and cells from DMD patients and animal models that express a different dystrophin isoform – these include liver (Howland and Challberg, 1973, Katyare *et al.*, 1978), heart (Zhang *et al.*, 2008, Lewis *et al.*, 2010) and brain (Bresolin *et al.*, 1994, Tracey *et al.*, 1995, Tracey *et al.*, 1996a, Tracey *et al.*, 1996b, Tuon *et al.*, 2010). Collectively, the literature strongly suggests that DMD is characterised by a systemic metabolic impairment, which is central to the aetiology of the disease and not secondary to the pathophysiology as currently accepted.

In 1992, and following 30 years of collective clinical research, Bonsett and Rudman (Bonsett and Rudman, 1992) published a timely article in *Medical Hypotheses* that offered compelling evidence to highlight that DMD is predominantly underscored by metabolic impairment at the mitochondrial level, and that this can be anaplerotically “corrected” using high dose adenylosuccinic acid (ASA) treatment. Since this publication, and despite mounting literature indicating the same perturbations in animal models of DMD, metabolic therapy – with the exception of dietary creatine monohydrate supplementation – is still not a mainstay of DMD treatment. This literature review explores the collective historical and contemporary literature describing the metabolic nuances of dystrophinopathy and the clinical evidence that suggests re-defining DMD as a metabolic myopathy and strategically treating it as such, could improve patient outcomes and quality of life.

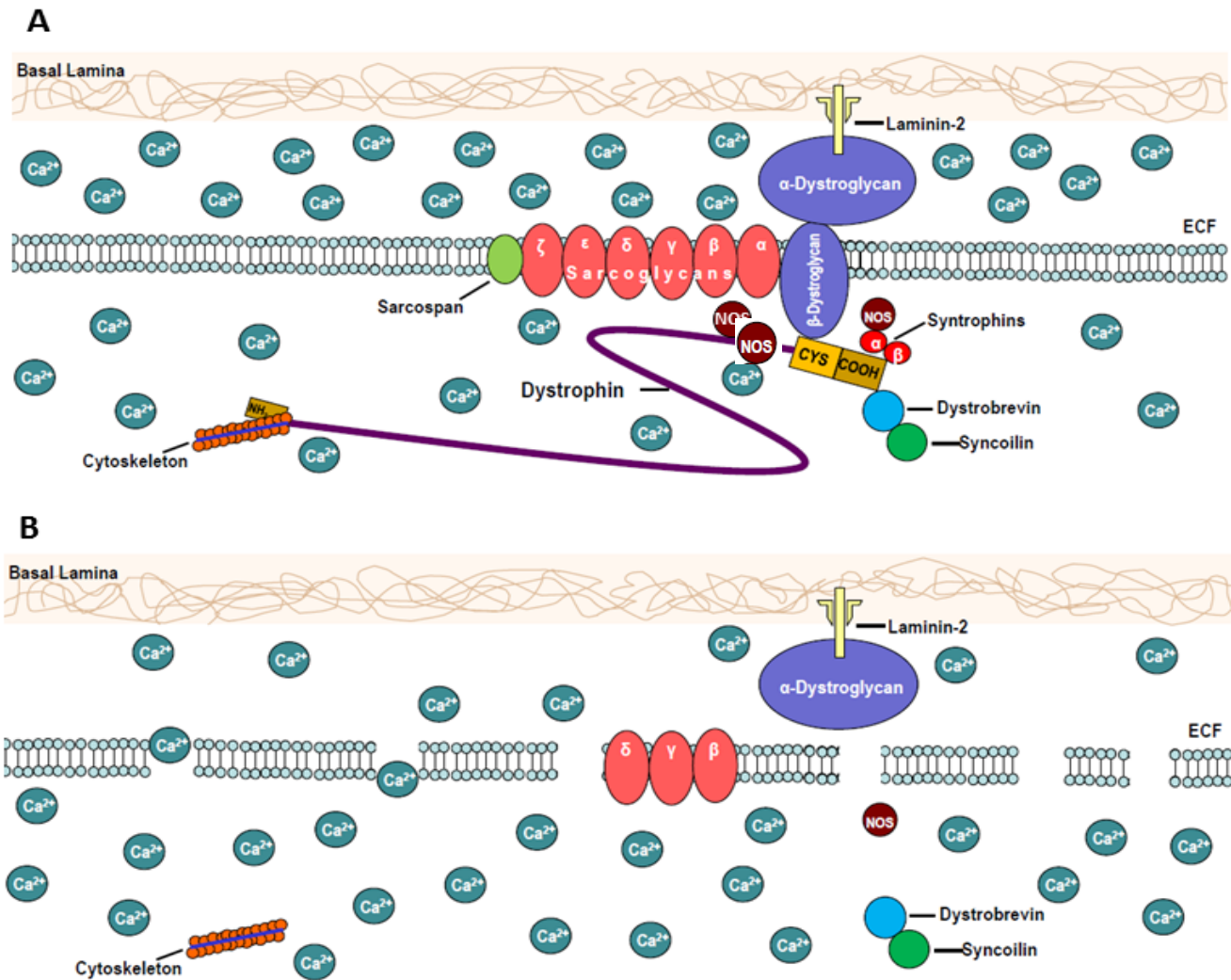


Figure 1.1. The location and role of the dystrophin protein in skeletal muscle. Dystrophin typically connects the cytoskeleton to the sarcolemmal complex of glycoproteins, reinforcing the sarcolemma and preventing excessive Ca²⁺ entry (A). In the absence of dystrophin (B) the sarcolemma becomes exceedingly porous and Ca²⁺ entry is unregulated.

1.2 Duchenne Muscular Dystrophy

1.2.1 Disease background

DMD was first described by Guillaume Duchenne in 1858 and some 125 years later, the origin of the disease, a mutation in the dystrophin gene at position 21 on the short arm of the X-chromosome (Hoffman *et al.*, 1987), was identified. The dystrophin gene is the largest gene in the human genome (2.6 million base pairs) and approximately 60% of mutations arise from large insertion/deletion frameshift errors while 40% arise from small frameshift errors or point mutations (Hoffman and Dressman, 2001). In either case, the mutation results in the ablation of dystrophin from the sarcolemma (DMD) or in the expression of a truncated dystrophin which is characteristic of Becker Muscular Dystrophy (BMD), a less severe form of muscular dystrophy. Typically, signs of DMD are evident between 2 and 5 years of age with developmental delays in ambulation and muscle weakness observed (Gardener-Medwin, 1980) along with a significant elevation in serum creatine kinase (CK) (Pennington, 1980, Moser, 1984). As the disease progresses, ambulation is lost and sufferers become wheelchair-bound by adolescence due to the primary degeneration of the lower limb and pelvic girdle muscles. Sufferers eventually succumb to cardiorespiratory failure in the third decade of life due to cardiac hypertrophy (Nigro *et al.*, 1990) and degeneration of the diaphragm which induces progressive cardiorespiratory failure. Currently, there is no cure for DMD, with corticosteroids, particularly deflazacort and prednisone, the treatment recommended to preserve muscle mass and function. Exon skipping therapy (Exondys51) has recently been approved in Europe and the US.

Dystrophin is a large and important cytoskeletal protein that structurally links the contractile apparatus to the sarcolemma and extracellular matrix through its interaction with the transmembranous protein β -dystroglycan (Figure 1.1). Dystrophin is purported to play a role in stabilising and maintaining membrane integrity during contraction (Campbell, 1995, Ozawa *et al.*, 1995) to prevent stretch-induced damage. Indeed, dystrophin-deficient skeletal muscle is more susceptible to damage (Menke and Jockusch, 1991, Cullen *et al.*, 1994), particularly during exercise (Clarke *et al.*, 1993), indicating the protective role dystrophin plays. In addition to this, dystrophin appears to play a vital role in dystrophin protein complex (DPC) assembly as its absence induces a secondary reduction in DPC proteins (Ohlendieck and Campbell, 1991). Overall, dystrophin-deficiency leads to a weakened and porous sarcolemmal membrane that induces a pathological cascade leading to repetitive muscle damage and degeneration.

It is well accepted that the instigator of the extensive skeletal muscle damage and degeneration is Ca^{2+} dysregulation. The unregulated and abnormal entry of Ca^{2+} into dystrophin-deficient myofibres results in a significantly elevated intracellular $[\text{Ca}^{2+}]$ (Turner *et al.*, 1988, Fong *et al.*, 1990, Mallouk *et al.*, 2000) which is poorly buffered (Salamino *et al.*, 1994). Ca^{2+} thus accumulates in various organelles, including the mitochondria, leading to cellular dysfunction, stimulation of Ca^{2+} -dependent proteolysis and phospholipidosis and extensive muscle damage. Initially, this muscle damage is repaired through the activation of satellite cells (dormant muscle cell precursors) but as muscle insult continues, it has been hypothesised that regenerative capacity diminishes, potentially due to reduced satellite cell number (Blau *et al.*, 1983, Sacco *et al.*, 2010). The imbalance between muscle degeneration and regeneration alters the histology of the muscle with large areas of phagocytic

cell invasion (Milhorat *et al.*, 1966), centronucleated fibres (Schmalbruch, 1984), fatty and connective tissue infiltrate (Moser, 1984) and fibre size variability including pseudohypertrophic fibres (Goldspink *et al.*, 1994), which together culminates in functional deficits and muscular weakness.

1.2.1.1 The C57BL/10 *mdx* mouse

The most commonly utilised animal model of DMD in research is the *mdx* (muscular dystrophy X-linked) mouse. The *mdx* mouse arose from a spontaneous mutation in the dystrophin gene resulting in the ablation of dystrophin from the sarcolemma as per human DMD (Bulfield *et al.*, 1984). Similar to human patients, the absence of dystrophin in the *mdx* mouse leads to increased intracellular $[Ca^{2+}]$ (Turner *et al.*, 1988), elevation of serum CK levels (Glesby *et al.*, 1988), metabolic abnormalities (Cole *et al.*, 2002, Passaquin *et al.*, 2002, Rybalka *et al.*, 2014), decreased muscle function (Dangain *et al.*, 1984, Brussee *et al.*, 1997, Vilquin *et al.*, 1998, van Putten *et al.*, 2010, Selsby *et al.*, 2011) significant inflammation (Carnwath *et al.*, 1987, Stedman *et al.*, 1991) and fibre size variability and centronucleation of fibres (Coulton *et al.*, 1988, McGeachie *et al.*, 1993). However, the *mdx* mouse differs phenotypically from the human condition. A stark phenotypic difference between human DMD and that evident in the *mdx* mouse is the disease progression. Muscular damage and degeneration is prominent in the early life of the *mdx* mouse. At around 5 days of age, musculature of the head, trunk and girdle display early signs of myofibre necrosis (De la Porte *et al.*, 1999). Hindlimb musculature is involved in degeneration and necrosis around 3-4 weeks of age, with peak damage occurring at 24-28 days (DiMario *et al.*, 1991). Coinciding with this massive degeneration is the proliferation of satellite cells around 3 weeks of age (McGeachie

et al., 1993) and within the proceeding 4-6 weeks, muscles are fully repaired and regenerated (Anderson *et al.*, 1988, Karpati *et al.*, 1988, Nagel *et al.*, 1990, DiMario *et al.*, 1991). Unlike human dystrophin-deficient skeletal muscle, proliferation of these satellite cells remains constant throughout the majority of the *mdx* mouse's lifespan – which is comparable to healthy, wild-type mice (Muntoni *et al.*, 1993) – and only begins to become insufficient around 18 months of age (McGeachie *et al.*, 1993), at which time skeletal muscle weakens, atrophies and becomes infiltrated with fibrotic tissue (Pastoret and Sebillé, 1993, Hayes and Williams 1998, Hakim *et al.*, 2011). Thus, while similar to human DMD, this loss of regenerative capacity and accumulation of histopathological abnormalities in *mdx* skeletal muscle very late in life and therefore lacks compatibility with DMD sufferers for which muscle wasting is progressive and cumulative over the life span. Overall, the *mdx* mouse displays a milder disease phenotype (Karpati *et al.*, 1988, Kaminski *et al.*, 1992, Marques *et al.*, 2007, Willmann *et al.*, 2009) which may be due to the upregulated expression of the dystrophin homologue utrophin (Helliwell *et al.*, 1992, Tinsley *et al.*, 1996), the maintenance of the satellite cell pool or the quadruped locomotion of the mice. .

One muscle that does display a similarly severe phenotype to human DMD is the diaphragm, which accrues damage throughout the *mdx* mouse lifespan (Stedman *et al.*, 1991). Characteristically, the diaphragm features damage, degeneration, fibrosis and collagen deposition around 6 months of age and it progressively worsens as the *mdx* mouse ages (Stedman *et al.*, 1991, Louboutin *et al.*, 1993). It is believed that these similarities are due to the significant proportion of fast-twitch fibres in the diaphragm – which are preferentially affected in DMD (Webster *et al.*, 1988) – and the constant contractions to enable respiration (Gillis *et al.*, 1996). To compensate for this progressive damage, there is a fibre shift to a more oxidative phenotype (De

la Porte *et al.*, 1999). Although there are limitations to the *mdx* mouse, especially as the most phenotypically similar muscle (i.e. the diaphragm) requires extensive time to accumulate damage, it is the most characterised model and allows for long-term studies due to a typically normal lifespan. Investigations using the double knockout mouse, which lacks both dystrophin and utrophin at the sarcolemma (Deconinck *et al.*, 1997, Grady *et al.*, 1997), highlights how important this feature is, as these mice die prematurely due to the severe pathology (Rafael *et al.*, 1998) and make it impossible to characterise long-term effects of potential therapeutics.

1.2.2 DMD as a metabolic myopathy

The earliest literature of Meryon (Meryon, 1852) and Duchenne (Duchenne, 1861) – who are renowned for reporting the first cases of DMD and the collective pathological manifestations of the disease, respectively – described the gross anatomical observations of DMD skeletal muscle fibres. A prominent feature of these fibres was intrafibrillar lipid accumulation. In whole fibre preparations, lipids are present extensively within the sarcoplasm and attached to the sarcolemma, and leach into the extracellular fluid from damaged fibres (Figure 1.2A) (Bonsett, 1979, Bonsett and Rudman, 1994). This feature has previously been reported in histological preparations using fat-specific stains (Harriman and Reed, 1972, Pearce, 1966). Intracellular lipid droplets are a normal feature of healthy skeletal muscle, albeit in lesser abundance, in which they are located proximal to the sarcoplasmic reticulum and mitochondria to act as energy reservoirs (Watt and Hoy, 2012). As skeletal muscle has a high affinity for fatty acid oxidation as ATP demand increases, these reservoirs act as important regulators of cellular energy homeostasis during metabolic stress. The early work of Charles Bonsett's laboratory on cultured human myocytes highlighted an equal propensity for healthy and DMD cells to produce

intracellular lipid droplets when supplemented with 20% foetal bovine serum (FBS) (Bonsett, 1979). Due to the nutrient dense profile of the serum supplement, this finding likely reflects the consequence of superfluous nutrient supply to the cell. While reducing the FBS concentration induced concurrent reductions in lipid accumulation in the healthy myocytes until lipid accumulation was absent, DMD myocytes continued to produce lipid droplets irrespective of serum concentration (Bonsett, 1979). This highlights a reduced capacity for metabolism that culminates in enhanced production of lipids at the cellular level (Figure 1.2B). Intramyofibrillar lipid accumulation is also characteristic of obese, type 2 diabetic patients and aged skeletal muscle (He *et al.*, 2001, Goodpaster *et al.*, 2000, Sinha *et al.*, 2002, Hilton *et al.*, 2008, Delmonico *et al.*, 2009) indicating similar metabolic dysfunction amongst these disease states.

In a further study by the same laboratory (Bonsett and Rudman, 1984), individual enzyme sites within the glycolytic and TCA cycle systems were systematically tested for dysfunction. The addition of 0.03M isocitrate to dystrophic cells induced significant intracellular lipid production which was not evident in healthy cells nor observed following the addition of other intermediates of glycolysis and TCA cycling (Bonsett and Rudman, 1984). The addition of 0.06M isocitrate to healthy myocytes induced some lipid formation while a 0.09M concentration was proven toxic. The authors deduced that their data was reflective of an isocitrate dehydrogenase (IDH) dysfunction/deficiency that may be related to the energy-sensing component of the enzyme, as the addition of the allosteric activator adenosine diphosphate (ADP) had no effect on isocitrate-stimulated lipid production, nor did addition of the allosteric inhibitor ATP. IDH exists both in the cytosol (IDH1) and the mitochondria (IDH 2 and 3). IDH1 and 2 may be the contributing factors to this increased intracellular fat as

nicotinamide adenine dinucleotide phosphate (NADPH), a precursor molecule involved in lipid synthesis (as reviewed in (Dulloo *et al.*, 2004)), is produced via the reaction. Indeed, dysfunctional IDH1 and 2 has been implicated in inducing increased lipid precursors and decreased TCA intermediates in cancerous cells (Reitman *et al.*, 2011). Thus IDH1 and 2 may also be dysfunctional in dystrophic muscle. IDH3, which is allosterically regulated by ATP, ADP and nicotinamide adenine dinucleotide (NAD), appears to also be dysregulated in dystrophic muscle as the addition of NAD, a co-factor of IDH3, significantly reduced the presence of intracellular fat droplets (Bonsett and Rudman, 1984). Whether this reduction in intracellular fat droplets is a direct effect of NAD shuttling across the mitochondrial membrane or via an indirect pathway (i.e. NAD-induced SIRT activation) is unknown. Nonetheless, this suggests that supplying the appropriate co-factor stimulates IDH3 activity and potentially stimulates the breakdown of these fat droplets to fuel TCA cycling.

1.3 Metabolic System Deficits in DMD

In human DMD muscle, a significant global down-regulation in the energy pathways has been demonstrated (Timmons *et al.*, 2005). Dystrophin-deficient skeletal muscle is characterised by severe perturbations in myocellular energy homeostasis with resting ATP levels consistently reported as ~50% of healthy control muscle (Ronzoni, 1958, Vignos Jr and Warner, 1963, Shuttlewood and Griffiths, 1982, Tamari, 1982, Cole *et al.*, 2002). In intensely exercised, healthy skeletal muscle, physiological fatigue mechanisms ensure that ATP demand does not exceed production capacity – a ~40% drop in resting ATP levels appears to be the critical maintenance threshold such to trigger these mechanisms and reduce demand on the metabolic system (as reviewed in (Allen *et al.*, 2008)).

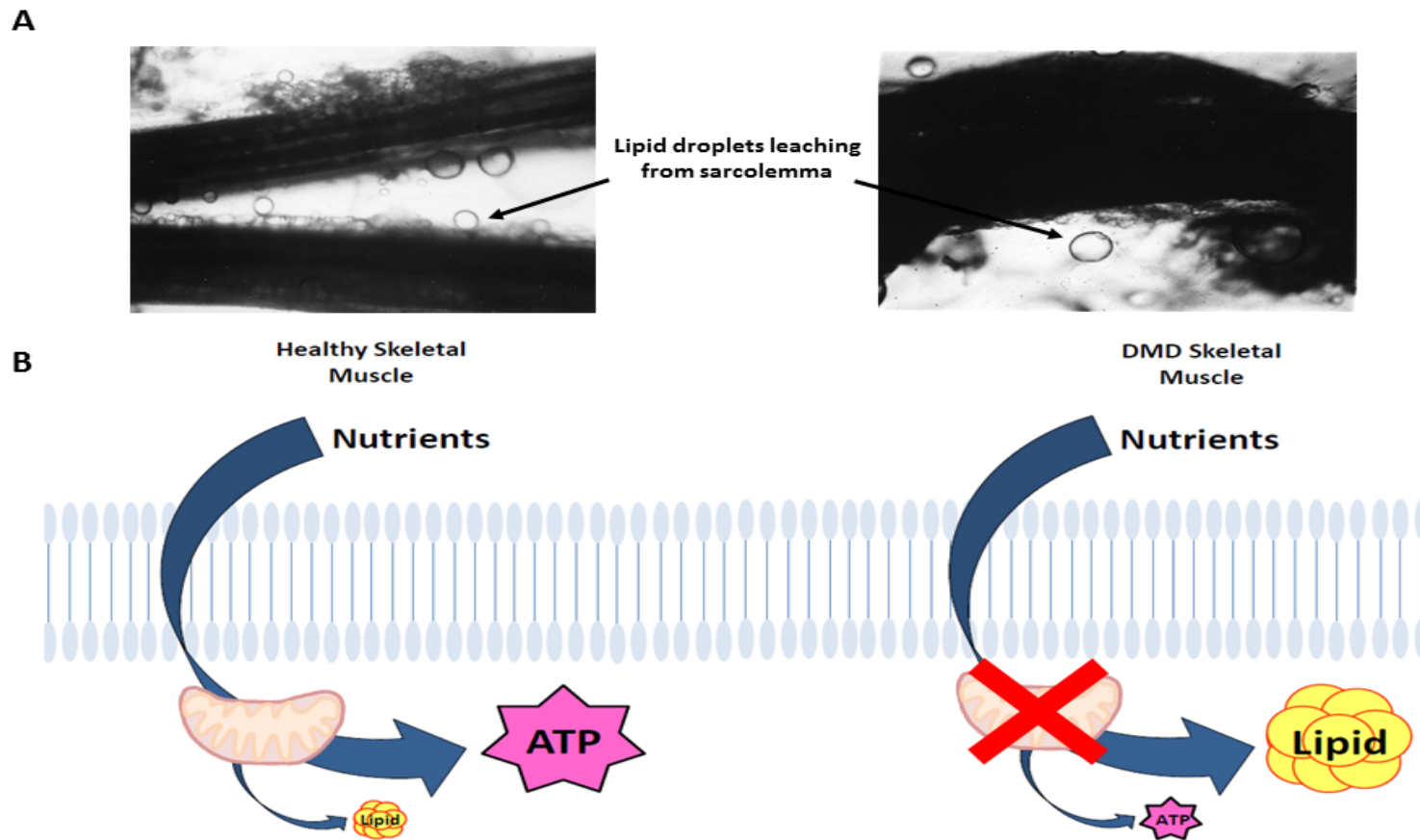


Figure 1.2. Accumulation of intramyofibrillar lipids is a feature of dystrophin-deficient skeletal muscle. Lipid droplets are evident in the sarcoplasm, the sarcolemma and leaching into the extracellular fluid of isolated dystrophin-deficient myofibres (Photographs courtesy of C.A. Bonsett (Bonsett, 1969); reproduced with the permission of C.C. Thomas Publisher Ltd). In a hypothetical model to explain this phenomenon (B), nutrients are typically oxidised to synthesise ATP in healthy skeletal muscle (left) with minimal directed to intracellular lipid production. In dystrophic muscle (right), the capacity to utilise nutrients for ATP synthesis is significantly impaired which coincides with an increased propensity to produce intracellular lipid (adapted from Bonsett, unpublished).

Thus, compared to healthy skeletal muscle, resting dystrophin-deficient muscle consistently maintains sub-threshold ATP levels which are likely incompatible with long-term cell survival.

A plethora of deficits in the cellular energy system have been reported in dystrophin-deficient skeletal muscle from human patients and animal models (as summarised in Table 1.1), which would both individually and collectively contribute to this failure of energy homeostasis. These are reviewed hereafter.

1.3.1 Macronutrient Uptake

Macronutrients represent the most primary form of cellular ATP potential, and as such, their delivery, uptake into, and storage within skeletal muscle fibres is integral to proper metabolic function and ATP synthesis. Skeletal muscle metabolism is highly dependent upon fatty acid oxidation and glucose metabolism, with amino acid oxidation usually contributing minimally (as reviewed in (Jeukendrup, 2003)). All pathways however, supplement metabolism synergistically in response to increasing energy demand and decreasing energy stores. Thus, deficits in macronutrient uptake and/or storage could be responsible for the energy homeostasis imbalances observed in dystrophic muscle, particularly since dystrophin is normally associated with the sarcolemma and thought to regulate membrane trafficking processes such as those required for glucose and amino acid uptake into cells.

Dystrophin-deficiency results in the secondary loss of neuronal nitric oxide synthase (nNOS) (Brenman *et al.*, 1995). One of the key roles of nNOS in skeletal muscle is the generation of nitric oxide (NO), which is a key intracellular signaling molecule with strong metabolic regulatory capacity that has effects on skeletal muscle contraction, blood flow, glucose uptake and metabolism (McConnell and

Kingwell, 2006, Mashimo and Goyal, 1999). In healthy muscles, nNOS is localised to the subsarcolemma via the DPC, with binding sites on dystrophin and the syntrophins (Figure 1.1A). The absence of dystrophin disrupts the formation of the DPC (Ohlendieck and Campbell, 1991) and affects nNOS localisation (Brenman *et al.*, 1995, Chang *et al.*, 1996). As nNOS exists unbound in the cytosol of *mdx* skeletal muscle and subsequently becomes a substrate for the calpain proteases, a 25-fold decrease in nNOS activity has been observed (Chang *et al.*, 1996, Kameya *et al.*, 1999, Li *et al.*, 2011). In the skeletal muscle of DMD patients, nNOS is absent in the pellet fraction of biopsy samples (confirmed by both enzyme assay and Western blot) (Brenman *et al.*, 1995, Chang *et al.* 1996) and is significantly reduced in the *mdx* mouse (Leary *et al.*, 1998, Thomas *et al.*, 1998, Vaghy *et al.*, 1998, Judge *et al.*, 2006). Additionally, nNOS mRNA in human DMD (Arning *et al.*, 2004) and *mdx* muscle is significantly decreased (Chang *et al.*, 1996, Crosbie *et al.*, 1998), with neither nNOS expression nor activity increasing as per normal during the regeneration of *mdx* skeletal muscle at 14 (post-necrotic) weeks of age (Chang *et al.*, 1996). As a consequence, endogenous NO production is significantly decreased (Gücüyener *et al.*, 2000, Kasai *et al.*, 2004, Barton *et al.*, 2005).

nNOS-generated NO has a key role in facilitating glucose uptake by stimulating glucose transporter 4 (GLUT4) translocation at rest (Balon and Nadler, 1997) and during contraction (Bradley *et al.*, 1999). Despite the reduction of nNOS in *mdx* skeletal muscle, basal (resting) glucose uptake has been shown to be equivalent to control muscle (Maclennan *et al.*, 1991a, Chinet *et al.* 1994, Even *et al.*, 1994) with GLUT4 expression also normal in young animals (Olichon-Berthe *et al.*, 1993, Raith *et al.*, 2013). However, GLUT4 expression (and its mRNA) decreases in the

Table 1.1. Summary of the metabolic deficits in the metabolic pathways of dystrophic skeletal muscle.

	Defect Description	DMD Model	References
Macronutrient Uptake & Availability	Normal glucose uptake but ↓ glucose content	Human DMD & <i>mdx</i> mouse	(Nishio <i>et al.</i> , 1990, Griffin <i>et al.</i> , 2001, Sharma <i>et al.</i> , 2003)
	↓ GLUT4 mRNA & protein expression in aged diaphragm	<i>mdx</i> mouse	(Olichon-Berthe <i>et al.</i> , 1993)
	↓ Gluconeogenic precursors (alanine & glutamine)	Human DMD	(Nishio <i>et al.</i> , 1990, Hankard, 1998, Sharma <i>et al.</i> , 2003)
	↑ Fructose content	Human DMD	(Ellis, 1972)
Glycolysis	↓ Glucose-6-Phosphate	Human DMD	(Hess, 1965)
	↓ Phosphofructokinase activity, ↓ sensitivity to allosteric regulation	Human DMD & <i>mdx</i> mouse	(Hess, 1965, Di Mauro, 1967, Chi <i>et al.</i> , 1987, Lilling and Beitner, 1991, Wehling-Henricks <i>et al.</i> , 2009)
	↓ Aldolase	Human DMD	(Dreyfus, 1954, Thomson, 1960, Hess, 1965)
	↓ Pyruvate kinase activity	Human DMD	(Chi <i>et al.</i> , 1987, Zatz <i>et al.</i> , 1991)
	↓ Lactate dehydrogenase	Human DMD	(Hess, 1965, Cao <i>et al.</i> , 1965, Di Mauro, 1967)
	↓ Lactate production & acidification	Human DMD & <i>mdx</i> mouse	(Ellis, 1980, Cole <i>et al.</i> , 2002, Sharma <i>et al.</i> , 2003)
Glycogen Storage & Utilisation	↑ Glycogen content	Human DMD & <i>mdx</i> mouse	(Watkins and Cullen, 1987, Cullen and Jaros, 1988, Stapleton <i>et al.</i> , 2014)
	↓ Phosphorylase activity	Human DMD & <i>mdx</i> mouse	(Dreyfus, 1954, Ronzoni <i>et al.</i> , 1960, Hess, 1965, Di Mauro, 1967, Mastaglia and Kakulas, 1969, Ellis, 1980, Petell <i>et al.</i> , 1984, Engel, 1986, Chi <i>et al.</i> , 1987, Chen <i>et al.</i> , 2000, Carberry <i>et al.</i> , 2013, Stapleton <i>et al.</i> , 2014)
	↓ Phosphoglucomutase activity	Human DMD & <i>mdx</i> mouse	(Chi <i>et al.</i> , 1987, Matsumura <i>et al.</i> , 2013)
Fat Oxidation	↓ Palmitate oxidation	Human DMD patients & carriers	(Lin, 1972, Shumate <i>et al.</i> , 1982, Carroll <i>et al.</i> , 1985)
	↓ Palmitoylcarnitine & malate oxidation	Human DMD	(Borum <i>et al.</i> , 1977, Carrier and Berthillier, 1980, Shumate <i>et al.</i> , 1982, Carroll <i>et al.</i> , 1983, Scholte <i>et al.</i> , 1985, Sharma <i>et al.</i> , 2003, Le Borgne <i>et al.</i> , 2012)
	↓ Total carnitine	Human DMD	(Borum <i>et al.</i> , 1977, Carrier and Berthillier, 1980, Shumate <i>et al.</i> , 1982, Carroll <i>et al.</i> , 1983, Sharma <i>et al.</i> , 2003, Le Borgne <i>et al.</i> , 2012)
	↓ Fatty acid transport into mitochondria	Human DMD	(Le Borgne <i>et al.</i> , 2012)
Creatine Phosphagen System	↓ PCr concentration	Human DMD & <i>mdx</i> mouse	(Ronzoni, 1958, Fitch and Moody, 1969, Samaha, 1981, Newman <i>et al.</i> , 1982, Griffiths <i>et al.</i> , 1985, Dunn <i>et al.</i> , 1991, Pulido <i>et al.</i> , 1998, Sharma <i>et al.</i> , 2003)
	↓ Cr concentration	Human DMD & <i>mdx</i> mouse	(Ronzoni, 1958, Fitch and Moody, 1969, Griffin <i>et al.</i> , 2001, Sharma <i>et al.</i> , 2003, Martins-Bach <i>et al.</i> , 2012)
	↓ TCr	Human DMD & <i>mdx</i> mouse	(Ronzoni, 1958, Ionasescu <i>et al.</i> , 1981, Louis <i>et al.</i> , 2004)
	↓ PCr/Pi	Human DMD	(Newman <i>et al.</i> , 1982, Griffiths <i>et al.</i> , 1985, Younkin <i>et al.</i> , 1987)
	↓ PCr/ATP	Human DMD	(Newman <i>et al.</i> , 1982, Griffiths <i>et al.</i> , 1985, Kemp <i>et al.</i> , 1993)
	↑ Urinary Cr excretion (due to ↓ turnover)	Human DMD	(Benedict <i>et al.</i> , 1955)
Purine Nucleotide Cycle	↓ IMP concentration	Human DMD	(Camiña <i>et al.</i> , 1995)
	↓ Adenylate kinase content & activity	<i>mdx</i> mouse	(Ge <i>et al.</i> , 2003)
	↑ Uric acid excretion	Human DMD	(de Bruyn <i>et al.</i> , 1980, Bertorini <i>et al.</i> , 1981, Camiña <i>et al.</i> , 1995)

diaphragm of older *mdx* mice (Olichon-Berthe *et al.*, 1993), which is important clinically since the diaphragm is the only *mdx* muscle to undergo progressive degenerative wasting throughout the lifespan as per the human disease (Stedman *et al.*, 1991). Decreased mRNA expression in the older *mdx* mice suggests that disease progression may affect protein expression of GLUT4 and therefore the ability to bring glucose into muscle fibres. There is, however, no evidence in the literature to indicate abnormalities in the transport of fatty- or amino-acids across dystrophin-deficient membranes. In contrast to the gastrointestinal perturbations that demonstrably impair digestion and nutrient absorption (outside the scope of this review; Miyatake *et al.*, 1989, Mule *et al.*, 1999), macronutrient uptake at the level of skeletal muscle does not appear to be a major contributor to the impaired metabolism observed.

1.3.2 Glycolysis

Despite glycolysis only contributing 2 ATP molecules for every glucose molecule oxidised under anaerobic conditions, proper glycolytic function is essential to support the TCA cycle. The end-product of glycolysis, pyruvate, can be oxidised to yield acetyl CoA via pyruvate dehydrogenase (PDH) and subsequently transported into the mitochondria to enter the TCA cycle and produce reducing equivalents that feed the ETC (Figure 1.3). Therefore, dysfunction in any glycolytic enzyme (or the overall glycolytic process (Vignos Jr and Lefkowitz, 1959)) would both reduce anaerobic ATP production and affect downstream metabolic reactions for aerobic ATP synthesis.

Although it has been shown that the capacity to uptake glucose is normal in dystrophic muscle (Maclennan *et al.*, 1991a, Chinet *et al.*, 1994, Even *et al.*, 1994),

the concentration of available cytoplasmic glucose in dystrophic human and *mdx* mouse muscle is decreased (Nishio *et al.*, 1990, Griffin *et al.*, 2001, Sharma *et al.*, 2003). The availability of cytoplasmic glucose is relied upon once the available ATP, phosphocreatine (PCr) and glycogen (glycogen storage in dystrophic muscle reviewed in section 1.3.2.1) is exhausted (i.e. during exercise and starvation). This decreased glucose concentration in the presence of normal glucose uptake capacity reflects a reduced capacity for gluconeogenesis as substrates including alanine and glutamine are decreased in dystrophic muscle (Nishio *et al.*, 1990, Hankard, 1998, Sharma *et al.*, 2003). This may reflect either caloric shortage in that the availability of gluconeogenic precursors is decreased or that fibre degeneration results in the loss of these substrates (Nishio *et al.*, 1990), potentially to the bloodstream.

DMD muscle exhibits a significant down-regulation in both glycogen and carbohydrate (summarised in Figure 1.3) metabolism (Timmons *et al.*, 2005, Kotelnikova *et al.*, 2012). More specifically, in both DMD and *mdx* muscle samples, phosphofructokinase (PFK) activity is demonstrably decreased (Hess, 1965, Di Mauro, 1967, Chi *et al.*, 1987, Lilling and Beitner, 1991, Wehling-Henricks *et al.*, 2009). PFK is the rate-limiting enzyme of glycolysis and is highly regulated by metabolites. In healthy muscle, PFK is inhibited by high concentrations of ATP and activated by ADP and other by-products of ATP hydrolysis (as reviewed in (Wegener and Krause, 2002)). As ATP concentration is diminished in dystrophic muscle, PFK activity should, logically, be increased to promote ATP synthesis and energy balance. However, altered allosteric regulation of PFK has been observed in *mdx* muscle (Wehling-Henricks *et al.*, 2009) suggesting that PFK fails to respond appropriately to normal stimuli. Despite the soluble and cytoskeleton-bound PFK enzymes being distributed normally, the sensitivity of PFK to its allosteric regulators

is reduced (Lilling and Beitner, 1991). This indicates a functional change in PFK properties and/or its modulation, which significantly reduces its activity and likely contributes to the overall metabolic deficit in dystrophic muscle. It is probable that PFK deactivation is strongly associated with the nNOS delocalization described earlier, as the two enzymes co-localise at the sarcolemma in healthy muscle suggesting a regulatory role for NO on PFK activity (Wehling-Henricks *et al.*, 2009). Reintroduction of nNOS into *mdx* skeletal muscle has shown some benefit in improving glucose and glycogen metabolism (in addition to reducing membrane degradation and muscle inflammation) (Wehling *et al.*, 2001, Wehling-Henricks *et al.*, 2009), such to improve exercise tolerance which was attributed to the positive allosteric effect nNOS exhibited on PFK (Wehling-Henricks *et al.*, 2009).

Deficits in adolase (Dreyfus, 1954, Thomson, 1960, Hess, 1965), pyruvate kinase (PK) (Chi *et al.*, 1987, Zatz *et al.*, 1991a) and lactate dehydrogenase (LDH) (Hess, 1965, Cao *et al.* 1965, Di Mauro, 1967) activity, alongside a decrease in glucose-6-phosphate content (Hess, 1965), have also been observed in DMD skeletal muscle. The increased leakiness of the sarcolemma results in the loss of some enzymes, including adolase, to the blood stream where increased plasma activity has been reported in dystrophic patients (Dreyfus, 1954, Thomson and Guest, 1963, Vignos Jr and Warner, 1963, Di Mauro, 1967, Shaw, 1967). Loss of adolase abundance may limit downstream enzymatic activity by reducing substrate availability, particularly to phosphoglycerate kinase, which produces ATP via substrate-level phosphorylation. In a possible bid to alleviate this reduced propensity for glucose oxidation, increased fructose metabolism may be occurring in dystrophic muscle. In human dystrophin-deficient (DMD) and dystrophin-positive mutant carrier muscle, fructose levels are significantly elevated compared to control muscle and other neuromuscular diseases

(Ellis, 1972). It was suggested that this may be a secondary pathway to glucose metabolism that is necessary in the dystrophic condition (Ellis, 1972). However, it is more likely that this increased fructose content is reflective of an incapacity to metabolise it into products (glyceraldehyde and dihydroxyacetone phosphate) that are channelled into glycolysis (as reviewed in (Johnson *et al.*, 2009, Tornheim and Ruderman, 2011)) thus ensues a failure to expand glycolytic flux.

1.3.2.1 Glycogen Storage and Utilisation

Muscle glycogen is a valuable reservoir of glucose that can be channelled into glycolysis to assist in processes including Ca^{2+} handling and contraction. Compared to lipid oxidation, glycogen oxidation is advantageous as it is quickly activated, yields more ATP per molecule utilised and produces ATP at a faster rate (as reviewed in (Connett and Sahlin, 2010)). Therefore glycogenolysis is an important supplementary pathway to support and stimulate glycolysis in muscle.

There are conflicting reports regarding the glycogen content in dystrophic muscle (Vignos Jr and Warner, 1963, Hess, 1965, Duma, 1967, Mastaglia and Kakulas, 1969, Watkins and Cullen, 1987, Cullen and Jaros, 1988, Maclennan *et al.*, 1991, Stapleton *et al.*, 2014). This discrepancy may be accounted for by the chronological/pathological time points at which the biopsies were taken. It has been shown that glycogen content increases during times of skeletal muscle regeneration (Engel, 1986), thus this could account for the increased glycogen content observed in both human and *mdx* dystrophic samples (Watkins and Cullen, 1987, Cullen and Jaros, 1988, Maclennan *et al.*, 1991a, Stapleton *et al.*, 2014). In contrast, increased glycogen storage may reflect the decreased capacity for glycolysis. There would be no value in flooding the glycolytic pathway with glucose derived from glycogen if it

cannot be efficiently utilised downstream and may reflect dystrophic muscle prioritising what is essential for muscle survival.

During increased glycolytic demand, glycogen stores are utilised to increase glucose availability. However, it appears that dystrophic muscle is unable to accomplish this (Timmons *et al.*, 2005) as there are severe deficits in phosphorylase (Dreyfus, 1954, Ronzoni *et al.*, 1960, Hess, 1965, Di Mauro, 1967, Mastaglia and Kakulas, 1969, Ellis, 1980, Petell *et al.*, 1984, Chi *et al.*, 1987, Chen *et al.*, 2000, Carberry *et al.*, 2013, Stapleton *et al.*, 2014) and to a lesser extent, phosphoglucomutase (Chi *et al.*, 1987, Matsumura *et al.*, 2013), the enzymes of glycogenolysis. These deficits, which are particularly pronounced in phosphorylase, exist despite it normally being stimulated by elevations in $[Ca^{2+}]$ (Tornheim and Ruderman, 2011). Increased membrane permeability results in significantly increased $[Ca^{2+}]$ content in dystrophic muscle and organelles (Bodensteiner and Engel, 1978, Glesby *et al.*, 1988, Dunn and Radda, 1991). In times of transient increases in cytosolic and mitochondrial $[Ca^{2+}]$ (i.e. exercise), Ca^{2+} positively stimulates various aspects of metabolism to match ATP production to demand, however this is not apparent in the dystrophic condition. Together, these deficits in glycogenolysis indicate a decreased capacity to supply additional glucose to fuel glycolysis in dystrophic muscle. Overall, dystrophic muscle appears to be unable to proactively utilise any pathway of carbohydrate metabolism, which would place further strain on the already impaired oxidative metabolism.

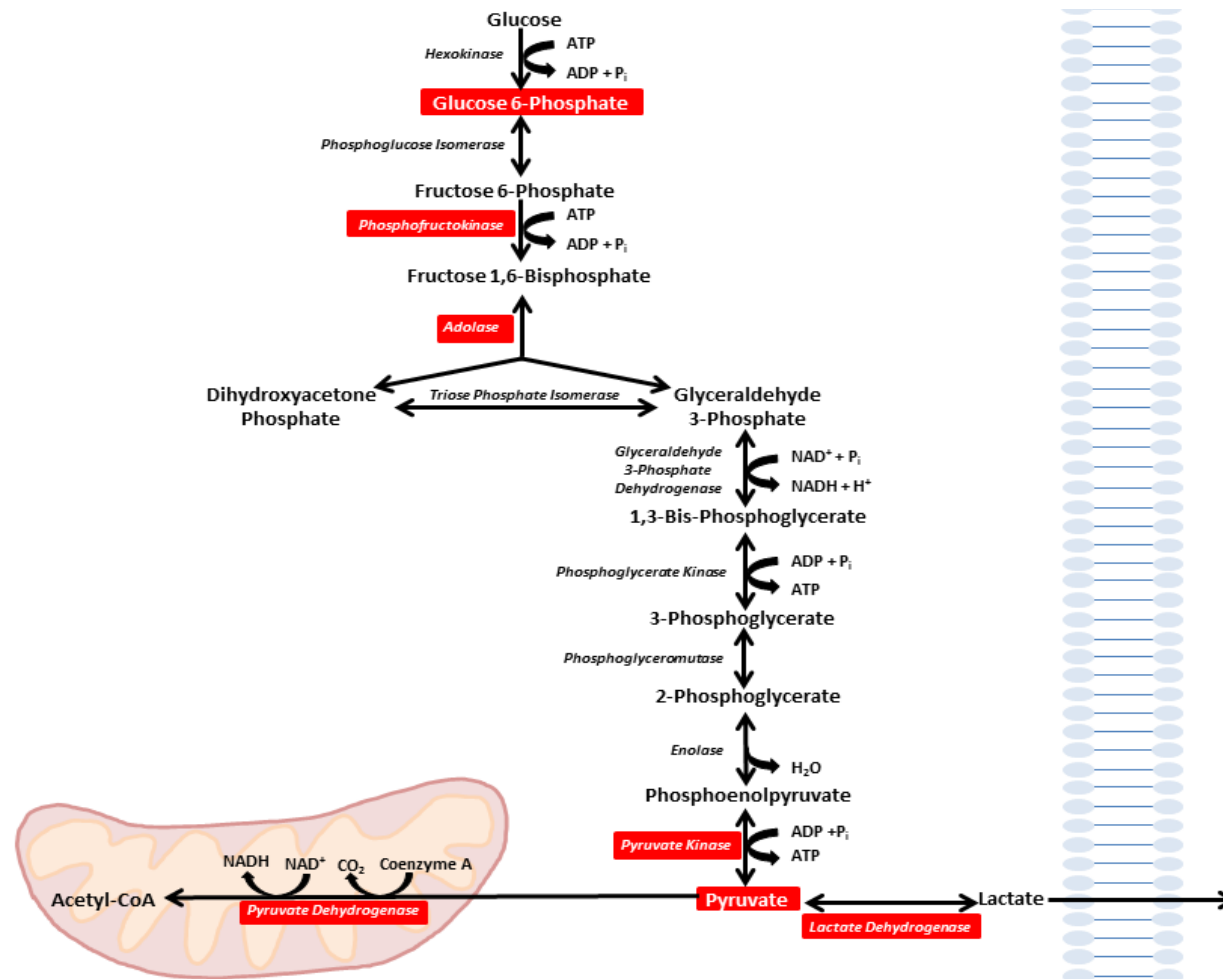


Figure 1.3. Glycolytic impairment in dystrophin-deficient skeletal muscle. Glycolysis involves the sequential conversion of glucose to pyruvate which can either be channelled into mitochondrial oxidative phosphorylation as acetyl CoA or excreted from the muscle as lactate. In dystrophic muscle, various glycolytic impairments have been observed (as indicated by those enclosed in solid boxes with white writing).

1.3.3 Fat oxidation

β -oxidation is the major pathway for saturated fatty acid catabolism that occurs in the mitochondria, producing acetyl CoA, nicotinamide adenine dinucleotide (NADH) and flavin adenine dinucleotide (FADH₂). The ATP yield that can be generated from the reducing equivalents produced from β -oxidation is large as it stimulates both the TCA cycle and the ETC.

Deficits in fat oxidation have been reported in various muscular dystrophy animal models and human samples. Prior to the discovery of the *mdx* mouse, hereditary models of muscular dystrophy were commonly used. In isolated mitochondria from the 129/ReJ-dy mice strain, acetylcarnitine (Jato-Rodriguez *et al.*, 1975, Liang, 1986), palmitylcarnitine (Jato-Rodriguez *et al.*, 1975, Liang, 1986) and palmitate (Jato-Rodriguez *et al.*, 1975) oxidation are reduced by up to 80% with decreased oxidation of acetylcarnitine and palmitate apparent in the BIO 14.6 dystrophic hamster (Wrogemann *et al.*, 1973). Furthermore, in C57BL/6J-*dy*^{2J}*dy*^{2J} hindlimb muscles, oleoyl CoA oxidation is diminished (Kang *et al.*, 1986) while in the *mdx* mouse, a markedly reduced thermogenic response from octanoate oxidation has been reported (Even *et al.*, 1994). It is worthwhile noting that these impairments of fat oxidation are observed in hereditary models that do not lack dystrophin but rather other glycoproteins associated with the sarcolemma. This indicates that metabolic impairment is independent of dystrophin-deficiency but may ostensibly be linked to the disassembly of sarcolemmal proteins. Of interest, the addition of acetyl-CoA improved octanoate oxidation highlighting that the delivery of acetyl-CoA may be impaired (Jato-Rodriguez *et al.*, 1975, Even *et al.*, 1994) and therefore impacting upon the formation of reducing equivalents that feed the ETC.

In muscle samples from early stage DMD patients, oxidation of palmitic acid is demonstrably reduced (Lin, 1972, Shumate *et al.*, 1982, Carroll *et al.*, 1985). Moreover, in dystrophin-expressing carriers of DMD, a similar reduction of palmitic acid oxidation is also observed (Lin, 1972) and provides another example of a metabolic defect that is related to the genotype but which is independent of dystrophin expression. Conversely, Scholte *et al.* (Scholte *et al.*, 1985) concluded that β -oxidation is normal in dystrophic mitochondria, despite reporting that samples pertaining to older patients had lower palmitate oxidation than controls. In contrast to this, decreased oxidation with a combination of palmitoylcarnitine and malate and decreased total carnitine (Borum *et al.*, 1977, Carrier and Berthillier, 1980, Shumate *et al.*, 1982, Carroll *et al.*, 1983, Scholte *et al.*, 1985, Sharma *et al.*, 2003, Le Borgne *et al.*, 2012), which impairs fatty acid transport (Le Borgne *et al.*, 2012), has been consistently reported in DMD patients. Moreover, mRNA expression of mitochondrial enzymes associated with lipid oxidation have been shown to be reduced in DMD cultured cells (Le Borgne *et al.*, 2012). It appears that this overall reduction in fat oxidation may be impairing the capacity to expand acetyl-CoA availability to TCA cycling and may partially explain why the increased lipid droplets observed in DMD cells (Bonsett, 1979) are unable to be oxidised.

1.3.4 Mitochondria

The fundamental role of the mitochondria is ATP synthesis, thus they are the major cellular regulators of energy homeostasis. More recently mitochondria have emerged as playing an important role in the regulation of initiating apoptotic cell death. Mitochondria are adept at sensing and responding to intracellular changes in energy balance to maintain homeostasis, but once the metabolic insult exceeds

regulatory capacity, mitochondrial dysfunction ensues. Prolonged mitochondrial stress can initiate apoptosis when dissipation of the mitochondrial membrane potential, release of cytochrome c and/or caspases and opening of the mitochondrial transition pore occurs (as reviewed in (Galluzzi *et al.*, 2012)).

Mitochondrial dysfunction in dystrophic skeletal muscle is well documented and a key contributor to the reductions (up to 50%) in resting ATP content (Ronconi, 1958, Vignos Jr and Warner, 1963, Samaha, 1981, Tamari, 1982, Newman *et al.*, 1982, Shuttlewood and Griffiths, 1982, Bertorini *et al.*, 1985, Dunn *et al.*, 1991, Lilling and Beitner, 1991, Camiña *et al.*, 1995, Cole *et al.*, 2002, Percival *et al.*, 2013, Rybalka *et al.*, 2014) with decreased ATP content in the brain of DMD patients also evident (Tracey *et al.*, 1995). An ~40% reduction in the amount of ATP produced per oxygen molecule (O₂) utilised by *mdx* mitochondria (Percival *et al.*, 2013) explicates the aforementioned ATP deficiency and indicates potential oxidative uncoupling or a reduction of available ADP for ATP rephosphorylation. However, there is conflicting data reporting either increases (Kemp *et al.*, 1993, Cole *et al.*, 2002) or decreases (Ronconi, 1958, Camiña *et al.*, 1995) in ADP content in dystrophic muscle. Either finding could be interpreted to affect ATP rephosphorylation - increased ADP (and inorganic phosphate (P_i)) (Griffiths *et al.*, 1985, Younkin *et al.*, 1987)) suggest an inability to rephosphorylate adequately, while decreased ADP could indicate that the potential to synthesise ATP is diminished potentially due to cytosolic ADP degradation. If the latter is correct, this may suggest an issue with adenine nucleotide translocase, in that ADP is not efficiently translocated across the mitochondrial membrane to participate in ATP rephosphorylation. Thus if ADP accumulates in the cytosol and fluxes through the PNC (refer to section 1.3.6), there

is the potential for adenine nucleotide loss that would reduce the ADP supply to the mitochondria.

1.3.4.1 The Tricarboxylic Acid Cycle & Electron Transport Chain

The TCA cycle and ETC work together in the mitochondria to produce the majority of ATP derived from the various linked macronutrient feeder pathways. As there is a deficit in ATP content in dystrophic mitochondria, it follows that the TCA cycle (and the pathways that feed into it) and/or the ETC are a significant cause of this deficit (summarised in Figure 1.4). Indeed, it has been demonstrated that human DMD muscle has a significant down-regulation of oxidative phosphorylation genes (Timmons *et al.*, 2005, Kotelnikova *et al.*, 2012).

In the majority of studies researching the oxidative capacity of human and animal dystrophic mitochondria (and even dystrophic cells), impaired handling of pyruvate is evident (Olson *et al.*, 1968, Martens *et al.*, 1980, Shumate *et al.*, 1982, Liang, 1986, Glesby *et al.*, 1988, Bhattacharya *et al.*, 1993, Chinet *et al.*, 1994, Kuznetsov *et al.*, 1998, Faist *et al.*, 2001, Onopiuk *et al.*, 2009, Rybalka *et al.*, 2014). Furthermore, the addition of substrates that stimulate the TCA cycle, including malate (Martens *et al.*, 1980, Glesby *et al.*, 1988, Bhattacharya *et al.*, 1993, Kuznetsov *et al.*, 1998, Faist *et al.*, 2001, Rybalka *et al.*, 2014) and glutamate (Olson *et al.*, 1968, Kuznetsov *et al.*, 1998, Rybalka *et al.*, 2014) (with glutamate content increased in *mdx* diaphragm (Griffin *et al.*, 2001)) have been consistently reported to produce lower oxidation rates compared to healthy controls, even in combination with other substrates. Addition of succinate, on the other hand, has been shown to either restore (Ionășescu *et al.*, 1967, Nylén and Wrogemann, 1983, Glesby *et al.*, 1988, Chinet *et al.*, 1994) or at least partially restore oxidation rates to control levels

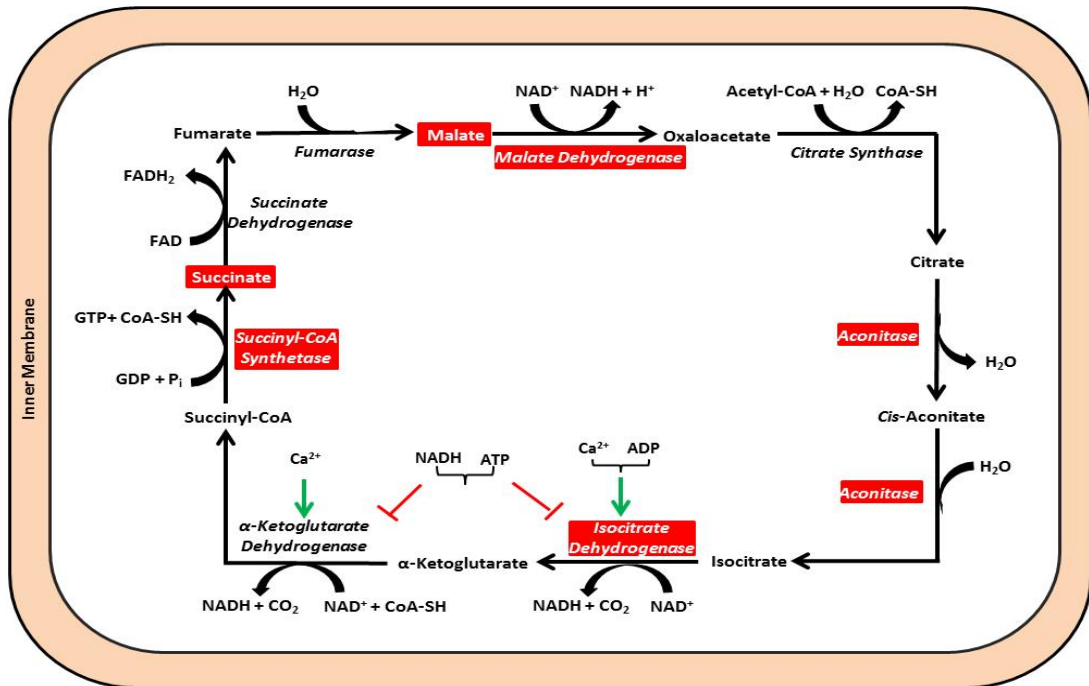
(Martens *et al.*, 1980, Bhattacharya *et al.*, 1993, Kuznetsov *et al.*, 1998, Rybalka *et al.*, 2014). This is a widely reported feature of dystrophin-deficient muscle metabolism and as published by us recently, indicates that the metabolic deficit may be located at complex I of the ETC (Rybalka *et al.*, 2014). Alternatively, as it appears that some enzymes of the TCA cycle do not function as normal – including succinic CoA synthetase, aconitase, malate dehydrogenase and IDH (Cao *et al.*, 1965, Chen *et al.*, 2000, Dudley *et al.*, 2006b, Carberry *et al.*, 2013, Matsumura *et al.*, 2013) – which would result in decreased production of reducing equivalents at the TCA level, the ability of succinate to restore oxidative phosphorylation may lie in its ability to bypass a defective TCA system and stimulate complex II of the ETC directly.

Various enzymes of the TCA cycle (in addition to complex V of the ETC) are regulated by increases in intramitochondrial $[Ca^{2+}]$ (Figure 1.4A). PDH (indirectly activated by Ca^{2+} -activated phosphatase), α -ketoglutarate dehydrogenase and IDH (at higher concentrations) are all allosterically activated as mitochondrial matrix $[Ca^{2+}]$ rises (as reviewed in (Gellerich *et al.*, 2010)). This results in the anaplerotic expansion of TCA-generated reducing equivalents and a greater chemiosmotic drive for, and faster speed of, ATP production at complex V. These enzymes should theoretically be stimulated in dystrophic muscle (as free intracellular Ca^{2+} is considerably higher at rest and during contraction (Turner *et al.*, 1988, MacLennan *et al.*, 1991b, Kämper and Rodemann, 1992, Bakker *et al.*, 1993, Hopf *et al.*, 1996) to increase Ca^{2+} buffering and remove the pathological stimulus. However, normal stimulation of these enzymes by increased $[Ca^{2+}]$ appears to be absent in dystrophic muscle as evidenced by decreased IDH activity (Dudley *et al.*, 2006b). If IDH fails to activate in response to the extremely high $[Ca^{2+}]$ observed in DMD, it may be that the other Ca^{2+} -sensitive enzymes are not responding appropriately either. The

consequence of this is reduced ATP production and Ca^{2+} buffering capacity leading to amplification of the pathological stimulus (i.e. $[\text{Ca}^{2+}]$). In contrast, it has been recently demonstrated that *mdx* mitochondria hypersensitively respond to a Ca^{2+} load to prematurely open the permeability transition pore (channel that initiates mitochondrial death) (Pauly *et al.*, 2012). This suggests that the inability of dystrophic mitochondria to respond to an overwhelming Ca^{2+} stimulus by ramping up ATP production, favours premature induction of pro-apoptotic pathways such that cell death is the only viable outcome (Figure 1.5).

The decreased oxidation rates of the substrates that channel through the TCA cycle appear to culminate at the ETC. In saponin-skinned *mdx* skeletal muscle fibres, the maximal rate of respiration, as stimulated by the addition of ADP, was nearly 50% lower regardless of the substrate used (Kuznetsov *et al.* 1998). Similarly, isolated dystrophic mitochondria showed only ~60% of maximal respiration control rates (Kuznetsov *et al.*, 1998 Percival *et al.*, 2013), while a biopsy from a DMD patient revealed similar respiratory deficits (Kuznetsov *et al.*, 1998). Additionally, reduced ADP-stimulated (Martens *et al.*, 1980, Nylén and Wrogemann, 1983, Bhattacharya *et al.*, 1993, Faist *et al.*, 2001, Passaquin *et al.*, 2002, Schuh *et al.*, 2012) and basal respiration has been reported (Wrogemann *et al.*, 1973, Passaquin *et al.*, 2002, Onopiuk *et al.*, 2009, Schuh *et al.*, 2012, Godin *et al.*, 2012), with further reductions observed as the disease progresses (Olson *et al.*, 1968). The ability of mitochondria to aptly respond to the increased $[\text{Ca}^{2+}]$ and requirements of dystrophic muscle appears to be further impaired as the spare respiratory reserve, which indicates the ability for the ETC to increase ATP production in response to metabolic challenge, is reduced by ~60% (Schuh *et al.*, 2012).

A



B

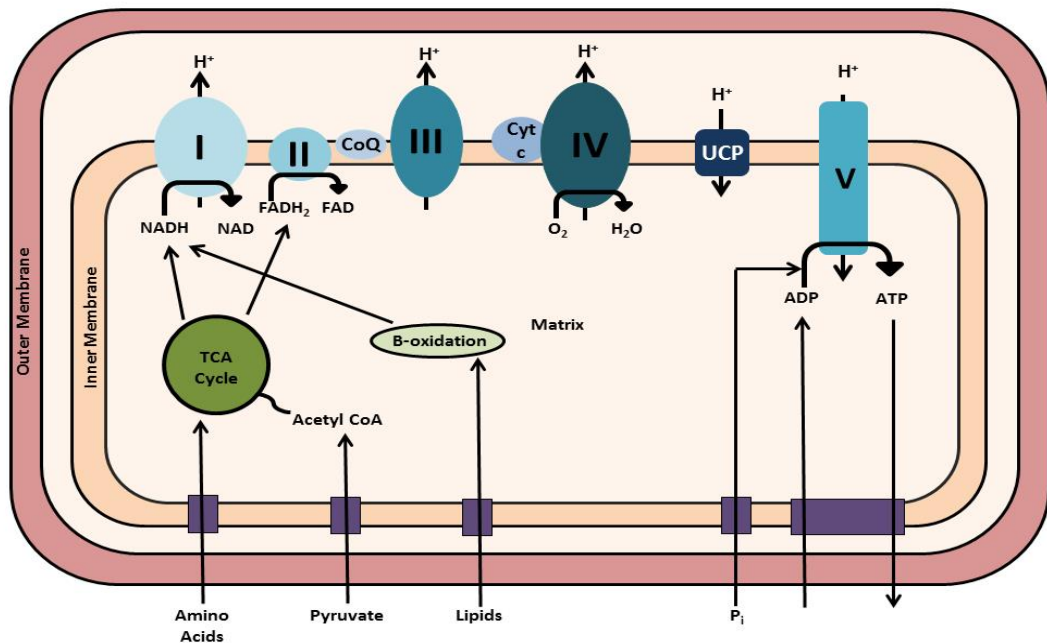


Figure 1.4. Widespread mitochondrial dysfunction in dystrophin-deficient skeletal muscle. The TCA cycle (A) produces reducing equivalents (NADH and FADH₂) which are fed into the ETC (B) for ATP synthesis. In dystrophic muscle, impairments in TCA enzyme activity and intermediate oxidation have been observed (as indicated by those enclosed in solid boxes with white writing). The ETC utilises the reducing equivalents produced by the TCA cycle (B) to synthesis ATP via the coupled flow of electrons to pumping of protons. In dystrophic muscle, impairments in the content and/or activity of all complexes, in particular complex I, have been observed and severely impacts upon the ATP producing capacity of the mitochondria.

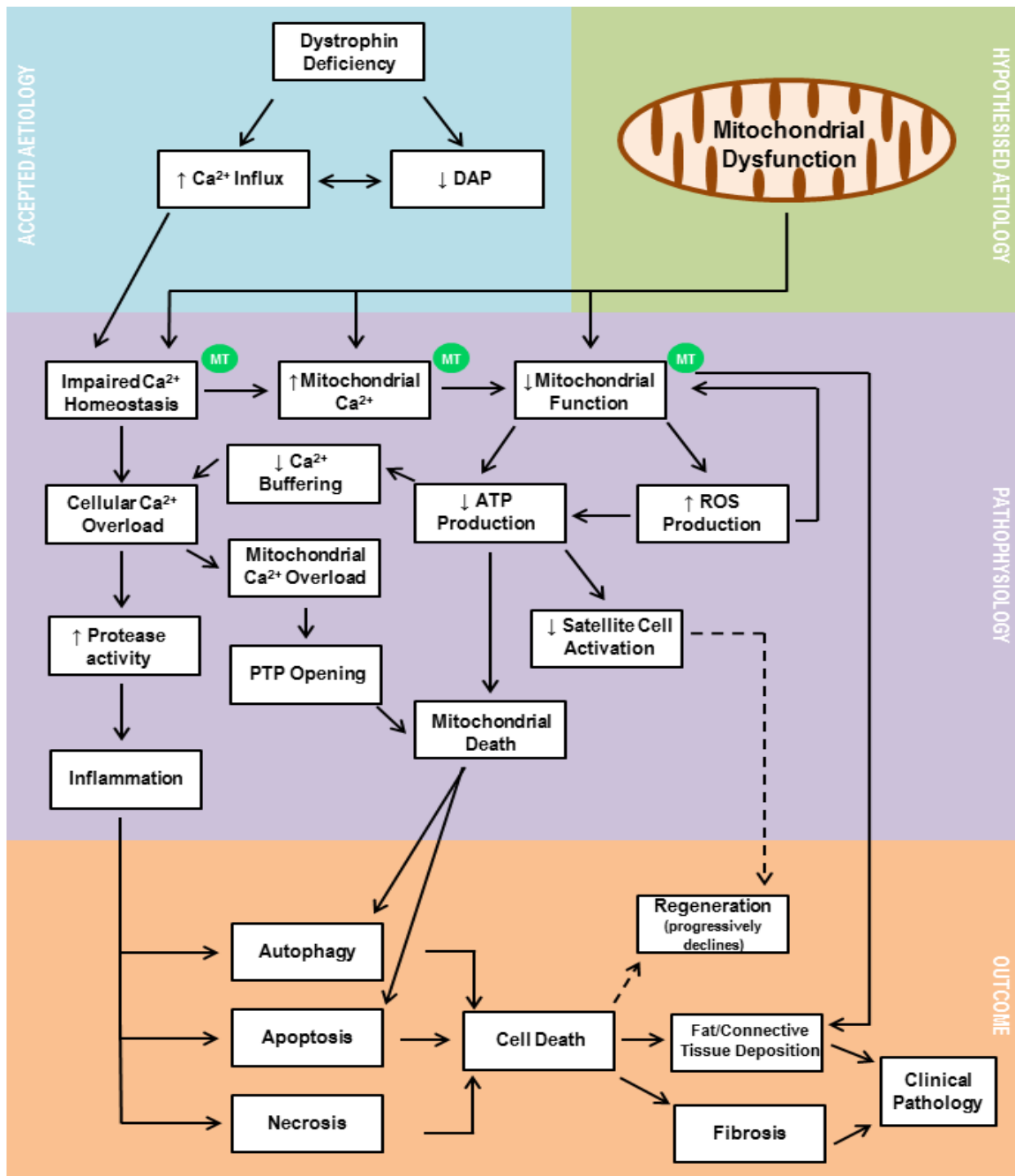


Figure 1.5. Challenging the accepted paradigm of DMD aetiology: the potential for metabolic therapy to anaplerotically “correct” dystrophin-deficiency-mediated pathology. In the accepted aetiology of DMD (blue box), the pathophysiology (purple box) and clinical outcomes (orange box) are the result of dystrophin- and dystrophin-associated protein (DAP)-complex-deficiency-mediated Ca^{2+} influx and homeostasis deregulation. Mitochondrial dysfunction is a secondary consequence of cellular Ca^{2+} overload. In our hypothesised aetiology of DMD (green box), inherent mitochondrial dysfunction is the precursor to dystrophic pathophysiology and not a secondary consequence of dystrophin-deficiency as currently accepted. Inherent mitochondrial dysfunction would limit the ATP production required to buffer Ca^{2+} from myofibres and organelles and maintain regenerative capacity, thus driving the clinical phenotype. The application of metabolic therapy (MT) (green circles) would target the impaired Ca^{2+} homeostasis, increased mitochondrial Ca^{2+} load and mitochondrial dysfunction to effectively buffer the Ca^{2+} influx induced by dystrophin/DAP-deficiency and prevent the subsequent pathophysiology.

The decreased respiration rate of dystrophic mitochondria from both human and various animal models may be mostly accounted for by the activities of the ETC enzymes (Figure 1.4B). In *mdx* fibres of the quadriceps, the activities of rotenone-sensitive NADH:cytochrome *c* reductase, succinate:cytochrome *c* reductase and cytochrome *c* oxidase were found to be 50% of that in normal fibres (Kuznetsov *et al.*, 1998), with a 20-35% reduction in the activities of complexes I, II and IV in *mdx* fibres of the tibialis anterior (Godin *et al.*, 2012) and an ~30% decrease in complex I activity in 129/ReJ-dy mitochondria following NADH addition (Martens *et al.*, 1980). Moreover, in both the fast-twitch EDL and slow-twitch soleus (SOL) of the *mdx* mouse, NADH activity is reduced (Jahnke *et al.*, 2012), with *mdx* myoblasts expressing a decreased complex III and V content (Onopiuk *et al.*, 2009). There is also a significant decrease in the expression of genes encoding the subunits of complexes I, II, III and IV in DMD muscle (Chen *et al.*, 2000). Ultimately, the maximal ATP synthesis rate is reduced by up to 75% in mitochondria isolated from dystrophic skeletal muscle (Percival *et al.*, 2013, Rybalka *et al.*, 2014). Similar respiratory dysfunction is observed in the brain of the *mdx* mouse. Decreased activity of complexes I and IV is observed throughout various sections of the brain (Tuon *et al.*, 2010) indicating that despite not being strongly involved in the pathological progression of the disease, the brain still manifests similar metabolic deficits as per the skeletal musculature.

In addition to the content and activity of isolated complexes of the mitochondrial respiratory chain, functional measures of mitochondrial performance are challenged in dystrophin-deficient skeletal muscle. Dystrophic mitochondria exhibit reduced respiratory control, ADP/oxygen (O) and P/O ratios (Ionășescu *et al.*, 1967, Olson *et al.*, 1968, Jato-Rodriguez *et al.*, 1972, Wrogemann *et al.*, 1973, Nylen

and Wrogemann, 1983, Liang, 1986, Glesby *et al.*, 1988, Bhattacharya *et al.*, 1993, Percival *et al.*, 2013), all of which indicate that dystrophic mitochondria are not as tightly coupled as healthy mitochondria, thus reducing the phosphorylation potential (Kemp *et al.*, 1993) as evidenced by the 40% reduction in ATP produced per O₂ molecule consumed (Percival *et al.*, 2013). This mismatch of ATP production to O₂ consumption infers uncoupled respiration. Uncoupling refers to any process that impacts upon the P/O ratio and subsequently depletes the potential energy. This includes loss of protons due to inefficient proton pumping by the ETC complexes, leak of electrons from the respiratory chain and activity of uncoupling proteins. Both uncoupling proteins and a leaky inner membrane promote proton loss from the intermembrane space of the mitochondria resulting in dissipation of the mitochondrial membrane potential ($\Delta\Psi$). While uncoupling is thought to provide protective effects as it can buffer reactive oxygen species (ROS) produced by electron leak from the respiratory chain, prolonged uncoupling can lead to severe mitochondrial impairment and death (as reviewed in (Kadenbach, 2003)).

The NAD/NADH ratio is an important regulator of metabolism (Stein and Imai, 2012). NAD is a cofactor at multiple sites of the TCA cycle and in glycolysis, where it is reduced to NADH and oxidised at complexes I, III and IV of the ETC. This generates the $\Delta\Psi$ which is the driving force for ATP production. Therefore, maintaining the NAD/NADH ratio is imperative, albeit seemingly difficult in dystrophic muscle due to the decreased total intramitochondrial NAD pool (Martens *et al.*, 1980). Moreover, as the NADH produced at the glycolytic level is dependent upon the malate-aspartate and glycerol-3-phosphate shuttles to enter the mitochondria, and these rely on glutamate oxidation (which is notably decreased in dystrophic

muscle (Olson *et al.*, 1968, Kuznetsov *et al.*, 1998, Rybalka *et al.*, 2014)), glycolysis-generated NADH may be largely prevented from contributing to respiration. Together, this indicates that the NAD/NADH ratio is unable to suitably modulate metabolic function due to other confounding factors that impair the maintenance of the NAD and NADH pool at the mitochondrial level.

1.3.4.2 Mitochondrial Morphology & Density

Mitochondria exist in two distinct pools – located beneath the sarcolemma (subsarcolemmal) and at the I band and intermyofibrillar space of the contractile apparatus (intermyofibrillar) (Hood, 2001). Subsarcolemmal mitochondria account for 10-15% of the mitochondrial pool and supply ATP for Ca²⁺ handling, ion transport, membrane function and the peripheral nuclei while also assisting with glucose homeostasis and lipid utilisation (Hood, 2001). Intermyofibrillar mitochondria constitute up to 90% of the mitochondrial pool and provide ATP for contraction. Intermyofibrillar mitochondria differ from subsarcolemmal mitochondria in that they maintain a higher respiratory rate via increased mitochondrial enzyme activity (Hood, 2001). Despite their differences, both pools of mitochondria share a networking system that allows them to translocate to areas of increased metabolic demand. Thus, mitochondria are extremely responsive to changes in isolated regions of the intracellular environment.

In *mdx* skeletal muscle, a decrease in mitochondrial mass has been reported (Godin *et al.*, 2012, Jahnke *et al.*, 2012). This is partnered with a decrease in the density of subsarcolemmal mitochondria and the accrual of intermyofibrillar mitochondria around necrotic and regenerating fibres with no change in overall mitochondrial number (Percival *et al.*, 2013). This suggests that either the

subsarcolemmal mitochondria are translocating to support the intermyofibrillar mitochondrial pool or require the presence of dystrophin for scaffolding to remain at their proper location. Decreased density would be detrimental as the subsarcolemmal mitochondria play a role in Ca^{2+} handling and lipid metabolism, which may partially explain the inability to appropriately handle the stress applied by Ca^{2+} and the deficits observed in β -oxidation. Moreover, in human DMD biopsies, an increased population of dense and dilated mitochondria have been observed (Mastaglia *et al.*, 1970, Cullen and Fulthorpe, 1975, Watkins and Cullen, 1987) along with changes in cristae shape and density (Pearce, 1966). Swollen mitochondria are also evident in the *mdx* mouse (Cullen and Jaros, 1988, Tidball *et al.*, 1995, Pauly *et al.*, 2012) along with morphologically abnormal cristae structure (Pauly *et al.*, 2012). While morphological changes of the mitochondria are generally resultant of fibres undergoing degeneration and necrosis, it appears this swollen morphology may exist outside of an environment conducive to swelling (Rybalka *et al.*, 2014). Isolated *mdx* mitochondria bathed in a Ca^{2+} -free environment have been shown to be more swollen than mitochondria isolated from healthy animals (Rybalka *et al.*, 2014). While this could be a residual effect of an extreme pre-isolation *in vivo* Ca^{2+} environment, it may also be an inherent feature of the disease as alterations in mitochondrial architecture, morphology and localisation are apparent in female DMD carriers that do not manifest dystrophinopathy (Afifi *et al.*, 1973). If so, this inherent swollen morphology would affect mitochondrial functionality, due to the altered cristae structure described previously (Afifi *et al.*, 1973), as changes in cristae shape have recently been shown to alter ETC supercomplex assembly (Cogliati *et al.*, 2013). Together, this decrease in mitochondrial mass and inherent swollen morphology strongly suggest that metabolic impairments in DMD are an inherent

feature of the genotype, and this is worsened by the persistent elevation of Ca^{2+} .

1.3.5 The Creatine Phosphagen System

The creatine phosphagen (Cr/PCr) system is an important buffering system to maintain ATP levels, especially during exercise (as reviewed in (Clark, 1997)). CK exists both in the cytosol and mitochondria and reversibly phosphorylates Cr to produce ADP and PCr at the expense of ATP hydrolysis; and dephosphorylates PCr to produce ATP and Cr using ADP as a substrate. Activity of the Cr/PCr system assists metabolism in a couple of ways: (1) mitochondrial CK is coupled to oxidative phosphorylation, therefore stimulating respiration and (2) phosphorylation of PCr minimises nucleotide loss by sequestering ADP before it is further dephosphorylated in the PNC. Thus, it is an important support system in skeletal muscle.

It has been consistently reported that there are significant deficiencies in the Cr/PCr system within dystrophic skeletal muscle (summarised in Figure 1.6). Decreases in PCr (Ronzoni, 1958, Vignos Jr and Warner, 1963, Fitch and Rahmanian, 1969, Samaha, 1981, Newman *et al.*, 1982, Griffiths *et al.*, 1985, Younkin *et al.*, 1987, Dunn *et al.*, 1991, Pulido *et al.*, 1998, Sharma *et al.*, 2003), Cr (Vignos Jr and Warner, 1963, Fitch and Rahmanian, 1969, Griffin *et al.*, 2001, Sharma *et al.*, 2003, Martins-Bach *et al.*, 2012) and total Cr content (Vignos Jr and Warner, 1963, Ionasescu *et al.*, 1981, Louis *et al.*, 2004), the PCr/ P_i (Newman *et al.*, 1982, Griffiths *et al.*, 1985, Younkin *et al.*, 1987,) and PCr/ATP ratios (Newman *et al.*, 1982, Kemp *et al.*, 1993 Griffiths *et al.*, 1995), along with increased activity of CK in blood (Hootan, 1966, Shaw, 1967, Drummond, 1979, Hamada *et al.*, 1981, Zatz *et al.*, 1991, Felber *et al.*, 2000) indicating its loss from muscle, are common nuances of dystrophic muscle. Indeed, it has been demonstrated in dystrophic mice (129

strain) that despite increased Cr uptake by the sodium-dependent Cr transporter (Fitch and Rahmanian, 1969), urinary Cr excretion is 2-fold greater (reflective of decreased turnover rate) compared to healthy mice (Fitch *et al.*, 1961), indicating a deficit in Cr rephosphorylation and retention (Fitch and Moody, 1969). Increased urinary Cr excretion is also observed in human dystrophic muscle (Benedict *et al.*, 1955) with shifts in the proportions of the 3 isoenzymes of CK (muscle, mitochondrial and brain) expressed in dystrophic muscle (Kuby *et al.*, 1977 Ionasescu *et al.*, 1981). The presence of the brain isoenzyme suggests that dystrophic muscle expresses a fetal muscle phenotype (Kuby *et al.*, 1977, Ionasescu *et al.*, 1981) which is most likely reflective of the ongoing regeneration occurring. As the Cr/PCr system assists in ATP rephosphorylation to fuel contraction and the sequestration of Ca²⁺ into the sarcoplasmic reticulum via the linked CK (Spitzer *et al.*, 1981), dysfunction in this system would be highly detrimental to dystrophic muscle.

The capacity to resynthesise ATP via the Cr/PCr system also appears to be impaired, as PCr content in dystrophic muscle has been shown to be reduced by up to 35% (Ronconi, 1958, Vignos Jr and Warner, 1963, Fitch and Rahmanian, 1969, Samaha, 1981, Newman *et al.*, 1982, Griffiths *et al.*, 1985, Younkin *et al.*, 1987, Dunn *et al.*, 1991, Pulido *et al.*, 1998, Felber *et al.*, 2000). PCr is an abundant form of high-energy in muscle (Clark, 1997), thus reduced PCr content in dystrophic muscle infers a reduced total phosphate pool. As PCr hydrolysis supports mitochondrial respiration in times when ATP utilisation outweighs ATP production (Figure 1.6), diminished substrate availability would exacerbate the capacity of dystrophic mitochondria to buffer transient metabolic stress. As such, improving the capacity of the Cr/PCr system to replenish depleted ATP stores and prevent ADP

loss through the PNC would be beneficial in dystrophic muscle, as has been consistently proven using dietary Cr supplementation (reviewed in section 1.7.1).

1.3.6 Purine Nucleotide Salvage & *De Novo* Synthesis

During metabolic stress – such as that evident during high-intensity exercise – and/or catabolism, when ATP rephosphorylation rate cannot match demand, purine nucleotides are systematically degraded to hypoxanthine, adenine and guanine within skeletal muscle (Figure 1.7). Following normal recovery conditions, up to 90% of them are capably resalvaged via the PNC to replete resting ATP stores. Consisting of three enzymes: adenosine monophosphate (AMP) deaminase, adenylosuccinate synthetase and adenylosuccinase; the PNC converts AMP to inosine monophosphate (IMP) and adenylosuccinate (and back to AMP), producing ammonia and fumarate in the cytosol (Lowenstein, 1972). Fumarate, which can also be converted to malate (Flanagan *et al.*, 1986) via cytosolic fumarase, is transported into the mitochondria via the malate-aspartate shuttle to anaplerotically expand the TCA cycle and increase ATP production. Further to this, the production of AMP from adenylosuccinate allows for the rephosphorylation of ADP via the adenylate kinase (AK) reaction which can then return to the mitochondria for the synthesis of ATP (Figure 1.7). Therefore, the PNC is an important cytosolic pathway which conserves purine nucleotides that can expand ATP synthesis.

As with the other metabolic pathways, deficits in enzyme activity of the PNC have been observed (summarised in Figure 1.8), albeit it has not been investigated in the *mdx* mouse model. In 129/ReJ-dy (Pennington, 1963), C57BL/6J-dy/dy (Sanada and Yamaguchi, 1979), C57BL/6J- $dy^{2J}dy^{2J}$ (Fitt and Parliament, 1982)

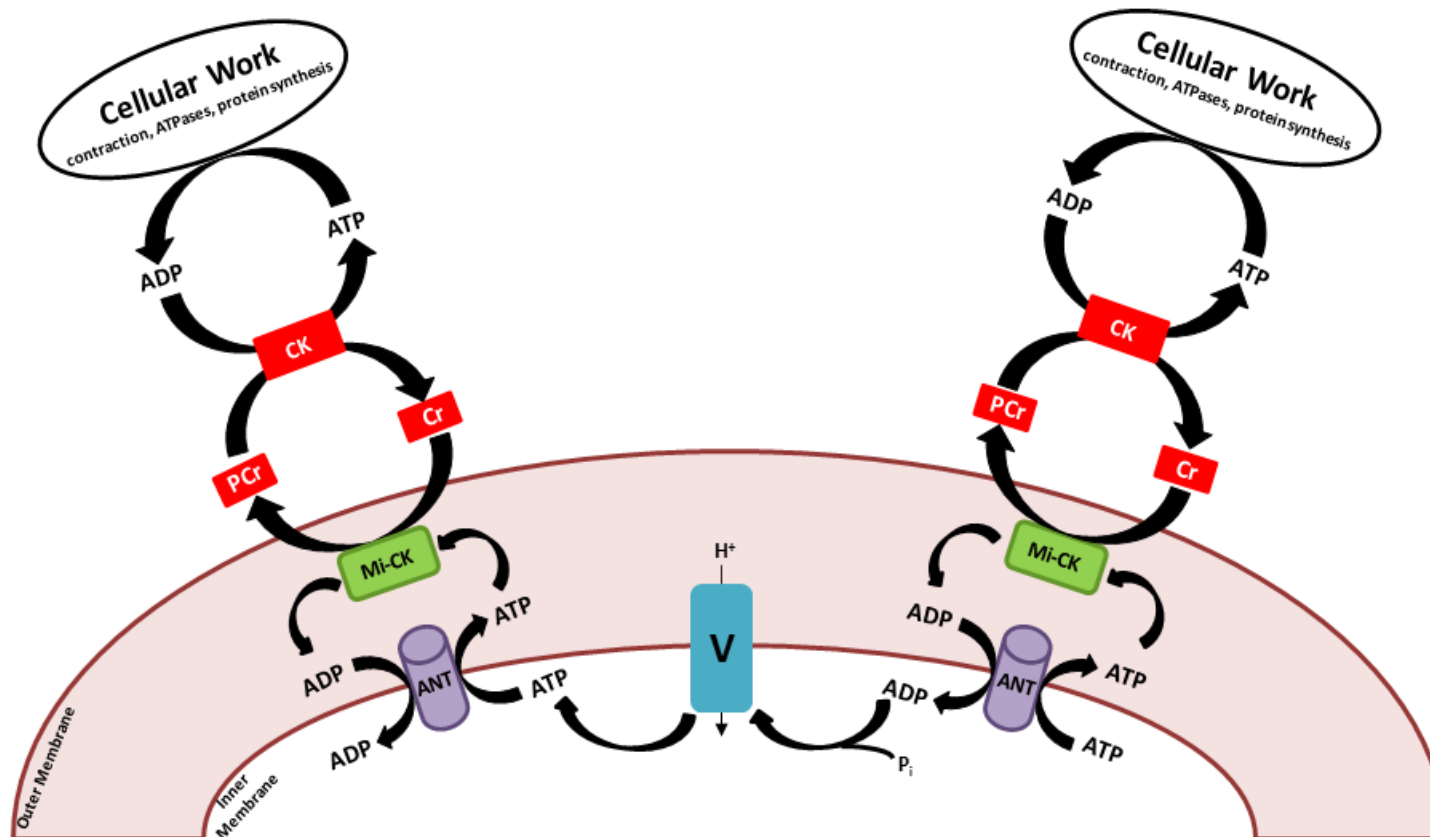


Figure 1.6. Creatine phosphagen (Cr/PCr) system function in skeletal muscle. The Cr/PCr system is involved in maintaining the energy pool in skeletal muscle, especially during acute metabolic stress. The translocation of ADP via adenine nucleotide translocase (ANT) into the mitochondrial matrix promotes the rephosphorylation of ATP via complex V of the ETC. This ATP is then translocated across the inner mitochondrial membrane and utilised by mitochondrial creatine kinase (Mi-CK), along with Cr, to produce PCr and ADP which can be shuttled back into ATP rephosphorylation at complex V. In the cytosol, CK rephosphorylates ADP produced during cellular work to replenish ATP stores. In dystrophin-deficient skeletal muscle, CK, PCr, Cr and functional ratios are impaired (as indicated by those enclosed in solid boxes with white writing).

and Bar Harbor (Pennington, 1961) dystrophic skeletal muscle, AMP deaminase activity demonstrably decreases with age. Similar findings are observed in human skeletal muscle biopsies from DMD patients (van Bennekom, 1984) in addition to decreased [IMP] (Camiña *et al.*, 1995). Additionally, the activity of adenylosuccinate synthetase is decreased (Sanada and Yamaguchi, 1979, Fitt and Parliament, 1982) subsequently reducing adenylosuccinate content in dystrophic muscle (Fitt and Parliament, 1982). This indicates a decreased capacity for the conversion of adenylosuccinate to AMP in the PNC which would (1) reduce the production of fumarate and anaplerosis of the TCA cycle; (2) reduce cycling of the PNC; and (3) decrease the availability of AMP for rephosphorylation. Therefore, targeting this pathway to increase anaplerotic capacity and increase the adenine nucleotide pool may be beneficial for metabolically impaired dystrophic muscle.

Two products of PNC activity, AMP and IMP, can be utilised as substrates for ATP (via ADP) resynthesis, or be further degraded if ADP levels exceed mitochondrial phosphorylation potential. With respect to salvage, AMP is rephosphorylated to ADP via AK. In dystrophic muscle, both the activity (Pennington, 1963, van Bennekom, 1984, Ge *et al.*, 2003) and content (Ge *et al.*, 2003) of AK is demonstrably decreased (Figure 1.7). Increased serum activity suggests that AK is lost from skeletal muscle as a direct consequence of the leaky dystrophin-deficient membrane (Hamada *et al.*, 1981). Decreased AK activity severely compromises the cellular capacity for purine salvage, thus increasing the flux of adenine nucleotides from skeletal muscle and increasing the need for *de novo* ATP synthesis. As such, AK is an important metabolic sensor and regulator of adenine nucleotide homeostasis (Ge *et al.*, 2003). When salvage is insufficient, IMP can be further degraded to inosine (which is normally absent in healthy muscle but observed in

50% of dystrophic muscle biopsies (Ronzoni, 1958)) and lost to the bloodstream as uric acid. This is an unfavourable outcome as both inosine and hypoxanthine can be resalvaged for upstream ATP rephosphorylation. To ensure cellular energy homeostasis, adenine nucleotides that are lost from skeletal muscle are repleted via *de novo* synthesis which is an extremely energy consuming process. *De novo* purine nucleotide synthesis utilises ribose-5-phosphate, a product of the pentose phosphate pathway, which is sequentially converted in a series of steps to produce IMP, a precursor for AMP and guanosine monophosphate.

While *de novo* synthesis does produce intermediates that can be funnelled into ATP rephosphorylation (i.e. fumarate, ADP and IMP), it also consumes a considerable amount of ATP (6 molecules). Therefore, the loss of purines would be highly detrimental as use of this pathway would induce further ATP demand from an already small ATP pool in dystrophic muscle. Indeed, increased uric acid excretion in the urine has been reported in DMD (de Bruyn *et al.*, 1980, Bertorini *et al.*, 1981, Camiña *et al.*, 1995) indicating loss of essential purines from dystrophic muscle, and perhaps more importantly, a failure of the cellular metabolic systems to maintain energy homeostasis. As intensely exercised muscle generally exhibits transient increases in urinary excretion of purines due to higher ATP turnover, this data suggests that the metabolic profile of dystrophic muscle is consistent with extreme metabolic stress (Bertorini *et al.*, 1981), albeit persistently.

1.4 Dystrophic muscle does not respond normally to master energy signals

In healthy skeletal muscle, ATP depletion induced by metabolic, nutritional and/or environmental stressors (including intense exercise and hypoglycaemia) stimulates ATP-producing pathways to restore energy homeostasis (as reviewed in

(Viollet *et al.*, 2003)). One important regulator of this switch from ATP-consuming (anabolic) to ATP-producing (catabolic) pathways is adenosine monophosphate-activated protein kinase (AMPK), a major sensor of cellular energy status. Induced by rises in the AMP/ATP ratio (Figure 1.7), AMPK stimulates glucose uptake, glycolysis, fatty acid oxidation (Viollet *et al.*, 2003, Wang *et al.*, 2011) and various TCA cycle and ETC enzymes (Winder *et al.*, 2000), while also modulating expression of a suite of genes – including PGC-1 α – that increase mitochondrial biogenesis. Thus, AMPK activation favours the oxidative fibre phenotype, which is highly beneficial in dystrophic muscle as this fibre type is less affected by the disease (Webster *et al.*, 1988) and therefore may offer protection from damage. In addition, AMPK appears to play a significant role in muscle remodelling as it stimulates autophagy. Autophagy is a catabolic pathway that breaks down cellular components when they are in excess or damaged, or, to provide fuel sources in times of metabolic challenge (as reviewed in (Neel *et al.*, 2012)). Therefore, AMPK is a positive stimulator of metabolism, controlling the supply of fuel to various metabolic pathways and initiating remodelling to improve muscle structure and function.

Considering that AMPK positively modulates metabolism, stimulates targeted remodelling of muscle to improve oxidative capacity and is activated by ATP depletion, AMPK activation should, theoretically, be enhanced in dystrophic skeletal muscle. Indeed, Pauly *et al.* demonstrate a higher basal AMPK activation in *mdx* diaphragm, highlighting that metabolic stress-induced signalling pathways are appropriately activated in dystrophic muscle (Pauly *et al.*, 2012). However, when the AMPK-activator metabolite 5'-aminoimidazole-4-carboxamide-1- β -D-ribofuranoside (AICAR) was given to *mdx* myotubes *in vitro* and to 6 week old *mdx* mice via daily intraperitoneal injection, AMPK activation was further enhanced compared to

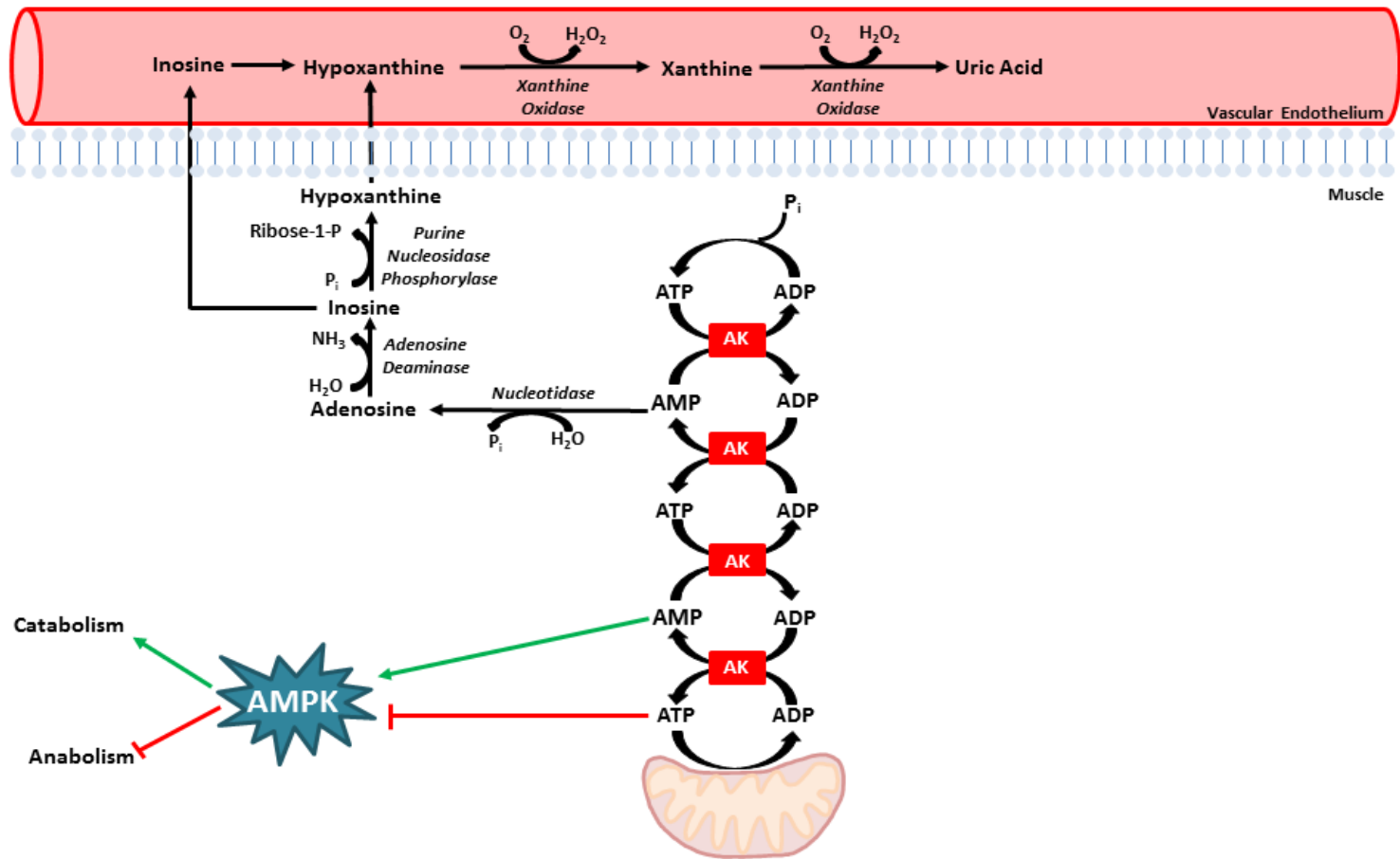


Figure 1.7. Adenylate kinase (AK) dysregulation in dystrophin-deficient skeletal muscle. AK dysfunction leads to the accumulation of AMP during metabolic stress and the irreversible loss of adenine nucleotides from skeletal muscle as hypoxanthine/inosine. This leads to increased serum concentration and renal excretion of uric acid. High AMP levels also activate the metabolic sensor molecule AMP-activated protein kinase (AMPK) to inhibit anabolic- and stimulate catabolic-signalling pathways to increase nutrient availability to metabolism and reduce energy expenditure.

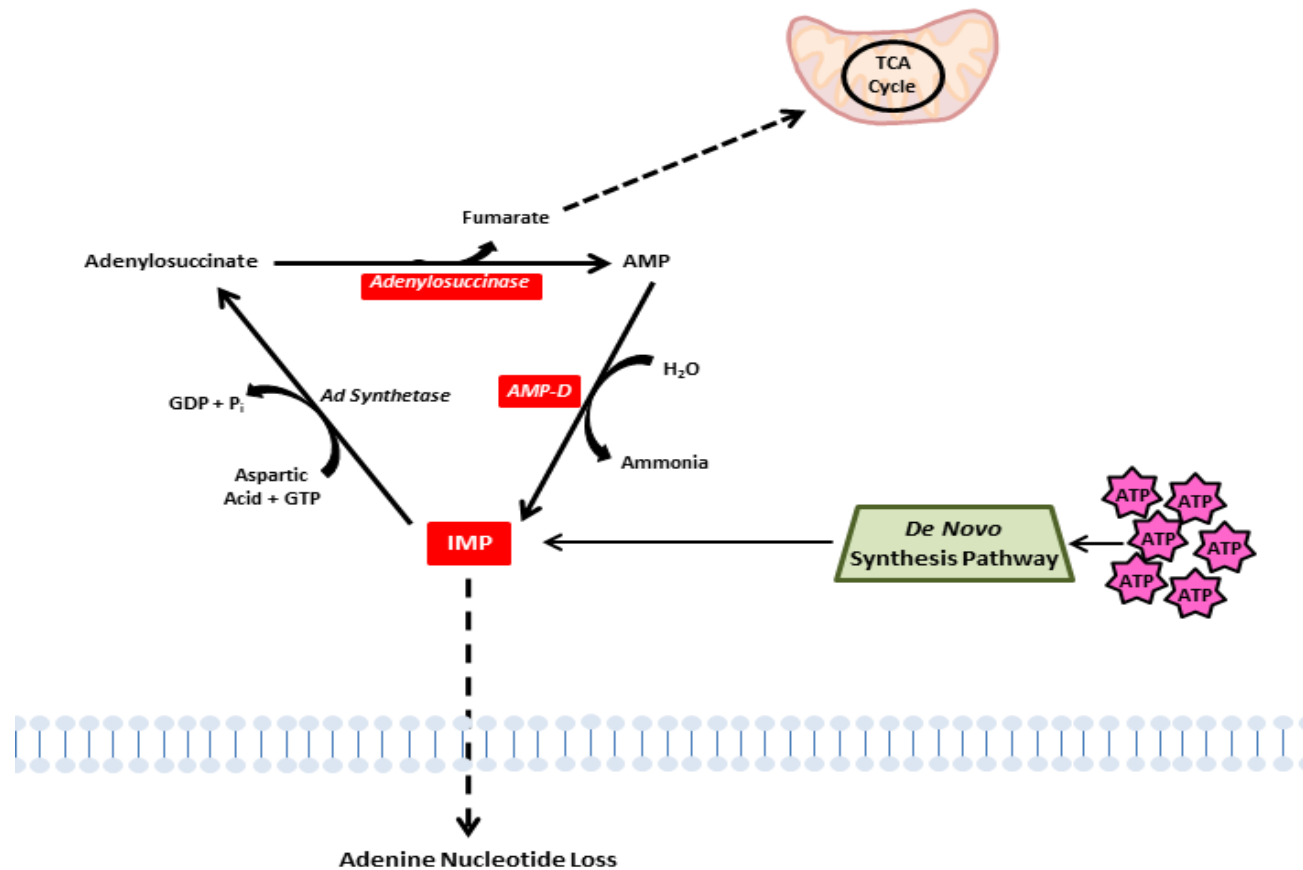


Figure 1.8. The consequences of dysfunctional Purine Nucleotide Cycle (PNC) activity in dystrophin-deficient skeletal muscle. In healthy skeletal muscle, the PNC cycles IMP (from degraded adenine nucleotides) to re-salvage AMP, ADP and ATP while stimulating mitochondrial function via fumarate production. In dystrophin-deficient skeletal muscle, key enzymes of the PNC are dysfunctional (as indicated by those in solid boxes with white writing) which leads to the degradation and loss of IMP from skeletal muscle as hypoxanthine/inosine and reduced stimulation of the mitochondrial TCA cycle (as indicated by broken arrows). The muscle must then rely on *de novo* synthesis to replenish the adenine nucleotide pool at the expense of ATP consumption.

untreated conditions. In the *mdx* mice in particular, AICAR treatment had several beneficial effects including increased activation of autophagic signalling proteins, maximal force production and time to permeability transition pore opening in response to Ca^{2+} challenge (Pauly *et al.*, 2012). Most noteworthy however, was that despite AICAR inducing an ~50% increase in activated AMPK, only minimal increases were observed in acetyl CoA carboxylase phosphorylation (the downstream target of AMPK activity) and this failed to induce any changes in oxidative metabolism including activity of citrate synthase, cytochrome oxidase and mitochondrial O_2 consumption. This data importantly highlights that while dystrophin-deficient muscle can ably detect metabolic stress, the downstream response of the metabolic systems to AMPK-regulation fails to improve ATP synthesis to abate this stress.

The plasticity of the skeletal musculature in response to isolated and chronic exposure to metabolic stress is afforded via the induction of a slow-type oxidative phenotype. In a study that compared global gene expression responses between skeletal muscle from metabolically-challenged endurance-trained (6 weeks) individuals who had been previously sedentary, and DMD patients, ~90 genes were shown to be modulated identically (Timmons *et al.*, 2005). This highlights that strong metabolic challenge is a feature of dystrophinopathy and that it invokes similar responses as per chronic endurance exercise. However, while the expression of genes regulating oxidative phosphorylation was increased following endurance training as expected, they were differentially down regulated in muscle from DMD patients (Timmons *et al.*, 2005). These included genes of carbohydrate, glycogen and mitochondrial metabolism (Timmons *et al.*, 2005). Thus, while DMD muscle adapts on a genetic level to metabolic stress as per endurance trained athletes, this

stress seems not to induce the regular adaptations at the mitochondrial level to enhance the ATP production capacity of the skeletal musculature. It has been well established in the literature that inducing type I oxidative fibre type transformations pharmacologically and genetically, affords therapeutic value to dystrophin-deficient skeletal muscle by reducing the rate of disease progression (Chakkalakal *et al.*, 2003, Chakkalakal *et al.*, 2004, Angus *et al.*, 2005, Chakkalakal *et al.*, 2006), as type II fibres are preferentially affected (Webster *et al.*, 1988, Karpati *et al.*, 1988). This can be promoted by the activation of AMPK (Ljubicic *et al.*, 2011, Ljubicic *et al.*, 2012, Jahnke *et al.*, 2012, Ljubicic and Jasmin, 2013, Al-Rewashdy *et al.*, 2014) and its downstream targets (Handschin *et al.*, 2007, Selsby *et al.*, 2012, Bueno Júnior *et al.*, 2012, Godin *et al.*, 2012). However, a recent study by Al-Rewashdy *et al.* (Al-Rewashdy *et al.*, 2014) suggests that the beneficial effects of a slow type I phenotype is functionally related to enhanced utrophin A expression as in dystrophin/utrophin double knock-out mice, AICAR administration afforded no benefit – in comparison, therapeutic benefit was observed in *mdx* mice. Thus whether AMPK activation can suitably induce benefits at the mitochondrial level to buffer metabolic demand remains unclear.

Another important role more recently identified for AMPK is regulation of the targeted removal of dysfunctional organelles/structures via autophagy. It has been observed that *mdx* diaphragm is laden with dysfunctional mitochondria characterised by morphological abnormalities and an increased propensity to open the permeability transition pore (Pauly *et al.*, 2012). The removal of dysfunctional mitochondria is strongly regulated in healthy skeletal muscle (Sandri, 2010), albeit background mitophagic activity is typically low due to the relatively low ratio of unhealthy/healthy mitochondria. However, in dystrophic skeletal muscle, there is reduced propensity for

sufficient and/or functional mitophagy leading to the accumulation of defective mitochondria, particularly in the subsarcolemmal pool (De Palma *et al.*, 2014). Ineffective autophagic signalling induction has been demonstrated in *mdx* (De Palma *et al.*, 2014) and human DMD (Pauly *et al.*, 2012, De Palma *et al.*, 2014) skeletal muscle with AMPK activation seemingly central to the problem. Both AICAR and low protein diet-induced AMPK activation demonstrably increases the activity of pro-autophagic pathways and ameliorates the dystrophic condition (Pauly *et al.*, 2012), indicating that improving the clearance of dysfunctional mitochondria is beneficial. Thus while Pauly *et al.* (Pauly *et al.*, 2012) have demonstrated enhanced endogenous AMPK signalling in dystrophin-deficient skeletal muscle, it appears insufficient to match the extent of mitochondrial pathology evident in DMD without therapeutic support.

1.5 The Dystrophin-ATP Connection: Is a mitochondrial disease at the heart of DMD?

Several hypothetical review and original research papers have both historically and more recently proposed that the lack of dystrophin protein may not be the primary cause of the progressive and fatal degeneration observed in DMD, but rather a co-morbidity (Bonsett and Rudman, 1992, Lucas-Heron, 1995, Onopiuk *et al.*, 2009, Kelly-Worden and Thomas, 2014, Górecki, 2016). Within this review, a plethora of mitochondrial defects (in addition to many others of substrate feeder pathways that are allosterically regulated by the functional capacity of the mitochondria) have been described that are also commonly observed in mitochondrial diseases and in senescence. Indeed, DMD shares common metabolic and mitopathological features with various mitochondrial diseases and with aged skeletal muscle (Baron *et al.*, 2011), including often comparable symptomology. In

addition a more recent study has shown that mitochondrial dysfunction exists in “pre” dystrophin-deficient myoblasts prior to the “typical” cascade of events that are commonly believed to cause the progressive muscle degeneration and wasting evident in DMD (Onopiuk *et al.*, 2009). Collectively, this literature importantly suggests a mitochondrial aetiology of DMD, and is discussed in more detail herein.

Because skeletal muscle accounts for ~40-50% of body weight and ~30% of oxygen consumption at rest, it is an important regulator of overall metabolism. As such, mitochondrial deficits manifest vastly in the skeletal musculature (in addition to brain, heart and liver) and are characteristic of many mitochondrial diseases. Mitochondrial disease can arise from mutations in the maternally inherited mitochondrial DNA (mtDNA), and less commonly in the nuclear DNA. mtDNA resides in the matrix and encodes for the hydrogen pumping regions of the respiratory chain complexes, highlighting its integral role in the regulation of metabolism (as reviewed in (Wallace, 1999)). However due to its proximity to the respiratory chain, mtDNA is extremely vulnerable to mutation, most commonly by ROS produced by the respiratory complexes (Yakes and Van Houten, 1997, Lin *et al.*, 2003). Initially, this has minimal effect on mitochondrial function, until the number of mutant mtDNA outnumber wild-type mtDNA. As mutant mtDNA accumulates, the bioenergetic capacity of the cell diminishes. Several diseases including mitochondrial encephalomyopathy, lactic acidosis and stroke-like episodes (MELAS), Leigh’s syndrome and the classical mitochondrial dystrophies result from mtDNA mutations and manifest themselves as multisystemic diseases. These mitochondrial diseases share common features with DMD including mental impairment, skeletal muscle weakness, cardiomyopathy and multisystem metabolic dysfunction (as reviewed in (Wallace, 1999, DiMauro and Davidzon, 2005)). Reduced activities of complex I, III,

IV and V of the ETC, increased ROS production and decreased ATP synthesis are common nuances of mitochondrial diseases and DMD (DiMauro and Davidzon, 2005). The fact that dystrophin is encoded and expressed normally in these diseases, but that they share clinical features with dystrophinopathy indicates the potential for a common disease origin not relating to dystrophin-deficiency.

As the majority of ETC complexes (excluding complex II) are partially encoded by mtDNA and reports exist that describe mitochondrial dysfunction in DMD carriers that express dystrophin (Bonilla *et al.*, 1988), maternal mtDNA inheritance would be a likely theoretical origin of such a mitochondrial mutation. Female carriers of the dystrophin gene mutation on one of their X chromosomes commonly express normal levels of dystrophin (albeit sporadic dystrophin-deficient fibres have been reported (Bonilla *et al.*, 1988)). As such, they do not manifest DMD. However, despite lacking phenotypic pathology, deficits in mitochondrial responses to exercise have been reported. Carriers are unable to perform muscle work at the same level as controls and their P_i/PCr ratio is higher for corresponding work levels (Barbiroli *et al.*, 1992a, Barbiroli *et al.*, 1992b). This supports an inability of the mitochondria to sufficiently replenish the Cr/PCr system during activity. Post-exercise recovery of the PCr/ P_i ratio is also much slower in carriers (Barbiroli *et al.*, 1992b), demonstrating that mitochondrial insufficiency is also apparent at rest. Additionally, sharp increases in serum CK activity are observed following exercise in carriers but are absent in healthy exercised individuals (Stephens and Lewin, 1965, Thomson, 1969). Notably, the co-occurrence of a mtDNA mutation in a family with extensive history of DMD has also been observed (Wong *et al.*, 2004), which adds further credence to the ideation of mtDNA mutation underscoring DMD pathology.

If not inherited, another likely origin of mtDNA mutation is via the rapidly progressive accumulation of ROS-induced mutations that are not too dissimilar to those that underscore senescence as described in the popular *mtDNA accumulation theory of aging* (reviewed in (Hiona and Leeuwenburgh, 2008)). Aging muscle shares many symptomatic characteristics of dystrophic muscle including fatigability, muscular weakness and atrophy, and mitochondrial dysfunction. In aging muscle, it appears that accumulation of mutant mtDNA leads to mitochondria that are characterised by decreased oxidative capacity, increased oxidative stress and decreased ATP synthesis (as reviewed in (Wallace, 1999, Dirks *et al.*, 2006)) which impairs muscular function. Of note, a characteristic feature of senescent mitochondria is a reduction in spare respiratory capacity (Desler *et al.*, 2012) which renders mitochondria unable to adapt to increased energy demand, thus promoting fatigue, exercise intolerance and progressive muscle wasting (sarcopenia) which are all symptoms of DMD. Indeed, both aged and dystrophic muscles display deregulation of the same genes involved in metabolism (Baron *et al.*, 2011) which highlights once more the possibility of mtDNA mutation involvement in DMD.

Perhaps one of the more compelling pieces of evidence that mitochondrial dysfunction is an inherent feature of DMD is a recent finding by Onopiuk and colleagues (Onopiuk *et al.*, 2009). Using myoblasts from control and *mdx* mice, it was observed that *mdx* myoblasts exhibit changes to several mitochondrial functional parameters including decreased basal oxygen consumption, increased mitochondrial membrane potential and ROS production (~70% higher) and decreased complex III and V content (Onopiuk *et al.*, 2009). Remarkably, these metabolic changes are observed at a time when dystrophin is yet to be expressed in myoblasts (Klamut *et al.*, 1989). In both control and *mdx* myoblasts, dystrophin

expression was negligible, despite an mRNA transcript evident in control myoblasts (Onopiuk *et al.*, 2009). Myoblasts express a different metabolic phenotype to myotubes including a greater dependence on glycolysis (Leary *et al.*, 1998). Glycolysis pacifies ~60% of energy demand (Leary *et al.*, 1998) and *mdx* myoblasts demonstrably produce more lactate (Onopiuk *et al.*, 2009) indicating heavy reliance on glycolytic flux. This appears to be pertinent to *mdx* myoblasts as the basal rate of respiration following the addition of glucose and pyruvate was depressed compared to controls (Onopiuk *et al.*, 2009), suggesting that further oxidation of intermediates in the mitochondria is impaired. The authors concluded that the metabolic dysfunction in *mdx* myoblasts is independent of dystrophin-deficiency as deficits were observed in *mdx* myoblasts prior to the time of dystrophin expression.

1.6 Clinical Case Studies

There are now several case studies in the literature documenting either dual mtDNA and nuclear dystrophin gene mutations in family pedigrees (Wong *et al.*, 2004) or dystrophin gene abnormalities with pseudometabolic presentation (Romero *et al.*, 2001, Veerapandiyam *et al.*, 2010). A case study by Wong and colleagues (Wong *et al.*, 2004) describes the presentation of an adolescent male with a strong family history of DMD but who does not express the genotype himself, with complicated seizure disorder, congenital heart disease and developmental delay. Suspected mitochondrial respiratory chain disorder was confirmed with sensitive DNA analysis, in which low levels of heteroplasmic A3243G mutation was detected in the mtDNA. The diagnosis of MELAS disorder was made following respiratory enzyme analysis that revealed significantly elevated complex IV activity without gross mitochondrial cytopathy (albeit some mitochondria displayed altered cristae

structure and were morphometrically abnormal). The patient carried low mutant loads in all tissues analysed – 6%, 8%, 12%, 17% and 9% for blood, hair follicle, buccal mucosa, skeletal muscle and skin fibroblast cultures, respectively. The mutation appeared to have occurred *de novo* as it was not detected in the maternal mtDNA from blood, hair follicle or buccal mucosa cells, albeit this could not be confirmed given the relatively low mutant load found in the patient. Similar cases of mtDNA mutation in the background of other, more severe nuclear gene mutations (such as cystic fibrosis and spinal muscular atrophy) have been reported by the same group (Lam *et al.*, 1997, Wong *et al.*, 2003) highlighting the propensity for dual mitochondrial and nuclear gene mutations that are difficult to diagnose due to broad and often competing symptomologies.

The pseudometabolic presentation of DMD due to missense mutations in the dystrophin gene has also been documented. Romero and colleagues (Romero *et al.*, 2001) report three male adolescents presenting with exercise-induced myalgia, muscle stiffness, and myoglobinuria following strenuous exercise – all symptoms of metabolic diseases including glycogen storage disorder, fatty acid oxidation disorder and mitochondrial cytopathy. All patients were found to have a hemizygous T-to-C mutation in exon 15 of the DMD gene resulting in an amino acid substitution of leucine to proline at codon 575. Immunohistochemical staining of dystrophin and other proteins of the DPC was normal as was western blot analysis for dystrophin quantity and size. A further two reports of the same missense mutation inducing recurrent rhabdomyolysis has been reported (Aartsma-Rus *et al.*, 2006). These case studies highlight symptoms characteristic of metabolic disease that are seemingly induced by dystrophin gene point mutations but which are not phenotypically associated with dystrophin protein expression abnormalities.

Most recently, several studies by the same group have documented the clinical history of canine models of muscular dystrophy (Zucconi *et al.*, 2010, Zatz *et al.*, 2015, Vieira *et al.*, 2015b) and dystrophin-deficient human DMD patients (Zatz *et al.*, 2014) that express a mild disease phenotype and in some instances, a normal lifespan, despite the absence of dystrophin. Zucconi *et al.* (Zucconi *et al.*, 2010) and Zatz *et al.* (Zatz *et al.*, 2015) describe the clinical history of a golden retriever muscular dystrophy dog, Ringo, and his male offspring, Sulfair, who display absent dystrophin production, unremarkable utrophin regulation, hallmark histopathological features of skeletal musculature and extreme elevations in serum CK levels as per phenotypically normal severely-affected dogs, but are seemingly able to buffer this to maintain muscle mass, ambulation and a normal life span. Ringo died at 11 years of age from dilated cardiomyopathy – this is in stark contrast to the 1-2 year life span of severely affected littermates. A similar canine colony has been reported in a Labrador retriever muscular dystrophy model (Vieira *et al.*, 2015b) which also displays the absence of dystrophin – albeit the precise mutation on the dystrophin gene was not elucidated in this study – and are asymptomatic. This protection seems related to the overexpression of the *Jagged1* gene which enhances skeletal muscle proliferative capacity and therefore repair and regeneration of damaged muscle (Vieira *et al.*, 2015a). Finally, in human DMD patients, Zatz *et al.* (Zatz *et al.*, 2014) have reported half-brothers with comparable, minimal (near absent) levels of dystrophin expression, elevated serum CK levels and pathological histological parameters, but who express widely variable phenotypic progression of DMD. While one brother has progressed through a normal disease course with onset of symptoms at 3 years, diagnosis at 7 years and loss of ambulation at 9 years, the older brother shows mild signs of muscle weakness and physical dysfunction with

mild calf hypertrophy, but maintains normal ambulatory capacity at 16 years of age. The same paper describes a third case of an unrelated male 16 year old adolescent who displayed normal phenotypic DMD at age 7 years when diagnosis was made, but who now displays only mild weakness and calf hypertrophy and is fully ambulatory. Other isolated case studies exist documenting the complete absence of dystrophin expression but a mild DMD phenotype (Dubowitz, 2006, Castro-Gago, 2015). Collectively, these clinical cases strongly suggest that the loss of dystrophin expression is not the sole contributor to the pathological deterioration of skeletal muscle in DMD, and while indeed promoting sarcolemmal leakiness and significant damage, dystrophin-deficiency can be effectively buffered by adaptive mechanisms in some instances.

1.7 Could metabogenic therapy be a plausible DMD treatment avenue?

Although the collective literature over the past 50 years has carefully documented the plethora of metabolic abnormalities consistently observed in DMD patients, genetic carriers and genotypically identical animal models of the disease, the significance of this data has been largely ignored. As a cure for DMD remains currently elusive, every effort must be made to consider all possibilities for improved characterisation and treatment of the disease. The literature highlights a very probable aetiological nuance at the mitochondrial level that manifests in multiple deficiencies of various metabolic pathways to culminate in severe ATP insufficiency. Of course, it cannot be denied that changes induced by dystrophin-deficiency, including disruption of the DPC and failed Ca^{2+} homeostasis, play a role in the severe and progressive muscle wasting characteristic of DMD. However, if mitochondrial defects do underlie DMD aetiology, then re-defining DMD as a

metabolic myopathy and strategically treating it as such could improve patient outcomes and quality of life. Thus, there is a need to investigate potential metabolic therapies to rectify metabolic dysfunction.

In recent years, the investigation of metabolic therapies as viable treatment options for DMD has increased in popularity. For example within the past 5 years, treatment with Resveratrol – a red wine polyphenol (Langcake and Pryce, 1977) that stimulates mitochondrial biogenesis (Selsby *et al.*, 2012) and decreases oxidative stress (Hori *et al.*, 2013) – in the *mdx* mouse has shown great promise as it reduces muscle damage (Hori *et al.*, 2011), muscle inflammation (Gordon *et al.*, 2012) and promotes mitochondrial biogenesis and a fibre type shift to an oxidative phenotype (Ljubacic *et al.*, 2014). Similarly, the polyphenol Quercetin improves muscle function, reduces dystrophic skeletal and cardiac muscle pathology and stimulates the expression of oxidative genes (Hollinger *et al.*, 2012, Hollinger *et al.*, 2015, Ballmann *et al.*, 2015a, Ballman *et al.*, 2015b, Selsby *et al.*, 2015). From these limited studies, it appears that increasing the mitochondrial pool/density/capacity for ATP production is critical to improving the dystrophic condition, and further investigation of these compounds in DMD patients is clearly warranted. Other metabogenic therapeutic options, including creatine, Idebenone and allopurinol, have been more extensively investigated in both animal models and human patients and the findings are discussed below.

1.7.1 Creatine supplementation

Given that the Cr/PCr system is an important buffering system that maintains ATP levels during metabolic stress, Cr supplementation has been investigated to elucidate its capacity to improve metabolic stress in dystrophic muscle. In healthy

and exercised skeletal muscle, Cr supplementation has been shown to increase the total Cr pool (and PCr levels), increase lean tissue content and increase strength (Kreider *et al.*, 1998, Volek *et al.*, 1999, Cribb *et al.*, 2007a, Cribb *et al.*, 2007b, Cooke *et al.*, 2009). Similar positive benefits have been observed in clinical trials with DMD patients, in animal models of DMD and in dystrophin-deficient cell culture. In a 9 year old DMD boy, oral Cr supplementation reduced the abnormally high P_i/PCr and ATP/PCr ratios (Felber *et al.*, 2000) that had been described in the literature previously (Griffiths *et al.*, 1985, Younkin *et al.*, 1987) and observed in the patient prior to supplementation. In addition, increased muscle strength, decreased falls and participation in 50m walks and stair climbs was observed (Felber *et al.*, 2000). Of interest, cessation of Cr supplementation decreased the subjects' performance, but the benefits were regained when supplementation recommenced (Felber *et al.*, 2000). This indicates that metabolic support via replenishing the Cr pool is beneficial to dystrophic muscle.

In *mdx* mice, Cr supplementation demonstrably increases PCr levels (Pulido *et al.*, 1998), reduces cytosolic $[Ca^{2+}]$ fluctuations (Pulido *et al.*, 1998), stimulates myotube hypertrophy (Pulido *et al.*, 1998), decreases muscle necrosis and improves mitochondrial respiration (Passaquin *et al.*, 2002) and muscle architecture (Louis *et al.*, 2004). These improvements were observed predominantly in fast-twitch *mdx* muscle fibres (Louis *et al.*, 2004, Passaquin *et al.*, 2002) (which are generally affected first by the dystrophinopathy (Webster *et al.*, 1988)) and attributed to increased activity of the sarcoplasmic reticulum Ca^{2+} -ATPase and the mitochondrial adenine nucleotide translocator (Passaquin *et al.*, 2002, Pulido *et al.*, 1998). Additionally, increased strength (Tarnopolsky and Martin, 1999, Tarnopolsky *et al.*, 2004), fat-free mass (Tarnopolsky *et al.*, 2004) and increased PCr/P_i ratio, PCr and

ATP peaks (³¹P MRS) (Banerjee *et al.*, 2010) have been observed following Cr supplementation in DMD patients. Together, these results support the theory that the inability of mitochondria to sufficiently respond to metabolic challenge is a key contributor to the demise of dystrophic skeletal muscle, but that metabolic support can improve the condition.

1.7.2 Allopurinol

In an effort to limit the loss of adenine nucleotides from skeletal muscle as hypoxanthine, allopurinol treatment has been extensively investigated. Allopurinol works via its metabolite oxipurinol which inhibits the activity of xanthine oxidase in vascular endothelium (Hellsten-Westling, 1993). This moderates the conversion of purines to uric acid to maintain relatively high plasma hypoxanthine concentrations relative to the muscle, thereby theoretically reducing the flux of purines from skeletal muscle. This would afford beneficial effects to dystrophic skeletal muscle by reducing the need for purine repletion via *de novo* synthesis and promoting the re-circulation of hypoxanthine into ATP-synthesising pathways (Thomson and Smith, 1978). As there is increased uric acid excretion (and therefore a need for purine salvage) and a requirement for energy support in DMD patients, supplementation with allopurinol poses major benefits.

During a 6-12 week trial of 100 mg allopurinol in 16 DMD boys, significant improvements in manual function was observed which was maintained for a subsequent 6 months (Thomson and Smith, 1978a). Biochemical studies have demonstrated similar benefits – following body weight-corrected supplementation of DMD patients, improvement in levels of metabolites that can stimulate ATP resynthesis was observed (Castro-Gago *et al.*, 1987). Improvements in the

concentrations of ATP (Thomson and Smith, 1978a, Camiña *et al.*, 1995), ADP, GTP, guanosine diphosphate, IMP, adenylosuccinate, adenine, hypoxanthine and guanine has also been noted following a trial using age-matched patients (Camiña *et al.*, 1995). This improvement in energy potential was partnered with an increase in the charge of dystrophic mitochondria from 51% in the placebo group to 83% in allopurinol-treated patients respectively (Camiña *et al.*, 1995). This data suggests that the capacity for ATP production is significantly improved by inhibiting purine catabolism.

In the quadriceps, biceps and adductor muscles, allopurinol treatment of $10\text{mg}\cdot\text{kg}^{-1}\cdot\text{day}^{-1}$ showed either stabilisation or improvement in strength of DMD patients in the earliest phases of the disease (de Bruyn *et al.*, 1980). As expected, decreased uric acid excretion was observed even in the later stages of the disease. However, Kulakowski *et al.* (Kulakowski *et al.*, 1981) and Tamari *et al.* (Tamari *et al.*, 1982) only noted functional and biochemical improvement in some patients (generally in the earlier stage of the disease) following 6 months of therapy (Kulakowski *et al.*, 1981, Tamari *et al.*, 1982), highlighting that allopurinol treatment might not afford the widespread benefit that was originally touted.

Numerous researchers have subsequently failed to replicate the beneficial effects of allopurinol described in previous experiments as an effective treatment for DMD. One of the first to reject the findings of Thomson and Smith (Thomson and Smith, 1978a) was Bakouche *et al.* (Bakouche *et al.*, 1979) who gave a variety of muscular dystrophy patients (including DMD) 100 mg of allopurinol daily for a month and 300 mg daily for a subsequent two months and observed no overall improvement (Bakouche *et al.*, 1979). It should be noted, however, that the age of patients utilized in this study was in excess of 20 years, which is a significantly older

cohort compared to any other study that had previously investigated allopurinol. Given the progressive nature of DMD and the relative lifespan of sufferers, it is unlikely that this treatment would be beneficial at this stage of disease progression.

However, in ambulatory dystrophic males from 6 to 12 years of age, no significant improvement in functional muscle tests or serum CK was observed following supplementation with 100 mg allopurinol daily for one year either (Mendell and Wiechers, 1979). To increase sample size, all 6 patients received allopurinol for a further 8 weeks to no avail, therefore the authors concluded allopurinol to have no therapeutic effect (Mendell and Wiechers, 1979). Similarly, following 8 months of daily doses of 150 mg allopurinol in DMD boys aged 5 to 13, no clinical improvement but rather a deterioration was observed in functional and strength tests (Doriguzzi *et al.*, 1981). Comparable findings were observed following x2-three month trials of 100 mg allopurinol daily (Hunter *et al.*, 1983).

In another trial that supplemented allopurinol based on weight (no dose exceeding 150 mg daily) for 12 months, no clinical improvement in muscle and pulmonary function tests and serum CK and PK levels were observed by the authors despite a decrease in blood uric acid levels (Stern *et al.*, 1981). Furthermore, following daily 200-300 mg doses of allopurinol for 6 weeks (Griffiths *et al.*, 1985) and 300 mg daily for 18 months (Bertorini *et al.*, 1985), no improvement in phosphate metabolites (including ATP levels), functional measurements and strength were observed again despite decreased excretion of uric acid. Overall, these studies report comparable findings using similar assessment techniques and were reported in quick succession indicating that allopurinol therapy may not be a useful adjunct therapy for the treatment of DMD.

The majority of studies that have deemed allopurinol therapy to be ineffective for DMD treatment noted a deterioration of muscle function during and following the supplementation period (Stern *et al.*, 1981, Doriguzzi *et al.*, 1981, Hunter *et al.*, 1983, Bertorini *et al.*, 1985, Griffiths *et al.*, 1985). This may be reflective of the age of participants in these trials and to the extent of disease progression at commencement of the trial, with the baseline measurements of these studies indicating that younger patients were able to perform better on functional tests and generally saw some sort of improvement. It is well-known that as DMD progresses, muscle wastage intensifies with the culmination of fibrotic, non-functional muscle tissue and concomitant strength decline (Ziter *et al.*, 1977). Therefore, the inclusion of DMD patients of older age and who are non-ambulatory (or thereabouts) limits the potential of such metabolic therapies as there is a significant reduction in treatable muscle mass. This may explain the conflicting findings and highlights the need for clinical trials to implement early intervention strategies when considering metabolically-targeted therapies and their ability to maintain long term efficacy.

While preventing the degradation and loss of hypoxanthine from dystrophic muscle may not be possible, potentially due to the inability of hypoxanthine to be re-taken up into skeletal muscle, targeting the PNC further up the metabolic milieu could be of therapeutic benefit. A seminal study that illustrates the critical role of ATP depletion in dystrophinopathy comprised of a 10 year clinical trial of ASA treatment which maintained muscle function and strength in DMD patients (Bonsett and Rudman, 1992). This study importantly highlights the necessity for further investigation into the ways in which metabolic capacity can be enhanced to improve the phenotypic progression of DMD and the quality of life of patients.

1.7.3 Idebenone

As discussed in section 1.3.4.1, there appears to be a significant dysfunction/impairment at the level of complex I of the ETC which results in reduced oxidation of complex I substrates and mitochondrial ATP production capacity (Olson *et al.*, 1968, Martens *et al.*, 1980, Glesby *et al.*, 1988, Bhattacharya *et al.*, 1993, Kuznetsov *et al.*, 1998, Faist *et al.*, 2001, Rybalka *et al.*, 2014). This, however, can be partially attenuated through the inhibition of complex I and channelling of complex II substrates into the ETC (Ionăşescu *et al.*, 1967, Martens *et al.*, 1980, Nylen and Wrogemann, 1983, Glesby *et al.*, 1988, Bhattacharya *et al.*, 1993, Chinet *et al.*, 1994, Kuznetsov *et al.*, 1998, Giorgio *et al.*, 2012, Rybalka *et al.*, 2014) indicating a potential site for therapeutic intervention to stimulate ATP production in dystrophic muscle.

Idebenone is a synthetic analogue of coenzyme Q10 (CoQ10) that has antioxidant properties and can modulate mitochondrial ATP production (as reviewed in (Gueven *et al.*, 2015)). Idebenone is an inhibitor of complex I (Sugiyama and Fujita, 1985, Degli Esposti *et al.*, 1996, Brière *et al.*, 2004), therefore eliciting its effect on respiration in a complex I-independent manner and promoting complex II and III respiration (Degli Esposti *et al.*, 1996). This feature of Idebenone would be particularly beneficial in dystrophic muscle considering the overt complex I dysfunction. Additionally, Idebenone is reduced by NADH-quinone oxidoreductase I, a cytoplasmic enzyme that is involved in the detoxification of quinones to prevent ROS production (Haefeli *et al.*, 2011, Giorgio *et al.*, 2012). The reduction of Idebenone results in an active form which enters the mitochondria and is re-oxidised by complex III thereby stimulating complex III activity which can improve ATP

production and the $\Delta\Psi$ in the presence of a dysfunctional complex I (Erb *et al.*, 2012, Haefeli *et al.*, 2011, Giorgio *et al.*, 2012). These characteristics of Idebenone highlight it as a strong therapeutic candidate for DMD.

Overall, literature regarding Idebenone and DMD is limited. This is perhaps due to the commercialisation endeavour by Santhera Pharmaceuticals, which has seen the recent approval of Idebenone (Raxone®) as the first indication specific treatment for DMD by the European Medical Association (EMA). Long term administration of Idebenone in the *mdx* mouse (4 weeks to 10 months of age, 200mg/kg) improved cardiac function, decreased cardiac inflammation and fibrosis and increased voluntary running capacity (Buyse *et al.*, 2008). From these preclinical findings, a phase IIa double-blind randomised clinical trial was conducted in DMD patients to investigate the tolerability and efficacy of Idebenone on cardiac and respiratory function (Buyse *et al.*, 2011). Daily supplementation of Idebenone (450mg) in DMD boys aged 8-16 resulted in significant respiratory function improvements and trends for improved cardiac function compared to the placebo group. These clinical findings led to a phase III double-masked, randomised, multicentre clinical trial which investigated the capacity of Idebenone to delay respiratory decline in DMD patients (Buyse *et al.*, 2015). In these 31 DMD boys, who were not receiving glucocorticoids, daily administration of Idebenone (900mg) for 12 months mitigated the fall in peak expiratory flow indicating a delay in disease progression. Considering that Idebenone – a mitochondrial-targeted drug that demonstrably attenuates a key clinical marker of disease progression – is the only approved, indication specific treatment for DMD in Europe, and is currently being evaluated by the Food and Drug Administration (F.D.A) in the U.S., highlights the value of metabogenic therapies as future treatments for DMD.

1.7.4 New metabogenic therapies for the treatment of DMD

Considering the vast metabolic impairments in dystrophin-deficient muscle, and the necessity for adequate ATP production to buffer Ca^{2+} , prevent damage and facilitate regeneration, metabolically targeted therapies are pertinent to improving the dystrophic condition and potentially patient quality of life. Stimulating various metabolic pathways and/or metabolic checkpoints to support mitochondrial function appears to be crucial to improving the dystrophic condition. Despite the vast improvements observed following treatment with various metabolic therapies, there is a need to investigate other candidates which may afford greater therapeutic benefit. Two potential candidate therapies are: (1) NO therapy and (2) ASA therapy.

1.7.4.1 The dystrophin-metabolism connection – nNOS

An increasingly popular therapeutic target for the treatment of DMD is the nNOS-NO deficiency. nNOS is an enzyme usually localised to the sarcolemma attached to the DPC, however in the absence of dystrophin, there is a secondary reduction of nNOS (Brenman *et al.*, 1995, Chang *et al.*, 1996). The loss of nNOS from the sarcolemma reduces overall nNOS content in dystrophic muscle (Leary *et al.*, 1998, Thomas *et al.*, 1998, Vaghy *et al.*, 1998, Judge *et al.*, 2006) resulting in decreased nNOS activity (Leary *et al.*, 1998, Thomas *et al.*, 1998, Vaghy *et al.*, 1998, Judge *et al.*, 2006) and NO production (Gücüyener *et al.*, 2000, Kasai *et al.*, 2004, Barton *et al.*, 2005). The loss of nNOS protein and subsequently NO production capacity and bioavailability, is detrimental to dystrophic muscle for two reasons. Firstly, NO is an important signalling molecule involved in many biological processes including metabolism, blood flow and regulation of muscle function and

mass (McConell *et al.*, 2012). Secondly, the nNOS protein itself interacts with PFK, a regulatory enzyme of glycolysis, and is capable of increasing its activity by 60-fold (Wehling-Henricks *et al.*, 2009) thereby increasing glycolytic rate and capacity. The loss of association between nNOS and PFK in dystrophin-deficient muscle may help to explain the fatigability of dystrophic muscle (Frascarelli *et al.*, 1988, Wineinger *et al.*, 1998) and may partially or fully account for the various glycolytic impairments observed (Vignos Jr and Lefkowitz, 1959, Chi *et al.*, 1987, Wehling-Henricks *et al.*, 2009). As it appears that NO plays an important role in metabolism and the maintenance of skeletal muscle mass, restoring NO bioavailability in dystrophin-deficient muscle may be beneficial (summarised in Table 1.2).

NO is an important signalling molecule that elicits a myriad of physiological effects through the production of cyclic guanosine monophosphate (cGMP) and/or S-nitrosylation of thiol residues of cysteine groups. cGMP is a second messenger produced by the binding of NO to the enzymatic receptor soluble guanylyl cyclase (sGC) (Buglioni and Burnett Jr, 2015). The increase in cytoplasmic cGMP activates downstream cGMP specific protein kinases, cation channels and phosphodiesterases (PDE) which then exert various biological effects (Buglioni and Burnett Jr, 2015). NO also mediates its effects through S-nitrosylation, a post-translational modification of proteins that modulates enzyme activity, protein stability and localisation (Treuer and Gonzalez, 2015). Since the secondary dissociation of nNOS from the sarcolemma in dystrophic skeletal muscle reduces NO bioavailability, which would impair a multitude of physiological processes that may contribute to disease progression, various techniques to increase NO production have been investigated.

1.7.4.1.1 Increasing NO bioavailability

Considering that nNOS delocalisation from the sarcolemma does not completely obliterate the nNOS protein in dystrophic skeletal muscle (Chang *et al.*, 1996), substrate availability, in the form of L-arginine, may be a limiting factor to nNOS-dependent NO production (Figure 1.9). L-arginine administration in the *mdx* mouse demonstrably improves sarcolemmal integrity as indicated by increased utrophin (Chaubourt *et al.*, 1999, Voisin *et al.*, 2005, Barton *et al.*, 2005, Hnia *et al.*, 2008, Vianello *et al.*, 2013, Vianello *et al.*, 2014) and DPC protein expression (Voisin *et al.*, 2005, Barton *et al.*, 2005, Hnia *et al.*, 2008, Vianello *et al.*, 2013, Vianello *et al.*, 2014), reduced Evans Blue Dye (EBD) uptake – a marker of skeletal muscle membrane damage – (Barton *et al.*, 2005, Archer *et al.*, 2006, Vianello *et al.*, 2013, Vianello *et al.*, 2014) and decreased serum CK levels – a clinical marker of muscle damage and disease progression (Voisin *et al.*, 2005, Vianello *et al.*, 2013, Vianello *et al.*, 2014). In DMD patients, the combination of L-arginine and the pharmacological AMPK-activator, metformin, decreased resting energy expenditure, shifted energy metabolism substrate preference to fatty acids, reduced oxidative stress and improved motor function (Hafner *et al.*, 2015). NO is a known activator of AMPK, highlighting that promoting both the production of NO (i.e. with L-arginine) and the downstream metabolic responses that are normally modulated by NO (i.e. with metformin) can improve the metabolism and function of dystrophic skeletal muscle. Histologically, L-arginine was also shown to improve many of the characteristic myopathological hallmarks in *mdx* mice (a genetically homologous murine model of DMD) including reductions in fatty and fibrotic tissue and collagen deposition (Voisin *et al.*, 2005, Hnia *et al.*, 2008, Guerron *et al.*, 2010, Vianello *et al.*, 2013),

inflammatory cell infiltration (Hnia *et al.*, 2008) and necrosis (Barton *et al.*, 2005, Voisin *et al.*, 2005, Vianello *et al.*, 2013). Functional improvements in grip strength (Vianello *et al.*, 2013, Vianello *et al.*, 2014), less decrement in strength with age (Guerron *et al.*, 2010), and improved respiratory function (Voisin *et al.*, 2005, Vianello *et al.*, 2013) were also observed. In addition to these functional improvements, L-arginine reduced dystrophic muscle fatigability (Vianello *et al.*, 2014) and improved contractile function (Voisin *et al.*, 2005, Vianello *et al.*, 2013) which resulted in an increased capacity to exercise (Archer *et al.*, 2006). Whilst L-arginine administration appears to be beneficial both in the *mdx* mouse and DMD patients, the significantly reduced nNOS content evident in DMD patients suggests that there is a limited therapeutic application for L-arginine unless concomitant increases in nNOS expression could be achieved. This is especially true since L-arginine administration alone, especially in high doses, can have adverse side effects (Böger and Bode-Böger, 2001). Indeed, a recent paper describing metabolic biomarkers of DMD demonstrates significantly elevated serum arginine concentrations in DMD patients as the disease progresses, highlighting the possibility of an ineffective uptake and metabolism via nNOS at the skeletal muscle level (Boca *et al.*, 2016).

1.7.4.1.2 Restoring nNOS protein expression

Restoring nNOS levels in dystrophic skeletal muscle has proven to be beneficial (Table 1.2). Transgenic nNOS overexpressors bred with the *mdx* mouse significantly mitigates membrane damage as reflected by a reduction in inflammation, macrophage and neutrophil infiltration, centronucleation of fibres and membrane lesions (Wehling *et al.*, 2001, Nguyen and Tidball, 2003). Introduction of

this nNOS transgene also extends protective effects to the dystrophic heart by reducing fibrosis and macrophage infiltration in conjunction with improving impulse conduction (Wehling-Henricks *et al.*, 2005); and to the neuromuscular junction through improvements in neuromuscular junction size and architecture in the presence of α -syntrophin (Shiao *et al.*, 2004). Remarkably, nNOS restoration in dystrophin/utrophin knockout mice (which phenotypically resemble DMD) increased survival rate while reducing macrophage infiltration and the fibrotic and connective tissue content of skeletal muscle (Wehling-Henricks and Tidball, 2011). Therefore, increased expression of nNOS has a protective effect on maintaining muscle architecture and preventing membrane lysis through the normalised NO production (Tidball and Wehling-Henricks, 2004). Moreover, transfection with a modified muscle specific nNOS μ isoform resulted in increased expression of utrophin and other DPC proteins (including α -syntrophin and β -dystroglycan) which induced localised NO production at the sarcolemma and protect against contraction-induced damage and fatigue (Rebolledo *et al.*, 2015). The upregulation of utrophin seems to protect dystrophic *mdx* muscle from progressive damage as utrophin expression increases as *mdx* mice age (Pons *et al.*, 1994) – this likely explains how the use of this skeletal muscle-specific nNOS without increased dystrophin expression, improved the dystrophic phenotype. Additionally, insertion of a mini-dystrophin gene via a dual adeno-associated viral vector which increases mini-dystrophin expression and restores nNOS at the sarcolemma (Zhang and Duan, 2011), improved contraction-induced ischemia and mitigated the loss of force production and muscle damage (Lai *et al.*, 2009, Zhang *et al.*, 2013). Therefore, increased presence of the nNOS protein, irrespective of localisation within the cell, can improve various characteristics of the dystrophic condition. However, there may be limited long-term therapeutic potential

for nNOS overexpression as a delocalised nNOS (from the sarcolemmal DPC) becomes a substrate of calpains (Laine and de Montellano, 1998). As calpains are enzymes that stimulate protein damage, and are particularly active in DMD pathology, increased calpain activity may significantly reduce unbound nNOS expression. This indicates that there is a necessity for dual upregulation of nNOS and dystrophin to minimise unbound nNOS as a target for calpains which would promote the disease phenotype.

1.7.4.1.3 Inhibition of phosphodiesterase activity

Given that enhancing NO production capacity is beneficial in dystrophic muscle yet there are complexities associated with re-insertion/establishment of dystrophin and nNOS expression, other mechanisms to increase NO bioavailability have been investigated. One such avenue is the inhibition of the PDE family which breakdown phosphodiester bonds in second messenger molecules. Specific PDEs hydrolyse cGMP thereby degrading it and decreasing cGMP second messenger capacity. Since NO activates cGMP cycling, and its production and bioavailability is reduced in dystrophic muscle, pharmacologically prolonging/amplifying the cGMP signal would have likely benefits in NO-deficient cells (Figure 1.9).

Inhibition of PDE5A has been commonly investigated in the *mdx* mouse as PDE5A is present not only in vascular smooth muscle (Wallis *et al.*, 1999), but also skeletal muscle (Bloom, 2002) and to a lesser extent cardiac muscle (Senzaki *et al.*, 2001), thereby allowing for a systemic effect of a prolonged NO signal. Treatment with Tadalafil, a pharmacological PDE5 inhibitor, was shown to be beneficial in overcoming functional ischaemia following contraction and was partnered with reduced contraction-induced sarcolemmal damage and muscle fibre death (Asai *et*

al., 2007). Tadalafil treated *mdx* muscles also demonstrated histological improvements with a decrease in EBD uptake, fibrotic infiltration, centronucleated fibres and fibre size variability (Asai *et al.*, 2007, De Arcangelis *et al.*, 2016) suggesting less damage and prevention of muscle degeneration. Additionally, exercise-induced damage was minimised in Tadalafil treated mice as evidenced by reduced Ca^{2+} accumulation (De Arcangelis *et al.*, 2016). Functionally, time to exhaustion from treadmill running and EDL strength were concomitantly improved following Tadalafil treatment (De Arcangelis *et al.*, 2016) in addition to an increase in post-exercise activity (Kobayashi *et al.*, 2008). PGC-1 α expression was also increased following Tadalafil treatment alongside an enhanced expression of various ETC genes suggestive of a fibre type shift to an oxidative phenotype (De Arcangelis *et al.*, 2016). Considering the vast mitochondrial and oxidative metabolism deficiencies observed in dystrophic muscle (Timpani *et al.*, 2015), upregulation of mitochondrial and oxidative genes would likely be beneficial to dystrophic muscle.

Similar results have been observed with the alternative PDE5A inhibitor, Sildenafil. In *mdx* mice, Sildenafil demonstrably increased specific force, reduced collagen I, fibronectin and TNF α infiltration, and improved sarcolemmal integrity of the diaphragm (Percival *et al.*, 2012). However, these improvements did not result in changes to mitochondrial function nor improvements in ATP production as originally hypothesised (Percival *et al.*, 2013). In the *mdx* heart, Sildenafil appears to induce protective effects by reducing membrane permeability and altering the expression of proteins implicated in beneficial cardiac remodelling (Khairallah *et al.*, 2008). Functionally, Sildenafil normalises heart rate responses to increasing workload (Khairallah *et al.*, 2008) and reverses ventricular dysfunction (Adamo *et al.*, 2010).

Together, these studies suggest that amplification of the typically NO-dependent cGMP signal through PDE inhibition benefits both skeletal and cardiac function and mitigates various characteristics of the dystrophic condition in the *mdx* mouse. Recently, however, a Phase 3 clinical trial of Tadalafil in DMD boys was prematurely stopped following the absence of improvements in skeletal muscle function and adverse changes to left ventricle volumes. This indicates that the specific targeting of PDE receptors is not a translatable therapeutic avenue in human DMD patients. While the inhibition of PDE5 is seemingly protective against dystrophin-deficiency-induced damage in mouse models of DMD, it has recently been demonstrated that BMD patients, who express a truncated version of dystrophin, are also deficient in PDE5 (Witting *et al.*, 2014). This deficiency suggests that as per nNOS, the expression of PDE receptors is intimately linked with dystrophin and/or DPC expression. As such, no improvements in cardiac function, blood flow to the skeletal muscle during exercise, or quality of life were observed in BMD patients (Witting *et al.*, 2014). Given the totality of this evidence, the capacity to exploit PDE's pharmacotherapeutically is therefore limited.

1.7.4.1.4 NO donors

Since L-arginine and PDE activation are both dependent upon the presence of key enzymes/proteins associated with the sarcolemma, and more specifically, the DPC, promoting NO production through the use of NO donors may be of greater benefit to bypass this defective/inefficient protein system. As there is limited nNOS present in dystrophin-deficient skeletal muscle, this significantly impairs the capacity for NO production in the muscle. Therefore, even with PDE inhibition, the availability of NO would still be significantly diminished. Thus, the use of NO donors is an

attractive therapeutic treatment option as they have the capacity to markedly increase systemic NO availability beyond the capacity to endogenously produce it within dystrophic muscle (Figure 1.9).

Indeed, 6 months delivery of a nitric ester derivative of sedative alkyl alcohol (administered at 40mg/kg 5 days/week) has been shown to enhance the vascular density of skeletal muscle, as well as exercise performance and strength in *mdx* mice, with a marked decrease in the free intracellular Ca^{2+} concentration of skeletal muscle (Wang and Lu, 2013). In addition, the NO-donating nitric ester increased muscle fibre size while concomitantly reducing the population of regenerating fibres, suggestive of decreased damage (Wang and Lu, 2013). Similarly, 7 months of 30mg/kg naproxcinod, a non-steroidal anti-inflammatory drug (NSAID) with NO-donating properties, in food, had a beneficial effect on the running capacity of *mdx* mice with both time to exhaustion and whole body strength improved (Miglietta *et al.*, 2015). These functional improvements were partnered with better muscle architecture displaying decreased inflammation, fibrosis and collagen infiltrate in both skeletal and cardiac muscle (Miglietta *et al.*, 2015). Longer term administration of naproxcinod (at 21mg/kg/day in food for 9 months) induced similar improvements in the strength and histological properties of cardiac muscle leading to the functional normalisation of ejection fraction time, and systolic blood pressure (Uaesoontrachoon *et al.*, 2014). Considering the anti-inflammatory effects of the aforementioned NO-donors, combining a NO donor with NSAIDs could enhance the beneficial effects of NO. Three months of a HCT 1026-enriched diet (NO donor derived from flurbiprofen; 45mg/kg/day) significantly improved blood flow and alleviated functional ischaemia in *mdx* mice (Thomas *et al.*, 2012). A longer term supplementation regimen of the same drug (30 mg/kg/day in food for 12 months)

was shown to reduce muscular damage, with a concomitant decrease in serum CK levels and improved mobility of *mdx* mice (Brunelli *et al.*, 2007). Moreover, the addition of isosorbide dinitrate (30mg/kg/day) with ibuprofen (50 mg/kg/day) has been shown to induce significant protection of the dystrophic heart by normalising left ventricle mass and wall thickness, maintaining cardiomyocyte number and reducing cross sectional area, decreasing fibrotic tissue content and inflammatory cell infiltration and improving overall cardiac function in the *mdx* mouse (Sciorati *et al.*, 2013). Isosorbide dinitrate alone (66mg/kg), or in combination with prednisone (1mg/kg) for 18 days, also demonstrably improves sarcolemmal integrity, decreases the presence of calcified fibres and stimulates regeneration in the *mdx* diaphragm, however without the addition of ibuprofen, it promoted an increase in heart weight (Mizunoya *et al.*, 2011) which was not observed previously (Sciorati *et al.*, 2013). An increase in cardiac mass, without improvements in cardiac function, is considered an adverse effect of treatment which would promote the normal, progressive cardiac hypertrophy observed in DMD patients. Ibuprofen seems to abate this adverse effect since a safety study in DMD patients using 12 months of isosorbide dinitrate (40mg/day) and ibuprofen (400mg/day) maintained cardiac function and reduced systemic inflammatory markers (D'Angelo *et al.*, 2012). Given there is the capacity for non-specific, systemic NO-donors to adversely affect cardiac tissue, the use of skeletal muscle targeted NO donation would be beneficial. Indeed, oral administration of MyoNovin (80mg/kg) – a NO donor that specifically donates NO to skeletal muscle – for 18 days induces similar effects to isosorbide dinitrate in *mdx* mice without the adversity of cardiac hypertrophy induction (Mizunoya *et al.*, 2011). Given that uncontrolled and excessive NO delivery can induce pathological effects including inflammation, mitochondrial dysfunction and myocardial damage (Pacher *et*

al., 2007), these data suggest that manipulation of the NO-donation delivery system may be pivotal to mitigating the unwanted side effects of NO donor therapy.

1.7.4.1.5 Could nitrate therapy be beneficial?

Recently, it has emerged that dietary supplementation with nitrate increases endogenous NO production via a nNOS-independent pathway (Figure 1.9). Nitrate is an inorganic anion that is abundant in green leafy vegetables including beetroot, lettuce and spinach (Gangolli *et al.*, 1994) and also in carrot, beetroot and pomegranate juices (Hord *et al.*, 2009). The nitrate anion is inert but once ingested, nitrate is reduced by the commensal bacteria in the enterosalivary pathway (Doel *et al.*, 2005) into the bioactive nitrite, which then circulates in the blood. Although bioactive, nitrite is further converted to NO via several enzymatic pathways in the blood and tissues, including xanthine oxidase, myoglobin and haemoglobin (Kim-Shapiro and Gladwin, 2014), to exert a range of physiological effects. Thus, this pathway is complementary to nNOS-derived NO production. Additionally, there is benefit to this nitrate-nitrite-NO pathway as it is reversible (Lundberg *et al.*, 2015). NO can be oxidised back to nitrate by myoglobin and haemoglobin and therefore the capacity to cycle back to nitrate allows for a constant reservoir of NO (Affourtit *et al.*, 2015). Moreover, since chronic increases in NO bioavailability can be toxic and induce systemic pathology (Pacher *et al.*, 2007), having an inactive reservoir of buffered NO would be beneficial. Therefore, enhancing the nitrate-nitrite-NO pathway represents a potential pathway that could be exploited to significantly enhance NO availability in dystrophic muscle in a controlled and buffered manner.

Recent studies suggest that nitrate supplementation enhances health and skeletal muscle performance. A 3 day oral supplementation of sodium nitrate

(0.1mmol/kg/day) in healthy males revealed that nitrate significantly improved skeletal muscle mitochondrial bioenergetics by increasing mitochondrial efficiency and decreasing proton leak; and reduced whole body oxygen consumption following submaximal exercise (Larsen *et al.*, 2011). Moreover, a 7 day supplementation regimen in drinking water of healthy mice (~3.75µmol/day) significantly improved skeletal muscle contractility, particularly of the EDL, by increasing expression of Ca²⁺ handling proteins and free myoplasmic Ca²⁺ during contraction (Hernández *et al.*, 2012). Similar improvements in contractile function have also been observed in humans following acute supplementation with nitrate-rich beetroot juice (0.6g/300 ml), with the authors noting improved excitation-contraction coupling (at low frequencies) and increased explosive force production in quadriceps (Haider and Folland, 2014). Acute beetroot supplementation also demonstrably reduced whole body oxygen consumption (Lansley *et al.*, 2011b, Cermak *et al.*, 2012b, Bond Jr *et al.*, 2013, Whitfield *et al.*, 2016), promoted fatigue resistance (Bailey *et al.*, 2009, Bond *et al.*, 2012, Hoon *et al.*, 2015, Aucouturier *et al.*, 2015) and improved performance times (Bond *et al.*, 2012, Cermak *et al.*, 2012a, Lansley *et al.*, 2011a). Similar data has been observed using dietary sodium nitrate supplementation. Eighteen days of sodium nitrate administered in drinking water (0.7mM), was shown to stimulate mitochondrial biogenesis (peroxisome proliferator-activated receptor β/δ and PGC-1 α expression) which enhanced fatty acid oxidation, indicating that acute exposure to nitrate supplementation has a modulatory effect on bioenergetics (Ashmore *et al.*, 2015).

The benefits of nitrate supplementation also extend to disease states. In chronic obstructive pulmonary disease patients, acute beetroot juice supplementation improved exercise capacity and decreased blood pressure (Berry *et*

al., 2015, Kerley *et al.*, 2015). Similar findings – in addition to increased tissue oxygenation – were observed in peripheral artery disease patients (Kenjale *et al.*, 2011). Considering that dystrophic muscle is in a comparable metabolically-stressed state to exercising muscle in that there is an increased metabolic demand and sarcoplasmic $[Ca^{2+}]$, and that nitrate supplementation can elicit positive physiological responses in diseased tissue, investigating such a therapy for DMD is essential. Moreover, the positive effects elicited through increased NO bioavailability in dystrophin-deficient skeletal muscle highlights the potential for NO donation through nitrate supplementation as a viable therapeutic option.

1.7.4.2 ASA supplementation

As detailed in section 1.3.6, the PNC is an important metabolic pathway that assists in the maintenance of the adenine nucleotide pool to ensure ATP production can match ATP demand at all times. In addition, the PNC plays a supportive role for oxidative metabolism as it anaplerotically expands the TCA cycle through the production of fumarate (Figure 1.10). In dystrophic muscle, the compromised metabolic capacity suggests that exploitation of this pathway may result in maintenance of the adenine nucleotide pool which could minimise metabolic stress and support mitochondrial ATP production.

A seminal study that illustrates the critical role of ATP depletion in dystrophinopathy comprised a 10 year clinical trial of ASA treatment in both DMD and BMD patients (Bonsett and Rudman, 1992). ASA stimulates the PNC producing fumarate to fuel TCA cycling and adenine nucleotides that can increase ADP re-synthesis and availability to mitochondrial ATP production. Significant improvements were observed in a patient with BMD, a milder form of DMD in which there is

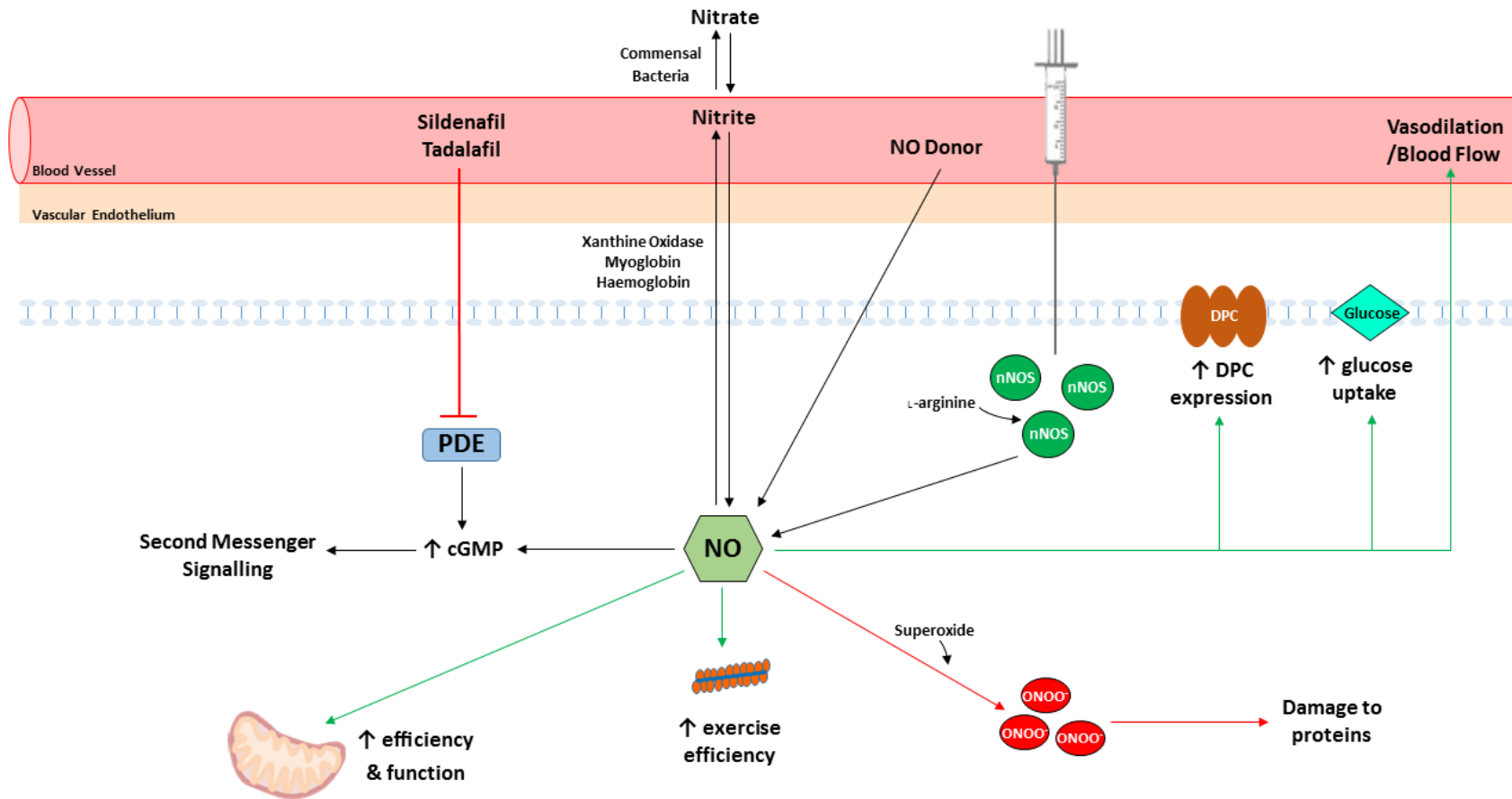


Figure 1.9. Schematic of methods utilised to increase NO bioavailability in dystrophic skeletal muscle and the downstream effects. Increasing NO bioavailability through restoration of nNOS, NO donation and inhibition of PDE has led to increases in mitochondrial function, exercise capacity stabilisation of the membrane. A potential consequence of increased NO bioavailability is peroxynitrite (ONOO⁻) formation which can lead to damage.

Table 1.2. Summary of methods utilised to increase NO production dystrophic muscle.

Method/Mechanism	Dosage Range	Model	Effects	Other	Reference
<p>nNOS restoration</p> <p>Breeding with transgenic nNOS overexpressors</p> <p>Transfection with nNOS</p>	N/A	<p><i>mdx</i> mouse</p> <p>Dystrophin/utrophin knockout mouse</p> <p><i>mdx</i> mouse</p>	<p>Skeletal muscle: reduces inflammation, macrophage and neutrophil infiltration, damage</p> <p>Cardiac muscle: reduces fibrosis, macrophage infiltration, improves impulse conduction</p> <p>Skeletal muscle: increases DPC expression, NO production, reduces damage and fatigue, prevents force production loss</p>		<p>Wehling <i>et al.</i>, 2001; Nguyen & Tidball, 2003; Shiao <i>et al.</i>, 2004; Tidball & Wehling-Henricks, 2004; Wehling-Henricks <i>et al.</i>, 2005; Lai <i>et al.</i>, 2009; Wehling-Henricks & Tidball, 2011; Zhang & Duan, 2011; Zhang <i>et al.</i>, 2013; Rebolledo <i>et al.</i>, 2015</p>
<p>L-arginine supplementation</p>	200-1000mg/kg/day	<p>DMD patients</p> <p><i>mdx</i> mouse</p>	<p>Skeletal muscle: increases DPC expression, reduces damage, fibrotic and fatty tissue infiltration, inflammatory cell infiltration, oxidative stress, improves grip strength, contractile function and reduces fatigability</p>	<p>Administered in combination with metformin and prednisone</p>	<p>Chaubourt <i>et al.</i>, 1999; Voisin <i>et al.</i>, 2005; Barton <i>et al.</i>, 2005; Archer <i>et al.</i>, 2006; Hnia <i>et al.</i>, 2008; Gueron <i>et al.</i>, 2010; Vianello <i>et al.</i>, 2013; Vianello <i>et al.</i>, 2014; Hafner <i>et al.</i>, 2015</p>

<p>PDE inhibition</p> <p>Sildenafil</p> <p>Tadalafil</p>	<p>0.7-80mg/kg/day</p> <p>30-300mg/kg/day</p>	<p>DMD patients</p> <p><i>mdx</i> mouse</p>	<p>Skeletal muscle: reduces collagen and inflammatory cell infiltration, improves sarcolemmal integrity</p> <p>Cardiac muscle: reduces membrane permeability, induces cardiac remodelling, improves heart function</p> <p>Skeletal muscle: improves functional ischaemia, reduces contraction-induced damage, fibrotic infiltration, histological variability, improves exercise performance, increases expression of ETC genes</p>		<p><i>Asai et al., 2007;</i> <i>Khairallah et al., 2008;</i> <i>Kobayashi et al., 2008;</i> <i>Adamo et al., 2010;</i> <i>Percival et al., 2012;</i> <i>Percival et al., 2013;</i> <i>Witting et al., 2014;</i> <i>De Arcangelis et al., 2016</i></p>
<p>NO donation</p>	<p>21-80mg/kg/day</p>	<p><i>mdx</i> mouse</p>	<p>Skeletal muscle: increases vascularisation, blood flow, exercise performance and strength, decreases free Ca²⁺ concentration, damage, inflammation, fibrotic and collagenous infiltration,</p> <p>Cardiac muscle: decreases damage, inflammation, fibrotic and collagenous infiltration, improves cardiac function and architecture</p>	<p>Administered in combination with NSAIDs</p>	<p><i>Brunelli et al., 2007;</i> <i>Mizunoya et al., 2011;</i> <i>D'Angelo et al., 2012;</i> <i>Thomas et al., 2012;</i> <i>Sciorati et al., 2013;</i> <i>Wang & Lu, 2013;</i> <i>Uaesoontrachoon et al., 2014;</i> <i>Miglietta et al., 2015</i></p>

reduced, yet present, dystrophin at the sarcolemma. Muscle damage and degeneration is less severe in comparison to the pathology associated with DMD however muscle weakness and impaired function is evident. Increasing daily doses of ASA ($30 \text{ mg.kg}^{-1}.\text{day}^{-1}$ to $200 \text{ mg.kg}^{-1}.\text{day}^{-1}$) reduced serum CK levels in a BMD patient who commenced supplementation from 6 years of age. Upon discontinuation of ASA, CK levels increased 70 fold within 2 weeks and the patient resumed daily ASA administration to maintain CK levels with the normal range. During this time, the BMD patient was able to participate in exercise due to increased energy levels and stamina without any muscle weakness or pain. Histologically, following 4 years of ASA treatment, a reduction in the ratio of regenerating area to necrotic area was evident in muscle biopsies obtained from the vastus lateralis of the BMD patient (Bonsett and Rudman, 1992).

Increasing dosage of daily ASA treatment ($25\text{mg.kg}^{-1}.\text{day}^{-1}$ to $600\text{mg.kg}^{-1}.\text{day}^{-1}$) induced vast improvements in a DMD patient who commenced supplementation from 2.5 years of age. Instantaneous increases in energy, endurance and stamina were observed following commencement of ASA supplementation with significant maintenance of muscle strength and function (i.e. able to stand erect, walk without falling and rise from the floor) noted over the supplementation period. In addition, ASA induced a four-fold reduction in serum CK levels indicative of reduced muscle damage, and improved the typical DMD histopathological hallmarks including the ratio of regeneration compared to necrosis (Bonsett and Rudman, 1992). Such improvements in the dystrophic condition readily subsided upon discontinuation of ASA supplementation highlighting that ongoing support of the mitochondria is pivotal to mitigating disease progression.

A prominent feature of a muscle biopsy taken from the DMD patient some 4.5 years following commencement of ASA supplementation was a lack of fatty tissue infiltration. Characteristic of dystrophic disease progression is accumulation of fatty tissue (Pearce, 1966, Harriman and Reed, 1972, Bonsett, 1979) which may be reflective of a higher propensity for dystrophic muscle to produce lipids. As mentioned in section 1.2.2., culturing of healthy and DMD human myocytes revealed that in the presence of decreasing concentrations of FBS, lipid production became negligible in healthy cultures while DMD cultures continued to produce lipid droplets irrespective of serum concentration (Bonsett, 1979). The enhanced ability to produce lipid droplets in DMD myocytes was pinpointed to a dysfunction at the level of IDH in the TCA cycle which was eliminated following the addition 1.2×10^{-6} M ASA (Bonsett and Rudman, 1984). ASA's ability to improve multiple facets of the dystrophic phenotype appears to lie in its capacity to support both the TCA cycle and the adenine nucleotide pool.

Recently, evidence has emerged in the literature that ASA has a strong modulatory role over organismal energy storage. There is the potential that increased production of this metabolite promotes energy utilisation as it has recently been identified to stimulate exocytosis of insulin from pancreatic β cells (Gooding *et al.*, 2015). Inhibition of adenylosuccinase, which limits the production of adenylosuccinate, hindered glucose-stimulated insulin secretion indicating that adenylosuccinate plays a role in energy sensing. Furthermore, infusion of adenylosuccinate into patch-clamped pancreatic β cells stimulated insulin secretion as effectively as glucose, and promoted insulin secretion in glucose-insensitive human diabetic pancreatic β cells (Gooding *et al.*, 2015). Given adenylosuccinate plays a role in energy utilisation, and dystrophic muscle is in an energy-deprived

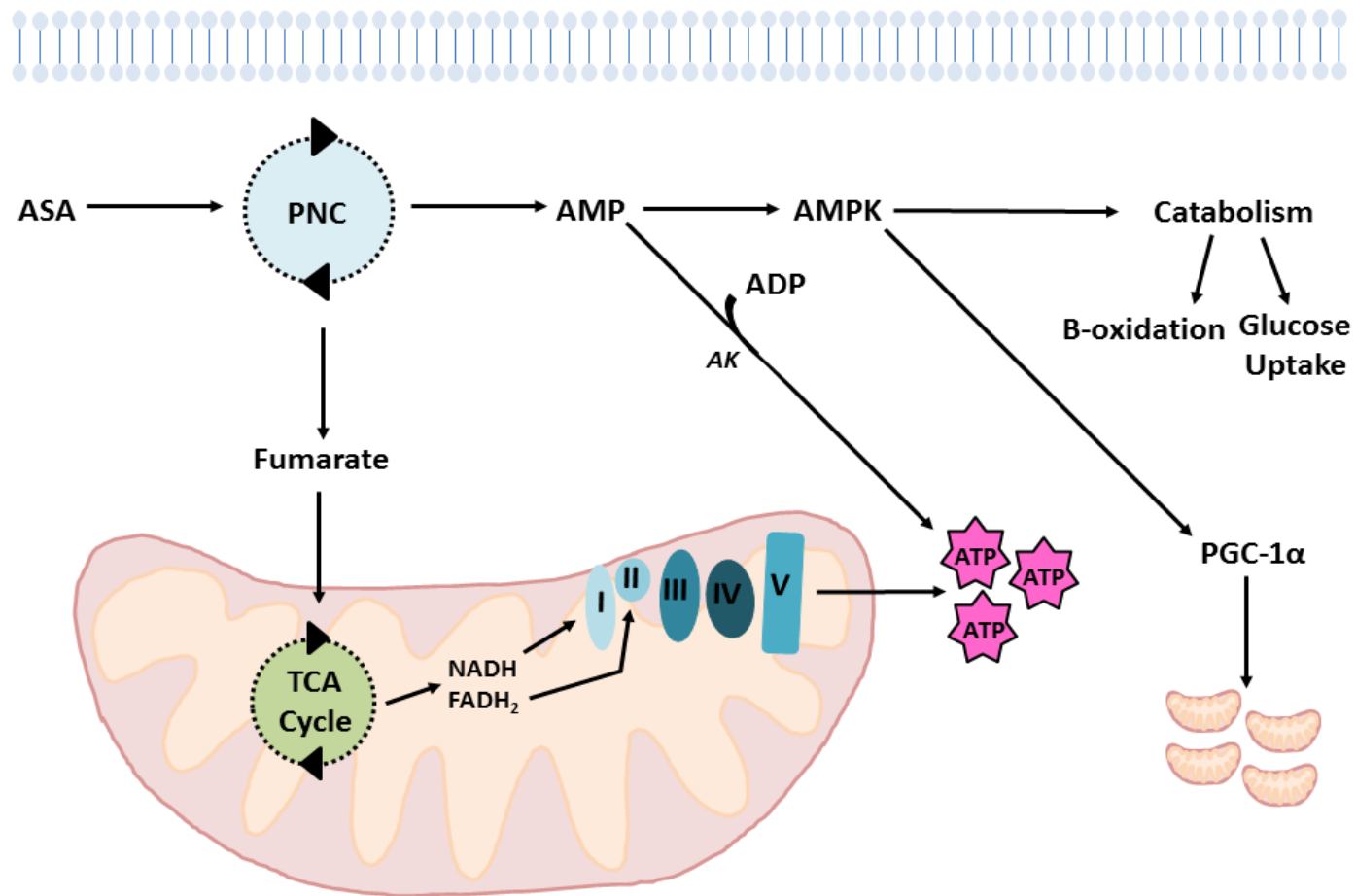


Figure 1.10. Proposed effects of ASA supplementation. ASA supplementation would stimulate purine nucleotide cycle (PNC) activity which would produce fumarate. Fumarate can be shuttled into the mitochondria and anaplerotically expand the TCA cycle which would produce reducing equivalents (NADH and FADH₂) that are used at the electron transport chain to increase ATP production. Additionally, stimulation of the PNC would increase adenosine monophosphate (AMP) content activating adenosine monophosphate-activated protein kinase (AMPK) and promoting catabolic pathways and mitochondrial biogenesis (PGC-1α).

state there is need to further investigate the ways in which metabolic capacity can be enhanced by ASA to improve the phenotypic progression of DMD and the quality of life of patients. Despite the success in the small clinical trial of ASA, the limited clinical evaluations and anecdotal evidence (increases in energy and stamina), in addition to the inclusion of only one DMD patient who completed the study long-term, indicates the need for a re-evaluation of ASA. Specifically, there is a need to assess the efficiency of ASA therapy in a proof-of-concepts study to fully elucidate the therapeutic potential of ASA. Reinvestigation of ASA is critical for the DMD community given the significant findings in the small clinical trial indicate a strong therapeutic potential.

1.8 Concluding comments

From the literature, it is evident that there is extensive metabolic dysfunction in dystrophin-deficient skeletal muscle that appears to play a significant role in disease progression. Considering that current treatment options are limited and associated with various side effects, there is a critical need to develop new treatment strategies targeting metabolism and mitochondrial function. Metabolic therapy has the potential to provide energy needed to prevent muscle damage to preserve muscle architecture leading to maintenance of muscle function and strength. Of particular interest to us is the extent to which NO signalling and PNC pathways can be exploited to overcome, or at least enhance, metabolic dysfunction in dystrophic muscle. This thesis will evaluate the therapeutic potential of two candidate treatments – sodium nitrate and ASA – in a bid to instigate the availability of new and effective treatment options for DMD patients.

Chapter Two

Aims & Hypotheses

2.1 Principal aim and hypothesis

The principal aim of this thesis is to experimentally evaluate the potential of two metabolic therapies (nitrate/nitrite and ASA) as treatments for DMD using the dystrophic *mdx* mouse. In particular, this thesis will focus on the effects of the therapies on glucose uptake, mitochondrial metabolism and muscle architecture. This thesis will also evaluate the potential for nitrate/nitrite and ASA to ameliorate metabolic dysfunction in immortalised myoblasts derived from human DMD patients. It is hypothesised that treatment with these metabolic therapies will improve dystrophic mitochondrial function and thus to moderate muscle damage and enhance repair.

2.1.1 Part One Aims and Hypotheses

The overarching aim of Part One (Chapters 4 and 5) is to investigate the effect of enhancing NO bioavailability in dystrophic *mdx* mice and in cultured DMD cells, with sodium nitrate/nitrite therapy.

The specific aim of Chapter 4 is to investigate the effect of an 8 week dietary nitrate supplementation regimen in the dystrophic *mdx* mouse model of DMD. In particular, we will examine the effect of increasing NO bioavailability on glucose uptake, mitochondrial metabolism, oxidative stress (through hydrogen peroxide (H₂O₂) and peroxynitrite (ONOO⁻) formation) and muscle architecture. It is hypothesised that nitrate therapy will improve glucose uptake in both dystrophin-negative and -positive EDL and soleus muscles, and that it will improve mitochondrial respiration in *mdx* gastrocnemius (both red and white portions). Additionally, it is hypothesised that nitrate supplementation will reduce

H₂O₂ production in *mdx* gastrocnemius and moderate muscle damage in the *mdx* TA as evidenced by reduced fibre size variability, centronucleation of fibres and immune cell infiltration.

The specific aim of Chapter 5 is to investigate the acute effect of nitrite (a reduced form of nitrate) treatment in cultured human DMD myoblasts. In particular, we examined the effect of 24 hours, 3 days and 7 days of nitrite treatment on mitochondrial respiration, viability and superoxide (O₂⁻) production. It is hypothesised that acute nitrite supplementation will improve mitochondrial respiration and mitochondrial viability in control and DMD myoblasts. As a direct result of improved mitochondrial performance, we hypothesise that acute nitrite supplementation will decrease mitochondrial O₂⁻ production in DMD myoblasts.

2.1.2 Part Two Aims and Hypotheses

The overarching aim of Part Two (Chapters 6 and 7) is to investigate the effect of ASA therapy in dystrophic *mdx* mice and in cultured DMD cells, on metabolism and the progression of muscular dystrophy.

The specific aim of Chapter 6 is to investigate the effect of an 8 week ASA treatment regimen in the dystrophic *mdx* mouse model of DMD. In particular, we will examine the effect of ASA on glucose uptake, mitochondrial metabolism and superoxide production; the bioenergetic profile of the muscle; and the various histopathological features of DMD. It is hypothesised that ASA therapy will improve glucose uptake in both dystrophin-negative and -positive EDL and soleus and that it will improve mitochondrial respiration in *mdx* isolated flexor digitorum brevis fibres. Additionally, it is hypothesised that ASA

supplementation will reduce mitochondrial (O_2^-) oxidative stress in *mdx* flexor digitorum brevis fibres as a direct consequence of improvements in mitochondrial function. Histologically, it is hypothesised that ASA supplementation will attenuate muscle damage (as evidenced by reduced fibre size variability and centronucleation of fibres) and reduce fat infiltration and fibrosis of the *mdx* TA. As a consequence of an improved bioenergetical profile and capacity for ATP-dependent Ca^{2+} buffering, it is also hypothesised that ASA will reduce Ca^{2+} accumulation within *mdx* TA fibres.

The specific aim of Chapter 7 is to investigate the acute effect of ASA treatment in cultured human DMD myoblasts. In particular, we will examine the effect of 24 hours, 3 days and 7 days of ASA treatment on mitochondrial respiration, viability and O_2^- production. It is hypothesised that acute ASA supplementation will improve mitochondrial respiration and viability in control and DMD myoblasts. Additionally, it is hypothesised that acute ASA supplementation will decrease mitochondrial O_2^- production in DMD myoblasts.

Chapter Three

Methods

3.1 Mdx mouse model experiments

3.1.1 Animals

For both animal studies, the dystrophin-positive C57BL/10ScSn (CON) mouse and dystrophin-negative C57BL/10*mdx* (*mdx*) mouse were utilised (males only). The *mdx* mouse is the most commonly utilised model of DMD due to being genetically homologous and lacking dystrophin at the sarcolemma. Animals were purchased from The Animal Resources Centre (Western Australia, Australia) and housed at the Western Centre for Health, Research and Education animal facility (Sunshine Hospital, Victoria, Australia) on a 12:12 hour light-dark cycle in individually ventilated cages (4-5 per cage). The animal facility temperature was maintained between 20 and 25°C with humidity maintained at 40%. All animals were acclimatised for a week prior to the supplementation period and at all times, animals were permitted *ad libitum* access to food and water and were weighed weekly. All experimental procedures were approved by the Victoria University Animal Ethics Experimentation Committee (ethics numbers 13/003 and 14/003) and conformed to the Australian Code of Practice for the care and use of animals for scientific purposes.

3.1.1.1 Dietary supplementation

In both supplementation studies, 3 week old male CON and *mdx* mice were randomly assigned into four groups ($n=16$ per group) by an animal technician (to remove experimenter bias; Kilkenney *et al.*, 2010, McGrath and Lilley, 2015) and allowed to acclimatise for one week prior to the

commencement of the supplementation period (Figure 3.1). Animals assigned to the unsupplemented groups (CON and *mdx* UNSUPP) were provided with non-autoclaved standard rodent chow (Speciality Feeds, Western Australia, Australia) and RO (reverse osmosis to remove impurities) drinking water. Animals assigned to the supplemented groups (CON and *mdx* NITR or ASA) were provided the same chow but the RO drinking water was supplemented with either sodium nitrate or ASA. Both food and drinking water were monitored and replaced weekly, with supplemented water made up fresh on the day of being changed.

Sodium nitrate (NITR) supplementation

In the NITR supplementation study, RO water was supplemented with 1mM (85mg/mL; equivalent to ~3.75 μ mol/day) of sodium NITR (S5506, Sigma Aldrich). This supplementation rate has been previously utilised in mice (Carlström *et al.*, 2010, Hernández *et al.*, 2012) and has been shown to significantly increase the pool of nitrogen species in both plasma and tissue (Carlström *et al.*, 2010) and to have beneficial effects on energy metabolism and other mitochondrial parameters (Larsen *et al.*, 2011, Ashmore *et al.*, 2015, Lansley *et al.*, 2011, Bailey *et al.*, 2009).

ASA supplementation

In the first clinical trial to test the efficacy of ASA (Bonsett and Rudman, 1992), the supplementation range approved was 1mg/kg/day to 1g/kg/day. We aimed to administer a dose of 25mg/kg/day in mice as this was the only specified dose that was delivered via a non-intravenous route (Bonsett and

Rudman, 1992). Additionally, as there is no data regarding the half-life, clearance and toxicity of ASA, we selected this dose to be within the lower half of the range approved for the clinical trial in DMD boys (Bonsett and Rudman, 1992). After taking into account blood volume and average daily water intake of a mouse, the dose was calculated to be 3000µg/mL.

A staggered supplementation protocol was employed to enable the detection of toxic and adverse effects in mice as this has yet to be established in mice. Mice were initially supplemented with 3µg/mL of ASA for 3 days and this was increased to 30µg/mL for 4 days, and 300µg/mL of ASA for one week. Since no adverse effects were observed, a dosage of 3000µg/mL for 6 weeks was delivered for the remainder of the supplementation period.

3.1.1.2 Surgeries

Following the supplementation period, mice underwent non-survival surgery. Mice were anaesthetised via intraperitoneal injection of sodium pentobarbitone (60mg/kg) and surgery was performed once the plantar reflex could not be detected. Following removal of muscles to be analysed on the day, the remainder of the muscles and organs (including the heart and diaphragm) were surgically excised, weighed and snap frozen for future analysis.

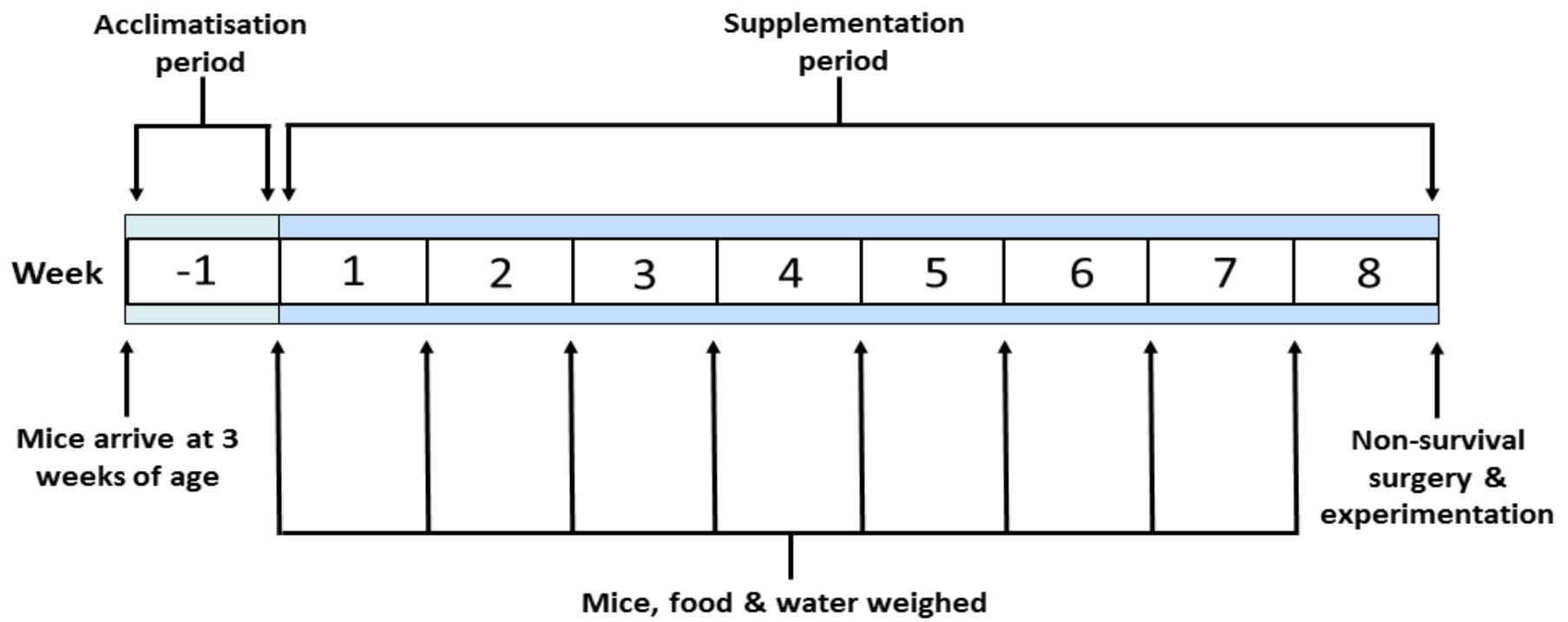


Figure 3.1. Supplementation protocol.

3.1.2 Glucose uptake (GU)

3.1.2.1 Muscle dissection and contraction protocol

In deeply anaesthetised mice, the predominantly fast-twitch extensor digitorum longus (EDL) and predominantly slow-twitch soleus (SOL) proximal and distal tendons in each hindlimb were tied with 4/0 surgical silk. Once all four muscles were tied, the right EDL and SOL were surgically excised tendon-to-tendon and placed in separate muscle baths containing warmed (30°C) Krebs basal buffer (118.5mM NaCl, 24.7mM NaHCO₃, 4.74mM KCl, 1.18mM MgSO₄, 2.5mM CaCl₂, 8mM mannitol, 2mM Na pyruvate, 0.01% BSA; pH 7.4) bubbled with carbogen (95% O₂, 5% CO₂). The left EDL and SOL were then excised and placed into muscle baths prepared in the same manner. The proximal tendon was attached to a force transducer with the distal tendon attached to a hook (Figure 3.2) and muscles were incubated for 20 minutes to equilibrate in the bath.

Single muscle baths were stimulated via square wave electrical pulses sufficient to recruit all motor units and produce maximum force in the contracting muscle. Stimulation, delivered by platinum electrodes flanking the muscles, and subsequent recording of the force output were obtained from a custom-built muscle analysis system (Zultek Engineering, Victoria, Australia). Following determination of optimal length (L_0) of each muscle via a succession of isometric twitch contractions, the left EDL and SOL were stimulated to contract for a total of 10 minutes (pulse durations of 350msec and 500msec for EDL and SOL, respectively at a frequency of 60 Hz; Figure 3.3 and 3.4). This protocol maintains muscle viability and elicits maximal GU (Merry *et al.*, 2010). The right EDL and SOL were not stimulated to

contract during the 10 minute contraction period, and were utilised to measure basal GU.

3.1.2.2 Radioactive determination of GU

Following 5 minutes of contraction, the Krebs basal buffer was exchanged for warmed Krebs buffer with the addition of 2-Deoxy-D-[1,2-³H]glucose (0.128 μ Ci/mL, Perkin Elmer) and D-[¹⁴H]mannitol (0.083 μ Ci/mL, Perkin Elmer) in both resting and contracting muscle baths. At the end of the 10 minute contraction protocol, muscles were placed immediately in ice-cold Krebs basal buffer to stop further GU, blotted on filter paper and snap frozen in liquid nitrogen. Whole muscles were then weighed, digested for 10 minutes at 95°C in 135 μ L of 1M NaOH, neutralised with 135 μ L of 1M HCl and centrifuged for 5 minutes at 13,000G. 200 μ L of supernatant was added to 4mL of inorganic scintillation fluid (UltimaGold, Perkin Elmer) in scintillation vials and radioactivity was measured in a β -scintillation counter (Tri-Carb 2810, Perkin Elmer).

GU was calculated (Hong *et al.*, 2015) using the formula:

$$\text{Glucose uptake} = (\text{2DG transfer/weight} \times 1000) \times 12$$

Where:

2DG transfer = amount of radioactive 2DG uptaken into muscle sample

Weight = weight of muscle in mg



Figure 3.2. Muscle dissection and contractile bath setup. Panels A and B demonstrate the tied proximal and distal tendons of EDL and SOL respectively. Panel C shows the contractile baths housing the EDL (bath 1 and 3) and SOL (bath 2 and 4) during equilibration time with Panels D and E showing close-ups of EDL and SOL, respectively.

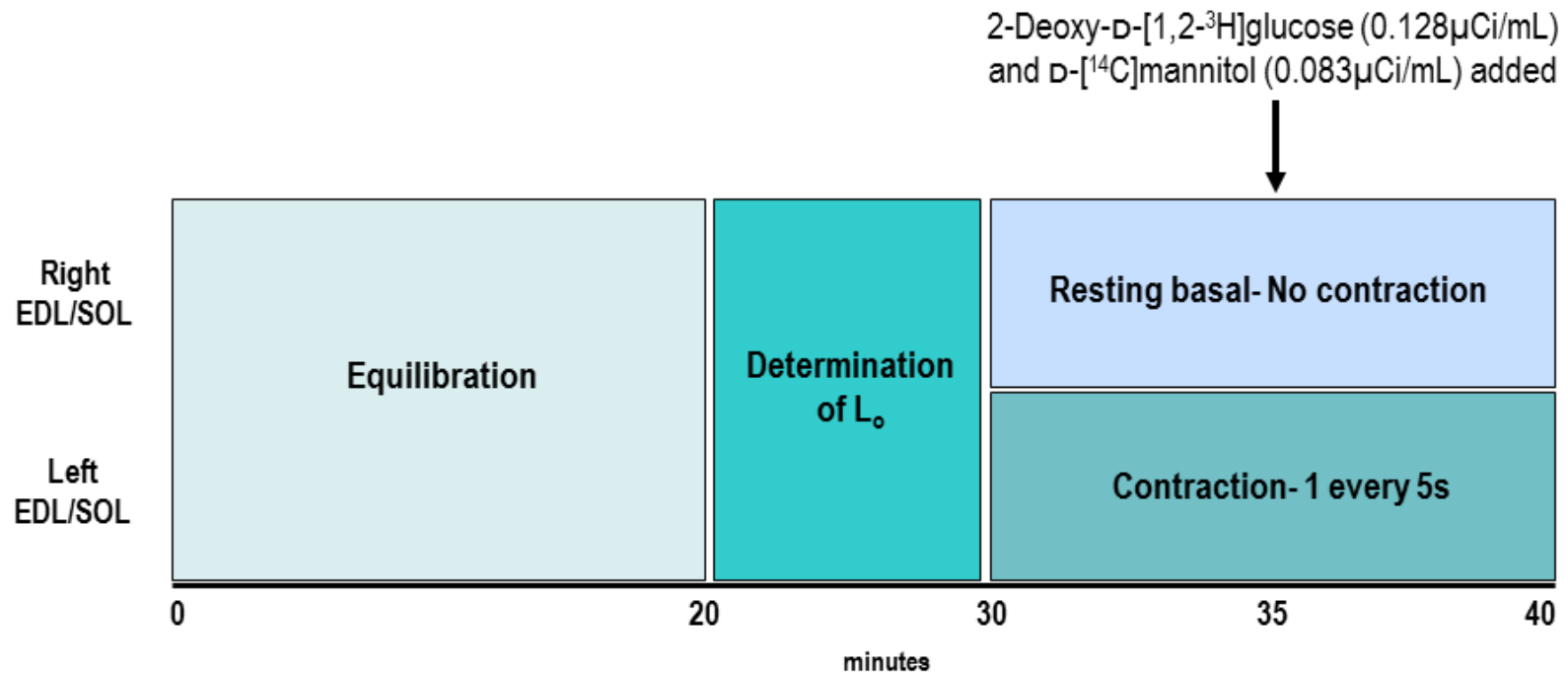


Figure 3.3. Timeline of contraction protocol to determine glucose uptake (GU). Both right and left EDL and SOL were allowed to equilibrate in the muscle baths for 20 minutes before the optimal length (L_o) of each muscle was determined. At the 30 minute mark, the left EDL and SOL underwent contractions every 5 seconds while the right EDL and SOL received no stimulation. At the 35 minute mark, radioactive tracers were added to all muscles and at 40 minutes muscle were snap frozen for later GU analysis.

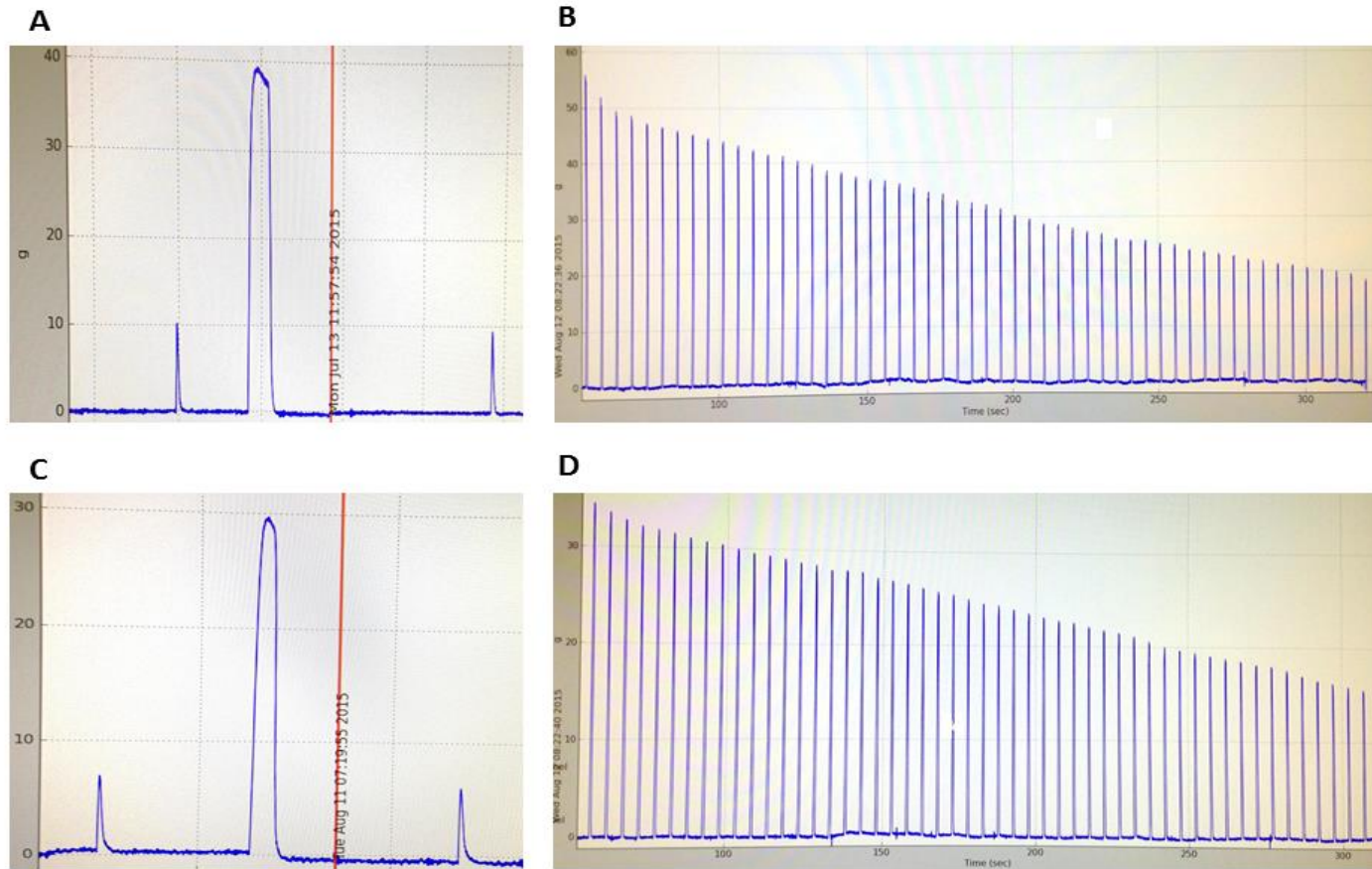


Figure 3.4. Examples traces obtained during glucose uptake (GU) experimentation. Following determination of the optimal length (L_o) of each muscle, twitch and tetanic stimuli were delivered to the muscles to ensure that muscles would not slip during the 10 minute contraction protocol and that the true optimal length was determined. (Panel A- EDL, Panel C-SOL). During the 10 minutes of contraction, the force produced decreases in both EDL (B) and SOL (D).

3.1.3 Mitochondrial respirometry/metabolism

3.1.3.1 Measurement of mitochondrial respiration

Mitochondrial respiration was determined using different methods in each study. In the NITR supplementation study, mitochondrial respiration was assessed using the Oxygraph O2K high resolution respirometer (Oroboros Instruments, Innsbruck, Austria) and was performed by a collaborator at the Institute of Sports, Exercise and Active Living (ISEAL, Victoria University). This methodology was employed due to the capacity of measuring mitochondrial respiration and oxidative stress (in the form of hydrogen peroxide (H₂O₂) production) simultaneously which is important considering NO can promote oxidative stress. In addition, this methodology is advantageous as the permeabilisation of the fibre bundles bypass deficits in substrate transport across the membrane.

In the ASA supplementation study, mitochondrial respiration was assessed using the XF24-3 Flux Analyser (Seahorse Bioscience, MA, USA). An advantage of this method is that both oxidative and glycolytic metabolic function can be assessed in intact fibres. This is important given ASA influences both anaerobic and aerobic metabolism.

Mitochondrial respirometry using the Oroboros Oxygraph

For the NITR study, left and right gastrocnemius were excised from anaesthetised mice and separated into red (slow-twitch; RG) and white (fast-twitch; WG) portions to allow for comparison with the fast-twitch EDL and slow-twitch SOL utilised for GU determination. Following separation, red and white portions were immediately placed into ice-cold BIOPS (7.23mM K₂EGTA, 2.77mM CaK₂EGTA,

5.77mM Na₂ATP, 6.56mM MgCl₂·6H₂O, 20mM taurine, 15mM phosphocreatine, 20mM imidazole, 0.5mM dithiothreitol, 50mM K⁺-MES; pH 7.1). Muscle fibres were mechanically separated from a small portion of muscle (remaining gastrocnemius was snap frozen for later western blot analysis and citrate synthase activity) in ice-cold BIOPS to maximise fibre surface area and transferred into ice-cold BIOPS supplemented with saponin (50µg/mL) for 30 minutes. Separated fibres were agitated to permeabilise the sarcolemma and allow diffusion of subsequent assay substrates before being thrice washed with agitation in ice-cold respiration buffer (110mM K⁺-MES, 35mM KCl, 1mM EGTA, 5mM K₂HPO₄, 3mM MgCl₂·6H₂O, 0.05mM pyruvate, 0.02mM malate, 5 mg/mL BSA; pH 7.4).

Electron transport chain (ETC) and oxidative phosphorylation (OXPHOS) function and H₂O₂ emission was measured by the Oxygraph O2k high resolution respirometer (Oroboros Instruments, Innsbruck, Austria) via a substrate, uncoupler, inhibitor titration (SUIT) protocol at 37°C. Briefly, the SUIT protocol commenced with titrations of complex I substrates malate (2mM final concentration) and pyruvate (10mM), followed by the complex II substrate succinate (10mM) to determine LEAK (state 4) respiration. Titrations of ADP (0.25, 1 and 5mM) assessed OXPHOS (state 3) capacity with the addition of cytochrome *c* (10µM) testing mitochondrial membrane integrity and titration of FCCP (0.025µM; (carbonyl cyanide-*p*-trifluoromethoxyphenylhydrazine)) determining maximal respiration. Respiration was inhibited by the addition of rotenone (1µM) and antimycin A (5µM) to inhibit complex I and complex III, respectively. Finally, complex IV capacity was evaluated via addition of TMPD (N,N,N',N'-tetramethyl-*p*-phenylenediamine; 0.5mM, Sigma Aldrich) and ascorbate (2mM, Sigma Aldrich; Figure 3.5).

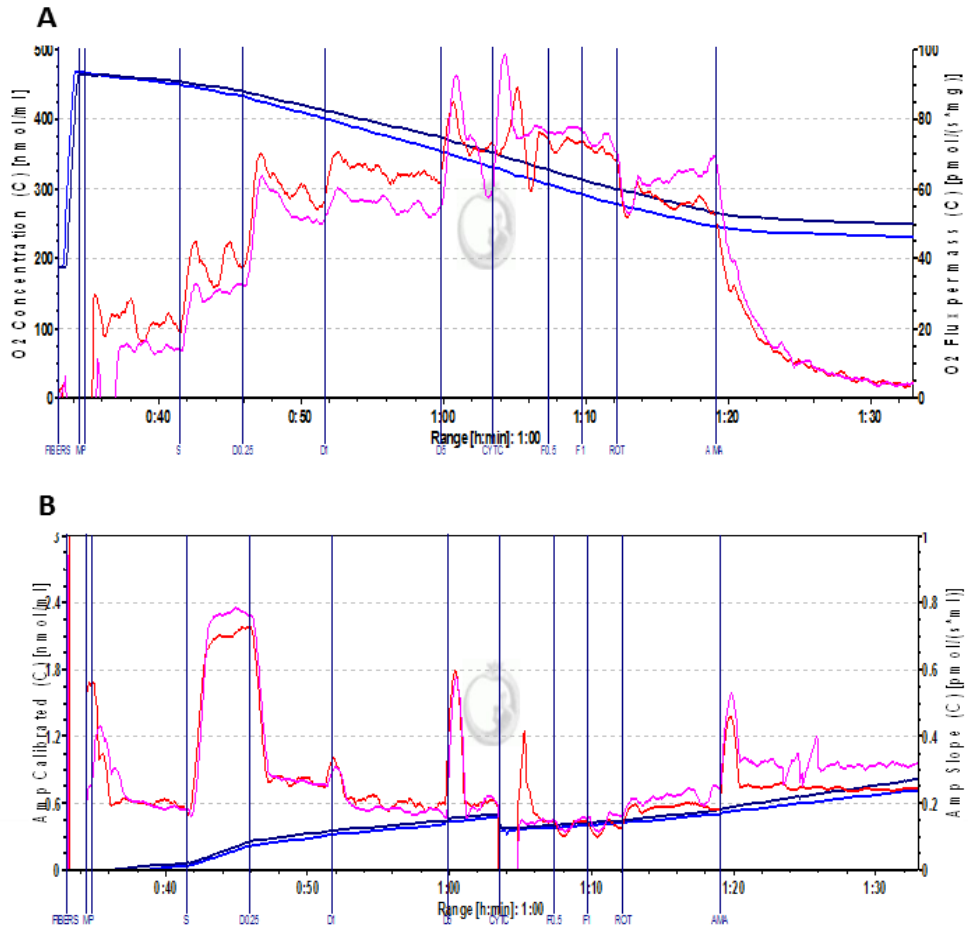


Figure 3.5. Representative traces of mitochondrial respiration (A) and hydrogen peroxide (H₂O₂) emission (B) from the Oxygraph respirometer.

Mitochondrial & glycolytic metabolism using the Extracellular Flux Analyser

Isolation of flexor digitorum brevis (FDB) fibres

FDB fibres were isolated according to procedures described by Schuh *et al.* (Schuh *et al.*, 2012). FDB (see Figure 3.6) was surgically excised from both paws of anaesthetised mice and incubated in 1 mL of pre-warmed dissociation media (DMEM, Gibco 10566016; 2% FBS, Bovogen Biologicals; 4mg/mL collagenase A, Roche 10103586001; 50µg/mL gentamycin, Sigma Aldrich G1397) for 1 hour and 45 minutes (37°C, 5% CO₂). Following the dissociation period, FDB bundles were placed into ~1.5 mL of incubation media (DMEM, Gibco 10566016; 2% FBS, Bovogen Biologicals; 50µg/mL gentamycin, Sigma Aldrich G1397) and bundles were triturated with pipette tips of decreasing bore size to yield single fibres. To avoid hypercontraction of fibres, fibres were triturated no more than 10 times before being returned into the dissociation media for a further 15 minutes and triturated again to liberate the remaining fibres. Any undigested FDB bundles or debris were removed from the media using forceps.



Figure 3.6. Indication of the position of FDB in the sole of the foot

Seeding of isolated FDB fibres

To facilitate fibre adherence to Seahorse XF24 cell culture V7 microplates (Seahorse Bioscience, MA, USA), all wells of the microplate were coated with 5µL of extracellular matrix (Sigma Aldrich, E1270) diluted in DMEM (1:1). Diluted extracellular matrix was evenly dispersed throughout the wells by tapping the microplate and then allowed to air dry for 30 minutes in a sterile biohazard hood.

A 75µL aliquot of isolated fibres were placed into the coated wells (all samples were run in triplicate) and confluency was determined using a light microscope. If ~60% of the well bottom was not covered by isolated FDB fibres, an additional 50µL aliquot of fibres was dispensed into wells. Isolated fibres were incubated for 30 minutes to promote adherence to the extracellular matrix. When adherence was achieved, additional incubation media was added to each well to give a final volume of 180µL and the microplate was returned to the incubator overnight. Four background control wells (matrigel only) were included on each microplate to serve as a temperature control for the experiment.

Establishing an energetic profile of isolated FDB fibres

The primary measures of mitochondrial function in isolated FDB fibres (oxygen consumption rate (indicative of mitochondrial metabolism; OCR) and extracellular acidification rate (indicative of anaerobic glycolytic metabolism; ECAR)) were performed on the XF24-3 Extracellular Flux Analyser (Seahorse Bioscience, MA, USA) according to the methods of Schuh *et al.* (Schuh *et al.*, 2012). The XF24 Flux Analyser employs real-time measurements of dissolved O₂ and pH via probes that emit excitation wavelengths (O₂ at 532nm, pH at 470nm) and the fluorescent

signal is detected by photodetectors (O_2 at 650nm, pH at 530nm) (Wu *et al.* 2007). OCR and ECAR measurements are taken following the lowering of the probes into a Sensor Cartridge which forms a temporary micro chamber ($\sim 7\mu\text{L}$), and following the probes being raised, the medium is re-oxygenated to allow for multiple measurements (Rogers *et al.*, 2011).

To obtain the best metabolic profile of the mitochondria, OCR and ECAR is measured over various respiratory states (Figure 3.7). Basal (state 2) respiration is substrate-driven (through the addition of glucose in the media) and indicates an idling ETC using endogenous ADP and includes OCR driven by leak of protons (H^+) through uncoupled mitochondria (i.e. via uncoupling proteins and/or a leaky inner mitochondrial membrane). State 4 respiration is driven by the addition of oligomycin, an inhibitor of complex V, and defines the contribution of H^+ leak to respiration. State 3 uncoupled respiration is stimulated by FCCP, a known ETC uncoupler that induces maximal respiration by driving H^+ out of the intermembrane space causing the collapse of mitochondrial membrane potential ($\Delta\Psi$) thus driving electron transport at its maximum. Pyruvate is subsequently delivered to ensure ample substrate availability to support maximal respiration and ensure that maximal OCR measured is not limited by substrate. Finally, inhibited respiration is measured following the addition of rotenone and antimycin A (acting on complex I and III, respectively) which inhibit electron flow along – and respiration by – the ETC, and enables the measurement of non-mitochondrial OCR as a background control. Together, these measurements can be used to calculate the contribution of OCR to ATP production and the spare respiratory capacity, and to calculate the coupling efficiency of the mitochondria.

Additionally, an indication of anaerobic glycolytic metabolism can be obtained through the measurement of ECAR. The conversion of glucose to lactate produces H^+ ions and the efflux of these H^+ ions from the cell results in acidification of the extracellular environment. Therefore, ECAR is an indirect measurement of glycolytic flux. Glycolytic flexibility can also be assessed following the addition of oligomycin as ECAR dramatically increases to compensate for the inhibition of complex V and therefore oxidative ATP production. The response to this metabolic stress indicates how well glycolysis can respond to meet ATP demand.

To a pre-hydrated XF24 Sensor Cartridge (Seahorse Bioscience, MA, USA), 75 μ L of oligomycin (20 μ g/mL, Sigma Aldrich) was added to injection port A (to give a final assay concentration of 2 μ g/mL), 82 μ L of FCCP (4 μ M, Sigma Aldrich) and sodium pyruvate (100mM, Sigma Aldrich) was added to injection port B (to give a final assay concentration of 400nM and 10mM respectively) and 92 μ L antimycin A (10 μ M, Sigma Aldrich) was added to injection port C (to give a final assay concentration of 1 μ M). Into the injection ports corresponding to the background control wells, equivalent volumes of measurement buffer was added. The cartridge was incubated at 37⁰C for 10 minutes prior to commencement of the assay.

Following overnight incubation of the microplate with isolated FDB fibres, 105 μ L of incubation media was removed from each well and replaced with 1000 μ L of pre-warmed measurement buffer (120mM NaCl, 3.5mM KCl, 1.3mM CaCl₂, 0.4 mM KH₂PO₄, 1mM MgCl₂, 5mM HEPES, 2.5mM D-glucose and 0.5mM L-carnitine; pH 7.4) to wash the fibres of any incubation media. One thousand μ L was removed from each well and replaced with 600 μ L of measurement buffer to give a final volume of 675 μ L per well. Six hundred and seventy-five μ L of measurement buffer was added

to the background control wells and the microplate was returned to the incubator for 2 hours for pH and temperature equilibration.

OCR and ECAR were determined for various respiratory states via a SUIT protocol. A SUIT loaded Sensor Cartridge was inserted into the XF24 Analyser and calibration of the XF24 Analyser commenced. Once calibration was completed, the loaded microplate was inserted into the XF24 Analyser and the mitochondrial stress test was commenced (refer to Table 3.1 for complete protocol). Following an equilibration period, basal OCR and ECAR were measured using a cycle consisting of a 3 minute mix, 2 minute wait, 3 minute measure cycle, that was looped 3 times. Following this, Port A, B, C and D were sequentially injected into the wells, with a full cycle read between each injection.

Table 3.1. Protocol utilized to measure OCR and ECAR in the XF24 Analyser

Command	Time (min)	Port	Stimulator/Inhibitor	Measurement
Calibrate	10			
Equilibrate				
Mix	3			Basal Respiration
Wait	2			
Measure	3			
Mix	3			
Wait	2			
Measure	3			
Mix	3			
Wait	2			
Measure	3			
Inject		A	Oligomycin	Uncoupled Respiration
Mix	3			
Wait	2			
Measure	3			
Mix	3			
Wait	2			
Measure	3			
Mix	3			
Wait	2			
Measure	3			
Inject		B	FCCP and Pyruvate	Maximal Respiration
Mix	3			
Wait	2			
Measure	3			
Mix	3			
Wait	2			
Measure	3			
Mix	3			
Wait	2			
Measure	3			
Inject		C	Antimycin A	Inhibited Respiration
Mix	3			
Wait	2			
Measure	3			
Mix	3			
Wait	2			
Measure	3			
Mix	3			
Wait	2			
Measure	3			

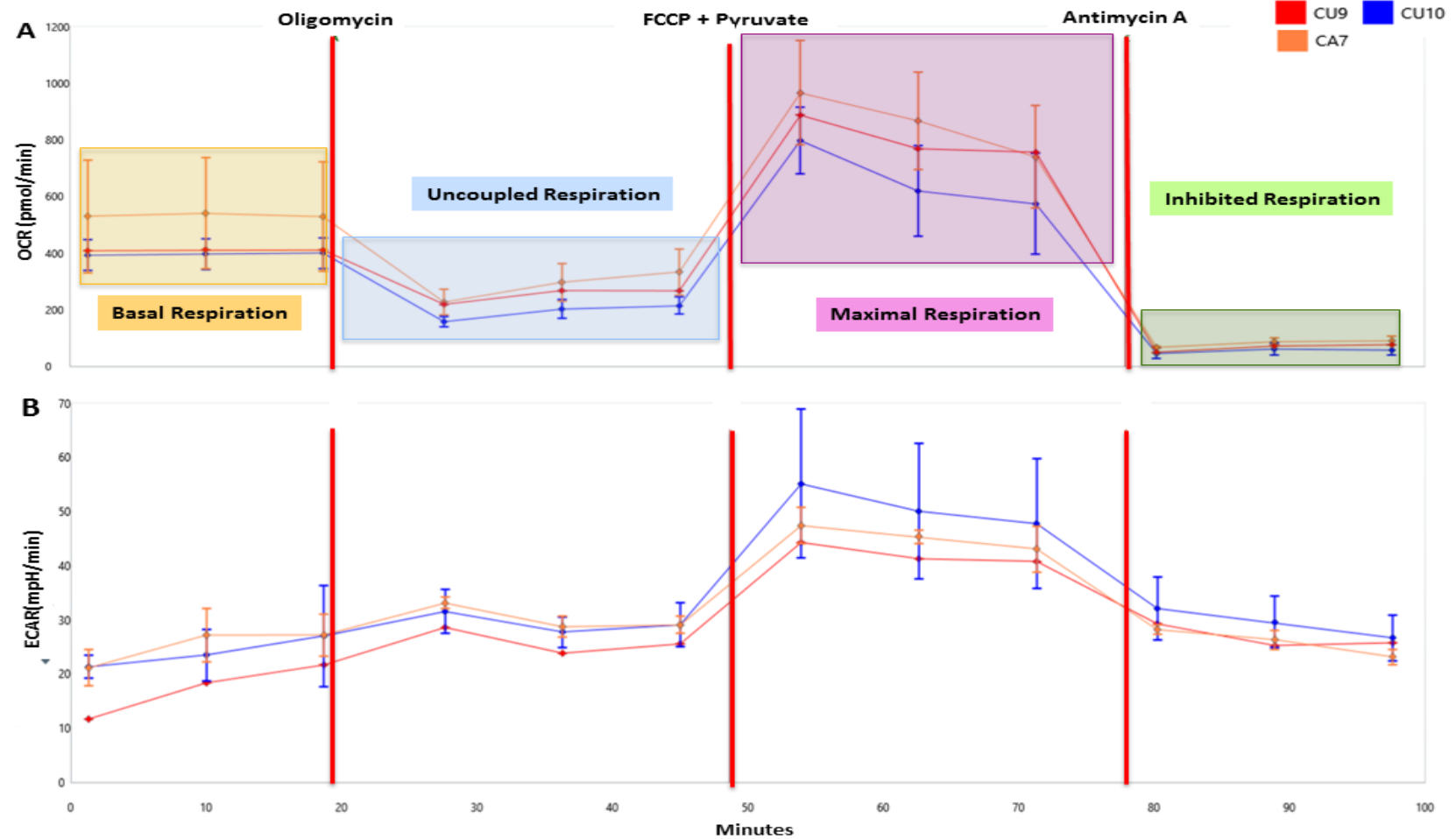


Figure 3.7. Representative traces of oxygen consumption rate (OCR, A) and extracellular acidification rate (ECAR, B) in isolated FDB fibres. Following basal respiration (yellow box), stimulators and inhibitors were injected in sequence – oligomycin to induce uncoupled respiration (blue box), FCCP and pyruvate to induce maximal respiration (purple box) and antimycin A to induce inhibited respiration (green box). CON UNSUPP (red and blue); CON ASA (orange).

Derivation of data

While the OCR and ECAR readings from the respiratory states can be analysed and presented, they are not presented in this thesis as there was no capacity to control for variable fibre number plating in each well, nor could the data be corrected for protein content (as per Schuh *et al.*, 2012). Therefore, coupling efficiency, ATP production, spare respiratory capacity, the metabolic potential and bioenergetic health index have been presented as these parameters are internally corrected for basal respiration and thus the fibre plating density of each well (see Table 3.2).

Table 3.2. Metabolic parameters employed to assess the metabolic/mitochondrial effects of the supplementation periods

Parameter	Definition	Calculation
Coupling Efficiency	A marker of how efficiently O ₂ consumption is matched to ATP production	$\frac{\text{State 4 Respiration}}{\text{Basal Respiration}} \times 100$
ATP Production	Following the addition of oligomycin, the decrease in OCR represents the fraction of basal respiration that was dedicated to ATP production	Basal Respiration – State 4 Respiration
Spare Respiratory Capacity	An indicator of the capacity of the mitochondria to respond to metabolic demand	(State 3 Respiration – Basal Respiration) x 100
Metabolic Potential	A measure of metabolic flexibility (via respiration and glycolysis) to meet energy demand	$\frac{\text{State 3 OCR or ECAR}}{\text{Basal OCR or ECAR}} \times 100$
Bioenergetic Health Index	An indicator of overall bioenergetic health and dysfunction	$\log \frac{\text{Spare Respiratory Capacity} \times \text{ATP Production}}{\text{Inhibited Respiration} \times \text{Proton Leak}}$

3.1.3.2 Mitochondrial content, viability and metabolites

Markers of mitochondrial biogenesis (AMPK, PGC-1 α and PGC-1 β) and ETC complex expression

To assess the mitochondrial pool and the stimulation of mitochondrial biogenesis, AMPK- α (rabbit, 1:1000, Gene Signalling, 2535S) – and its phosphorylated form phospho-AMPK (rabbit, 1:1000, Gene Signalling, 2603S) – PGC-1 α (mouse, 1:1000, Merck Millipore, ST1202) and PGC-1 β (rabbit, 1:3000, Abcam, ab176328) were analysed through semi-quantitative western blot analysis. For this analysis, only quadriceps from the ASA supplementation study were utilised. To assess if differences in respiration parameters were reflective of changes in mitochondrial ETC density, subunits of each of the complexes of the ETC were assessed. The Total OXPHOS Antibody Cocktail (mouse, 1:1000, Abcam, ab110413) consisted of primary antibodies against the following proteins: NADH Dehydrogenase (Ubiquinone) 1 Beta Sub-complex, 8 (NDUFB8; Complex I), Succinate Dehydrogenase Assembly Factor 4 (SDH8; Complex II), Ubiquinol-Cytochrome-C Reductase Complex Core Protein 2 (UQCRC2; Complex III), Mitochondrially Encoded Cytochrome C Oxidase I (MTOC1; Complex IV) and Mitochondrial ATP Synthase Subunit Alpha (ATPSA; Complex V). For this analysis, quadriceps from the ASA supplementation study and red and white gastrocnemius from the nitrate study were utilised.

Frozen muscles were homogenized with a Polytron homogenizer (Kinematica AG, Lucerne, Switzerland) for 20 seconds in ice-cold WB buffer (40mM Tris, pH 7.5; 1mM EDTA; 5mM EGTA; 0.5% Triton X-100; 25mM β -glycerophosphate; 25mM NaF; 1mM Na₃VO₄; 10 μ g/ml leupeptin; and 1mM PMSF), and the whole

homogenate was used for further analysis. Sample protein concentrations were determined with a DC protein assay kit (Bio-Rad Laboratories, Hercules, CA, USA), and equivalent amounts of protein (15µg) from each sample were dissolved in Laemmli buffer, heated for 5 min at 37°C and subjected to electrophoretic separation on SDS-PAGE acrylamide gels. Following electrophoretic separation, proteins were transferred to a PVDF membrane, blocked with 5% powdered milk in Tris-buffered saline containing 0.1% Tween 20 (TBST) for 1 h followed by an overnight incubation at 4°C with primary antibody dissolved in TBST containing 1% bovine serum albumin (BSA). After overnight incubation, the membranes were washed for 30 min in TBST and then probed with the appropriate peroxidase-conjugated secondary antibody (1:10000 for anti-mouse (ETC complexes), 1:20000 for anti-mouse (PCG-1α) and 1:5000 for anti-rabbit (AMPK-α, phosphor-AMPK, PCG-1β)) for 1 h at room temperature. Following 30 min of washing in TBST, the blots were developed with a DARQ CCD camera mounted to a Fusion FX imaging system (Vilber Lourmat, Germany) using ECL Prime reagent (Amersham, Piscataway, NJ, USA). Once the image was captured, the membranes were stained with Coomassie Blue to verify equal loading of total protein in all lanes. Densitometric measurements were carried out using Fusion CAPT Advance software (Vilber Lourmat, Germany). Coomassie Blue was utilised to normalise the protein of interest. For all data, except for the AMPK/Total AMPK ratio, the protein of interest was normalised to the signal intensity of Coomassie Blue. For the AMPK/Total AMPK ratio, 4 gels were run with 2 sequences of 4 (CON UNSUPP, CON SUPP, *mdx* UNSUPP and *mdx* SUPP) samples and an additional 6 CON UNSUPP samples. Every sample was normalised to the mean of the 8 controls on the gel.

Assessment of mitochondrial viability

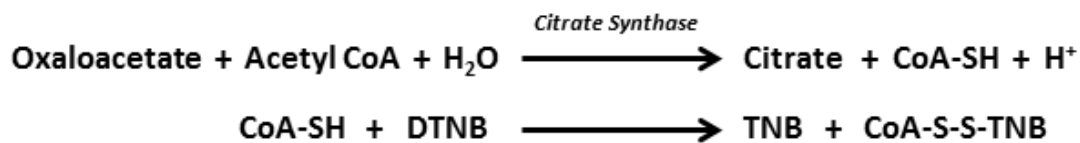
Mitochondrial viability was assessed using the fluorescent probes MitoTracker Green and Red (Molecular Probes). MitoTracker Green is a non-selective mitochondrial dye that labels all mitochondria irrespective of the mitochondrial membrane potential while MitoTracker Red is only uptaken into actively respiring mitochondria. Mitochondrial viability is calculated as a ratio of active mitochondria (MitoTracker Red) to total mitochondrial pool (MitoTracker Green).

One hundred μL of isolated FDB fibres were plated onto a matrigel coated 96 well microplate (all samples were run in triplicate) and confluency was determined using a light microscope. If ~60% of the well bottom was not covered by isolated FDB fibres, an additional 50 μL aliquot of fibres was dispensed into the well. For wells that did not receive the additional 50 μL of fibres, 50 μL of incubation media was added and the microplate was incubated overnight.

Ten minutes prior to the addition of the MitoTracker dyes, FCCP and antimycin A (final concentration of 3 μM each) were added to the positive control wells. As FCCP induces the collapse of the mitochondrial membrane potential and antimycin A inhibits complex III function, mitochondrial viability decreases as evidenced by a reduction in the intensity of MitoTracker Red fluorescence. Following this, a cocktail of MitoTracker Green and Red (final concentration of 200nM and 50nM, respectively) in Flurobrite media (100 μL total, ThermoFischer) was added to each well and incubated at 37°C for 30 minutes. Fibres were then washed twice with Flurobrite media and imaged on an inverted microscope (Olympus, Tokyo, Japan) using FITC and TRITC filters and standardised exposure time. The intensity of red and green fluorescence of each image was analysed using ImageJ (NIH, USA).

Citrate synthase (CS) activity

CS is the first enzyme of the TCA cycle that catalyses the production of citrate through the reaction of acetyl CoA and oxaloacetate. As CS is localised to the mitochondrial matrix, it is a marker of oxidative metabolism and thus mitochondrial density. CS activity can be determined by the following reactions (Srere, 1969):



The by-product of CS activity, CoA-SH, reacts with 5,5'-dithiobis-2-nitrobenzoic acid (DTNB) producing the yellow product 5-thio-2-nitrobenzoic acid (TNB) which is measured spectrophotometrically at 412nm.

The CS assay was run on an X-Mark Microplate Reader (Bio-Rad Laboratories, Australia) in a 96-well clear-bottom microplate. Samples were added to the microplate with 230µL of reagent cocktail (100mM Tris Buffer, 1mM DTNB, 3mM Acetyl CoA) and the reaction was initiated by the addition of 10mM oxaloacetate. The assay was read at 412 nm for 5 minutes with a reading taken every 30 seconds. RG and WG from the NITR study and FDB fibres from the ASA study were utilized for CS activity.

CS activity was calculated by the following formula:

$$CS = \frac{\text{Absorbance} \times \text{volume}}{E}$$

Where:

Absorbance = change in absorbance per minute
Volume = total volume in well
E = extinction coefficient (13.6 as determined by Srere 1969)

Metabolites

Since ASA reportedly expands the PNC cycle, thereby increasing the production of AMP and fumarate which can lead to increased ATP production, we assessed various metabolites in ASA supplemented samples to investigate if there is changes in the metabolite production and utilisation of other metabolic pathways.

Freeze-drying

At least 20mg of frozen TA were cut in liquid nitrogen to ensure that approximately 5mg of dry muscle was maintained following the drying process. Cut samples were placed into cryule tubes and into a -40°C freeze dryer (Edwards Modulo, Edwards High Vacuum, Britain, England) for a minimum of 48 hours. Following the freeze-drying process, samples were weighed to determine the dry weight. Samples were stored in a room temperature dessicator until required.

Metabolite extraction

ATP-PCr, Cr and Lactate

Two mg of powdered sample was weighed into an eppendorf tube with 250µL of 0.5M perchloric acid (PCA) and 1mM ethylenediaminetetra-acetic acid (EDTA) added thereafter. Tubes were vortexed and settled on ice for 10 minutes before being placed in a 0°C centrifuge and spun for 2 minutes at 28,000 RPM (28,837 g). Two hundred µL of supernatant was placed into a new eppendorf tube with 50µL of 2.1M KHCO_3^- and after 5 minutes on ice, the tube was re-centrifuged at the same settings. Supernatant was collected and stored in cryovials at -80°C until required.

Glycogen

One mg of powdered sample was weighed into an eppendorf tube and 250µL of hydrochloric acid added thereafter. Tubes were incubated for 2 hours at 100°C and agitated half way through the incubation period. 750µL of 0.667M sodium hydroxide was added to tubes to neutralise the reaction. Samples were stored at -80°C until required.

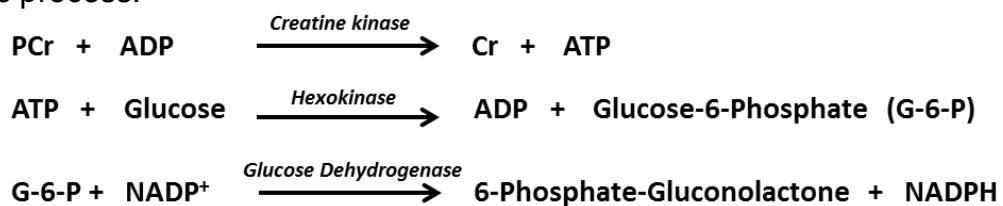
Metabolite analysis

ATP-CP, Cr, lactate and glycogen metabolite analysis was adapted from Lowry and Passonneau (Lowry and Passonneau, 1972) to be performed in 96 well plates and measured using a Fluroskan plate reader (ThermoFisher, USA). For all metabolites, a NADH standard curve was established on a UV-visible spectrophotometer at 340nm to compare the change in fluorescence of the internal

standards against the standard curve. Internal standards for different for each metabolite analysis – ATP and PCr for ATP-PCR analysis, PCr for Cr analysis, lactate for lactate analysis and glucose for glycogen analysis.

ATP-PCr

ATP and PCr content was determined in samples using a three-step enzymatic process:



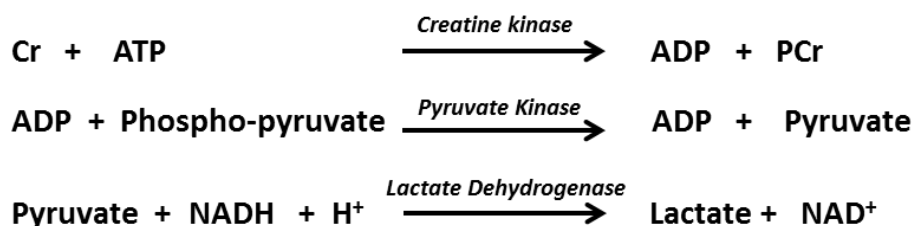
Once the standard curve was generated, 10µL of blank, ATP, PCr and NADH standards and sample were pipetted into 96 well plates in addition to the reagent cocktail (Table 3.3). The first reading indicates NADPH concentration through the presence of G-6-P dehydrogenase in the reagent cocktail. The second reading was recorded following the addition of dilute hexokinase which produces G-6-P – the substrate for the third reaction – and a 30 minute incubation at room temperature. The subtraction of reading one from reading two indicates the change in NADPH concentration which correlates with ATP concentration. Following the addition of CK and ADP to the well, and a 60 minute incubation at room temperature, the third reading is recorded. The NADPH produced from this reaction is reflective of PCr in the sample.

Table 3.3. Reagent cocktail for ATP-CP metabolite analysis

Reagent	Final Concentration
Tris buffer (pH 8.1)	50mM
Magnesium chloride	1mM
Dithiothreitol	0.5mM
Glucose	100µM
Nicotinamide adenine dinucleotide phosphate (NADP)	50µM
G-6-P dehydrogenase	-

Cr

Cr content was determined in samples using a three-step enzymatic process:



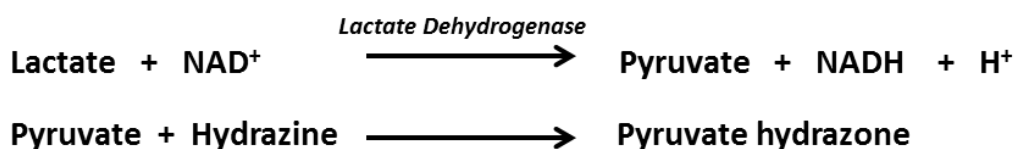
Following generation of the standard curve, 30µL of reagent blank, PCr standard or sample were pipetted into 96 well plates in addition to the reagent cocktail (Table 3.4). The first reading, following a 15 minute incubation at room temperature, indicates residual NADH concentration. The second reading was recorded following the addition of CK (in 0.05% BSA) and a 60 minute incubation at room temperature which produces pyruvate, the substrate for the third reaction, which is measured 15 minutes after the second reading.

Table 3.4. Reagent cocktail for Cr metabolite analysis

Reagent	Final Concentration
Imidazole (pH 7.4)	50mM
Magnesium chloride	5mM
Potassium chloride	30mM
Phosphoenolpyruvic acid	0.1mM
ATP	0.2mM
LDH	1µg/mL
PK	5µg/mL

Lactate

Lactate content was determined in samples using a two-step enzymatic process:



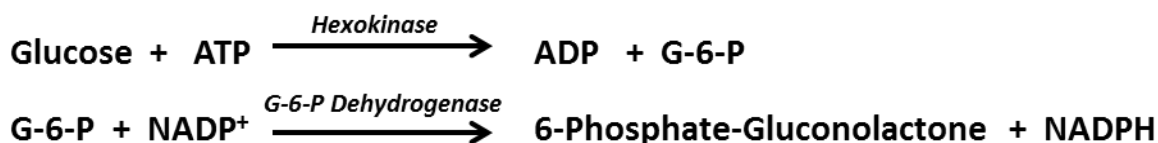
The reagent cocktail (Table 3.5) was pipetted into 96 well plates and the plates were incubated for 30 minutes before the first reading without any samples. Following this, 5µL of reagent blank, lactate standard or sample were pipetted into the plate and incubated at room temperature for 60 minutes before the second reading.

Table 3.5. Reagent cocktail for lactate metabolite analysis

Reagent	Final Concentration
Hydrazine	100mM
Glycine	100mM
NAD ⁺	0.5mM
Phosphoenolpyruvic acid	0.1mM
LDH	25mg/mL

Glycogen

Glycogen content was determined in samples using a two-step enzymatic process:



Following generation of the standard curve, 5µL of reagent blank, glucose standard or sample were pipetted into 96 well plates in addition to the reagent cocktail (Table 3.6) and the first reading was measured. The second reading was recorded following the addition of dilute hexokinase and a 60 minute incubation at room temperature.

Table 3.6. Reagent cocktail for glycogen metabolite analysis

Reagent	Final Concentration
Tris buffer	50mM
Magnesium chloride	1mM
Dithiothreitol	0.5mM
ATP	0.3mM
NADP ⁺	50µM
G-6-P Dehydrogenase	-

Oxygen (O₂) radical production

Superoxide (O₂⁻)

Uncoupled respiration results in the loss of electrons that can interact with O₂ and form O₂⁻ anions. Elevated production of this ROS can be detrimental to cellular function and can be measured by the superoxide indicator MitoSOX Red (Molecular Probes). MitoSOX is selective to mitochondria and fluoresces red when oxidised by mitochondrial O₂⁻. Teamed with a MitoTracker Green dye, O₂⁻ production, per volume of mitochondria, can be measured/assessed.

One hundred µL of isolated FDB fibres were plated onto a matrigel coated 96 well microplate (all samples were run in triplicate) and confluency was determined using a light microscope. If ~60% of the well bottom was not covered by isolated FDB fibres, an additional 50µL aliquot of fibres was dispensed into the well. For wells that did not receive the additional 50µL of fibres, 50µL of incubation media was added and the microplate was incubated overnight.

Five minutes prior to the addition of the MitoTracker dyes, antimycin A (final concentration of 3µM) was added the positive control wells. Antimycin A inhibits complex III, inducing reverse electron flow along the ETC which culminates in O₂⁻ production at complex I, to drive maximal MitoSox fluorescence. Following this, MitoSOX (final concentration of 5µM) in HBSS/Ca²⁺/Mg²⁺ buffer (10mM HEPES, 150mM NaCl, 5mM KCl, 1mM MgCl, 1.8mM CaCl₂, pH 7.4) was added to each well and incubated at 37°C for 30 minutes. MitoSOX was removed and fibres were counterstained with MitoTracker Green (as described in “*Assessment of mitochondrial viability*” (p111)). Fibres were then washed twice with Flurobrite and

imaged on an inverted microscope (Olympus, Tokyo, Japan) using FITC and TRITC filters and a standardised exposure time. The intensity of red and green fluorescence of each image was analysed using ImageJ software.

Hydrogen peroxide (H_2O_2)

H_2O_2 emission was simultaneously measured throughout the SUIT protocol via optical sensors (Oroboros O2k-Fluorescence LED-2 Module, Anton Paar, Graz, Austria). H_2O_2 emission was quantified via the reaction with Amplex UltraRed (25 μ M; Molecular Probes, Invitrogen) and horseradish peroxidase (2.5 U.mL⁻¹) at 525nm wavelength. Superoxide produced during the SUIT protocol was converted to H_2O_2 via the addition of superoxide dismutase (2.5U.mL⁻¹, Sigma Aldrich).

Peroxynitrite ($ONOO^-$)

Increased NO production can lead to formation of reactive nitrogen species during oxidative stress. The combination of a O_2^- anion with NO produces $ONOO^-$ a radical that initiates the nitration of tyrosine residues in proteins which mediates damage. As NITR supplementation increases NO availability and oxidative stress is a feature of dystrophic muscle, $ONOO^-$ levels were indirectly measured through 3-nitrotyrosine, a product of $ONOO^-$ nitration of proteins.

Embedded TA's were sectioned as described in "*Sample preparation*" (p122) and fixed with 4% formaldehyde for 30 minutes at room temperature. After incubation with blocking serum (0.1M PBS, 0.1% triton X-100, 10% donkey serum) for 1 hour at room temperature, sections were then labelled with primary anti-3-nitrotyrosine antibody (rabbit, 1:200) overnight at room temperature. After washing three times with a 0.1M PBS and 0.1% triton X-100 solution, samples were

incubated with the secondary antibody (anti-rabbit Alexa Fluor 647, 1:100, Abacus ALS, UK) for 2 hours at room temperature. A pan nuclei marker DAPI (4',6-diamidino-2-phenylindole) was added to the tissue sections and incubated for 2 minutes at room temperature, tissues were washed three times with a 0.1M PBS and 0.1% triton X-100 solution and mounted with fluorescent mounting medium.

Confocal microscopy was performed at excitation wavelengths of 640nm for Alexa 647 and 406nm for Alexa 405. Eight random images (20x magnification, total 2mm² area) from each animal were captured and the microscope was calibrated to standardise the minimum baseline fluorescence for imaging nitrotyrosine immunoreactivity. Images were analysed using ImageJ software to determine the number of DAPI positive nuclei and nitrotyrosine positive fibres.

Nuclear factor (erythroid-derived 2)-like 2 (Nrf2)

Recent observations that enhanced fumarate content can stimulate antioxidant gene upregulation through stimulation of Nrf2 (Ashrafian *et al.*, 2012) led us to investigate if ASA therapy had a similar effect. Nrf2 was assessed via semi-quantitative western blot analysis as outlined in section 3.1.3.2 (primary antibody, rabbit, 1:1000, Gene Signalling, 12721; secondary, 1:5000, Vector Laboratories, PI-1000).

3.1.4 Immunolabelling and histology

3.1.4.1 Immunolabelling of dystrophin-associated proteins

Dystrophin and dystrophin-associated proteins were assessed in both the NITR and ASA studies. Dystrophin-deficiency was confirmed in the *mdx* mouse and assessed in NITR and ASA supplemented samples to assess if either NITR or ASA therapy is a genetic modifier of dystrophin expression. The ablation of dystrophin from the sarcolemma results in the secondary loss of nNOS. Therefore, we utilised nNOS staining to assess if increased NO availability through nitrate supplementation can modulate nNOS protein expression. Finally, utrophin expression was assessed in the ASA study. The capacity for *mdx* muscles to escape cumulative damage and degeneration has been associated with increased utrophin expression. Therefore, we assessed if ASA has an effect on utrophin expression which may improve sarcolemmal integrity.

Sample preparation

Following excision, the right tibialis anterior (TA) was covered in optimal cutting temperature (OCT) compound (Sakura Finetek) and frozen in liquid nitrogen-cooled isopentane (Sigma Aldrich). Frozen muscles were stored at -80°C until required.

On the day of experimentation, embedded TA's were cryo-sectioned at -20°C on a cryostat microtome (Leica Microsystems, Wetzlar, Germany). TA'S were cut at the mid-belly of the muscle using a scalpel and one half was mounted onto a chuck using OCT. $10\mu\text{m}$ transverse sections were mounted onto glass slides (Menzel-

Glaser, Braunschweig, Germany) and fixed for 5 minutes using the Cytofix/Cytoperm Plus kit (BD Biosciences).

After incubation with blocking serum (0.1M PBS, 0.1% triton X-100, 10% FBS) for 1 hour at room temperature, sections were then labelled with the primary antibody (dystrophin and nNOS from Abcam, utrophin from Santa Cruz Technology, Table 3.7) overnight at room temperature. After washing three times with a 0.1M PBS and 0.1% triton X-100 solution, samples were incubated with the secondary antibody (Jackson ImmunoResearch, Table 3.7) for 2 hours at room temperature. Tissues were washed three times with a 0.1M PBS and 0.1% triton X-100 solution and mounted with fluorescent mounting medium (DAKO, Australia). Slides were dried overnight in a container to prevent photo-bleaching.

Microscopy

Confocal microscopy was performed on an Eclipse Ti confocal laser scanning system (Nikon, Tokyo, Japan). Fluorophores were visualized using a 488 nm excitation filter for Alexa 488 or FITC and a 559 nm excitation filter for Alexa 594 or Rhodamine Red. Z-series images were acquired at a nominal thickness of 0.5µm (512x512 pixels). The intensity of dystrophin and nNOS fluorescence was measured with ImageJ software from eight randomly captured images (total area size 2mm²) per animal at 20x magnification (Figure 3.8).

Table 3.7. Antibody details for immunolabelling.

Primary Antibody	Dilution	Incubation Time	Secondary Antibody	Dilution	Incubation Time
rabbit anti-dystrophin	1:400	Overnight	donkey anti-rabbit Alexa 488	1:200	2 hours
goat anti-nNOS	1:200	Overnight	donkey anti-goat Alexa 594	1:200	2 hours
goat anti-utrophin	1:200	Overnight	donkey anti-goat Alexa 488	1:100	2 hours

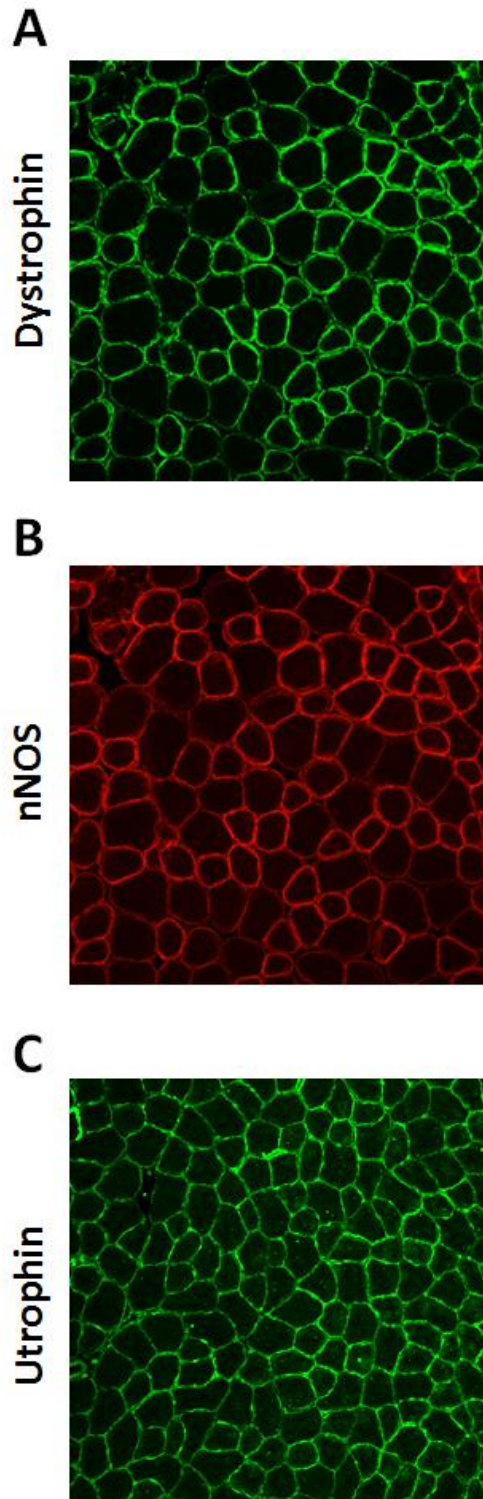


Figure 3.8. Representative images of immunohistochemical analysis of TA. Representative images of dystrophin (A), nNOS (B) and utrophin (C) in CON UNSUPP TA. .

3.1.4.2 Histology

Sample preparation and microscopy

Embedded TA's were prepared as outlined in section "*Sample preparation*" (p122) but were not fixed. Images were captured either using the Zeiss Axio Imager Z2 microscope (Carl Zeiss MicroImaging GmbH, Germany) at 20x magnification or on an inverted microscope (Olympus, Tokyo, Japan) at 4x magnification using a standardised exposure time. For each slide, three random images were taken in a blinded fashion.

Haematoxylin & Eosin (H&E)

Slides were stained using a standard H&E staining protocol as outlined in Table 3.8 and mounted with DPx (BDH, Poole, UK; Figure 3.9). To determine mean fibre size and frequency distribution of fibre size, 200 fibres (or as many whole fibres in the image) were individually circled on the three random images of each slide on a Microsoft Surface tablet using ImageJ. If there was not 200 fibres in the image, all of the whole fibres in the image were circled. Damaged area, as indicated by areas of mass nuclei infiltration, were traced and % of damaged area was calculated using the total area of muscle. Finally, of all the measured fibres, centronucleated fibres were counted to determine % of regenerating fibres (Shavlakadaze *et al.*, 2004).

Table 3.8. Protocol utilised for Haematoxylin & Eosin staining of TA

Solution	Time
100% ethanol	2 mins
90% ethanol	2 mins
Tap water	30 secs
Hematoxylin	30 secs
Tap water	30 secs
Tap water	Rinse
Scott's tap water	1 min
Eosin (1%)	1 min 45 secs
Tap water	1 min
100% ethanol	1 min
100% ethanol	1 min
Histolene	4 mins

Oil Red O (ORO)

Lipid infiltration and accumulation in dystrophic muscle is a characteristic of disease progression. In studies by Bonsett (Bonsett and Rudman, 1984, Bonsett and Rudman, 1992), ASA administration significantly reduced lipid production and therefore we employed ORO (Abcam) staining to assess the effect of ASA supplementation on lipid infiltration and accumulation in dystrophic muscle.

Slides were stained using an ORO protocol as outlined in Table 3.9 and mounted with 10% glycerol in PBS. Analysis was performed in two ways: (1) counting ORO-positive fibres in 3 random sections of the sample and (2) quantifying staining intensity of the whole muscle. Both analyses were performed on ImageJ.

Table 3.9. Protocol utilised for Oil Red O staining of TA

Solution	Time
3.7% formaldehyde	60 mins
Milli Q	1 min 30 secs
Oil Red O	30 mins
Milli Q	1 min 30 secs
Haematoxylin	45 secs
Tap water	Rinse

Alizarin Red

The loss of dystrophin from the sarcolemma leads to overwhelming Ca^{2+} accumulation in dystrophic fibres which stimulates a myriad of damage pathways. Therefore, Ca^{2+} content of muscle fibres from the TA was assessed using Alizarin Red (TMS-008-C, Merck Millipore), a dye which chelates with calcium to form Alizarin Red S- Ca^{2+} complexes. Slides were stained as outlined in Table 3.10 and mounted with DPx. Staining intensity of three random areas was assessed on ImageJ.

Table 3.10. Protocol utilised for Alizarin Red staining of TA

Solution	Time
Alizarin Red	2 mins
100% Acetone	20 dips
1:1 Acetone-Xylene	20 dips
Xylene	1 min

Succinate Dehydrogenase (SDH)

As mitochondrial oxidative capacity is affected in DMD, we assessed the oxidative nature of TA muscle fibres to elucidate if ASA supplementation has an effect through the activity of SDH. SDH is an enzyme located in the mitochondria that oxidises succinate to fumarate. This reaction, in the presence of nitro blue tetrazolium, is demonstrated by the formation of a blue-purple product with fibres more intensely coloured indicating highly oxidative fibres.

Slides were incubated in working solution (0.05M sodium succinate, 0.05M PBS, 0.05% nitro blue tetrazolium, pH 7.6, Sigma Aldrich) for 60 minutes at 37°C, fixed in formal saline (0.9% NaCl, 10% formaldehyde, Sigma Aldrich) and mounted with glycerol jelly (Sigma Aldrich, Table 3.11). Analysis was performed by quantifying the staining intensity of the whole muscle on ImageJ.

Table 3.11. Protocol utilised for SDH staining of TA

Solution	Time
SDH working solution	60 mins
Milli Q	Wash
Formal saline	10 dips
Milli Q	Wash

Gomori Trichrome

Since connective/fibrotic tissue infiltration occurs as DMD progresses, we assessed the presence of connective/fibrotic tissue within the muscle using a Gomori Trichrome (LG) stain (HT10316, Sigma Aldrich). Gomori Trichrome stain distinguishes three muscle components: (1) muscle (red/pink), (2) nuclei (blue/black) and (3) collagen (green-blue).

Slides were stained as outlined in Table 3.12 and mounted with DPx. The intensity of red (muscle), blue (nuclei) and green (collagen) staining of three random areas of each image was analysed using an automated RGB histogram on ImageJ. The proportion of green staining (fibrotic area) was calculated as a percentage of total RGB staining (Lee *et al.*, 2013).

Table 3.12. Protocol utilised for Gomori Trichrome staining of TA.

Solution	Time
Haematoxylin	1 min
Tap water	Wash
Gomori Trichrome stain	30 secs
Tap water	20 dips
0.2% acetic acid	20 dips
95% ethanol	30 secs
95% ethanol	30 secs
100% ethanol	30 secs
100% ethanol	30 secs
Xylene	1 min

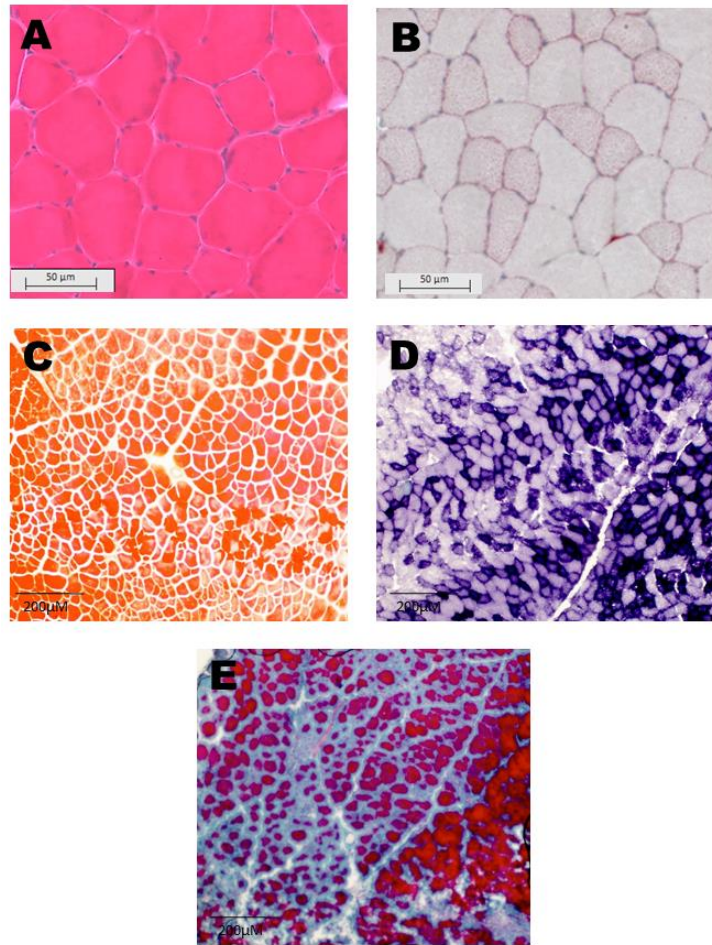


Figure 3.9. Representative images of histological analysis. Representative images of H&E (A), ORO (B), Alizarin Red (C), SDH (D) and Gomori Trichrome (E).

3.2 Cell experiments

Cell culture experiments were performed for further investigation of the acute metabolic effects of ASA and nitrate. In the following experiments, sodium nitrite was utilised *in lieu* of nitrate to overcome any limitations in the conversion of nitrate to nitrite (and finally to NO) as this conversion process is generally performed by the commensal bacteria. Therefore, we administered nitrite in the following cell experiments, as it is a known NO donor (Hindley *et al.*, 1997).

Immortalised human skeletal muscle cell lines were generously donated by Drs. Vincent Mouly and Gillian Butler-Browne of the Institut de Myologie (Paris, France) via Dr. Jason White (Murdoch Children's Research Institute, Melbourne, Australia). Dystrophin-positive (CON) muscle cells were derived from the paraspinal muscles of a 12 year old female and the dystrophin-negative (DMD) muscle cells derived from the fascia-lata of a 10 year old male with a deletion in exon 52 of the dystrophin gene. These human skeletal muscle cells were immortalised via transfection of the telomerase gene.

For all assays, excluding the determination of ASA and nitrite dosages and mitochondrial respiration assay, 3 time-points were utilised (24 hours, 3 days and 7 days of supplementation). This was performed to assess the acute effects of ASA and nitrite treatment.

3.2.1 Cell culture maintenance

Both CON and DMD cells were grown and maintained in growth medium containing low glucose 199 media (1:5, Gibco 11150059), high glucose Dulbecco's modified eagle medium (DMEM) (4:5, Gibco 10566016), fetuin (25µg/mL; Sigma Aldrich F2379), human epidermal growth factor (5ng/mL; Sigma Aldrich E9644), basic human fibroblast growth factor (0.5ng/mL; Sigma Aldrich F0291), insulin (5µg/mL; Sigma Aldrich I5500), dexamethasone (0.2µg/mL; Sigma Aldrich D4902), gentamycin (50µg/mL; Gibco 15750060) and FBS (20%; Bovogen Biologicals). Cells were seeded at 90-100,000 cells per well of a 24 well cell culture plate and passaged every 3 days. All cell experimentation was performed on undifferentiated myoblasts.

3.2.2 Determination of ASA and nitrite dosages

Assays were performed in CON myoblasts to establish the maximum tolerable dose of both ASA and nitrite to be utilised in all cell culture experiments. For both ASA and nitrite, a range of concentrations between 10nM and 1mM were investigated. Two methods were employed to determine the optimal concentration: (1) crystal violet staining, which binds to DNA to indicate cell viability and (2) real-time monitoring of cell proliferation using the xCELLigence Real Time Cell Analysis (RTCA) system (ACEA Biosciences, San Diego, CA).

3.2.2.1 Crystal violet assay

CON myoblasts were grown for 4 days in either media only, media with milli Q (MQ; vehicle) or increasing concentrations of ASA or nitrite. Cells were washed with PBS and then incubated with 0.1% crystal violet solution for 10 minutes. The staining

solution was removed and 1% SDS was added to solubilise the stain. Absorbance was read at 570 nm on an X-Mark Microplate Reader (Bio-Rad Laboratories, Australia) with a higher absorbance indicating higher cell viability.

3.2.2.2 Cell proliferation assay

The xCELLigence RTCA MP system is a non-invasive and label-free method used to quantify cell viability through calculation of the Cell Index. The Cell Index is determined by the measurement of electrical impedance across the microelectrodes on the bottom of the 16 well E-plates and therefore changes in cell adherence and proliferation are reflected by the Cell Index. For example, during the initial adhesion of cells to the bottom of the plate, electrical impedance across the microelectrodes increases significantly. This is reflected by a rapid increase in the Cell Index. In contrast, the detachment of cells from the plate due to cellular death is reflected by a significant decrease in the Cell Index. This occurs as the electrical impedance of the microelectrodes is reduced. This method overcomes limitations to other cell viability assays as it is non-invasive, does not require addition of reagents and the measurement of electrical impedance occurs in real-time within the incubator environment, without experimental interference.

CON myoblasts were seeded at a density of 5000 cells per well and plates were inserted into the xCELLigence RTCA MP system. Cells were allowed to adhere for 24 hours, after which time 50 μ L of either media only, media with MQ or increasing concentrations of ASA or nitrite were added. The Cell Index was measured every 30 minutes for 4 days.

3.2.3 Determination of mitochondrial viability

Mitochondrial viability was assessed by the same method employed in “*Assessment of mitochondrial viability*” (p111). CON and DMD myoblasts were seeded at a density of 5000 cells per well and either 1mM of ASA or nitrite was added to the wells. Plates were left to incubate for either 24 hours, 3 days or 7 days with media replaced every 3 days. The same protocol was followed as in section “*Assessment of mitochondrial viability*” (p111) however the positive controls were left to incubate for 15 minutes before the addition of the MitoTracker dyes.

3.2.4 Determination of mitochondrial O_2^- production

Mitochondrial O_2^- production was assessed by the same method employed in “*Superoxide (O_2^-)*” (p119) CON and DMD myoblasts were seeded at a density of 5000 cells per well and either 1mM of ASA or nitrite was added to the wells. Plates were left to incubate for either 24 hours, 3 days or 7 days with media replaced every 3 days.

3.2.5 Mitochondrial & glycolytic metabolism using the Extracellular Flux Analyser

Mitochondrial respiration and glycolytic flux was assessed using the Extracellular Flux Analyser as outlined in “*Mitochondrial & glycolytic metabolism using the Extracellular Flux Analyser*” (p101) with some minor modifications. On gelatin-coated (0.5%) Seahorse XF24 cell culture V7 microplates, CON (25,000 cells per well) and DMD myoblasts (15,000 cells per well) were seeded and incubated with 250 μ L of

either 1mM ASA or nitrite for 24 hours. Myoblasts were seeded at different densities due to the observation that 25,000 DMD myoblasts per well depleted O₂ in the wells and therefore affected the measurement of OCR. Thus, after experiments to determine optimal seeding density (data not shown), 15,000 myoblasts per well was determined to be the highest number of cells possible with inducing O₂ depletion. In addition, CON seeding density could not be reduced to match DMD myoblasts as the OCR would be lower than required. Following the 24 hour incubation period, 200µL of media was removed from each well and replaced with 1000 µL of pre-warmed assay buffer (DMEM XF assay media (Seahorse Bioscience, 102365-10), 25mM glucose and 1mM sodium pyruvate; pH 7.4) to wash the cells of any growth media. 1000 µL was removed from each well and replaced with 625 µL of assay buffer to give a final volume of 675 µL per well. 675 µL of assay buffer was added to the background control wells and the microplate was returned to a non-CO₂ incubator for 1 hour for pH and temperature equilibration.

To a pre-hydrated XF24 Sensor Cartridge, 50µL of oligomycin (30µM) was added to injection port A (to give a final assay concentration of 3 µM), 55µL of FCCP (30µM) was added to injection port B (to give a final assay concentration of 3µM) and 60µL antimycin A (10µM) and rotenone (20µM) was added to injection port C (to give a final assay concentration of 1µM and 2µM, respectively). The loaded Sensor Cartridge was incubated at 37°C for 10 minutes and then inserted into the XF24 Analyser for calibration. Once calibration was completed, the loaded microplate was inserted into the XF24 Analyser and the mitochondrial stress test was commenced (refer to Table 3.1 for complete protocol). The OCR and ECAR readings from the various respiratory states were analysed as described in “*Derivation of data*” (p108).

3.3 Statistical analysis

All results are presented as mean \pm standard error of the mean in the text, tables and figures. Two-way ANOVA was utilised to detect between strain (animal and cell) and supplementation differences and a three-way ANOVA was utilised to detect between strain, supplementation and GU type (basal vs contraction) differences. When a main effect or an interaction was detected, unpaired T-tests were used to determine differences between individual groups using SPSS (version 21). An α value of 0.05 was considered significant.

Part One

Nitrate/Nitrite Therapy

Chapter Four

Evaluation of Nitrate Therapy in the *mdx* Mouse

Publications from this chapter:

1. **Timpani et al.** Attempting to compensate for reduced nNOS protein with nitrate supplementation cannot overcome metabolic dysfunction but rather has detrimental effects in dystrophin-deficient *mdx* muscle, Under Review in *Neurotherapeutics*
2. **Timpani et al.** (2015) Glucose uptake & mitochondrial function following 8 weeks of dietary nitrate supplementation in the dystrophin-deficient *mdx* mouse. *Neuromuscular Disorders Supplement: World Muscle Society Proceedings*, 25(2).

Presentations from this chapter:

1. **Timpani et al.** (2015). Glucose uptake & mitochondrial function following 8 weeks of dietary nitrate supplementation in the dystrophin-deficient *mdx* mouse. Melbourne, Victoria, Australia. **Poster** presentation at The Australian Society for Medical Research Victorian Student Symposium.
2. **Timpani et al.** (2015). Glucose uptake & mitochondrial function following 8 weeks of dietary nitrate supplementation in the dystrophin-deficient *mdx* mouse. Brighton, England. **Poster** presentation at the 20th World Muscle Society Conference.

4.1 Introduction

DMD is a progressive X-linked (Monaco *et al.*, 1985) neuromuscular disease affecting 1 in 3,500 live male births (Emery, 1991), which arises from the ablation of the cytoskeletal protein, dystrophin (Hoffman *et al.*, 1987). Dystrophin deficiency causes alterations to the myofibre architecture leading to membrane lesions, Ca^{2+} accumulation, muscular weakness and cyclic bouts of degeneration and regeneration until the regenerative capacity of the muscle is unable to match demand for repair (Heslop *et al.*, 2000). Damaged muscle is eventually replaced with fibrous and/or fatty connective tissue leading to a decrease in muscle function, with cardiorespiratory failure ensuing by the third decade of life (Eagle *et al.*, 2002).

Mitochondrial and metabolic dysfunction have been increasingly implicated in the pathogenesis of DMD although it is not known if these abnormalities are associated with dystrophin deficiency, the pathophysiological sequelae caused by dystrophin deficiency, or completely independent of dystrophin deficiency (Timpani *et al.*, 2015). Indeed, the only obvious physical link between dystrophin and the intracellular metabolic pathways is via nNOS whereby ablation of dystrophin from the sarcolemma induces the secondary loss of the dystrophin-associated proteins (Ohlendieck and Campbell, 1991) including nNOS (Brenman *et al.*, 1995, Chang *et al.*, 1996). nNOS produces NO, a key signalling molecule in skeletal muscle that regulates various biological processes including blood flow, contraction, mass, satellite cell activation, Ca^{2+} handling and GU, in addition to mitochondrial metabolism, gene expression and ROS production (McConnell *et al.*, 2012). In dystrophic muscle, the dissociation of nNOS from the sarcolemma results in reduced nNOS content (Leary *et al.*,

1998, Thomas *et al.*, 1998, Vaghy *et al.*, 1998, Judge *et al.*, 2006), activity (Chang *et al.*, 1996, Kameya *et al.*, 1999, Li *et al.*, 2011) and NO production (Gücüyener *et al.*, 2000, Kasai *et al.*, 2004, Barton *et al.*, 2005). Importantly, this loss of nNOS has been shown to contribute to the progression of the dystrophic condition and to the deficits in metabolic function. For example, nNOS is a positive allosteric regulator of PFK, the rate limiting enzyme of the glycolytic pathway (Wehling-Henricks *et al.*, 2009), and therefore plays a critical role in regulating glucose metabolism. Interestingly, DMD is not only associated with impairments in glycolysis (Vignos Jr and Lefkowitz, 1959, Chi *et al.*, 1987, Wehling-Henricks *et al.*, 2009) but also in β -fatty acid oxidation, the TCA cycle and the electron transport system (ETS) (for detailed reviewed see (Timpani *et al.*, 2015)). Collectively, these metabolic impairments result in reduced energy production (Rybalka *et al.*, 2014), with reports of ATP content being 50% lower under resting conditions (Austin *et al.*, 1992, Cole *et al.*, 2002). Given that nNOS localisation and NO signalling are known to be important for metabolic control, the loss of nNOS and NO bioavailability might be key to metabolic deregulation in dystrophic skeletal muscle. Therefore, increasing NO availability has the potential to be of therapeutic benefit.

In an attempt to normalise NO production, several studies have reintroduced nNOS into dystrophic skeletal muscle which demonstrably reduces muscle damage and inflammation (Wehling *et al.*, 2001, Tidball and Wehling-Henricks, 2004). As gene therapy for nNOS transfection is not yet available in humans, other strategies to restore NO availability have been investigated. Several studies have shown that supplementation with NO donors, often combined with anti-inflammatory drugs, results in reduced damage, necrosis

and inflammation and improved muscle blood flow, function/strength and repair (Voisin *et al.*, 2005, Brunelli *et al.*, 2007, Mizunoya *et al.*, 2011, Vianello *et al.*, 2014, Archer *et al.*, 2006, Uaesoontrachoon *et al.*, 2014, Thomas *et al.*, 2012, Anderson and Vargas, 2003) in dystrophin-deficient skeletal muscle. While these findings may suggest a positive effect of increasing NO availability, it is difficult to control the delivery of NO to the skeletal muscle with pharmacological donors and also to separate the effects of the NO donor from those of the anti-inflammatory co-treatment. Another approach to increase NO availability has been to supplement with the nNOS substrate, L-arginine (Barton *et al.*, 2005); however, the potential for L-arginine to increase NO production is limited by the lowered nNOS protein in dystrophic skeletal muscle. An alternative method to increase NO availability, that is independent of nNOS activity, is supplementation with nitrate (NITR). Specifically, dietary NITR can be reduced to nitrite by commensal bacteria of the oral cavity and gastrointestinal tract, with nitrite being subsequently reduced to NO via several enzymatic pathways in the blood and tissues (Lundberg *et al.*, 2008). This mechanism is complementary to NOS-derived NO production and, importantly, represents a pathway that could be exploited to increase NO availability in dystrophic muscle.

To date, no studies have investigated the effect of NITR supplementation on metabolic function in dystrophic muscle; however, recent studies suggest that NITR supplementation has the potential to improve metabolic function in skeletal muscle. For example, Larsen *et al.* demonstrated that NITR supplementation in healthy, young males led to increased plasma NO concentration and subsequently, downstream metabolic adaptations including increased mitochondrial efficiency, reduced proton leak and ultimately

increased ATP production capacity (Larsen *et al.*, 2011). Similar data has been derived in mice during fatty acid oxidation (Ashmore *et al.*, 2015). In addition, there is some evidence that NITR supplementation can increase exercise efficiency in humans (Bailey *et al.*, 2009, Larsen *et al.*, 2007, Bailey *et al.*, 2010) and exercise capacity in some disease conditions such as peripheral arterial disease, where NO production is reduced (Kenjale *et al.*, 2011). Most pertinently, increasing NO bioavailability through administration of sodium nitrite mitigates functional ischemia in Becker Muscular Dystrophy patients (Nelson *et al.*, 2015) suggesting that expansion of the NITR-nitrite-NO pool in DMD may also be beneficial. The results from these studies prompted us to investigate whether increasing NO availability via NITR supplementation, which has been previously proven to increase plasma (Larsen *et al.*, 2011, Carlström *et al.*, 2010) and skeletal muscle (Ashmore *et al.*, 2015) NO levels and elicit beneficial mitochondrial adaptations at the skeletal muscle level (Larsen *et al.*, 2011, Carlström *et al.*, 2010), would improve mitochondrial function and rectify energy homeostasis dysregulation in dystrophic muscle. Therefore, we investigated whether an established dietary NITR supplementation regimen (Carlström *et al.*, 2010) could improve GU, mitochondrial function, ROS emission and muscle architecture in healthy (control; CON) and dystrophic (*mdx*) mouse models. We hypothesised that NITR supplementation would (1) increase GU in the contracting muscles from CON and *mdx* mice; (2) improve mitochondrial function in *mdx* mice and; (3) improve the muscle architecture of *mdx* mice.

4.2 Methods

4.2.1 Ethical approval

All experimental procedures were approved by the Victoria University Animal Ethics Experimentation Committee and conformed to the Australian Code of Practice for the Care and Use of Animals for Scientific Purposes.

4.2.2 Animals and supplementation

Three week-old male C57Bl/10ScSn (normal wild-type strain; CON; n=32) and C57Bl/10*mdx* (*mdx*; n=32) mice were randomly assigned into four groups: unsupplemented (CON UNSUPP (n=16) and *mdx* UNSUPP (n=16)) and supplemented (CON NITR (n=16) and *mdx* NITR (n=16)). Mice in the supplemented groups were given 85mg.L⁻¹ (1mM) sodium NITR (Carlström *et al.*, 2010) *ad libitum* in drinking water for 8 weeks and mice in the unsupplemented groups were given drinking water without NITR. The dose of NITR is comparable to doses studied in human experiments, is achievable through a normal diet (Hernández *et al.*, 2012), and is proven to increase the plasma NITR-nitrite-NO pool (Carlström *et al.*, 2010, Larsen *et al.*, 2011).

4.2.3 Muscle dissection and contraction protocol

White EDL and red SOL muscles were surgically extracted in deeply anaesthetised mice and placed into individual muscle baths containing Krebs basal buffer bubbled with carbogen (95% O₂, 5% CO₂) at 30°C. Optimal length (L₀) for each muscle was determined using a custom built muscle analysis system and the left EDL and SOL were then stimulated to contract for a total of

10 minutes (pulse durations of 350msec and 500msec for EDL and SOL, respectively at a frequency of 60 Hz).The right EDL and SOL were not stimulated in order to measure basal GU. See section 3.1.2.1 for more detail.

4.2.4 Glucose uptake (GU)

Following 5 minutes of contraction, the Krebs basal buffer was exchanged for Krebs buffer with 2-Deoxy-D-[1,2-³H]glucose (0.128 μ Ci/mL) and D-[¹⁴H]mannitol (0.083 μ Ci/mL) in both resting and contracting muscles. At the end of the 10 minute contraction protocol, muscles were immediately submerged in ice-cold Krebs basal buffer to stop further GU. Radioactivity and GU was calculated as previously in section 3.1.2.2.

4.2.5 Mitochondrial respiration and hydrogen peroxide (H₂O₂) emission measurements

Muscle fibres from white and red portions of the gastrocnemius were mechanically separated and agitated to permeabilise the sarcolemma to allow diffusion of subsequent assay substrates. ETS respiration, OXPHOS and H₂O₂ emission were measured by the Oxygraph O2k high resolution respirometer (Oroboros Instruments, Innsbruck, Austria) via a SUIT protocol at 37°C as described in section 3.1.3.

4.2.6 Western blot analysis of mitochondrial respiratory chain proteins

Mitochondrial respiratory chain proteins were analysed in homogenised gastrocnemius samples as described in section 3.1.3.2. Images were captured on a DARQ CCD camera mounted to a Fusion FX imaging system and once the

images were captured, the membranes were stained with Coomassie Blue to verify equal loading of total protein in all lanes.

4.2.7 Citrate Synthase (CS) Activity

Homogenised RG and WG samples were utilised to measure CS activity as described in section 3.1.3.2. CS activity was calculated using the extinction coefficient of 13.6 (Srere, 1969) and CS activity was normalised to whole muscle protein concentration.

4.2.8 Histological Analysis

Embedded TA's were cryo-sectioned (10µm) at -20°C using a Leica (CM1950) cryostat and mounted onto glass slides (Menzel-Glaser).

4.2.8.1 Dystrophin, nNOS and nitrotyrosine immunolabelling

Dystrophin and nNOS immunolabelling was performed on fixed slides as described in section 3.1.4.1. Confocal microscopy was performed on an Eclipse Ti confocal laser scanning system (Nikon, Japan) and the intensity of dystrophin, nNOS and nitrotyrosine fluorescence was quantified using ImageJ software (NIH, USA).

4.2.8.2 Haematoxylin & Eosin Staining

Air-dried slides were using a haematoxylin and eosin (H&E) staining protocol described in section 3.1.4.2. Slides were imaged using a Zeiss Axio

Imager Z2 microscope at 20x magnification and images were analysed using ImageJ software.

4.2.9 Statistics

Results are presented as mean \pm standard error of the mean. Two-way ANOVA was utilised to detect between strain and supplementation differences. A three-way ANOVA was utilised to detect differences between strain, supplementation and GU type. When a main effect or an interaction was detected, unpaired T-tests were used to determine differences between individual groups using SPSS (version 21). An α value of 0.05 was considered significant.

4.3 Results

4.3.1 Effect of NITR supplementation on body weight, food and water consumption and muscle weights

Throughout the 8 week supplementation period, greater weight gains were observed in the *mdx* groups compared to CON ($p < 0.0001$; Figure 4.1), with NITR having no effect in *mdx* mice ($p > 0.05$). NITR did, however, stimulate weight gain in CON ($p < 0.05$). No significant difference in food or water consumption was observed between any group over the supplementation period (Figure 4.2A & B, respectively; $p > 0.05$) except at week two where food consumption was greater in CON UNSUPP compared to all groups ($p < 0.05$). Overall, individual hind limb muscle weights were greater in the *mdx* compared to CON strain ($p < 0.0001$; Table 4.1) with NITR having minimal effects ($p > 0.05$; except for right plantaris and lungs, $p < 0.05$).

4.3.2 Immunolabelling of dystrophin and nNOS

To confirm the deficiency of both dystrophin and nNOS in *mdx* skeletal muscle, the presence of dystrophin and nNOS protein (Figure 4.3) was determined in the TA. Indeed, dystrophin was only evident in CON TA (Figure 4.3A and C) and was absent from *mdx* TA ($p < 0.0001$ compared to CON). Similarly, nNOS was only evident in CON TA (Figure 4.3A^I and C^I) and was completely absent from dystrophin-deficient *mdx* fibres ($p < 0.0001$). Co-localisation of dystrophin and nNOS was only observed in CON (Figure 4.3A^{II} and C^{II}) and NITR had no effect on either dystrophin or nNOS staining ($p > 0.05$).

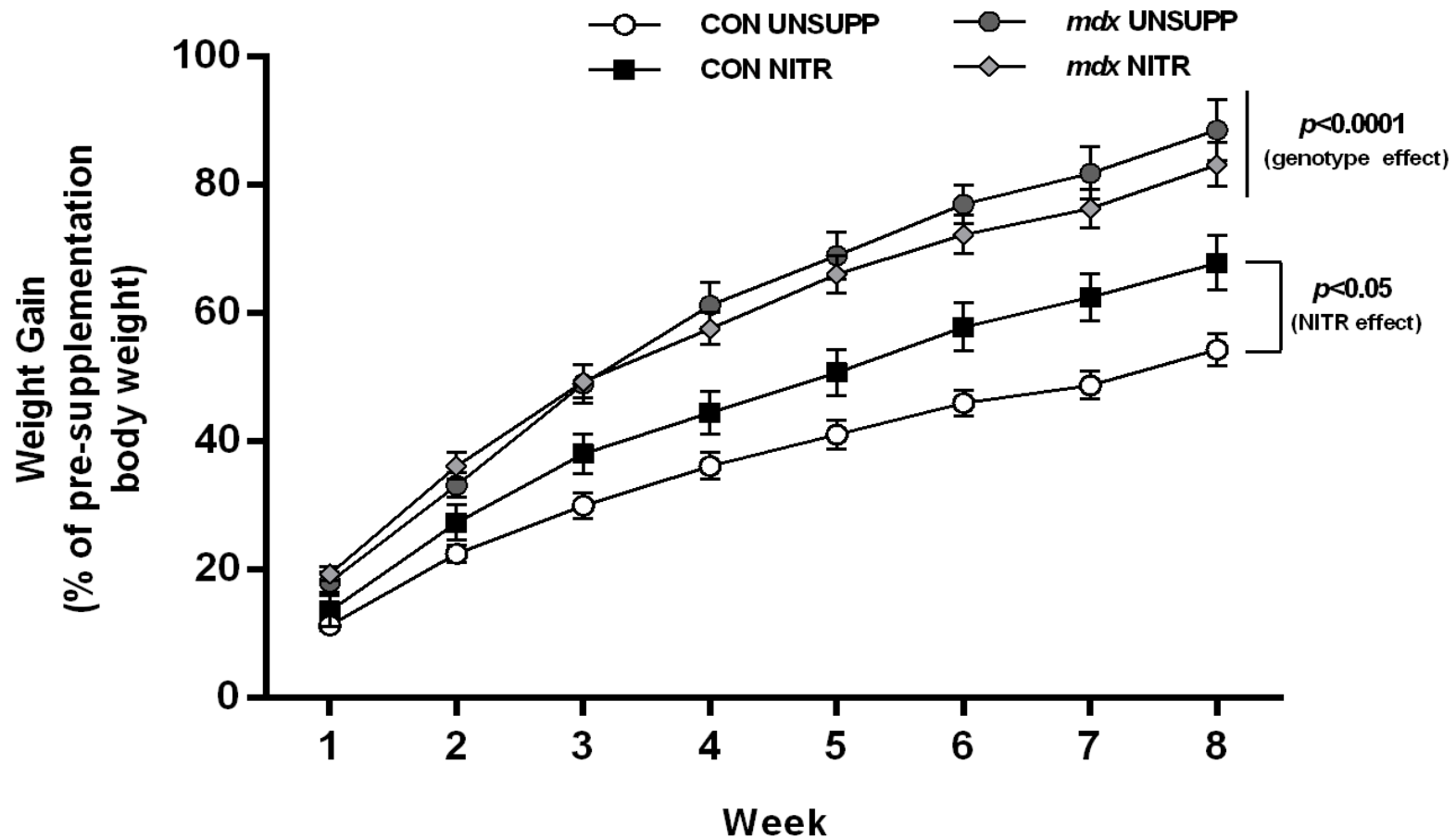


Figure 4.1. Body weight of unsupplemented (UNSUPP) and NITR-supplemented mice over the supplementation period. Changes in body weight are shown as a percentage of pre-supplementation weight. Overall, *mdx* mice gained more weight over the 8 week supplementation period compared to control (CON) ($p < 0.0001$). NITR had no effect on *mdx* weight gain but did increase weight gain in CON compared to CON UNSUPP ($p < 0.05$). $n = 14-16$ per group.

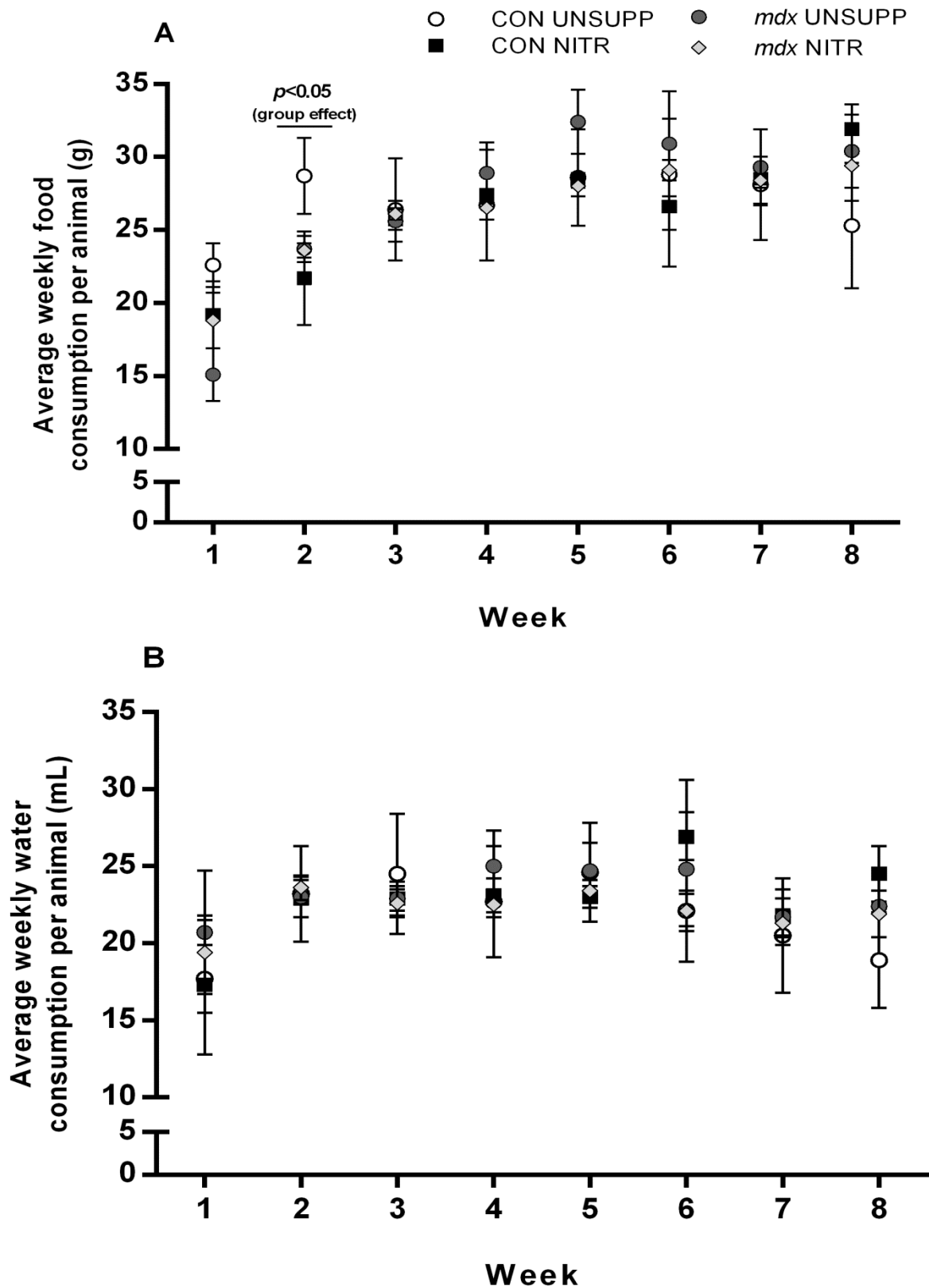
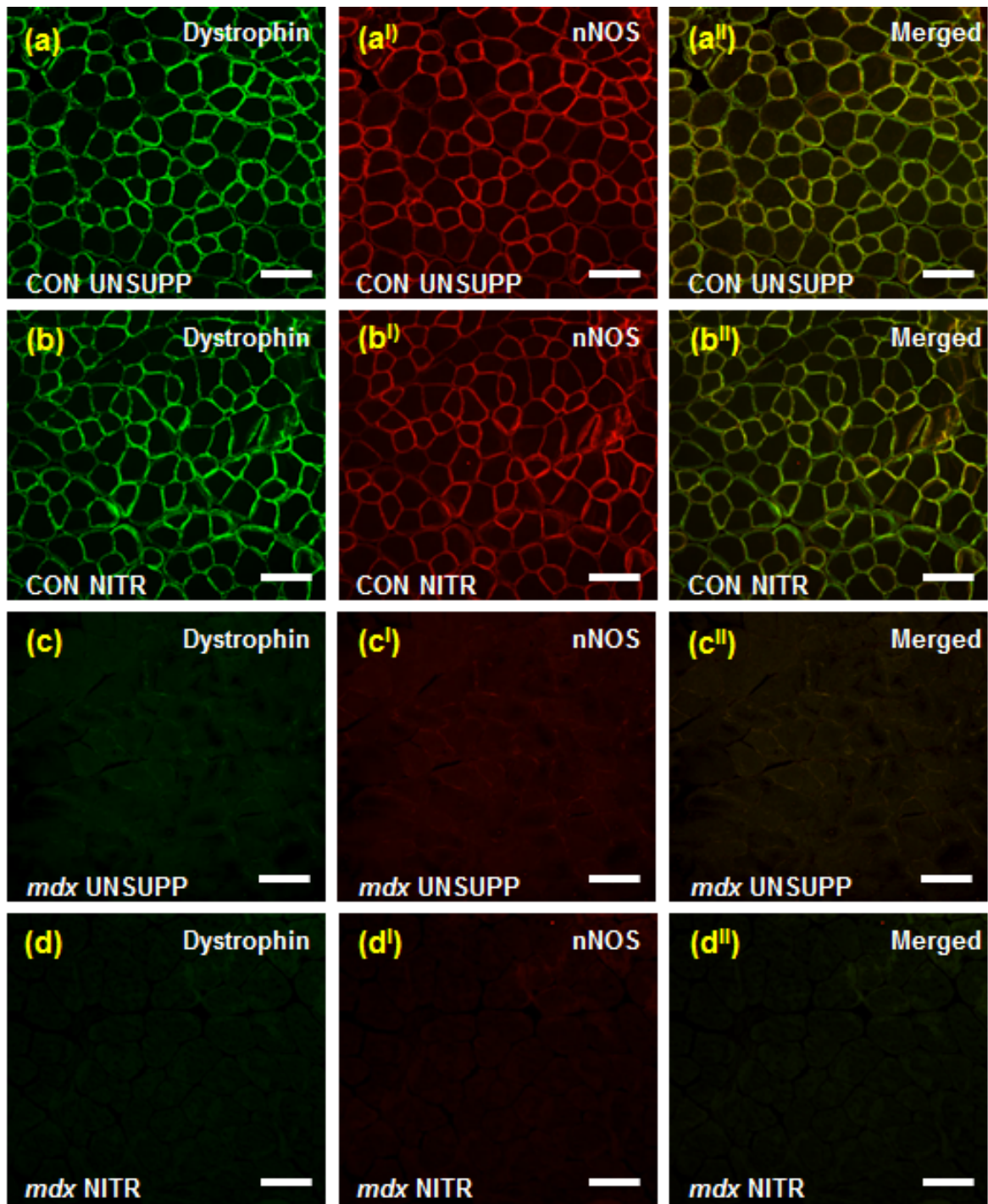


Figure 4.2. Average food and water consumption of unsupplemented (UNSUPP) and NITR supplemented mice over the supplementation period. Over the 8 week supplementation period, food and water consumption did not differ between unsupplemented and supplemented animals ($p > 0.05$) except for food consumption during week two where CON UNSUPP consumed more than all groups ($p < 0.05$). $n = 14-16$ per group.

Table 4.1. Weights of muscles and organs from unsupplemented and NITR supplemented mice over the supplementation period.

	CON		<i>mdx</i>		<i>p</i> values	
	UNSUPP	NITR	UNSUPP	NITR	Genotype	Supplement
Diaphragm	69.2 ± 5.36	65.36 ± 2.46	95.29 ± 6.2 ^^^^	96.65 ± 7.95 ^^^^	<0.0001	0.12416
EDL (L)	11.6 ± 1.1	11.34 ± 0.31	14.67 ± 0.83 ^^^^	14.77 ± 0.93 ^^^^	<0.0001	0.42482
EDL (R)	12.4 ± 1.22	12.57 ± 0.77	15.48 ± 1.38 ^^^^	16.1 ± 0.79 ^^^^	<0.0001	0.41849
Gastrocnemius (L)						
Red	18.9 ± 1.98	18.18 ± 1.03	16.84 ± 1.95	16.98 ± 1.31	0.15566	0.43008
White	126.3 ± 3.94	127.05 ± 2.99	153.32 ± 2.89 ^^^^	152.98 ± 3.47 ^^^^	<0.0001	0.46076
Gastrocnemius (R)						
Red	20.5 ± 1.85	19.58 ± 1.4	13.74 ± 1.62 ^^	14.87 ± 1.67 ^^	<0.01	0.25852
White	130.9 ± 4.76	126.35 ± 2.52	165.97 ± 4.28 ^^^^	159.88 ± 3.06 ^^^^	<0.0001	0.12507
Heart	143.58 ± 3.03	145.25 ± 2.74	138.37 ± 4.91 ^^	131.11 ± 2.55 ^^	<0.01	0.28402
Liver	1414.94 ± 44.56	1429.81 ± 34.44	1552.72 ± 56.95 ^^	1521.26 ± 45.4 ^^	<0.01	0.44240
Lungs	173.59 ± 4.94	183.66 ± 6.3 #	169.02 ± 5.84 ^	171.15 ± 2.28 ^#	<0.05	<0.05
Plantaris (L)	21.29 ± 1.44	20.77 ± 0.91	22.8 ± 0.92	21.18 ± 0.96	0.19290	0.17287
Plantaris (R)	18.15 ± 0.65	18.34 ± 0.65 #	21.11 ± 0.87 ^	21.55 ± 1.08 ^#	<0.05	<0.05
Quadriceps (L)	200.49 ± 6.52	200.9 ± 6.81	244.98 ± 8.82 ^^^^	249.58 ± 10.69 ^^^^	<0.0001	0.07543
Quadriceps (R)	184.62 ± 10.27	183.31 ± 7.25	246.63 ± 9.9 ^^^^	240.05 ± 12.11 ^^^^	<0.0001	0.33653
Soleus (L)	9.04 ± 0.98	10.34 ± 0.52	13.47 ± 1.33 ^^^^	13.65 ± 0.78 ^^^^	<0.0001	0.24223
Soleus (R)	9.78 ± 0.81	10.33 ± 0.58	14.9 ± 1.39 ^^^^	13.25 ± 0.63 ^^^^	<0.0001	0.35716
TA (L)	47.8 ± 2.13	47.51 ± 1.57	71.38 ± 2.29 ^^^^	67.42 ± 1.57 ^^^^	<0.0001	0.26890
TA (R)	46.89 ± 1.73	46.49 ± 1.46	68.89 ± 2.05 ^^^^	66.98 ± 2.4 ^^^^	<0.0001	0.35714

Overall, the weights of muscles and organs from *mdx* mice were different from control (CON) mice. All weights are expressed in mg. ^significant difference from CON mice $p < 0.05$; ^^significant difference from CON mice $p < 0.01$; ^^^significant difference from CON mice $p < 0.0001$; # significant difference from UNSUPP mice $p < 0.05$. $n = 12-16$ per group.



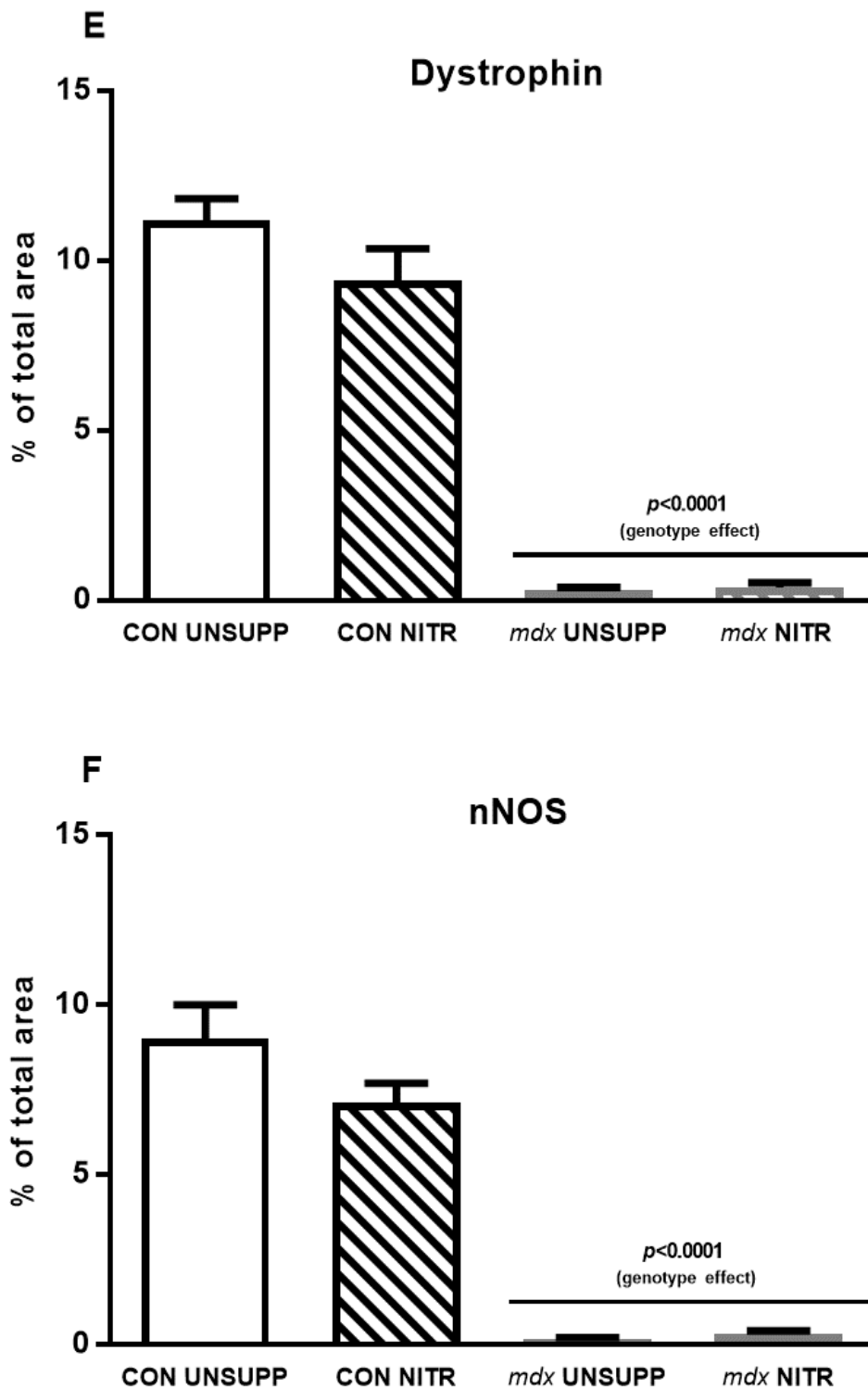


Figure 4.3. Proportion of dystrophin and neuronal nitric oxide synthase (nNOS) immunoreactivity in unsupplemented (UNSUPP) and supplemented control (CON) and *mdx* tibialis anterior (TA). Dystrophin (green) was evident in both CON UNSUPP (A) and CON NITR (B) but not in *mdx* UNSUPP (C) and *mdx* NITR (D) sections. Similarly, nNOS was only evident in CON UNSUPP (A^I) and CON NITR (B^I) but not in *mdx* UNSUPP (C^I) and *mdx* NITR (D^I) sections. Merged images A^{II} and B^{II} indicate co-localisation of dystrophin and nNOS in CON UNSUPP and CON NITR but not in *mdx* UNSUPP (C^{II}) and *mdx* NITR (D^{II}) sections. The proportion of dystrophin and nNOS was significantly higher in CON compared to *mdx* ($p < 0.0001$, E & F). NITR had no effect in either dystrophin (E) or nNOS (F) expression in CON or *mdx* mice. Scale bars= 100 μ m, $n = 3-4$ per group.

4.3.3 Effect of NITR supplementation on GU

NO has been proposed to play a role in contraction-stimulated GU and as such, we first investigated the effect of NITR supplementation on GU in CON and *mdx* muscles. This is the first instance of contraction-induced GU being measured in the *mdx* mouse and we demonstrated no difference in basal- or contraction-induced GU between CON and *mdx* UNSUPP EDL ($p>0.05$, Figure 4.4A). As expected, contraction induced an increase in GU in the EDL's of CON UNSUPP (55%), CON NITR (61%), *mdx* UNSUPP (35%) and *mdx* NITR (51%) compared to basal conditions ($p<0.05$, Figure 4.4A). NITR supplementation significantly increased contraction-induced GU in CON EDL muscles ($p<0.05$; Figure 4.4A) however in contrast, NITR reduced both basal- and contraction-induced GU in *mdx* muscles ($p<0.05$; Figure 4.4A). Contrary to the EDL, contraction did not stimulate further GU beyond that observed in basal conditions for any group in the SOL (all less than 20%, $p>0.05$, Figure 4.4B). While NITR had no effect on basal or contraction-induced GU in CON SOL muscles ($p>0.05$; Figure 4.4B), NITR further reduced both basal and contraction-induced GU in *mdx* SOL muscles ($p<0.05$). Combined, these data suggest that NITR supplementation has a negative effect on GU in both *mdx* EDL and SOL which may lead to impairments in downstream glycolysis and oxidative metabolism.

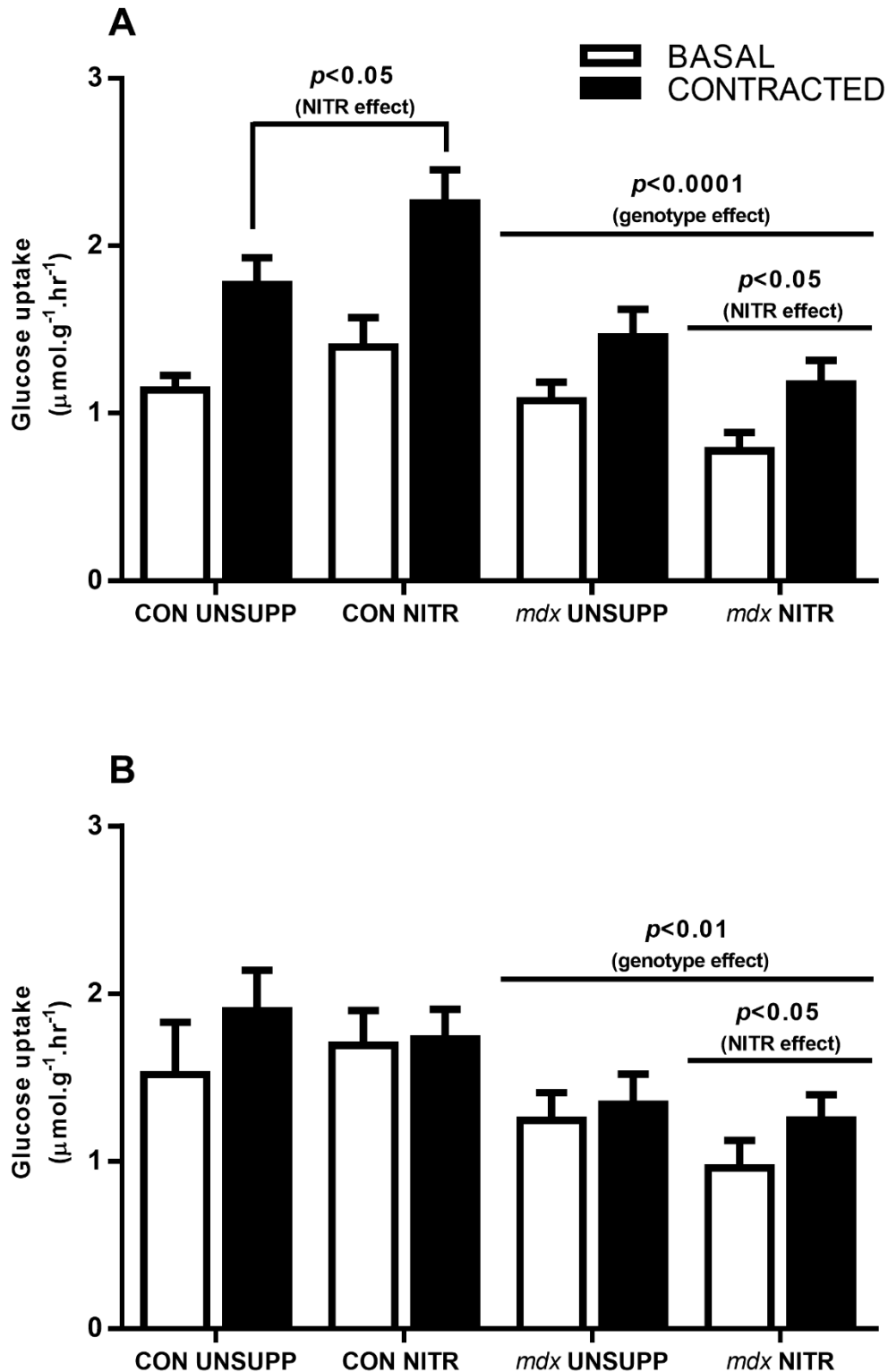


Figure 4.4. Glucose uptake (GU) in isolated extensor digitorum longus (EDL) and soleus (SOL) from unsupplemented (UNSUPP) and NITR supplemented control (CON) and *mdx* mice. In all groups, contraction-induced GU significantly compared to basal conditions ($p < 0.05$, A). NITR increased contraction-induced GU in CON EDL ($p < 0.05$) but in contrast, reduced both basal- and contraction-induced GU in *mdx* EDL ($p < 0.05$). For the SOL, both basal- and contraction-induced GU (B) were comparable ($p > 0.05$). NITR reduced basal GU in *mdx* SOL ($p < 0.05$) but had no effect in CON SOL. CON UNSUPP $n=9-13$; CON NITR $n=11$; *mdx* UNSUPP $n=11$; *mdx* NITR $n=10-12$.

4.3.4 Effect of NITR supplementation on mitochondrial function

4.3.4.1 Respirometry

Next, we examined the effect of NITR on parameters of mitochondrial function. First, we measured state 4 leak respiration which, in the absence of ADP, indicates the contribution of proton leak to respiration. In the presence of pyruvate and malate (CI), state 4 leak respiration was significantly lower in *mdx* white (WG) ($p < 0.05$; Figure 4.5A) and red gastrocnemius (RG) ($p < 0.01$; Figure 4.6A) muscles compared to their respective controls. In the presence of pyruvate, malate and succinate (CI+II), state 4 leak respiration was significantly higher than CI respiration across all groups, in both WG and RG muscles ($p < 0.0001$; Figure 4.5A and 4.6A, respectively). NITR supplementation had no effect on either CI or CI+II state 4 leak respiration in CON or *mdx* muscles (Figure 4.5A and 4.6A).

Next, the effect of NITR on coupled OXPHOS capacity was examined in WG and RG muscles by assessing maximal ADP-stimulated state 3 respiration in the presence of excess malate, pyruvate and succinate (complex I and II (CI+II) substrates). As shown in Figure 4.5, state 3 respiration was significantly depressed in *mdx* WG by ~20% ($p < 0.05$; Figure 4.5A) and in *mdx* RG by 25% ($p < 0.001$; Figure 4.6A) compared to CON. NITR supplementation, however, had no effect on State 3 respiration in either muscle (Figure 4.5A and 4.6A).

Maximal ETS capacity was then assessed by the addition of the uncoupling agent FCCP, which dissipates the mitochondrial membrane potential ($\Delta\Psi$). This parameter gives an indication of the maximal respiration in the uncoupled state. FCCP-induced maximal uncoupled respiration was significantly lower in *mdx* WG

($p < 0.05$; Figure 4.5A) and RG ($p < 0.001$; Figure 4.6A) compared to their respective controls; however, there was no effect of NITR on this parameter.

Next, we measured the activity of CIV (cytochrome C oxidase), the terminal oxidase of the ETS and the site of O₂ reduction to water. As shown in Figure 4.6, CIV activity was not different between UNSUPP CON and *mdx* WG muscles (Figure 4.5A); however, in the RG muscles, CIV activity was significantly lower in *mdx* UNSUPP compared to CON UNSUPP ($p < 0.01$; Figure 4.6A). NITR induced a significant increase in CIV activity in CON WG muscles ($p < 0.01$; Figure 4.5A) but reduced CIV activity in both CON and *mdx* RG muscles ($p < 0.01$; Figure 4.6A).

Finally, the respiratory control ratio (state 3 respiration divided by state 4 respiration; RCR) was calculated. The RCR is an indicator of the extent to which oxygen consumption is coupled to ATP production and therefore mitochondrial efficiency, with a higher RCR indicating better coupling. No difference in RCR was observed between CON and *mdx* WG ($p > 0.05$, Figure 4.5B). In contrast, *mdx* RG respiring on CI+II had a significantly lower RCR compared to CON ($p < 0.0001$) and NITR decreased the RCR further ($p < 0.01$, Figure 4.6B). This highlights that in oxidative red muscle at least, *mdx* mitochondria are more uncoupled and that this uncoupling is exacerbated by NITR.

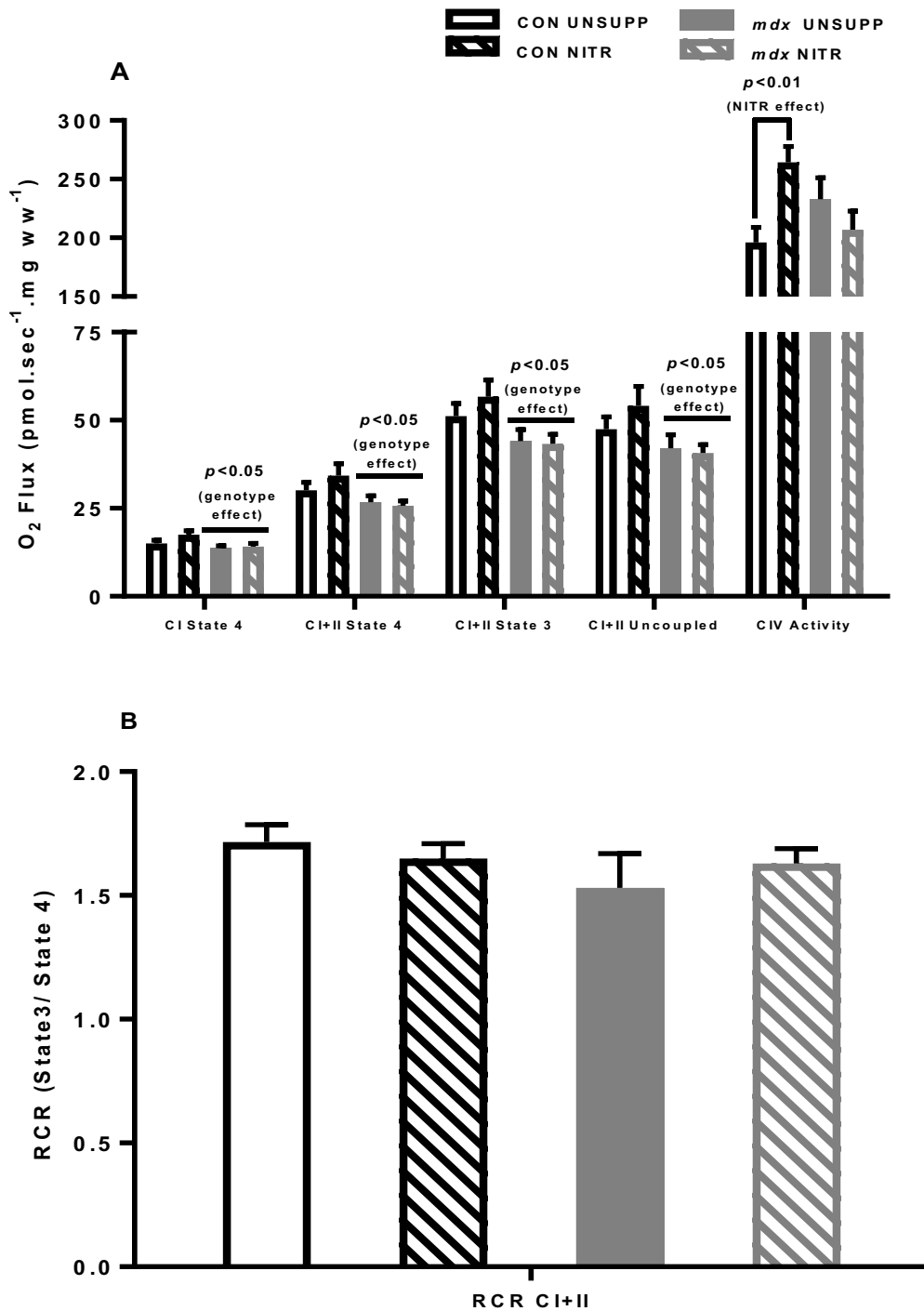


Figure 4.5. Mitochondrial function in intact, permeabilised muscle fibres from the white portion of gastrocnemius (WG) from unsupplemented (UNSUPP) and NITR-supplemented control (CON) and *mdx* mice. State 4 leak respiration (A) is significantly reduced in *mdx* compared to CON WG, irrespective of substrate combination ($p < 0.05$). ADP-stimulated state 3 respiration (A) is significantly reduced in *mdx* compared to CON WG ($p < 0.05$) with NITR having no effect. FCCP-stimulated uncoupled respiration (A) is significantly reduced in *mdx* WG compared with CON ($p < 0.05$). CIV activity (A) was significantly reduced in *mdx* UNSUPP compared to CON UNSUPP ($p < 0.01$). The respiratory control ratio (RCR; B), an indicator of the coupling of O₂ consumption and ATP production at the ETS, was comparable between CON and *mdx* WG. $n = 11-13$ per group.

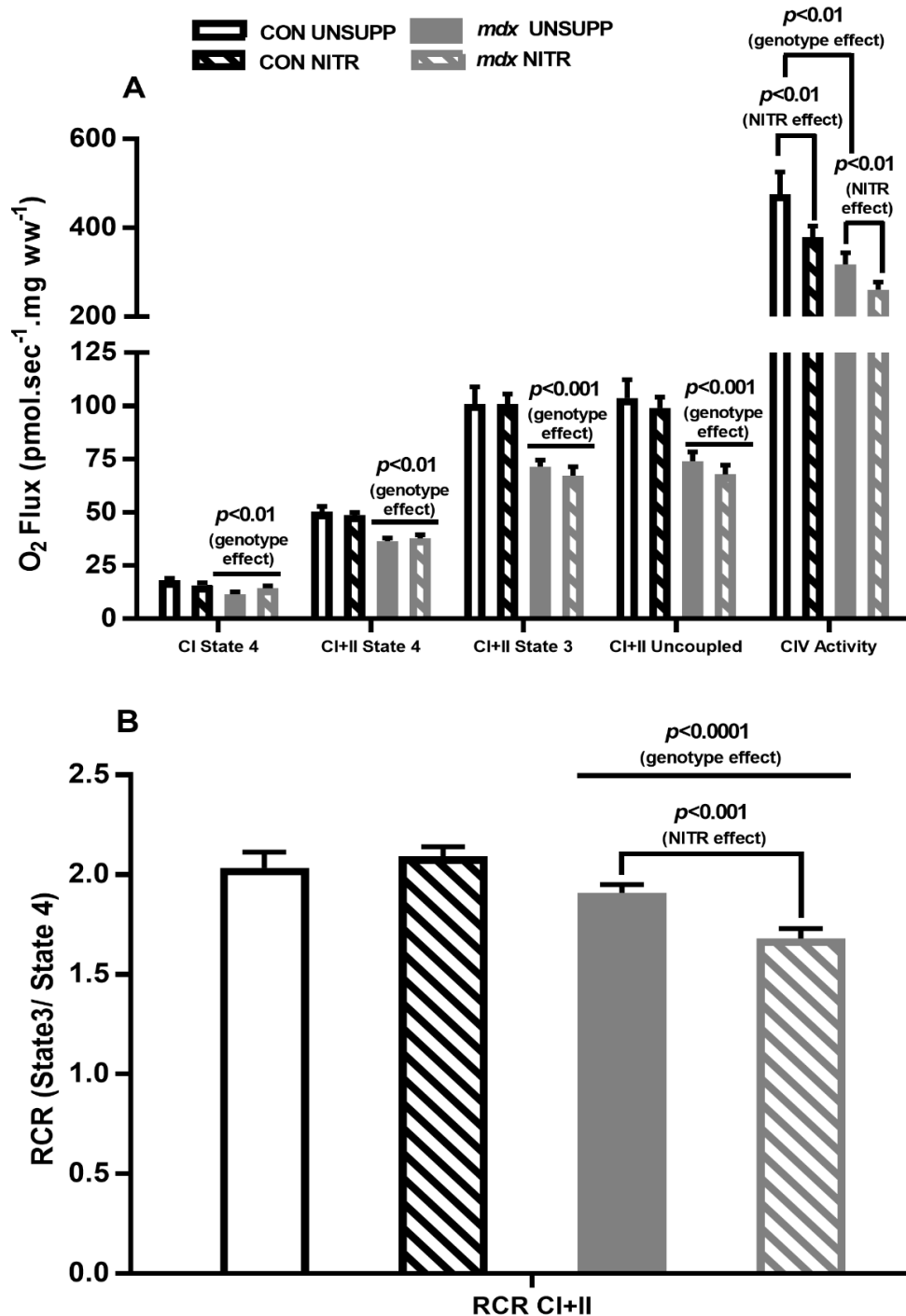


Figure 4.6. Mitochondrial function in intact, permeabilised muscle fibres from the red portion of gastrocnemius (RG) from unsupplemented (UNSUPP) and NITR supplemented control (CON) and *mdx* mice. State 4 leak respiration (A) is significantly reduced in *mdx* compared to CON RG, irrespective of substrate combination ($p < 0.01$). ADP-stimulated state 3 respiration (A) is significantly reduced in *mdx* compared to CON RG ($p < 0.001$) with NITR having no effect on phosphorylating respiration. FCCP-stimulated uncoupled respiration (A) is significantly reduced in *mdx* compared with CON ($p < 0.001$). CIV activity (A) is significantly reduced in *mdx* UNSUPP compared to CON UNSUPP ($p < 0.01$) with NITR inducing a significant decrease in both CON and *mdx* ($p < 0.01$). The respiratory control ratio (RCR; B) in *mdx* RG during CI+II-stimulated respiration is lower compared to CON ($p < 0.0001$) with NITR decreasing the RCR in *mdx* muscle ($p < 0.01$ and $p < 0.001$ respectively). $n = 11-13$ per group.

4.3.4.2 Electron transport chain complex expression

To determine whether the genotypic differences and NITR supplementation-induced changes in respiration parameters were associated with differences in mitochondrial ETS complex densities, the abundance of representative proteins from each of the five ETS complexes were measured using semi-quantitative Western blotting (Figure 4.7 and 4.8). In WG muscles, despite state 3, state 4 and maximal uncoupled respiration being lower in *mdx* muscles (Figure 4.5), the relative abundance of representative proteins from complexes I to V were not lower. In fact, to the contrary, proteins from CII, CIII, CIV and CV were significantly elevated in *mdx* UNSUPP WG muscles compared to CON UNSUPP muscles (Figure 4.7). Interestingly, the NITR-induced increase in CIV respiratory activity (Figure 4.5A) was not associated with a significant increase in the abundance of the CIV protein (Figure 4.7D). NITR supplementation did, however, lead to an increase in representative proteins in WG muscles for CI, CII, CIII and CV in CON but not *mdx* muscles (Figure 4.7).

Unlike the WG muscles, the lower state 3, state 4, uncoupled respiration and CIV activity found in RG *mdx* muscles (Figure 4.6) was accompanied by a reduction in representative proteins for CI, CII, CIV and CV compared with CON; however, NITR supplementation had no effect on any of these proteins in either CON or *mdx* RG muscles (Figure 4.8).

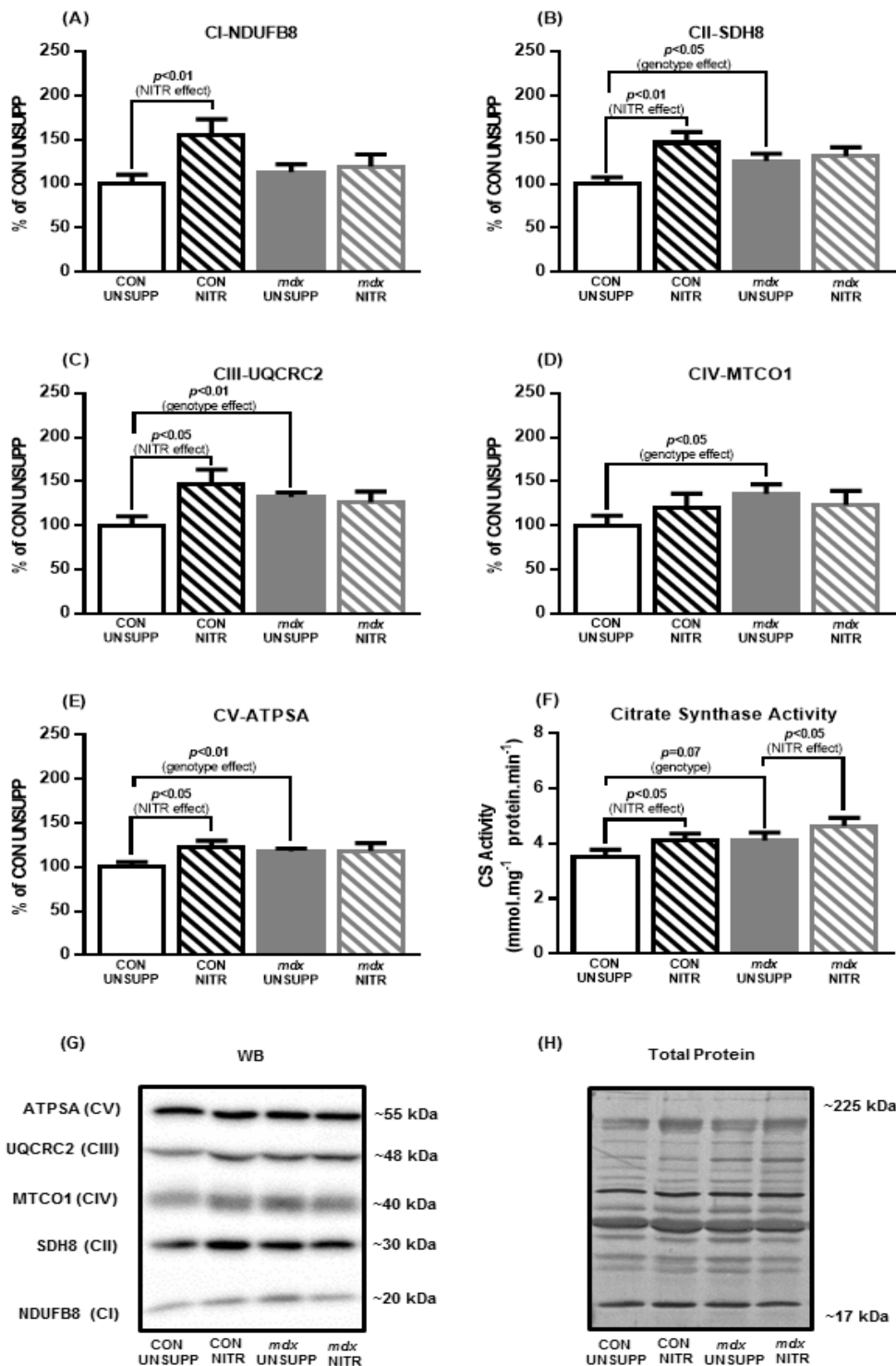


Figure 4.7. Mitochondrial respiratory chain complex proteins, and citrate synthase (CS) activity, from the white portion of gastrocnemius (WG) from unsupplemented (UNSUPP) and NITR-supplemented control (CON) and *mdx* mice. In *mdx* UNSUPP WG, expression of CII ($p < 0.05$; B), CIII ($p < 0.01$; C), CIV ($p < 0.05$; D) and CV ($p < 0.01$; E) were greater compared to CON UNSUPP. NITR induced an increase in CI ($p < 0.01$; A), CII ($p < 0.01$; B), CIII ($p < 0.05$; C) and CV ($p < 0.05$; E) subunits in CON WG but not in *mdx* WG. NITR also increased CS activity (F) in both CON and *mdx* WG ($p < 0.05$) with a trend for CS activity to be higher in *mdx* UNSUPP compared to CON ($p = 0.07$). Representative western blots of proteins from each of the five mitochondrial respiratory complexes (G) with coomassie blue stains of the respective western blots to demonstrate equal loading of the total protein (H). $n = 8$ per group.

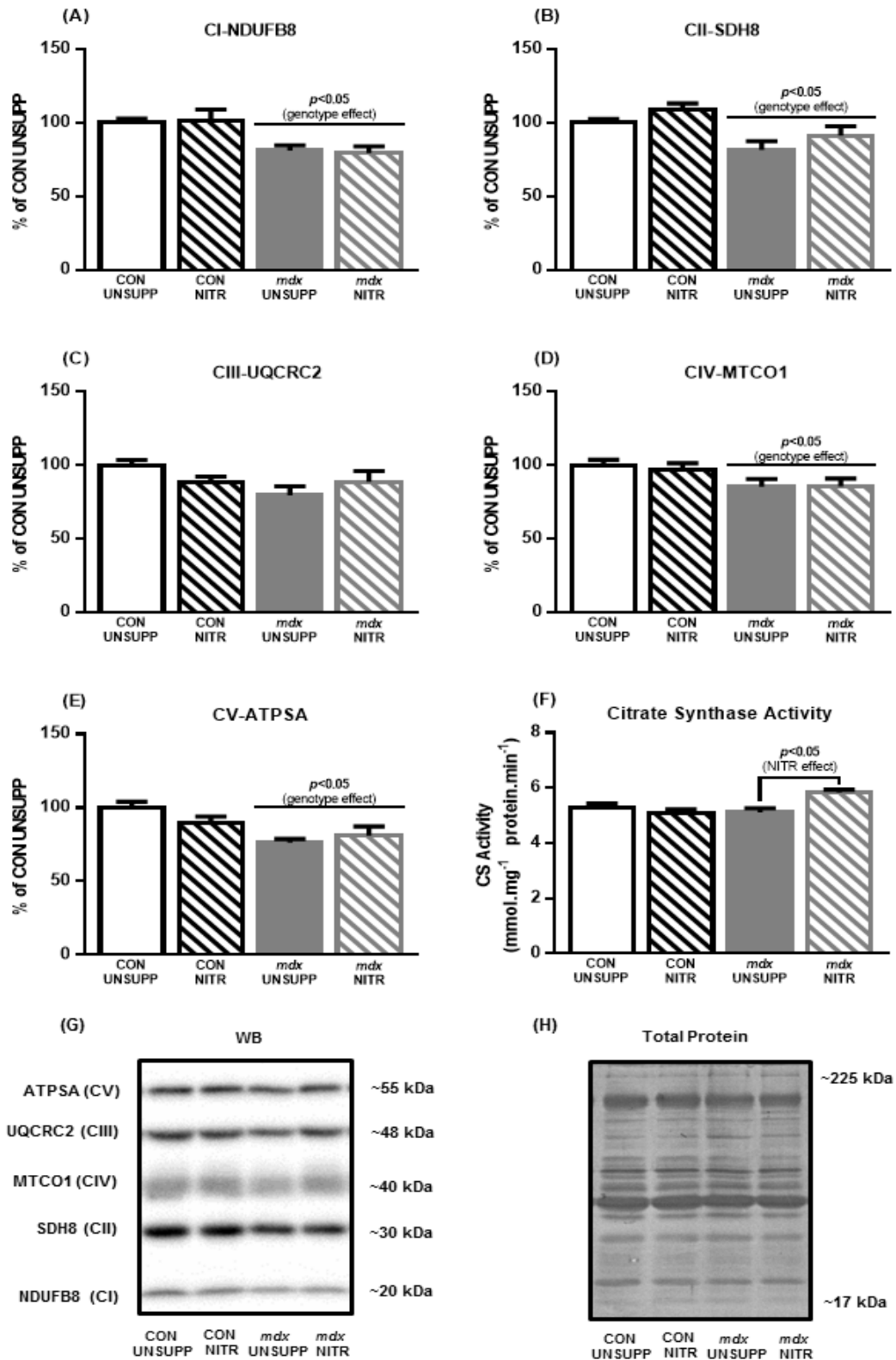


Figure 4.8. Mitochondrial respiratory chain complex proteins, and citrate synthase (CS) activity, from the red portion of gastrocnemius (RG) from unsupplemented (UNSUPP) and NITR supplemented control (CON) and *mdx* mice. Overall, expression of CI, CIII, CIV and CV subunits were decreased in *mdx* RG compared to CON ($p < 0.05$; A, C, D, E respectively). NITR increased CS activity in *mdx* RG but not in CON ($p < 0.05$; F). Representative western blots of proteins from each of the five mitochondrial respiratory complexes (G) with coomassie blue stains of the respective western blots to demonstrate equal loading of the total protein (H). $n = 8$ per group.

4.3.4.3 Citrate synthase activity

Finally, we measured citrate synthase (CS) activity in WG and RG muscles as a co-marker of mitochondrial content alongside mitochondrial ETC proteins (Larsen *et al.*, 2012) (Figure 4.7F and 4.8F, respectively). As shown in Figure 4.7F, there was a trend for CS activity to be higher in *mdx* UNSUPP compared to CON UNSUPP WG muscles. Moreover, NITR increased CS activity in both CON and *mdx* WG muscles. In the RG muscles there was no difference in CS activity between UNSUPP CON and *mdx* mice; however, NITR increased CS activity in RG muscles from *mdx* mice. Overall, NITR did not improve the capacity to phosphorylate ATP or maximal respiratory capacity in dystrophic muscle despite increasing CS activity, suggesting that NITR may have an alternative effect on mitochondrial function such as ROS generation.

4.3.5 Effect of NITR supplementation on ROS production in red and white gastrocnemius

The effect of NITR supplementation on the production of the mitochondrial ROS superoxide (O_2^-), was measured in intact and permeabilised fibres from WG and RG simultaneously with respiration. In the presence of excess O_2^- dismutase, O_2^- is converted to hydrogen peroxide (H_2O_2), which reacts with Amplex Red to produce the red fluorescent product, resorufin. A trend for decreased H_2O_2 emission was detected in *mdx* UNSUPP WG during state 3 respiration compared to CON UNSUPP muscles ($p=0.065$; Figure 4.9A) with NITR having no effect in either strain ($p>0.05$; Figure 4.9A). NITR did, however, induce a decrease in H_2O_2 emission during state 4 leak respiration in CON WG muscle fibres respiring on CI substrates ($p<0.05$; Figure 4.9A). When respiring on CI+CII substrates, there was significantly greater H_2O_2

emission in all groups during state 4 leak respiration compared to CI substrates only in WG fibres ($p < 0.0001$; Figure 4.9A). Importantly, NITR significantly decreased H_2O_2 emission in both CON and *mdx* WG muscles respiring on CI+II substrates ($p < 0.05$; Figure 4.9A). There was no difference in H_2O_2 emission in WG between any groups during FCCP-stimulated maximal uncoupled respiration ($p < 0.05$; Figure 4.9A).

In *mdx* RG fibres, there was significantly less H_2O_2 emission during state 3 respiration ($p < 0.05$; Figure 4.9B) compared to CON fibres; however, there was no effect of NITR on this parameter ($p > 0.05$). Similar to WG fibres, H_2O_2 emission was higher when respiring on CI+CII substrates compared to CI substrates across all groups during state 4 leak respiration ($p < 0.0001$), however, NITR only reduced H_2O_2 emission in *mdx* fibres ($p < 0.001$; Figure 4.9B). NITR also reduced H_2O_2 emission in *mdx* RG fibres during FCCP uncoupled respiration ($p < 0.05$; Figure 4.9B). While our data suggests that NITR reduces mitochondrial ROS production in dystrophic muscle, it is possible that increased NO bioavailability may sequester O_2^- from the O_2^- dismutase reaction to increase reactive nitrogen species (RNS).

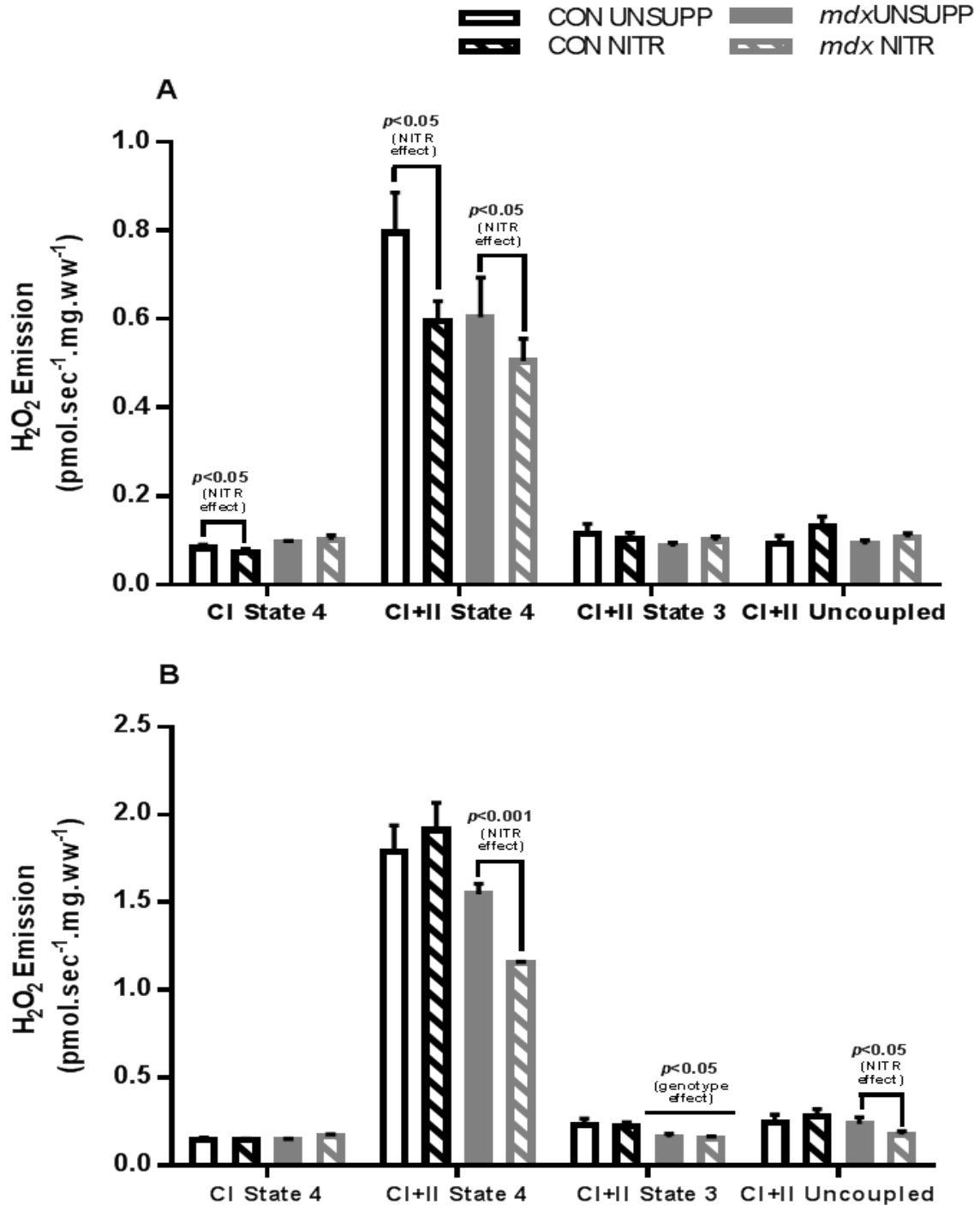


Figure 4.9. Hydrogen peroxide (H_2O_2) emission in intact fibres from the white (WG; A) and red (RG; B) portions of gastrocnemius from unsupplemented (UNSUPP) and NITR-supplemented control (CON) and *mdx* mice. In WG, NITR induced a decreased H_2O_2 emission during state 4 leak respiration (A) in CON during CI-stimulated respiration and in both CON and *mdx* during CI+II-stimulated respiration ($p < 0.05$). In WG, no significant difference was detected in H_2O_2 emission during ADP-stimulated state 3 respiration (A). There was no significant difference in H_2O_2 emission during FCCP-stimulated uncoupled respiration (A) in WG. In RG (B), NITR induced a decrease in H_2O_2 emission during state 4 leak respiration in *mdx* muscle during CI+II-stimulated respiration ($p < 0.001$). In *mdx* RG (B), H_2O_2 emission during ADP-stimulated state 3 respiration was significantly less compared to CON WG ($p < 0.05$) with NITR having no effect ($p > 0.05$). H_2O_2 emission during FCCP respiration was significantly lower in *mdx* RG (B) compared to all other groups ($p < 0.05$). $n = 11-13$ per group.

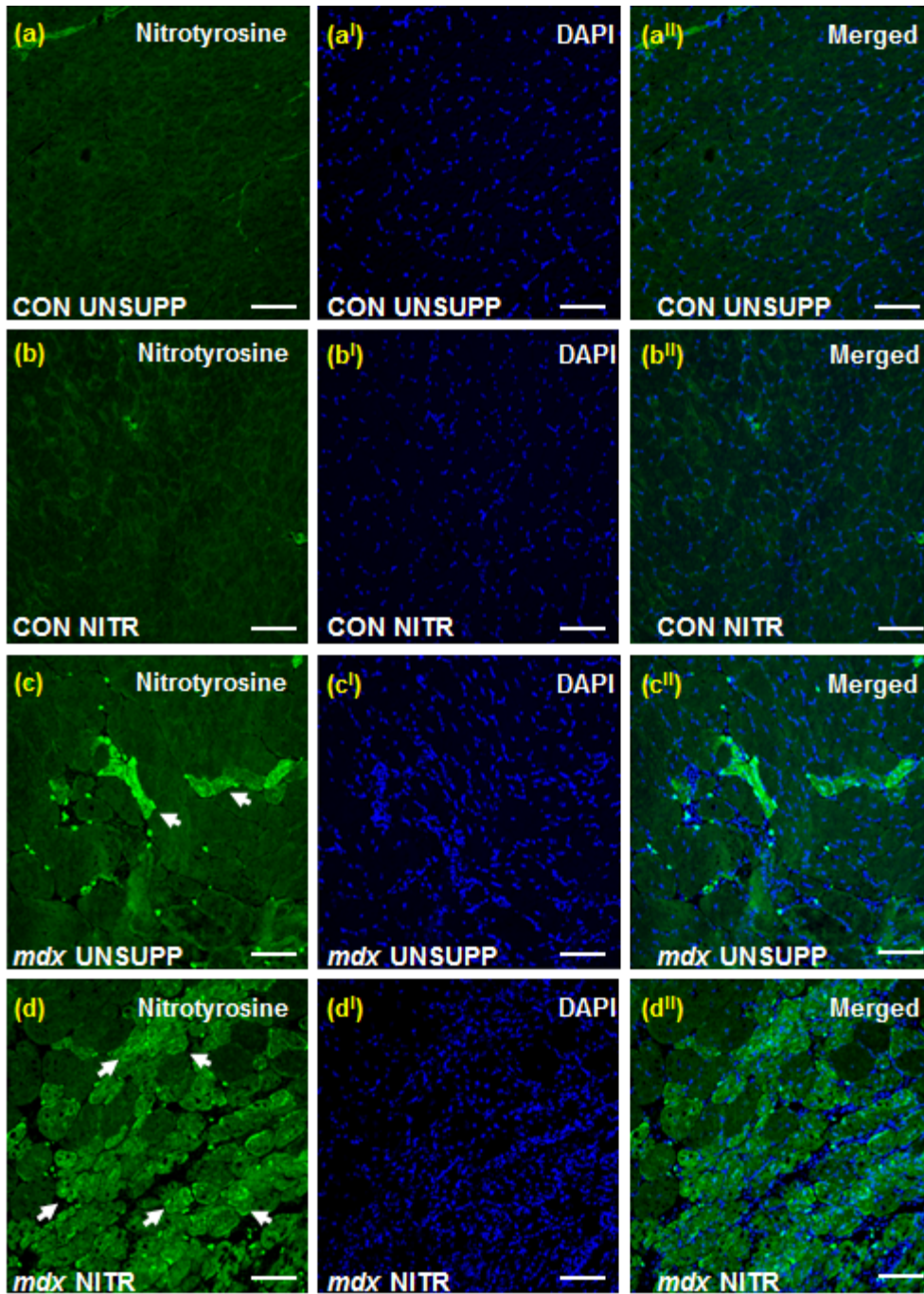
4.3.6 Effect of NITR supplementation on peroxynitrite production

NO is known to rapidly react with O_2^- resulting in the production of the highly RNS, peroxynitrite ($ONOO^-$), and given that elevated ROS is present in *mdx* muscle (Disatnik *et al.*, 1998), we investigated whether $ONOO^-$ production could account for the reduced H_2O_2 emission observed in our study. Increased $ONOO^-$ can result in increased protein nitration of tyrosine residues, potentially leading to altered protein function. Therefore, as an indirect marker of oxidative/nitrosative stress, we measured the effect of NITR on levels of nitrotyrosine via immunohistochemical staining of TA muscles. *Mdx* muscles had significantly higher nitrotyrosine staining compared to CON muscles ($p < 0.0001$) and NITR increased nitrotyrosine staining in both CON ($p < 0.05$) and *mdx* ($p < 0.0001$) TA (Figure 4.10E). Importantly, NITR induced a dramatically greater increase in nitrotyrosine production in *mdx* muscles (2775% in *mdx* versus 82% increase in CON) which was associated with increased DAPI-stained nuclei in NITR supplemented *mdx* TA ($p < 0.0001$, Figure 4.10F).

4.3.7 Effect of NITR supplementation on muscle architecture

Finally, we assessed the effect of NITR on muscle fibre histopathology. As expected, intact *mdx* muscle fibres were significantly larger than fibres from CON muscles (Figures 4.11B and C) which is representative of pseudohypertrophy, a hallmark histopathological feature of dystrophin-deficient muscle. Interestingly, there was a strong trend for NITR supplementation to increase the number of fibres between 6000 and 7499 μm^2 ($p = 0.068$; Figure 4.11B) and increase total mean fibre size ($p = 0.093$; Figure 4.11C). The area of damage, as indicated by areas of inflammatory cell/nuclei infiltration, was significantly higher in *mdx* ($p < 0.01$; Figure 4.11D) compared to CON TA sections and NITR significantly increased the damage

area in *mdx* muscle ($p < 0.01$). Centronucleated fibres, a marker of muscle cell regeneration, were significantly higher in *mdx* muscle ($p < 0.0001$; Figure 4.11E) with NITR further increasing regeneration area in *mdx* sections ($p < 0.01$). These results suggest that NITR supplementation enhances muscle damage, but also regeneration, in *mdx* TA but not in CON, which seems reflective of the increased ONOO⁻ production.



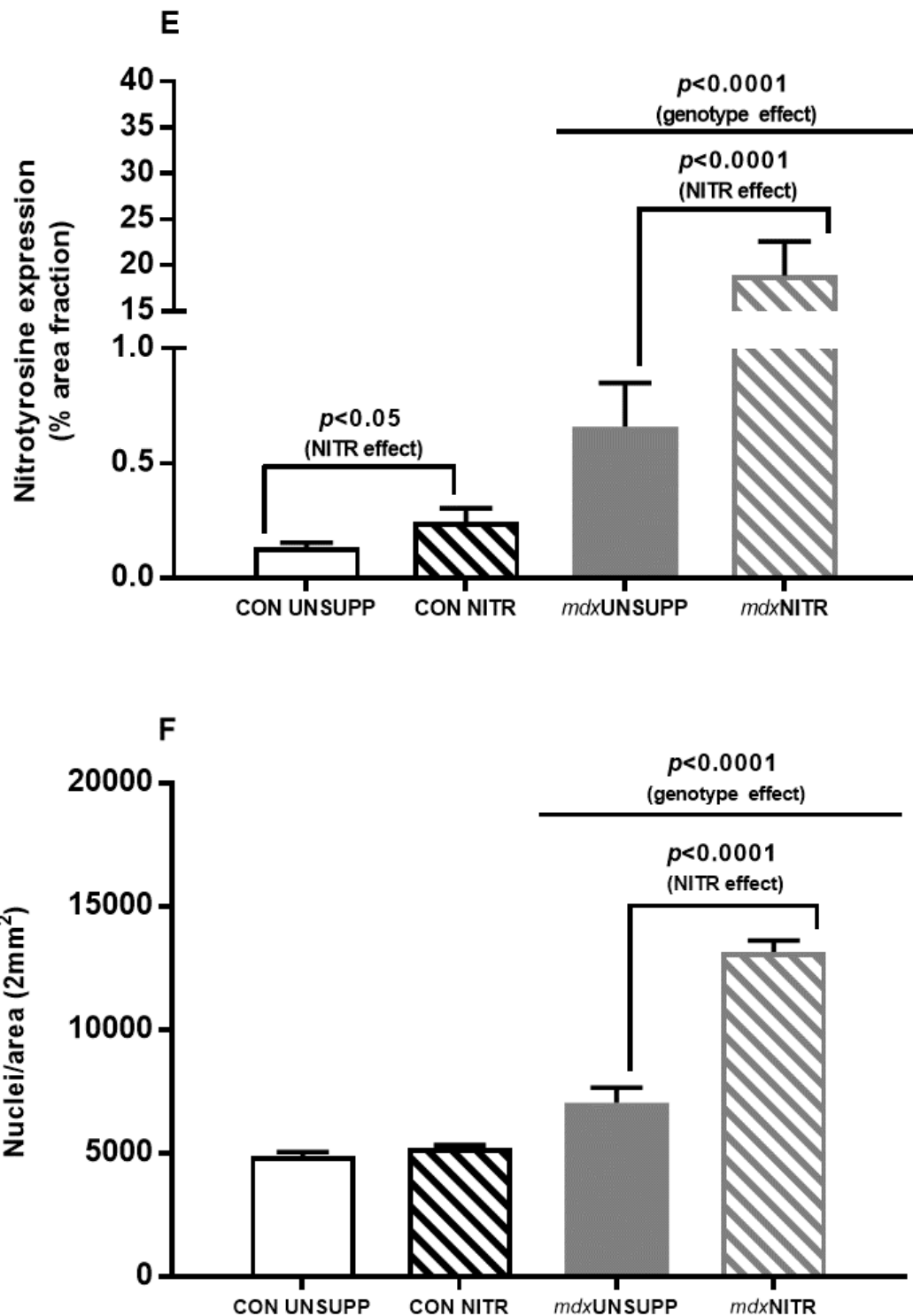


Figure 4.10. Immunohistological analysis of tibialis anterior (TA) from unsupplemented (UNSUPP) and NITR supplemented control (CON) and *mdx* mice. Sections were labelled with nitrotyrosine (green) and DAPI (blue) and merged to identify co-localisation. Representative images reveal nitrotyrosine present in CON NITR, *mdx* UNSUPP and *mdx* NITR (B, C and D respectively) with DAPI positive nuclei in all groups (A-D¹). NITR increased nitrotyrosine in CON ($p < 0.05$) and *mdx* ($p < 0.0001$; E) TA with NITR increasing DAPI-positive nuclei in *mdx* TA ($p < 0.0001$; F). Scale bars= 100 μ m, $n = 3-4$ per group

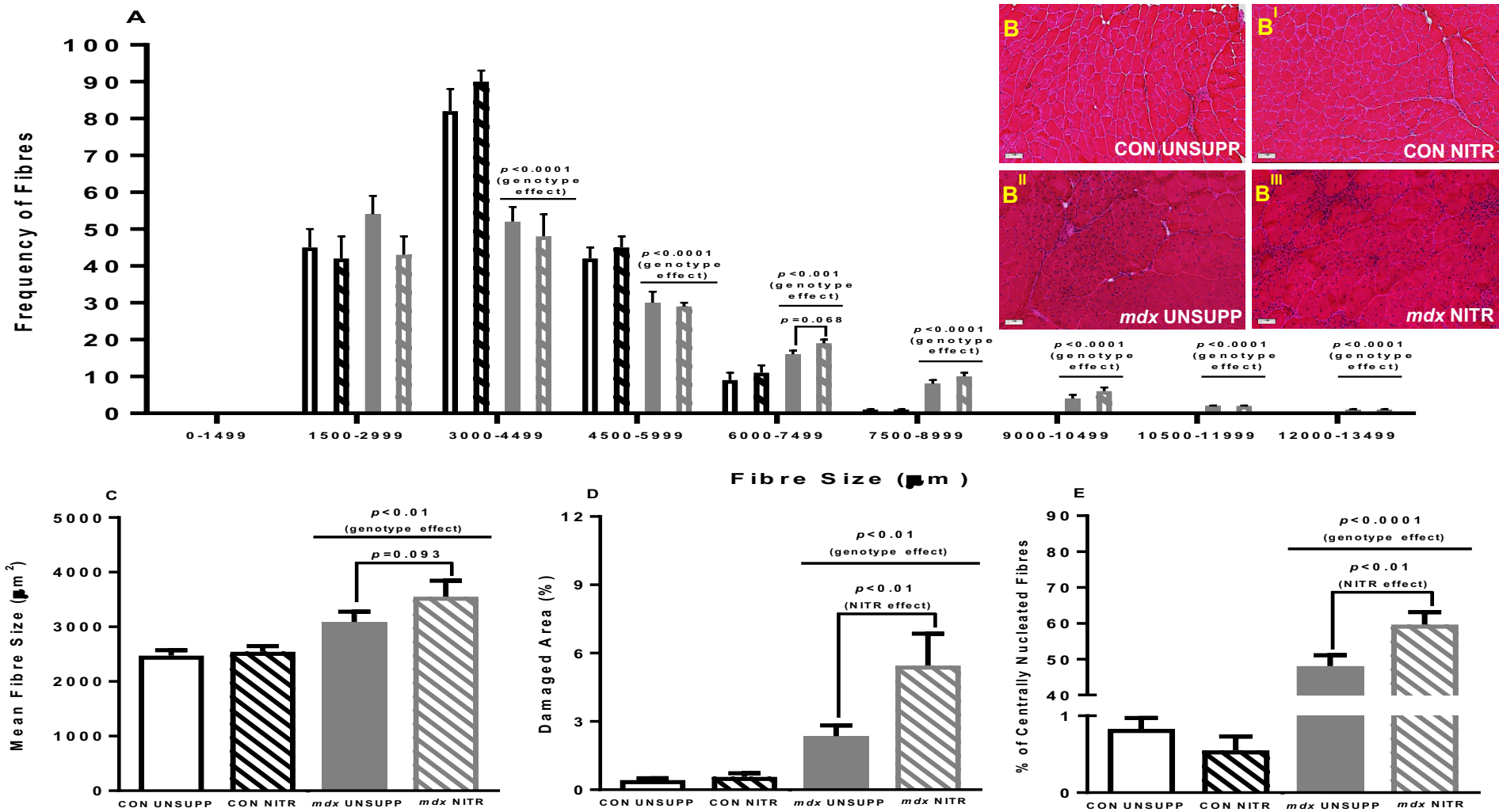


Figure 4.11. Histological analysis of tibialis anterior (TA) from unsupplemented (UNSUPP) and NITR supplemented control (CON) and *mdx* mice. The frequency histogram (B) indicates an increase in fibre size of *mdx* TA with fibres more frequent from 6000-12000 µm ($p < 0.0001$). NITR had no effect on the distribution of CON or *mdx* fibres but there was a trend for an increased number of fibres around 6000 µm ($p = 0.068$). Mean fibre size (C) was significantly greater in *mdx* TA ($p < 0.01$) with a trend for NITR to increase fibre size in *mdx* TA ($p = 0.093$). Damaged area (D) and percentage of centronucleated fibres (E) was significantly higher in *mdx* TA ($p < 0.01$ and $p < 0.0001$ respectively) with NITR stimulating further damage and regeneration ($p < 0.01$). $n = 10-12$ per group.

4.4 Discussion

Mutation of the dystrophin gene presents a clinical phenotype of muscular atrophy, physical impairment and premature death, with underlying dysregulation of Ca^{2+} homeostasis and metabolism implicated in promoting the cycle of damage. While the absence of dystrophin causes DMD, it appears that severe metabolic impairments play a key role in exacerbating disease progression. Considering NO can modulate metabolism and the enzymatic source of skeletal muscle NO production (nNOS) is reduced with dystrophin deficiency, we questioned whether promoting NITR-derived NO bioavailability, which has been previously proven to increase plasma NO levels (Larsen *et al.*, 2011) and elicit mitochondrial adaptations in skeletal muscle (Larsen *et al.*, 2011, Carlström *et al.*, 2010), could overcome this metabolic dysfunction. This is the first study to date to investigate NITR supplementation as a potential therapy for DMD and we show that the severe metabolic perturbations in dystrophin-deficient skeletal muscle could not be overcome by enhancing nNOS-independent NO production. Instead, our data suggests that chronically increasing NO bioavailability without restoring nNOS protein expression and its regulatory role on metabolism, in fact, promotes pathological muscle damage, potentially via a peroxynitrite (ONOO^-)-dependent mechanism.

In this study we investigated if impaired macronutrient uptake may be a contributing factor to the mitochondrial dysfunction in dystrophic muscle, as compromised transport of substrates across the sarcolemma could be a consequence of the loss of dystrophin and its associated complex which includes nNOS, from the membrane. Specifically, we have investigated glucose uptake (GU) as it is well established that GU during rest and contraction is

regulated by NO (Merry *et al.*, 2010b). The secondary loss of dystrophin-associated nNOS was confirmed in *mdx* TA via immunolabelling.

Concurrently, we have demonstrated that both basal- and contraction-induced GU in both *mdx* UNSUPP EDL and SOL is comparable to CON. We have demonstrated in our study that NITR increases contraction-induced GU in CON EDL but has no effect in CON SOL. Indeed, we have shown previously that there are greater effects of NOS inhibition on EDL than SOL (Merry *et al.*, 2010a), likely because of a greater comparative nNOS expression in fast-twitch versus slow-twitch muscles (Merry *et al.*, 2010a, Kobzik *et al.*, 1994) and the higher antioxidant enzymes in slow-twitch muscles which may buffer the effects of NO (Ji *et al.*, 1992). In both CON EDL and SOL muscles, however, NITR did not affect basal GU rate. This could infer that the NITR dosage administered in our study is sufficient to modulate non-cGMP-dependent contraction-induced GLUT-4 mediated GU (Richter *et al.*, 2013) but perhaps not cGMP-dependent GLUT-1 basal (Ren *et al.*, 1993) events. A notable limitation of our study is that we did not quantify cGMP levels in EDL and SOL muscles. However, in light of a recent study which demonstrated that even low dose (0.35mM) NITR therapy for ~2 weeks (in comparison to the 1mM NITR dosage for 8 weeks administered in our study) was sufficient to induce ~3-fold increases in cGMP levels in rat skeletal muscle, this seems unlikely. Rather, basal GU is likely regulated in the first instance by glucose utilisation, thus increasing NO signalling without the normal simultaneous increase in muscle work (and thus glucose utilisation) results in an unchanged basal GU. Unexpectedly and in contrast to CON EDL, NITR reduced basal GU in *mdx* EDL and SOL. Taken with the fact that NITR stimulated contraction-induced GU in CON but further depressed it in *mdx*

muscle, our data suggests that NITR-derived NO is being diverted away from its bio-modulatory effects on GU. Presumably, this is because in *mdx* muscle, in which O_2^- production is notoriously increased (Disatnik *et al.*, 1998), NITR-generated NO is being sequestered into ONOO⁻ production instead of cGMP activation, thus reducing the proportional NO available to GU signalling, despite an increased NITR-nitrite-NO pool.

We have assessed various indices of mitochondrial respiratory function in permeabilised red (RG) and white (WG) gastrocnemius fibre bundles. Permeabilisation of intact muscle bundles and delivery of optimal substrate concentrations allows for the measurement of the mitochondrial capacity independent of substrate delivery capacity. Indeed, even in this optimised environment, we demonstrate a severely reduced capacity (up to 25% of CON) to phosphorylate ADP in both WG and RG from the *mdx* mouse. This is consistent with others (Kuznetsov *et al.*, 1998, Passaquin *et al.*, 2002) who have reported similar depressions in ADP-stimulated phosphorylating respiration in *mdx* skeletal muscle fibres. When the $\Delta\Psi$ is collapsed via FCCP-induced uncoupling, *mdx* mitochondria from the RG responded with a lower maximal respiration. Together with a reduced CIV activity, our data suggest that mitochondria from dystrophic muscle are less metabolically flexible compared with their healthy counterparts and may indicate a failure to buffer metabolic stress associated with dystrophinopathy, and explain the exercise intolerance observed in DMD patients (Kemp *et al.*, 1993). NITR did not improve phosphorylating or maximal uncoupled respiration in either CON or *mdx* skeletal muscle but did decrease CIV activity in both CON and *mdx* RG. CIV inhibition is an established effect of reversible competitive binding of NO to heme-copper

sites *in lieu* of O₂, on CIV, in addition to CI and CIII (Brown and Borutaite, 1999, Brunori *et al.*, 2004, Sarti *et al.*, 2003). Despite the inhibitory effect of NITR-derived NO on CIV activity and therefore ETS respiratory capacity, the lack of effect on phosphorylating and maximal uncoupled respiration was unexpected, since NITR has been previously shown to improve various mitochondrial properties through stimulation of mitochondrial biogenesis and improved coupling of O₂ consumption to ATP production (Larsen *et al.*, 2011). Since NO is a highly reactive molecule that, to exert its biological role, must be produced in close proximity to its effector targets, the exogenous NO source afforded by NITR supplementation in our study may not be penetrating the muscle fibres sufficiently, or in sufficient concentration, to modulate mitochondrial function. This is particularly true of the mitochondrial function governed by nuclear gene regulation such as mitochondrial biogenesis and uncoupling. Aquilano *et al.* for instance, have demonstrated that the loss of nNOS-generated NO production nearby the nucleus is a causative factor of the impairment of mitochondrial biogenesis in skeletal muscle (Aquilano *et al.*, 2014). Thus, while we have evidence of NITR-derived NO penetrating the mitochondria to induce regulatory adaptations such as inhibition of CIV activity, overall respiratory capacity, which is dictated predominantly by mitochondrial density and coupling, is seemingly unaffected, even in CON mice. This is likely due to the chronic supplementation period and particular dosage employed in our study. For example, similar to our study, Hezel *et al.* did not observe any changes in mitochondrial parameters following 17 months of NITR supplementation in healthy mice (Hezel *et al.*, 2015). In contrast, others have shown beneficial mitochondrial modulation following much shorter supplementation periods (Larsen *et al.*, 2011, Nisoli *et*

al., 2004). In particular, Ashmore *et al.* have demonstrated that NITR dosage is important to the control of the nuclear signalling of mitochondrial biogenesis in which a low (0.35mM) dose increased peroxisome proliferator-activated receptor (PPAR) β/δ signalling but not mitochondrial functional adaptations; a medium (0.7mM) dose increased PPAR β/δ signalling, PPAR γ -coactivator 1 α (PGC-1 α) expression and mitochondrial fatty acid oxidation; while a high (1.4mM) dose reduced PPAR β/δ , increased CS activity but had no additive effect on mitochondrial fatty acid oxidation over the medium dose following 14-18 days supplementation (Ashmore *et al.*, 2015). These data highlight that the promotion of mitochondrial biogenesis might be an acute, dose-specific response to shorter-term increases in skeletal muscle NO signalling which may switch off or become desensitised in response to more chronic, prolonged increases in NO production.

The reduced capacity for *mdx* skeletal muscle to phosphorylate ADP and to ramp up respiration during times of metabolic stress may be reflective of uncoupled respiration. It would be expected that state 4 respiration is greater in dystrophic muscle to act as a buffering mechanism (Brand and Esteves, 2005) to mitigate increased ROS production (Disatnik *et al.*, 1998, Whitehead *et al.*, 2008). However, state 4 respiration was significantly less in both WG and RG of *mdx* mice. While the RCR was comparable to CON in *mdx* WG, it was lower in *mdx* RG respiring on CI+II substrates highlighting that respiratory control is compromised in the muscle that is most dependent upon mitochondrial oxidative ATP production (i.e. red oxidative muscle). When considered in context of a depressed state 3 and 4 respiration, tighter respiratory control would be required to maintain the $\Delta\Psi$ and drive for ATP synthesis, especially

given the heightened energy requirements of dystrophic muscle. Indeed, our observations of a depolarised $\Delta\Psi$ in isolated *mdx* mitochondria (C.A. Timpani, A. Hayes and E. Rybalka, unpublished observations) indicate insufficient coupling to maintain the drive for ATP synthesis in red muscle at least. Intriguingly, NITR decreased the RCR only in *mdx* RG under both CI and CI+II-mediated respiration. As CIV activity and expression are reduced in *mdx* gastrocnemius (Kuznetsov *et al.*, 1998, Jongpiputvanich *et al.*, 2005), the further suppression of CIV activity via NITR-derived NO may induce hyperpolarisation of the mitochondrial membrane potential as the reduced consumption of O₂ at CIV would lead to accumulation of protons in the intermembrane space. If this were the case, inducing uncoupling (as suggested by the decreased RCR) may be a beneficial adaptation to ETS dysfunction, to prevent potential hyperpolarisation of the $\Delta\Psi$ which is an initiator of mitochondria-mediated apoptosis (Nagy *et al.*, 2007). Certainly, the role of NITR-derived NO in the regulation of mitochondrial coupling efficiency is unclear since some studies have demonstrated an enhanced coupling efficiency of human skeletal muscle (Larsen *et al.*, 2011) while others have shown a reduced coupling efficiency of rodent skeletal muscle (Ashmore *et al.*, 2015). Despite the obvious species differences between these studies, these data highlight that NITR-derived NO has a modulatory role on the expression of uncoupling protein 3 and adenine nucleotide translocase expression, and seemingly regulates the leakiness of several respiratory complexes – all of which contribute to the coupled state of skeletal muscle mitochondria. However, this role requires further elucidation.

A reduced mitochondrial pool (particularly viable mitochondria) could also explain the decreased OXPHOS capacity of dystrophic skeletal muscle in our study, and should be positively modulated by NITR-induced NO signalling of nuclear factors associated with mitochondrial biogenesis (Ashmore *et al.*, 2015). As such, we have assessed mitochondrial complex protein (I-V) expression and citrate synthase (CS) activity as markers of mitochondrial density. While we saw no differences in CS activity of RG and WG between *mdx* and CON strains in our study, we did see a reduction in the expression of CI, CII, CIV and CV in *mdx* RG compared to CON. This could reflect a reduced mitochondrial pool or at the very least, a reduced propensity for mitochondrial respiration. In WG however, mitochondrial ETC complex expression and CS activity was comparable between *mdx* and CON strains suggesting a reduced respiratory capacity despite comparable mitochondrial density in *mdx* muscle. We (Rybalka *et al.*, 2014) and others (Chi *et al.*, 1987, Jongpiputvanich *et al.*, 2005, Kuznetsov *et al.*, 1998) have previously reported this, highlighting that a reduced mitochondrial density does not account for the decreased mitochondrial respiration associated with dystrophin-deficiency but rather, that the mitochondrial pool is intrinsically defective. While NITR had no effect on complex expression in RG from either strain, most complexes, except CIV, were upregulated in NITR-supplemented CON but not NITR-supplemented *mdx* WG. In fact, the only observed effect of NITR in WG that was consistent across strains was an increased CS activity, and this was reproducible in the RG from *mdx* but not CON mice. Our finding is curious since a recent study has demonstrated that a high (1.4mM) NITR diet increases CS activity in red SOL muscle from healthy mice, albeit a low (0.35mM) and medium (0.7mM) diet did

not (Ashmore et al., 2015). The current study supplemented mice with 1mM NITR, in between the medium and high dose used by Ashmore et al., suggesting that there are variations in the response of different fibre types to NITR-derived NO dosages, in which type II fibres are more responsive to a lower NO concentration. Irrespective, changes in mitochondrial CS activity and ETC complex expression induced by NITR did not translate to improved mitochondrial respiration in either CON or *mdx* muscles. For CON muscle, this likely reflects the chronic nature of the supplementation protocol in which persistently increased NO within the skeletal muscle both enhances the capacity for mitochondrial respiratory function (i.e. via upregulated ETC complex expression) but simultaneously inhibits the activity of ETC complex proteins (such as CIV activity observed in our study) with the net effect being an unchanged mitochondrial respiration. For dystrophic muscle, the failure of the mitochondria to respond to metabolic regulation might be due to defective mitochondria with a fundamentally suppressed respiratory – and subsequently ATP synthesis – capacity as described by us previously (Rybalka et al., 2014). This idea is supported by the data of Pauly et al. which demonstrated that the pharmacological activation of AMPK, a known positive regulator of mitochondrial biogenesis, increased autophagy, force production and Ca²⁺ handling but had no typical downstream effect on oxidative metabolism in *mdx* mice (Pauly et al., 2012). Taken with our data, this suggests that downstream metabolic processes, particularly at the level of the ETS, are unable to respond to metabolic regulation due to an inherent defect in *mdx* mitochondria.

We found in various respiratory states that NITR reduced H₂O₂ production in *mdx* but not CON skeletal muscle. This would immediately seem

to be beneficial, as ROS production is elevated in dystrophic muscle (Disatnik *et al.*, 1998) and NO reduces oxidative stress at the level of the ETS (Cho *et al.*, 2001). However excessive NO can lead to the generation of RNS in the presence of O_2^- . In addition to the inhibition of CIV, NO inhibits electron transfer at CI and CIII of the ETS (Poderoso *et al.*, 1996), producing O_2^- anions that interact with NO to produce $ONOO^-$ which can induce cellular damage (Beckman *et al.*, 1990). In our study, we have demonstrated elevated nitrotyrosine content in *mdx* muscle, which is consistent with increased $ONOO^-$ production, and this was dramatically exacerbated by NITR (2775% increase). The increased nitrotyrosine labelling corresponded with an increased area of damage in NITR-supplemented *mdx* TA sections. In previous studies, NO donor therapy has been shown to reduce the area of damage in dystrophic muscle, but as NO donors are typically given in combination with anti-inflammatories (Brunelli *et al.*, 2007, Uaesoontrachoon *et al.*, 2014), our data suggests that the anti-inflammatory component of these co-compounds is perhaps the more pertinent effector. NITR also increased the proportion of centronucleated fibres in *mdx* muscles, which has been previously observed with NO donors (Brunelli *et al.*, 2007, Mizunoya *et al.*, 2011) and is reflective of an enhanced regenerative capacity in response to NITR-induced damage. NO is a known stimulator of satellite cell proliferation, which is crucial to skeletal muscle regeneration following damage (Anderson, 2000) and is notably defective in dystrophin-deficient muscle. As dystrophic muscle is in a state of enhanced oxidative stress, and has no nNOS protein to modulate metabolic flux, superfluous NITR-derived NO bioavailability appears detrimental to dystrophic muscle by promoting excess $ONOO^-$ formation which, in turn, may exceed

antioxidant buffering capacity to promote muscle damage and escalate pathology. It is also possible that the absence of nNOS protein expression, its translocational capacity to deliver NO to specific intracellular sites and the metabolic modulatory effects it exerts, may account for the deleterious effect that NITR had on dystrophic muscle histopathology in our study, since breeding transgenic overexpressing nNOS mice with the *mdx* strain results in significant improvements to dystrophic muscle architecture (Wehling *et al.*, 2001, Tidball and Wehling-Henricks, 2004). NITR therapy, however, might be beneficial for the stimulation of satellite cell replication and dystrophic skeletal muscle regeneration, especially if mitochondrial O_2^- production could be pharmacologically attenuated and RNS-induced damage prevented (such as with antioxidant therapy).

4.5 Conclusion

In summary, our study is the first to demonstrate that an 8 week supplementation regimen of NITR in drinking water cannot overcome the metabolic dysfunction observed in the *mdx* mouse model of DMD. We are the first to examine contraction-induced GU in the *mdx* model and to demonstrate that NITR supplementation reduces otherwise normal GU in *mdx* muscles and cannot positively modulate mitochondrial function. Although NITR supplementation reduced mitochondrial H₂O₂ emission, it induced mitochondrial uncoupling in RG, increased muscle fibre nitrosylation (and therefore ONOO⁻ radicals) and promoted skeletal muscle damage. Our data is consistent with recent literature linking NO to muscle soreness (Radak *et al.*, 2012). Together this suggests that enhancing endogenous NO production via exogenous NITR therapy is contraindicative for the treatment of DMD. This is potentially due to the fact that there is no concomitant increase in nNOS protein expression and its regulatory role over metabolic flux control, and, that excessive ROS promotes RNS production which actually reduced NO bioavailability. This is in stark contrast to previous findings of significant improvements in the dystrophic condition following NO donor therapy, and in Becker patients following nitrite supplementation, suggesting that long-term NITR/NO supplementation requires better characterisation, particularly in conditions of heightened oxidative and/or metabolic stress such as in DMD. Our data is of particular importance because NITR therapy is currently in clinical trials for the treatment of DMD patients.

Chapter Five

Evaluation of Nitrite Therapy in Human DMD Myoblasts

5.1 Introduction

The imbalance between muscle damage and muscle repair (Decary *et al.*, 2000) in DMD favours the replacement of functional muscle with non-functional fatty and connective tissue. Such a loss of skeletal muscles leads to muscle weakness and poor quality of life with DMD sufferers becoming wheelchair bound by early adolescence. It has been hypothesised that the inability to adequately regenerate damaged muscle is through the exhaustion of the satellite cell pool (Blau *et al.*, 1983, Sacco *et al.*, 2010). Satellite cells are quiescent stem cells located between the basal lamina and sarcolemma of muscle fibres (Mauro, 1961) and are responsible for adult muscle growth and regeneration (Lepper *et al.*, 2011, Sambasivan *et al.*, 2011). Satellite cells are activated in response to muscle injury and, once they enter the cell cycle, they proliferate into myoblasts, the myogenic progenitors, which fuse into myotubes and with damaged myofibres, to repair them (Yin *et al.*, 2013).

While the satellite cell exhaustion hypothesis provides a rational explanation for the reduced regenerative capacity of dystrophic muscle, it is in contrast to the observation that satellite cell number is increased in both DMD patients (aged 2-13 years; Kottlors and Kirschner, 2010, Bankolé *et al.*, 2013) and aged (15 month old) *mdx* EDL (Boldrin *et al.*, 2015). This suggests that depletion of the satellite cell pool is not the origin of impaired muscle regenerative capacity. The recent observations that dystrophic satellite cells have a reduced capacity to commit to myogenic lineage (Biressi *et al.*, 2014, Dumont *et al.*, 2015) but rather promote a fibrogenic program (Biressi *et al.*,

2014), suggests that dystrophic satellite cells are dysfunctional and have a reduced capacity to induce muscle repair. In addition to these observations, the increased number of satellite cells in dystrophic muscle indicates that there may be an impairment in the satellite cells capacity to participate in cell cycle progression to form myoblasts. Quiescent satellite cells are characterised by low mitochondrial number, activity and exhibit a depressed metabolic state (Inoue *et al.*, 2010, Mantel *et al.*, 2010, Norddahl *et al.*, 2011) which must be overcome during satellite cell activation to support satellite cell progression through the cell cycle. As we (Rybalka *et al.*, 2014) and others (Passaquin *et al.*, 2002, Onopiuk *et al.*, 2009) have demonstrated impaired metabolism in differentiated muscle which culminates in reduced ATP content (Austin *et al.*, 1992, Cole *et al.*, 2002), it is plausible that dystrophic mitochondria cannot respond appropriately to the increased metabolic demand of active satellite cell cycling, thereby inhibiting appropriate cell progression into myoblasts. In addition, NO plays a pivotal role in the activation of satellite cells (Anderson, 2000, Anderson and Pilipowicz, 2002, Tatsumi *et al.*, 2006, Wozniak and Anderson, 2006) and therefore reduced NO production by nNOS in dystrophin-deficient skeletal muscle may contribute to reduced satellite cell activity. As myoblasts are important for repairing muscle damage, which is a substantial characteristic of dystrophic muscle, it is essential that there is sufficient energy and NO bioavailability to support satellite cell activity and to ensure myoblasts have the bioenergetical and chemical means to adequately repair damaged muscle.

In chapter 4, we investigated the effect of increasing NO bioavailability via an 8 week nitrate NITR supplementation regimen in the *mdx* mouse and

demonstrated this chronic NITR supplementation protocol was detrimental, in particular to skeletal muscle histology. Our observations are in contrast to those who have documented beneficial effects of NITR supplementation (Carlström *et al.*, 2010, Larsen *et al.*, 2011, Ashmore *et al.*, 2015) but may be accounted for by the differences in supplementation time. More importantly, the differences may be reflective of the utilisation of dystrophin- and nNOS-positive muscle in the aforementioned studies. Given that dystrophin-deficient cells have an associated secondary reduction of nNOS (Leary *et al.*, 1998, Thomas *et al.*, 1998, Vaghy *et al.*, 1998, Judge *et al.*, 2006) – and therefore may not be able to handle chronic NO production without a concomitant increase in nNOS protein as observed in Chapter 4 – an acute supplementation regimen to increase NO bioavailability may be better tolerated by DMD myoblasts and elicit positive effects on mitochondrial function. Therefore, we investigated the effects of an acute (24 hours, 3 days and 7 days) nitrite exposure on mitochondrial function and superoxide (O_2^-) production in dystrophin-positive and dystrophin-negative myoblasts. We hypothesised that acute nitrite exposure would (1) improve mitochondrial function and (2) decrease mitochondrial O_2^- in dystrophin-negative myoblasts.

5.2 Methods

5.2.1 Cell culture maintenance

As described in section 3.2.1, dystrophin-positive (CON) and dystrophin-negative (DMD) immortalised human skeletal muscle cells were grown at a density of 90-100,000 cells per well. Every 3 days, the skeletal muscle cells were passaged.

5.2.2 Determination of nitrite dosage

In the following myoblast experiments, sodium nitrite was utilised *in lieu* of nitrate. The conversion of nitrate to nitrite typically occurs via commensal bacteria in the oral cavity upon dietary consumption. As this is absent in a cell culture model, we administered nitrite as it is a known NO donor.

To establish the maximal tolerable dose of nitrite to be employed in the myoblast experiments, we performed dose response curves (10nM to 1mM) on CON myoblasts via two methods – (1) crystal violet staining to assess cell viability and (2) the xCELLigence system (ACEA Biosciences, San Diego, CA) to assess real-time monitoring of cell proliferation.

5.2.2.1 Crystal violet assay

For 4 days, CON myoblasts were grown in either media, media with MQ H₂O (vehicle) or increasing concentrations of nitrite (10nM-1mM). Crystal violet staining was performed and absorbance was read at 570 nm on an X-Mark Microplate Reader (Bio-Rad Laboratories, Australia) as described in section 3.2.2.1.

5.2.2.2 Cell proliferation assay

CON myoblasts were seeded at a density of 5000 cells per well and plates were inserted into the xCELLigence RTCA MP system. Once myoblasts were adhered to the plate, 50µL of either media, media with MQ H₂O (vehicle) or increasing concentrations of nitrite were added to the well. The Cell Index was measured every 30 minutes for 4 days as described in section 3.2.2.2.

5.2.3 Determination of mitochondrial viability

Mitochondrial viability of untreated (UNSUPP) and treated CON and DMD myoblasts was assessed by the fluorescent MitoTracker dyes Green and Red. Myoblasts (5000 per well) were incubated with or without 1mM of nitrite for 24 hours, 3 days or 7 days with media replaced every 3 days. Mitochondrial viability was assessed as described in section 3.2.3 and myoblasts were imaged on an inverted microscope (Olympus, Tokyo, Japan). Images were analysed using ImageJ software and mitochondrial viability was calculated (the ratio of red (live) to green (total) fluorescence).

5.2.4 Determination of mitochondrial superoxide (O₂⁻) production

Mitochondrial O₂⁻ production of untreated and treated CON and DMD myoblasts was assessed using the fluorescent probe, MitoSOX Red. Myoblasts (5000 cells per well) were incubated with or without 1mM of nitrite for 24 hours, 3 days or 7 days with media replaced every 3 days. Mitochondrial O₂⁻ production was determined as described in section 3.2.4 and myoblasts were

imaged as stated in section 5.2.3. Mitochondrial O_2^- production was calculated as the ratio of red (O_2^-) to green (mitochondrial density) ratio.

5.2.5 Measurement of mitochondrial & glycolytic metabolism using the Extracellular Flux Analyser

CON and DMD myoblasts were plated (25,000 and 15,000 cells per well, respectively, to prevent O_2 depletion in wells with DMD myoblasts) on gelatin-coated (0.5%) Seahorse XF24 cell culture V7 microplates. Following 24 hours of incubation either with or without 1mM nitrite, media was removed from each well and replaced with pre-warmed assay buffer. Mitochondrial (oxygen consumption rate; OCR) and glycolytic (extracellular acidification rate; ECAR) metabolism was measured as described in section 3.2.5.

5.2.6 Statistics

Results are presented as mean \pm standard error of the mean. Two-way ANOVA was utilised to detect between genotype (i.e. CON and DMD) and treatment (i.e. vehicle and nitrite) differences. When a main effect or an interaction was detected, unpaired T-tests were used to determine differences between individual groups using SPSS (version 21). An α value of 0.05 was considered significant.

5.3 Results

5.3.1 Effect of acute nitrite supplementation on cell viability

We first needed to establish the maximal dose of nitrite that was tolerable in myoblasts to determine what dose would be utilised in the proceeding experiments without causing cellular dysfunction and death. To determine this, we employed two methods: (1) crystal violet staining and (2) real-time cell monitoring.

Compared to unsupplemented myoblasts (both untreated and vehicle-treated), nitrite increased the crystal violet absorbance reading, but it was not dose-specific ($p < 0.01$, Figure 5.1). While crystal violet staining is a simple and efficient method to measure cell viability, it has limitations in that it is an end-point assay and only reveals what is occurring at that time point. Therefore, we employed an additional method which involves real time (temporal) measurements of cell viability to complement the crystal violet assay and to confirm that there is no detrimental effect of nitrite (up to 1mM) on the myoblasts.

The xCELLigence system utilises microelectrodes on well bottoms to sense changes in impedance. These impedance readings are converted by the software into the Cell Index with a higher Cell Index reflecting a greater cell number (Kho *et al.*, 2015). We present the Cell Index over a total of 60 hours, during the proliferative phase of cell growth and 24 hours after the addition of nitrite, in 12 hour blocks (Figure 5.2). At 0 hours, no significant difference was observed between unsupplemented myoblasts (both untreated and vehicle-treated) and nitrite supplemented myoblasts at any concentration ($p > 0.05$,

Figure 5.2A). A trend, however, was detected for 100nM nitrite to decrease the cell index from 10nM nitrite supplemented myoblasts ($p=0.053$). At 12, 24, 36, 48 and 60 hours, no difference in the cell index was observed between unsupplemented and nitrite-supplemented myoblasts ($p>0.05$, Figure 5.2B-F). As we observed no detrimental effects of nitrite on cell viability in either method, we proceeded with the maximal tolerable dose (that we investigated) of 1mM nitrite for the following experiments.

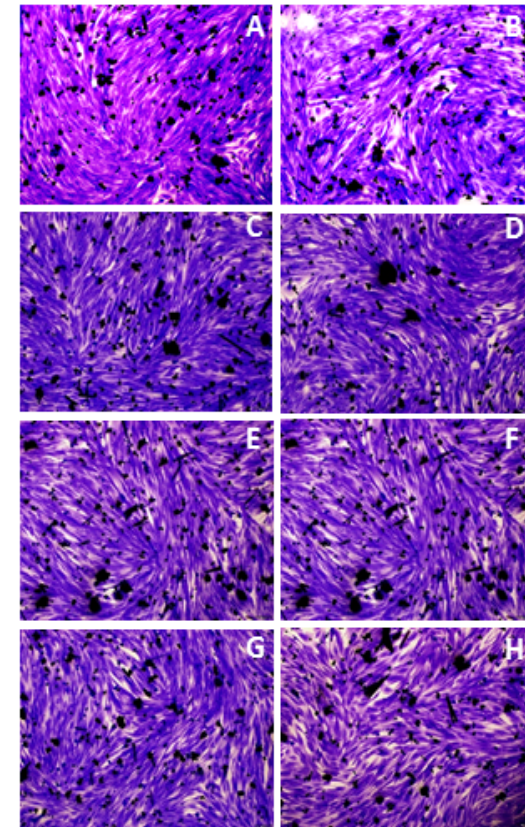
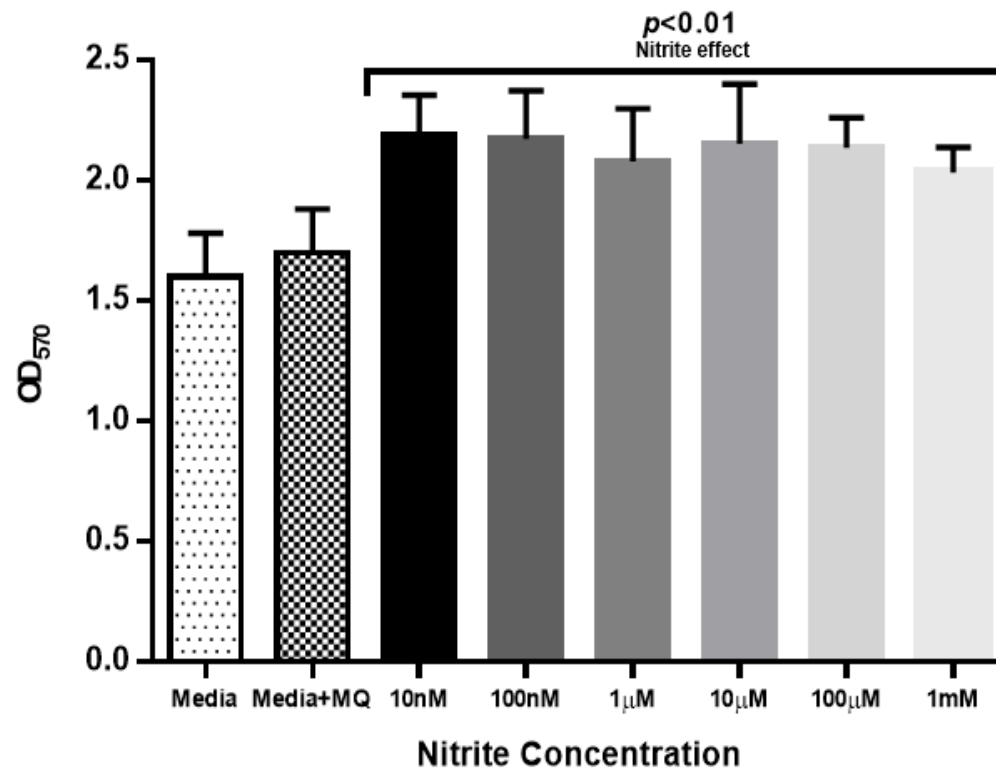


Figure 5.1. Cell viability, as determined by crystal violet staining, in unsupplemented and nitrite supplemented control (CON) myoblasts. Following 4 days of nitrite supplementation, cell viability increased compared to unsupplemented (media and media + Milli Q (MQ)) myoblasts ($p < 0.01$). $n = 3$ per group.

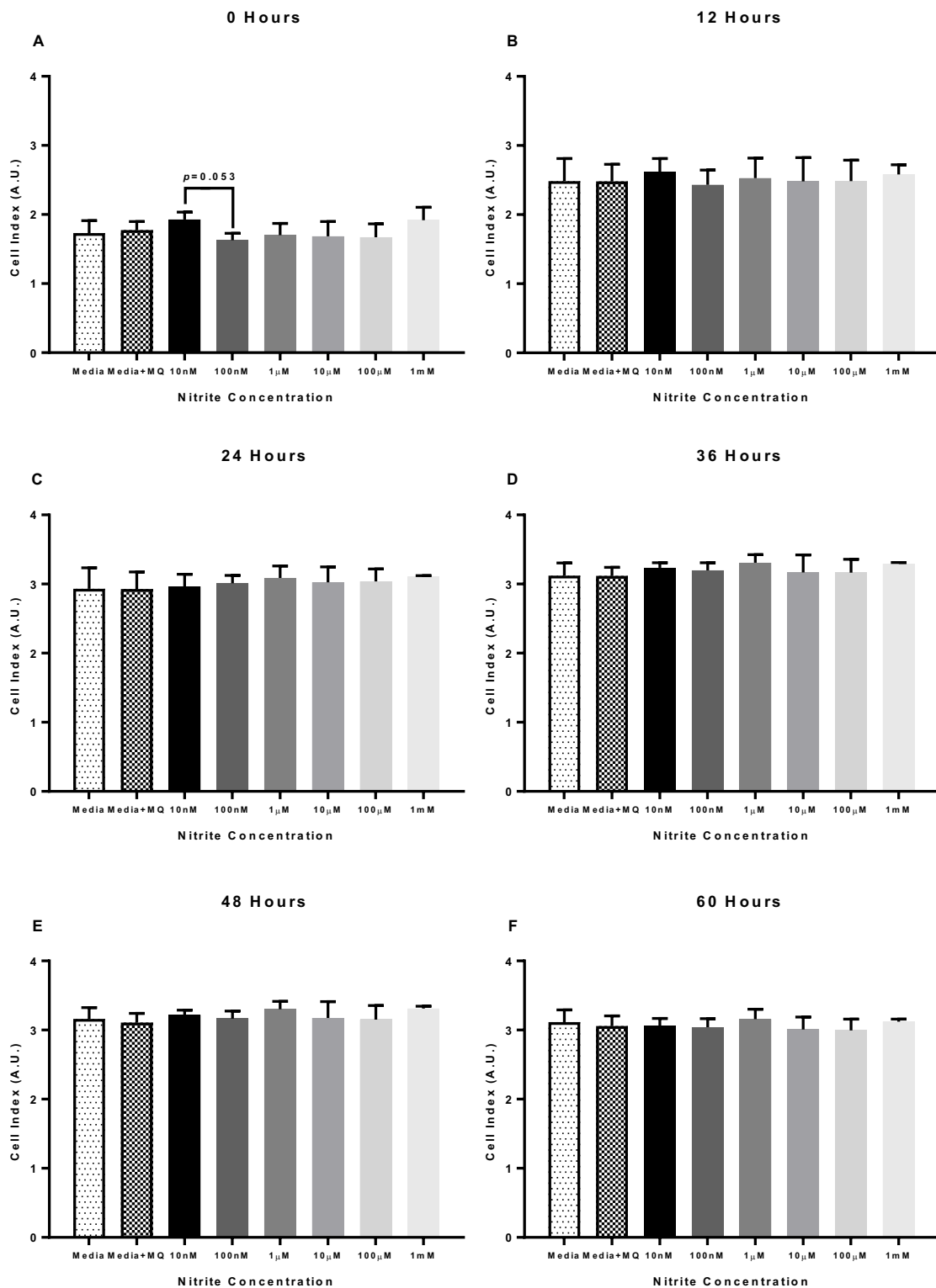


Figure 5.2. Cell Index (viability), as determined by real-time monitoring, in unsupplemented and nitrite supplemented control (CON) myoblasts. Cell Index, which was determined every 12 hours for 60 hours during the proliferative phase of cell growth, was not significantly different between unsupplemented (media and media + Milli Q (MQ)) and nitrite supplemented myoblasts ($p < 0.01$, A-F). $n = 3$ per group.

5.3.2 The effect of acute nitrite supplementation on mitochondrial viability

As NO has been documented to modulate mitochondrial function (Larsen *et al.*, 2011), we first assessed the effect of acute nitrite supplementation on mitochondrial viability using the fluorophores MitoTracker Red (active, healthy mitochondria) and MitoTracker Green (total mitochondrial pool). At the 24 hour time point, mitochondrial viability was 38% less in DMD compared to CON myoblasts ($p < 0.0001$, Figure 5.3A), however nitrite increased mitochondrial viability by 14% in DMD myoblasts only ($p < 0.01$). At 3 days, mitochondrial viability was 27% less in DMD myoblasts compared to CON ($p < 0.0001$, Figure 5.3B). As observed at the 24 hour time point, nitrite treatment improved mitochondrial viability in DMD myoblasts by 15% ($p < 0.01$), however, it was detrimental in CON myoblasts and reduced mitochondrial viability by ~10% ($p < 0.01$). At 7 days, no difference in mitochondrial viability was observed between CON and DMD myoblasts ($p > 0.05$, Figure 5.3C), however nitrite treatment was capable of increasing the mitochondrial viability in both CON and DMD myoblasts by ~4% and ~2%, respectively ($p < 0.05$).

As MitoTracker Green accumulates in all mitochondria irrespective of the $\Delta\psi$, we utilised this fluorophore to examine the effect of acute nitrite treatment on the total mitochondrial pool, since NO is a reported stimulator of mitochondrial biogenesis (Nisoli *et al.*, 2004). At 24 hours, the total mitochondrial pool was ~17% greater in DMD myoblasts compared to CON ($p < 0.01$, Figure 5.4A) with nitrite treatment having no effect in either CON or DMD myoblasts ($p > 0.05$). The mitochondrial pool, at 3 days, was still larger in DMD myoblasts (by ~72%) compared to CON ($p < 0.05$, Figure 5.4B). Nitrite treatment enhanced mitochondrial pool density at 3 days in both CON and DMD myoblasts by 58% and 21% respectively ($p < 0.01$). Interestingly, by 7 days, the mitochondrial pool was 15% lower in DMD myoblasts

compared to CON ($p < 0.0001$, Figure 5.4C). While 7 days of nitrite treatment increased the mitochondrial pool by ~6% in CON myoblasts ($p < 0.05$), there was no significant effect observed in DMD myoblasts – albeit a trend for nitrite treatment to reduce the mitochondrial pool at 7 days was detected ($p = 0.055$).

5.3.3 The effect of acute nitrite supplementation on mitochondrial superoxide (O_2^-) production

As we observed in Chapter 4 that NO has a regulatory role on cellular radical production, we assessed the effect of acute nitrite treatment on mitochondrial O_2^- production. At 24 hours, mitochondrial O_2^- production was 78% higher in DMD myoblasts compared to CON ($p < 0.01$, Figure 5.5A), and nitrite treatment stimulated further O_2^- production in both CON and DMD myoblasts by 40% and 83%, respectively ($p < 0.05$). At 3 days, O_2^- production was again higher in DMD UNSUPP myoblasts (by 77%) compared to CON ($p < 0.001$, Figure 5.5B). In both CON and DMD myoblasts, nitrite treatment significantly reduced mitochondrial O_2^- production by 72% and 66%, respectively ($p < 0.01$). Similar to 3 days, at 7 days, mitochondrial O_2^- production was 194% higher in DMD UNSUPP myoblasts compared to CON UNSUPP ($p > 0.01$, Figure 5.5C) and nitrite treatment was able to reduce mitochondrial O_2^- production in both CON and DMD myoblasts by 49% and 93%, respectively ($p < 0.001$).

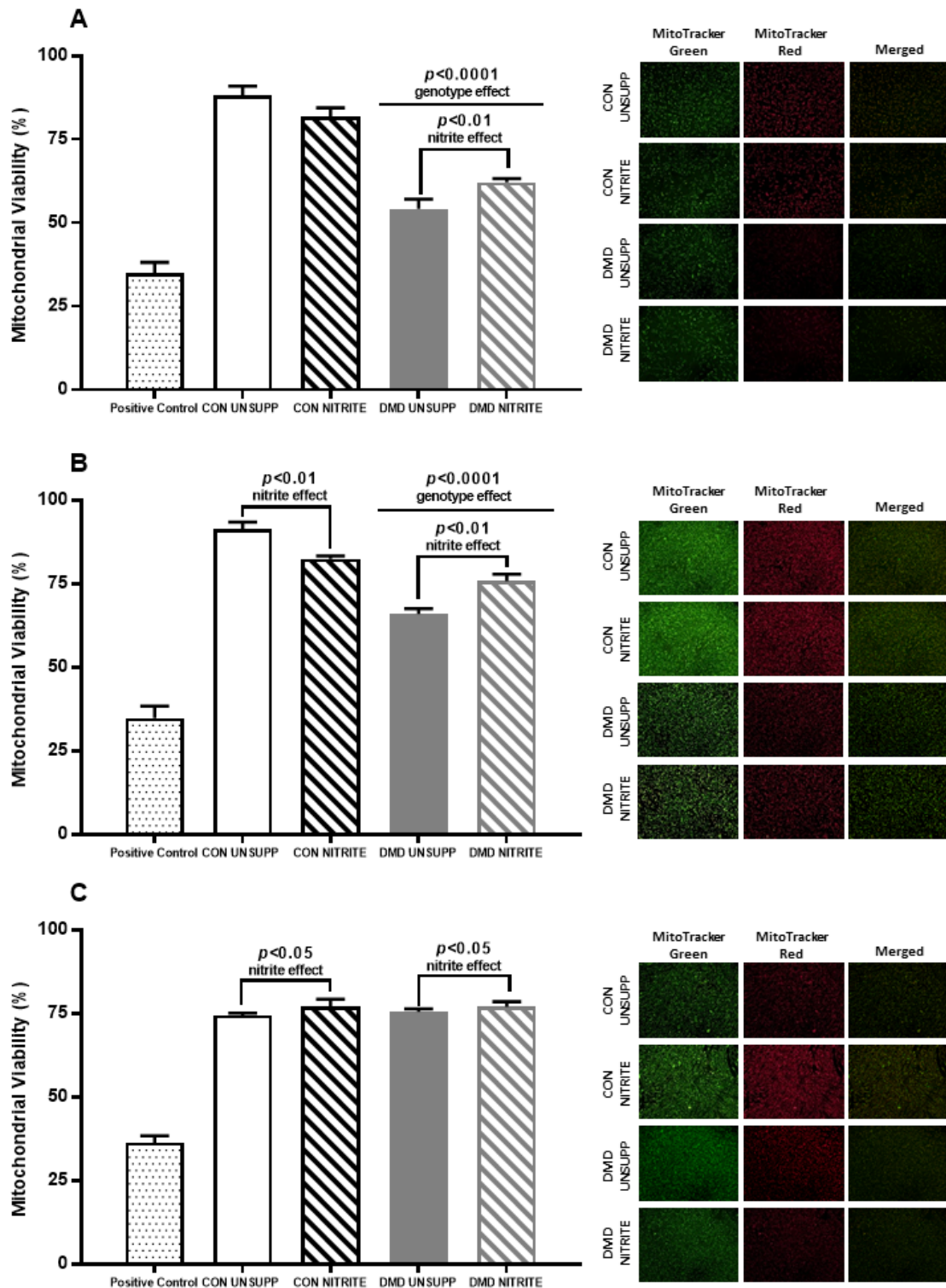


Figure 5.3. Mitochondrial viability of unsupplemented and nitrite supplemented control (CON) and DMD myoblasts. Positive control of FCCP and antimycin A. Mitochondrial viability was reduced in DMD myoblasts at 24 hours (A) and 3 days (B) compared to CON ($p < 0.0001$) with nitrite supplementation increasing mitochondrial viability at both time points in DMD myoblasts ($p < 0.01$, A & B). At 3 days, nitrite reduced mitochondrial viability in CON myoblasts ($p < 0.01$, B). At 7 days, no difference in mitochondrial viability was observed between CON UNSUPP and DMD UNSUPP myoblasts ($p > 0.05$, C) with nitrite increasing mitochondrial viability in both CON and DMD lines ($p < 0.05$). $n = 4$ per group.

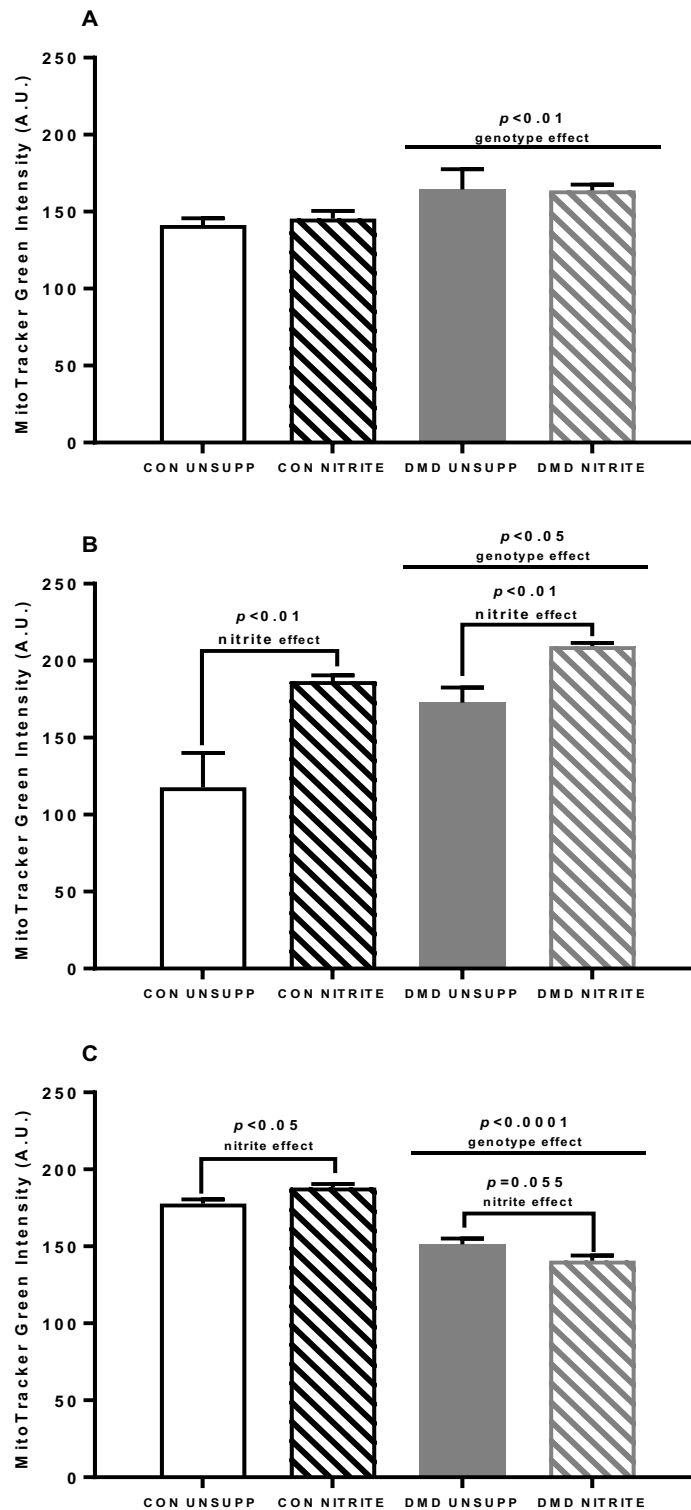


Figure 5.4. Total mitochondrial pool of unsupplemented (UNSUPP) and nitrite supplemented control (CON) and DMD myoblasts. The mitochondrial pool was greater in DMD UNSUPP myoblasts at 24 hours compared to DMD UNSUPP ($p < 0.01$, A) and nitrite had no effect in either cell type ($p > 0.05$). At 3 days, the mitochondrial pool was greater in DMD myoblasts compared to CON ($p < 0.05$, B) with nitrite increasing the mitochondrial pool in both CON and DMD myoblasts ($p < 0.01$). At 7 days, the mitochondrial pool was significantly less in DMD myoblasts compared to CON ($p > 0.0001$, C) with nitrite increasing mitochondrial pool in CON myoblasts ($p < 0.05$). In contrast, a trend for nitrite to decrease the mitochondrial pool was detected in DMD myoblasts ($p = 0.055$). $n = 4$ per group.

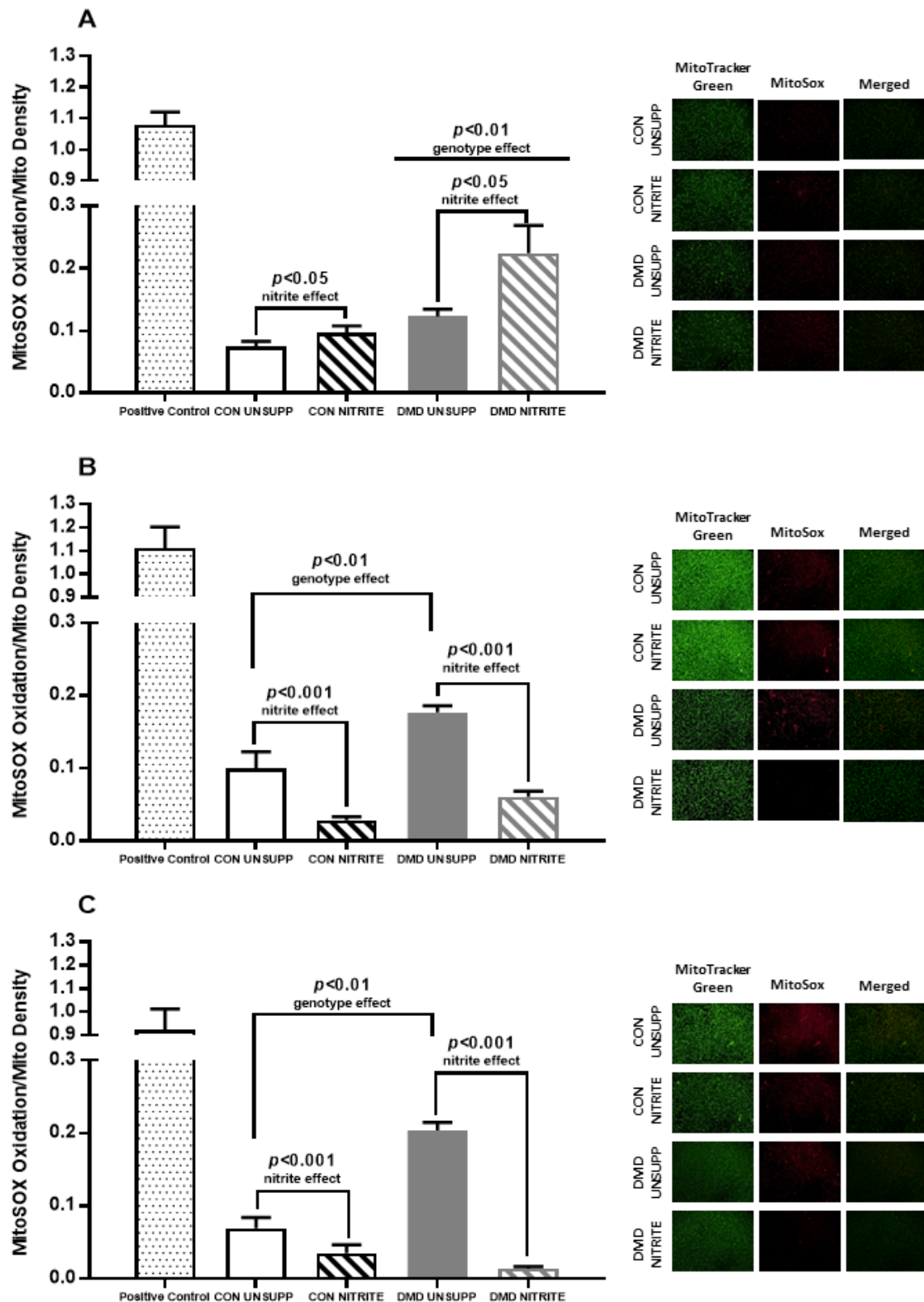


Figure 5.5. Mitochondrial superoxide (O_2^-) production of unsupplemented (UNSUPP) and nitrite supplemented control (CON) and DMD myoblasts. Positive control is antimycin A. Mitochondrial O_2^- production was greater in DMD myoblasts compared to CON at 24 hours ($p < 0.01$, A) with nitrite increasing O_2^- production in both CON and DMD myoblasts ($p < 0.05$). At 3 days, mitochondrial O_2^- production was greater in DMD UNSUPP myoblasts compared to CON UNSUPP ($p < 0.01$, B) with nitrite supplementation decreasing O_2^- production in both CON and DMD myoblasts ($p < 0.001$). At 7 days, O_2^- production was elevated in DMD UNSUPP compared to CON UNSUPP myoblasts ($p < 0.01$, C) with nitrite decreasing O_2^- production in both CON and DMD myoblasts ($p < 0.001$). $n = 4$ per group.

5.3.4 The effect of acute nitrite supplementation on oxidative and glycolytic metabolism

In Chapter Four, we demonstrated that chronic NITR supplementation in the *mdx* mouse was unable to modulate mitochondrial respiration parameters in red and white gastrocnemius fibre bundles. One limitation of the methods we employed in Chapter Four, however, was that NITR/nitrite was not provided in the assay medium. As NO is a very transient molecule, and fibre bundles were assayed ~2-4 hours after surgical excision from the blood supply containing the NITR, there is the potential that NO levels decreased during this time. Therefore, in this chapter we have assessed oxidative and glycolytic metabolic indices in the presence of nitrite to elucidate if acute (24 hour) increases in NO availability are able to positively modulate mitochondrial function. In our preliminary studies, we observed that comparable seeding densities of 25,000 myoblasts were not a viable plating density of DMD myoblasts since 25,000 myoblasts induced O₂ depletion during respiration (data not shown). Therefore, we have utilised different seeding densities in these experiments to overcome this, and we have presented these data corrected for a plating density of 5,000 myoblasts.

Using a mitochondrial stress test, we first investigated oxidative metabolism via the measurement of OCR in myoblasts across various respiratory states. Basal respiration was 192% higher in DMD myoblasts compared to CON ($p < 0.001$, Figure 5.6A) and nitrite treatment had no effect on this measure in either CON or DMD myoblasts ($p > 0.05$). Remarkably, a 6.5-fold higher proton leak was observed in DMD myoblasts compared to CON ($p < 0.0001$, Figure 5.6B), and nitrite was unable to reduce this in DMD myoblasts. As we observed with basal and proton leak OCR,

maximal and non-mitochondrial respiration was 190% and 178% higher, respectively, in DMD myoblasts compared to CON ($p < 0.0001$, Figure 5.6C & D, respectively). Nitrite treatment had no effect on maximal respiration in either CON or DMD myoblasts ($p > 0.05$, Figure 5.6C), however, nitrite did further stimulate non-mitochondrial respiration in DMD myoblasts by 63% ($p < 0.05$, Figure 5.6D).

Next, we assessed anaerobic glycolytic flux through the measurement of the ECAR in myoblasts across the various respiratory states. In DMD myoblasts, basal ECAR was 110% higher compared to CON myoblasts ($p < 0.01$, Figure 5.7A) and nitrite treatment stimulated this measure further in DMD myoblasts (by 96%; $p < 0.05$) but had no effect in CON ($p > 0.05$). Associated with increased basal ECAR, was a 210% increase in ECAR during oligomycin-induced inhibition of Complex V in DMD myoblasts compared to CON ($p < 0.0001$, Figure 5.7B). While nitrite had no effect on this measure in CON myoblasts ($p > 0.05$), nitrite further stimulated ECAR by 86% in DMD myoblasts ($p < 0.05$). During maximal (Figure 5.7C) and complete inhibition of oxidative metabolism (Figure 5.7D), ECAR was 123% and 114% higher, respectively, in DMD myoblasts compared to CON ($p < 0.0001$ and $p < 0.001$, respectively). Acute nitrite treatment had no effect on maximal ECAR in CON myoblasts ($p > 0.05$, Figure 5.7C) but did further increase the ECAR in DMD myoblasts (by 81%; $p < 0.05$). Similarly, nitrite had no effect on ECAR during the inhibition of oxidative metabolism in CON myoblasts ($p > 0.05$, Figure 5.7D) but did increase ECAR in DMD myoblasts 2-fold ($p < 0.01$, Figure 5.7D).

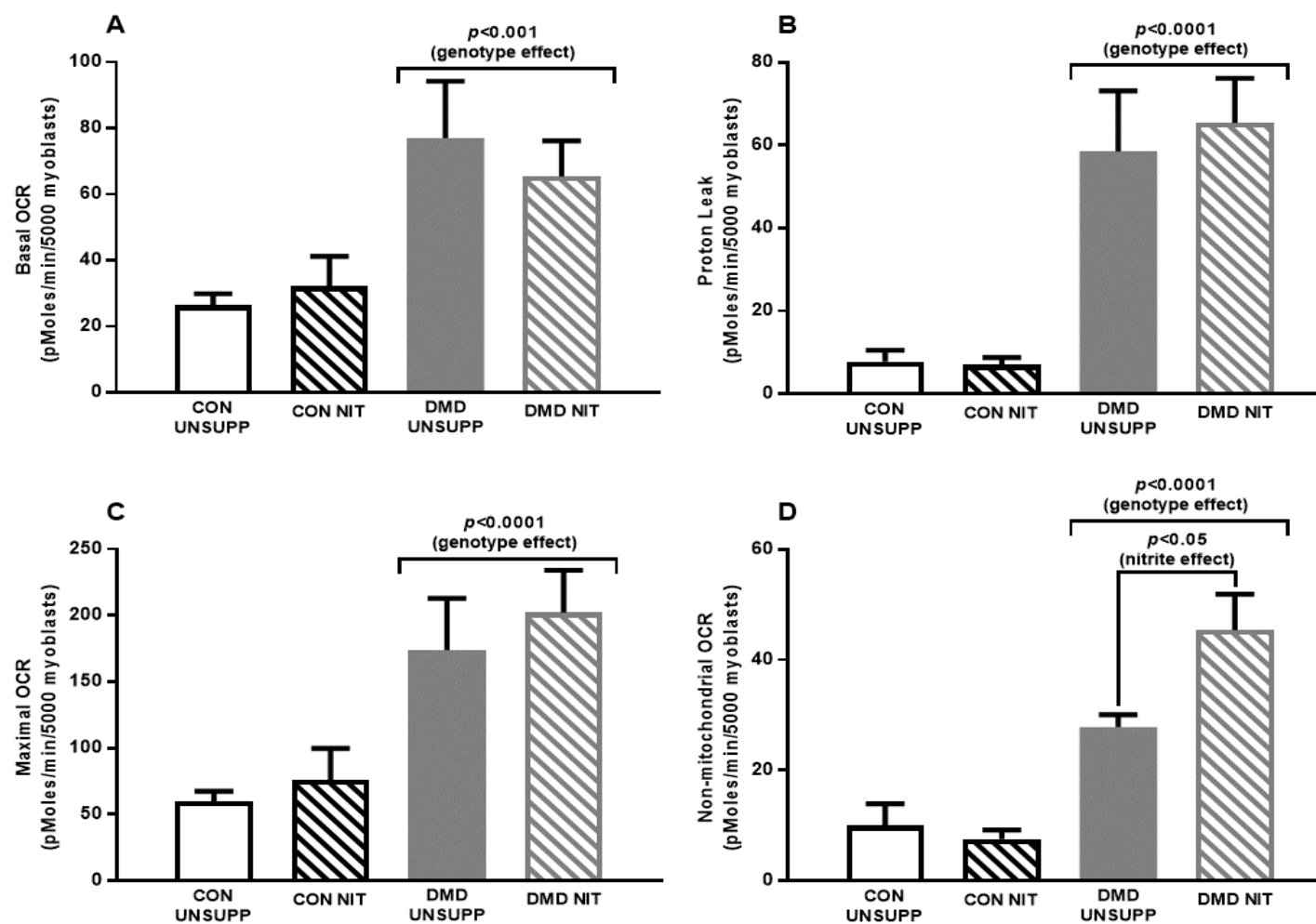


Figure 5.6. Oxygen consumption rate (OCR) of unsupplemented (UNSUPP) and nitrite (NIT) supplemented control (CON) and Duchenne Muscular Dystrophy (DMD) myoblasts. Data is presented as per 5000 myoblasts due to different plating densities of CON and DMD myoblasts following 24 hours of incubation with and without NIT. Basal respiration was significantly higher in DMD myoblasts compared to CON ($p < 0.001$, A) and nitrite had no effect in either cell line ($p > 0.05$). OCR during proton leak was higher in DMD myoblasts compared to CON ($p < 0.0001$, B) with nitrite having no effect in either cell line ($p > 0.05$). In DMD myoblasts, maximal OCR (C) and non-mitochondrial respiration (D) was also greater in DMD myoblasts ($p < 0.0001$) and nitrite further increased non-mitochondrial respiration in DMD myoblasts ($p < 0.05$). $n = 7-8$ CON UNSUPP, $n = 6$ CON NIT, $n = 5$ DMD UNSUPP, $n = 5$ DMD NIT.

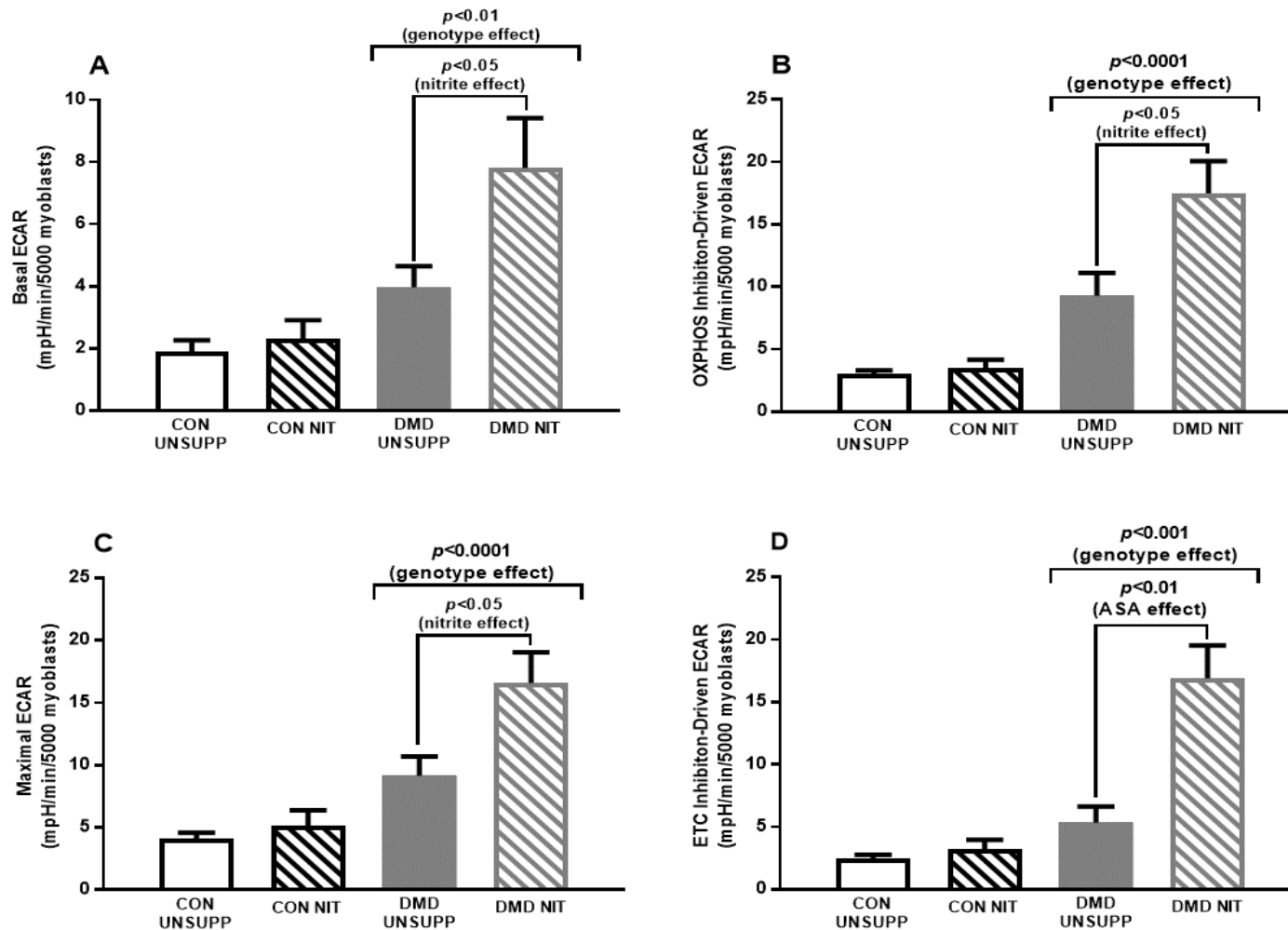


Figure 5.7. Extracellular acidification rate (ECAR) of unsupplemented (UNSUPP) and nitrite (NIT) supplemented control (CON) and Duchenne Muscular Dystrophy (DMD) myoblasts. Data is presented as per 5000 myoblasts due to different plating densities of CON and DMD myoblasts following 24 hours of incubation with and without NIT. Basal ECAR (A) and ECAR driven by inhibition of Complex V (B) was significantly higher in DMD myoblasts compared to CON ($p < 0.01$ and $p < 0.0001$ respectively) and nitrite further stimulated ECAR in both measures in DMD myoblasts only ($p < 0.05$). Maximal ECAR was higher in DMD myoblasts compared to CON ($p < 0.0001$, C) and nitrite stimulated maximal ECAR further in DMD myoblasts ($p < 0.05$). In DMD myoblasts, ECAR driven by inhibition of oxidative metabolism was greater in DMD myoblasts ($p < 0.05$ respectively) and nitrite further increased non-mitochondrial respiration in DMD myoblasts ($p < 0.01$). $n = 7-8$ CON UNSUPP, $n = 6$ CON NIT, $n = 5$ DMD UNSUPP, $n = 5$ DMD NIT.

We next calculated several mitochondrial functional indices using the OCR and ECAR measurements derived over the various respiratory states. In DMD myoblasts, the proportion of respiration attributed to ATP production (expressed as a % of basal respiration) was severely reduced (by 40%) in DMD myoblasts compared to CON ($p > 0.0001$, Figure 5.8A) and nitrite treatment exacerbated this by a further 48%; ($p < 0.05$). Next, we determined the spare respiratory capacity of myoblasts to elucidate the maximal capacity of the mitochondria to respond to depletion of the $\Delta\psi$ following chemical uncoupling i.e. a simulation of metabolic stress. Interestingly, and despite the depression of ATP production-associated mitochondrial respiration in DMD myoblasts, the spare (reserve) respiratory capacity was comparable to CON myoblasts ($p > 0.05$, Figure 5.8B). Nitrite treatment increased the spare respiratory capacity in DMD myoblasts by 28% ($p < 0.05$), but in contrast, had no effect on the spare respiratory capacity in CON myoblasts ($p > 0.05$). Next, we determined the coupling efficiency, which is a measure of the degree to which mitochondrial respiration is coupled to ATP production. The coupling efficiency of DMD myoblasts was one-third of compared to CON myoblasts ($p < 0.0001$, Figure 5.8C), highlighting a significant electron and proton leak from the mitochondrial respiratory chain. While nitrite had no effect on the coupling efficiency of CON myoblasts ($p > 0.05$), acute nitrite supplementation further uncoupled the mitochondria of DMD myoblasts (by 82%; $p < 0.0001$). Reflective of the reduced ATP production rate and coupling efficiency in DMD myoblasts, the bioenergetical health index (BHI) was only 10% of that observed in CON myoblasts ($p < 0.0001$, Figure 5.8D). While acute nitrite treatment was unable to improve the BHI of DMD myoblasts ($p > 0.05$, Figure 5.8D), it reduced the BHI of CON myoblasts by 15% ($p < 0.01$). Next, we determined the metabolic potential of the OCR and ECAR, which demonstrates the flexibility of

response to FCCP-induced mitochondrial uncoupling and depletion of the $\Delta\Psi$ for mitochondrial oxidative and cytosolic anaerobic metabolism, respectively. Both the oxidative and the glycolytic metabolic potential was comparable between CON and DMD myoblasts ($p>0.05$, Figure 5.9A and B, respectively) and acute nitrite supplementation had no effect on either measure ($p>0.05$).

Finally, we created metabolic phenograms to show the overall metabolic phenotype of FDB fibres under basal (resting) and stressed (FCCP-induced) conditions and to highlight the transitional capacities of mitochondrial respiration and glycolytic flux. At rest, untreated CON and DMD myoblasts resided in a low metabolic activity state and acute nitrite treatment had no effect on the metabolic phenotype in CON myoblasts (Figure 5.10A). In contrast, nitrite treated DMD myoblasts shifted their basal/resting metabolic state to a higher (more metabolic) phenotype (Figure 5.10A) which is reflective of the increased basal ECAR (Figure 5.7). Under metabolic stress (FCCP-induced), untreated CON myoblasts remained in a low metabolic state with nitrite transitioning the metabolic phenotype to a more aerobic one (Figure 5.10B). No differences between the rise (change in OCR), run (change in ECAR) or gradient was detected between untreated and nitrite treated CON myoblasts ($p>0.05$, Figure 5.10B). During metabolic stress, untreated DMD myoblasts transitioned to a predominantly aerobic state and nitrite treatment transitioned DMD myoblasts to a more metabolically active phenotype compared to untreated myoblasts (Figure 5.10B). This was highlighted by a 79% incremental increase in the rise (OCR) during metabolic stress-induced transition in nitrite-treated compared to untreated DMD myoblasts ($p<0.05$). The transition gradients (basal to stressed) were higher in DMD myoblasts compared to CON ($p<0.05$) and this was

resultant of DMD myoblasts relying more heavily upon increases in glycolysis, as evidenced by the larger run compared to untreated DMD myoblasts ($p < 0.05$).

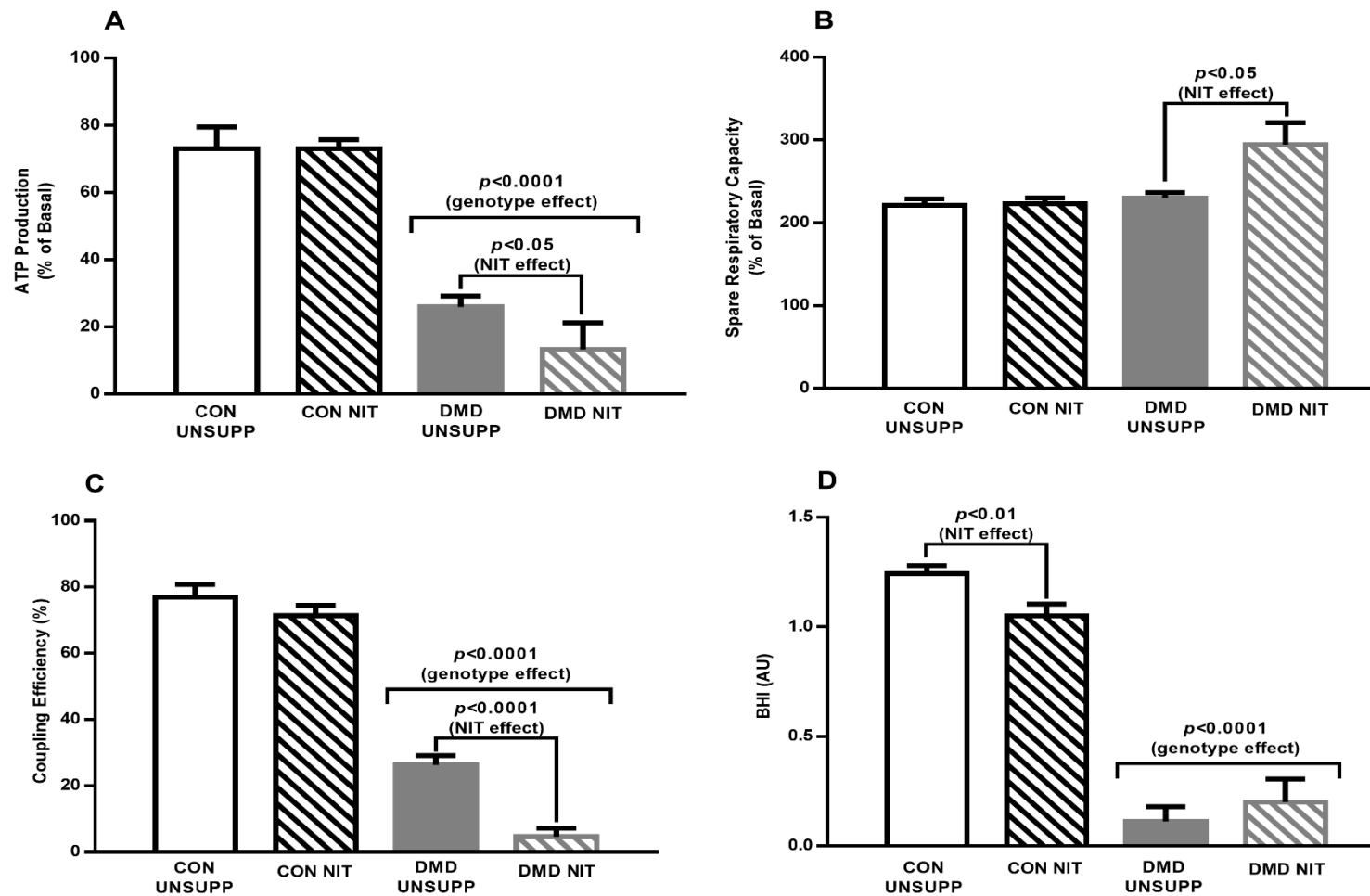


Figure 5.8. Mitochondrial function of unsupplemented (UNSUPP) and nitrite (NIT) supplemented control (CON) and Duchenne Muscular Dystrophy (DMD) myoblasts. ATP production was significantly less in DMD myoblasts compared to CON ($p < 0.0001$, A) with nitrite decreasing ATP production further ($p < 0.05$). Spare respiratory capacity was not different between CON UNSUPP and DMD UNSUPP myoblasts ($p > 0.05$, B) and while nitrite had no effect in CON ($p < 0.05$), nitrite decreased spare respiratory capacity further in DMD myoblasts ($p < 0.0001$). In DMD myoblasts, coupling efficiency was less compared to CON myoblasts ($p < 0.0001$, C) and nitrite decreased this further ($p < 0.0001$). The bioenergetic health index (BHI) of myoblasts was significantly lower in DMD compared to CON ($p < 0.0001$, D) with nitrite decreasing the BHI in CON myoblasts. $n = 7-8$ CON UNSUPP, $n = 6$ CON NIT, $n = 5$ DMD UNSUPP, $n = 5$ DMD NIT.

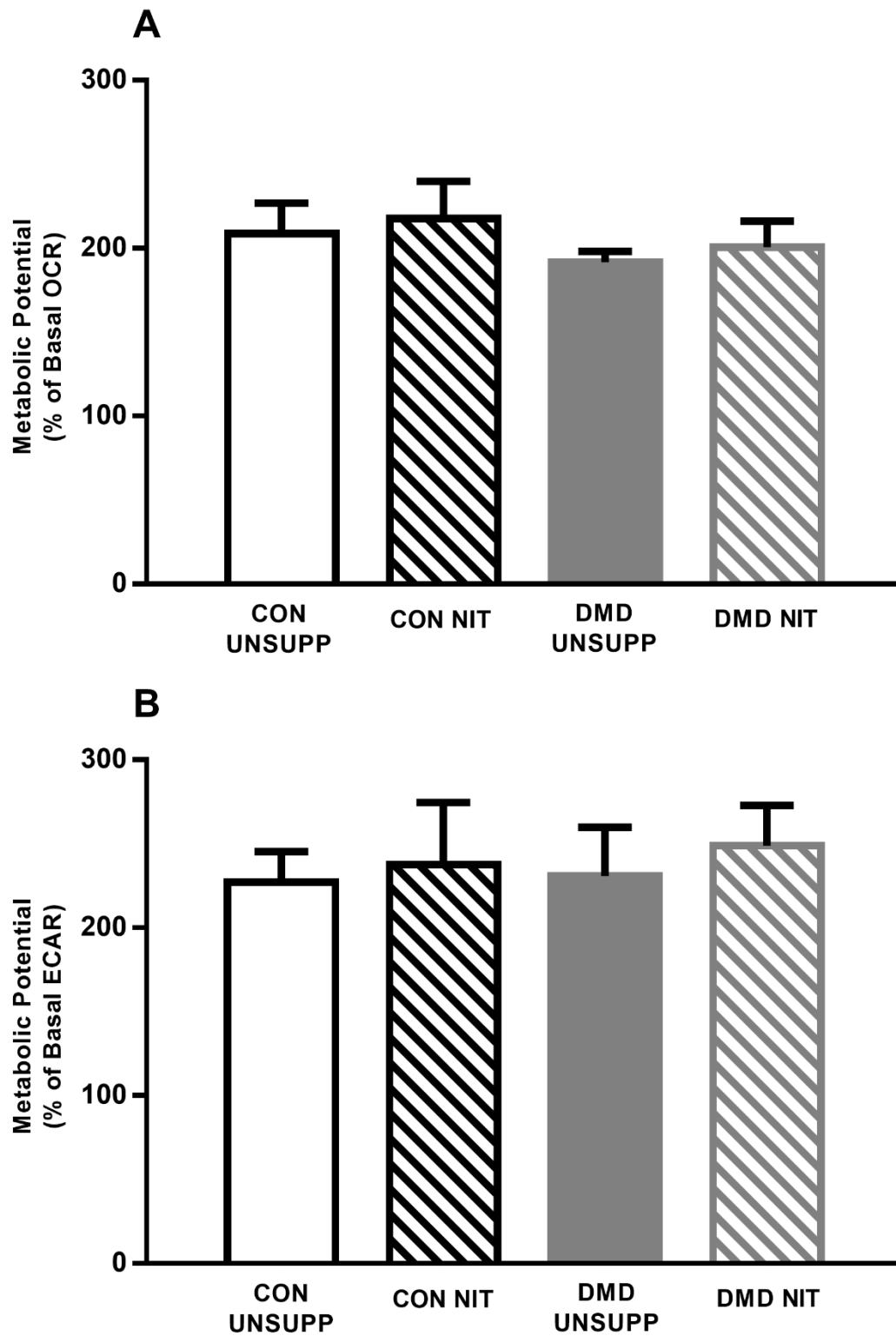
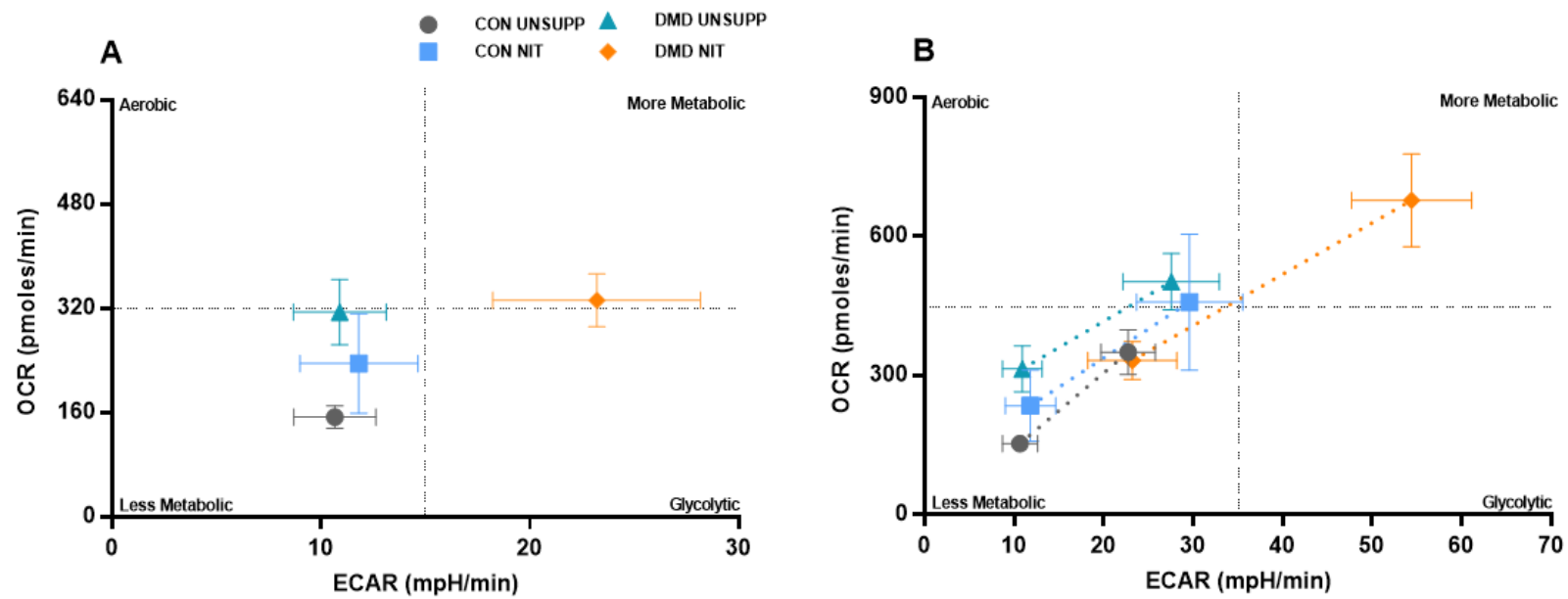


Figure 5.9. Metabolic potential of unsupplemented (UNSUPP) and nitrite (NIT) supplemented control (CON) and Duchenne Muscular Dystrophy (DMD) myoblasts. No significant difference in oxidative (A) or glycolytic metabolic potential (B) was observed between CON and DMD myoblasts ($p > 0.05$). Nitrite had no effect in either cell line ($p > 0.05$). $n = 7-8$ CON UNSUPP, $n = 6$ CON NIT, $n = 5$ DMD UNSUPP, $n = 5$ DMD NIT.



	CON UNSUPP	CON NIT	DMD UNSUPP	DMD NIT
Rise (OCR)	195.12 ± 21.65	223.58 ± 72.31	229.01 ± 27.45	410.33 ± 76.88 #
Run (ECAR)	15.02 ± 3.54	17.76 ± 3.21	16.63 ± 3.64	27.56 ± 4.44 #
Gradient	10.89 ± 1.03	8.72 ± 0.65	16.76 ± 5.47 ^	15.1 ± 2.44 ^

Figure 5.10. Metabolic phenograms of unsupplemented (UNSUPP) and nitrite (NIT) supplemented control (CON) and Duchenne Muscular Dystrophy (DMD) myoblasts. During basal respiration (A), CON UNSUPP, CON NIT and DMD UNSUPP myoblasts resided in a less metabolic phenotype with DMD NIT myoblasts residing in a more metabolic state. Under stressed conditions (B), CON UNSUPP and DMD NIT myoblasts remained in their basal phenotypes (less metabolic and more metabolic respectively) with CON NIT and DMD UNSUPP shifting to an aerobic phenotype. Rise, changes in oxygen consumption rate (OCR), was higher in nitrite treated DMD myoblasts compared to DMD UNSUPP ($p < 0.05$) with run (change in extracellular acidification rate (ECAR)) greater in DMD myoblasts compared to CON ($p < 0.05$). Overall, gradient was greater in DMD myoblasts compared to CON ($p < 0.05$). ^ significant difference from CON myoblasts $p < 0.05$, # significant difference from UNSUPP mice $p < 0.05$. $n = 7-8$ CON UNSUPP, $n = 6$ CON NIT, $n = 5$ DMD UNSUPP, $n = 5$ DMD NIT.

5.4 Discussion

The well-documented metabolic dysfunction in dystrophin-deficient skeletal muscle (Timpani *et al.*, 2015) may be a significant contributing factor to the inability to adequately repair muscle damage in dystrophin-deficient muscle. As muscle damage is a predominant pathological feature of the disease which drives the loss of functional muscle and the gain of non-functional fatty and fibrotic tissue – potentiating the clinical symptoms of progressive decline of physical function and quality of life – there is a need to facilitate/support reparative pathways in a bid to overcome this. One such way could be by improving the metabolic ATP producing capacity of myoblasts, since ATP content is an important regulator of satellite cell activity. Given NO is a known modulator of mitochondrial function (Larsen *et al.*, 2011), and it plays an important role in satellite cell activation (Anderson, 2000, Anderson and Pilipowicz, 2002, Tatsumi *et al.*, 2006, Wozniak and Anderson, 2006), we investigated an acute nitrite treatment protocol in human dystrophin-positive (CON) and dystrophin-negative (DMD) myoblasts. We demonstrated that DMD myoblasts are metabolically compromised and that acute nitrite supplementation cannot modulate this to culminate in enhanced ATP production capacity despite increased glycolytic flux and mitochondrial viability and reduced mitochondrial O₂⁻ production.

In accordance with previous studies (Olson *et al.*, 1968, Martens *et al.*, 1980, Bhattacharya *et al.*, 1993, Glesby *et al.*, 1988, Kuznetsov *et al.*, 1998, Faist *et al.*, 2001, Griffin *et al.*, 2001, Rybalka *et al.*, 2014), this study has demonstrated that dystrophic mitochondria are significantly impaired. When exposed to the mitochondrial stress test, the OCR of DMD myoblasts was significantly higher compared to CON myoblasts over all respiratory states (basal, proton leak, maximal

and non-mitochondrial), and this was evident in a mitochondrial pool that was less viable. In this instance, radical-induced proton leak would drive a higher respiratory rate (i.e. OCR) in an attempt to maintain the $\Delta\Psi$ and ATP-production capacity. However, the severely reduced ATP production capacity, coupling efficiency and BHI suggests that the $\Delta\Psi$ cannot be maintained, thus reducing the viable mitochondrial pool (i.e. MitoTracker Red fluorescence). Thus, respiratory drive favours proton leak in DMD myoblasts, apparently via leaky ETC complexes and/or heightened activity of inducible uncoupling (i.e. via adenosine nucleotide translocase (ANT) in response to elevated O_2^- production). Either of these are likely mechanisms since Percival *et al.* have shown no changes in the skeletal muscle uncoupling protein isoform, UCP3 (Percival *et al.*, 2013). Complex I of the ETC is considered to be the main source of O_2^- production in the mitochondria (Turrens *et al.*, 1980, Hansford *et al.*, 1997, Liu *et al.*, 2002, St-Pierre *et al.*, 2002, Han *et al.*, 2003, Talbot *et al.*, 2004). We have previously demonstrated that Complex I in isolated mitochondria from the *mdx* mouse is dysfunctional and, when it is the main catalyst of mitochondrial respiration, ATP production is severely impaired. However, when Complex I is inhibited (with rotenone), and Complex II-driven respiration is predominant, this deficiency is ameliorated. When considered in context with the findings of this chapter and the recent identification of a novel protein that regulates the assembly and maturation of Complex I (Fiedorczuk *et al.*, 2016), as well as the pace of electron transport and oxidative phosphorylation which is deficient in Complex I-related mitopathologies, our data highlight that a Complex I electron leak is a likely promoter of O_2^- production and mitochondrial dysfunction. For dystrophin-deficient myoblasts, mitochondrial dysfunction and a compromised bioenergetical status would compromise proliferative capacity and the capacity for skeletal muscle repair. Previous studies

have highlighted the importance of functional mitochondria and adequate energy production for the proliferation, differentiation and fusion of myoblasts into myotubes which is an important step in the repair process (Herzberg *et al.*, 1993, Korohoda *et al.*, 1993, Rochard *et al.*, 1996; 2000).

Contrary to our hypothesis that acute nitrite treatment could improve the mitochondrial dysfunction evident in DMD myoblasts, our data shows that nitrite further enhances O_2^- production and reduces the mitochondrial coupling efficiency in DMD myoblasts. While it is postulated that mild uncoupling of mitochondrial respiration is protective against oxidative stress (Skulachev, 1996), we have demonstrated that DMD myoblasts are extremely uncoupled to begin with and nitrite treatment further reduces the mitochondrial coupling efficiency to a mere ~5% of CON. Naturally, this was reflected by a low BHI of DMD myoblasts. It is curious that we observed these effects alongside a heightened nitrite-induced mitochondrial viability. Perhaps an explanation could be that nitrite concomitantly increases autophagic clearance of “dead” mitochondria while at the same time inducing mitochondrial biogenesis of “new” mitochondria, such that the total pool remains constant. However, since DMD mitochondria appear to be intrinsically defective, mitochondrial dysfunction persists and continues to be promoted by nitrite in a futile cycle. Clearly, a thorough investigation of the regulatory role nitrite-generated NO plays in the modulation of mitochondrial dysfunction and pool cycling, is required to confirm this idea.

Aside from reducing the BHI, and in stark contrast to DMD myoblasts, nitrate had no effect on mitochondrial respiration parameters in CON myoblasts. Our findings are in contrast to Larsen *et al.* who demonstrated that increased NO bioavailability induced beneficial modulation of respiration in the vastus lateralis of

healthy humans (Larsen *et al.*, 2011). However, this discrepancy may be explained by the difference in treatment time which was 3 days in Larsen *et al.* (Larsen *et al.*, 2011) compared to 24 hours at which time we measured respiration. Moreover, our conflicting results may reflect the use of a cell line that is derived from only one person. It is unknown if this individual has a genetic particularity that prevents the “normal” responses to increased NO bioavailability.

Dystrophin-deficient myoblasts appear to compensate for mitochondrial dysfunction through the enhancement of anaerobic glycolysis (ECAR) in a bid to protect against bioenergetical crisis. ECAR was higher under all respiratory states in DMD myoblasts, and, during FCCP-induced stress, a greater reliance on ECAR was evident (as indicated by the larger run during metabolic transition from resting to stressed states). In the resting state, glycolytic enhancement does not appear to benefit downstream oxidative ATP production since we did not observe an increased ATP production capacity despite elevated ECAR and OCR in DMD myoblasts. Rather, pyruvate is converted to lactate and the glycolytic flux rate is significantly enhanced. Interestingly, nitrite treatment of DMD myoblasts further enhanced glycolytic flux, an affect that was not observed in CON myoblasts suggesting a genotype-specific effect. It is plausible that nitrite-derived NO might specifically act on a deficient dystrophin-nNOS-phosphofructokinase (PFK) system in DMD muscle (Leary *et al.*, 1998, Thomas *et al.*, 1998, Vaghy *et al.*, 1998, Firestein & Bredt, 1999, Judge *et al.*, 2006, Wehling-Henricks *et al.*, 2009) as opposed to an intact system capable of independent and localised NO production (as would be the case in CON myoblasts), to enhance anaerobic glycolysis. PFK is the rate-limiting enzyme of glycolysis and reduced activity of PFK has been documented in DMD patients (Chi *et al.*, 1988) which is potentially due to the loss of allosteric regulation by nNOS, and

therefore NO, in dystrophin-deficient muscle (Wehling-Henricks *et al.*, 2009). Alternatively or complementarily, an enhanced drive to maintain the bioenergetical status of DMD myoblasts in the face of mitochondrial dysfunction which was promoted by nitrite treatment could be the primary regulator of nitrite-induced glycolytic flux enhancement observed in our study. In this instance, stimulating glycolytic flux would mitigate the impaired ATP production rate at the mitochondrial level. Such a scenario is unlikely in CON myoblasts and, without an appropriate stimulus, they would not need to enhance glycolysis as ATP demand is adequately being matched by oxidative metabolism.

Such an increase in glycolytic flux should lead to enhanced delivery of pyruvate into the mitochondria and therefore enhanced respiration in DMD myoblasts, however we did not observe this in nitrite-treated DMD myoblasts, except for an increase in spare respiratory capacity. While improved spare respiratory capacity following NO donor administration has been previously documented (Cerqueira *et al.*, 2012), the mechanism behind this is unclear. It is peculiar that nitrite treatment only modulated one mitochondrial parameter and in a stimulatory manner, since NO is known to inhibit respiration through its competitive, yet reversible, binding to Complex IV of the ETC (Cleeter *et al.*, 1994, Brown and Cooper, 1994, Boveris *et al.*, 2000, Poderoso *et al.*, 1996). Larsen *et al.* has demonstrated an improved coupling efficiency of skeletal muscle mitochondria following 3 days of nitrate supplementation of healthy humans (Larsen *et al.*, 2011), which could explain an improved spare capacity (i.e. less background proton leak thus a higher $\Delta\Psi$ to deplete and drive maximal OCR following FCCP administration). However, we have shown that acute 24 hour exposure enhances mitochondrial

uncoupling in DMD myoblasts. Notably, this effect was only observed in DMD myoblasts, and thus seems likely related to the mitochondrial pathology.

A characteristic of dystrophin-deficient skeletal muscle is oxidative stress (Hauser *et al.*, 1995, Ragusa *et al.*, 1997, Disatnik *et al.*, 1998, Rodriguez and Tarnopolsky, 2003, Tidball and Wehling-Henricks, 2007, Selsby, 2011, Terrill *et al.*, 2012) which leads to lipid and protein peroxidation (Haycock *et al.*, 1996, Disatnik *et al.*, 1998, Dudley *et al.*, 2006, Messina *et al.*, 2006) and muscle damage. In the present study, our data highlights that dystrophin-deficient myoblasts have a propensity to produce O_2^- over ATP due to poor coupling efficiency at 24 hours. Our assessment of mitochondrial O_2^- production indicates that O_2^- remains elevated at both 3 and 7 days. Nitrite treatment ameliorated the mitochondrial O_2^- production at 3 and 7 days in DMD myoblasts and similarly, reduced O_2^- production in CON myoblasts at these time points. While supraphysiological NO concentrations are typically considered to stimulate a pro-oxidant environment (Joshi *et al.*, 1999), NO has been shown to promote antioxidant gene expression through upregulation of inducible-NOS (iNOS) (Yu *et al.*, 2008). iNOS is typically expressed in response to immunostimulatory signalling (Aktan, 2004) which is absent in an *in vitro* skeletal muscle cell culture environment. However, iNOS expression is demonstrably induced in cultured muscle cells via a TNF- α -dependent pathway (Yu *et al.*, 2008). In the presence of a NO donor, TNF- α induced the expression of iNOS and the antioxidant genes *Sod3* and *Cat*, which transcribe the proteins superoxide dismutase and catalase, respectively, resulting in reduced oxidative stress (Yu *et al.*, 2008). A similar mechanism may be occurring in our study particularly since we demonstrated increased non-mitochondrial respiration in nitrite treated DMD myoblasts. Non-mitochondrial respiration refers to cytosolic O_2 consumption and it has been

documented that upregulation of antioxidant activity, to buffer radicals, increases cytosolic O_2 consumption (Winterbourn and Metodiewa, 1994, Kesler *et al.*, 2010). If nitrite treatment is inducing the upregulation of antioxidant expression through the TNF- α /iNOS pathway, then this may explain the elevated non-mitochondrial OCR in DMD myoblasts. However, for this to have occurred a similar increase in cytosolic O_2 consumption would also need to be evident in nitrite treated CON myoblasts, and it was not. Another potential reason for the amelioration of O_2^- production following nitrite treatment in CON and DMD myoblasts is the formation of other radicals, namely $ONOO^-$. In Chapter 4, while we observed that NITR reduced H_2O_2 production, this was actually accompanied by a drastic increase in $ONOO^-$ production in *mdx* TA. Similar sequestration of O_2^- into $ONOO^-$ formation may also be occurring in CON and DMD myoblasts and accounting for non-mitochondrial O_2 consumption. While we have not examined nitrite radical production in this study, such experiments seem a likely future direction.

In DMD myoblasts, the impaired metabolic integrity (in the form of elevated O_2^- production, reduced ATP production capacity and coupling) was reflected as reduced mitochondrial viability (at 24 hours). Changes in mitochondrial viability can be an indicator of impending mitochondrial demise and induction of cellular apoptosis (Liu *et al.*, 1996, Susin *et al.*, 1999). The reduced mitochondrial viability in DMD myoblasts suggests possible initiation of apoptosis. As myofibre death leads to functional muscle loss in DMD, mitigating this mitochondrial dysfunction may limit the induction of apoptosis. We demonstrated that acute nitrite supplementation at all time points (24 hours, 3 days and 7 days), enhanced mitochondrial viability in DMD myoblasts, albeit this did not correlate with improved coupling or ATP production rate following 24 hours of nitrite treatment. This improvement in mitochondrial viability

was, however, associated with an increase in the total mitochondrial pool at 24 hours suggesting that mitochondrial biogenesis may have been stimulated by nitrite treatment. Indeed, it has been well established that increasing NO bioavailability (between 1-14 days) induces PGC-1 α expression (Nisoli *et al.*, 2004, Lira *et al.*, 2010, Mo *et al.*, 2012, Ashmore *et al.*, 2015) and may be the mechanism for the increased mitochondrial pool observed at 24 hours and 3 days in nitrite treated DMD myoblasts. However, it is peculiar that we did not observe a nitrite-induced increase in the mitochondrial pool at 7 days but rather a trend for nitrite to reduce the mitochondrial pool. This seems to be a genotype-specific effect as nitrite treatment in CON myoblasts expanded the mitochondrial pool at both 3 and 7 days. The observations of Ljubacic *et al.* have demonstrated elevated basal levels of PGC-1 α in the *mdx* mouse (Ljubacic *et al.*, 2011), which we too have confirmed (see Chapter 6). This may suggest that there is limited scope to further upregulate PGC-1 α and downstream mitochondrial biogenesis signalling past the 3 day time point. It would be interesting to investigate this via western blot analysis to confirm this hypothesis.

5.5 Conclusions

In summary, our study demonstrates that DMD myoblasts exhibit severe metabolic perturbations that acute nitrite supplementation cannot overcome to improve ATP production capacity. This is despite comparable oxidative and glycolytic metabolic potentials to CON myoblasts, highlighting that the mitochondria of dystrophin-deficient myoblasts are intrinsically defective. Importantly, this data provides a mechanistic explanation for the observed reductions in proliferative and reparative capacity of DMD myoblasts (Blau *et al.*, 1983, Melone *et al.*, 2000) and highlights the key role that mitochondria play in supporting these processes. Nitrite treatment improved mitochondrial viability at all time points and ameliorated mitochondrial O_2^- production at 3 and 7 days in DMD myoblasts. Despite this, nitrite had no positive modulation on downstream mitochondrial respiration, but rather promoted the already severe uncoupling and reduced capacity for ATP production observed. Together, these data suggest that, although beneficial effects on mitochondrial pool density and viability were observed at some time points, enhancing NO bioavailability in DMD myoblasts may be detrimental at the level of respiratory chain. This may be due to either (1) the lack of nNOS protein expression, which exerts a modulatory role on metabolism; or (2) an intrinsically defective mitochondria associated with the DMD pathology and/or aetiology; particularly since nitrite treatment was not detrimental to dystrophin- and nNOS-positive CON myoblasts. In addition to our observations of the detrimental effects of chronic NO supplementation in the *mdx* mouse, our data strongly indicates that NITR/NIT therapy is contraindicative for the treatment of DMD.

Part Two

ASA Therapy

Chapter Six

Evaluation of ASA therapy in the *mdx* Mouse

6.1 Introduction

Characterised by muscular weakness and degeneration, DMD is a rare neuromuscular disorder that arises from the loss of dystrophin at the sarcolemma (Hoffman *et al.*, 1987). Ca^{2+} dysregulation appears to contribute to the pathology of DMD (Bodensteiner and Engel, 1978, Jackson *et al.*, 1985, Turner *et al.*, 1991, Imbert *et al.* 1996, Alderton and Steinhardt, 2000, Robert *et al.* 2001, Vandebrouck *et al.*, 2002, William *et al.* 2007) which leads to activation of Ca^{2+} -dependent enzymes (Haycock *et al.*, 1996, Disatnik *et al.*, 1998, Dudley *et al.*, 2006a, Messina *et al.*, 2006) and the stimulation of muscle damage and degeneration. The replacement of muscle with fatty and/or fibrous connective tissue consequentially leaves DMD sufferers wheelchair bound by early adolescence (Eagle *et al.*, 2002). A characteristic of dystrophin-deficient muscle is metabolic dysfunction that is evident in various metabolic pathways (Dreyfus, 1954, Chi *et al.*, 1987, Chinet *et al.*, 1994, Glesby *et al.*, 1988, Kuznetsov *et al.*, 1998, Rybalka *et al.*, 2014). While it is widely accepted that this metabolic dysfunction is a secondary consequence of the disease sequelae, we have published a hypothesis that places metabolic, and in particular mitochondrial dysfunction, as a core aetiological problem. Emerging evidence suggests that this dysfunction may be an inherent feature of the disease. In particular, the observations of Onopiuk *et al.* that metabolic dysfunction is present in dystrophic myoblasts (Onopiuk *et al.*, 2009) and Rybalka *et al.* that ATP production rate is affected in dystrophic mitochondria in the presence of a healthy and optimal extracellular environment (Rybalka *et al.*, 2014).

Decades ago, before the discovery of the ablation of dystrophin as the cause of DMD, metabolic therapy was extensively investigated as DMD was considered to be a predominantly metabolic myopathy. One such metabolic therapy of interest is the purine nucleotide ASA which was briefly investigated in a Phase I clinical trial for both Duchenne and Becker MD (Bonsett and Rudman, 1992). Following administration of this component of the PNC, which produces fumarate that can be shuttled into the mitochondria to expand the TCA cycle, patients anecdotally reported instantaneous increases in energy, stamina and endurance. Functionally, ASA supplementation maintained the ability to stand erect, rise from the floor and walk without falling which was accompanied with decreased serum CK levels and improvements in histopathological hallmarks indicating a reduction in muscle damage (Bonsett and Rudman, 1992). Strikingly, a significant reduction in fatty tissue infiltration was observed in muscle biopsies taken at multiple time points during the 4 year ASA trial. The replacement of functional muscle with fatty and connective tissue is a feature of disease progression and leads to reduced physical capacity. Indeed, explants of dystrophic muscle from DMD patients produce excessive lipid compared to healthy muscle cells (Bonsett, 1979) however this was ameliorated in the presence of ASA (Bonsett *et al.*, 1984).

The ability of ASA to improve key features of DMD, including the maintenance of muscle function, may arise from its capacity to promote purine salvage and anaerobic metabolism via purine nucleotide cycling and anaplerotic expansion of the TCA cycle. Together, this would converge to increase substrate delivery to the ETC and promote ATP production. Recently, it has been demonstrated that ASA stimulates exocytosis of insulin from pancreatic β cells, and that

inhibition of adenylosuccinase, the enzyme that produces ASA in the PNC, impairs glucose-stimulated insulin secretion (Gooding *et al.*, 2015). This suggests that ASA may play a role in enhancing the activation of energy producing pathways which would be beneficial to overcome the chronic metabolic compromise observed in Chapters 4 and 5, and by us (Rybalka *et al.*, 2014) and others (Olson *et al.*, 1968, Martens *et al.*, 1980, Bhattacharya *et al.*, 1993, Glesby *et al.*, 1988, Kuznetsov *et al.*, 1998, Faist *et al.*, 2001, Griffin *et al.*, 2001, Rybalka *et al.*, 2014).

A major limitation in the clinical trial investigating ASA is that the clinical evidence is very much anecdotal in that only one DMD patient completed the study long term. Thus, properly evaluating the efficacy of ASA therapy to ameliorate muscular dystrophy is timely. Thus, the aim of this study was to experimentally evaluate, in a proof-of-concept study, the therapeutic potential of ASA for the treatment of DMD. We investigated the effects of an 8 week ASA supplementation regimen in healthy (control; CON) and dystrophic (*mdx*) mouse models and specifically, assessed whether ASA supplementation could improve GU, mitochondrial function and muscle architecture. We hypothesised that expansion of the TCA cycle through ASA supplementation would: (1) enhance GU in contracting muscles of both CON and *mdx* mice; (2) improve mitochondrial respiration and reduce mitochondrial O₂⁻ production in *mdx* mice and; (3) reduce the histological hallmarks of DMD including muscle damage and lipid and fibrotic infiltration in *mdx* mice.

6.2 Methods

6.2.1 Ethical approval

All experimental procedures were approved by the Victoria University Animal Ethics Experimentation Committee and conformed to the Australian Code of Practice for the Care and Use of Animals for Scientific Purposes.

6.2.2 Animals and supplementation

Male C57Bl/10ScSn (normal wild-type strain; CON; $n=32$) and C57Bl/10*mdx* (*mdx*; $n=32$) mice were randomly assigned into four groups: unsupplemented (CON UNSUPP ($n=16$) and *mdx* UNSUPP ($n=16$)) and supplemented (CON ASA ($n=16$) and *mdx* ASA ($n=16$)). Mice in the supplemented groups were given 3000 μ g/mL ASA *ad libitum* in drinking water for 8 weeks. This dose of ASA reflects the only recorded dose administered to DMD patients via a non-intravenous dose (25mg/kg/day) (Bonsett and Rudman, 1992).

6.2.3 Muscle dissection and contraction protocol to induce GU

The muscle dissection and contraction protocol was performed as previously described in section 3.1.2.1. (Timpani *et al.*, 2016). White EDL and red SOL muscles were utilised for radioactive GU analysis following determination of optimal length (L_0) and a contraction protocol. The left EDL and SOL were stimulated to contract (contraction-induced GU) for a total of 10 minutes (pulse durations of 350msec and 500msec for EDL and SOL, respectively at a frequency of 60 Hz) while the right EDL and SOL were not

stimulated (basal GU). Following 5 minutes of contraction, Krebs buffer with 2-Deoxy-D-[1,2-³H]glucose (0.128 μ Ci/mL) and D-[¹⁴H]mannitol (0.083 μ Ci/mL) was placed in both resting and contracting muscle baths and muscles were snap frozen. GU was calculated (Hong *et al.*, 2015) in both rested and contracted muscles as described in section 3.1.2.2.

6.2.4 Mitochondrial respiration measurements

Left and right FDB were excised from anaesthetised mice and dissociated as described in section 3.1.3. Fibres were aliquoted onto coated Seahorse XF24 cell culture V7 microplates and incubated overnight. Incubation media was replaced with pre-warmed measurement buffer and OCR and ECAR was determined for various respiratory states as described in section 3.1.3.

6.2.5 Mitochondrial viability and superoxide production

Mitochondrial viability and O₂⁻ production in isolated FDB fibres was assessed by the fluorescent MitoTracker dyes Green and Red and MitoSOX Red. Isolated FDB fibres were plated onto a matrigel coated 96 well microplate and incubated overnight. Mitochondrial viability and O₂⁻ production were assessed as described in section 3.1.3.2. Images were captured on an inverted microscope (Olympus, Tokyo, Japan) and images were analysed using ImageJ software (NIH, USA).

6.2.6 Western blot analysis of metabolic stress (AMPK), mitochondrial biogenesis (PGC-1 α/β) and respiratory chain proteins (CI-V)

Western blot analysis of metabolic stress, mitochondrial biogenesis and respiratory chain proteins was performed in homogenised quadriceps as previously described in section 3.1.3.2 (Timpani *et al.*, 2016). Images were captured (Fusion FX imaging system, Vilber Lourmat, Germany) once the blots were developed with ECL Prime reagent (Amersham, Piscataway, NJ, USA) and membranes were then stained with Coomassie Blue. Analysis was performed using Fusion CAPT Advance software (Vilber Lourmat, Germany). For the ETC, PGC-1 α and $-\beta$, AMPK and Total AMPK protein analysis, data is normalised to the signal intensity of Coomassie Blue. For the AMPK/Total AMPK ratio, the data is normalised to the mean of the 8 CON UNSUPP samples run on each gel.

6.2.7 Citrate synthase (CS) activity

CS activity was measured in homogenised FDB fibres as a marker of mitochondrial capacity as described in section 3.1.3.2. CS activity was measured spectrophotometrically (412nm, 25°C, 5 mins) and calculated using the extinction coefficient of 13.6 (Srere, 1969).

6.2.8 Metabolites

ATP, PCr, Cr, lactate and glycogen metabolites were assessed in freeze-dried and crushed left TA. Metabolite analysis was performed in 96 well plates using a method adapted from Lowry and Passonneau (Lowry and Passonneau, 1972).

6.2.9 Histopathology Analysis

The right TA was covered in optimal cutting temperature compound (Sakura Finetek) and snap frozen in liquid nitrogen-cooled isopentane. TA's were sectioned on a cryostat (10µm, -20°C, Leica CM1950) and mounted onto glass slides (Menzel-Glaser).

6.2.9.1 Haematoxylin & Eosin (H&E) staining

Air-dried slides were stained using a standard H&E protocol described in section 3.1.4.2 and (Timpani *et al.*, 2016). Slides were imaged at 20x magnification (Zeiss Axio Imager Z2 microscope) and analysed for fibre size, damaged area (measured as areas of myofibril demise and inflammatory cell infiltration (Shavlakadze *et al.*, 2004)) and centronucleated fibres.

6.2.9.2 Oil Red O (ORO) staining

To assess lipid accumulation, slides were stained with ORO for 30 minutes and counterstained with haematoxylin as described in section 3.1.4.2.

Slides were imaged at 10x magnification (Zeiss Axio Imager Z2 microscope) and analysed using ImageJ software to detect staining intensity.

6.2.9.3 Gomori Trichrome staining

To assess connective tissue (fibrotic) infiltration, Gomori Trichrome staining (HT10316, Sigma Aldrich) was employed. Sections were incubated in Gomori Trichrome for 30 secs as described in section 3.1.4.2 and slides were imaged at 4x magnification (Olympus, Tokyo, Japan). The intensity of RGB staining (red=muscle, green=connective tissue, blue=nuclei) was quantified using ImageJ and the proportion of green staining (fibrotic area) was calculated as a percentage of total RGB staining (Lee *et al.* 2013).

6.2.9.4 Alizarin Red staining

To assess the relative Ca²⁺ content of the TA, sections were stained with Alizarin red (Merck Millipore) as described in section 3.1.4.2. Slides were imaged at 4x magnification (Olympus, Tokyo, Japan) and analysed using ImageJ software to detect staining intensity of Alizarin Red dye.

6.2.9.5 Succinate dehydrogenase (SDH) staining

To assess if there were any changes in oxidative capacity of TA (Sheehan and Hrapchak, 1980), the activity of SDH was assessed through histochemical analysis as described in section 3.1.4.2. Slides were incubated in working solution for 60 mins at 37°C and slides were imaged at 4x magnification (Olympus, Tokyo, Japan). Whole sections were scanned for SDH positive area

and the number of deep purple (SDH positive) and total fibres was counted to calculate percentage of oxidative fibres.

6.2.9.6 *Dystrophin and utrophin immunolabelling*

To assess if ASA is a genetic modifier of dystrophin and utrophin expression, we assessed the presence of dystrophin and utrophin in TA sections. As described in section 3.1.4.1, slides were labelled with primary dystrophin and utrophin antibodies overnight at room temperature and incubated with secondary antibodies for 2 hours at room temperature. Slides were mounted imaged via confocal microscopy.

6.2.10 Nrf2 quantification

Elevated fumarate content has been shown to stimulate Nrf2 activity (Ashrafian *et al.*, 2012) and prompted us to assess Nrf2 content in ASA-treated muscle. Nrf2 content was quantified via western blot analysis of homogenised quadriceps as described in section 3.1.3.2.

6.2.11 Statistics

Results are presented as mean \pm standard error of the mean. A two-way ANOVA was utilised to detect between genotype and supplementation differences. For GU, was utilised to detect between genotype, supplementation and GU type (basal vs contraction) differences. When a main effect or an interaction was detected, unpaired T-tests were used to determine differences

between individual groups using SPSS (version 21). An α value of 0.05 was considered significant.

6.3 Results

6.3.1 Effect of ASA supplementation on body weight, food and water consumption, and muscle and organ weights

As the tolerance of ASA in rodents is unknown, mice were supplemented with a staggered protocol. Mice received 3µg/mL of ASA for 3 days and this was increased to 30µg/mL for 4 days. The following week, mice were supplemented with 300µg/mL of ASA and a dosage of 3000µg/mL was delivered for the remainder of the supplementation period (6 weeks). Based off the average water intake, the average estimated daily exposure of mice during the first 7 days was 2.99±0.10 mg/kg/day for CON mice and 3.04±0.19 mg/kg/day for *mdx* mice. In the second week, the estimated daily exposure of mice was 35.89±2.48 mg/kg/day for CON mice and 40.20±2.20 mg/kg/day for *mdx* mice. Finally, the estimated daily exposure for the final 6 weeks of supplementation was 325.74±11.43 mg/kg/day for CON mice and 335.64±50.42 mg/kg/day for *mdx* mice. When scaled for the ~12 times higher metabolic rate of mice, the estimated daily exposure in humans would be ~27mg/kg/day and ~28mg/kg/day based off of CON and *mdx* data. This is slightly above what we aimed to achieve (25mg/kg/day).

Throughout the 8 week supplementation period, weight gain (displayed as a % of pre-supplementation body weight) was not different between CON and *mdx* strains (Figure 6.1) and ASA had no significant effect. However, post-treatment body weights following the conclusion of the supplementation period was different, with *mdx* mice being heavier compared to CON mice ($p < 0.01$,

Figure 6.2A). ASA reduced the post-treatment body weight of *mdx* ($p < 0.05$, Figure 6.2A) but not CON mice ($p > 0.05$), and this effect was independent of food and water consumption which was comparable between strain or supplementation protocol (Figure 6.3). Overall, hind limb muscle weights (EDL, gastrocnemius, quadriceps, SOL and TA) were heavier in the *mdx* strain compared to CON ($p < 0.0001$; Table 6.1), with ASA having virtually no effect on muscle weights in either strain.

As limited research has been conducted with ASA, we measured heart, diaphragm, lung and liver weight to determine potential effects on the cardiorespiratory system. While heart weight was reduced in *mdx* mice compared to CON ($p < 0.05$; Figure 6.2B) diaphragm and liver weight was increased in *mdx* mice compared to CON ($p < 0.0001$, Table 6.1). No difference in lung weight was observed ($p > 0.05$; Table 6.1). In *mdx* mice, ASA reduced the heart ($p < 0.05$; Figure 6.2B) and lung weights by ~2% and ~5%, respectively ($p < 0.01$; Table 6.1), but had no effect on diaphragm or liver weight ($p > 0.05$). Heart weight/body weight ratio was ~5% lower in *mdx* mice compared to CON with the reduction in heart weight in *mdx* ASA mice contributing to a further 5% decrease in the heart weight/body weight ratio ($p < 0.05$; Figure 6.2C).

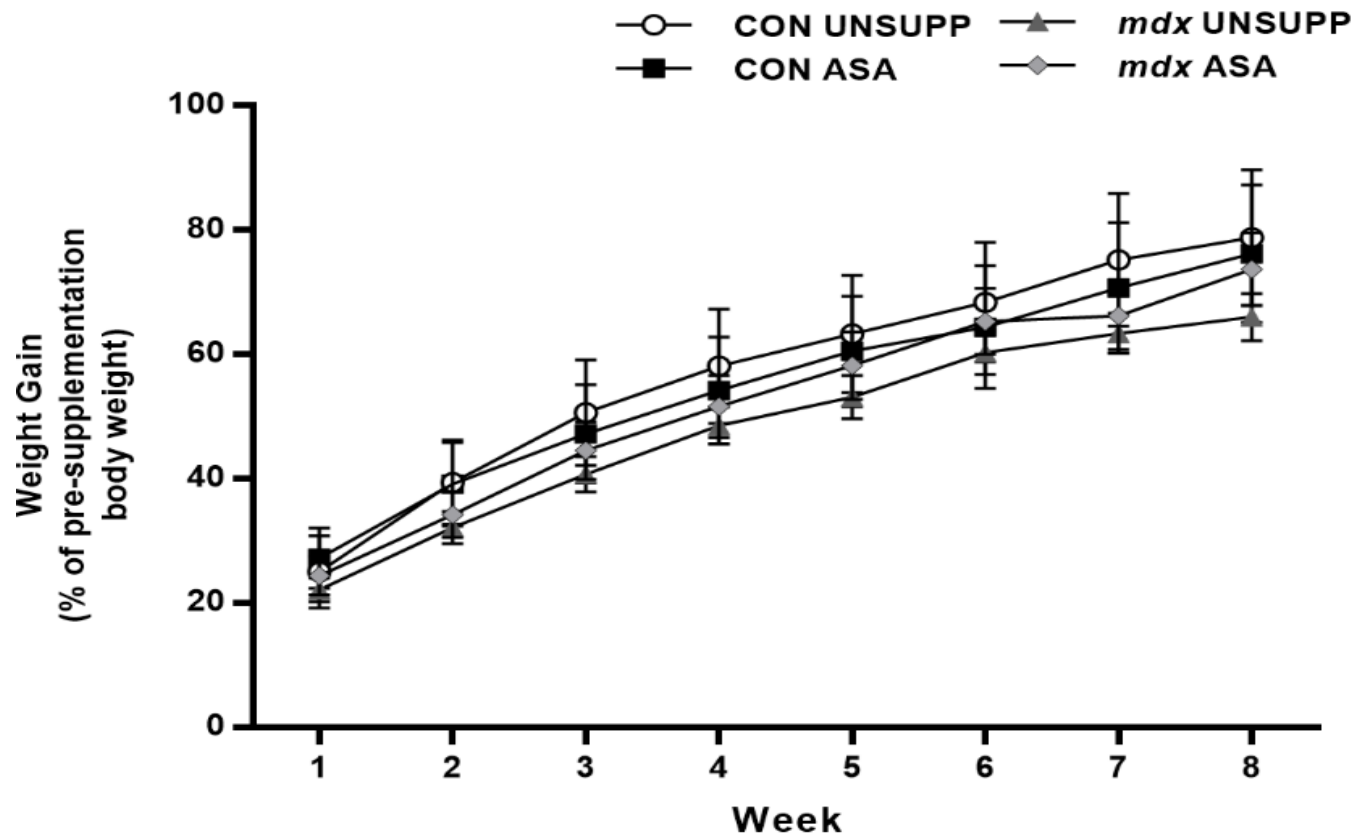


Figure 6.1. Weight gain of unsupplemented (UNSUPP) and adenylosuccinic acid (ASA) supplemented mice over the supplementation period. Changes in body weight are shown as a percentage of pre-supplementation weight. Overall, there was no difference in weight gain over the 8 week supplementation period in any group. $n=16$ per group.

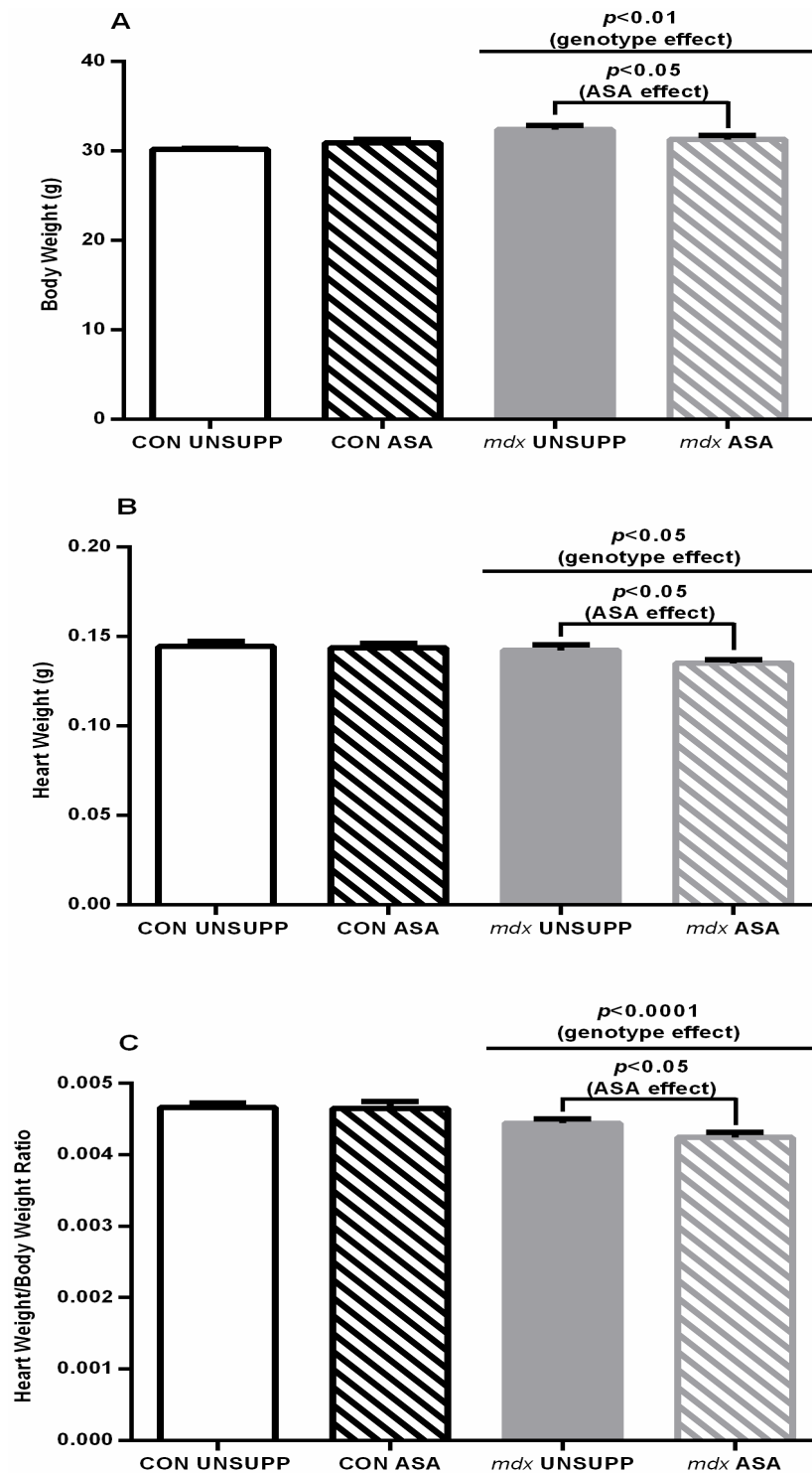


Figure 6.2. Final body weight, heart weight and heart weight to body weight ratio of unsupplemented (UNSUPP) and adenylosuccinic (ASA) supplemented mice. Final body weight was significantly higher in *mdx* mice compared to CON ($p < 0.01$, A) with ASA reducing body weight of *mdx* mice ($p < 0.05$). Heart weight was significantly lower in *mdx* mice compared to CON ($p < 0.05$, B) with ASA reducing heart weight in *mdx* mice ($p < 0.05$). The heart to body weight ratio was significantly lower in *mdx* mice compared to CON ($p < 0.0001$, B) with ASA reducing the heart to body weight ratio further in *mdx* mice ($p < 0.05$). $n = 12$ CON UNSUPP, $n = 14$ CON ASA, $n = 14$ *mdx* UNSUPP, $n = 15$ *mdx* ASA.

Table 6.1. Post-treatment muscle and organ weight from unsupplemented (UNSUPP) and adenylosuccinic acid (ASA) supplemented mice.

	CON		mdx		p values	
	UNSUPP	ASA	UNSUPP	ASA	Genotype	Supplement
Diaphragm	83.9±4.44	72.27 ± 6.87	108.69±4.29 ^^^^	110.01±5.11 ^^^^	<0.0001	0.23992
EDL (L)	12.4± 0.69	12.86 ± 0.46	17.41±0.8 ^^^^	16.13±0.85 ^^^^	<0.0001	0.26142
EDL (R)	11.57±0.88	12.26 ± 0.28	17.24±0.94 ^^^^	15.56±0.74 ^^^^	<0.0001	0.25701
Gastrocnemius (L)	147.01±7.48	142.14 ± 3.84	183.01±6.45 ^^^^	174.18±5.66 ^^^^ #	<0.0001	0.13076
Gastrocnemius (R)	154.15±4.8	155.16 ± 5.17	192.85±8.92 ^^^^	177.39±4.26 ^^^^	<0.0001	0.14414
Heart	144.48±2.99	143.75 ± 2.57	142.19±3.07 ^	135.12 ± 1.85 ^ #	<0.05	0.04583
Liver	1495.08±43.88	1603.18±49.51	1794.73± 43.42 ^^^^	1724.66±55.09 ^^^^	<0.0001	0.44239
Lungs	204.78±9.75	183.09±7.97 ##	195.72±6.91	176.96±5.45 ##	0.171	0.00436
Plantaris (L)	20.18±1.25	19.96±1.18	22.31± 0.81 ^	22.06±1.16 ^	0.01539	0.4597
Plantaris (R)	32.57±2.45	18.97±1.07	22.99±0.64 ^	21.98±0.93 ^	0.02343	0.14288
Quadriceps (L)	197.82 ± 11.39	198.99±7.02	289.92±9.54 ^^^^	279.91 ± 8.87 ^^^^	<0.0001	0.32215
Quadriceps (R)	190.12 ± 10.81	182.73±7.86	263.75±8.17 ^^^^	262.68±10.27 ^^^^	<0.0001	0.3423
Soleus (L)	11.36±0.54	11.76± 0.54	15.65±0.58 ^^^^	15.5 ± 0.69 ^^^^	<0.0001	0.45146
Soleus (R)	10.76±0.65	11.38±0.45	14.2±0.53 ^^^^	14.52±0.77 ^^^^	<0.0001	0.35649
Spleen	119.46±4.83	124.26± 4.24	125.08±3.58	117.56±4.00	0.3831	0.33078
TA (L)	48.67±3.24	49.74±2.3	74.67±2.94 ^^^^	69.7±2.26 ^^^^	<0.0001	0.20576
TA (R)	52.66±3.79	50.81± 1.63	72.59±2.04 ^^^^	71.71±2.4 ^^^^	<0.0001	0.12306

^ significant difference from CON mice $p<0.05$; ^^^^ significant difference from CON mice $p<0.0001$; # significant difference of CON and *mdx* ASA mice from UNSUPP mice $p<0.05$; ## significant difference of CON and *mdx* ASA mice from UNSUPP mice $p<0.05$ $n=7-14$ CON UNSUPP, $n=11-16$ CON ASA, $n=10-16$ *mdx* UNSUPP, $n=11-16$ *mdx* ASA.

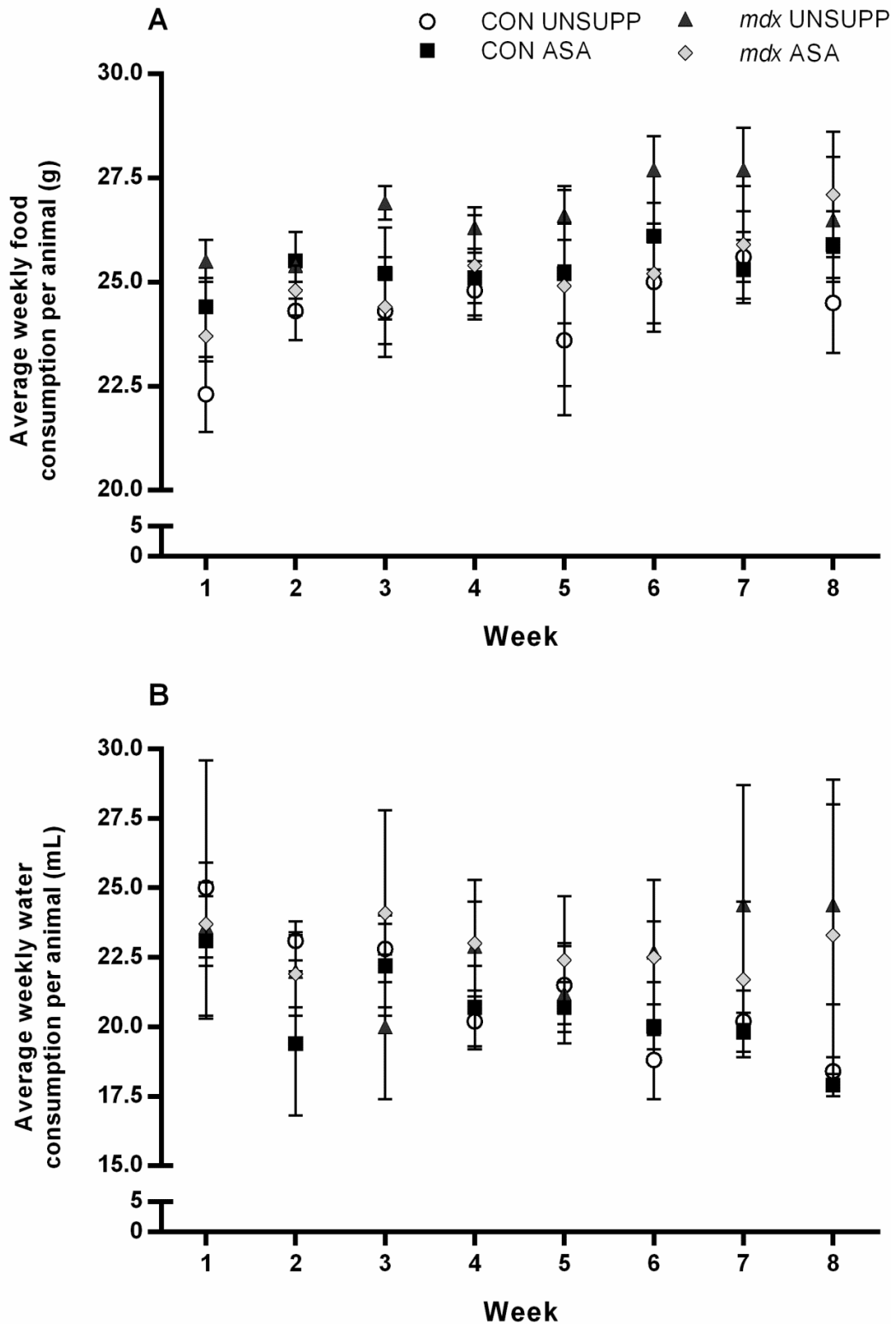


Figure 6.3. Average food and water consumption of unsupplemented (UNSUPP) and adenylosuccinic acid (ASA) supplemented mice during the supplementation period. Over the 8 week supplementation period, food and water consumption did not differ between unsupplemented and supplemented animals ($p > 0.05$). $n = 16$ per group.

6.3.2 Effect of ASA supplementation on GU

The recent evidence demonstrating that ASA can modulate insulin secretion from the pancreas suggests a regulatory role of ASA in systemic glucose homeostasis and utilisation. This prompted us to investigate whether ASA has an effect on GU (both basal- and contraction-induced) and if so, if it could normalise GU in *mdx* muscles. In the *mdx* EDL, GU (both basal- and contraction-induced) was depressed compared to CON ($p < 0.01$, Figure 6.4A) and a similar reduction was observed in *mdx* SOL muscles ($p < 0.0001$; Figure 6.4B). There was no effect of ASA on either basal- or contraction-induced GU across the genotypes and muscles ($p > 0.05$; Figure 6.4). As per Chapter 4, this data highlights an impaired capacity for basal- and contraction-induced GU in both the *mdx* EDL and SOL which could not be modulated by ASA supplementation.

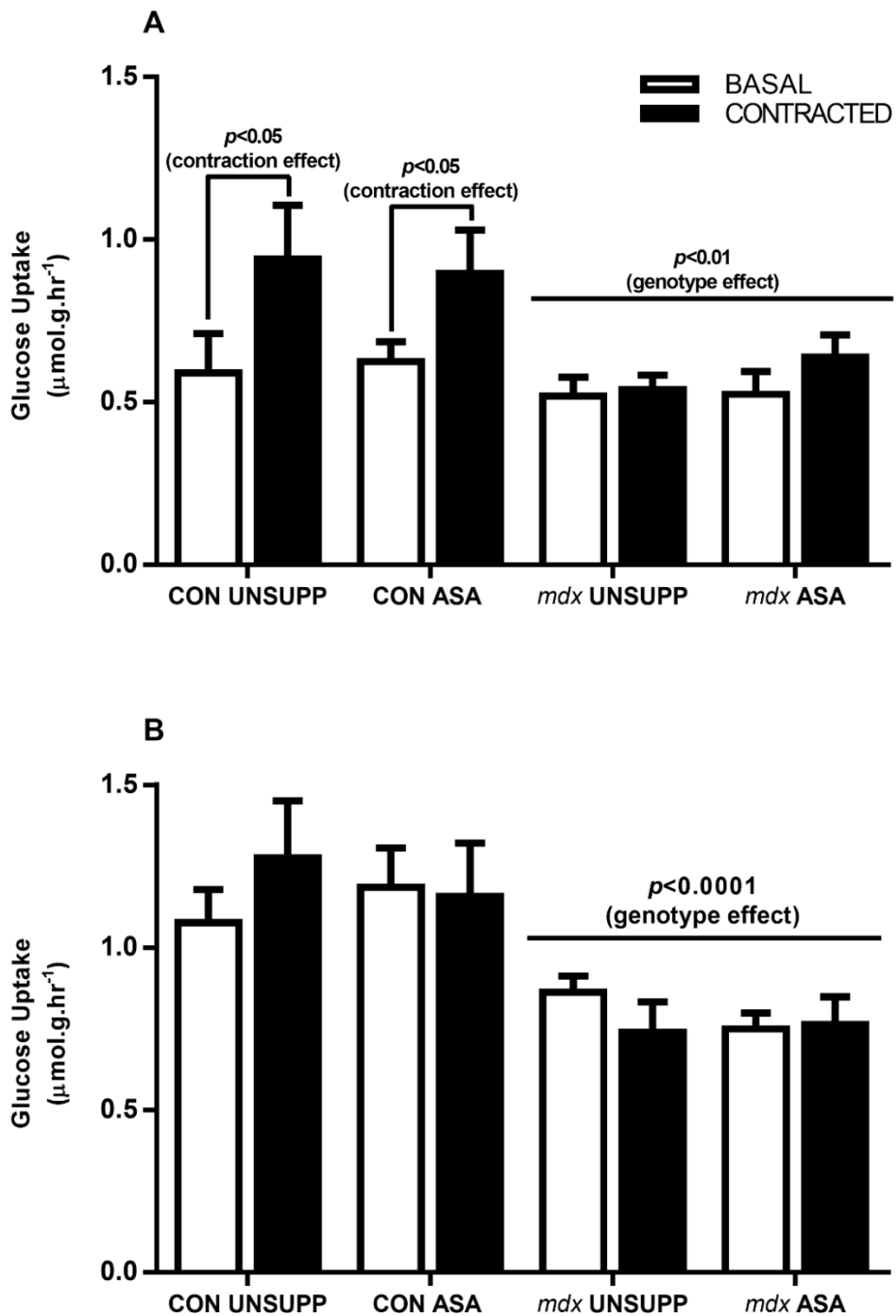


Figure 6.4. Glucose uptake (GU) in isolated extensor digitorum longus (EDL) and soleus (SOL) from unsupplemented (UNSUPP) and adenylosuccinic acid (ASA) supplemented control (CON) and *mdx* mice. In *mdx* EDL, both basal- and contraction-induced GU were significantly reduced compared to CON EDL ($p < 0.01$, A). For the SOL, both basal- and contraction-induced GU were significantly reduced in the *mdx* compared to CON groups ($p < 0.0001$, B). There was no effect of ASA in any strain or muscle type ($p > 0.05$). For EDL basal GU: $n = 9$ CON UNSUPP, $n = 11$ CON ASA, $n = 10$ *mdx* UNSUPP, $n = 16$ *mdx* ASA. For EDL contraction-induced GU: $n = 10$ CON UNSUPP, $n = 14$ CON ASA, $n = 6$ *mdx* UNSUPP, $n = 15$ *mdx* ASA. For SOL basal GU: $n = 11$ CON UNSUPP, $n = 15$ CON ASA, $n = 10$ *mdx* UNSUPP, $n = 16$ *mdx* ASA. For SOL contraction-induced GU: $n = 8$ CON UNSUPP, $n = 12$ CON ASA, $n = 7$ *mdx* UNSUPP, $n = 13$ *mdx* ASA.

6.3.3 Effect of ASA supplementation on metabolism

6.3.3.1 *Respirometry*

Considering the significant improvements in energy and stamina observed in the clinical trial of ASA (Bonsett and Rudman, 1992), and the capacity of purine nucleotide cycling to generate fumarate for anaplerosis, we next investigated the effect of ASA on mitochondrial functional indices in dissociated FDB fibres. As we could not reliably quantify protein content of the wells to internally correct respiration values for mitochondrial density, due to very low protein concentrations (Schuh *et al.*, 2012), here we present respiration parameters that are internally corrected for basal respiration rate and thus mitochondrial content.

Using a mitochondrial stress test, we first determined the metabolic potential of the OCR and ECAR, which demonstrates the flexibility of response to FCCP-induced mitochondrial uncoupling and depletion of the inner-mitochondrial membrane potential ($\Delta\Psi$), for mitochondrial oxidative and cytosolic anaerobic metabolism, respectively. The oxidative metabolic potential, which assesses the capacity to ramp up oxidative metabolism during metabolic stress, was 18% less in *mdx* compared to CON FDB fibres ($p < 0.01$, Figure 6.5A). ASA had no effect on this measure in either strain of mice. In contrast, the glycolytic metabolic potential, which assesses the capacity to ramp up glycolysis during metabolic stress, was 113% higher in *mdx* compared to CON FDB fibres ($p < 0.01$, Figure 6.5B). Again, ASA had no effect on this measure in either strain.

Next, we assessed the mitochondrial coupling efficiency of dissociated FDB fibres, which highlights the extent to which ATP production at Complex V is matched

to oxygen consumption at Complex IV. There was no difference in the coupling efficiency between mouse strains and ASA had no effect on this measure in either strain (Figure 6.7C). We also assessed the Bioenergetical Health Index (BHI), a predictive marker of the overall metabolic responsiveness to stress (Chacko *et al.*, 2014). In *mdx* FDB fibres, the BHI was ~18% less than that of CON FDB fibres ($p < 0.01$, Figure 6.5D) and ASA had no effect on the BHI in either CON or *mdx* fibres. Next, we measured citrate synthase (CS) activity in FDB fibres as a rudimentary marker of mitochondrial functional capacity (Reichmann *et al.*, 1985, Larsen *et al.*, 2012). There was no difference in the CS activity between CON and *mdx* FDB fibres (Figure 6.5E). ASA did, however, increase CS activity by 24% in CON fibres ($p < 0.05$) but had no effect in *mdx* fibres ($p > 0.05$).

Finally, we created metabolic phenograms to show the overall metabolic phenotype of FDB fibres under basal (resting) and stressed (FCCP-induced) conditions and to highlight the transitional capacities of mitochondrial respiration and glycolytic flux. Under basal conditions (Figure 6.6A), CON UNSUPP fibres maintained a more glycolytic phenotype that was moderately metabolic, with ASA shifting CON fibres to a higher basal metabolic and glycolytic state. At rest, *mdx* UNSUPP FDB fibres were highly metabolic, and ASA restored the basal metabolic phenotype to one comparable to CON UNSUPP fibres (Figure 6.6A). During FCCP-induced stress conditions (Figure 6.6B), both CON UNSUPP and ASA fibres transitioned into a highly metabolic phenotype. *Mdx* UNSUPP and ASA fibres also responded to FCCP-induced metabolic stress by transitioning to a more metabolic phenotype however the gradient associated with this transition was significantly less, with a smaller increase in OCR (rise) compared to CON ($p < 0.05$, Figure 6.6B). ASA

reduced the run (the change in ECAR) in *mdx* fibres by 48% compared to *mdx* UNSUPP ($p < 0.05$).

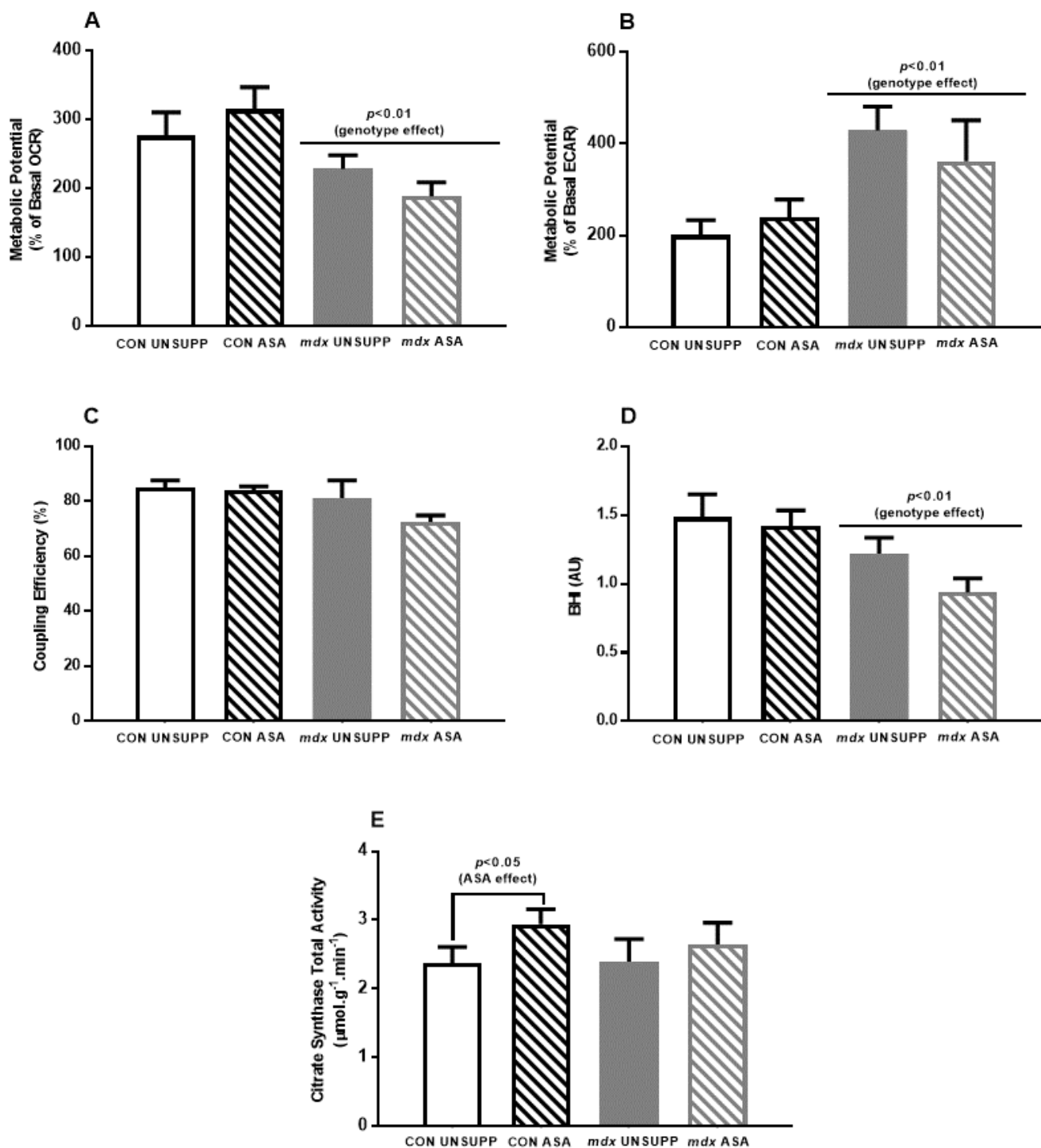
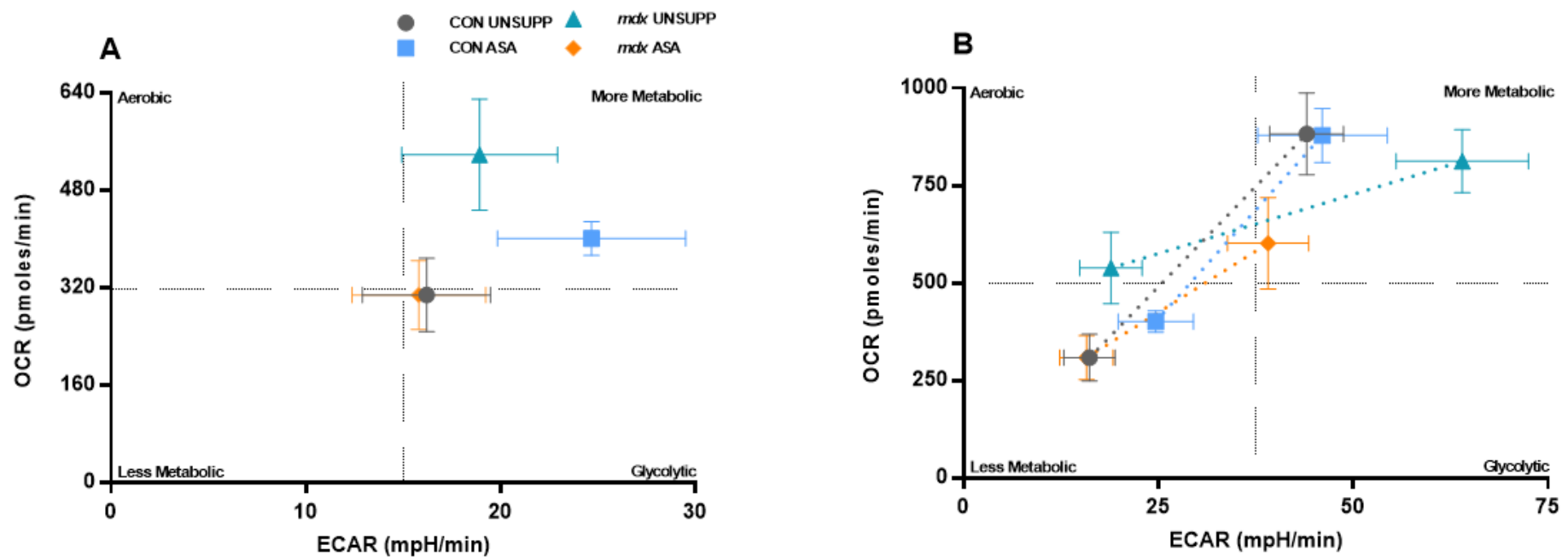


Figure 6.5. Mitochondrial function in isolated flexor digitorum brevis (FDB) fibres from unsupplemented (UNSUPP) and adenylosuccinic acid (ASA) supplemented control (CON) and *mdx* mice. Oxidative metabolic potential was significantly less in *mdx* fibres compared to CON ($p < 0.01$, A) while glycolytic metabolic potential was greater ($p < 0.01$, B) and ASA had no effect ($p > 0.05$). No differences in coupling efficiency was observed between CON and *mdx* FDB fibres ($p > 0.05$, C). The bioenergetical health index (BHI) of isolated FDB fibres was significantly lower in *mdx* compared to CON ($p < 0.01$) with ASA having unable to improve the BHI in either strain. In CON fibres, ASA increased citrate synthase (CS) activity ($p < 0.05$, E) with ASA having no effect in *mdx* fibres ($p > 0.05$). $n = 9-11$ CON UNSUPP, $n = 9-10$ CON ASA, $n = 10-14$ *mdx* UNSUPP, $n = 10-15$ *mdx* ASA.



	CON UNSUPP	CON ASA	mdx UNSUPP	mdx ASA
Rise (OCR)	490.56 ± 77.65	500.61 ± 51.26	270.63 ± 52.24 ^^	240.83 ± 63.06 ^^
Run (ECAR)	26.94 ± 6.54	26.87 ± 5.24	48.05 ± 6.03 ^	24.89 ± 2.67 #
Gradient	28.51 ± 5.91	31.73 ± 7.74	8.93 ± 1.98 ^	10.04 ± 1.77 ^

Figure 6.6. Metabolic phenograms of isolated flexor digitorum brevis (FDB) fibres from unsupplemented (UNSUPP) and adenylosuccinic acid (ASA) supplemented control (CON) and *mdx* mice. During basal respiration (A), CON UNSUPP and *mdx* ASA fibres resided in a predominantly glycolytic phenotype with CON ASA and *mdx* UNSUPP fibres residing in a more metabolic state. Under stressed conditions, CON FDB fibres had a larger increase in oxygen consumption rate (OCR; rise) compared to *mdx* fibres ($p < 0.01$). The increase in extracellular acidification rate (ECAR; run) during FCCP-induced stressed was larger in *mdx* UNSUPP fibres compared to CON UNSUPP ($p < 0.05$) and ASA reduced the run in *mdx* fibres ($p < 0.05$). Overall, the gradient was greater in CON fibres compared to *mdx* fibres ($p < 0.05$, B) with ASA having no effect. $n = 9$ CON UNSUPP, $n = 9$ CON ASA, $n = 10-11$ *mdx* UNSUPP, $n = 10-11$ *mdx* ASA.

6.3.3.2 Mitochondrial Viability and Superoxide (O_2^-) Production

Since ASA increases purine nucleotide cycling and cytosolic fumarate production, which did not appear to stimulate mitochondrial metabolism in our FDB fibres, we have investigated other potential effectors of increased fumarate production. Mitochondrial viability, which was determined by the ratio of live mitochondria (MitoTracker red) to the total mitochondrial pool (MitoTracker green), was comparable between CON UNSUPP and *mdx* UNSUPP FDB fibres (Figure 6.9A). While ASA had no effect on mitochondrial viability in CON fibres, it did increase the viability of the mitochondrial pool in *mdx* fibres by 17% ($p < 0.05$, Figure 6.7A). We also assessed the total mitochondrial pool (MitoTracker green) and demonstrated that, while the mitochondrial pool was not different between CON UNSUPP and *mdx* UNSUPP fibres (Figure 6.7B), ASA increased the pool in both CON and *mdx* fibres by 55% and 208% respectively ($p < 0.01$, Figure 6.7B).

Next we assessed the effect of ASA on mitochondrial O_2^- production to assess whether ASA could modulate oxidative stress. No differences in mitochondrial O_2^- production were detected between CON UNSUPP and *mdx* UNSUPP fibres (Figure 6.7C). In CON FDB fibres, ASA increased O_2^- production by 28% ($p < 0.05$) but in contrast, decreased O_2^- production in *mdx* fibres by 26% ($p < 0.05$). Together, these data suggest that, while ASA does not improve downstream mitochondrial respiration in FDB fibres, ASA can promote mitochondrial viability and improve the redox status of the cell.

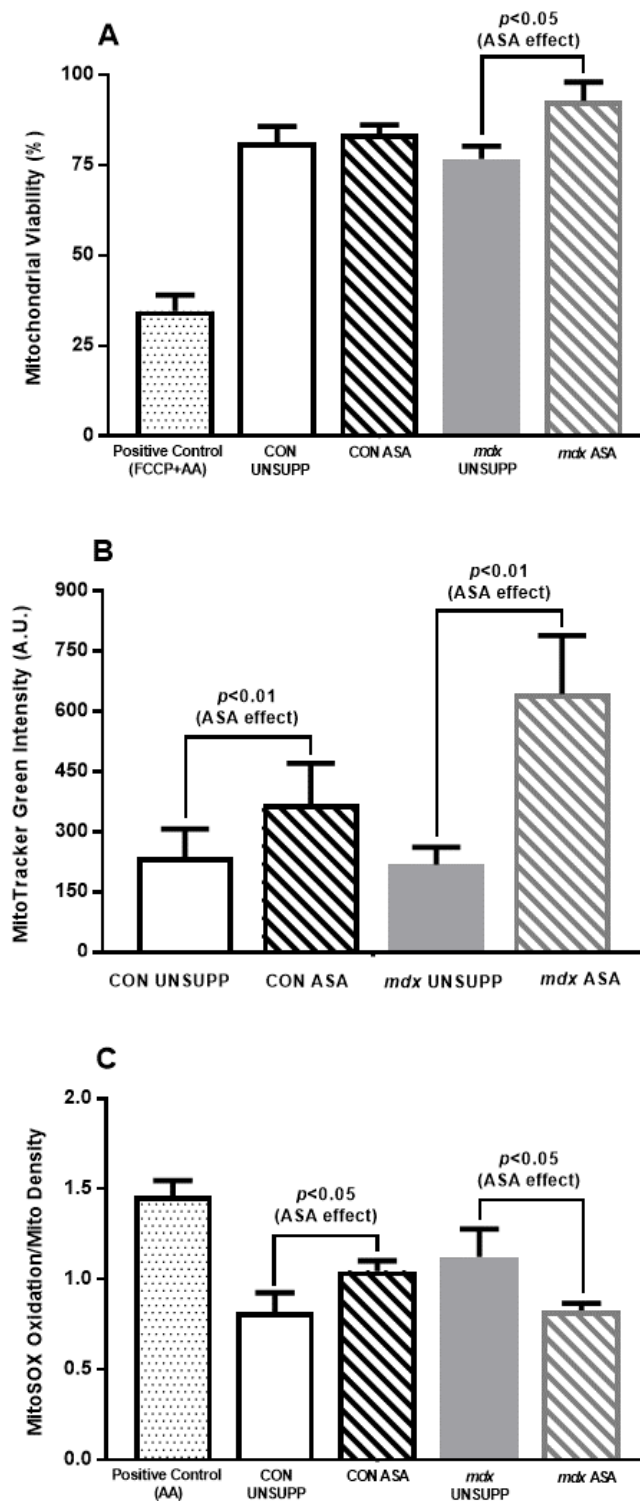


Figure 6.7. Mitochondrial viability, pool and superoxide (O_2^-) production of isolated flexor digitorum brevis (FDB) fibres from unsupplemented (UNSUPP) and adenylosuccinic acid (ASA) supplemented control (CON) and *mdx* mice. There was no difference in mitochondrial viability between CON UNSUPP, CON ASA and *mdx* UNSUPP fibres ($p > 0.05$, A) and ASA increased mitochondrial viability in *mdx* fibres ($p < 0.05$). In both CON and *mdx* fibres, ASA increased the total mitochondrial pool compared to UNSUPP fibres ($p < 0.01$, B). In CON fibres, ASA increased O_2^- production ($p < 0.05$, C) with ASA decreasing O_2^- production in *mdx* fibres ($p < 0.05$). For mitochondrial viability and mitochondrial pool: $n = 3$ CON UNSUPP, $n = 6$ CON ASA, $n = 9$ *mdx* UNSUPP, $n = 8$ *mdx* ASA. For mitochondrial O_2^- production: $n = 3$ CON UNSUPP, $n = 6$ CON ASA, $n = 6$ *mdx* UNSUPP, $n = 8$ *mdx* ASA.

6.3.3.3 Electron Transport Chain (ETC) Complex Expression

We next assessed ETC complex expression to elucidate if ASA could modulate respiratory chain density. As we did not have sufficient FDB fibres following respiratory analysis, we utilised the quadriceps for Western blot analysis due to a similar fibre type composition (Armstrong & Phelps, 1984, Pickett-Gies *et al.* 1986, Burkholder *et al.* 1994, Kuznetsov *et al.* 1996). In all subunits quantified from CI to CV, no difference was detected between CON and *mdx* quadriceps ($p>0.05$, Figure 6.8). ASA had no effect on the expression of any of the mitochondrial complex subunits assessed in either strain.

6.3.3.4 Metabolites

We next evaluated the metabolite content of TA to assess if ASA could influence the metabolic signature of the skeletal muscle. The Cr, PCr, Total intramuscular creatine (TCr), ATP and lactate content was comparable between CON UNSUPP and *mdx* UNSUPP (Figure 6.9A-E). While ASA had no effect on Cr content in *mdx* TA (Figure 6.9A), ASA reduced Cr content by 21% in CON TA ($p<0.05$). ASA induced an increase in the intramuscular PCr content of both CON and *mdx* TA by, 61% and 33%, respectively ($p<0.01$, Figure 6.9B). Similarly, TCr content was positively modulated by ASA with a 17% and 13% increase in CON and *mdx* TA, respectively ($p<0.05$, Figure 6.9C). While ASA had no effect on the ATP content of *mdx* TA (Figure 6.9D), there was a trend for ASA to increase ATP content in CON samples ($p=0.05$). Finally, glycogen content was 47% higher in *mdx* TA compared to CON ($p<0.01$, Figure 6.9F) however was not affected by ASA in either strain.

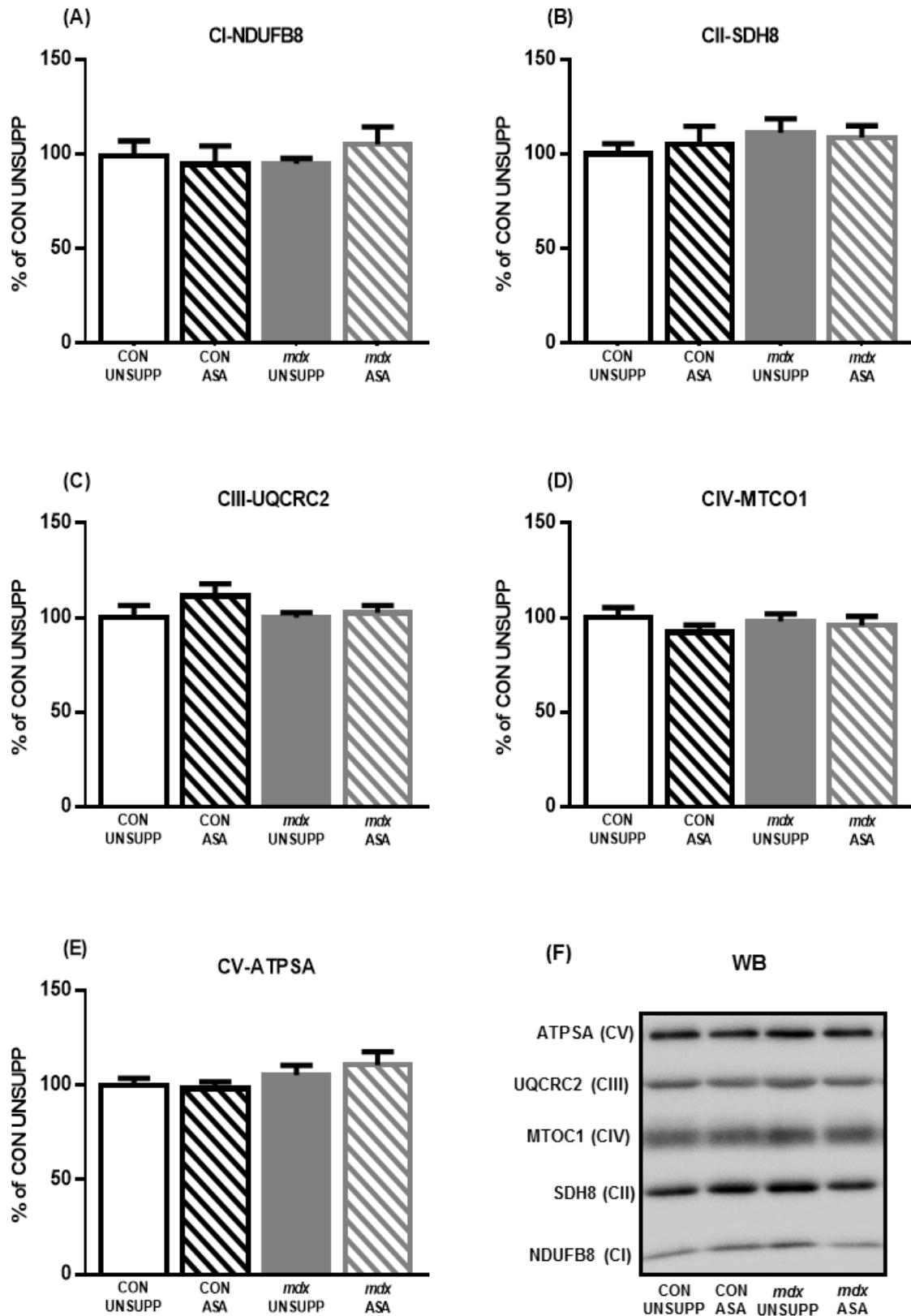


Figure 6.8. Mitochondrial respiratory chain complex proteins of the quadriceps from unsupplemented (UNSUPP) and adenylosuccinic acid (ASA) supplemented control (CON) and *mdx* mice. No significant difference was detected between CON and *mdx* quadriceps in any subunit of the ETC complexes ($p > 0.05$, A-E). Representative western blots of proteins from each of the five mitochondrial respiratory complexes (F). $n = 8$ per group.

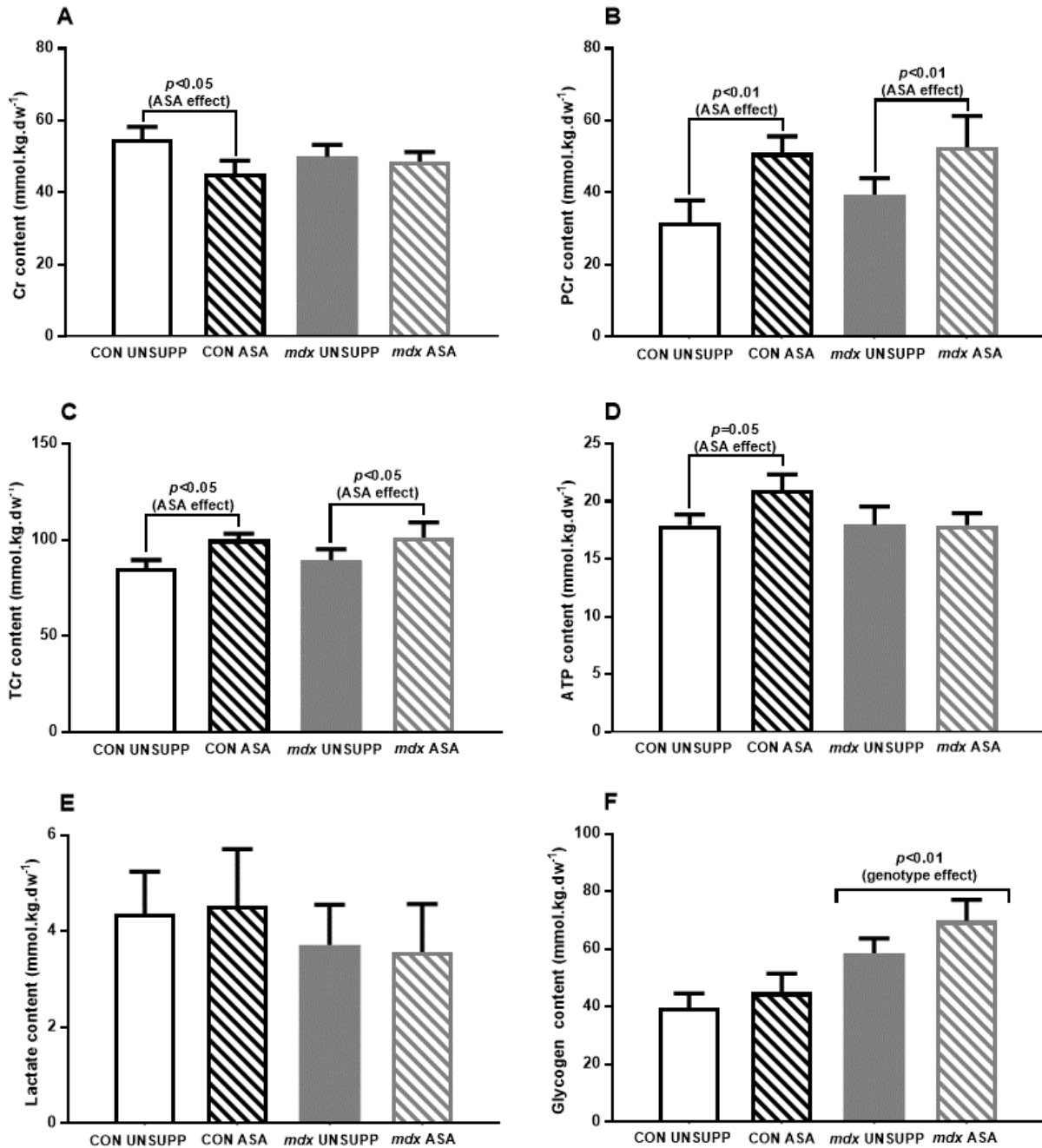


Figure 6.9. Intramuscular creatine (Cr), phosphocreatine (PCr), total creatine (TCr), adenosine triphosphate (ATP), lactate and glycogen content of unsupplemented (UNSUPP) and adenylosuccinic acid (ASA) supplemented control (CON) and *mdx* mice. No significant difference in Cr content was detected between CON UNSUPP and *mdx* UNSUPP tibialis anterior (TA) ($p>0.05$, A) with ASA increasing Cr content in CON only ($p<0.05$). While PCr content was comparable between CON UNSUPP and *mdx* UNSUPP TA ($p>0.05$, B), ASA increased PCr content in both CON and *mdx* tissues ($p<0.01$). Similarly, although no genotypic differences were detected ($p>0.05$, C), ASA increased TCr content in both CON and *mdx* TA ($p<0.05$). ATP content was not different between CON UNSUPP and *mdx* UNSUPP TA ($p<0.05$, D) with a trend for ASA to increase ATP content in CON detected ($p=0.056$). Lactate content was comparable between CON and *mdx* TA ($p>0.05$, E) and ASA had no effect. Overall, glycogen content was greater in *mdx* TA compared to CON ($p<0.01$, F) and ASA had no effect in either genotype. For Cr: $n=7$ CON UNSUPP, $n=9$ CON ASA, $n=8$ *mdx* UNSUPP, $n=8$ *mdx* ASA.

6.3.3.5 Metabolic stress signalling

During metabolic stress, when ATP cannot be resynthesised sufficiently to match metabolic demand, ADP is rapidly degraded to AMP. The rising AMP level activates AMPK to modulate various responses to support ATP production in mitochondrial biogenesis, lipid metabolism and autophagy. Therefore, we assessed metabolic stress signalling pathways in the quadriceps muscle to assess whether ASA treatment could stimulate an upregulation of these pathways given purine nucleotide cycling stimulates AMP production, along with fumarate. Phosphorylated AMPK (P-AMPK), which indicates AMPK activation, was similar between CON UNSUPP and *mdx* UNSUPP quadriceps (Figure 6.10A). ASA reduced metabolic stress-associated P-AMPK in CON muscle only (by 47%; $p < 0.05$), having no effect in *mdx* quadriceps. Total AMPK protein was also comparable between the strains, and ASA had no effect on this measure (Figure 6.10B). The ratio of P-AMPK to total AMPK was also comparable between CON UNSUPP and *mdx* UNSUPP (Figure 6.10C) and while there was no effect on *mdx* quadriceps, there was a strong trend for ASA to reduce the ratio in CON quadriceps ($p = 0.058$). Expression of the downstream regulators of mitochondrial biogenesis, PGC-1 α and -1 β , was elevated in *mdx* quadriceps by 34% and 149%, respectively compared to CON quadriceps ($p < 0.05$, Figure 6.11A and B respectively). ASA increased the protein content of both PGC-1 α and - β in CON quadriceps by 23% and 47% respectively ($p < 0.05$), but in contrast, had no effect on *mdx* samples.

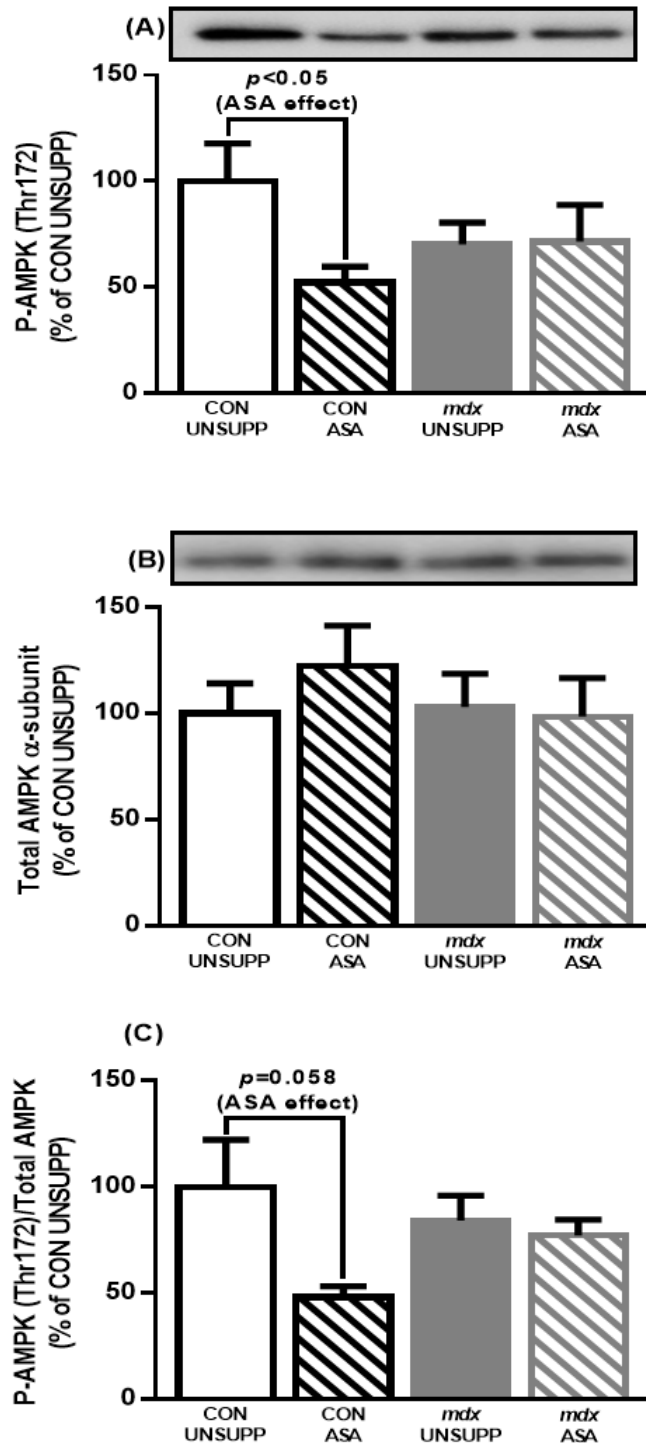


Figure 6.10. AMPK protein content of quadriceps from unsupplemented (UNSUPP) and adenylosuccinic acid (ASA) supplemented control (CON) and *mdx* mice. Phosphorylated AMPK (P-AMPK) was not different between CON UNSUPP and *mdx* UNSUPP quadriceps ($p > 0.05$, A) with ASA decreasing P-AMPK in CON only ($p < 0.05$). No difference in Total AMPK was detected between either strain or supplementation regimes ($p > 0.05$, B) with no difference in P-/Total AMPK ratio observed between CON UNSUPP and *mdx* UNSUPP ($p > 0.05$, C). While ASA had no effect on *mdx* quadriceps, there was a trend for ASA to decrease the ratio in CON quadriceps ($p = 0.058$). $n = 7$ CON UNSUPP, $n = 6$ CON ASA, $n = 8$ *mdx* UNSUPP, $n = 7$ *mdx* ASA.

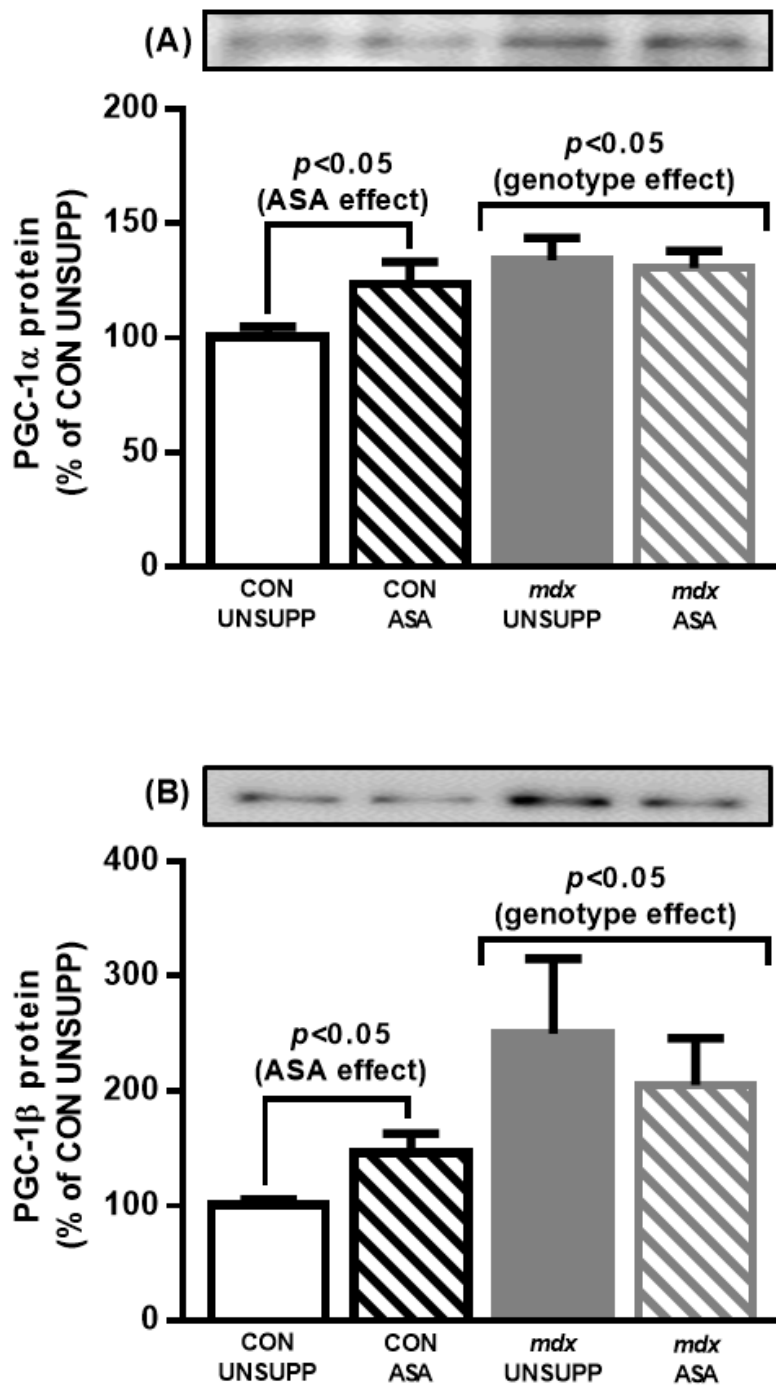


Figure 6.11. PGC-1 α and -1 β protein content of quadriceps from unsupplemented (UNSUPP) and adenylosuccinic acid (ASA) supplemented control (CON) and *mdx* mice. PGC-1 α and - β protein content was higher in *mdx* quadriceps compared to CON ($p < 0.05$, A and B respectively) with ASA increasing both PGC-1 α and - β protein in CON only ($p < 0.05$). For PGC-1 α : $n = 8$ CON UNSUPP, $n = 6$ CON ASA, $n = 6$ *mdx* UNSUPP, $n = 6$ *mdx* ASA. For PGC-1 β : $n = 8$ CON UNSUPP, $n = 8$ CON ASA, $n = 7$ *mdx* UNSUPP, $n = 7$ *mdx* ASA.

6.3.4 Effect of ASA supplementation on histopathology

We assessed the effect of ASA on the histopathological features of dystrophic muscle since the clinical trial of ASA supplementation in DMD patients resulted in maintenance of muscle function and strength (Bonsett and Rudman, 1992). The most likely explanation for these improvements is reduced damage, fat and fibrotic tissue infiltration and/or enhanced regeneration.

6.3.4.1 Haematoxylin and Eosin (H&E)

The mean fibre size was 17% larger in *mdx* UNSUPP TA compared to CON UNSUPP ($p < 0.05$, Figure 6.12A). This increase in mean fibre size was associated with a shift in fibre size distribution to the right in dystrophic *mdx* UNSUPP TA as there was a higher frequency of fibres with a larger CSA (6000-13499 μm^2 , $p < 0.0001$, Figure 6.12A and 6.13). ASA supplementation reduced the mean fibre size in both CON and *mdx* TA by 7% and 21%, respectively ($p < 0.05$, Figure 6.12A). In particular, a decrease in the number of fibres number between 6000 and 13499 μm^2 was observed in *mdx* ASA TA ($p < 0.05$, Figure 6.13) which shifted the fibre size distribution to the left. As expected, the proportional area of damage within TA sections was significantly higher in *mdx* compared to CON ($p < 0.001$; Figure 6.12B) and this was correlated with an elevated number of DAPI-positive nuclei ($p < 0.01$, Figure 6.18C). Remarkably, ASA reduced the damaged area by 46% in *mdx* muscle ($p < 0.05$, Figure 6.12B), which was reflected by a reduced number of DAPI-positive nuclei ($p < 0.05$, Figure 6.18), and suggests a reduction of inflammatory/immune cell infiltration. In ASA treated *mdx* TA, the reduction in damaged area corresponded with a concomitant reduction (by 29%) in centronucleated fibres (an indicator of muscle regeneration) compared to *mdx* UNSUPP ($p < 0.01$, Figure 6.12C).

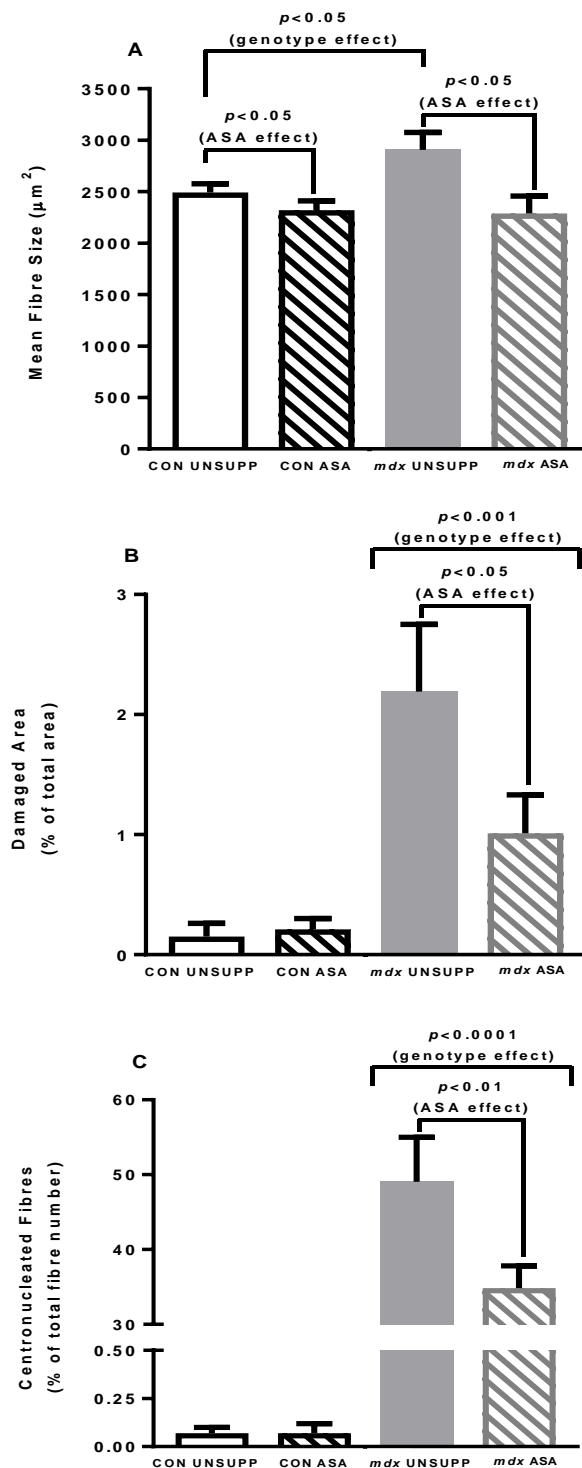


Figure 6.12. Histological analysis of tibialis anterior (TA) from unsupplemented (UNSUPP) and adenylosuccinic acid (ASA) supplemented control (CON) and *mdx* mice. Mean fibre size was larger in *mdx* UNSUPP TA compared to CON UNSUPP ($p < 0.05$, A) with ASA decreasing mean fibre size in both CON and *mdx* fibres ($p < 0.05$). Damaged area (B) and percentage of centronucleated fibres (C) was significantly higher in *mdx* TA compared to CON ($p < 0.001$ and $p < 0.0001$ respectively) with ASA decreasing damage and regeneration in *mdx* TA ($p < 0.05$ and $p < 0.01$ respectively). $n = 9$ CON UNSUPP, $n = 9$ CON ASA, $n = 10$ *mdx* UNSUPP, $n = 11$ *mdx* ASA.

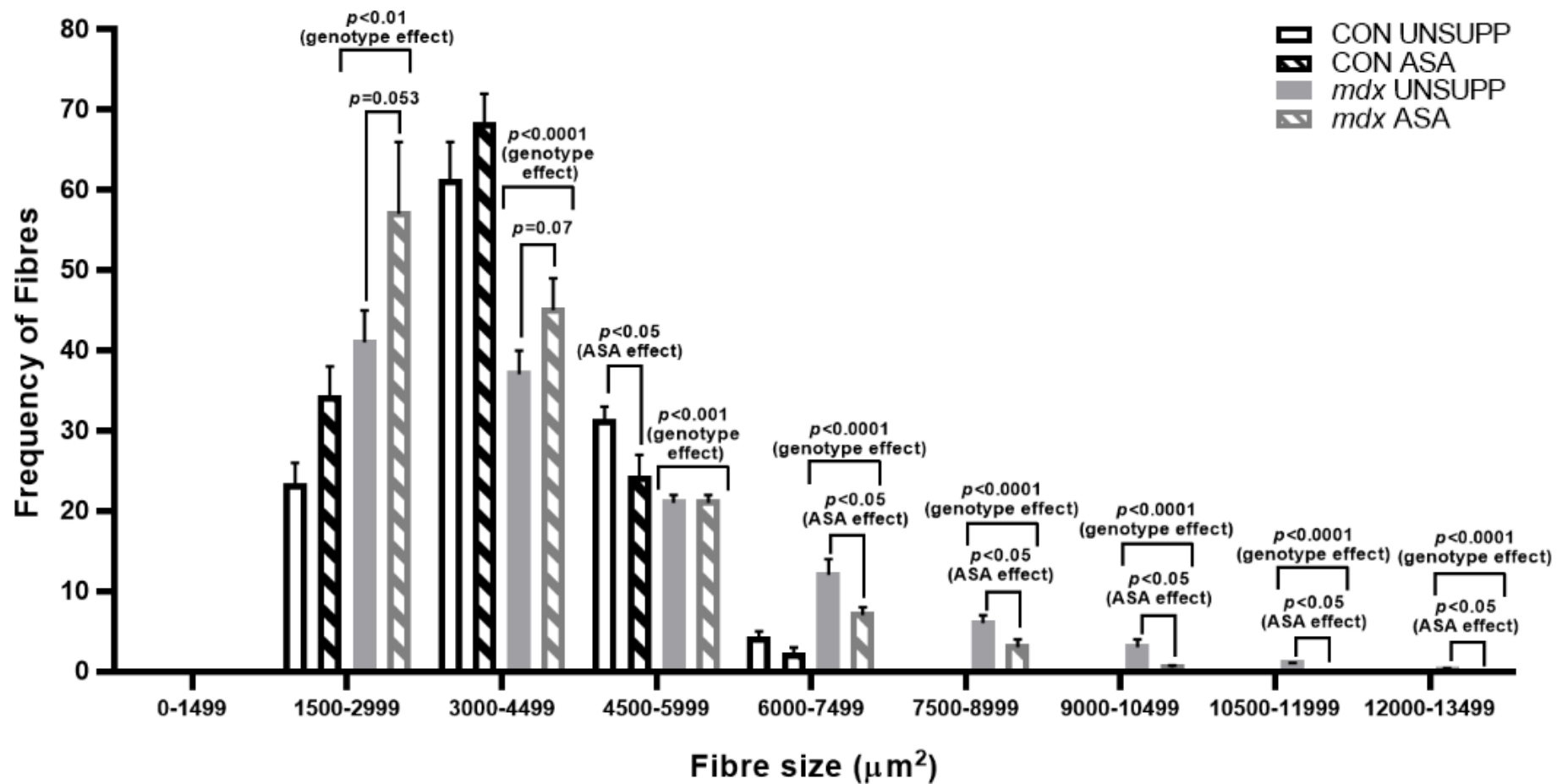


Figure 6.13. Histogram of tibialis anterior (TA) fibre size distribution from unsupplemented (UNSUPP) and adenylosuccinic acid (ASA) supplemented control (CON) and *mdx* mice. The frequency histogram indicates an increase in fibre size of *mdx* TA with fibres more frequent from 6000-13499µm compared to CON ($p < 0.0001$). ASA reduced fibre size frequency from 6000-13499µm in *mdx* ASA compared to *mdx* UNSUPP ($p < 0.05$). $n = 9$ CON UNSUPP, $n = 9$ CON ASA, $n = 10$ *mdx* UNSUPP, $n = 11$ *mdx* ASA.

6.3.4.2 Oil Red O (ORO)

Previously it has been demonstrated that ASA reduces lipid production in dystrophic explants (Bonsett, 1979) and therefore, we assessed the effect of ASA on lipid infiltration in dystrophic muscle. Lipid infiltration was quantified by scanning whole cross-sections for staining intensity to assess the overall ORO positive area of the TA. In *mdx* TA, the ORO positive area was 34% higher compared to CON TA ($p < 0.001$, 6.14A) and ASA reduced the ORO positive area by 9% compared to *mdx* UNSUPP ($p < 0.05$). In addition, the proportion of fibres infiltrated with intramuscular lipids were assessed in three random sections of the muscle. Compared to CON, *mdx* TA had 27% more ORO positive fibres ($p < 0.001$, Figure 6.14B) and ASA reduced this in *mdx* TA by 16% ($p < 0.05$) such that there was no difference from CON UNSUPP animals.

6.3.4.3 Gomori Trichrome

Next we assessed the effect of ASA on connective/fibrotic tissue infiltration in dystrophic muscle, as connective/fibrotic tissue accumulation is a feature of disease progression. In *mdx* UNSUPP TA, connective/fibrotic tissue was 15% greater compared to CON UNSUPP ($p < 0.001$, Figure 6.15) and remarkably, ASA normalised the connective/fibrotic tissue content in *mdx* TA to CON levels ($p < 0.0001$).

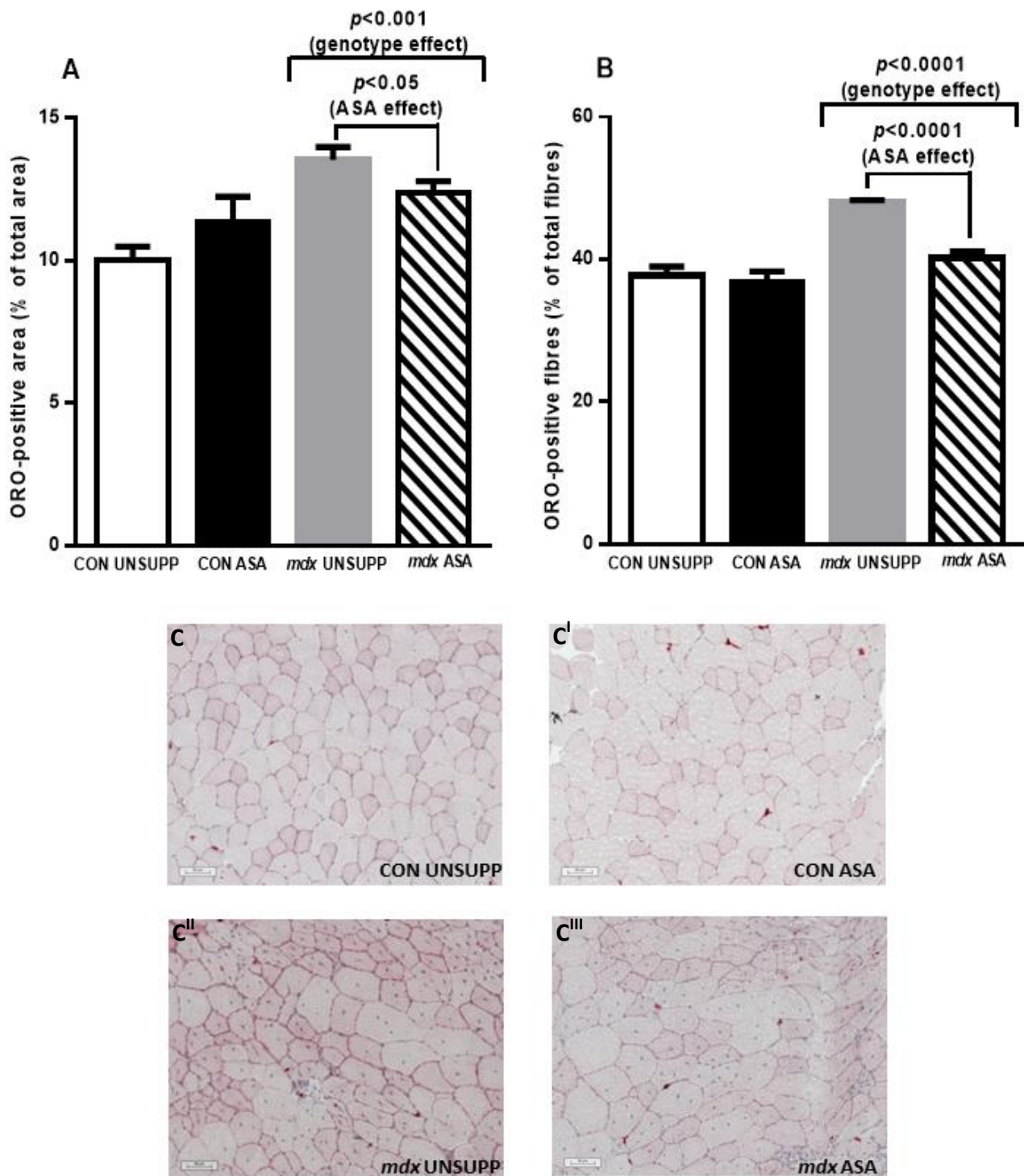


Figure 6.14. Assessment of lipid accumulation in tibialis anterior (TA) from unsupplemented (UNSUPP) and adenylosuccinic acid (ASA) supplemented control (CON) and *mdx* mice. Oil Red O (ORO) positive area of *mdx* TA was significantly higher compared to CON ($p < 0.001$, A) with ASA reducing ORO positive area of *mdx* TA compared to *mdx* UNSUPP ($p < 0.05$). ORO positive fibres of *mdx* TA was significantly higher compared to CON ($p < 0.0001$, B) with ASA reducing ORO positive area of *mdx* TA compared to *mdx* UNSUPP ($p < 0.0001$). Panels C-C^{III} are representative pictures of ORO staining in each group. $n = 11$ CON UNSUPP, $n = 11$ CON ASA, $n = 12$ *mdx* UNSUPP, $n = 12$ *mdx* ASA.

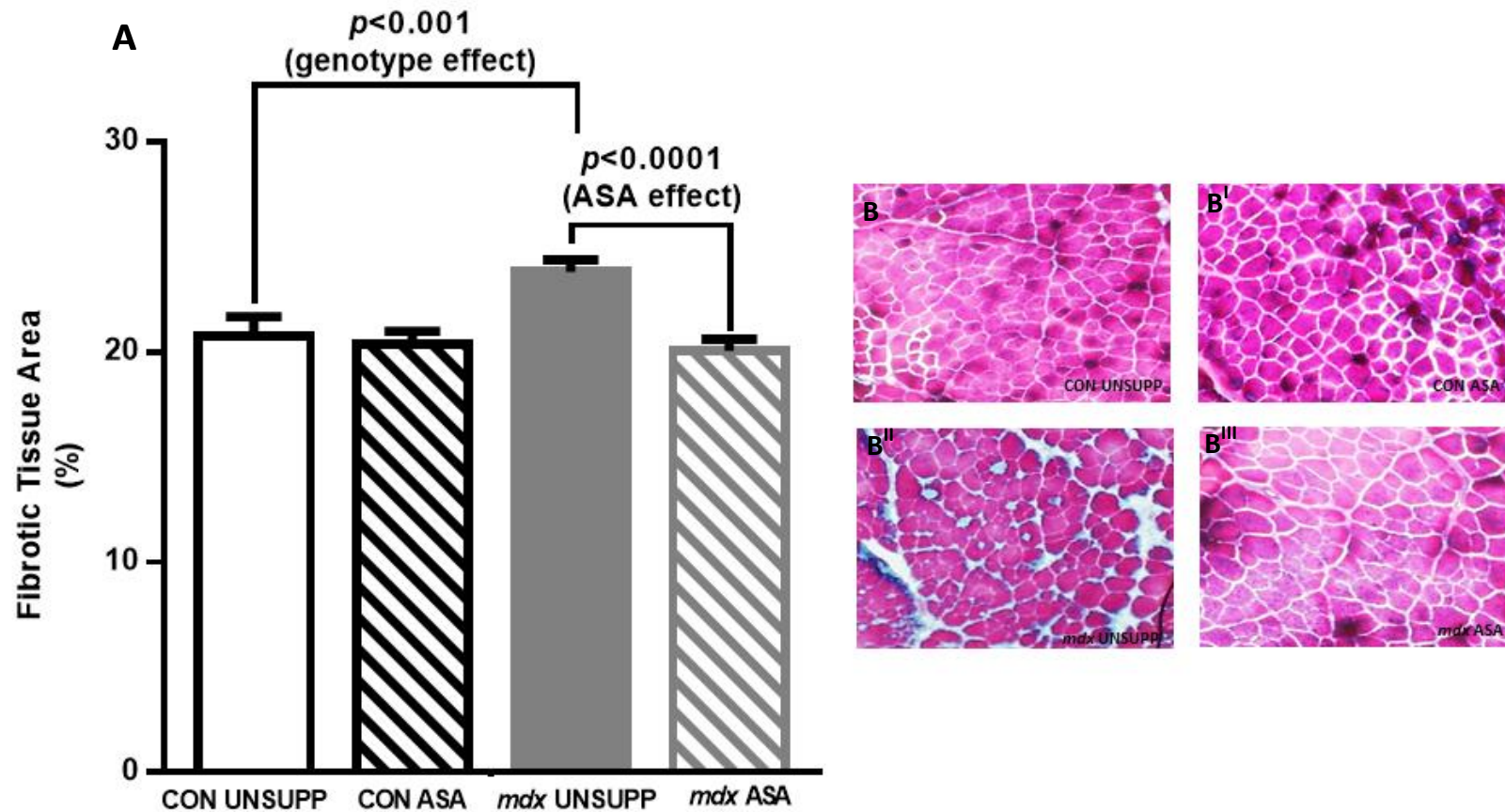


Figure 6.15. Assessment of connective/fibrotic tissue in tibialis anterior (TA) from unsupplemented (UNSUPP) and adenylosuccinic acid (ASA) supplemented control (CON) and *mdx* mice. Fibrotic tissue was significantly higher in *mdx* UNSUPP TA compared to CON UNSUPP ($p < 0.001$, A) with ASA reducing fibrotic tissue of *mdx* TA compared to *mdx* UNSUPP ($p < 0.0001$). Panels B-B''' are representative pictures of gomori staining in each group. $n = 8$ CON UNSUPP, $n = 10$ CON ASA, $n = 9$ *mdx* UNSUPP, $n = 11$ *mdx* ASA.

6.3.4.4 Alizarin Red

Since Ca^{2+} dysregulation is a well-documented consequence of dystrophin-deficiency and is a driver of the pathological muscle degeneration in DMD, we investigated whether ASA could positively modulate this important pathological feature. Intramuscular Ca^{2+} content, as assessed by the staining intensity of Alizarin Red, was 62% higher in *mdx* UNSUPP compared to CON UNSUPP TA ($p < 0.0001$, Figure 6.16) as expected. Although, ASA had no effect on the Ca^{2+} content of CON TA ($p > 0.05$), ASA treatment positively modulated Ca^{2+} content in *mdx* TA, reducing it by 15% ($p < 0.001$).

6.3.4.5 Succinate Dehydrogenase (SDH)

SDH, a component of the TCA cycle and the ETC, is a marker of oxidative fibre type with deep purple fibres being characteristic of Type I fibres and lighter purple fibres being indicative of Type IIa fibres. Assessing the TA cross-sectional area for SDH staining indicates the total mitochondrial content of all fibres types. SDH staining of the entire cross-section was initially quantified and we demonstrated that there was no difference in SDH positive area between CON UNSUPP and *mdx* UNSUPP (Figure 6.17A). Chronic ASA supplementation increased the SDH positive area of the TA in both CON and *mdx* samples by 25% and 46% respectively ($p < 0.0001$).

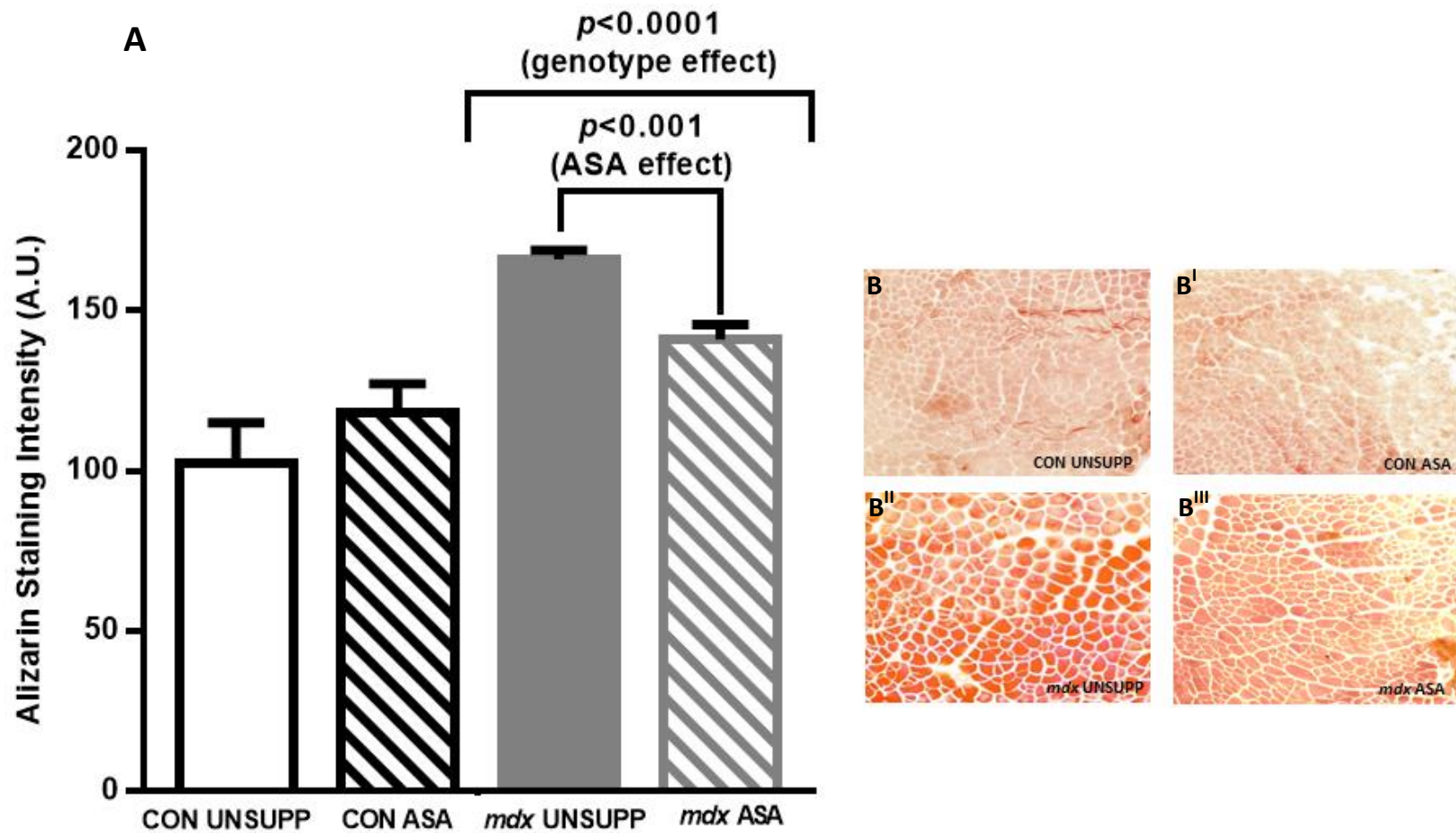


Figure 6.16. Assessment of calcium (Ca^{2+}) content in tibialis anterior (TA) from unsupplemented (UNSUPP) and adenylosuccinic acid (ASA) supplemented control (CON) and *mdx* mice. Ca^{2+} content was significantly higher in *mdx* TA compared to CON ($p < 0.0001$, A) with ASA reducing Ca^{2+} content in *mdx* TA compared to *mdx* UNSUPP ($p < 0.001$). Panels B-B''' are representative pictures of Alizarin red staining in each group. $n=10$ CON UNSUPP, $n=10$ CON ASA, $n=11$ *mdx* UNSUPP, $n=10$ *mdx* ASA.

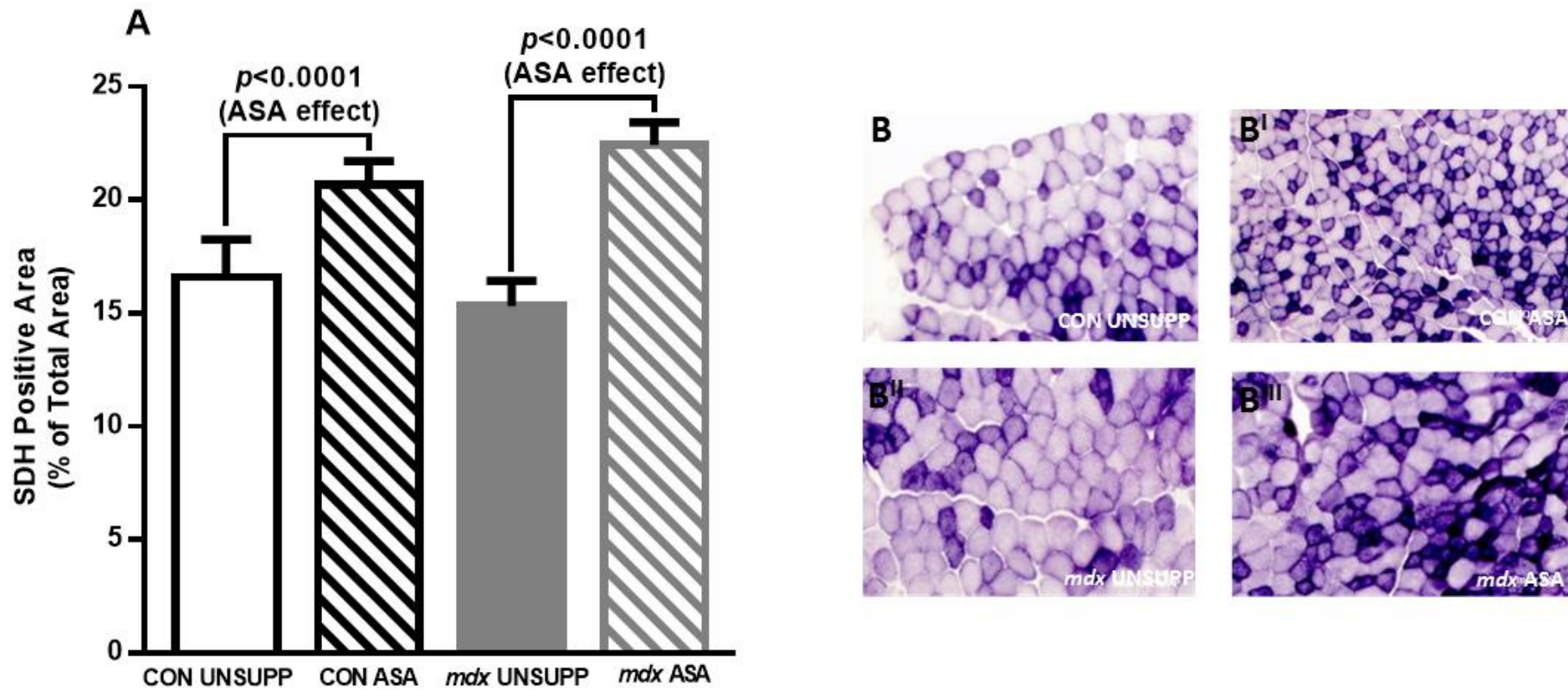


Figure 6.17. Assessment of succinate dehydrogenase (SDH) in tibialis anterior (TA) from unsupplemented (UNSUPP) and adenylosuccinic acid (ASA) supplemented control (CON) and *mdx* mice. SDH positive area was not significantly difference between CON UNSUPP and *mdx* UNSUPP ($p>0.05$, A) with ASA increasing SDH positive area in both CON and *mdx* TA ($p<0.0001$). Panels B-B^{III} are representative pictures of SDH staining in each group. $n=11$ CON UNSUPP, $n=12$ CON ASA, $n=11$ *mdx* UNSUPP, $n=12$ *mdx* ASA.

6.3.4.6 Dystrophin and utrophin expression

Finally, we examined the potential of ASA to act as a genetic modifier of DMD due to the beneficial effects observed in histopathology. In particular, we assessed dystrophin and utrophin expression in TA. Utrophin expression was investigated as it is a genetic modifier of the DMD phenotype, commonly upregulated in the *mdx* mouse resulting in a milder phenotype, and induced via AMPK activation. As expected, dystrophin protein abundance was essentially negligible (10-fold reduction) in *mdx* TA compared to CON ($p < 0.0001$, Figure 6.18A) with utrophin protein 2-fold less in *mdx* TA ($p < 0.0001$, Figure 6.18B). While ASA had no effect on dystrophin in either CON or *mdx* TA ($p > 0.05$, Figure 6.18A), there was a trend for ASA to decrease utrophin expression in *mdx* TA ($p = 0.073$, Figure 6.18B). This data highlights that enhanced utrophin expression is not a mechanism via which ASA improves the histopathology of DMD in *mdx* mice.

6.3.5 Effect of ASA supplementation on Nrf2

Initially, we hypothesised that the improvements documented in the clinical trial of ASA were associated with enhancement of metabolism, however, we did not observe this. We did, however, observe remarkable improvements in histopathology in the *mdx* mouse but this was not via a metabolic or utrophin-dependent pathway. In an attempt to elucidate a potential mechanism behind these histological improvements in the *mdx* mouse, we assessed nuclear factor (erythroid-derived 2)-like 2 (Nrf2), a transcription factor that has various biological effects, including improvement of cellular redox status (Gao *et al.*, 2014), and can be activated via elevated cytosolic fumarate (Ashrafian *et al.*, 2012). Basal levels of Nrf2 were

comparable between CON UNSUPP and *mdx* UNSUPP quadriceps (Figure 6.19) and ASA supplementation increased Nrf2 content by ~12% in both CON and *mdx* samples ($p < 0.05$). This data suggests that the mechanism underlying the ASA-induced improvements in the histopathology observed in this study, may be mediated through Nrf2 activation.

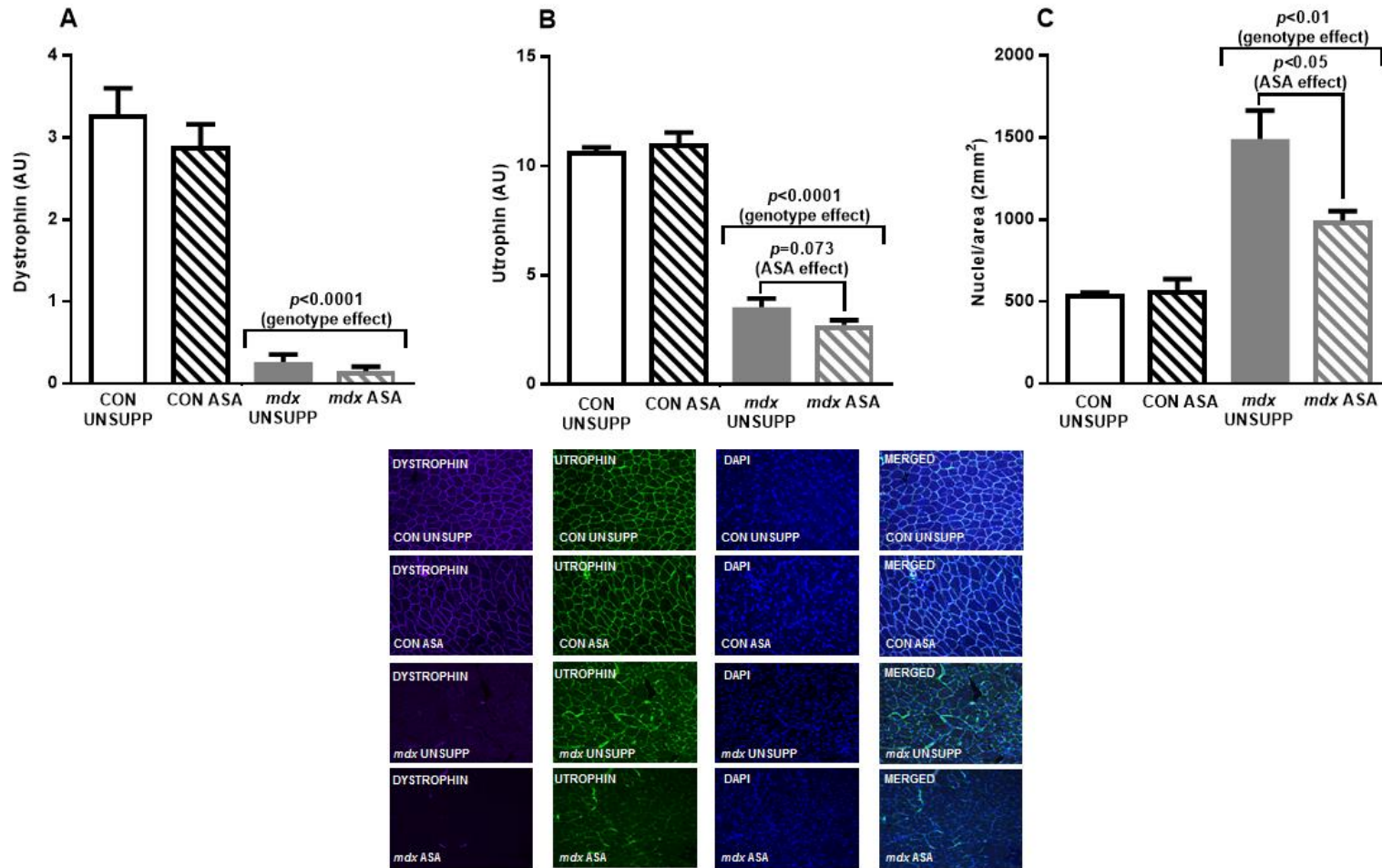


Figure 6.18. Proportion of dystrophin and utrophin immunoreactivity in unsupplemented (UNSUPP) and supplemented control (CON) and *mdx* tibialis anterior (TA). Dystrophin (purple, A) and utrophin (green, B) was significantly less in *mdx* TA compared to CON ($p < 0.0001$). ASA had no effect on dystrophin expression ($p > 0.05$, A) however there was a trend for ASA to decrease utrophin expression in *mdx* ASA compared to *mdx* ($p = 0.073$, B). DAPI-positive nuclei were greater in *mdx* TA compared to CON ($p < 0.01$, C) with ASA reducing nuclei number in *mdx* sections ($p < 0.05$). Scale bars = 100 μ m, $n = 3$ per group.

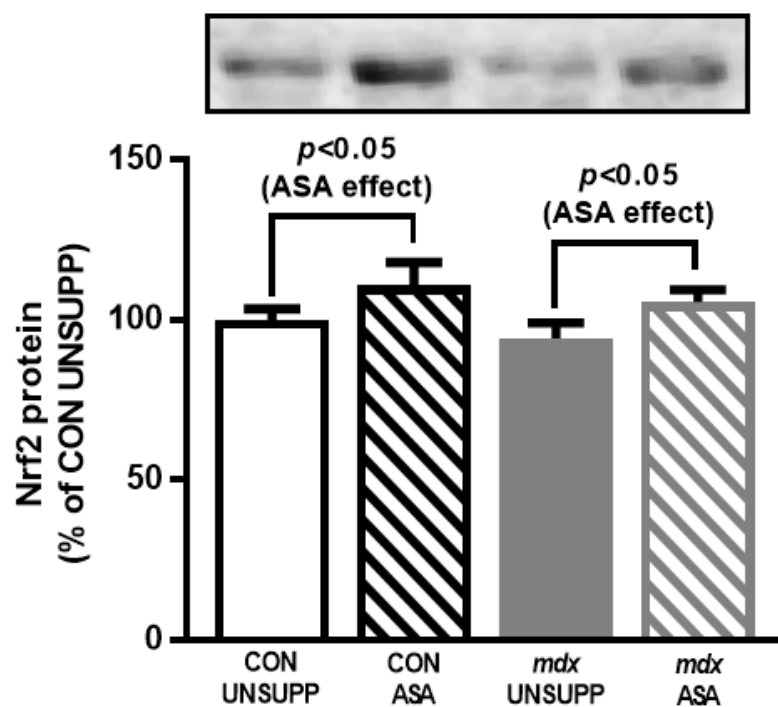


Figure 6.19. Nrf2 protein content of quadriceps from unsupplemented (UNSUPP) and adenylosuccinic acid (ASA) supplemented control (CON) and *mdx* mice. Nrf2 protein content was comparable between CON UNSUPP and *mdx* UNSUPP quadriceps ($p > 0.05$) and ASA increased protein content in both CON and *mdx* ($p < 0.05$). $n = 8$ CON UNSUPP, $n = 6$ CON ASA, $n = 6$ *mdx* UNSUPP, $n = 6$ *mdx* ASA.

6.4 Discussion

While dystrophin-deficiency underpins DMD pathology, we have hypothesised that metabolic dysfunction may be a core aetiological problem that promotes disease progression (Timpani *et al.* 2015). Considering the pivotal role that the mitochondria play in determining cell life and death, and the severe metabolic perturbations documented in the *mdx* mouse, we investigated the potential of metabolic therapy to improve the metabolism, bioenergetical status and histopathological features of dystrophin-deficient skeletal muscle. In particular, we examined the efficacy of the purine nucleotide ASA, which has previously been demonstrated to have beneficial effects in DMD patients including maintenance of muscle function and strength (Bonsett and Rudman, 1992). As there is minimal research regarding ASA, and there is a need for new therapeutic options for the DMD community, we have re-evaluated the potential of ASA as a candidate for the treatment of DMD. This is the first study to experimentally evaluate the therapeutic potential of ASA in an animal model of DMD and we show therapeutic efficacy in mitigating the various histopathological features of muscular dystrophy, albeit apparently independent of metabolic regulation.

A striking finding in our study was that ASA therapy ameliorated key histopathological features of dystrophin-deficient muscle. Importantly, ASA reduced pseudohypertrophy, damaged area, and therefore regenerative features (centronucleated fibres), fibrotic and lipid tissue infiltration and Ca^{2+} content in *mdx* TA. These histopathological features are most prominent as the disease progresses [49, 50, 51, 52, 53] and potentiate the deterioration of the functional capacity of skeletal muscle [54, 55]. These histological improvements in ASA-treated *mdx* TA

are a promising sign of ASA's capacity to ameliorate the progression of DMD and maintain skeletal muscle function. Functional measurements, including grip strength and contractile properties, remain to be assessed in the *mdx* mouse to confirm our positive histopathology data. Together, the reduced damage, lipid and connective tissue infiltration in *mdx* skeletal muscle following ASA treatment in our study suggests improvements in muscle integrity and quality which likely explains the maintenance of muscle strength and function in ASA-treated DMD and BMD patients [18]. These improvements are independent of upregulated utrophin expression in *mdx* TA.

Recently, it has been demonstrated that ASA has a role in glucose-stimulated insulin secretion (Gooding *et al.*, 2015) suggesting that ASA is involved in the regulation of glucose homeostasis, and potentially, glucose utilisation at the tissue level. Since the dependency of energy resynthesis on purine nucleotide cycling increases concomitantly with muscle contraction intensity (Broberg and Sahlin, 1989), we have investigated the capacity for ASA to modulate contraction-induced GU in both the fast-twitch EDL and the slow-twitch SOL. Both basal- and contraction-induced GU is depressed in *mdx* EDL and SOL indicating that impaired macronutrient (glucose) uptake may be a contributing factor to the mitochondrial deficits observed in dystrophic skeletal muscle. ASA was unable to overcome this depression in *mdx* EDL and SOL, having no effect on GU in either basal or contraction states in CON muscles indicating that ASA's modulatory effect on GU may be insulin-dependent only.

As metabolic dysfunction is a well-documented characteristic of dystrophic muscle, and we hypothesise that this contributes significantly to disease progression, we assessed the effect of ASA supplementation on various mitochondrial indices in

isolated FDB fibres. Determination of the BHI – which is a predicative marker of metabolic responsiveness to stress derived from spare respiratory capacity, ATP production, proton leak and non-mitochondrial respiration (Chacko *et al.*, 2014) – indicates that metabolic dysfunction exists in FDB fibres from the *mdx* mouse. In particular, this appears to stem from a reduced capacity to utilise oxidative metabolism during metabolic stress. This was reflected in the metabolic phenogram in which there was a reduced capacity to increase overall metabolism through the ramping up of OCR (as indicated by the smaller gradient), despite maintaining a more active metabolic phenotype in the basal/resting state. This reduced capacity for oxidative metabolism was observed in the presence of increased PGC-1 α (which has been previously observed (Ljubicic *et al.*, 2011)) and PGC-1 β protein in *mdx* UNSUPP quadriceps muscle. As there was no downstream increase in mitochondrial respiration, nor a difference in CS activity, SDH staining or the total mitochondrial pool (assessed by MitoTracker Green) in *mdx* muscle, this suggests that, despite an increased signal, dystrophin-deficient muscles are unable to respond appropriately to this signalling to expand the mitochondrial pool. While we did not observe differences in the expression of subunits of the ETC complexes between CON and *mdx* quadriceps (which would indicate a potential reason for the inability to increase ATP production), it is plausible that expression of other subunits of the ETC complexes are depressed or functional impairments of the complexes exist. We have previously demonstrated that Complex I-mediated respiration is severely impaired in *mdx* skeletal muscle, irrespective of substrate supply, but that this can be ameliorated with Complex I inhibition and stimulation of Complex II respiration (Rybalka *et al.*, 2014). This finding, when considered in context with the current study's demonstration of no differences in various subunits of the ETC, suggests that

functional impairments, particularly at Complex I, may be responsible for the impaired mitochondrial respiration.

Of note, *mdx* fibres appear to compensate for their lack of flexibility in oxidative metabolism by increasing their reliance on anaerobic glycolysis. This is evident while transitioning to higher metabolic states in response to, and during, metabolic stress. This suggests that anaerobic metabolism is not as severely affected as oxidative metabolism in dystrophic muscle – especially in the presence of exogenously administered pyruvate. However, to what extent this compensation by anaerobic metabolism exists *in vivo* and can be facilitated by adequate GU is unknown. Our GU data certainly suggests that during contraction in particular, the capacity for anaerobic metabolism to compensate for mitochondrial dysfunction during heightened metabolic demand would be limited. A potential way in which this depressed facilitation of GU into the muscle could be overcome to ensure that substrate supply for glycolytic flux is apt, would be the utilisation of glycogen stores. In this study, we have demonstrated that intramuscular glycogen content is elevated in *mdx* TA and this finding is supported by others (Watkins and Cullen, 1987, Cullen and Jaros, 1988, Stapleton *et al.*, 2014). Therefore, elevated glycogen content indicates a potential source of glucose readily available to dystrophic muscle. However, the activity of phosphorylase, the enzyme that breaks down glycogen, is reduced in dystrophin-deficient skeletal muscle (Dreyfus, 1954, Ronzoni *et al.*, 1960, Hess, 1965, Di Mauro, 1967, Mastaglia and Kakulas, 1969, Ellis, 1980, Petell *et al.*, 1984, Engel, 1986, Chi *et al.*, 1987, Chen *et al.*, 2000, Carberry *et al.*, 2013, Stapleton *et al.*, 2014). Thus it is unlikely that the compensatory upregulation of glycolytic flux is evident *in vivo* in *mdx* mice.

We hypothesised that ASA could improve the metabolic status of dystrophic muscle by enhancing PNC function and thus purine nucleotide salvage, but particularly, by increasing fumarate production and anaplerosis of the TCA cycle. Despite having previously demonstrated an impaired mitochondrial ATP production rate in isolated dystrophic mitochondria bathed in optimal TCA substrate cocktails (Rybalka *et al.*, 2014), we and others (Ionășescu *et al.*, 1967, Martens *et al.*, 1980, Nylen and Wrogemann, 1983, Glesby *et al.*, 1988, Bhattacharya *et al.*, 1993, Chinet *et al.*, 1994, Kuznetsov *et al.*, 1998) have shown a partial amelioration of this mitochondrial dysfunction by stimulating Complex II with succinate. Thus we predicted in this study that promoting anaplerosis could at the very least, enhance SDH activity and the respiratory capacity of Complex II-mediated OXPHOS. However, our data demonstrates that ASA therapy was unable to modulate any of the mitochondrial parameters measured in FDB fibres, and this was despite improving the viability and the density of the mitochondrial pool (as detected by MitoTracker dyes in dissociated FDB fibres). This was unexpected as the clinical trial of ASA in DMD and BMD patients anecdotally reported increases in stamina and energy levels, while functional measurements were maintained (Bonsett and Rudman, 1992). This is suggestive that ASA can improve muscle fatigability properties. We did observe, however, that ASA induced changes in PCr content and the TCr pool suggesting manipulation of the Cr/PCr system to improve buffering capacity to assist in the maintenance of ATP levels.

The lack of effect of ASA at the mitochondrial level may be due to a few reasons. Firstly, it is unknown how long lasting the effects of ASA are. The improvements observed in the DMD and BMD patients in Bonsett and Rudman's Phase I clinical trial were measured during the treatment period, which constituted

infusion of ASA into the bloodstream via a miniature insulin pump (Bonsett and Rudman, 1992). In contrast, our mitochondrial measurements were made in FDB fibres removed from the *in vivo* (and ASA) environment some 24 hours earlier. Potentially, this purine metabolite has a short half-life and therefore any downstream anaplerotic effects on the TCA cycle and mitochondrial respiration would not be observed in this experimental time frame. Secondly, as ASA supplementation theoretically stimulates PNC activity and increases fumarate production, it is unknown whether delivery of fumarate and/or malate into the mitochondria is affected in dystrophic muscle. The chronic supplementation period may have a negative modulatory effect on the fumarate/malate shuttle – a similar observation has been documented in Cr supplementation studies where chronic Cr delivery downregulates the Cr transporter (Loike *et al.* 1988, Guerrero-Ontiveros and Wallimann, 1998, Murphy *et al.* 2001). While this may be a possible scenario in the *mdx* skeletal muscle, it is unlikely to explain the results observed in CON mice, as ASA stimulated CS activity suggesting that transport of fumarate/malate is evident. This finding indicates a genotype-specific effect. Thirdly, assuming a normal fumarate/malate transport system, another obstacle may exist in the incorporation of fumarate into the TCA cycle. Dysfunction exists in many of the TCA cycle enzymes including malate dehydrogenase (Cao *et al.*, 1965) which is involved in the breakdown of malate to oxaloacetate following the conversion of fumarate to malate. Therefore, – expansion of the TCA substrate pool may be futile in the presence of a dysfunction mitochondrial TCA cycle.

Since fumarate can be converted by fumarase in both the mitochondria and the cytosol (Akiba *et al.*, 1984), it is possible that ASA-generated fumarate is being directed into cytosolic reactions rather than into the mitochondria. As fumarate

conversion is non-specific, there may be an increased propensity for the cytosolic conversion and utilisation of fumarate, which would limit any potential downstream effects on mitochondrial respiration. This seems to be specifically relevant to the *mdx* mouse as ASA supplementation in CON mice did elicit modulation of some metabolic parameters. ASA reduced metabolic stress signalling (as demonstrated by lower P-AMPK protein) and stimulated mitochondrial biogenesis as evidenced by the elevated protein expression of PGC-1 α and β and increased CS activity. Moreover, ASA manipulated the Cr/PCr system in CON mice which led to a trend towards enhanced ATP production. Together, this data strongly suggests that ASA-generated fumarate is likely sequestered into a mitochondrial route in CON mice. However without metabolic demand, this seems to induce enhanced O₂⁻ production as opposed to ATP generation. This is presumably because (1) ATP demand is being met; and (2) purine salvage is enhanced alleviating the role of mitochondria in maintaining the bioenergetical status of the muscle. In contrast, fumarate may be directed into cytosolic reactions in the *mdx* mouse.

While ASA had no effect on various mitochondrial properties in this study, it did enhance mitochondrial viability and reduce O₂⁻ production in *mdx* FDB fibres. Oxidative stress is a well-documented feature of dystrophic muscle (Disatnik *et al.*, 1998), potentially due to the down-regulation of redox genes (Khairallah *et al.*, 2012). However we unexpectedly demonstrated similar mitochondrial O₂⁻ production between CON and *mdx* FDB fibres. As we did not measure other pathways of radical production, nor antioxidant levels, it cannot be concluded that oxidative stress was not evident in *mdx* skeletal muscle. The reduction of mitochondrial O₂⁻ production via ASA is a positive finding in this study as radical production in dystrophin-deficient muscle is undesirable due to the potential negative downstream effects on

mitochondrial respiration. It has been previously demonstrated that fumarate content and cytosolic fumarase activity affects the redox status of the cell to promote the antioxidant status (Pinto and Bartley, 1969, Laplante *et al.*, 1997, (Raimundo *et al.*, 2011). If fumarate is being sequestered into cytosolic reactions in ASA treated *mdx* mice, this may account for the reduced mitochondrial O_2^- production. Additionally, the recent observation that elevated intracellular fumarate content is cardioprotective through the activation of Nrf2 (Ashrafian *et al.*, 2012) may also indicate a potential mechanism for the reduced mitochondrial O_2^- production in ASA treated *mdx* FDB fibres as we have observed increased Nrf2 protein. Further investigation however is warranted to confirm that the increased Nrf2 protein expression is correlated with increased Nrf2 activity and activation of downstream target genes.

As this study is the first to experimentally evaluate ASA in a murine model, we closely monitored body weight and food and water consumption throughout the treatment period. No difference in weekly weight gain or food and water consumption was observed throughout the supplementation period, although ASA did reduce final body weights of *mdx* mice. While this was not reflected in differences in muscle weights, we did observe a decrease in lipid content of ASA treated *mdx* TA's. This is consistent with a previous study that demonstrated reduced lipid production by dystrophic muscle cells following ASA administration (Bonsett and Rudman, 1984). While this was hypothetically instigated by increased isocitrate dehydrogenase (IDH) activity and support of oxidative ATP production in the aforementioned study, our data does not support this hypothesis due to the lack of effect on mitochondrial functional indices – albeit we did not measure IDH activity directly. In context of our other findings, the reduced lipid content in ASA treated *mdx* muscle may also reflect Nrf2 activation, which alters expression of lipid metabolism genes (Yates *et al.*,

2009) leading to increased β -oxidation. The stimulation of β -fat oxidation may explain the reduced lipid content observed in our study as it is plausible that the lipid accumulation in dystrophic skeletal muscle is a result of a combination of enhanced lipid production (Bonsett and Rudman, 1984) and poor fatty acid oxidation (Sharma *et al.*, 2003, Lin CH, 1972, Shumate *et al.*, 1982, Carroll *et al.*, 1985). Indeed, Nrf2 deficiency leads to lipid accumulation in the liver (steatosis) (Chowdhry *et al.*, 2010, Sugimoto *et al.*, 2010, Zhang *et al.*, 2010) therefore suggesting that the reduced lipid content in ASA-treated *mdx* TA is through upregulation of β -oxidation. Together, the reduced damage, lipid and connective tissue infiltration in *mdx* skeletal muscle following ASA treatment suggests improvements in muscle integrity and quality which may explain the maintenance of muscle strength and function in ASA-treated DMD and BMD patients (Bonsett and Rudman, 1992).

6.5 Conclusion

In summary, our study is the first to experimentally evaluate 8 weeks of dietary ASA therapy in *mdx* mice and demonstrate a remarkable capacity for ASA to ameliorate the histopathological hallmarks of DMD. This included a reduction in intramuscular Ca^{2+} content, muscle damage and lipid and fibrotic tissue infiltration. In stark contrast to our hypothesis, ASA had no modulatory effect on metabolic function but did reduce mitochondrial O_2^- production, improve the total content and viability of the mitochondrial pool and improve the overall metabolic signature of dystrophic skeletal muscle. While the precise mechanism of action and a full characterisation of the antioxidant effects of ASA via Nrf2 activation requires further elucidation, our data highlights ASA as a strong therapeutic candidate for the treatment of DMD.

Chapter Seven

Evaluation of ASA Therapy in Human DMD
Myoblasts

7.1 Introduction

The first indication of the therapeutic potential of ASA as a treatment for DMD was described in 1984 by Dr's. Bonsett and Rudman (Bonsett and Rudman, 1984, Bonsett, 1979). After documenting severe fatty tissue replacement of the paraspinal, abdominal, pelvic girdle and lower limb muscles of a 16 year old DMD patient (Bonsett, 1963), Dr's. Bonsett and Rudman aimed to elucidate the reason behind this gain in non-functional tissue within the skeletal muscle architecture. They demonstrated a higher propensity for skeletal muscle explants from DMD patients to produce intracellular lipid and hypothesised that this defect had a biochemical basis with a preference of the skeletal muscle to produce lipid instead of ATP (Bonsett, 1979). Thereafter, they tested various metabolic pathways, via the addition of metabolites from glycolysis, the TCA cycle and *de novo* ATP synthesis pathways, to elucidate the metabolic pathway with the potential defect (Bonsett and Rudman, 1984). Although the addition of various metabolite substrates of the TCA cycle reduced lipid production in DMD muscles, it was the addition of ASA to the culture medium that eliminated lipid production completely. While the exact mechanism as to how ASA was effective in lipid elimination was not determined in their study, it was hypothesised that ASA was capable of modifying ADP, AMP and ATP concentrations and thereby enhancing the metabolic state. Indeed, ASA is an important intermediate in the purine nucleotide salvage pathway which drives the recovery of IMP to AMP while concurrently inducing mitochondrial anaplerosis via fumarate production.

In Chapter 6, we investigated the potential of a chronic 8 week ASA supplementation regimen to overcome metabolic dysfunction in the *mdx* mouse as a proof-of-principle mechanism for the clinical efficacy observed by Bonsett & Rudman (Bonsett and Rudman, 1992). In stark contrast to our hypothesis, ASA did not have an effect on mitochondrial respiration but did improve dystrophic muscle histopathology – including decreased muscle damage, lipid, connective tissue and intracellular Ca²⁺ accumulation. Our data thus suggests a metabolic-independent mechanism of action. These histological improvements may indeed explain the maintenance of skeletal muscle function and strength observed in the clinical trial of ASA in DMD and BMD patients (Bonsett and Rudman, 1992). However, our data is not consistent with the self-reported instantaneous increases in energy and stamina since we found no evidence of modifications to mitochondrial respiration. The reported instantaneous improvements in energy suggest that ASA may elicit its effects in an acute time-dependent manner. This is further suggested by the mitigation of lipid production in DMD explants following acute (24 hour) incubation with ASA (Bonsett and Rudman, 1984). In chapter 6, we assayed FDB fibres in an exogenous media that lacked ASA and we hypothesised that the lack of effect on mitochondrial respiration may reflect the potentially transient nature of ASA modulation. In this study, we aimed to elucidate this through the utilisation of acute ASA treatment on human-derived dystrophin-positive and dystrophin-negative myoblasts to mimic real-time delivery of ASA to the skeletal muscle via the bloodstream. In particular, we investigated the effects of acute (24 hours, 3 days and 7 days) ASA treatment on mitochondrial function, viability and O₂⁻

production in dystrophin-positive and dystrophin-negative myoblasts. We hypothesised that acute ASA exposure would (1) improve mitochondrial function, (2) improve mitochondrial viability and (3) decrease mitochondrial O_2^- in dystrophin-negative myoblasts; and thus promote an overall improvement in mitochondrial health.

7.2 Methods

7.2.1 Cell culture maintenance

Immortalised dystrophin-positive (CON) and dystrophin-negative (DMD) skeletal muscle myoblasts were grown in growth medium as described in section 3.2.1 and seeded at a density of 90-100,000 cells per well. Myoblasts were passaged every 3 days.

7.2.2 Determination of ASA dosage

The maximal tolerable dose of ASA (10nM to 1mM) in CON myoblasts was determined via two methods – (1) crystal violet staining; and (2) the xCELLigence system. Both methods assess cell viability however crystal violet staining is an end-point assay whereas the xCELLigence system involves real-time monitoring of changes in the Cell Index (a measurement calculated to reflect cell number and growth).

7.2.2.1 Crystal violet assay

CON myoblasts were grown in either media, media with MQ H₂O (vehicle) or increasing concentrations of ASA (dissolved in H₂O). Following 4 days incubation, cells were stained with 0.1% crystal violet solution as described in section 3.2.2.1 and absorbance was read at 570 nm on an X-Mark Microplate Reader (Bio-Rad Laboratories, Australia).

7.2.2.2 Cell proliferation assay

Using a non-invasive and label-free method (xCELLigence RTCA MP system), cell viability was quantified through calculation of the Cell Index. CON myoblasts were seeded at 5000 cells per well and once adhered, 50 μ L of either media, media with MQ or increasing concentrations of ASA were added. Plates were inserted into the xCELLigence RTCA MP system and the Cell Index was measured every 30 minutes for 4 days. The data presented is for 60 hours during the proliferative phase of cell growth.

7.2.3 Determination of mitochondrial viability

Using the fluorescent MitoTracker dyes Green and Red, mitochondrial viability was assessed in treated and untreated CON and DMD cells. Myoblasts were seeded at 5000 cells per well with 1mM of ASA for 24 hours, 3 days or 7 days and on the day of experimentation, mitochondrial viability was determined as described in section 3.2.3. Myoblasts were imaged on an inverted microscope (Olympus, Tokyo, Japan) and images were analysed using ImageJ.

7.2.4 Determination of mitochondrial superoxide (O₂⁻) production

Using the fluorescent dye MitoSOX Red, we assessed mitochondrial O₂⁻ production in treated and untreated CON and DMD cells. Myoblasts were seeded at 5000 cells per well with 1mM of ASA for 24 hours, 3 days or 7 days

and on the day of experimentation, mitochondrial O_2^- production was measured as described in section 3.2.4. Myoblasts were imaged and analysed as described above.

7.2.5 Mitochondrial & glycolytic metabolism using the Extracellular Flux Analyser

On gelatin-coated (0.5%) Seahorse XF24 cell culture V7 microplates, CON and DMD myoblasts were plated (25,000 and 15,000 cells per well, respectively) and incubated for 24 hours with 1mM ASA. Oxygen consumption rate (OCR) and extracellular acidification rate (ECAR) was determined as described in section 3.2.5.

7.2.6 Statistics

Results are presented as mean \pm standard error of the mean. A two-way ANOVA was utilised to detect between genotype (CON and DMD) and treatment differences. When a main effect or an interaction was detected, unpaired T-tests were used to determine differences between individual groups using SPSS (version 21). An α value of 0.05 was considered significant.

7.3 Results

7.3.1 Effect of acute ASA supplementation on cell viability

We first established the maximal tolerable dose (10nM-1mM) of ASA in CON myoblasts to determine the dosage suitable for the proceeding studies without causing cellular dysfunction and death. Cell viability was first quantified through crystal violet staining. Following 4 days of incubation, relative crystal violet absorbance, and therefore cell viability, was greater in ASA-treated CON myoblasts compared to untreated and vehicle-treated myoblasts irrespective of ASA concentration ($p < 0.01$, Figure 7.1). No significant difference in cell viability was detected between ASA concentrations.

Next we assessed real-time monitoring of cell viability in the form of the Cell Index. The Cell Index is presented for a total of 60 hours during the proliferative phase of cell growth, divided into 12 hour blocks. At 0 and 12 hours, there was no difference in the Cell Index observed between untreated, vehicle-treated and ASA- treated myoblasts at any concentration (Figure 7.2A and B, respectively). At 24 hours, ASA-treated myoblasts maintained a higher Cell Index compared to untreated and vehicle-treated myoblasts ($p < 0.05$, Figure 7.2C). At 36 hours, 1mM ASA increased the Cell Index in treated myoblasts compared to untreated and vehicle-treated myoblasts ($p < 0.05$, Figure 7.2D), with a similar trend observed at 48 hours ($p = 0.093$, Figure 7.2E). No significant difference in the Cell Index was detected at 60 hours, between

unsupplemented and ASA supplemented CON myoblasts ($p>0.05$, Figure 7.2F).

As both experiments demonstrated no detrimental effect of 1mM ASA supplementation on cell viability, we proceeded with the maximal tolerable dose (we investigated) for the following experiments. From these assays, our data suggests that ASA improves cell viability and stimulates generative capacity of myoblasts.

7.3.2 The effect of acute ASA supplementation on mitochondrial viability

In Chapter 6, we observed that 8 weeks of chronic ASA supplementation improved the mitochondrial viability of isolated FDB fibres in the *mdx* mouse. We therefore assessed mitochondrial viability, through the addition of MitoTracker Red (active, healthy mitochondria) and MitoTracker Green (total mitochondrial pool), in DMD myoblasts to investigate the effects of acute ASA supplementation.

At the 24 hour time point, mitochondrial viability was reduced by 38% in DMD myoblasts compared to CON ($p<0.0001$, Figure 7.3A) and there was a trend for ASA to increase mitochondrial viability in both CON and DMD myoblasts ($p=0.085$). A similar reduction (~27%) in mitochondrial viability in was also observed at 3 days DMD myoblasts (compared to CON; $p<0.0001$, Figure 7.3B) and could not be improved by ASA treatment ($p>0.05$). In contrast, the viability of the mitochondrial pool was restored at 7 days in DMD myoblasts to

CON levels (Figure 7.3C). As observed at 3 days, ASA had no effect on mitochondrial viability in either CON or DMD myoblasts.

Associated with the increased mitochondrial viability observed in ASA supplemented FDB fibres (Chapter 6), was an increase in the total mitochondrial pool (MitoTracker Green). We therefore assessed the effect of acute ASA treatment on the mitochondrial pool density. At 24 hours, the mitochondrial pool was approximately 17% larger in DMD myoblasts compared to CON ($p < 0.0001$, Figure 7.4A) and there was a trend for ASA to increase the mitochondrial pool in both CON and DMD myoblasts at this time point ($p = 0.061$). At 3 days, mitochondrial pool density was ~72% higher in DMD compared to CON myoblasts ($p < 0.001$, Figure 7.4B) and ASA treatment had no effect on the mitochondrial pool in either CON or DMD myoblasts ($p > 0.05$). In contrast, at 7 days, the mitochondrial pool was ~6% lower in DMD compared to CON myoblasts ($p < 0.001$, Figure 7.4C) and ASA treatment stimulated the expansion of the mitochondrial pool in both CON and DMD myoblasts by 4% and 14%, respectively ($p < 0.05$).

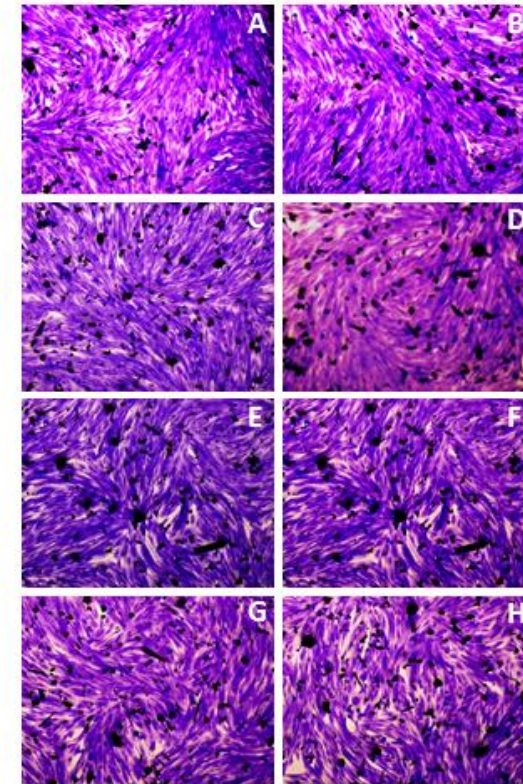
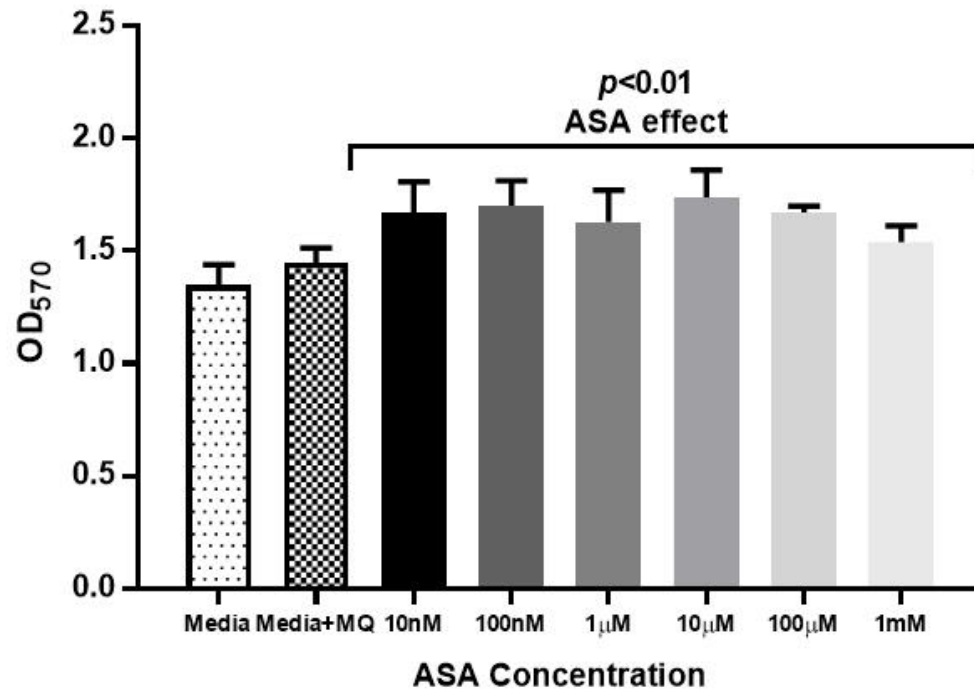


Figure 7.1. Cell viability, as determined by crystal violet staining, in unsupplemented and adenylosuccinic acid (ASA) supplemented control (CON) myoblasts. Following 4 days of ASA supplementation, cell viability increased compared to unsupplemented (media and media + MQ) myoblasts ($p < 0.01$). There was a trend for 1mM ASA to decrease cell viability compared to 10µM ($p = 0.096$) and 100µM ($p = 0.068$). $n = 3$ per group.

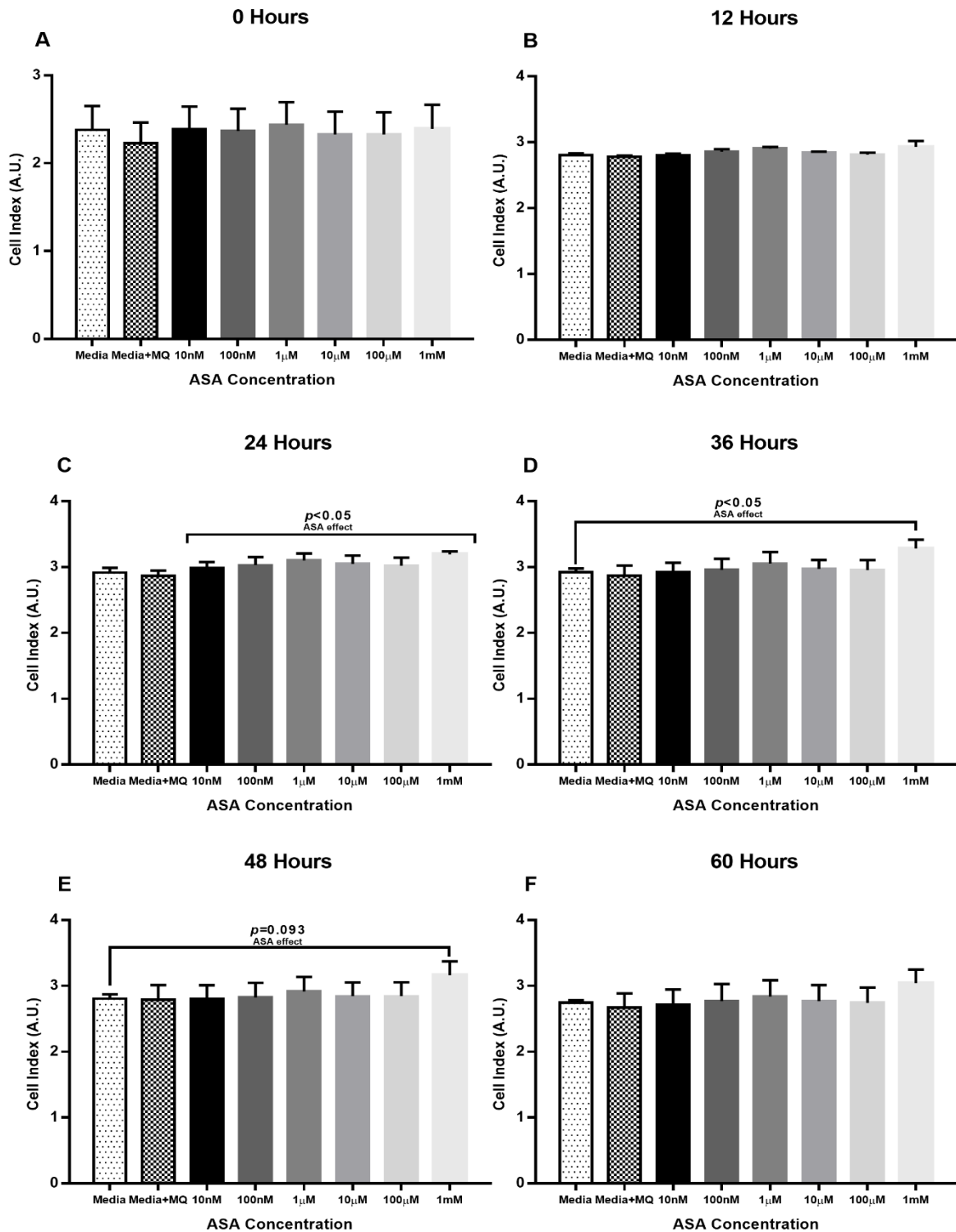


Figure 7.2. Cell Index (viability), as determined by real-time monitoring, in unsupplemented and adenylosuccinic acid (ASA) supplemented control (CON) myoblasts. Cell Index, which was determined every 12 hours for 60 hours during the proliferative phase of cell growth, was not significantly different between unsupplemented (media and media + MQ) and ASA supplemented myoblasts at 0, 12 and 60 hours ($p > 0.05$, A, B and F respectively). At 24 hours, ASA treatment increased the Cell Index compared to unsupplemented myoblasts ($p < 0.05$, C). At 36 hours, 1mM ASA increased the Cell Index compared to media only treated myoblasts ($p < 0.05$, D) with a similar trend detected at 48 hours ($p = 0.093$, E). $n = 3$ per group.

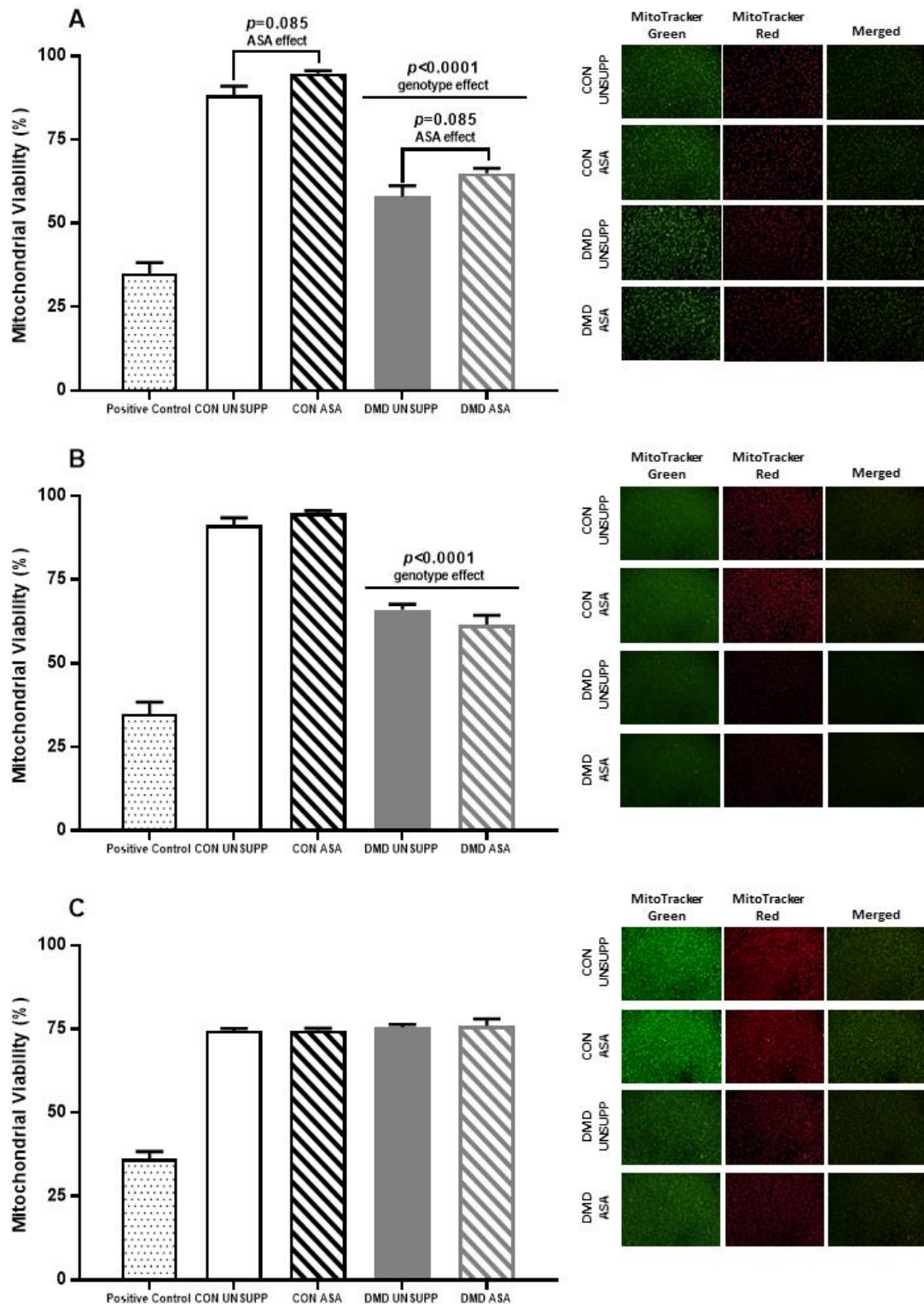


Figure 7.3. Mitochondrial viability of unsupplemented (UNSUPP) and adenylosuccinic acid (ASA) supplemented control (CON) and Duchenne Muscular Dystrophy (DMD) myoblasts. Mitochondrial viability was less in DMD myoblasts at 24 hours (A) and 3 days (B) compared to CON ($p < 0.0001$) with a trend for ASA supplementation to increase mitochondrial viability in both cell lines at 24 hours detected ($p = 0.085$, A). At 7 days, mitochondrial viability was comparable between CON and DMD myoblasts ($p > 0.05$, C) with ASA having no effect in either CON or DMD lines ($p > 0.05$). $n = 4$ per group.

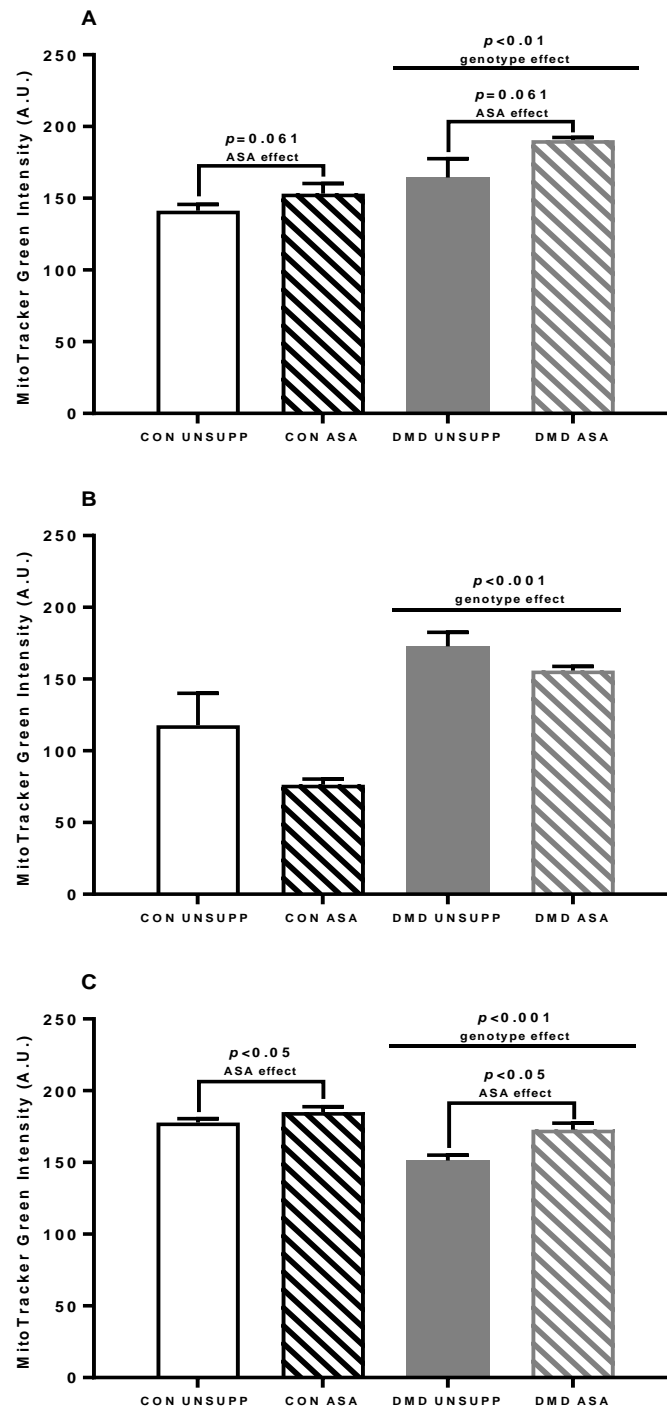


Figure 7.4. Total mitochondrial pool of unsupplemented (UNSUPP) and adenylosuccinic acid (ASA) supplemented control (CON) and Duchenne Muscular Dystrophy (DMD) myoblasts. The mitochondrial pool was greater in DMD myoblasts at 24 hours compared to CON ($p < 0.01$, A) with a trend for ASA to increase the mitochondrial pool in both CON and DMD myoblasts detected ($p = 0.061$). At 3 days, the mitochondrial pool was greater in DMD myoblasts compared to CON ($p < 0.001$, B) and ASA had no effect in either cell line ($p < 0.05$). At 7 days, the mitochondrial pool was significantly less in DMD myoblasts compared to CON ($p > 0.001$, C) with ASA increasing the mitochondrial pool in both CON and DMD myoblasts ($p < 0.05$). $n = 4$ per group.

7.3.3 The effect of acute ASA supplementation on mitochondrial superoxide (O₂⁻) production

Since we observed in Chapter 6 that chronic ASA supplementation reduced mitochondrial O₂⁻ production in *mdx* FDB fibres, we assessed the effect of acute ASA supplementation on mitochondrial O₂⁻ production. At 24 hours, mitochondrial O₂⁻ production was 78% higher in DMD myoblasts compared to CON ($p < 0.0001$, Figure 7.5A) and ASA stimulated a further 64% increase in mitochondrial O₂⁻ production in DMD myoblasts ($p < 0.01$). At 3 days, however, mitochondrial O₂⁻ production was comparable between untreated CON and DMD myoblasts ($p > 0.05$, Figure 7.5B) and ASA treatment reduced O₂⁻ production in DMD myoblasts by ~14% ($p < 0.05$). At 7 days, mitochondrial O₂⁻ production was 194% higher in DMD myoblasts compared to CON ($p > 0.0001$, Figure 7.5C), with ASA reducing mitochondrial O₂⁻ production in CON and DMD myoblasts by 66% and 20%, respectively ($p < 0.001$).

7.3.4 The effect of acute ASA supplementation on oxidative and glycolytic metabolism

Although we did not observe improvements in mitochondrial respiration following 8 weeks of ASA supplementation in the *mdx* mouse, we assessed oxidative and glycolytic metabolic indices following an acute (24 hour) supplementation period to elucidate if ASA can stimulate metabolism. This acute setting may demonstrate downstream effects on mitochondrial respiration

as the 24 incubation with ASA in DMD skeletal muscle explants inhibited lipid production (Bonsett and Rudman, 1984) suggesting modulation of mitochondrial activity. In an attempt to overcome the limitations stated in Chapter 6, we included 1mM ASA in the media during the assay. As we utilised different seeding densities in these experiments – due to a seeding density of 25,000 DMD myoblasts inducing oxygen depletion in the wells during respiration – we have presented these data corrected for a plating density of 5,000 myoblasts.

First, we investigated oxidative metabolism via the measurement of OCR in myoblasts across various respiratory states using a mitochondrial stress test. Basal respiration was shown to be 192% higher in DMD compared to CON myoblasts ($p < 0.001$, Figure 7.6A), however, ASA treatment had no effect on this measure in either CON or DMD myoblasts. Associated with this increased basal respiration was a 6.5-fold increase in OCR associated with proton leak (i.e. OCR not attributable to ATP production) in DMD compared to CON myoblasts ($p < 0.0001$, Figure 7.6B) and ASA was unable to reduce this in DMD myoblasts. Maximal respiration, as induced by the addition of FCCP which uncouples the mitochondria to deplete the $\Delta\psi$, was 190% higher in DMD myoblasts compared to CON ($p < 0.001$, Figure 7.6C) and non-mitochondrial respiration was 178% higher in DMD myoblasts compared to CON ($p < 0.0001$, Figure 7.6D). While ASA had no effect on maximal respiration in either CON or DMD myoblasts (Figure 7.6C), ASA enhanced the non-mitochondrial respiration in DMD myoblasts by 33% ($p < 0.05$, Figure 7.6D).

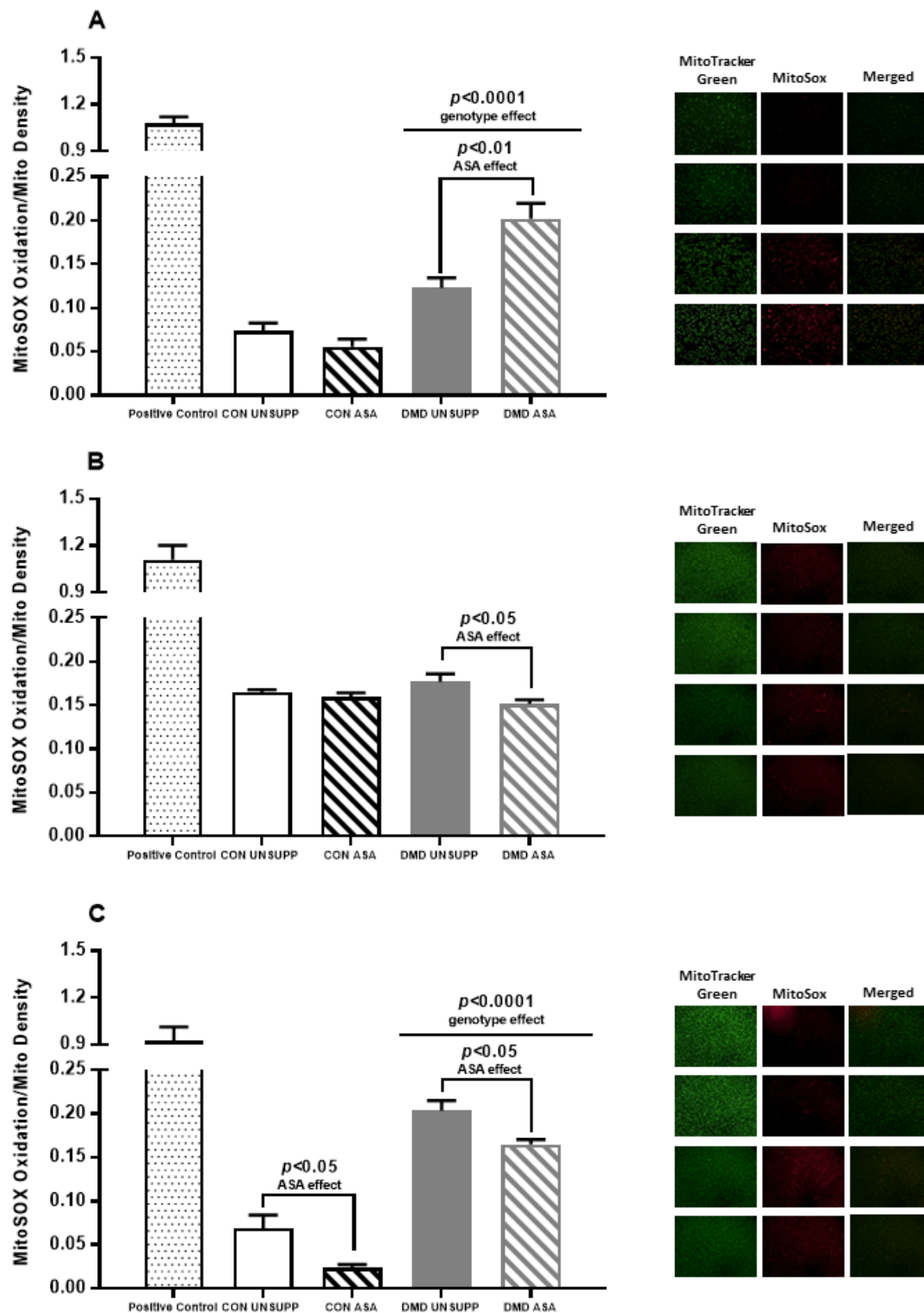


Figure 7.5. Mitochondrial superoxide (O_2^-) production of unsupplemented (UNSUPP) and adenylosuccinic acid (ASA) supplemented control (CON) and Duchenne Muscular Dystrophy (DMD) myoblasts. Mitochondrial O_2^- production was greater in DMD myoblasts compared to CON at 24 hours ($p < 0.0001$, A) with ASA increasing O_2^- production in DMD myoblasts only ($p < 0.001$). At 3 days, mitochondrial O_2^- production was comparable between CON and DMD myoblasts ($p > 0.05$, B) with ASA supplementation decreasing O_2^- production in DMD myoblasts ($p < 0.05$). At 7 days, O_2^- production was greater in DMD myoblasts compared to CON ($p > 0.0001$, C) with ASA decreasing O_2^- production in both CON and DMD myoblasts ($p < 0.05$). $n = 4$ per group.

Next, we assessed anaerobic glycolytic flux through the measurement of the ECAR in myoblasts across the various respiratory states induced by the mitochondrial stress test. Basal ECAR was demonstrably 110% higher in DMD compared to CON myoblasts ($p < 0.01$, Figure 7.7A) and this was not affected by ASA treatment in either genotype. During oligomycin-induced inhibition of Complex V, ECAR increased from the basal state in both CON and DMD myoblasts to compensate for the inhibition of oxidative ATP production. While a 210% higher ECAR was observed in DMD compared to CON myoblasts ($p < 0.0001$, 7.7B), ASA treatment had no effect on ECAR in either genotype. During maximal (Figure 7.7C) and complete inhibition of oxidative metabolism (Figure 7.7D), ECAR was 123% and 114% higher, respectively, in DMD compared to CON myoblasts ($p < 0.0001$ and $p < 0.01$, respectively). Acute ASA supplementation had no effect on maximal ECAR in either CON or DMD myoblasts ($p > 0.05$, Figure 7.7C) but did, however, increase ECAR in CON and DMD myoblasts during inhibition of oxidative metabolism by 37% and 108%, respectively ($p < 0.05$, Figure 7.7D).

Using the derived OCR and ECAR measurements over the various respiratory states, we calculated several mitochondrial functional indices to elucidate if the changes in these basic respiration parameters had an effect on overall mitochondrial function. The ATP production capacity (expressed as a % of basal respiration) was severely reduced (by 40%) in DMD compared to CON myoblasts ($p < 0.0001$, Figure 7.8A). ASA treatment was demonstrably detrimental in DMD myoblasts and decreased the ATP production capacity by a further 51% ($p < 0.05$), albeit it had no effect on the ATP production capacity of CON myoblasts. Next, we determined the spare respiratory capacity during metabolic stress induced by chemical uncoupling of

the mitochondria with FCCP. Unexpectedly, the spare respiratory capacity of CON and DMD myoblasts was comparable (Figure 7.8B) with ASA having no effect on either genotype ($p>0.05$). The coupling efficiency, a determinant of the extent to which oxygen consumption reflects ATP production at Complex V, was, however, significantly reduced in DMD compared to CON myoblasts (by 66%, $p<0.0001$, Figure 7.8C). While ASA had no effect on the coupling efficiency of CON myoblasts ($p>0.05$), it was further detrimental to DMD myoblasts by suppressing the coupling efficiency to ~10% ($p<0.05$). The decreased ATP production rate and coupling efficiency of DMD myoblasts was reflected by a significantly lower Bioenergetical Health Index (BHI) compared to CON myoblasts ($p<0.0001$, Figure 7.8D). ASA was unable to improve the BHI in DMD myoblasts ($p>0.05$) or in CON myoblasts ($p>0.05$). Next we investigated the flexibility of the oxidative and glycolytic pathways to respond appropriately to energy requirements during FCCP-induced metabolic stress. Both the oxidative metabolic potential and the glycolytic metabolic potential were comparable between CON and DMD myoblasts ($p>0.05$, Figure 6,9A and B respectively) and ASA had no effect on either oxidative or glycolytic metabolic potential in either genotype.

Finally, we utilised metabolic phenograms to indicate the metabolic phenotype of myoblasts under basal (rest) and stressed (FCCP-induced) conditions. When presented together, the metabolic phenogram indicates how the cell responds to metabolic stress through mitochondrial respiration and glycolytic flux. As expected during resting metabolism, both CON groups, irrespective of their treatment, displayed low metabolic activity (Figure 7.10A). While DMD UNSUPP myoblasts also displayed low metabolic activity at rest, ASA treatment shifted their basal metabolic

state to a more glycolytic phenotype (Figure 7.10A). Under metabolic stress (FCCP-induced), CON UNSUPP myoblasts remained in a lower comparative metabolic state while ASA induced transition to more a metabolic phenotype (Figure 7.10B). Similarly, DMD UNSUPP and ASA myoblasts also transitioned to a more active metabolic phenotype during FCCP-induced stress. While the overall gradients (basal to stressed) were comparable between CON and DMD myoblasts ($p>0.05$), DMD myoblasts relied more on increases in glycolysis to fuel their metabolic demand, as evidenced by the larger run ($p<0.05$).

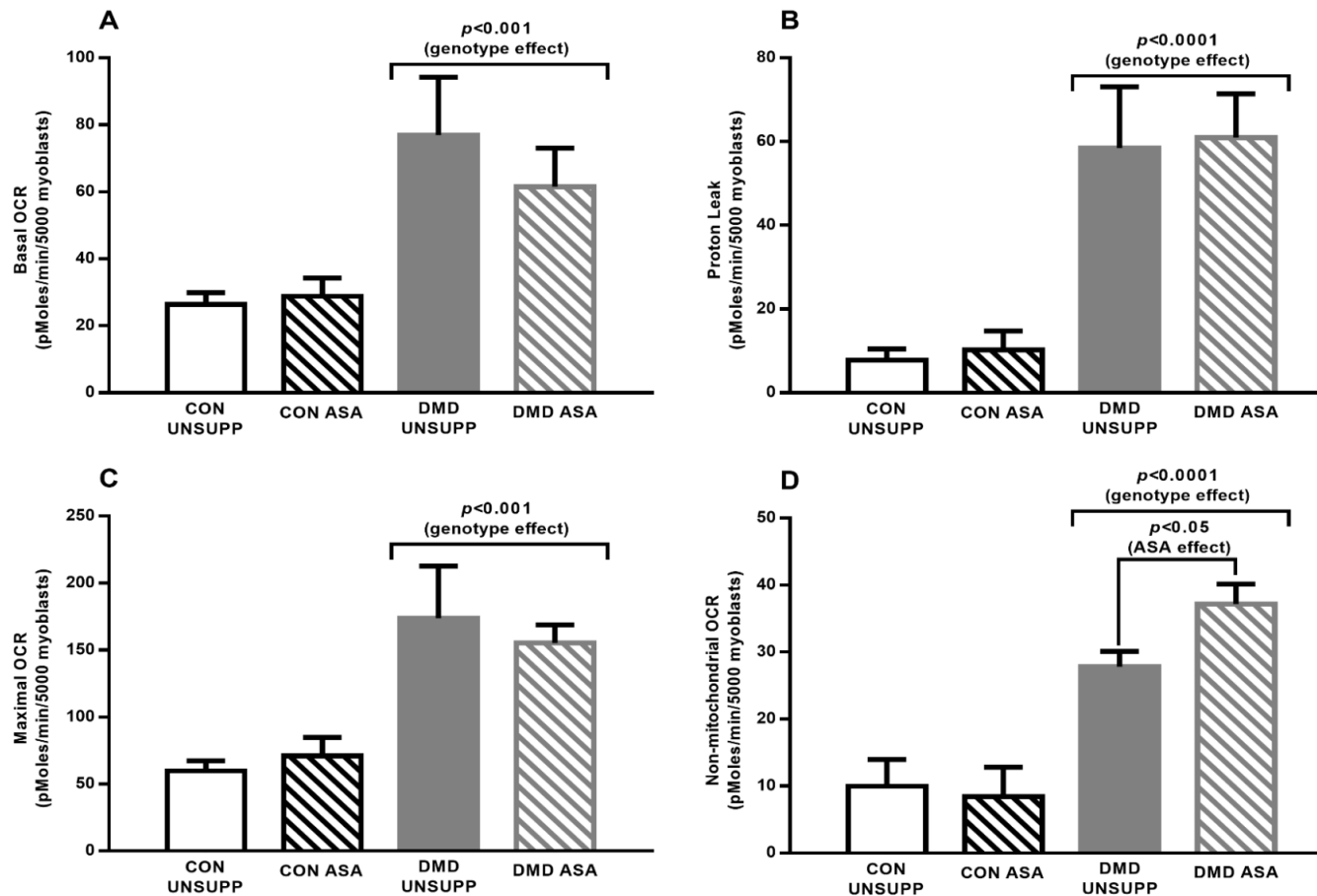


Figure 7.6. Oxygen consumption rate (OCR) of unsupplemented (UNSUPP) and adenylosuccinic acid (ASA) supplemented control (CON) and Duchenne Muscular Dystrophy (DMD) myoblasts. Basal respiration was significantly higher in DMD myoblasts compared to CON ($p < 0.001$, A) and ASA had no effect in either cell line ($p > 0.05$). OCR during proton leak was higher in DMD myoblasts compared to CON ($p < 0.0001$, B) with ASA having no effect in either cell line ($p > 0.05$). In DMD myoblasts, maximal OCR (C) and non-mitochondrial respiration (D) was also greater in DMD myoblasts ($p < 0.001$ and $p < 0.0001$ respectively) and ASA further increased non-mitochondrial respiration in DMD myoblasts ($p < 0.05$). $n = 7-8$ CON UNSUPP, $n = 6$ CON ASA, $n = 5$ DMD UNSUPP, $n = 5$ DMD ASA.

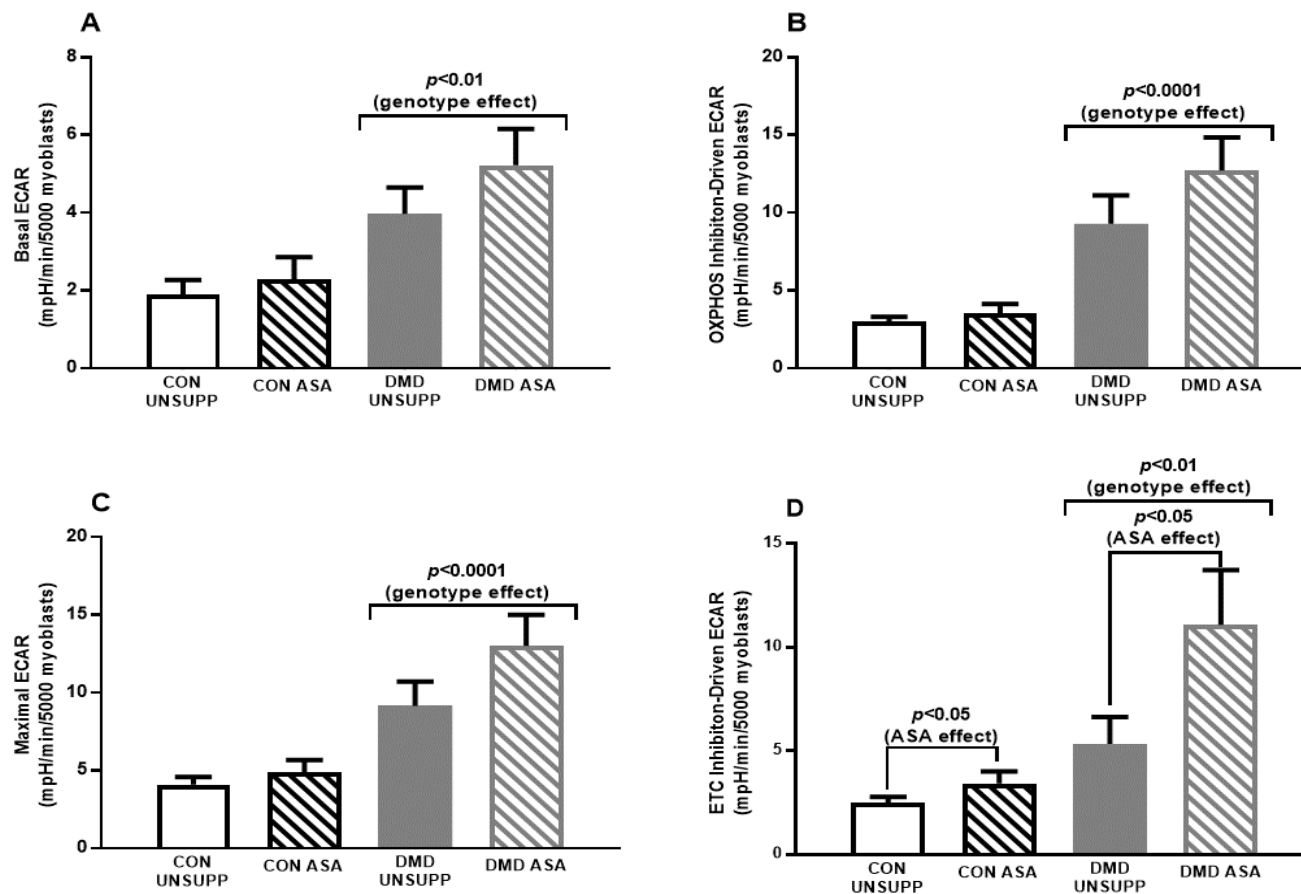


Figure 7.7. Extracellular acidification rate (ECAR) of unsupplemented (UNSUPP) and adenylosuccinic acid (ASA) supplemented control (CON) and Duchenne Muscular Dystrophy (DMD) myoblasts. Basal ECAR (A) and ECAR driven by inhibition of Complex V (B) was significantly higher in DMD myoblasts compared to CON ($p < 0.01$ and $p < 0.0001$ respectively) and ASA had no effect in either cell line ($p > 0.05$). Maximal ECAR was higher in DMD myoblasts compared to CON ($p < 0.0001$, C) and ASA had no effect in either CON or DMD myoblasts ($p > 0.05$). In DMD myoblasts, ECAR driven by inhibition of oxidative metabolism was greater in DMD myoblasts ($p < 0.01$) and ASA further increased non-mitochondrial respiration in both CON and DMD myoblasts ($p < 0.05$). $n = 7-8$ CON UNSUPP, $n = 6$ CON ASA, $n = 5$ DMD UNSUPP, $n = 5$ DMD ASA.

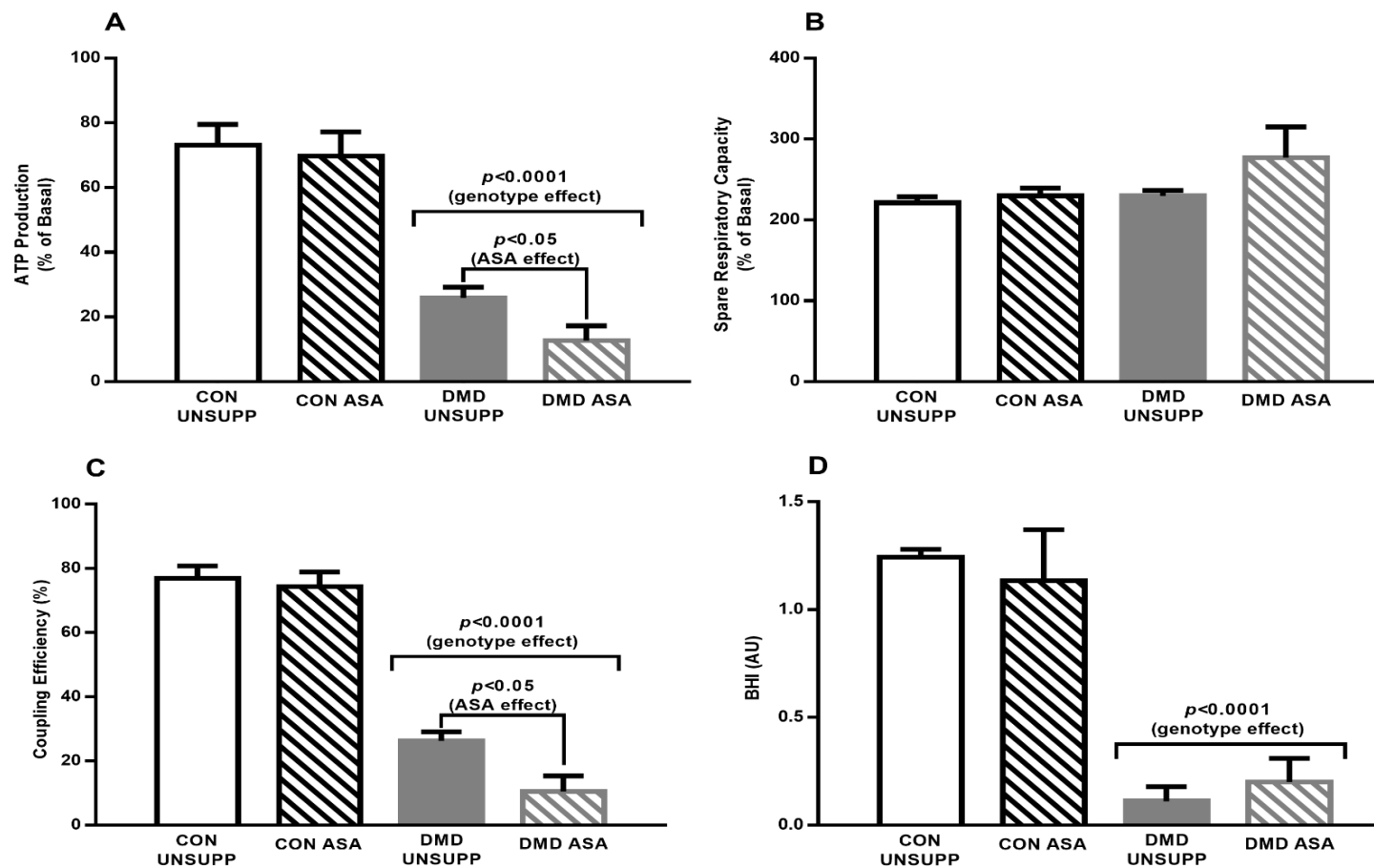


Figure 7.8. Mitochondrial function of unsupplemented (UNSUPP) and adenylosuccinic acid (ASA) supplemented control (CON) and Duchenne Muscular Dystrophy (DMD) myoblasts. ATP production was significantly less in DMD myoblasts compared to CON ($p < 0.0001$, A) with ASA decreasing ATP production further ($p < 0.05$). Spare respiratory capacity was not different between CON and DMD myoblasts ($p > 0.05$, B) with ASA having no effect in either cell line ($p > 0.05$). In DMD myoblasts, coupling efficiency was less compared to CON myoblasts ($p < 0.0001$, C) and ASA decreased this further ($p < 0.05$). The bioenergetical health index (BHI) of myoblasts was significantly lower in DMD myoblasts compared to CON ($p < 0.0001$, D) with ASA having no effect ($p > 0.05$). $n = 7-8$ CON UNSUPP, $n = 6$ CON ASA, $n = 5$ DMD UNSUPP, $n = 5$ DMD ASA.

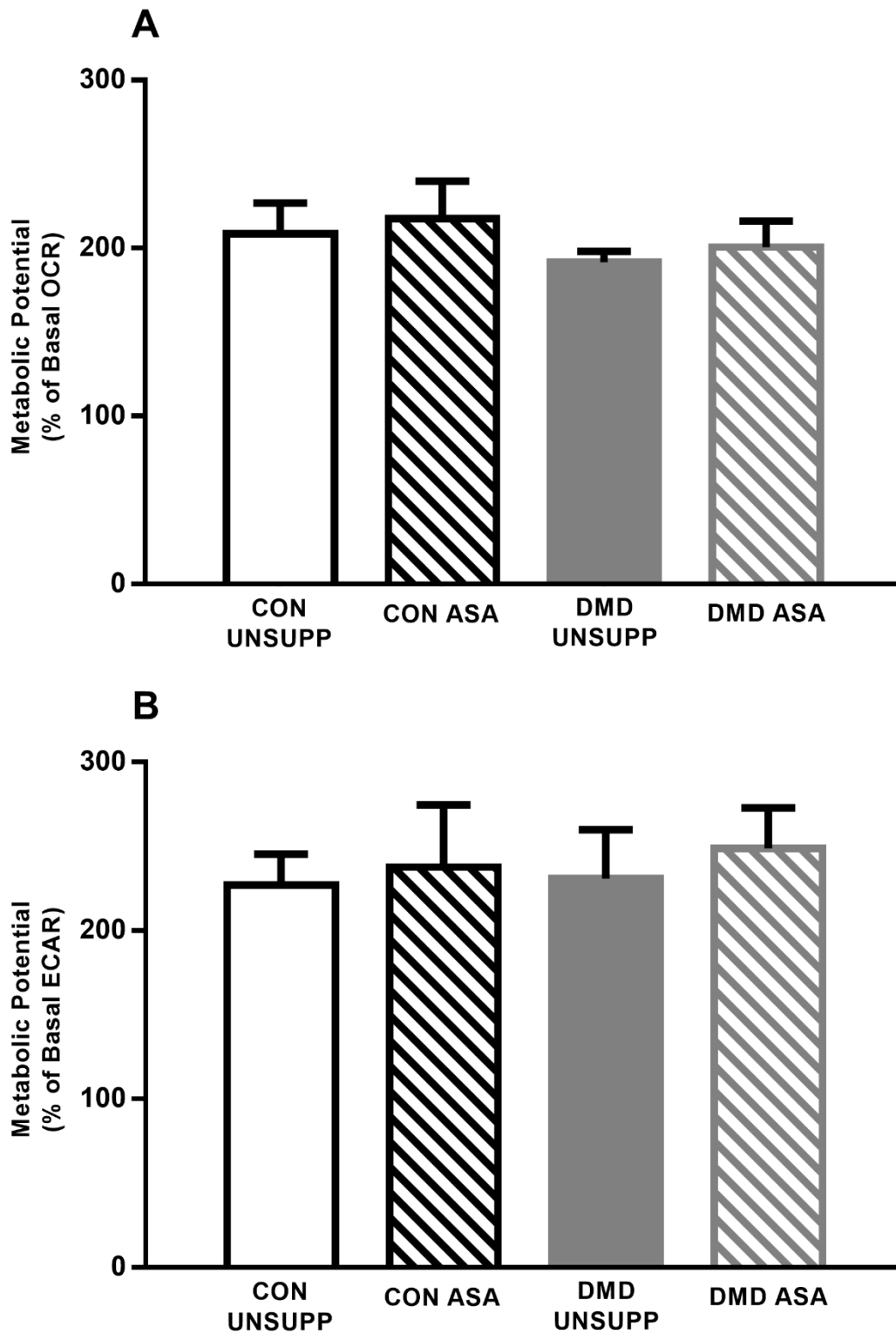
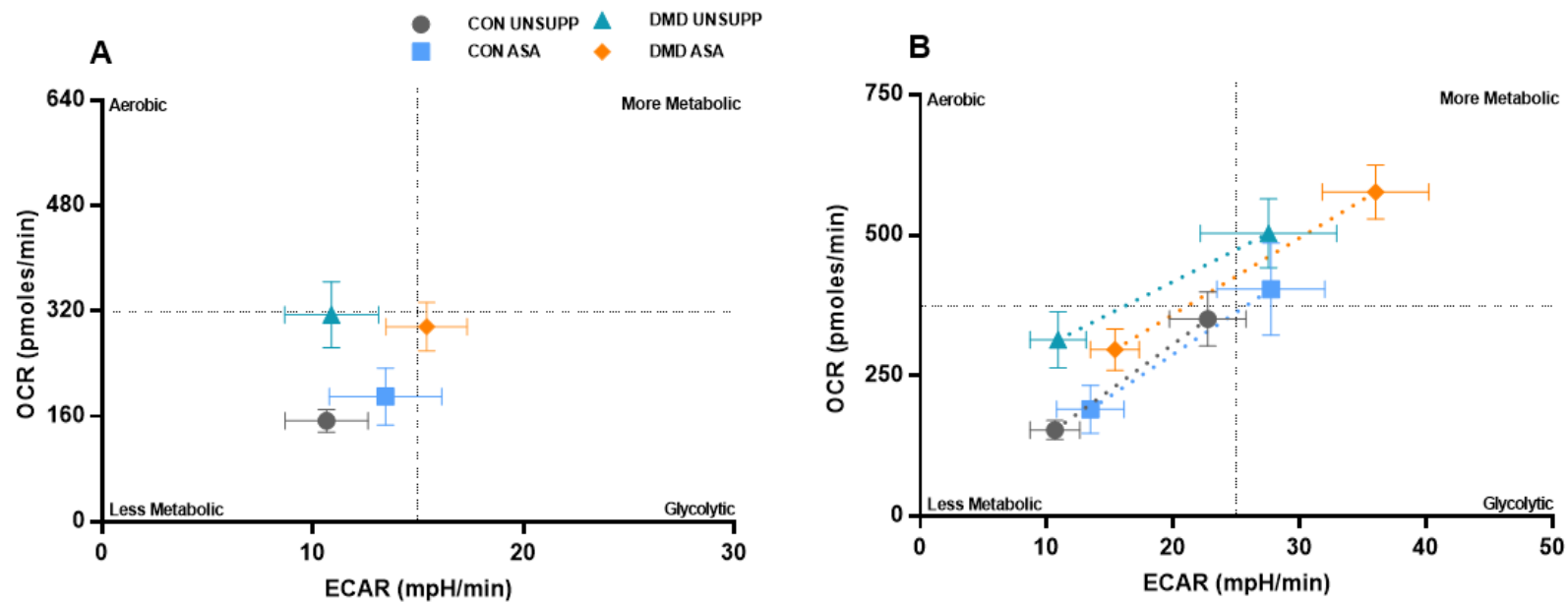


Figure 7.9. Metabolic potential of unsupplemented (UNSUPP) and adenylosuccinic acid (ASA) supplemented control (CON) and Duchenne Muscular Dystrophy (DMD) myoblasts. No significant different in oxidative (A) or glycolytic metabolic potential (B) was observed between CON and DMD myoblasts ($p>0.05$). ASA had no effect in either cell line ($p>0.05$). $n= 7-8$ CON UNSUPP, $n= 6$ CON ASA, $n=5$ DMD UNSUPP, $n=5$ DMD ASA.



	CON UNSUPP	CON ASA	DMD UNSUPP	DMD ASA
Rise (OCR)	195.12 ± 21.65	214.14 ± 44.14	229.01 ± 27.45	247.38 ± 8.14
Run (ECAR)	15.02 ± 3.54	14.27 ± 2.28	16.63 ± 3.64 ^	20.56 ± 3.20 ^
Gradient	10.89 ± 1.03	15.68 ± 3.53	16.76 ± 5.47	13.5 ± 1.92

Figure 7.10. Metabolic phenograms of unsupplemented (UNSUPP) and adenylosuccinic acid (ASA) supplemented control (CON) and Duchenne Muscular Dystrophy (DMD) myoblasts. During basal respiration (A), CON UNSUPP, CON ASA and DMD UNSUPP myoblasts resided in a less metabolic phenotype with DMD ASA myoblasts residing in a glycolytic state. Under stressed conditions (B), CON UNSUPP myoblasts remained in a less metabolic phenotype with ASA shifting the phenotype to more metabolic in CON myoblasts. Both DMD UNSUPP and DMD ASA shifted to a more metabolic phenotype. No difference in rise (change in oxygen consumption rate; OCR) or gradient was observed between the cell lines ($p>0.05$), however, run (change in extracellular acidification rate; ECAR) was greater in DMD myoblasts compared to CON ($p<0.05$). ASA had no effect on rise, run or gradient ($p>0.05$). ^ significant difference from CON myoblasts $p<0.05$. $n= 7-8$ CON UNSUPP, $n= 6$ CON ASA, $n=5$ DMD UNSUPP, $n=5$ DMD ASA.

7.4 Discussion

Central to our hypothesis is that metabolic dysfunction is a core aetiological problem in dystrophin-deficient skeletal muscle and therefore treatment options for DMD should include metabolically targeted therapies (Timpani *et al.*, 2015). One promising therapeutic candidate, of metabolic origin, is ASA which was examined in a small clinical trial and demonstrated significant improvements in DMD and BMD patients with maintenance of muscle function and strength (Bonsett and Rudman, 1992). Despite this, following the discovery of dystrophin-deficiency as the cause of DMD (Hoffman *et al.*, 1987), the experimental evaluation of ASA was abandoned (as was other metabolic therapy-related research) and has not been investigated since. As we observed remarkable improvements in muscle histology following chronic ASA supplementation of the *mdx* mouse, yet few metabolic changes, we were interested in investigating the acute effects of ASA treatment on metabolism in human dystrophin-positive (CON) and dystrophin-negative (DMD) myoblasts. In this chapter, we have again demonstrated that DMD myoblasts are severely metabolically compromised but that acute ASA supplementation cannot moderate this metabolic deficiency. Our data highlights that ASA is therapeutically active via a metabolism-independent pathway.

As the mitochondria have been implicated as key players in apoptotic signalling and cell death (Liu *et al.*, 1996, Susin *et al.*, 1999), any early detectable changes in mitochondrial viability would suggest impending mitochondrial and cellular demise as mitochondria are unable to meet cellular energy demands. From our study, the reduced mitochondrial viability at 24 hours and 3 days could be

indicative of impending cellular death in DMD myoblasts. Indeed, increased apoptotic activity has been observed in skeletal muscle of the *mdx* mouse (Pal *et al.*, 2014). However, mitochondrial viability recovers at 7 days to be comparable with CON myoblasts. It would be interesting to investigate if this recovered mitochondrial viability is because mitochondria improve (1) coupling of their respiration to ATP production and therefore (2) produce less O₂⁻. In addition, this poor mitochondrial viability was associated with an increased mitochondrial pool at 24 hours and 3 days and a decreased pool at 7 days. From the outset, this data seems to conflict as it would be anticipated that a larger mitochondrial pool is required to meet the metabolic demands of the cells and therefore greater mitochondrial viability would be associated with this. However, this does not seem to be the case in DMD myoblasts. A larger mitochondrial pool might be reflective of one of two things: (1) a greater cell density, due to faster proliferative rate, culminating in more mitochondria in the assay; or (2) a higher mitochondrial density per myoblast. However, since DMD myoblasts exhibit a reduced proliferative rate (Blau *et al.*, 1983, Melone *et al.*, 2000), our increased mitochondrial pool is unlikely due to increased myoblast number, at least at the 24 hour time point. As we (in Chapter 6) and others (Ljubcic *et al.*, 2011) have demonstrated elevated basal levels of the mitochondrial biogenesis stimulator PGC-1 α , it is most likely that the increased mitochondrial pool is through PGC-1 α activation. Despite the capacity to increase the mitochondrial pool in dystrophic muscle, there is no positive modulation of oxidative metabolism that results in improved ATP production. Therefore, the data suggests that dystrophin-negative myoblasts stimulate the biogenesis of defective mitochondria and the biogenesis of defective mitochondria cannot be overcome by acute ASA treatment.

The comparable mitochondrial viability at 7 days between CON and DMD myoblasts was an unexpected result, especially because this was demonstrated in a smaller mitochondrial pool in dystrophin-deficient myoblasts. Autophagy, a degradative process that removes cytotoxic proteins and damaged/dysfunctional organelles, may be responsible for the reduction of mitochondria in DMD myoblasts, thus maintaining a higher viability in lesser mitochondrial pool. As autophagy is additionally activated in response to nutrient stress (Sandri *et al.*, 2013), and dystrophic muscle is characterised by a reduced ATP production capacity – as highlighted in this Chapter and by us previously (Rybalka *et al.*, 2014) – and content (Cole *et al.*, 2002, Austin *et al.*, 1992), autophagy could be heightened in our DMD cell culture model to ensure the healthiest mitochondria are maintained while defective mitochondria are destroyed in DMD myoblasts. Indeed, stimulation of autophagy in the *mdx* mouse elicits positive effects on muscle function and composition (De Palma *et al.*, 2012, Pauly *et al.*, 2012, Bibee *et al.*, 2014, Li *et al.*, 2012). However, recently it has been documented that autophagic activity is reduced in DMD patients and *mdx* mice (Pal *et al.*, 2014, De Palma *et al.*, 2012, Li *et al.*, 2012, Spitali *et al.*, 2013) indicating a reduced capacity for the removal of dysfunctional and damaged organelles. This reduction in autophagic capacity has been linked to hyperactivity of the Akt/mammalian target of rapamycin (mTOR) pathway (De Palma *et al.*, 2012, Dogra *et al.*, 2006, Peter and Crosbie, 2006, Eghtesad *et al.*, 2011) which is involved in muscle growth and hypertrophy. While activation of the Akt/mTOR pathway is important in dystrophic muscle as a compensatory mechanism to increase muscle mass, persistent activation of this pathway leads to the inhibition of autophagy (De Palma *et al.*, 2012). Furthermore,

as oxidative stress has been observed to further inhibit autophagy induction in the *mdx* mouse (Pal *et al.*, 2014), and our observation of higher levels of mitochondrial O_2^- production could suggest possible oxidative stress in DMD myoblasts, this could potentially exclude increased autophagic activity in DMD myoblasts at this time point. Further investigation would be required to confirm this.

Oxidative and glycolytic metabolism was assessed following 24 hours of ASA treatment as it is well established that oxidative (Olson *et al.*, 1968, Martens *et al.*, 1980, Bhattacharya *et al.*, 1993, Glesby *et al.*, 1988, Kuznetsov *et al.*, 1998, Faist *et al.*, 2001, Griffin *et al.*, 2001, Rybalka *et al.*, 2014) and glycolytic (Dreyfus, 1954, Thomson, 1960, Cao *et al.*, 1965, Hess, 1965, Di Mauro, 1967, Ellis, 1980, Lilling and Beitner, 1991, Zatz *et al.*, 1991, Wehling-Henricks *et al.*, 2009) deficits are features of dystrophic muscle and that this significantly impacts cellular energy levels (Cole *et al.*, 2002, Austin *et al.*, 1992). All measurements of OCR (basal, proton leak, maximal and non-mitochondrial) were significantly higher in DMD myoblasts compared to CON. This observation is quite interesting considering that, despite having a larger mitochondrial pool density at 24 hours, a significant proportion of this pool was non-viable. Therefore, the remaining viable mitochondria are respiring excessively, (basally 1.5-fold higher than CON) in an attempt to address the cellular metabolic stress. However, this appears to be futile as higher proportions of respiration are attributed to proton leak. The elevated proton leak is most likely a response to the higher mitochondrial O_2^- production and indicates that O_2 is being sequestered away from ATP generation into radical production and importantly proton leak is depleting the $\Delta\Psi$, the driver of ATP production at Complex V. Indeed, we observed a severely depressed ATP production capacity (40% lower compared

to CON myoblasts), which is consistent with our previous findings in isolated mitochondria from the *mdx* mouse (Rybalka *et al.*, 2014), and a severely reduced mitochondrial coupling efficiency of DMD myoblasts. As myoblasts are central to the facilitation of muscle repair, the requirement for which is elevated in DMD, our data suggests that repair under these circumstances might be compromised. The reduced number of viable mitochondria that favour O_2^- production over ATP generation in DMD myoblasts could: (1) affect how quickly repair can occur or (2) result in an inadequate repair of the muscle. In either scenario, this would promote loss of skeletal muscle integrity and strength.

It would be anticipated that the higher metabolic demand of DMD myoblasts, – due to increased proton leak and reduced ATP production – in conjunction with dysfunction at the level of ETC, would result in a depressed maximal respiratory capacity (Schuh *et al.*, 2012). Our results however, indicate otherwise as we demonstrated comparable maximal respiratory capacity between CON and DMD myoblasts, suggesting that they maintain metabolic flexibility. This is in contrast to our observations in Chapter 6 where isolated FDB fibres from the *mdx* mouse exhibited reduced oxidative metabolic capacity but a compensatory increase in glycolytic capacity. While we did not replicate these results in DMD myoblasts, we did demonstrate increased ECAR throughout all respiratory states and a greater dependency on ECAR (as indicated by a larger run in the metabolic phenotypes) in the face of chemically-induced metabolic stress. Glycolytic flux is upregulated during the metabolic triad of stress (increased radical production, reduced ATP production and coupling) in an attempt to overcome limited energy production. This seems to be evident in dystrophin-deficient skeletal muscle as an increased ECAR, however

appears to be insufficient to match ATP demand as indicated by the reduced BHI of DMD myoblasts. This inability to match ATP demand despite upregulation of glycolysis may be reflective of the glycolytic nature of proliferating cells (i.e. myoblasts). In proliferating cells, glycolysis is limited not by ATP production but ATP consumption (Scholnick *et al.*, 1973). In the case of DMD myoblasts, the inability for glycolysis to satisfy cellular energy demands may be due to: (1) the reduced ATP content, and therefore the ATP available to drive glycolytic flux since several glycolytic reactions consume ATP or; (2) functional deficits of various glycolytic enzymes (Dreyfus, 1954, Thomson, 1960, Cao *et al.*, 1965, Hess, 1965, Di Mauro, 1967, Ellis, 1980, Lilling and Beitner, 1991, Zatz *et al.*, 1991, Wehling-Henricks *et al.*, 2009).

While acute ASA treatment had no significant effect on mitochondrial viability at any time point – which is in contrast to our observations in the *mdx* mouse (Chapter 6) – ASA reduced mitochondrial O_2^- following 3 and 7 days of treatment. It is well documented that increased respiration through Complex II of the ETC generates excessive O_2^- production (Turrens and Boveris, 1980, Liu *et al.*, 2002, Kushnareva *et al.*, 2002, Hansford *et al.*, 1997, Votyakova and Reynolds, 2001) through the reversal of electron flow to Complex I (Liu *et al.*, 2002, Hansford *et al.*, 1997, Votyakova and Reynolds, 2001, Han *et al.*, 2003). As the fumarate produced by the cycling of the PNC could theoretically stimulate anaplerosis of the TCA cycle, it is possible that acute ASA treatment generates downstream TCA cycle metabolites, succinate included. We did observe enhanced mitochondrial uncoupling in ASA-treated DMD myoblasts, suggesting anaplerotic expansion of the TCA cycle induced by ASA. While Complex II-driven respiration may be preferable in dystrophic

mitochondria (we have demonstrated Complex I dysfunction (Rybalka *et al.*, 2014), which can be ameliorated through Complex II-driven respiration (Chinet *et al.*, 1994, Glesby *et al.*, 1988, Nylen and Wrogemann, 1983, Ionășescu *et al.*, 1967)), the enhanced O_2^- production is potentially detrimental in already oxidatively stressed dystrophic muscles (Disatnik *et al.*, 1998, Grosso *et al.*, 2008). An indicator of elevated oxidative stress in DMD myoblasts, in addition to the increased mitochondrial O_2^- production, is the higher non-mitochondrial OCR. This measurement is taken following the addition of rotenone and antimycin A (to inhibit Complex I and III respectively) which prevents ETC O_2 consumption. Any O_2 consumed at this point occurs in the cytosol and is typically very low, as indicated in CON myoblasts. However, the excessive non-mitochondrial OCR seems likely reflective of increased antioxidant activity, in particular GSH as it consumes O_2 to buffer radicals (Winterbourn and Metodiewa, 1994, Kesler *et al.*, 2010). While there is no consensus if antioxidant activity is elevated in DMD to compensate for increased radical production (Hunter and Mohamed, 1996, Ragusa *et al.*, 1996, Dorchies *et al.*, 2006, Chahbouni *et al.*, 2011), our data suggests that it may be. Interestingly, ASA-treatment further stimulated non-mitochondrial OCR by 33% in DMD myoblasts. We have shown increased Nrf2 protein content in *mdx* mice following chronic ASA supplementation in Chapter 6 and Nrf2 is known to upregulate various antioxidants (Reddy *et al.*, 2007, Reddy *et al.*, 2008, Higgins *et al.*, 2009, Miller *et al.*, 2012), therefore this may account for the increased non-mitochondrial OCR. However, further investigation of the antioxidant status of the cell is required to elucidate if this is true.

Our data, in both Chapter 6 and 7, seems to disprove the hypothesis of Bonsett and Rudman that ASA exerts its therapeutic potential in DMD muscle via promotion of mitochondrial function and the cellular metabolic status (Bonsett and Rudman, 1984, Bonsett and Rudman, 1992). One alternative explanation for this is the possibility that unbuffered ASA was administered in the clinical trials conducted by Bonsett & Rudman as no specific details were given regarding this (Bonsett and Rudman, 1992). Very recent evidence indicates that an acidotic environment modulates metabolism through the reduction of glycolytic flux and upregulation of fatty acid oxidation which induces protein hyperacetylation that limits Complex I function (Corbet *et al.*, 2016). It may be that the acidic profile of unbuffered ASA acted through a similar mechanism. In addition, it may explain the remarkable effects of ASA on lipid production in DMD explants (Bonsett and Rudman, 1984) since acidosis stimulates fatty acid oxidation which might explain the reduction of lipid content within DMD skeletal muscle following ASA therapy. As such, a modern day investigation of the fatty acid oxidation capacity of DMD myoblasts is warranted.

7.5 Conclusion

In summary, our study demonstrates severe metabolic perturbations in DMD myoblasts that acute ASA supplementation cannot moderate. At 3 and 7 days, ASA treatment was effective at reducing O_2^- production in DMD myoblasts but was unable to improve mitochondrial viability. At 24 hours, however, ASA supplementation was detrimental and stimulated further mitochondrial O_2^- production in DMD myoblasts. When considered in context with reductions in coupling efficiency and ATP production rate, our data suggests that acute ASA treatment in DMD myoblasts may promote further pathology which is in contrast to previous findings. While this data suggests that longer exposure to ASA could elicit positive effects on downstream mitochondrial respiration, due to the reductions in mitochondrial O_2^- production, further investigation is required at the 3 and 7 day time points to confirm this. This is particularly important to assess as we observed no detrimental effects of ASA on mitochondrial respiration in a chronic supplementation regimen of the *mdx* mouse. The findings in this chapter suggest that there may be time-dependent effects of ASA.

Chapter Eight

Conclusions, Limitations & Future Directions

8.1 Conclusions

Our working hypothesis challenges the currently accepted paradigm of DMD in that the severe metabolic perturbations are not secondary to the absence of dystrophin from the sarcolemma of skeletal muscle but rather a core aetiological problem. As such, we believe that treating DMD as a predominantly metabolic disease, and tailoring therapeutic options to allay metabolic stress, would lead to significant improvements in dystrophic pathology including prevention of muscle damage and heightened capacity for muscular repair. Thus, the broad aim of this thesis was to evaluate and characterise the potential of the metabolic therapies, ASA and nitrate, as viable future treatment options for DMD with emphasis on their capacity to moderate key features of the disease including metabolic dysfunction and histopathology.

This thesis has demonstrated that dystrophin-deficient skeletal muscle, in particular human dystrophin-deficient myoblasts, are metabolically compromised. This poor ability to utilise respiration for ATP generation favours O_2^- production and results in severely uncoupled mitochondria. This scenario was observed in DMD myoblasts (Chapters 5 and 7) and in the red portion of gastrocnemius derived from the *mdx* mouse (Chapter 4) but not in the white portion of gastrocnemius (Chapter 4) nor the predominantly glycolytic FDB (Chapter 6). This suggests a fibre-type dependent effect and likely reflects the mitochondrial density of myoblasts and oxidative fibres whereby the denser the mitochondrial population, the more evident the mitochondrial dysfunction is. These data provide credence for the investigation of the potential of metabolic therapies to alleviate this systemic metabolic crisis and highlight the severity of mitochondrial dysfunction in dystrophin-deficient skeletal muscle.

In Part One of this thesis, the value of increasing NO bioavailability in hind limb skeletal muscles derived from the dystrophin-deficient *mdx* mouse, and immortalised myoblasts derived from DMD patients was assessed. As NO production is affected in dystrophin-deficient skeletal muscle – due to the secondary reduction of the NO-producing sarcolemmal protein nNOS – and NO is a known modulator of metabolism, we investigated the capacity of NO donation via the NITR-nitrite-NO pathway to improve dystrophic metabolism. In the *mdx* mouse, chronic NITR supplementation had no beneficial modulatory effect on GU or mitochondrial respiration but rather further depressed GU in the *mdx* EDL. The lack of effect on metabolic processes stimulated the investigation of enhanced NO bioavailability on other features of the disease. Interestingly, while NITR reduced H₂O₂ emission in *mdx* gastrocnemius, this was associated with a concomitant increase in ONOO⁻ and enhanced muscle damage (as observed in *mdx* TA). From this study, the data suggests that chronic NITR supplementation is detrimental and promotes further pathology in the *mdx* mouse. To assess if these findings were potentially due to the utilisation of a chronic supplementation period, we assessed NO donation via nitrite treatment in an acute setting. Despite nitrite treatment improving glycolytic flux and mitochondrial viability, and reducing mitochondrial O₂⁻ production, nitrite was unable to overcome metabolic dysfunction at the level of the ETC. Rather, nitrite escalated mitochondrial dysfunction by reducing coupling efficiency and consequently, the ATP production capacity. Together, the findings from Chapters 4 and 5 suggest an inability of dystrophin-deficient skeletal muscle to appropriately manage exogenously derived NO bioavailability which is in stark contrast to previous studies that support NO donation as a viable therapeutic

option for DMD (Wang and Lu, 2013, Uaesoontrachoon *et al.*, 2014, Miglietta *et al.*, 2015). Since nitrite had few effects on metabolic parameters in dystrophin- and nNOS-positive (i.e. control) skeletal muscle, our data suggests an important regulatory role of the nNOS protein and/or mitochondrial oxygen radical production (specifically O_2^-) in modulating the biological effects of NO. Therefore, without a concomitant increase in nNOS protein expression and in the presence of profound mitochondrial uncoupling and oxygen radical production, we have concluded that expansion of the NITR-nitrite-NO pool as a therapeutic option for DMD is unsuitable as it escalates histopathology and mitochondrial dysfunction. This is an important finding since NITR supplementation is currently under investigation in clinical trials for the treatment of DMD patients.

Part Two of this thesis stemmed from previous observations in a clinical trial of ASA in a very small population of DMD and BMD patients in which maintenance of muscular function and strength was maintained. This remarkable observation stimulated our experimental re-evaluation of the efficacy of ASA in the *mdx* mouse and DMD myoblasts to mitigate features of the disease. We also sought to confirm the hypothetical mechanism of ASA action. Chronically, ASA supplementation of the *mdx* mouse had no modulatory effect on GU or mitochondrial respiration, which was in contrast to our hypothesis. However, ASA did improve mitochondrial viability, the PCr and TCr content and reduced mitochondrial O_2^- production in *mdx* FDB fibres. At the histopathological level, ASA therapy had remarkable results, mitigating muscle damage, fat and fibrotic tissue infiltration as well as intramuscular Ca^{2+} content. We initially hypothesised that amelioration of muscular dystrophy would be a

result of improved metabolic (specifically mitochondrial) function. However, since ASA did not positively affect any mitochondrial parameters, our data suggests that the therapeutic mechanism is independent of mitochondrial anaplerosis. In search of an alternative mechanism, we subsequently investigated disease modifiers of muscular dystrophy. Since ASA participates in purine nucleotide cycling to salvage IMP from degradation and drive AMP→ADP→ATP (adenine nucleotide) salvage, we next examined the activation of AMPK, a known inducer of the surrogate dystrophin-related protein, utrophin. The upregulation of utrophin demonstrably results in improved sarcolemmal integrity and the amelioration of muscular dystrophy, and is a proposed mechanism for the milder pathology observed in the mdx mouse, which exhibits a higher utrophin content. In mdx muscle, ASA did not affect either AMPK phosphorylation or utrophin expression, however, highlighting that this is also not the mechanism of action. Since purine nucleotide cycle metabolism of ASA generates fumarate, and a cytosolic fumarase enzyme has been identified (Yogev *et al.*, 2010) and associated with a cellular stress response via the activation of Nrf2 (nuclear factor (erythroid-derived 2)-like 2, as opposed to nuclear respiratory factor 2) (Ashrafian *et al.*, 2012), we next investigated this pathway as a potential mechanism of action. Importantly, this thesis has provided the first preliminary evidence that ASA elicits its therapeutic efficacy through the upregulation of Nrf2 expression, which has various functions in oxidatively-stressed cells including upregulation of the antioxidant suite (in particular glutathione), heat shock proteins and other molecular chaperones. While we are yet to confirm the downstream activation of cytoprotective pathways, ASA treatment did improve mitochondrial viability and

reduce mitochondrial O_2^- production in both chronically supplemented *mdx* muscles and in acutely treated DMD myoblasts, highlighting the attenuation of oxidative stress and damage which is consistent with Nrf-2-mediated effects. In contrast to these positive data, ASA had a negative effect on mitochondrial coupling and ATP production capacity in DMD myoblasts presumably due to the anaplerotic expansion of a defective mitochondrial pool, but had no effect on mitochondrial parameters in *mdx* FDB fibres. Our data disproves the hypothesis of Bonsett and Rudman (Bonsett and Rudman, 1992) demonstrating that ASA elicits its effects through a metabolism-independent mechanism. Irrespective of its mechanism of action, our data highlights ASA as a strong candidate for the therapeutic treatment of DMD.

In conclusion, this thesis is the first to provide experimental evidence of ASA efficacy for the treatment of DMD and to elucidate a potential mechanism through which it elicits cytoprotective effects in dystrophin-deficient muscle. The outstanding histological improvements in ASA-treated *mdx* TA showcases a potential new therapeutic option for the treatment of DMD. In contrast, our data suggests that expansion of the NITR-nitrite-NO pool to enhance NO bioavailability in dystrophin-deficient skeletal muscle is not a practical therapy for DMD as it escalates muscular dystrophy, specifically via the generation of reactive nitrogen species ($ONOO^-$). Unexpectedly, both metabolic therapies were unable to overcome DMD-associated metabolic dysfunction despite having positive modulatory effects on mitochondrial O_2^- production and viability. This suggests that (1) the mode of action of the treatments is not as we hypothesised (i.e. through a metabolic pathway) or (2) that dystrophic mitochondria may be inherently defective and therefore unable to respond to

any potential enhancement of respiration. The latter is supported by the observations of an enhanced anaerobic glycolytic flux as a compensatory mechanism to support ATP production during the oxidative crisis observed in dystrophin-deficient as compared to dystrophin-positive (i.e. control) muscle. This thesis provides important evidence for a future direction of therapeutic investigation for the treatment of DMD and warrants a more rigorous preclinical evaluation of the efficacy of ASA to alleviate other clinical markers (i.e. muscle strength, function and whole body muscle mass and quality) of DMD.

8.2 Limitations

The data provided in this thesis indicates one metabolic therapy (NITR/nitrite) as an unlikely future prospect for the treatment of DMD while the other (ASA) is highlighted as a strong therapeutic candidate. Despite these very distinct findings, there are limitations associated with each Chapter.

Animal studies (Chapter 4 & 6)

1. A common limitation in both dietary supplementation studies performed in the *mdx* mouse was the lack of analysis of the diaphragm. The diaphragm is considered the most phenotypically comparable muscle between *mdx* and human muscular dystrophy, which progressively accumulates damage (Stedman *et al.*, 1991). Therefore, the diaphragm is a particularly useful muscle to give insight into possible effects the treatments might have in the human condition. One major reason for the lack of diaphragmatic analysis was the age of mice utilised (up to 12 weeks of age). This is well short of the

time (6 months) when damage begins to appear in the *mdx* diaphragm (Stedman *et al.*, 1991, Louboutin *et al.*, 1993). Despite this, histological evaluation in both studies (NITR and ASA) would have been insightful and helped to confirm the detrimental effects observed following NITR therapy and beneficial effects observed following ASA therapy.

2. Another limitation common to both dietary supplementation studies was the length of supplementation and age of mice. There is the potential that we may have observed different results if the supplementation period was shorter (i.e. an acute study) or if we had supplemented younger or older mice. Beginning supplementation from a younger time point (i.e. 18 days) would provide insight into the effects of the therapies during the peak time of muscle damage whereas supplementation at an older age (i.e. 12 months) would indicate the effects on the diaphragm and longevity.
3. The use of drinking water as a vehicle for mice to receive both NITR and ASA did not allow us to control the amount consumed and therefore deliver a precise dosage. This methodology was employed due to the chronic nature (i.e. duration) of the supplementation period and the goal of delivering a continuous supply of both therapies throughout the day, as opposed to daily one-off dosages i.e. via oral gavage or intraperitoneal or intravenous injection. There may be significant variability among the water ingestion of individual animals (which were housed in boxes of 4-5) and therefore variability in the concentrations of NITR and ASA ingested, and then made available to the skeletal muscle for uptake.
4. Associated with limitation 2, is the lack of quantification of plasma and intramuscular NO/cGMP and ASA/fumarate concentrations to confirm

therapy dosages were absorbed from the GI tract into the blood, and from the blood into the muscle. We are currently assessing the nitrate/nitrite and cGMP content of plasma and muscles via high performance liquid chromatography and mass spectrometry to finalise reviewer recommendations for our *Neurotherapeutics* paper (Chapter 4), however, this analysis was unable to be completed in time for thesis submission. Once these measurements have been determined, this will allow us to unequivocally confirm that oral NITR supplementation can expand the NITR-nitrite-NO pool. We intend to undertake similar analyses to confirm ASA and fumarate concentrations in plasma and muscle samples derived in Chapter 6.

5. A significant limitation to the measurement of GU and mitochondrial respirometry in *mdx* skeletal muscle (Chapters 4 and 6) was the absence of NO/ASA from the media during the assays. As both NO and ASA are transient components of complex biochemical pathways within the muscle, it is probable that the lack of effects on GU and respirometry are attributable to the removal of these tissues from the blood supply in the animal and the lack of exogenous NO and ASA in the assay. We did attempt to overcome this limitation during our myoblast experiments and supplied both nitrite and ASA to the media during respiration analysis.
6. Due to the analysis of GU in both right and left EDL and SOL, we were unable to perform contractile function experiments in these muscles. Such data would have been valuable to be able to correlate muscular function with changes in the histopathology. Since muscle function and strength decline

as the disease progresses, measurement of such clinical features to flesh out the full effect of these metabolic therapies would have been ideal.

7. Along the line of Limitation 5, we did not measure serum creatine kinase (CK) in our animal studies, which constitutes the primary clinical marker of DMD progression in human patients. We did take blood with the intention of measuring CK, however due to the full muscle and organ harvests performed in our studies, we were often left with too little serum with which to perform this assay.

Chapter 6

8. A limitation of our analysis of mitochondrial respiration in FDB fibres was that we stimulated maximal respiration using both FCCP and pyruvate, thus bypassing the depressed capacity to bring glucose into the muscle fibres during metabolic stress. Typically, FCCP is the stimulant utilised to assess maximal respiration however we added pyruvate to ensure that maximal respiration was not limited by substrate supply (as per Schuh *et al.*, 2012). A limitation to the tandem addition of FCCP and pyruvate is that we did not independently assess the capacity for glucose influx into the fibres and subsequently the mitochondria to drive respiration during metabolic stress. If pyruvate had been injected after FCCP administration, this would have allowed us to assess the intrinsic capacity for maximal (uncoupled) respiration (i.e. glucose uptake and glycolysis facilitated) first, and then to ensure that maximal respiration was not limited by substrate flux into the mitochondria from glycolysis.

9. A limitation of our metabolite analyses was that not all muscles were snap frozen immediately after extraction. This event only occurred if problems had arisen with GU analysis (i.e. dissected muscle had to be re-tied in the baths due to slippage of knots). Therefore, these slight differences in time between muscle extraction and being snap frozen may have affected metabolite content. Ideally, we should have selected key muscles for metabolomics analyses and snap frozen them *in situ* prior to removal from the blood supply.

Myoblast studies (Chapters 5 & 7)

10. While the use of human-derived muscle cells is a beneficial model for the assessment of both nitrite and ASA, there is a limitation regarding the capacity to make disease-specific conclusions. As large variation in the genetic and molecular signatures exists between DMD patients, the conclusions drawn in these studies are only patient-specific.

11. There is a low experimental sample size throughout the myoblasts studies (chapters 5 and 7). Limited by time, these were the only experiments that could be performed within the timeframe and therefore, additional experiments are required to reduce the variability of the data and complete further analysis.

12. To establish the dose of nitrite and ASA in our cell culture experiments, we only performed dose-response testing in CON myoblasts. A limitation with this is that we did not assess the cell viability and Cell Index of DMD myoblasts with increasing doses of nitrite and ASA (nor with time) and therefore, we may have utilised a dose that was detrimental to dystrophin-deficient myoblasts. In addition, as the Cell Index reflects proliferative rate,

utilising DMD myoblasts in this assay would allow us to compare growth rates in CON and DMD myoblasts, and in particular, assess whether nitrate and ASA could modulate growth rate. Furthermore, it is unlikely that the dose utilised (1mM) reflects what skeletal muscle would be exposed to *in vivo*. Therefore, experimentation using a lower dose would potentially be a better option for these experiments.

13. Cell media was replaced every 3 days for these experiments, and at this time, fresh nitrite or ASA was also added. This may be a limitation due to the transient nature of both NO and ASA in that after 24 hours for example, levels of nitrite and ASA may have been depleted significantly.
14. Mitochondrial respiration was only performed at 24 hours. Measuring mitochondrial respiration at 3 days and 7 days for both supplementation studies would have potentially enabled explanation of the mitochondrial O₂⁻ production results.
15. The variation in responses between the *in vivo* (animal) and *in vitro* (cell) experiments regarding ASA supplementation may suggest that the mode of action of ASA is tissue specific. The majority of ASA may be metabolised in the liver and this may explain why different responses were observed in chapter 6 and 7. Therefore, muscle cells may have a lower capacity to convert ASA into fumarate *in vitro*.

8.3 Future Directions

The findings from this thesis have demonstrated that metabolic therapy, in particular ASA, is a novel therapeutic treatment avenue that warrants further investigation. From these remarkable outcomes, several ideas to fully characterise the mechanisms behind ASA-induced improvements in the *mdx* mouse have been elucidated.

1. We have derived a small metabolite profile/signature for untreated and ASA-treated skeletal muscle which has focussed predominantly on energy stores and indicators of glycolytic flux capacity. A logical future direction would be to derive a complete metabolic signature of these muscles. Characterising metabolites of the TCA cycle, specifically fumarate and malate, would obviously elucidate if ASA is capable of anaplerotically expanding the TCA cycle. Further to this, quantifying cytosolic and mitochondrial pools of fumarate and malate would help to determine if, as we have hypothesised, fumarate is sequestered away from the mitochondria and into cytosolic cellular stress reactions. However, it would be interesting to assess the effect that both dystrophin-deficiency and ASA therapy has on the entire cytosolic and mitochondrial metabolomes, using metabolomics.
2. As we have shown that ASA seemingly mediates its therapeutic effect through a Nrf2-dependent mechanism, further investigation is warranted to assess the downstream cytoprotective mechanisms. For example, since Nrf2 has been shown to increase GSH level and antioxidant gene expression, it would be valuable to assess GSH levels, and in particular, the GSH:GSSG ratio which is an established marker of cellular redox status, in the *mdx* mouse. In addition, investigating the suite of antioxidant genes that

Nrf2 activates, including heme oxygenase 1, NAD(P)H quinone oxidoreductase 1 and sulfiredoxin 1, would allow for a better characterisation of the redox status of ASA-treated skeletal muscle and would help to pinpoint the exact mechanisms behind the remarkable improvements in histopathology in dystrophin-deficient skeletal muscle.

3. The reduced lipid content of ASA-treated *mdx* TA, and the observations that Nrf2 modulates lipid metabolism, warrants further investigation. In Chapter 6, we only assessed oxidative metabolism and glycolysis through measurements of OCR and ECAR that was stimulated by glucose (basal and leak respiration) and pyruvate (maximal and non-mitochondrial respiration). We did not investigate if ASA had a modulatory effect on β -oxidation. Thus, assessing this metabolic pathway may elucidate if the reduced lipid content in *mdx* TA is a result of enhanced β -oxidation.
4. In contrast to Bonsett and Rudman, who delivered ASA via a miniature insulin pump (Bonsett and Rudman, 1992), we delivered ASA in the drinking water of mice. A limitation to our delivery method was that we could not control the amount of water consumed by the mice and therefore did not precisely control the dose of ASA ingested. Despite this, we did observe significant effects in the *mdx* mouse using this delivery method. However we postulate that a more precise delivery method could enhance the efficacy of ASA. Thus, investigating various delivery methods and dosage regimens would allow us to determine the optimal way to supply ASA.
5. A comparative study between ASA, dimethyl fumarate and sulforaphane (all activators of Nrf2) would be of great interest to assess if ASA is a more potent activator of the Nrf2-dependent cytoprotective response or has dual

therapeutic effects on *mdx* muscle histopathology and antioxidant capacity. In addition, such a study would assist in determining the primary pathway through which ASA acts – if increased fumarate production is the primary mediator, ASA would be comparable to dimethyl fumarate; or if ASA activates Nrf-2 through a fumarate-independent pathway, ASA would be comparable to sulforaphane.

6. In the small clinical trial of ASA, the one DMD patient who remained in the study until it ended began treatment at 2.5 years of age. This may be a confounding factor to the improvements observed in this patient as, at this age, disease pathology would be minimal. Therefore, the efficacy and potency of ASA may be enhanced when administered at a time where muscle composition is largely functional and not infiltrated by non-functional fatty and connective tissue. Importantly, this indicates the relevance of therapeutic intervention in very young mice (and children). A challenge associated with this, however, is choosing an appropriate age to begin the supplementation regimen in *mdx* mice. As mice are not weaned until 3 weeks of age, and this coincides with the onset of damage, the only option to supplement mice would be through lactation (i.e. via maternal supplementation). However, it is unknown if ASA can permeate breast milk, and more importantly this would not be the preferred mode of delivery in young DMD sufferers. Therefore, a study utilising the dystrophin-utrophin of *mdx/telomerase* knockout mouse may be a useful way to overcome this as in these models, disease progression is more reflective of the human condition i.e. it progresses throughout a shorter lifespan. Such a study would thus highlight when therapeutic ASA intervention is most effective at limiting

the disease phenotype and if and when there is a time at which it no longer affords therapeutic value.

7. In ASA-treated CON mice, we demonstrated an increase in mitochondrial biogenesis markers and high energy metabolite content (i.e. PCr and ATP) in skeletal muscle. This suggests that ASA has modulatory effects even in cells that exhibit no metabolic stress. Given this, our data suggests that ASA may have the potential to be a valuable ergogenic aid during exercise and therefore exercise studies using healthy (dystrophin-positive) skeletal muscle and animal models would be fascinating. In addition, since the data in this thesis highlights that ASA may mediate its effects through a Nrf2-dependent pathway, this suggests a potential application for the treatment of other diseases characterised by heightened oxidative stress (i.e. Parkinson's disease, Multiple Sclerosis). Thus, studies investigating the therapeutic potential of ASA for other indications is an exciting avenue for future study.

Chapter Nine

References

- AARTSMA-RUS, A., VAN DEUTEKOM, J. C., FOKKEMA, I. F., VAN OMMEN, G. J. B. & DEN DUNNEN, J. T. 2006. Entries in the Leiden Duchenne muscular dystrophy mutation database: An overview of mutation types and paradoxical cases that confirm the reading-frame rule. *Muscle & nerve*, 34, 135-144.
- ADAMO, C. M., DAI, D.-F., PERCIVAL, J. M., MINAMI, E., WILLIS, M. S., PATRUCCO, E., FROEHNER, S. C. & BEAVO, J. A. 2010. Sildenafil reverses cardiac dysfunction in the mdx mouse model of Duchenne muscular dystrophy. *Proceedings of the National Academy of Sciences*, 107, 19079-19083.
- AFFOURTIT, C., BAILEY, S. J., JONES, A. M., SMALLWOOD, M. J. & WINYARD, P. G. 2015. On the mechanism by which dietary nitrate improves human skeletal muscle function. *Frontiers in physiology*, 6.
- AFIFI, A. K., BERGMAN, R. A. & ZELLWEGER, H. 1973. A possible role for electron microscopy in detection of carriers of Duchenne type muscular dystrophy. *Journal of Neurology, Neurosurgery & Psychiatry*, 36, 643-650.
- AKIBA, T., HIRAGI, K. & TUBOI, S. 1984. Intracellular distribution of fumarase in various animals. *Journal of biochemistry*, 96, 189-195.
- AKTAN, F. 2004. iNOS-mediated nitric oxide production and its regulation. *Life sciences*, 75, 639-653.
- ALDERTON, J. M. & STEINHARDT, R. A. 2000. Calcium influx through calcium leak channels is responsible for the elevated levels of calcium-dependent proteolysis in dystrophic myotubes. *Journal of Biological Chemistry*, 275,

9452-9460.

ALLEN, D. G., LAMB, G. & WESTERBLAD, H. 2008. Skeletal muscle fatigue: cellular mechanisms. *Physiological reviews*, 88, 287-332.

AL-REWASHDY, H., LJUBICIC, V., LIN, W., RENAUD, J.-M. & JASMIN, B. J. 2014. Utrophin A is Essential in Mediating the Functional Adaptations of mdx Mouse Muscle Following Chronic AMPK Activation. *Human Molecular Genetics*.

ANDERSON, J. & PILIPOWICZ, O. 2002. Activation of muscle satellite cells in single-fiber cultures. *Nitric Oxide*, 7, 36-41.

ANDERSON, J. E. 2000. A role for nitric oxide in muscle repair: nitric oxide-mediated activation of muscle satellite cells. *Molecular biology of the cell*, 11, 1859-1874.

ANDERSON, J. E., BRESSLER, B. H. & OVALLE, W. K. 1988. Functional regeneration in the hindlimb skeletal muscle of the mdx mouse. *Journal of Muscle Research and Cell Motility*, 9, 499-515.

ANDERSON, J. E. & VARGAS, C. 2003. Correlated NOS-1 μ and myf5 expression by satellite cells in mdx mouse muscle regeneration during NOS manipulation and deflazacort treatment. *Neuromuscular Disorders*, 13, 388-396.

ANDREETTA, F., BERNASCONI, P., BAGGI, F., FERRO, P., OLIVA, L., ARNOLDI, E., CORNELIO, F., MANTEGAZZA, R. & CONFALONIERI, P. 2006. Immunomodulation of TGF-beta1 in mdx mouse inhibits connective tissue proliferation in diaphragm but increases inflammatory response:

implications for antifibrotic therapy. *Journal of neuroimmunology*, 175, 77-86.

ANGUS, L. M., CHAKKALAKAL, J. V., MÉJAT, A., EIBL, J. K., BÉLANGER, G., MEGENEY, L. A., CHIN, E. R., SCHAEFFER, L., MICHEL, R. N. & JASMIN, B. J. 2005. Calcineurin-NFAT signaling, together with GABP and peroxisome PGC-1 α , drives utrophin gene expression at the neuromuscular junction. *American Journal of Physiology-Cell Physiology*, 289, C908-C917.

AQUILANO, K., BALDELLI, S. & CIRIOLO, M. R. 2014. Nuclear recruitment of neuronal nitric-oxide synthase by α -syntrophin is crucial for the induction of mitochondrial biogenesis. *Journal of Biological Chemistry*, 289, 365-378.

ARCHER, J. D., VARGAS, C. C. & ANDERSON, J. E. 2006. Persistent and improved functional gain in mdx dystrophic mice after treatment with L-arginine and deflazacort. *The FASEB Journal*.

ARMSTRONG, R. & PHELPS, R. 1984. Muscle fiber type composition of the rat hindlimb. *American Journal of Anatomy*, 171, 259-272.

ARNING, L., JAGIELLO, P., SCHARA, U., VORGERD, M., DAHMEN, N., GENCIKOVA, A., MORTIER, W., EPPLEN, J. T. & GENCIK, M. 2004. Transcriptional profiles from patients with dystrophinopathies and limb girdle muscular dystrophies as determined by qRT-PCR. *Journal of neurology*, 251, 72-78.

ASAI, A., SAHANI, N., KANEKI, M., OUCHI, Y., MARTYN, J. J. & YASUHARA, S. E. 2007. Primary role of functional ischemia, quantitative evidence for the two-hit mechanism, and phosphodiesterase-5 inhibitor therapy in mouse

muscular dystrophy. *PLoS One*, 2, e806.

ASHMORE, T., ROBERTS, L. D., MORASH, A. J., KOTWICA, A. O., FINNERTY, J., WEST, J. A., MURFITT, S. A., FERNANDEZ, B. O., BRANCO, C. & COWBURN, A. S. 2015. Nitrate enhances skeletal muscle fatty acid oxidation via a nitric oxide-cGMP-PPAR-mediated mechanism. *BMC biology*, 13, 1.

ASHRAFIAN, H., CZIBIK, G., BELLAHCENE, M., AKSENTIJEVIĆ, D., SMITH, A. C., MITCHELL, S. J., DODD, M. S., KIRWAN, J., BYRNE, J. J. & LUDWIG, C. 2012. Fumarate is cardioprotective via activation of the Nrf2 antioxidant pathway. *Cell metabolism*, 15, 361-371.

AUCOUTURIER, J., BOISSIÈRE, J., PAWLAK-CHAOUCH, M., CUVELIER, G. & GAMELIN, F.-X. 2015. Effect of dietary nitrate supplementation on tolerance to supramaximal intensity intermittent exercise. *Nitric Oxide*, 49, 16-25.

AUSTIN, L., DE NIESE, M., MCGREGOR, A., ARTHUR, H., GURUSINGHE, A. & GOULD, M. 1992. Potential oxyradical damage and energy status in individual muscle fibres from degenerating muscle diseases. *Neuromuscular Disorders*, 2, 27-33.

BAILEY, S. J., FULFORD, J., VANHATALO, A., WINYARD, P. G., BLACKWELL, J. R., DIMENNA, F. J., WILKERSON, D. P., BENJAMIN, N. & JONES, A. M. 2010. Dietary nitrate supplementation enhances muscle contractile efficiency during knee-extensor exercise in humans. *Journal of Applied Physiology*, 109, 135-148.

BAILEY, S. J., WINYARD, P., VANHATALO, A., BLACKWELL, J. R., DIMENNA, F.

- J., WILKERSON, D. P., TARR, J., BENJAMIN, N. & JONES, A. M. 2009. Dietary nitrate supplementation reduces the O₂ cost of low-intensity exercise and enhances tolerance to high-intensity exercise in humans. *Journal of Applied Physiology*, 107, 1144-1155.
- BAKKER, A., HEAD, S., WILLIAMS, D. & STEPHENSON, D. 1993. Ca²⁺ levels in myotubes grown from the skeletal muscle of dystrophic (mdx) and normal mice. *The Journal of Physiology*, 460, 1-13.
- BAKOUICHE, P., CHAOUAT, D. & NICK, J. 1979. Allopurinol not effective in muscular dystrophy. *The New England journal of medicine*, 301, 785.
- BALLMANN, C., BEYERS, R., DENNEY, T., SELSBY, J. & QUINDRY, J. 2015. Effect of chronic dietary quercetin enrichment on cardiac function in dystrophic mice. *The FASEB Journal*, 29, 1039.5.
- BALLMANN, C., HOLLINGER, K., SELSBY, J. T., AMIN, R. & QUINDRY, J. C. 2015. Histological and biochemical outcomes of cardiac pathology in mdx mice with dietary quercetin enrichment. *Experimental physiology*, 100, 12-22.
- BALON, T. W. & NADLER, J. L. 1997. Evidence that nitric oxide increases glucose transport in skeletal muscle. *Journal of Applied Physiology*, 82, 359-363.
- BANERJEE, B., SHARMA, U., BALASUBRAMANIAN, K., KALAIVANI, M., KALRA, V. & JAGANNATHAN, N. R. 2010. Effect of creatine monohydrate in improving cellular energetics and muscle strength in ambulatory Duchenne muscular dystrophy patients: a randomized, placebo-controlled^{< sup>} 31</sup> P MRS study. *Magnetic resonance imaging*, 28, 698-707.

- BANKOLÉ, L. C., FEASSON, L., PONSOT, E. & KADI, F. 2013. Fibre type-specific satellite cell content in two models of muscle disease. *Histopathology*, 63, 826-832.
- BARBIROLI, B., FUNICELLO, R., FERLINI, A., MONTAGNA, P. & ZANIOL, P. 1992. Muscle energy metabolism in female DMD/BMD carriers: A 31P-MR spectroscopy study. *Muscle & Nerve*, 15, 344-348.
- BARBIROLI, B., FUNICELLO, R., IOTTI, S., MONTAGNA, P., FERLINI, A. & ZANIOL, P. 1992. 31P-NMR spectroscopy of skeletal muscle in Becker dystrophy and DMD/BMD carriers: Altered rate of phosphate transport. *Journal of the Neurological Sciences*, 109, 188-195.
- BARON, D., MAGOT, A., RAMSTEIN, G., STEENMAN, M., FAYET, G., CHEVALIER, C., JOURDON, P., HOULGATTE, R., SAVAGNER, F. & PEREON, Y. 2011. Immune Response and Mitochondrial Metabolism Are Commonly Deregulated in DMD and Aging Skeletal Muscle. *PloS one*, 6, e26952.
- BARTON, E. R., MORRIS, L., KAWANA, M., BISH, L. T. & TOURSEL, T. 2005. Systemic administration of L-arginine benefits mdx skeletal muscle function. *Muscle & Nerve*, 32, 751-760.
- BECKMAN, J. S., BECKMAN, T. W., CHEN, J., MARSHALL, P. A. & FREEMAN, B. A. 1990. Apparent hydroxyl radical production by peroxynitrite: implications for endothelial injury from nitric oxide and superoxide. *Proceedings of the National Academy of Sciences*, 87, 1620-1624.
- BENEDICT, J. D., KALINSKY, H. J., SCARRONE, L. A., WERTHEIM, A. R. &

- STETTEN JR, D. 1955. The origin of urinary creatine in progressive muscular dystrophy. *Journal of Clinical Investigation*, 34, 141.
- BERRY, M. J., JUSTUS, N. W., HAUSER, J. I., CASE, A. H., HELMS, C. C., BASU, S., ROGERS, Z., LEWIS, M. T. & MILLER, G. D. 2015. Dietary nitrate supplementation improves exercise performance and decreases blood pressure in COPD patients. *Nitric Oxide*, 48, 22-30.
- BERTHILLIER, G., GAUTHERON, D. & ROBERT, J. 1967. Phosphorylated fractions and free adenine nucleotides of myopathic muscles in children]. *Comptes rendus hebdomadaires des séances de l'Académie des sciences. Série D: Sciences naturelles*, 265, 79.
- BERTORINI, T. E., PALMIERI, G. M. A., AIROZO, D., EDWARDS, N. L. & FOX, I. H. 1981. Increased Adenine Nucleotide Turnover in Duchenne Muscular Dystrophy. *Pediatr Res*, 15, 1478-1482.
- BHATTACHARYA, S. K., JOHNSON, P. L. & THAKAR, J. H. 1993. Reversal of impaired oxidative phosphorylation and calcium overloading in the in vitro cardiac mitochondria of CHF-146 dystrophic hamsters with hereditary muscular dystrophy. *Journal of the Neurological Sciences*, 120, 180-186.
- BIA, B. L., CASSIDY, P. J., YOUNG, M. E., RAFAEL, J. A., LEIGHTON, B., DAVIES, K. E., RADDA, G. K. & CLARKE, K. 1999. Decreased myocardial nNOS, increased iNOS and abnormal ECGs in mouse models of Duchenne muscular dystrophy. *Journal of molecular and cellular cardiology*, 31, 1857-1862.
- BIBEE, K. P., CHENG, Y.-J., CHING, J. K., MARSH, J. N., LI, A. J., KEELING, R.

- M., CONNOLLY, A. M., GOLUMBEEK, P. T., MYERSON, J. W. & HU, G. 2014. Rapamycin nanoparticles target defective autophagy in muscular dystrophy to enhance both strength and cardiac function. *The FASEB Journal*, 28, 2047-2061.
- BIRESSI, S., MIYABARA, E. H., GOPINATH, S. D., CARLIG, P. M. & RANDO, T. A. 2014. A Wnt-TGF β 2 axis induces a fibrogenic program in muscle stem cells from dystrophic mice. *Science translational medicine*, 6, 267ra176-267ra176.
- BLAU, H. M., WEBSTER, C. & PAVLATH, G. K. 1983. Defective myoblasts identified in Duchenne muscular dystrophy. *Proceedings of the National Academy of Sciences*, 80, 4856-4860.
- BLOOM, T. J. 2002. Cyclic nucleotide phosphodiesterase isozymes expressed in mouse skeletal muscle. *Canadian journal of physiology and pharmacology*, 80, 1132-1135.
- BOCA, S. M., NISHIDA, M., HARRIS, M., RAO, S., CHEEMA, A. K., GILL, K., SEOL, H., MORGENROTH, L. P., HENRICSON, E. & MCDONALD, C. 2016. Discovery of Metabolic Biomarkers for Duchenne Muscular Dystrophy within a Natural History Study. *PloS one*, 11, e0153461.
- BODENSTEINER, J. B. & ENGEL, A. G. 1978. Intracellular calcium accumulation in Duchenne dystrophy and other myopathies A study of 567,000 muscle fibers in 114 biopsies. *Neurology*, 28, 439-439.
- BÖGER, R. H. & BODE-BÖGER, S. M. 2001. The clinical pharmacology of L-arginine. *Annual review of pharmacology and toxicology*, 41, 79-99.

- BOLDRIN, L., ZAMMIT, P. S. & MORGAN, J. E. 2015. Satellite cells from dystrophic muscle retain regenerative capacity. *Stem cell research*, 14, 20-29.
- BOND, H., MORTON, L. & BRAAKHUIS, A. J. 2012. Dietary nitrate supplementation improves rowing performance in well-trained rowers.
- BOND JR, V., CURRY, B. H., ADAMS, R. G., MILLIS, R. M. & HADDAD, G. E. 2013. Cardiorespiratory function associated with dietary nitrate supplementation. *Applied Physiology, Nutrition, and Metabolism*, 39, 168-172.
- BONILLA, E., SCHMIDT, B., SAMITT, C. E., MIRANDA, A. F., HAYS, A. P., DE OLIVEIRA, A. B., CHANG, H. W., SERVIDEI, S., RICCI, E. & YOUNGER, D. S. 1988. Normal and dystrophin-deficient muscle fibers in carriers of the gene for Duchenne muscular dystrophy. *The American journal of pathology*, 133, 440.
- BONSETT, C., RUDMAN, A & ELLIOTT, AY 1979. Intracellular lipid in pseudohypertrophic muscular dystrophy tissue culture. *J Indiana State Med Assoc*, 72, 184-187.
- BONSETT, C. & RUDMAN, A. 1984. Duchenne's muscular dystrophy: a tissue culture perspective. *Indiana medicine: the journal of the Indiana State Medical Association*, 77, 446.
- BONSETT, C. & RUDMAN, A. 1992. The dystrophin connection—ATP? *Medical Hypotheses*, 38, 139-154.
- BONSETT, C. A. 1963. Psuedohypertrophic musuclar dystrophy. Distribution of

- degenerative features as revealed by an anatomical study. *Neurology*, 13, 728.
- BORDER, W. A. & NOBLE, N. A. 1994. Transforming growth factor β in tissue fibrosis. *New England Journal of Medicine*, 331, 1286-1292.
- BORUM, P. R., BROQUIST, H. P. & ROELOFS, R. I. 1977. Muscle carnitine levels in neuromuscular disease. *Journal of the neurological sciences*, 34, 279-286.
- BOVERIS, A., COSTA, L. E., PODEROSO, J. J., CARRERAS, M. C. & CADENAS, E. 2000. Regulation of mitochondrial respiration by oxygen and nitric oxide. *Annals of the New York Academy of Sciences*, 899, 121-135.
- BRADLEY, S. J., KINGWELL, B. A. & MCCONELL, G. K. 1999. Nitric oxide synthase inhibition reduces leg glucose uptake but not blood flow during dynamic exercise in humans. *Diabetes*, 48, 1815-1821.
- BRAND, M. D. & ESTEVES, T. C. 2005. Physiological functions of the mitochondrial uncoupling proteins UCP2 and UCP3. *Cell metabolism*, 2, 85-93.
- BRAND, M. D. & MURPHY, M. P. 1987. Control of electron flux through the respiratory chain in mitochondria and cells. *Biological Reviews*, 62, 141-193.
- BRENNAN, J. E., CHAO, D. S., XIA, H., ALDAPE, K. & BREDT, D. S. 1995. Nitric oxide synthase complexed with dystrophin and absent from skeletal muscle sarcolemma in Duchenne muscular dystrophy. *Cell*, 82, 743-752.
- BRESOLIN, N., CASTELLI, E., COMI, G., FELISARI, G., BARDONI, A., PERANI, D., GRASSI, F., TURCONI, A., MAZZUCHELLI, F. & GALLOTTI, D. 1994.

Cognitive impairment in Duchenne muscular dystrophy. *Neuromuscular Disorders*, 4, 359-369.

BRIÈRE, J.-J., SCHLEMMER, D., CHRETIEN, D. & RUSTIN, P. 2004. Quinone analogues regulate mitochondrial substrate competitive oxidation. *Biochemical and biophysical research communications*, 316, 1138-1142.

BROBERG, S. & SAHLIN, K. 1989. Adenine nucleotide degradation in human skeletal muscle during prolonged exercise. *Journal of applied physiology*, 67, 116-122.

BROOKE, M., FENICHEL, G., GRIGGS, R., MENDELL, J., MOXLEY, R., FLORENCE, J., KING, W., PANDYA, S., ROBISON, J. & SCHIERBECKER, J. 1989. Duchenne muscular dystrophy Patterns of clinical progression and effects of supportive therapy. *Neurology*, 39, 475-475.

BROOKE, M., GRIGGS, R., MENDELL, J., FENICHEL, G. & SHUMATE, J. 1981. The natural history of Duchenne muscular dystrophy: a caveat for therapeutic trials. *Transactions of the American Neurological Association*, 106, 195.

BROWN, G. C. & BORUTAITE, V. Nitric oxide, cytochrome c and mitochondria. *Biochemical Society Symposia*, 1999. Portland Press Limited, 17-25.

BROWN, G. C. & COOPER, C. 1994. Nanomolar concentrations of nitric oxide reversibly inhibit synaptosomal respiration by competing with oxygen at cytochrome oxidase. *FEBS letters*, 356, 295-298.

BRUNELLI, S., SCIORATI, C., D'ANTONA, G., INNOCENZI, A., COVARELLO, D., GALVEZ, B. G., PERROTTA, C., MONOPOLI, A., SANVITO, F.,

- BOTTINELLI, R., ONGINI, E., COSSU, G. & CLEMENTI, E. 2007. Nitric oxide release combined with nonsteroidal antiinflammatory activity prevents muscular dystrophy pathology and enhances stem cell therapy. *Proceedings of the National Academy of Sciences*, 104, 264-269.
- BRUNORI, M., GIUFFRÈ, A., FORTE, E., MASTRONICOLA, D., BARONE, M. C. & SARTI, P. 2004. Control of cytochrome c oxidase activity by nitric oxide. *Biochimica et Biophysica Acta (BBA)-Bioenergetics*, 1655, 365-371.
- BRUSSEE, V., TARDIF, F. & TREMBLAY, J. P. 1997. Muscle fibers of mdx mice are more vulnerable to exercise than those of normal mice. *Neuromuscular Disorders*, 7, 487-492.
- BUENO JÚNIOR, C. R., PANTALEÃO, L. C., VOLTARELLI, V. A., BOZI, L. H. M., BRUM, P. C. & ZATZ, M. 2012. Combined Effect of AMPK/PPAR Agonists and Exercise Training in *mdx* Mice Functional Performance. *PLoS ONE*, 7, e45699.
- BUGLIONI, A. & BURNETT JR, J. C. 2015. New Pharmacological Strategies to Increase cGMP. *Annual review of medicine*.
- BULFIELD, G., SILLER, W., WIGHT, P. & MOORE, K. J. 1984. X chromosome-linked muscular dystrophy (mdx) in the mouse. *Proceedings of the National Academy of Sciences*, 81, 1189-1192.
- BURKHOLDER, T. J., FINGADO, B., BARON, S. & LIEBER, R. L. 1994. Relationship between muscle fiber types and sizes and muscle architectural properties in the mouse hindlimb. *Journal of Morphology*, 221, 177-190.
- BUYSE, G., GOEMANS, N., VAN DER MIEREN, G., ERB, M., D'HOOGHE, J.,

- HERIJGERS, P., VERBEKEN, E., JARA, A., VAN DEN BERGH, A. & COURDIER-FRUH, I. 2008. TO 3 SNT-MC17/idebenone in Duchenne muscular dystrophy: long-term blinded controlled preclinical study in the mdx mouse followed by a 12 month double-blind randomized controlled trial in humans. *Neuromuscular Disorders*, 18, 832.
- BUYSE, G. M., GOEMANS, N., VAN DEN HAUWE, M., THIJS, D., DE GROOT, I. J., SCHARA, U., CEULEMANS, B., MEIER, T. & MERTENS, L. 2011. Idebenone as a novel, therapeutic approach for Duchenne muscular dystrophy: results from a 12 month, double-blind, randomized placebo-controlled trial. *Neuromuscul Disord*, 21, 396-405.
- BUYSE, G. M., VOIT, T., SCHARA, U., STRAATHOF, C. S., D'ANGELO, M. G., BERNERT, G., CUISSET, J.-M., FINKEL, R. S., GOEMANS, N. & MCDONALD, C. M. 2015. Efficacy of idebenone on respiratory function in patients with Duchenne muscular dystrophy not using glucocorticoids (DELOS): a double-blind randomised placebo-controlled phase 3 trial. *The Lancet*, 385, 1748-1757.
- CAMIÑA, F., NOVO-RODRIGUEZ, M. I., RODRIGUEZ-SEGADE, S. & CASTRO-GAGO, M. 1995. Purine and carnitine metabolism in muscle of patients with Duchenne muscular dystrophy. *Clinica Chimica Acta*, 243, 151-164.
- CAMPBELL, K. P. 1995. Three muscular dystrophies: loss of cytoskeleton-extracellular matrix linkage. *Cell*, 80, 675-679.
- CAO, A., MACCIOTTA, A., FIORELLI, G., MANNUCCI, P. & IDÉO, G. 1965. Chromatographic and electrophoretic pattern of lactate and malate

dehydrogenase in normal human adult and foetal muscle and in muscle of patients affected by Duchenne muscular dystrophy. *Enzymologia biologica et clinica*, 7, 156-166.

CARBERRY, S., BRINKMEIER, H., ZHANG, Y., WINKLER, C. K. & OHLENDIECK, K. 2013. Comparative proteomic profiling of soleus, extensor digitorum longus, flexor digitorum brevis and interosseus muscles from the mdx mouse model of Duchenne muscular dystrophy. *International Journal of Molecular Medicine*.

CARLSTRÖM, M., LARSEN, F. J., NYSTRÖM, T., HEZEL, M., BORNIQUEL, S., WEITZBERG, E. & LUNDBERG, J. O. 2010. Dietary inorganic nitrate reverses features of metabolic syndrome in endothelial nitric oxide synthase-deficient mice. *Proceedings of the National Academy of Sciences*, 107, 17716-17720.

CARNWATH, J. W. & SHOTTON, D. M. 1987. Muscular dystrophy in the mdx mouse: histopathology of the soleus and extensor digitorum longus muscles. *Journal of the neurological sciences*, 80, 39-54.

CARRIER, H. N. & BERTHILLIER, G. 1980. Carnitine levels in normal children and adults and in patients with diseased muscle. *Muscle & nerve*, 3, 326-334.

CARROLL, J. E., NORRIS, B. J. & BROOKE, M. H. 1985. Defective [U-14 C] palmitic acid oxidation in Duchenne muscular dystrophy. *Neurology*, 35, 96-7.

CARROLL, J. E., VILLADIEGO, A. & BROOKE, M. H. 1983. Increased long chain acyl CoA in Duchenne muscular dystrophy. *Neurology*, 33, 1507-1507.

- CASTRO-GAGO, M. 2015. Milder course in Duchenne patients with nonsense mutations and no.
- CERMAK, N. M., GIBALA, M. J. & VAN LOON, L. J. 2012. Nitrate supplementation's improvement of 10-km time-trial performance in trained cyclists. *International Journal of Sport Nutrition and Exercise Metabolism*, 22, 64.
- CERMAK, N. M., RES, P., STINKENS, R., LUNDBERG, J. O., GIBALA, M. J. & VAN LOON, L. J. 2012. No improvement in endurance performance after a single dose of beetroot juice. *International Journal of Sport Nutrition and Exercise Metabolism*, 22, 470.
- CERQUEIRA, F. M., CUNHA, F. M., LAURINDO, F. R. & KOWALTOWSKI, A. J. 2012. Calorie restriction increases cerebral mitochondrial respiratory capacity in a NO•-mediated mechanism: impact on neuronal survival. *Free Radical Biology and Medicine*, 52, 1236-1241.
- CHACKO, B. K., KRAMER, P. A., RAVI, S., BENAVIDES, G. A., MITCHELL, T., DRANKA, B. P., FERRICK, D., SINGAL, A. K., BALLINGER, S. W. & BAILEY, S. M. 2014. The Bioenergetic Health Index: a new concept in mitochondrial translational research. *Clinical science*, 127, 367-373.
- CHAHBOUNI, M., ESCAMES, G., LÓPEZ, L. C., SEVILLA, B., DOERRIER, C., MUÑOZ-HOYOS, A., MOLINA-CARBALLO, A. & ACUÑA-CASTROVIEJO, D. 2011. Melatonin treatment counteracts the hyperoxidative status in erythrocytes of patients suffering from Duchenne muscular dystrophy. *Clinical biochemistry*, 44, 853-858.

- CHAKKALAKAL, J. V., HARRISON, M.-A., CARBONETTO, S., CHIN, E., MICHEL, R. N. & JASMIN, B. J. 2004. Stimulation of calcineurin signaling attenuates the dystrophic pathology in mdx mice. *Human molecular genetics*, 13, 379-388.
- CHAKKALAKAL, J. V., MICHEL, S. A., CHIN, E. R., MICHEL, R. N. & JASMIN, B. J. 2006. Targeted inhibition of Ca²⁺/calmodulin signaling exacerbates the dystrophic phenotype in mdx mouse muscle. *Human molecular genetics*, 15, 1423-1435.
- CHAKKALAKAL, J. V., STOCKSLEY, M. A., HARRISON, M.-A., ANGUS, L. M., DESCHÊNES-FURRY, J., ST-PIERRE, S., MEGENEY, L. A., CHIN, E. R., MICHEL, R. N. & JASMIN, B. J. 2003. Expression of utrophin A mRNA correlates with the oxidative capacity of skeletal muscle fiber types and is regulated by calcineurin/NFAT signaling. *Proceedings of the National Academy of Sciences*, 100, 7791-7796.
- CHANG, W. J., IANNACCONE, S. T., LAU, K. S., MASTERS, B. S., MCCABE, T. J., MCMILLAN, K., PADRE, R. C., SPENCER, M. J., TIDBALL, J. G. & STULL, J. T. 1996. Neuronal nitric oxide synthase and dystrophin-deficient muscular dystrophy. *Proceedings of the National Academy of Sciences*, 93, 9142-9147.
- CHAUBOURT, E., FOSSIER, P., BAUX, G., LEPRINCE, C., ISRAËL, M. & DE LA PORTE, S. 1999. Nitric oxide and l-arginine cause an accumulation of utrophin at the sarcolemma: a possible compensation for dystrophin loss in Duchenne muscular dystrophy. *Neurobiology of disease*, 6, 499-507.

- CHEN, Y. W., ZHAO, P., BORUP, R. & HOFFMAN, E. P. 2000. Expression profiling in the muscular dystrophies: identification of novel aspects of molecular pathophysiology. *J Cell Biol*, 151, 1321-36.
- CHI, M. M. Y., HINTZ, C. S., MCKEE, D., FELDER, S., GRANT, N., KAISER, K. K. & LOWRY, O. H. 1987. Effect of Duchenne muscular dystrophy on enzymes of energy metabolism in individual muscle fibers. *Metabolism*, 36, 761-767.
- CHINET, A., EVEN, P. & DECROUY, A. 1994. Dystrophin-dependent efficiency of metabolic pathways in mouse skeletal muscles. *Cellular and Molecular Life Sciences*, 50, 602-605.
- CHO, H., MU, J., KIM, J. K., THORVALDSEN, J. L., CHU, Q., CRENSHAW, E. B., KAESTNER, K. H., BARTOLOMEI, M. S., SHULMAN, G. I. & BIRNBAUM, M. J. 2001. Insulin resistance and a diabetes mellitus-like syndrome in mice lacking the protein kinase Akt2 (PKB β). *Science*, 292, 1728-1731.
- CHO, H.-Y., REDDY, S. P., YAMAMOTO, M. & KLEEBERGER, S. R. 2004. The transcription factor NRF2 protects against pulmonary fibrosis. *The FASEB journal*, 18, 1258-1260.
- CHOWDHRY, S., NAZMY, M. H., MEAKIN, P. J., DINKOVA-KOSTOVA, A. T., WALSH, S. V., TSUJITA, T., DILLON, J. F., ASHFORD, M. L. & HAYES, J. D. 2010. Loss of Nrf2 markedly exacerbates nonalcoholic steatohepatitis. *Free Radical Biology and Medicine*, 48, 357-371.
- CLARK, J. F. 1997. Creatine and phosphocreatine: a review of their use in exercise and sport. *Journal of athletic training*, 32, 45.
- CLARKE, M., KHAKEE, R. & MCNEIL, P. L. 1993. Loss of cytoplasmic basic

fibroblast growth factor from physiologically wounded myofibers of normal and dystrophic muscle. *Journal of Cell Science*, 106, 121-133.

CLEETER, M., COOPER, J., DARLEY-USMAR, V., MONCADA, S., AND & SCHAPIRA, A. 1994. Reversible inhibition of cytochrome c oxidase, the terminal enzyme of the mitochondrial respiratory chain, by nitric oxide. *FEBS letters*, 345, 50-54.

CLEMENS, P., KOCHANEK, S., SUNADA, Y., CHAN, S., CHEN, H., CAMPBELL, K. & CASKEY, C. 1996. In vivo muscle gene transfer of full-length dystrophin with an adenoviral vector that lacks all viral genes. *Gene therapy*, 3, 965-972.

COGLIATI, S., FREZZA, C., SORIANO, MARIA E., VARANITA, T., QUINTANA-CABRERA, R., CORRADO, M., CIPOLAT, S., COSTA, V., CASARIN, A., GOMES, LIGIA C., PERALES-CLEMENTE, E., SALVIATI, L., FERNANDEZ-SILVA, P., ENRIQUEZ, JOSE A. & SCORRANO, L. 2013. Mitochondrial Cristae Shape Determines Respiratory Chain Supercomplexes Assembly and Respiratory Efficiency. *Cell*, 155, 160-171.

COLE, M., RAFAEL, J., TAYLOR, D., LODI, R., DAVIES, K. & STYLES, P. 2002. A quantitative study of bioenergetics in skeletal muscle lacking utrophin and dystrophin. *Neuromuscular Disorders*, 12, 247-257.

CONNETT, R. J. & SAHLIN, K. 2010. Control of Glycolysis and Glycogen Metabolism. *Comprehensive Physiology*. John Wiley & Sons, Inc.

COOKE, M. B., RYBALKA, E., WILLIAMS, A. D., CRIBB, P. J. & HAYES, A. 2009. Creatine supplementation enhances muscle force recovery after

- eccentrically-induced muscle damage in healthy individuals. *Journal of the International Society of Sports Nutrition*, 6, 1-11.
- CORBET, C., PINTO, A., MARTHERUS, R., DE JESUS, J. P. S., POLET, F. & FERON, O. 2016. Acidosis drives the reprogramming of fatty acid metabolism in cancer cells through changes in mitochondrial and histone acetylation. *Cell Metabolism*, 24, 311-323.
- COSSU, G. & SAMPAOLESI, M. 2007. New therapies for Duchenne muscular dystrophy: challenges, prospects and clinical trials. *Trends in molecular medicine*, 13, 520-526.
- COULTON, G. R., MORGAN, J. E., PARTRIDGE, T. A. & SLOPER, J. C. 1988. The mdx mouse skeletal muscle myopathy: I. A histological, morphometric and biochemical investigation. *Neuropathology and Applied Neurobiology*, 14, 53-70.
- CRIBB, P. J., WILLIAMS, A. D. & HAYES, A. 2007. A creatine-protein-carbohydrate supplement enhances responses to resistance training. *Medicine and Science in Sport and Exercise*, 39, 1960-1968.
- CRIBB, P. J., WILLIAMS, A. D., STATHIS, C. G., CAREY, M. F. & HAYES, A. 2007. Effects of whey isolate, creatine and resistance training on muscle hypertrophy. *Medicine & Science in Sports & Exercise*, 39, 298-307.
- CROSBIE, R. H., STRAUB, V., YUN, H.-Y., LEE, J. C., RAFAEL, J. A., CHAMBERLAIN, J. S., DAWSON, V. L., DAWSON, T. M. & CAMPBELL, K. P. 1998. mdx Muscle Pathology is Independent of nNOS Perturbation. *Human Molecular Genetics*, 7, 823-829.

- CULLEN, M. & FULTHORPE, J. 1975. Stages in fibre breakdown in Duchenne muscular dystrophy: an electron-microscopic study. *Journal of the Neurological Sciences*, 24, 179-200.
- CULLEN, M. & JAROS, E. 1988. Ultrastructure of the skeletal muscle in the X chromosome-linked dystrophic (mdx) mouse. *Acta neuropathologica*, 77, 69-81.
- CULLEN, M., WALSH, J. & NICHOLSON, L. 1994. Immunogold localization of the 43-kDa dystroglycan at the plasma membrane in control and dystrophic human muscle. *Acta neuropathologica*, 87, 349-354.
- D'ANGELO, M. G., GANDOSSINI, S., BONESCHI, F. M., SCIORATI, C., BONATO, S., BRIGHINA, E., COMI, G. P., TURCONI, A. C., MAGRI, F. & STEFANONI, G. 2012. Nitric oxide donor and non steroidal anti inflammatory drugs as a therapy for muscular dystrophies: evidence from a safety study with pilot efficacy measures in adult dystrophic patients. *Pharmacological Research*, 65, 472-479.
- DANGAIN, J. & VRBOVA, G. 1984. Muscle development in mdx mutant mice. *Muscle & nerve*, 7, 700-704.
- DE ARCANGELIS, V., STRIMPAKOS, G., GABANELLA, F., CORBI, N., LUVISETTO, S., MAGRELLI, A., ONORI, A., PASSANANTI, C., PISANI, C. & ROME, S. 2016. Pathways Implicated in Tadalafil Amelioration of Duchenne Muscular Dystrophy. *Journal of cellular physiology*, 231, 224-232.
- DE BRUYN, C., KULAKOWSKI, S., VAN BENNEKOM, C., RENOIRTE, P. & MÜLLER, M. 1980. Purine metabolism in Duchenne muscular dystrophy.

Advances In Experimental Medicine And Biology, 122, 177.

DE LA PORTE, S., MORIN, S. & KOENIG, J. 1999. Characteristics of skeletal muscle in mdx mutant mice. *International review of cytology*, 191, 99-148.

DE PALMA, C., MORISI, F., CHELI, S., PAMBIANCO, S., CAPPELLO, V., VEZZOLI, M., ROVERE-QUERINI, P., MOGGIO, M., RIPOLONE, M. & FRANCOLINI, M. 2012. Autophagy as a new therapeutic target in Duchenne muscular dystrophy. *Cell death & disease*, 3, e418.

DE PALMA, C., PERROTTA, C., PELLEGRINO, P., CLEMENTI, E. & CERVIA, D. 2014. Skeletal muscle homeostasis in Duchenne muscular dystrophy: modulating autophagy as a promising therapeutic strategy. *Frontiers in aging neuroscience*, 6.

DECARY, S., HAMIDA, C. B., MOULY, V., BARBET, J., HENTATI, F. & BUTLER-BROWNE, G. 2000. Shorter telomeres in dystrophic muscle consistent with extensive regeneration in young children. *Neuromuscular Disorders*, 10, 113-120.

DECONINCK, A. E., RAFAEL, J. A., SKINNER, J. A., BROWN, S. C., POTTER, A. C., METZINGER, L., WATT, D. J., DICKSON, J. G., TINSLEY, J. M. & DAVIES, K. E. 1997. Utrophin-Dystrophin-Deficient Mice as a Model for Duchenne Muscular Dystrophy. *Cell*, 90, 717-727.

DECONINCK, N., TINSLEY, J., BACKER, F. D., FISHER, R., KAHN, D., PHELPS, S., DAVIES, K. & GILLIS, J.-M. 1997. Expression of truncated utrophin leads to major functional improvements in dystrophin-deficient muscles of mice. *Nature medicine*, 3, 1216-1221.

- DEGLI ESPOSTI, M., NGO, A., GHELLI, A., BENELLI, B., CARELLI, V., MCLENNAN, H. & LINNANE, A. W. 1996. The interaction of Q analogs, particularly hydroxydecyl benzoquinone (idebenone), with the respiratory complexes of heart mitochondria. *Archives of biochemistry and biophysics*, 330, 395-400.
- DELLORUSSO, C., CRAWFORD, R. W., CHAMBERLAIN, J. S. & BROOKS, S. V. 2001. Tibialis anterior muscles in mdx mice are highly susceptible to contraction-induced injury. *Journal of Muscle Research & Cell Motility*, 22, 467-475.
- DELMONICO, M. J., HARRIS, T. B., VISSER, M., PARK, S. W., CONROY, M. B., VELASQUEZ-MIEYER, P., BOUDREAU, R., MANINI, T. M., NEVITT, M. & NEWMAN, A. B. 2009. Longitudinal study of muscle strength, quality, and adipose tissue infiltration. *The American journal of clinical nutrition*, 90, 1579-1585.
- DESLER, C., HANSEN, T. L., FREDERIKSEN, J. B., MARCKER, M. L., SINGH, K. K. & JUEL RASMUSSEN, L. 2012. Is there a link between mitochondrial reserve respiratory capacity and aging? *Journal of aging research*, 2012.
- DI MAURO, S., ANGELINI, CORRADO & CATANI, CLAUDIA 1967. Enzymes of the glycogen cycle and glycolysis in various human neuromuscular disorders. *J. Neurol. Neurosurg. Psychiat.*, 30, 411-415.
- DIMARIO, J. X., UZMAN, A. & STROHMAN, R. C. 1991. Fiber regeneration is not persistent in dystrophic (mdx) mouse skeletal muscle. *Developmental Biology*, 148, 314-321.

- DIMAURO, S. & DAVIDZON, G. 2005. Mitochondrial DNA and disease. *Annals of medicine*, 37, 222-232.
- DIRKS, A. J., HOFER, T., MARZETTI, E., PAHOR, M. & LEEUWENBURGH, C. 2006. Mitochondrial DNA mutations, energy metabolism and apoptosis in aging muscle. *Ageing research reviews*, 5, 179-195.
- DISATNIK, M. H., DHAWAN, J., YU, Y., BEAL, M. F., WHIRL, M. M., FRANCO, A. A. & RANDO, T. A. 1998. Evidence of oxidative stress in *mdx* mouse muscle: Studies of the pre-necrotic state. *Journal of the Neurological Sciences*, 161, 77-84.
- DOEL, J. J., BENJAMIN, N., HECTOR, M. P., ROGERS, M. & ALLAKER, R. P. 2005. Evaluation of bacterial nitrate reduction in the human oral cavity. *European journal of oral sciences*, 113, 14-19.
- DOGRA, C., CHANGOTRA, H., WERGEDAL, J. E. & KUMAR, A. 2006. Regulation of phosphatidylinositol 3-kinase (PI3K)/Akt and nuclear factor-kappa B signaling pathways in dystrophin-deficient skeletal muscle in response to mechanical stretch. *Journal of cellular physiology*, 208, 575-585.
- DORCHIES, O. M., WAGNER, S., VUADENS, O., WALDHAUSER, K., BUETLER, T. M., KUCERA, P. & RUEGG, U. T. 2006. Green tea extract and its major polyphenol (-)-epigallocatechin gallate improve muscle function in a mouse model for Duchenne muscular dystrophy. *American Journal of Physiology-Cell Physiology*, 290, C616-C625.
- DORIGUZZI, C., BERTOLOTTO, A., GANZIT, G. P., MONGINI, T. & PALMUCCI, L. 1981. Ineffectiveness of allopurinol in Duchenne Muscular Dystrophy.

Muscle & Nerve, 4, 176-178.

DREYFUS, J.-C., SCHAPIRA, GEORGES & SCHAPIRA, FANNY 1954.

Biochemical study of muscle in progressive muscular dystrophy. *J Clin Invest.* , 33, 794-797.

DRUMMOND, L. 1979. Creatine phosphokinase levels in the newborn and their use in screening for Duchenne muscular dystrophy. *Archives of disease in childhood*, 54, 362-366.

DUBOWITZ, V. 2006. Enigmatic conflict of clinical and molecular diagnosis in Duchenne/Becker muscular dystrophy. *Neuromuscular Disorders*, 16, 865-866.

DUCHENNE, G.-B. 1861. *De l'électrisation localisée et de son application à la pathologie*, Baillière.

DUCHENNE, G. B. 1868. *De la paralysie musculaire pseudo-hypertrophique ou paralysie myo-sclérosique*, P. Asselin.

DUDLEY, R. W., DANIALOU, G., GOVINDARAJU, K., LANDS, L., EIDELMAN, D. E. & PETROF, B. J. 2006. Sarcolemmal damage in dystrophin deficiency is modulated by synergistic interactions between mechanical and oxidative/nitrosative stresses. *The American journal of pathology*, 168, 1276-1287.

DUDLEY, R. W., KHAIRALLAH, M., MOHAMMED, S., LANDS, L., DES ROSIERS, C. & PETROF, B. J. 2006. Dynamic responses of the glutathione system to acute oxidative stress in dystrophic mouse (mdx) muscles. *American Journal of Physiology-Regulatory, Integrative and Comparative Physiology*,

291, R704-R710.

- DULLOO, A. G., GUBLER, M., MONTANI, J.-P., SEYDOUX, J. & SOLINAS, G. 2004. Substrate cycling between de novo lipogenesis and lipid oxidation: a thermogenic mechanism against skeletal muscle lipotoxicity and glucolipotoxicity. *International Journal of Obesity*, 28, S29-S37.
- DUMONT, N. A., WANG, Y. X., VON MALTZAHN, J., PASUT, A., BENTZINGER, C. F., BRUN, C. E. & RUDNICKI, M. A. 2015. Dystrophin expression in muscle stem cells regulates their polarity and asymmetric division. *Nature medicine*, 21, 1455-1463.
- DUNN, J. & RADDA, G. 1991. Total ion content of skeletal and cardiac muscle in the *mdx* mouse dystrophy: Ca^{2+} is elevated at all ages. *Journal of the Neurological Sciences*, 103, 226-231.
- EAGLE, M., BAUDOUIN, S. V., CHANDLER, C., GIDDINGS, D. R., BULLOCK, R. & BUSHBY, K. 2002. Survival in Duchenne muscular dystrophy: improvements in life expectancy since 1967 and the impact of home nocturnal ventilation. *Neuromuscular Disorders*, 12, 926-929.
- EGHTESAD, S., JHUNJHUNWALA, S., LITTLE, S. R. & CLEMENS, P. R. 2011. Rapamycin ameliorates dystrophic phenotype in *mdx* mouse skeletal muscle. *Molecular medicine*, 17, 917.
- ELLIS, D. 1980. Intermediary metabolism of muscle in Duchenne muscular dystrophy. *British Medical Bulletin*, 36, 165-172.
- EMERY, A. 1991. Population frequencies of inherited neuromuscular diseases--a world survey. *Neuromuscular disorders: NMD*, 1, 19.

- ENGEL, A. 1986. Duchenne Dystrophy. *In: ENGEL, A., BANKER, BQ (ed.) Myology*. New York McGraw-Hill.
- ERB, M., HOFFMANN-ENGER, B., DEPPE, H., SOEBERDT, M., HAEFELI, R. H., RUMMEY, C., FEURER, A. & GUEVEN, N. 2012. Features of idebenone and related short-chain quinones that rescue ATP levels under conditions of impaired mitochondrial complex I. *PLoS One*, 7, e36153.
- EVEN, P., DECROUY, A. & CHINET, A. 1994. Defective regulation of energy metabolism in mdx-mouse skeletal muscles. *Biochemical Journal*, 304, 649.
- FAIRCLOUGH, R. J., WOOD, M. J. & DAVIES, K. E. 2013. Therapy for Duchenne muscular dystrophy: renewed optimism from genetic approaches. *Nature Reviews Genetics*, 14, 373-378.
- FAIST, V., KÖNIG, J., HÖGER, H. & ELMADFA, I. 2001. Decreased mitochondrial oxygen consumption and antioxidant enzyme activities in skeletal muscle of dystrophic mice after low-intensity exercise. *Annals of nutrition and metabolism*, 45, 58-66.
- FELBER, S., SKLADAL, D., WYSS, M., KREMSER, C., KOLLER, A. & SPERL, W. 2000. Oral creatine supplementation in Duchenne muscular dystrophy: a clinical and ³¹P magnetic resonance spectroscopy study. *Neurological research*, 22, 145.
- FIRESTEIN, B. L. & BREDET, D. S. 1999. Interaction of neuronal nitric-oxide synthase and phosphofructokinase-M. *Journal of Biological Chemistry*, 274, 10545-10550.
- FITCH, C. D. & MOODY, L. G. Creatine metabolism in skeletal muscle V. An

- intracellular abnormality of creatine trapping in dystrophic muscle. Proceedings of the Society for Experimental Biology and Medicine. Society for Experimental Biology and Medicine (New York, NY), 1969. Royal Society of Medicine, 219-222.
- FITCH, C. D., OATES, J. D. & DINNING, J. S. 1961. The metabolism of creatine-1-C14 by mice with hereditary muscular dystrophy. *Journal of Clinical Investigation*, 40, 850.
- FITCH, C. D. & RAHMANIAN, M. Creatine entry into skeletal muscle of normal and of dystrophic mice. Proceedings of the Society for Experimental Biology and Medicine. Society for Experimental Biology and Medicine (New York, NY), 1969. Royal Society of Medicine, 236-239.
- FITT, P. S. & PARLIAMENT, M. B. 1982. Purine nucleotide cycle enzymes in dystrophic and normal mouse muscle. *Bioscience Reports*, 2, 177-183.
- FLANAGAN, W. F., HOLMES, E. W., SABINA, R. L. & SWAIN, J. L. 1986. Importance of purine nucleotide cycle to energy production in skeletal muscle. *American Journal of Physiology - Cell Physiology*, 251, C795-C802.
- FLORINI, J. R., EWTON, D. Z. & MAGRI, K. A. 1991. Hormones, growth factors, and myogenic differentiation. *Annual review of physiology*, 53, 201-216.
- FONG, P., TURNER, P. R., DENETCLAW, W. F. & STEINHARDT, R. A. 1990. Increased activity of calcium leak channels in myotubes of Duchenne human and mdx mouse origin. *Science (New York, NY)*, 250, 673.
- FRASCARELLI, M., ROCCHI, L. & FEOLA, I. 1988. EMG computerized analysis of localized fatigue in Duchenne muscular dystrophy. *Muscle & nerve*, 11, 757-

761.

- GALLUZZI, L., KEPP, O. & KROEMER, G. 2012. Mitochondria: master regulators of danger signalling. *Nature reviews Molecular cell biology*, 13, 780-788.
- GANGOLLI, S. D., VAN DEN BRANDT, P. A., FERON, V. J., JANZOWSKY, C., KOEMAN, J. H., SPEIJERS, G. J., SPIEGELHALDER, B., WALKER, R. & WISHNOK, J. S. 1994. Nitrate, nitrite and N-nitroso compounds. *European Journal of Pharmacology: Environmental Toxicology and Pharmacology*, 292, 1-38.
- GAO, B., DOAN, A. & HYBERTSON, B. M. 2014. The clinical potential of influencing Nrf2 signaling in degenerative and immunological disorders. *Clin Pharmacol*, 6, 19-34.
- GARDNER-MEDWIN, D. 1980. Clinical features and classification of the muscular dystrophies. *British medical bulletin*, 36, 109-116.
- GE, Y., MOLLOY, M. P., CHAMBERLAIN, J. S. & ANDREWS, P. C. 2003. Proteomic analysis of mdx skeletal muscle: Great reduction of adenylate kinase 1 expression and enzymatic activity. *Proteomics*, 3, 1895-1903.
- GELLERICH, F. N., GIZATULLINA, Z., TRUMBECKAITE, S., NGUYEN, H. P., PALLAS, T., ARANDARCIKAITE, O., VIELHABER, S., SEPPET, E. & STRIGGOW, F. 2010. The regulation of OXPHOS by extra-mitochondrial calcium. *Biochimica et Biophysica Acta (BBA)-Bioenergetics*, 1797, 1018-1027.
- GILLIS, J.-M. 1996. The mdx mouse: why diaphragm? *Muscle & nerve*, 19, 1230-1230.

- GIULIVI, C. 2003. Characterization and function of mitochondrial nitric-oxide synthase. *Free Radical Biology and Medicine*, 34, 397-408.
- GLESBY, M. J., ROSENMAN, E., NYLEN, E. G. & WROGEMANN, K. 1988. Serum CK, calcium, magnesium, and oxidative phosphorylation in mdx mouse muscular dystrophy. *Muscle & Nerve*, 11, 852-856.
- GNAIGER, E., LASSNIG, B., KUZNETSOV, A., RIEGER, G. & MARGREITER, R. 1998. Mitochondrial oxygen affinity, respiratory flux control and excess capacity of cytochrome c oxidase. *Journal of Experimental Biology*, 201, 1129-1139.
- GODIN, R., DAUSSIN, F., MATECKI, S., LI, T., PETROF, B. J. & BURELLE, Y. 2012. PGC1 α gene transfer restores mitochondrial biomass and improves mitochondrial calcium handling in post-necrotic mdx MOUSE skeletal muscle. *The Journal of Physiology*.
- GOLDSPINK, G., FERNANDES, K., WILLIAMS, P. E. & WELLS, D. J. 1994. Age-related changes in collagen gene expression in the muscles of mdx dystrophic and normal mice. *Neuromuscular Disorders*, 4, 183-191.
- GOODING, J. R., JENSEN, M. V., DAI, X., WENNER, B. R., LU, D., ARUMUGAM, R., FERDAOUSI, M., MACDONALD, P. E. & NEWGARD, C. B. 2015. Adenylosuccinate Is an Insulin Secretagogue Derived from Glucose-Induced Purine Metabolism. *Cell reports*, 13, 157-167.
- GOODMAN, C. A., HORVATH, D., STATHIS, C., MORI, T., CROFT, K., MURPHY, R. M. & HAYES, A. 2009. Taurine supplementation increases skeletal muscle force production and protects muscle function during and after high-

- frequency in vitro stimulation. *Journal of Applied Physiology*, 107, 144-154.
- GOODMAN, M. & LOWENSTEIN, J. 1977. The purine nucleotide cycle. Studies of ammonia production by skeletal muscle in situ and in perfused preparations. *Journal of Biological Chemistry*, 252, 5054-5060.
- GOODPASTER, B. H., THERIAULT, R., WATKINS, S. C. & KELLEY, D. E. 2000. Intramuscular lipid content is increased in obesity and decreased by weight loss. *Metabolism*, 49, 467-472.
- GORDON, B. S., WEED, P., LEARNER, E., SCHOENLING, D. & KOSTEK, M. C. 2012. Resveratrol decreases inflammation and oxidative stress in the mdx mouse model of duchenne muscular dystrophy. *The FASEB Journal*, 26, 823.12.
- GÓRECKI, D. C. 2016. Dystrophin: The dead calm of a dogma. *Rare Diseases*, 4, e1153777.
- GOSELIN, L. E., WILLIAMS, J. E., DEERING, M., BRAZEAU, D., KOURY, S. & MARTINEZ, D. A. 2004. Localization and early time course of TGF- β 1 mRNA expression in dystrophic muscle. *Muscle & nerve*, 30, 645-653.
- GRADY, R. M., TENG, H., NICHOL, M. C., CUNNINGHAM, J. C., WILKINSON, R. S. & SANES, J. R. 1997. Skeletal and cardiac myopathies in mice lacking utrophin and dystrophin: a model for Duchenne muscular dystrophy. *Cell*, 90, 729-738.
- GRIFFIN, J., WILLIAMS, H., SANG, E., CLARKE, K., RAE, C. & NICHOLSON, J. 2001. Metabolic profiling of genetic disorders: a multitissue ^1H nuclear magnetic resonance spectroscopic and pattern recognition study into

- dystrophic tissue. *Analytical biochemistry*, 293, 16-21.
- GRIFFITHS, R. D., CADY, E. B., EDWARDS, R. H. T. & WILKIE, D. R. 1985. Muscle energy metabolism in duchenne dystrophy studied by ³¹P-NMR: Controlled trials show no effect of allopurinol or ribose. *Muscle & Nerve*, 8, 760-767.
- GROSSO, S., PERRONE, S., LONGINI, M., BRUNO, C., MINETTI, C., GAZZOLO, D., BALESTRI, P. & BUONOCORE, G. 2008. Isoprostanes in dystrophinopathy: evidence of increased oxidative stress. *Brain and Development*, 30, 391-395.
- GÜCÜYENER, K., ERGENEKON, E., ERBAS, D., PINARLI, G. & SERDAROĞLU, A. 2000. The serum nitric oxide levels in patients with Duchenne muscular dystrophy. *Brain and Development*, 22, 181-183.
- GUERRERO-ONTIVEROS, M. L. & WALLIMANN, T. 1998. Creatine supplementation in health and disease. Effects of chronic creatine ingestion in vivo: down-regulation of the expression of creatine transporter isoforms in skeletal muscle. *Bioenergetics of the Cell: Quantitative Aspects*. Springer.
- GUERRON, A. D., RAWAT, R., SALI, A., SPURNEY, C. F., PISTILLI, E., CHA, H.-J., PANDEY, G. S., GERNAPUDI, R., FRANCA, D. & FARAJIAN, V. 2010. Functional and molecular effects of arginine butyrate and prednisone on muscle and heart in the mdx mouse model of Duchenne Muscular Dystrophy. *PloS one*, 5, e11220.
- GUEVEN, N., WOOLLEY, K. & SMITH, J. 2015. Border between natural product and drug: comparison of the related benzoquinones idebenone and

coenzyme Q 10. *Redox biology*, 4, 289-295.

HAEFELI, R. H., ERB, M., GEMPERLI, A. C., ROBAY, D., FRUH, I. C., ANKLIN, C., DALLMANN, R. & GUEVEN, N. 2011. NQO1-dependent redox cycling of idebenone: effects on cellular redox potential and energy levels. *PLoS One*, 6, e17963.

HAFNER, P., BONATI, U., ERNE, B., SCHMID, M., RUBINO, D., POHLMAN, U., PETERS, T., RUTZ, E., FRANK, S. & NEUHAUS, C. 2015. Improved Muscle Function in Duchenne Muscular Dystrophy through L-Arginine and Metformin: An Investigator-Initiated, Open-Label, Single-Center, Proof-Of-Concept-Study. *PloS one*, 11, e0147634-e0147634.

HAIDER, G. & FOLLAND, J. P. 2014. Nitrate supplementation enhances the contractile properties of human skeletal muscle. *Medicine and science in sports and exercise*, 46, 2234-2243.

HAKIM, C. H., GRANGE, R. W. & DUAN, D. 2011. The passive mechanical properties of the extensor digitorum longus muscle are compromised in 2-to 20-mo-old mdx mice. *Journal of applied physiology*, 110, 1656-1663.

HAMADA, M., OKUDA, H., OKA, K., WATANABE, T., UEDA, K., NOJIMA, M., KUBY, S. A., MANSHIP, M., TYLER, F. H. & ZITER, F. A. 1981. An aberrant adenylate kinase isoenzyme from the serum of patients with Duchenne muscular dystrophy. *Biochimica et Biophysica Acta (BBA) - Enzymology*, 660, 227-237.

HAN, D., CANALI, R., RETTORI, D. & KAPLOWITZ, N. 2003. Effect of glutathione depletion on sites and topology of superoxide and hydrogen peroxide

- production in mitochondria. *Molecular pharmacology*, 64, 1136-1144.
- HANDSCHIN, C., KOBAYASHI, Y. M., CHIN, S., SEALE, P., CAMPBELL, K. P. & SPIEGELMAN, B. M. 2007. PGC-1 α regulates the neuromuscular junction program and ameliorates Duchenne muscular dystrophy. *Genes & development*, 21, 770-783.
- HANKARD, R. G., HAMMOND, D., HAYMOND, M. W. & DARMAUN, D. 1998. Oral glutamine slows down whole body protein breakdown in Duchenne muscular dystrophy. *Pediatr Res*, 43, 222-6.
- HANSFORD, R. G., HOGUE, B. A. & MILDAZIENE, V. 1997. Dependence of H₂O₂ formation by rat heart mitochondria on substrate availability and donor age. *Journal of bioenergetics and biomembranes*, 29, 89-95.
- HARRIMAN, D. & REED, R. 1972. The incidence of lipid droplets in human skeletal muscle in neuromuscular disorders: A histochemical, electron-microscopic and freeze-etch study. *The Journal of pathology*, 106, 1-24.
- HARTEL, J. V., GRANCHELLI, J. A., HUDECKI, M. S., POLLINA, C. M. & GOSELIN, L. E. 2001. Impact of prednisone on TGF- β 1 and collagen in diaphragm muscle from mdx mice. *Muscle & nerve*, 24, 428-432.
- HAUSER, E., HOGER, H., BITTNER, R., WIDHALM, K., HERKNER, K. & LUBEC, G. 1995. Oxyradical damage and mitochondrial enzyme activities in the mdx mouse. *Neuropediatrics*, 26, 260-262.
- HAYCOCK, J. W., MAC NEIL, S., JONES, P., HARRIS, J. B. & MANTLE, D. 1996. Oxidative damage to muscle protein in Duchenne muscular dystrophy. *Neuroreport*, 8, 357-361.

- HAYES, A. & WILLIAMS, D. A. 1998. Contractile function and low-intensity exercise effects of old dystrophic (mdx) mice. *American Journal of Physiology-Cell Physiology*, 274, C1138-C1144.
- HE, J., WATKINS, S. & KELLEY, D. E. 2001. Skeletal muscle lipid content and oxidative enzyme activity in relation to muscle fiber type in type 2 diabetes and obesity. *Diabetes*, 50, 817-823.
- HEINO, J. & MASSAGUE, J. 1990. Cell adhesion to collagen and decreased myogenic gene expression implicated in the control of myogenesis by transforming growth factor beta. *Journal of Biological Chemistry*, 265, 10181-10184.
- HELLIWELL, T., MORRIS, G. & DAVIES, K. 1992. The dystrophin-related protein, utrophin, is expressed on the sarcolemma of regenerating human skeletal muscle fibres in dystrophies and inflammatory myopathies. *Neuromuscular Disorders*, 2, 177-184.
- HELLSTEN-WESTING, Y. 1993. Immunohistochemical localization of xanthine oxidase in human cardiac and skeletal muscle. *Histochemistry*, 100, 215-222.
- HENDGEN-COTTA, U. B., MERX, M. W., SHIVA, S., SCHMITZ, J., BECHER, S., KLARE, J. P., STEINHOFF, H.-J., GOEDECKE, A., SCHRADER, J. & GLADWIN, M. T. 2008. Nitrite reductase activity of myoglobin regulates respiration and cellular viability in myocardial ischemia-reperfusion injury. *Proceedings of the National Academy of Sciences*, 105, 10256-10261.
- HERNÁNDEZ, A., SCHIFFER, T. A., IVARSSON, N., CHENG, A. J., BRUTON, J.

- D., LUNDBERG, J. O., WEITZBERG, E. & WESTERBLAD, H. 2012. Dietary nitrate increases tetanic $[Ca^{2+}]_i$ and contractile force in mouse fast-twitch muscle. *The Journal of physiology*, 590, 3575-3583.
- HERZBERG, N. H., ZWART, R., WOLTERMAN, R. A., RUITER, J. P., WANDERS, R. J., BOLHUIS, P. A. & VAN DEN BOGERT, C. 1993. Differentiation and proliferation of respiration-deficient human myoblasts. *Biochimica et Biophysica Acta (BBA)-Molecular Basis of Disease*, 1181, 63-67.
- HESLOP, L., MORGAN, J. E. & PARTRIDGE, T. A. 2000. Evidence for a myogenic stem cell that is exhausted in dystrophic muscle. *Journal of Cell Science*, 113, 2299-2308.
- HESS, J. 1965. Phosphorylase activity and glycogen, glucose-6-phosphate, and lactic acid content of human skeletal muscle in various myopathies. *J Lab Clin Med*, 66, 452-463.
- HEZEL, M. P., LIU, M., SCHIFFER, T. A., LARSEN, F. J., CHECA, A., WHEELLOCK, C. E., CARLSTRÖM, M., LUNDBERG, J. O. & WEITZBERG, E. 2015. Effects of long-term dietary nitrate supplementation in mice. *Redox Biology*.
- HIGAKI, Y., HIRSHMAN, M. F., FUJII, N. & GOODYEAR, L. J. 2001. Nitric oxide increases glucose uptake through a mechanism that is distinct from the insulin and contraction pathways in rat skeletal muscle. *Diabetes*, 50, 241-247.
- HIGGINS, L. G., KELLEHER, M. O., EGGLESTON, I. M., ITOH, K., YAMAMOTO, M. & HAYES, J. D. 2009. Transcription factor Nrf2 mediates an adaptive

response to sulforaphane that protects fibroblasts in vitro against the cytotoxic effects of electrophiles, peroxides and redox-cycling agents.

Toxicology and applied pharmacology, 237, 267-280.

HILTON, T. N., TUTTLE, L. J., BOHNERT, K. L., MUELLER, M. J. & SINACORE, D. R. 2008. Excessive adipose tissue infiltration in skeletal muscle in individuals with obesity, diabetes mellitus, and peripheral neuropathy: association with performance and function. *Physical Therapy*, 88, 1336-1344.

HINDLEY, S., JUURLINK, B. H., GYSBERS, J. W., MIDDLEMISS, P. J., HERMAN, M. A. & RATHBONE, M. P. 1997. Nitric oxide donors enhance neurotrophin-induced neurite outgrowth through a cGMP-dependent mechanism. *Journal of neuroscience research*, 47, 427-439.

HIONA, A. & LEEUWENBURGH, C. 2008. The role of mitochondrial DNA mutations in aging and sarcopenia: implications for the mitochondrial vicious cycle theory of aging. *Experimental gerontology*, 43, 24-33.

HNIA, K., GAYRAUD, J., HUGON, G., RAMONATXO, M., DE LA PORTE, S., MATECKI, S. & MORNET, D. 2008. L-arginine decreases inflammation and modulates the nuclear factor- κ B/matrix metalloproteinase cascade in mdx muscle fibers. *The American journal of pathology*, 172, 1509-1519.

HOFFMAN, E. P., BROWN, R. H. & KUNKEL, L. M. 1987. Dystrophin: the protein product of the Duchenne muscular dystrophy locus. *Cell*, 51, 919-928.

HOFFMAN, E. P. & DRESSMAN, D. 2001. Molecular pathophysiology and targeted therapeutics for muscular dystrophy. *Trends in pharmacological*

sciences, 22, 465-470.

HOLLINGER, K., SHANELY, R. A., QUINDRY, J. C. & SELSBY, J. T. 2015. Long-term quercetin dietary enrichment decreases muscle injury in mdx mice. *Clinical Nutrition*, 34, 515-522.

HOLLINGER, K., SNELLA, E., SHANELY, R. A. & SELSBY, J. T. 2012. Dietary quercetin supplementation alleviates disease related muscle injury in dystrophic muscle. *The FASEB Journal*, 26, 255.4-255.4.

HOLMSTRÖM, K. M., BAIRD, L., ZHANG, Y., HARGREAVES, I., CHALASANI, A., LAND, J. M., STANYER, L., YAMAMOTO, M., DINKOVA-KOSTOVA, A. T. & ABRAMOV, A. Y. 2013. Nrf2 impacts cellular bioenergetics by controlling substrate availability for mitochondrial respiration. *Biology open*, 2, 761-770.

HONG, Y. H., FRUGIER, T., ZHANG, X., MURPHY, R. M., LYNCH, G. S., BETIK, A. C., RATTIGAN, S. & MCCONELL, G. K. 2015. Glucose uptake during contraction in isolated skeletal muscles from neuronal nitric oxide synthase μ knockout mice. *Journal of Applied Physiology*, 118, 1113-1121.

HOOD, D. A. 2001. Invited Review: contractile activity-induced mitochondrial biogenesis in skeletal muscle. *Journal of Applied Physiology*, 90, 1137-1157.

HOON, M. W., FORNUSEK, C., CHAPMAN, P. G. & JOHNSON, N. A. 2015. The effect of nitrate supplementation on muscle contraction in healthy adults. *European journal of sport science*, 15, 712-719.

HOOTAN, B. W., DC 1966. Adenosine 5'-triphosphate-creatine phosphotransferase from dystrophic mouse skeletal muscle: A genetic

- lesion associated with the catalytic-site thiol group. *Biochem. J.*, 100, 637-646.
- HOPF, F., TURNER, P., DENETCLAW, W., REDDY, P. & STEINHARDT, R. 1996. A critical evaluation of resting intracellular free calcium regulation in dystrophic mdx muscle. *American Journal of Physiology-Cell Physiology*, 271, C1325-C1339.
- HORD, N. G., TANG, Y. & BRYAN, N. S. 2009. Food sources of nitrates and nitrites: the physiologic context for potential health benefits. *The American journal of clinical nutrition*, 90, 1-10.
- HORI, Y. S., KUNO, A., HOSODA, R. & HORIO, Y. 2013. Regulation of FOXOs and p53 by SIRT1 modulators under oxidative stress. *PLoS One*, 8, e73875.
- HORI, Y. S., KUNO, A., HOSODA, R., TANNO, M., MIURA, T., SHIMAMOTO, K. & HORIO, Y. 2011. Resveratrol ameliorates muscular pathology in the dystrophic mdx mouse, a model for Duchenne muscular dystrophy. *Journal of Pharmacology and Experimental Therapeutics*, 338, 784-794.
- HOWLAND, J. L. & CHALLBERG, M. D. 1973. Altered respiration and proton permeability in liver mitochondria from genetically dystrophic mice. *Biochemical and Biophysical Research Communications*, 50, 574-580.
- HUNTER, J. R., GALLOWAY, J. R., BROOKE, M. M., KUTNER, M. H., RUDMAN, D., VOGEL, R. L., WARDLAW, C. F. & GERRON, G. G. 1983. Effects of allopurinol in Duchenne's muscular dystrophy. *Archives of Neurology*, 40, 294.
- HUNTER, M. I. S. & MOHAMED, J. B. 1986. Plasma antioxidants and lipid

- peroxidation products in Duchenne muscular dystrophy. *Clinica chimica acta*, 155, 123-131.
- IMBERT, N., COGNARD, C., DUPORT, G., GUILLOU, C. & RAYMOND, G. 1995. Abnormal calcium homeostasis in Duchenne muscular dystrophy myotubes contracting in vitro. *Cell Calcium*, 18, 177-186.
- INOUE, S.-I., NODA, S., KASHIMA, K., NAKADA, K., HAYASHI, J.-I. & MIYOSHI, H. 2010. Mitochondrial respiration defects modulate differentiation but not proliferation of hematopoietic stem and progenitor cells. *FEBS letters*, 584, 3402-3409.
- IONASESCU, R., KAEDING, L., FELD, R., WITTE, D., CANCELLA, P. & STERN, L. Z. 1981. Alterations in creatine kinase in fresh muscle and cell cultures in duchenne dystrophy. *Annals of neurology*, 9, 394-399.
- IONĂȘESCU, V., LUCA, N. & VUIA, O. 1967. Respiratory control and oxidative phosphorylation in the dystrophic muscle. *Acta Neurologica Scandinavica*, 43, 564-572.
- JACKSON, M. J., JONES, D. A. & EDWARDS, R. H. 1985. Measurements of calcium and other elements in muscle biopsy samples from patients with Duchenne muscular dystrophy. *Clinica chimica acta*, 147, 215-221.
- JAHNKE, V. E., VAN DER MEULEN, J. H., JOHNSTON, H. K., GHIMBOVSCHI, S., PARTRIDGE, T., HOFFMAN, E. P. & NAGARAJU, K. 2012. Metabolic remodeling agents show beneficial effects in the dystrophin-deficient mdx mouse model. *Skeletal muscle*, 2, 16.
- JATO-RODRIGUEZ, J., LIANG, C. R., LIN, C. H., HUDSON, A. J. &

- STRICKLAND, K. P. 1975. Comparison of the intermediary metabolism of fatty acids in denervated and dystrophic murine skeletal muscle. *Journal of Neurology, Neurosurgery & Psychiatry*, 38, 1083-1089.
- JEUKENDRUP, A. 2003. Modulation of carbohydrate and fat utilization by diet, exercise and environment. *Biochemical Society Transactions*, 31, 1270-1273.
- JI, L. L., FU, R. & MITCHELL, E. W. 1992. Glutathione and antioxidant enzymes in skeletal muscle: effects of fiber type and exercise intensity. *Journal of Applied Physiology*, 73, 1854-1859.
- JOHNSON, R. J., PEREZ-POZO, S. E., SAUTIN, Y. Y., MANITIUS, J., SANCHEZ-LOZADA, L. G., FEIG, D. I., SHAFIU, M., SEGAL, M., GLASSOCK, R. J. & SHIMADA, M. 2009. Hypothesis: could excessive fructose intake and uric acid cause type 2 diabetes? *Endocrine reviews*, 30, 96-116.
- JONGPIPITVANICH, S., SUEBLINVONG, T. & NORAPUCSUNTON, T. 2005. Mitochondrial respiratory chain dysfunction in various neuromuscular diseases. *Journal of clinical neuroscience*, 12, 426-428.
- JOSHI, M. S., PONTHER, J. L. & LANCASTER, J. R. 1999. Cellular antioxidant and pro-oxidant actions of nitric oxide. *Free Radical Biology and Medicine*, 27, 1357-1366.
- JUDGE, L. M., HARAGUCHILN, M. & CHAMBERLAIN, J. S. 2006. Dissecting the signaling and mechanical functions of the dystrophin-glycoprotein complex. *Journal of cell science*, 119, 1537-1546.
- KADDAI, V., GONZALEZ, T., BOLLA, M., LE MARCHAND-BRUSTEL, Y. &

- CORMONT, M. 2008. The nitric oxide-donating derivative of acetylsalicylic acid, NCX 4016, stimulates glucose transport and glucose transporters translocation in 3T3-L1 adipocytes. *American Journal of Physiology-Endocrinology and Metabolism*, 295, E162-E169.
- KADENBACH, B. 2003. Intrinsic and extrinsic uncoupling of oxidative phosphorylation. *Biochimica et Biophysica Acta (BBA) - Bioenergetics*, 1604, 77-94.
- KAMEYA, S., MIYAGOE, Y., NONAKA, I., IKEMOTO, T., ENDO, M., HANAOKA, K., NABESHIMA, Y.-I. & TAKEDA, S. I. 1999. α 1-syntrophin gene disruption results in the absence of neuronal-type nitric-oxide synthase at the sarcolemma but does not induce muscle degeneration. *Journal of Biological Chemistry*, 274, 2193-2200.
- KAMINSKI, H. J., AL-HAKIM, M., LEIGH, R. J., BASHAR, M. K. & RUFF, R. L. 1992. Extraocular muscles are spared in advanced Duchenne dystrophy. *Annals of neurology*, 32, 586-588.
- KÄMPER, A. & RODEMANN, H. 1992. Alterations of protein degradation and 2-D protein pattern in muscle cells of MDX and DMD origin. *Biochemical and biophysical research communications*, 189, 1484-1490.
- KANG, E. S., CAPACI, M. T., KANG, E. H., LAW, P. K. & CROSBY, G. 1986. Fatty acid metabolism and mitochondrial proteins in the C57BL/6J-^{dy}2J^{dy} dystrophic mice. *Comparative Biochemistry and Physiology Part B: Comparative Biochemistry*, 83, 545-550.

- KARPATI, G., CARPENTER, S. & PRESCOTT, S. 1988. Small-caliber skeletal muscle fibers do not suffer necrosis in mdx mouse dystrophy. *Muscle & nerve*, 11, 795-803.
- KASAI, T., ABEYAMA, K., HASHIGUCHI, T., FUKUNAGA, H., OSAME, M. & MARUYAMA, K. 2004. Decreased total nitric oxide production in patients with Duchenne muscular dystrophy. *Journal of biomedical science*, 11, 534-537.
- KATYARE, S. S., CHALLBERG, M. D. & HOWLAND, J. L. 1978. Energy coupling in liver mitochondria from dystrophic mice: Differential sensitivity of oxidative phosphorylation and Ca^{2+} uptake to K^{+} . *Metabolism*, 27, 761-769.
- KELLY-WORDEN, M. & THOMAS, E. 2014. Mitochondrial Dysfunction in Duchenne Muscular Dystrophy. *Open Journal of Endocrine and Metabolic Diseases*, 2014.
- KEMP, G., TAYLOR, D., DUNN, J., FROSTICK, S. & RADDA, G. 1993. Cellular energetics of dystrophic muscle. *Journal of the Neurological Sciences*, 116, 201-206.
- KENJALE, A. A., HAM, K. L., STABLER, T., ROBBINS, J. L., JOHNSON, J. L., VANBRUGGEN, M., PRIVETTE, G., YIM, E., KRAUS, W. E. & ALLEN, J. D. 2011. Dietary nitrate supplementation enhances exercise performance in peripheral arterial disease. *Journal of applied physiology*, 110, 1582-1591.
- KERLEY, C. P., CAHILL, K., BOLGER, K., MCGOWAN, A., BURKE, C., FAUL, J. & CORMICAN, L. 2015. Dietary nitrate supplementation in COPD: An acute,

- double-blind, randomized, placebo-controlled, crossover trial☆. *Nitric Oxide*, 44, 105-111.
- KESZLER, A., ZHANG, Y. & HOGG, N. 2010. Reaction between nitric oxide, glutathione, and oxygen in the presence and absence of protein: How are S-nitrosothiols formed? *Free Radical Biology and Medicine*, 48, 55-64.
- KHAIRALLAH, M., KHAIRALLAH, R., YOUNG, M., ALLEN, B., GILLIS, M., DANIALOU, G., DESCHEPPER, C., PETROF, B. & DES ROSIERS, C. 2008. Sildenafil and cardiomyocyte-specific cGMP signaling prevent cardiomyopathic changes associated with dystrophin deficiency. *Proceedings of the National Academy of Sciences*, 105, 7028-7033.
- KHAIRALLAH, R. J., SHI, G., SBRANA, F., PROSSER, B. L., BORROTO, C., MAZAITIS, M. J., HOFFMAN, E. P., MAHURKAR, A., SACHS, F. & SUN, Y. 2012. Microtubules underlie dysfunction in duchenne muscular dystrophy. *Science signaling*, 5.
- KHO, D., MACDONALD, C., JOHNSON, R., UNSWORTH, C. P., O'CARROLL, S. J., MEZ, E. D., ANGEL, C. E. & GRAHAM, E. S. 2015. Application of xCELLigence RTCA biosensor technology for revealing the profile and window of drug responsiveness in real time. *Biosensors*, 5, 199-222.
- KIM-SHAPIRO, D. B. & GLADWIN, M. T. 2014. Mechanisms of nitrite bioactivation. *Nitric Oxide*, 38, 58-68.
- KLAMUT, H., ZUBRZYCKA-GAARN, E., BULMAN, D., MALHOTRA, S., BODRUG, S., WORTON, R. & RAY, P. 1989. Myogenic regulation of dystrophin gene expression. *British medical bulletin*, 45, 681-702.

- KOBAYASHI, Y. M., RADER, E. P., CRAWFORD, R. W., IYENGAR, N. K., THEDENS, D. R., FAULKNER, J. A., PARIKH, S. V., WEISS, R. M., CHAMBERLAIN, J. S. & MOORE, S. A. 2008. Sarcolemma-localized nNOS is required to maintain activity after mild exercise. *Nature*, 456, 511-515.
- KOBZIK, L., REID, M. B., BREDET, D. S. & STAMLER, J. S. 1994. Nitric oxide in skeletal muscle. *Nature*, 372, 546-548.
- KOENIG, M., MONACO, A. P. & KUNKEL, L. M. 1988. The complete sequence of dystrophin predicts a rod-shaped cytoskeletal protein. *Cell*, 53, 219-228.
- KOMBAIRAJU, P., KERR, J. P., ROCHE, J. A., PRATT, S. J., LOVERING, R. M., SUSSAN, T. E., KIM, J.-H., SHI, G., BISWAL, S. & WARD, C. W. 2014. Genetic silencing of Nrf2 enhances X-ROS in dysferlin-deficient muscle. *Frontiers in physiology*, 5, 57.
- KOROHODA, W., PIETRZKOWSKI, Z. & REISS, K. 1992. Chloramphenicol, an inhibitor of mitochondrial protein synthesis, inhibits myoblast fusion and myotube differentiation. *Folia histochemica et cytobiologica/Polish Academy of Sciences, Polish Histochemical and Cytochemical Society*, 31, 9-13.
- KOTELNIKOVA, E., SHKROB, M. A., PYATNITSKIY, M. A., FERLINI, A. & DARASELIA, N. 2012. Novel Approach to Meta-Analysis of Microarray Datasets Reveals Muscle Remodeling-related Drug Targets and Biomarkers in Duchenne Muscular Dystrophy. *PLoS Comput Biol*, 8, e1002365.
- KOTTLORS, M. & KIRSCHNER, J. 2010. Elevated satellite cell number in Duchenne muscular dystrophy. *Cell and tissue research*, 340, 541-548.
- KREIDER, R. B., FERREIRA, M., WILSON, M., GRINDSTAFF, P., PLISK, S.,

- REINARDY, J., CANTLER, E. & ALMADA, A. 1998. Effects of creatine supplementation on body composition, strength, and sprint performance. *Medicine and Science in Sports and Exercise*, 30, 73-82.
- KUBY, S. A., KEUTEL, H. J., OKABE, K., JACOBS, H. K., ZITER, F., GERBER, D. & TYLER, F. H. 1977. Isolation of the human ATP-creatine transphosphorylases (creatine phosphokinases) from tissues of patients with Duchenne muscular dystrophy. *Journal of Biological Chemistry*, 252, 8382-90.
- KULAKOWSKI, S., RENOIRTE, P. & DE BRUYN, C. 1981. Dynamometric and biochemical observations in Duchenne patients receiving allopurinol. *Neuropediatrics*, 12, 92.
- KUMAR, A. & BORIEK, A. M. 2003. Mechanical stress activates the nuclear factor-kappaB pathway in skeletal muscle fibers: a possible role in Duchenne muscular dystrophy. *The FASEB Journal*, 17, 386-396.
- KURU, S., INUKAI, A., KATO, T., LIANG, Y., KIMURA, S. & SOBUE, G. 2003. Expression of tumor necrosis factor- α in regenerating muscle fibers in inflammatory and non-inflammatory myopathies. *Acta neuropathologica*, 105, 217-224.
- KUSHNAREVA, Y., MURPHY, A. N. & ANDREYEV, A. 2002. Complex I-mediated reactive oxygen species generation: modulation by cytochrome c and NAD(P)⁺ oxidation–reduction state. *Biochemical Journal*, 368, 545-553.
- KUZNETSOV, A. V., TIIVEL, T., SIKK, P., KAAMBRE, T., KAY, L., DANESHKAD, Z., ROSSI, A., KADAJA, L., PEET, N. & SEPPET, E. 1996. Striking

- Differences Between the Kinetics of Regulation of Respiration by ADP in Slow-Twitch and Fast-Twitch Muscles In Vivo. *European Journal of Biochemistry*, 241, 909-915.
- KUZNETSOV, A. V., WINKLER, K., WIEDEMANN, F., VON BOSSANYI, P., DIETZMANN, K. & KUNZ, W. S. 1998. Impaired mitochondrial oxidative phosphorylation in skeletal muscle of the dystrophin-deficient mdx mouse. *Molecular and cellular biochemistry*, 183, 87-96.
- LAI, Y., THOMAS, G. D., YUE, Y., YANG, H. T., LI, D., LONG, C., JUDGE, L., BOSTICK, B., CHAMBERLAIN, J. S. & TERJUNG, R. L. 2009. Dystrophins carrying spectrin-like repeats 16 and 17 anchor nNOS to the sarcolemma and enhance exercise performance in a mouse model of muscular dystrophy. *The Journal of clinical investigation*, 119, 624-635.
- LAINE, R. & DE MONTELLANO, P. R. 1998. Neuronal nitric oxide synthase isoforms alpha and mu are closely related calpain-sensitive proteins. *Mol Pharmacol*, 54, 305-12.
- LAM, C., LAU, C., WILLIAMS, J., CHAN, Y. & WONG, L. 1997. Mitochondrial myopathy, encephalopathy, lactic acidosis and stroke-like episodes (MELAS) triggered by valproate therapy. *European journal of pediatrics*, 156, 562-564.
- LANGCAKE, P. & PRYCE, R. J. 1977. The production of resveratrol and the viniferins by grapevines in response to ultraviolet irradiation. *Phytochemistry*, 16, 1193-1196.
- LANSLEY, K. E., WINYARD, P. G., BAILEY, S. J., VANHATALO, A.,

- WILKERSON, D. P., BLACKWELL, J. R., GILCHRIST, M., BENJAMIN, N. & JONES, A. M. 2011. Acute dietary nitrate supplementation improves cycling time trial performance. *Med Sci Sports Exerc*, 43, 1125-31.
- LANSLEY, K. E., WINYARD, P. G., FULFORD, J., VANHATALO, A., BAILEY, S. J., BLACKWELL, J. R., DIMENNA, F. J., GILCHRIST, M., BENJAMIN, N. & JONES, A. M. 2011. Dietary nitrate supplementation reduces the O₂ cost of walking and running: a placebo-controlled study. *Journal of Applied Physiology*, 110, 591-600.
- LAPLANTE, A., VINCENT, G., POIRIER, M. & DES ROSIERS, C. 1997. Effects and metabolism of fumarate in the perfused rat heart. A ¹³C mass isotopomer study. *American Journal of Physiology-Endocrinology And Metabolism*, 272, E74-E82.
- LARSEN, F., WEITZBERG, E., LUNDBERG, J. & EKBLUM, B. 2007. Effects of dietary nitrate on oxygen cost during exercise. *Acta physiologica*, 191, 59-66.
- LARSEN, F. J., SCHIFFER, T. A., BORNIQUEL, S., SAHLIN, K., EKBLUM, B., LUNDBERG, J. O. & WEITZBERG, E. 2011. Dietary inorganic nitrate improves mitochondrial efficiency in humans. *Cell metabolism*, 13, 149-159.
- LARSEN, S., NIELSEN, J., HANSEN, C. N., NIELSEN, L. B., WIBRAND, F., STRIDE, N., SCHRODER, H. D., BOUSHEL, R., HELGE, J. W. & DELA, F. 2012. Biomarkers of mitochondrial content in skeletal muscle of healthy young human subjects. *The Journal of physiology*, 590, 3349-3360.
- LE BORGNE, F., GUYOT, S., LOGEROT, M., BENEY, L., GERVAIS, P. &

- DEMARQUOY, J. 2012. Exploration of Lipid Metabolism in Relation with Plasma Membrane Properties of Duchenne Muscular Dystrophy Cells: Influence of L-Carnitine. *PLoS ONE*, 7, e49346.
- LEARY, S. C., BATTERSBY, B. J., HANSFORD, R. G. & MOYES, C. D. 1998. Interactions between bioenergetics and mitochondrial biogenesis. *Biochimica et Biophysica Acta (BBA) - Bioenergetics*, 1365, 522-530.
- LEE, A. S., ANDERSON, J. E., JOYA, J. E., HEAD, S. I., PATHER, N., KEE, A. J., GUNNING, P. W. & HARDEMAN, E. C. 2013. Aged skeletal muscle retains the ability to fully regenerate functional architecture. *Bioarchitecture*, 3, 25-37.
- LEE, D.-H., GOLD, R. & LINKER, R. A. 2012. Mechanisms of oxidative damage in multiple sclerosis and neurodegenerative diseases: therapeutic modulation via fumaric acid esters. *International journal of molecular sciences*, 13, 11783-11803.
- LEE, J.-M., SHIH, A. Y., MURPHY, T. H. & JOHNSON, J. A. 2003. NF-E2-related factor-2 mediates neuroprotection against mitochondrial complex I inhibitors and increased concentrations of intracellular calcium in primary cortical neurons. *Journal of Biological Chemistry*, 278, 37948-37956.
- LEPPER, C., PARTRIDGE, T. A. & FAN, C.-M. 2011. An absolute requirement for Pax7-positive satellite cells in acute injury-induced skeletal muscle regeneration. *Development*, 138, 3639-3646.
- LEWIS, C., JOCKUSCH, H. & OHLENDIECK, K. 2010. Proteomic profiling of the dystrophin-deficient MDX heart reveals drastically altered levels of key

- metabolic and contractile proteins. *BioMed Research International*, 2010.
- LI, A. J., BIBEE, K. P., MARSH, J. N., WEIHL, C. C. & WICKLINE, S. A. 2012. Mdx mice have a defect in autophagy that is restored by rapamycin-loaded nanoparticle treatment. *The FASEB Journal*, 26, 396.5.
- LI, D., YUE, Y., LAI, Y., HAKIM, C. H. & DUAN, D. 2011. Nitrosative stress elicited by nNOS μ delocalization inhibits muscle force in dystrophin-null mice. *The Journal of pathology*, 223, 88-98.
- LIANG, R. C. R. 1986. Studies on mitochondria from dystrophic skeletal muscle of mice. *Biochemical Medicine and Metabolic Biology*, 36, 172-178.
- LILLING, G. & BEITNER, R. 1991. Altered allosteric properties of cytoskeleton-bound phosphofructokinase in muscle from mice with X chromosome-linked muscular dystrophy (mdx). *Biochemical Medicine and Metabolic Biology*, 45, 319-325.
- LIN CH, H. A. S. K. 1972. Fatty acid oxidation by skeletal muscle mitochondria in Duchenne muscular dystrophy. *Life Sci II*, 11, 355-362.
- LIN, P.-H., LEE, S.-H., SU, C.-P. & WEI, Y.-H. 2003. Oxidative damage to mitochondrial DNA in atrial muscle of patients with atrial fibrillation. *Free Radical Biology and Medicine*, 35, 1310-1318.
- LINKER, R. A., LEE, D.-H., RYAN, S., VAN DAM, A. M., CONRAD, R., BISTA, P., ZENG, W., HRONOWSKY, X., BUKO, A. & CHOLLATE, S. 2011. Fumaric acid esters exert neuroprotective effects in neuroinflammation via activation of the Nrf2 antioxidant pathway. *Brain*, 134, 678-692.
- LIRA, V. A., BROWN, D. L., LIRA, A. K., KAVAZIS, A. N., SOLTOW, Q. A.,

- ZEANAH, E. H. & CRISWELL, D. S. 2010. Nitric oxide and AMPK cooperatively regulate PGC-1 α in skeletal muscle cells. *The Journal of physiology*, 588, 3551-3566.
- LIU, X., KIM, C. N., YANG, J., JEMMERSON, R. & WANG, X. 1996. Induction of apoptotic program in cell-free extracts: requirement for dATP and cytochrome c. *Cell*, 86, 147-157.
- LIU, Y., FISKUM, G. & SCHUBERT, D. 2002. Generation of reactive oxygen species by the mitochondrial electron transport chain. *Journal of neurochemistry*, 80, 780-787.
- LJUBICIC, V. & JASMIN, B. J. 2013. AMP-activated protein kinase at the nexus of therapeutic skeletal muscle plasticity in Duchenne muscular dystrophy. *Trends in Molecular Medicine*.
- LJUBICIC, V., KHOGALI, S., RENAUD, J.-M. & JASMIN, B. J. 2012. Chronic AMPK stimulation attenuates adaptive signaling in dystrophic skeletal muscle. *American Journal of Physiology-Cell Physiology*, 302, C110-C121.
- LJUBICIC, V., MIURA, P., BURT, M., BOUDREAULT, L., KHOGALI, S., LUNDE, J. A., RENAUD, J.-M. & JASMIN, B. J. 2011. Chronic AMPK activation evokes the slow, oxidative myogenic program and triggers beneficial adaptations in mdx mouse skeletal muscle. *Human molecular genetics*, ddr265.
- LOIKE, J. D., ZALUTSKY, D. L., KABACK, E., MIRANDA, A. F. & SILVERSTEIN, S. C. 1988. Extracellular creatine regulates creatine transport in rat and human muscle cells. *Proceedings of the National Academy of Sciences*, 85, 807-811.

- LOUBOUTIN, J. P., FICHTER-GAGNEPAIN, V., THAON, E. & FARDEAU, M. 1993. Morphometric analysis of mdx diaphragm muscle fibres. Comparison with hindlimb muscles. *Neuromuscular Disorders*, 3, 463-469.
- LOUFRANI, L., DUBROCA, C., YOU, D., LI, Z., LEVY, B., PAULIN, D. & HENRION, D. 2004. Absence of dystrophin in mice reduces NO-dependent vascular function and vascular density: total recovery after a treatment with the aminoglycoside gentamicin. *Arteriosclerosis, thrombosis, and vascular biology*, 24, 671-676.
- LOUIS, M., RAYMACKERS, J. M., DEBAIX, H., LEBACQ, J. & FRANCAUX, M. 2004. Effect of creatine supplementation on skeletal muscle of mdx mice. *Muscle & Nerve*, 29, 687-692.
- LOWENSTEIN, J. M. 1972. Ammonia Production in Muscle and Other Tissues: the Purine Nucleotide Cycle. *Physiological Reviews*, 52, 382-414.
- LOWRY, O. & PASSONNEAU, J. 1972. A flexible system m enzyme analysis. New York: Academic Press.
- LUCAS-HÉRON, B., MUSSINI, J.-M. & OLLIVIER, B. 1989. Is there a maturation defect related to calcium in muscle mitochondria from dystrophic mice and Duchenne and Becker muscular dystrophy patients? *Journal of the neurological sciences*, 90, 299-306.
- LUDTMANN, M. H., ANGELOVA, P. R., ZHANG, Y., ABRAMOV, A. Y. & DINKOVA-KOSTOVA, A. T. 2014. Nrf2 affects the efficiency of mitochondrial fatty acid oxidation. *Biochemical Journal*, 457, 415-424.
- LUNDBERG, J. O., GLADWIN, M. T. & WEITZBERG, E. 2015. Strategies to

- increase nitric oxide signalling in cardiovascular disease. *Nature Reviews Drug Discovery*, 14, 623-641.
- LUNDBERG, J. O., WEITZBERG, E. & GLADWIN, M. T. 2008. The nitrate-nitrite-nitric oxide pathway in physiology and therapeutics. *Nat Rev Drug Discov*, 7, 156-167.
- MACLENNAN, P. A., MCARDLE, A. & EDWARDS, R. 1991. Acute effects of phorbol esters on the protein-synthetic rate and carbohydrate metabolism of normal and mdx mouse muscles. *Biochemical Journal*, 275, 477.
- MAKRECKA-KUKA, M., KRUMSCHNABEL, G. & GNAIGER, E. 2015. High-resolution respirometry for simultaneous measurement of oxygen and hydrogen peroxide fluxes in permeabilized cells, tissue homogenate and isolated mitochondria. *Biomolecules*, 5, 1319-1338.
- MALLOUK, N., JACQUEMOND, V. & ALLARD, B. 2000. Elevated subsarcolemmal Ca^{2+} in mdx mouse skeletal muscle fibers detected with Ca^{2+} -activated K^{+} channels. *Proceedings of the National Academy of Sciences*, 97, 4950-4955.
- MAMCHAOU, K., TROLLET, C., BIGOT, A., NEGRONI, E., CHAOUCH, S., WOLFF, A., KANDALLA, P. K., MARIE, S., DI SANTO, J. & ST GUILY, J. L. 2011. Immortalized pathological human myoblasts: towards a universal tool for the study of neuromuscular disorders. *Skeletal muscle*, 1, 1.
- MANTEL, C., MESSINA-GRAHAM, S. & BROXMEYER, H. E. 2010. Upregulation of nascent mitochondrial biogenesis in mouse hematopoietic stem cells parallels upregulation of CD34 and loss of pluripotency: a potential strategy

- for reducing oxidative risk in stem cells. *Cell cycle*, 9, 2008-2017.
- MARANHAO, J. B., DE OLIVEIRA MOREIRA, D., MAURICIO, A. F., DE CARVALHO, S. C., FERRETTI, R., PEREIRA, J. A., SANTO NETO, H. & MARQUES, M. J. 2015. Changes in calsequestrin, TNF-a, TGF-b and MyoD levels during the progression of skeletal muscle dystrophy in mdx mice: a comparative analysis of the quadriceps, diaphragm and intrinsic laryngeal muscles.
- MARQUES, M. J., FERRETTI, R., VOMERO, V. U., MINATEL, E. & NETO, H. S. 2007. Intrinsic laryngeal muscles are spared from myonecrosis in the mdx mouse model of Duchenne muscular dystrophy. *Muscle & nerve*, 35, 349-353.
- MARTENS, M., JANKULOVSKA, L., NEYMARK, M. & LEE, C. 1980. Impaired substrate utilization in mitochondria from strain 129 dystrophic mice. *Biochimica et Biophysica Acta (BBA)-Bioenergetics*, 589, 190-200.
- MARTINS-BACH, A. B., BLOISE, A. C., VAINZOF, M. & RAHNAMAYE RABBANI, S. 2012. Metabolic profile of dystrophic mdx mouse muscles analyzed with in vitro magnetic resonance spectroscopy (MRS). *Magnetic resonance imaging*, 30, 1167-1176.
- MASHIMO, H. & GOYAL, R. 1999. Lessons from genetically engineered animal models. IV. Nitric oxide synthase gene knockout mice. *AMERICAN JOURNAL OF PHYSIOLOGY*, 277, G745-G750.
- MASTAGLIA, F. & KAKULAS, B. 1969. Regeneration in Duchenne muscular dystrophy: a histological and histochemical study. *Brain*, 92, 809-818.

- MATSAKAS, A., YADAV, V., LORCA, S. & NARKAR, V. 2013. Muscle ERRy mitigates Duchenne muscular dystrophy via metabolic and angiogenic reprogramming. *The FASEB Journal*, 27, 4004-4016.
- MATSUMURA, C. Y., PERTILLE, A., ALBUQUERQUE, T. C., SANTO NETO, H. & MARQUES, M. J. 2009. Diltiazem and verapamil protect dystrophin-deficient muscle fibers of MDX mice from degeneration: A potential role in calcium buffering and sarcolemmal stability. *Muscle & nerve*, 39, 167-176.
- MAURO, A. 1961. Satellite cell of skeletal muscle fibers. *The Journal of biophysical and biochemical cytology*, 9, 493-495.
- MCCONELL, G. K. & KINGWELL, B. A. 2006. Does nitric oxide regulate skeletal muscle glucose uptake during exercise? *Exercise and sport sciences reviews*, 34, 36-41.
- MCCONELL, G. K., RATTIGAN, S., LEE-YOUNG, R. S., WADLEY, G. D. & MERRY, T. L. 2012. Skeletal muscle nitric oxide signaling and exercise: a focus on glucose metabolism. *American Journal of Physiology - Endocrinology and Metabolism*, 303, E301-E307.
- MCDONALD, J. T., KIM, K., NORRIS, A. J., VLASHI, E., PHILLIPS, T. M., LAGADEC, C., DELLA DONNA, L., RATIKAN, J., SZELAG, H. & HLATKY, L. 2010. Ionizing radiation activates the Nrf2 antioxidant response. *Cancer research*, 70, 8886-8895.
- MCGEACHIE, J. K., GROUNDS, M. D., PARTRIDGE, T. A. & MORGAN, J. E. 1993. Age-related changes in replication of myogenic cells in mdx mice: quantitative autoradiographic studies. *Journal of the Neurological Sciences*,

119, 169-179.

- MEAKIN, P. J., CHOWDHRY, S., SHARMA, R. S., ASHFORD, F. B., WALSH, S. V., MCCRIMMON, R. J., DINKOVA-KOSTOVA, A. T., DILLON, J. F., HAYES, J. D. & ASHFORD, M. L. 2014. Susceptibility of Nrf2-null mice to steatohepatitis and cirrhosis upon consumption of a high-fat diet is associated with oxidative stress, perturbation of the unfolded protein response, and disturbance in the expression of metabolic enzymes but not with insulin resistance. *Molecular and cellular biology*, 34, 3305-3320.
- MELONE, M. A., PELUSO, G., PETILLO, O. & COTRUFO, R. 2000. Defective growth in vitro of Duchenne Muscular Dystrophy myoblasts: the molecular and biochemical basis. *Journal of cellular biochemistry*, 76, 118-132.
- MENDELL, J. R. & WIECHERS, D. O. 1979. Lack of benefit of allopurinol in duchenne dystrophy. *Muscle & Nerve*, 2, 53-56.
- MENKE, A. & JOCKUSCH, H. 1991. Decreased osmotic stability of dystrophin-less muscle cells from the mdx mouse. *Nature*, 349.
- MERRY, T. L., DYWER, R. M., BRADLEY, E. A., RATTIGAN, S. & MCCONELL, G. K. 2010. Local hindlimb antioxidant infusion does not affect muscle glucose uptake during in situ contractions in rat. *Journal of applied physiology*, 108, 1275-1283.
- MERRY, T. L. & MCCONELL, G. K. 2009. Skeletal muscle glucose uptake during exercise: a focus on reactive oxygen species and nitric oxide signaling. *IUBMB life*, 61, 479-484.
- MERRY, T. L., STEINBERG, G. R., LYNCH, G. S. & MCCONELL, G. K. 2010.

Skeletal muscle glucose uptake during contraction is regulated by nitric oxide and ROS independently of AMPK. *American Journal of Physiology-Endocrinology and Metabolism*, 298, E577-E585.

MERRY, T. L., WADLEY, G. D., STATHIS, C. G., GARNHAM, A. P., RATTIGAN, S., HARGREAVES, M. & MCCONELL, G. K. 2010. N-Acetylcysteine infusion does not affect glucose disposal during prolonged moderate-intensity exercise in humans. *The Journal of physiology*, 588, 1623-1634.

MERYON, E. 1852. On granular and fatty degeneration of the voluntary muscles. *Medico-chirurgical transactions*, 35, 73.

MESSINA, S., ALTAVILLA, D., AGUENNOUZ, M. H., SEMINARA, P., MINUTOLI, L., MONICI, M. C., BITTO, A., MAZZEO, A., MARINI, H. & SQUADRITO, F. 2006. Lipid peroxidation inhibition blunts nuclear factor- κ B activation, reduces skeletal muscle degeneration, and enhances muscle function in mdx mice. *The American journal of pathology*, 168, 918-926.

MESSINA, S., VITA, G., AGUENNOUZ, M., SFRAMELI, M., ROMEO, S., RODOLICO, C. & VITA, G. 2011. Activation of NF-KB pathway in Duchenne muscular dystrophy: relation to age. *Acta Myologica*, 30, 16.

MIGLIETTA, D., DE PALMA, C., SCIORATI, C., VERGANI, B., PISA, V., VILLA, A., ONGINI, E. & CLEMENTI, E. 2015. Naproxcinod shows significant advantages over naproxen in the mdx model of Duchenne Muscular Dystrophy. *Orphanet journal of rare diseases*, 10, 1.

MILHORAT, A., SHAFIQ, S. A. & GOLDSTONE, L. 1966. Changes in muscle

structure in dystrophic patients, carriers and normal siblings seen by electron microscopy; correlation with levels of serum creatinephosphokinase (CPK). *Annals of the New York Academy of Sciences*, 138, 246-292.

MILLER, C. J., GOUNDER, S. S., KANNAN, S., GOUTAM, K., MUTHUSAMY, V. R., FIRPO, M. A., SYMONS, J. D., PAINE, R., HOIDAL, J. R. & RAJASEKARAN, N. S. 2012. Disruption of Nrf2/ARE signaling impairs antioxidant mechanisms and promotes cell degradation pathways in aged skeletal muscle. *Biochimica et Biophysica Acta (BBA)-Molecular Basis of Disease*, 1822, 1038-1050.

MIZUNOYA, W., UPADHAYA, R., BURCZYNSKI, F. J., WANG, G. & ANDERSON, J. E. 2011. *Nitric oxide donors improve prednisone effects on muscular dystrophy in the mdx mouse diaphragm.*

MO, L., WANG, Y., GEARY, L., COREY, C., ALEF, M. J., BEER-STOLZ, D., ZUCKERBRAUN, B. S. & SHIVA, S. 2012. Nitrite activates AMP kinase to stimulate mitochondrial biogenesis independent of soluble guanylate cyclase. *Free Radical Biology and Medicine*, 53, 1440-1450.

MONACO, A. P., BERTELSON, C. J., MIDDLESWORTH, W., COLLETTI, C.-A., ALDRIDGE, J., FISCHBECK, K. H., BARTLETT, R., PERICAK-VANCE, M. A., ROSES, A. D. & KUNKEL, L. M. 1985. Detection of deletions spanning the Duchenne muscular dystrophy locus using a tightly linked DNA segment. *Nature*, 316, 842-845.

MOSER, H. 1984. Duchenne muscular dystrophy: pathogenetic aspects and genetic prevention. *Human genetics*, 66, 17-40.

- MOXLEY, R., ASHWAL, S., PANDYA, S., CONNOLLY, A., FLORENCE, J., MATHEWS, K., BAUMBACH, L., MCDONALD, C., SUSSMAN, M. & WADE, C. 2005. Practice Parameter: Corticosteroid treatment of Duchenne dystrophy Report of the Quality Standards Subcommittee of the American Academy of Neurology and the Practice Committee of the Child Neurology Society. *Neurology*, 64, 13-20.
- MUNTONI, F., MATEDDU, A., MARCHEI, F., CLERK, A. & SERRA, G. 1993. Muscular weakness in the mdx mouse. *Journal of the Neurological Sciences*, 120, 71-77.
- MUNTONI, F., MATEDDU, A., MARCHEI, F., CLERK, A. & SERRA, G. 1993. Muscular weakness in the mdx mouse. *Journal of the neurological sciences*, 120, 71-77.
- MURPHY, R., MCCONELL, G., CAMERON-SMITH, D., WATT, K., ACKLAND, L., WALZEL, B., WALLIMANN, T. & SNOW, R. 2001. Creatine transporter protein content, localization, and gene expression in rat skeletal muscle. *American Journal of Physiology-Cell Physiology*, 280, C415-C422.
- NAGEL, A., LEHMANN-HORN, F. & ENGEL, A. G. 1990. Neuromuscular transmission in the mdx mouse. *Muscle & nerve*, 13, 742-749.
- NAGY, G., KONCZ, A., FERNANDEZ, D. & PERL, A. 2007. Nitric oxide, mitochondrial hyperpolarization, and T cell activation. *Free Radical Biology and Medicine*, 42, 1625-1631.
- NELSON, M. D., ROSENBERRY, R., BARRESI, R., TSIMERINOV, E. I., RADER, F., TANG, X., MASON, O. N., SCHWARTZ, A., STABLER, T. & SHIDBAN,

- S. 2015. Sodium nitrate alleviates functional muscle ischaemia in patients with Becker muscular dystrophy. *The Journal of physiology*, 593, 5183-5200.
- NEWMAN, R. J., BORE, P. J., CHAN, L., GADIAN, D. G., STYLES, P., TAYLOR, D. & RADDA, G. K. 1982. Nuclear Magnetic Resonance Studies Of Forearm Muscle In Duchenne Dystrophy. *British Medical Journal (Clinical Research Edition)*, 284, 1072-1074.
- NGUYEN, H. X. & TIDBALL, J. G. 2003. Expression of a muscle-specific, nitric oxide synthase transgene prevents muscle membrane injury and reduces muscle inflammation during modified muscle use in mice. *The Journal of physiology*, 550, 347-356.
- NIGRO, G., COMI, L., POLITANO, L. & BAIN, R. 1990. The incidence and evolution of cardiomyopathy in Duchenne muscular dystrophy. *International journal of cardiology*, 26, 271-277.
- NISHIO, H., WADA, H., MATSUO, T., HORIKAWA, H., TAKAHASHI, K., NAKAJIMA, T., MATSUO, M. & NAKAMURA, H. 1990. Glucose, free fatty acid and ketone body metabolism in Duchenne muscular dystrophy. *Brain and Development*, 12, 390-402.
- NISOLI, E., FALCONE, S., TONELLO, C., COZZI, V., PALOMBA, L., FIORANI, M., PISCONTI, A., BRUNELLI, S., CARDILE, A. & FRANCOLINI, M. 2004. Mitochondrial biogenesis by NO yields functionally active mitochondria in mammals. *Proceedings of the National Academy of Sciences of the United States of America*, 101, 16507-16512.

- NISOLI, E., FALCONE, S., TONELLO, C., COZZI, V., PALOMBA, L., FIORANI, M., PISCONTI, A., BRUNELLI, S., CARDILE, A. & FRANCOLINI, M. 2004. Mitochondrial biogenesis by NO yields functionally active mitochondria in mammals. *Proceedings of the National Academy of Sciences of the United States of America*, 101, 16507-16512.
- NORDDAHL, G. L., PRONK, C. J., WAHLESTEDT, M., STEN, G., NYGREN, J. M., UGALE, A., SIGVARDSSON, M. & BRYDER, D. 2011. Accumulating mitochondrial DNA mutations drive premature hematopoietic aging phenotypes distinct from physiological stem cell aging. *Cell stem cell*, 8, 499-510.
- NYLEN, E. G. & WROGEMANN, K. 1983. Mitochondrial calcium content and oxidative phosphorylation in heart and skeletal muscle of dystrophic mice. *Experimental neurology*, 80, 69-80.
- OHLENDIECK, K. & CAMPBELL, K. P. 1991. Dystrophin-associated proteins are greatly reduced in skeletal muscle from mdx mice. *The Journal of Cell Biology*, 115, 1685-1694.
- OLICHON-BERTHE, C., GAUTIER, N., VAN OBERGHEEN, E. & LE MARCHAND-BRUSTEL, Y. 1993. Expression of the glucose transporter GLUT4 in the muscular dystrophic mdx mouse. *Biochemical Journal*, 291, 257.
- OLSON, E., VIGNOS, P., WOODLOCK, J. & PERRY, T. 1968. Oxidative phosphorylation of skeletal muscle in human muscular dystrophy. *J Lab Clin Med*, 71, 231.
- ONOPIUK, M., BRUTKOWSKI, W., WIERZBICKA, K., WOJCIECHOWSKA, S.,

- SZCZEPANOWSKA, J., FRONK, J., LOCHMÜLLER, H., GÓRECKI, D. C. & ZABŁOCKI, K. 2009. Mutation in dystrophin-encoding gene affects energy metabolism in mouse myoblasts. *Biochemical and Biophysical Research Communications*, 386, 463-466.
- OZAWA, E., YOSHIDA, M., SUZUKI, A., MIZUNO, Y., HAGIWARA, Y. & NOGUCHI, S. 1995. Dystrophin-associated proteins in muscular dystrophy. *Human Molecular Genetics*, 4, 1711-1716.
- PACHER, P., BECKMAN, J. S. & LIAUDET, L. 2007. Nitric oxide and peroxynitrite in health and disease. *Physiological reviews*, 87, 315-424.
- PAL, R., PALMIERI, M., LOEHR, J. A., LI, S., ABO-ZAHRAH, R., MONROE, T. O., THAKUR, P. B., SARDIELLO, M. & RODNEY, G. G. 2014. Src-dependent impairment of autophagy by oxidative stress in a mouse model of Duchenne muscular dystrophy. *Nature communications*, 5.
- PASSAQUIN, A. C., RENARD, M., KAY, L., CHALLET, C., MOKHTARIAN, A., WALLIMANN, T. & RUEGG, U. T. 2002. Creatine supplementation reduces skeletal muscle degeneration and enhances mitochondrial function in mdx mice. *Neuromuscular Disorders*, 12, 174-182.
- PASTORET C, S. A. 1993. Further aspects of muscular dystrophy in mdx mice. *Neuromuscular Disorders*, 3, 471-475.
- PAULY, M., DAUSSIN, F., BURELLE, Y., LI, T., GODIN, R., FAUCONNIER, J., KOECHLIN-RAMONATXO, C., HUGON, G., LACAMPAGNE, A. & COISY-QUIVY, M. 2012. AMPK activation stimulates autophagy and ameliorates muscular dystrophy in the mdx mouse diaphragm. *The American journal of*

- pathology*, 181, 583-592.
- PEARCE, G. 1966. Electron microscopy in the study of muscular dystrophy. *Annals of the New York Academy of Sciences*, 138, 138-150.
- PENNINGTON, R. 1961. Biochemistry of dystrophic muscle. Mitochondrial succinate-tetrazolium reductase and adenosine triphosphatase. *Biochemical Journal*, 80, 649.
- PENNINGTON, R. 1963. Biochemistry of dystrophic muscle. 2. Some enzyme changes in dystrophic mouse muscle. *Biochemical Journal*, 88, 64.
- PENNINGTON, R. J. T. 1980. Clinical biochemistry of muscular dystrophy. *British Medical Bulletin*, 36, 123-126.
- PERCIVAL, J. M., SIEGEL, M. P., KNOWELS, G. & MARCINEK, D. J. 2013. Defects in mitochondrial localization and ATP synthesis in the mdx mouse model of Duchenne muscular dystrophy are not alleviated by PDE5 inhibition. *Human Molecular Genetics*, 22, 153-167.
- PERCIVAL, J. M., WHITEHEAD, N. P., ADAMS, M. E., ADAMO, C. M., BEAVO, J. A. & FROEHNER, S. C. 2012. Sildenafil reduces respiratory muscle weakness and fibrosis in the mdx mouse model of Duchenne muscular dystrophy. *The Journal of pathology*, 228, 77-87.
- PETELL, J. K., MARSHALL, N. A. & LEBHERZ, H. G. 1984. Content and synthesis of several abundant glycolytic enzymes in skeletal muscles of normal and dystrophic mice. *International Journal of Biochemistry*, 16, 61-67.
- PETER, A. K. & CROSBIE, R. H. 2006. Hypertrophic response of Duchenne and limb-girdle muscular dystrophies is associated with activation of Akt

- pathway. *Experimental cell research*, 312, 2580-2591.
- PICKETT-GIES, C. A., CARLSEN, R. C., ANDERSON, L. J., ANGELOS, K. L. & WALSH, D. A. 1987. Characterization of the isolated rat flexor digitorum brevis for the study of skeletal muscle phosphorylase kinase phosphorylation. *Journal of Biological Chemistry*, 262, 3227-3238.
- PINTO, R. & BARTLEY, W. 1969. The effect of age and sex on glutathione reductase and glutathione peroxidase activities and on aerobic glutathione oxidation in rat liver homogenates. *Biochemical Journal*, 112, 109-115.
- PODEROSO, J. J., CARRERAS, C., LISDERO, C., RIOBÓ, N., SCHÖPFER, F. & BOVERIS, A. 1996. Nitric oxide inhibits electron transfer and increases superoxide radical production in rat heart mitochondria and submitochondrial particles. *Archives of biochemistry and biophysics*, 328, 85-92.
- PODEROSO, J. J., CARRERAS, M. A. C., LISDERO, C., RIOBÓ, N., SCHÖPFER, F. & BOVERIS, A. 1996. Nitric oxide inhibits electron transfer and increases superoxide radical production in rat heart mitochondria and submitochondrial particles. *Archives of biochemistry and biophysics*, 328, 85-92.
- PONS, F., ROBERT, A., MARINI, J. & LEGER, J. 1994. Does utrophin expression in muscles of mdx mice during postnatal development functionally compensate for dystrophin deficiency? *Journal of the neurological sciences*, 122, 162-170.
- PULIDO, S., PASSAQUIN, A., LEIJENDEKKER, W., CHALLET, C., WALLIMANN,

- T. & RÜEGG, U. 1998. Creatine supplementation improves intracellular Ca²⁺ handling and survival in mdx skeletal muscle cells. *FEBS letters*, 439, 357-362.
- RAFAEL, J. A., TINSLEY, J. M., POTTER, A. C., DECONINCK, A. E. & DAVIES, K. E. 1998. Skeletal muscle-specific expression of a utrophin transgene rescues utrophin-dystrophin deficient mice. *Nature genetics*, 19, 79-82.
- RAGUSA, R. J., CHOW, C. K., CLAIR, D. K. S. & PORTER, J. D. 1996. Extraocular, limb and diaphragm muscle group-specific antioxidant enzyme activity patterns in control and mdx mice. *Journal of the neurological sciences*, 139, 180-186.
- RAGUSA, R. J., CHOW, C. K. & PORTER, J. D. 1997. Oxidative stress as a potential pathogenic mechanism in an animal model of Duchenne muscular dystrophy. *Neuromuscular disorders*, 7, 379-386.
- RAIMUNDO, N., BAYSAL, B. E. & SHADEL, G. S. 2011. Revisiting the TCA cycle: signaling to tumor formation. *Trends in molecular medicine*, 17, 641-649.
- RAITH, M., VALENCIA, R. G., FISCHER, I., ORTHOFER, M., PENNINGER, J. M., SPULER, S., REZNICZEK, G. A. & WICHE, G. 2013. Linking cytoarchitecture to metabolism: sarcolemma-associated plectin affects glucose uptake by destabilizing microtubule networks in mdx myofibers. *Skeletal muscle*, 3, 14.
- RANDO, T. A. 2001. Role of nitric oxide in the pathogenesis of muscular dystrophies: a "two hit" hypothesis of the cause of muscle necrosis. *Microscopy research and technique*, 55, 223-235.

- RANGASAMY, T., GUO, J., MITZNER, W. A., ROMAN, J., SINGH, A., FRYER, A. D., YAMAMOTO, M., KENSLER, T. W., TUDER, R. M. & GEORAS, S. N. 2005. Disruption of Nrf2 enhances susceptibility to severe airway inflammation and asthma in mice. *The Journal of experimental medicine*, 202, 47-59.
- REBOLLEDO, D. L., KIM, M. J., WHITEHEAD, N. P., ADAMS, M. E. & FROEHNER, S. C. 2015. Sarcolemmal targeting of nNOS μ improves contractile function of mdx muscle. *Human molecular genetics*, ddv466.
- REDDY, N., KLEEBERGER, S., BREAM, J., FALLON, P., KENSLER, T., YAMAMOTO, M. & REDDY, S. 2008. Genetic disruption of the Nrf2 compromises cell-cycle progression by impairing GSH-induced redox signaling. *Oncogene*, 27, 5821-5832.
- REDDY, N., KLEEBERGER, S., BREAM, J., FALLON, P., KENSLER, T., YAMAMOTO, M. & REDDY, S. 2008. Genetic disruption of the Nrf2 compromises cell-cycle progression by impairing GSH-induced redox signaling. *Oncogene*, 27, 5821-5832.
- REDDY, N. M., KLEEBERGER, S. R., YAMAMOTO, M., KENSLER, T. W., SCOLLICK, C., BISWAL, S. & REDDY, S. P. 2007. Genetic dissection of the Nrf2-dependent redox signaling-regulated transcriptional programs of cell proliferation and cytoprotection. *Physiological genomics*, 32, 74-81.
- REICHMANN, H., HOPPELER, H., MATHIEU-COSTELLO, O., VON BERGEN, F. & PETTE, D. 1985. Biochemical and ultrastructural changes of skeletal muscle mitochondria after chronic electrical stimulation in rabbits. *Pflügers*

Archiv, 404, 1-9.

- REITMAN, Z. J., JIN, G., KAROLY, E. D., SPASOJEVIC, I., YANG, J., KINZLER, K. W., HE, Y., BIGNER, D. D., VOGELSTEIN, B. & YAN, H. 2011. Profiling the effects of isocitrate dehydrogenase 1 and 2 mutations on the cellular metabolome. *Proceedings of the National Academy of Sciences*, 108, 3270-3275.
- REN, J.-M., MARSHALL, B., GULVE, E., GAO, J., JOHNSON, D., HOLLOSZY, J. & MUECKLER, M. 1993. Evidence from transgenic mice that glucose transport is rate-limiting for glycogen deposition and glycolysis in skeletal muscle. *Journal of Biological Chemistry*, 268, 16113-16115.
- RICHTER, E. A. & HARGREAVES, M. 2013. Exercise, GLUT4, and skeletal muscle glucose uptake. *Physiological reviews*, 93, 993-1017.
- ROBERT, V., MASSIMINO, M. L., TOSELLO, V., MARSAULT, R., CANTINI, M., SORRENTINO, V. & POZZAN, T. 2001. Alteration in Calcium Handling at the Subcellular Level in mdx Myotubes. *Journal of Biological Chemistry*, 276, 4647-4651.
- ROCHARD, P., CASSAR-MALEK, I., MARCHAL, S., WRUTNIAK, C. & CABELLO, G. 1996. Changes in mitochondrial activity during avian myoblast differentiation: Influence of triiodothyronine or v-erbA expression. *Journal of cellular physiology*, 168, 239-247.
- ROCHARD, P., RODIER, A., CASAS, F., CASSAR-MALEK, I., MARCHAL-VICTORION, S., DAURY, L., WRUTNIAK, C. & CABELLO, G. 2000. Mitochondrial activity is involved in the regulation of myoblast differentiation

- through myogenin expression and activity of myogenic factors. *Journal of Biological Chemistry*, 275, 2733-2744.
- RODRIGUEZ, M. C. & TARNOPOLSKY, M. A. 2003. Patients with dystrophinopathy show evidence of increased oxidative stress. *Free Radical Biology and Medicine*, 34, 1217-1220.
- ROGERS, G. W., BRAND, M. D., PETROSYAN, S., ASHOK, D., ELORZA, A. A., FERRICK, D. A. & MURPHY, A. N. 2011. High throughput microplate respiratory measurements using minimal quantities of isolated mitochondria. *PloS one*, 6, e21746.
- ROMERO, N. B., DE LONLAY, P., LLENSE, S., LETURCQ, F., TOUATI, G., URTIZBEREA, J.-A., SAUDUBRAY, J. M., MUNNICH, A., KAPLAN, J. C. & RÉCAN, D. 2001. Pseudo-metabolic presentation in a Duchenne muscular dystrophy symptomatic carrier with 'de novo' duplication of dystrophin gene. *Neuromuscular Disorders*, 11, 494-498.
- RONZONI, E., WALD, S, BERG, L & RAMSEY, R 1958. Distribution of high energy phosphate in normal and dystrophic muscle. *Neurology*, 8, 359-368.
- RYBALKA, E., TIMPANI, C. A., COOKE, M. B., WILLIAMS, A. D. & HAYES, A. 2014. Defects in Mitochondrial ATP Synthesis in Dystrophin-Deficient Mdx Skeletal Muscles May Be Caused by Complex I Insufficiency. *PloS one*, 9, e115763.
- SACCO, A., MOURKIOTI, F., TRAN, R., CHOI, J., LLEWELLYN, M., KRAFT, P., SHKRELI, M., DELP, S., POMERANTZ, J. H. & ARTANDI, S. E. 2010. Short telomeres and stem cell exhaustion model Duchenne muscular

- dystrophy in mdx/mTR mice. *Cell*, 143, 1059-1071.
- SAKAMOTO, M., YUASA, K., YOSHIMURA, M., YOKOTA, T., IKEMOTO, T., SUZUKI, M., DICKSON, G., MIYAGOE-SUZUKI, Y. & TAKEDA, S. I. 2002. Micro-dystrophin cDNA ameliorates dystrophic phenotypes when introduced into mdx mice as a transgene. *Biochemical and biophysical research communications*, 293, 1265-1272.
- SALAMINO, F., SPARATORE, B., MELLONI, E., MICHETTI, M., VIOTTI, P., PONTREMOLI, S. & CARAFOLI, E. 1994. The plasma membrane calcium pump is the preferred calpain substrate within the erythrocyte. *Cell calcium*, 15, 28-35.
- SAMAHA FJ, D. B. N. B. 1981. Duchenne muscular dystrophy: adenosine triphosphate and creatine phosphate content in muscle. *Neurology*, 31, 916-919.
- SAMBASIVAN, R., YAO, R., KISSENPFENNIG, A., VAN WITTENBERGHE, L., PALDI, A., GAYRAUD-MOREL, B., GUENOU, H., MALISSEN, B., TAJBAKHSI, S. & GALY, A. 2011. Pax7-expressing satellite cells are indispensable for adult skeletal muscle regeneration. *Development*, 138, 3647-3656.
- SANADA, H. & YAMAGUCHI, M. 1979. A defect of purine nucleotide cycle in the skeletal muscle of hereditary dystrophic mice. *Biochemical and Biophysical Research Communications*, 90, 453-459.
- SANDRI, M. 2010. Autophagy in skeletal muscle. *FEBS letters*, 584, 1411-1416.
- SANDRI, M., COLETTI, L., GRUMATI, P. & BONALDO, P. 2013. Misregulation of

- autophagy and protein degradation systems in myopathies and muscular dystrophies. *J Cell Sci*, 126, 5325-5333.
- SARTI, P., GIUFFRÈ, A., BARONE, M. C., FORTE, E., MASTRONICOLA, D. & BRUNORI, M. 2003. Nitric oxide and cytochrome oxidase: reaction mechanisms from the enzyme to the cell. *Free Radical Biology and Medicine*, 34, 509-520.
- SCHMALBRUCH, H. 1984. Regenerated muscle fibers in Duchenne muscular dystrophy A serial section study. *Neurology*, 34, 60-60.
- SCHOLNICK, P., LANG, D. & RACKER, E. 1973. Regulatory mechanisms in carbohydrate metabolism IX. Stimulation of aerobic glycolysis by energy-linked ion transport and inhibition by Dextran sulfate. *Journal of Biological Chemistry*, 248, 5175-5182.
- SCHOLTE, H., LUYT-HOUWEN, I., BUSCH, H. & JENNEKENS, F. 1985. Muscle mitochondria from patients with Duchenne muscular dystrophy have a normal beta oxidation, but an impaired oxidative phosphorylation. *Neurology*, 35, 1396-1396.
- SCHUH, R. A., JACKSON, K. C., KHAIRALLAH, R. J., WARD, C. W. & SPANGENBURG, E. E. 2012. Measuring mitochondrial respiration in intact single muscle fibers. *American Journal of Physiology - Regulatory, Integrative and Comparative Physiology*, 302, R712-R719.
- SCIORATI, C., STASZEWSKY, L., ZAMBELLI, V., RUSSO, I., SALIO, M., NOVELLI, D., DI GRIGOLI, G., MORESCO, R. M., CLEMENTI, E. & LATINI, R. 2013. Ibuprofen plus isosorbide dinitrate treatment in the mdx mice

- ameliorates dystrophic heart structure. *Pharmacological Research*, 73, 35-43.
- SELSBY, J., BALLMANN, C. & QUINDRY, J. 2015. Long-term Dietary Quercetin Enrichment Improves Muscle Function in Dystrophic Skeletal Muscle. *The FASEB Journal*, 29, 1039.6.
- SELSBY, J. T. 2011. Increased catalase expression improves muscle function in mdx mice. *Experimental physiology*, 96, 194-202.
- SELSBY, J. T., MORINE, K. J., PENDRAK, K., BARTON, E. R. & SWEENEY, H. L. 2012. Rescue of dystrophic skeletal muscle by PGC-1 α involves a fast to slow fiber type shift in the mdx mouse. *PloS one*, 7, e30063.
- SENZAKI, H., SMITH, C. J., JUANG, G. J., ISODA, T., MAYER, S. P., OHLER, A., PAOLOCCI, N., TOMASELLI, G. F., HARE, J. M. & KASS, D. A. 2001. Cardiac phosphodiesterase 5 (cGMP-specific) modulates β -adrenergic signaling in vivo and is down-regulated in heart failure. *The FASEB Journal*, 15, 1718-1726.
- SHARMA, U., ATRI, S., SHARMA, M., SARKAR, C. & JAGANNATHAN, N. 2003. Skeletal muscle metabolism in Duchenne muscular dystrophy (DMD): an in-vitro proton NMR spectroscopy study. *Magnetic resonance imaging*, 21, 145-153.
- SHAVLAKADZE, T., WHITE, J., HOH, J. F., ROSENTHAL, N. & GROUNDS, M. D. 2004. Targeted expression of insulin-like growth factor-I reduces early myofiber necrosis in dystrophic mdx mice. *Molecular Therapy*, 10, 829-843.
- SHAW, R., PEARSON, CM, CHOWDHURY, SR, DREIFUSS FE 1967. Serum

- enzymes in sex-linked (duchenne) muscular dystrophy. *Archives of Neurology*, 16, 115-122.
- SHEEHAN, D. C. & HRAPCHAK, B. B. 1980. *Theory and practice of histotechnology*, Cv Mosby.
- SHIAO, T., FOND, A., DENG, B., WEHLING-HENRICKS, M., ADAMS, M. E., FROEHNER, S. C. & TIDBALL, J. G. 2004. Defects in neuromuscular junction structure in dystrophic muscle are corrected by expression of a NOS transgene in dystrophin-deficient muscles, but not in muscles lacking α - and β 1-syntrophins. *Human molecular genetics*, 13, 1873-1884.
- SHUMATE, J. B., CARROLL, J. E., BROOKE, M. H. & CHOKSI, R. M. 1982. Palmitate oxidation in human muscle: comparison to CPT and carnitine. *Muscle & nerve*, 5, 226-231.
- SHUTTLEWOOD, R. & GRIFFITHS, J. 1982. The purine nucleotide profile in mouse, chicken and human dystrophic muscle: an abnormal ratio of inosine plus adenine nucleotides to guanine nucleotides. *Clin. Sci*, 62, 113-115.
- SINHA, R., DUFOUR, S., PETERSEN, K. F., LEBON, V., ENOKSSON, S., MA, Y.-Z., SAVOYE, M., ROTHMAN, D. L., SHULMAN, G. I. & CAPRIO, S. 2002. Assessment of skeletal muscle triglyceride content by ¹H nuclear magnetic resonance spectroscopy in lean and obese adolescents relationships to insulin sensitivity, total body fat, and central adiposity. *Diabetes*, 51, 1022-1027.
- SKULACHEV, V. P. 1996. Role of uncoupled and non-coupled oxidations in maintenance of safely low levels of oxygen and its one-electron reductants.

Quarterly reviews of biophysics, 29, 169-202.

- SPITALI, P., GRUMATI, P., HILLER, M., CHRISAM, M., AARTSMA-RUS, A. & BONALDO, P. 2013. Autophagy is impaired in the tibialis anterior of dystrophin null mice. *PLOS Currents Muscular Dystrophy*.
- SPITZER, E., GROSSE, R., KUPRIJANOV, V. & PREOBRAZHENSKY, A. 1981. Demonstration of a digitalis-sensitive sarcolemmal Ca²⁺-pump functionally coupled with a membrane associated creatine phosphokinase. *Acta biologica et medica Germanica*, 40, 1111.
- SQUIRE, S., RAYMACKERS, J.-M., VANDEBROUCK, C., POTTER, A., TINSLEY, J., FISHER, R., GILLIS, J.-M. & DAVIES, K. 2002. Prevention of pathology in mdx mice by expression of utrophin: analysis using an inducible transgenic expression system. *Human Molecular Genetics*, 11, 3333-3344.
- SRERE, P. 1969. [1] Citrate synthase:[EC 4.1. 3.7. Citrate oxaloacetate-lyase (CoA-acetylating)]. *Methods in enzymology*, 13, 3-11.
- STAPLETON, D. I., LAU, X., FLORES, M., TRIEU, J., GEHRIG, S. M., CHEE, A., NAIM, T., LYNCH, G. S. & KOOPMAN, R. 2014. Dysfunctional Muscle and Liver Glycogen Metabolism in *mdx* Dystrophic Mice. *PLoS ONE*, 9, e91514.
- STEDMAN, H. H., SWEENEY, H. L., SHRAGER, J. B., MAGUIRE, H. C., PANETTIERI, R. A., PETROF, B., NARUSAWA, M., LEFEROVICH, J. M., SLADKY, J. T. & KELLY, A. M. 1991. The mdx mouse diaphragm reproduces the degenerative changes of Duchenne muscular dystrophy. *Nature*, 352, 536-539.

- STEIN, L. R. & IMAI, S.-I. 2012. The dynamic regulation of NAD metabolism in mitochondria. *Trends in Endocrinology & Metabolism*, 23, 420-428.
- STEPHENS, J. & LEWIN, E. 1965. Serum enzyme variations and histological abnormalities in the carrier state in Duchenne dystrophy. *Journal of neurology, neurosurgery, and psychiatry*, 28, 104.
- STEPHENSON, E. J., CAMERA, D. M., JENKINS, T. A., KOSARI, S., LEE, J. S., HAWLEY, J. A. & STEPTO, N. K. 2012. Skeletal muscle respiratory capacity is enhanced in rats consuming an obesogenic Western diet. *American Journal of Physiology-Endocrinology and Metabolism*, 302, E1541-E1549.
- STEPHENSON, E. J., STEPTO, N. K., KOCH, L. G., BRITTON, S. L. & HAWLEY, J. A. 2012. Divergent skeletal muscle respiratory capacities in rats artificially selected for high and low running ability: a role for Nor1? *Journal of applied physiology*, 113, 1403-1412.
- STERN, L. M., FEWINGS, J. D., BRETAG, A. H., BALLARD, F. J., TOMAS, F. M., COOPER, D. M. & GOLDBLATT, E. 1981. The progression of Duchenne muscular dystrophy: Clinical trial of allopurinol therapy. *Neurology*, 31, 422.
- ST-PIERRE, J., BUCKINGHAM, J. A., ROEBUCK, S. J. & BRAND, M. D. 2002. Topology of superoxide production from different sites in the mitochondrial electron transport chain. *Journal of Biological Chemistry*, 277, 44784-44790.
- SUGIMOTO, H., OKADA, K., SHODA, J., WARABI, E., ISHIGE, K., UEDA, T., TAGUCHI, K., YANAGAWA, T., NAKAHARA, A. & HYODO, I. 2010. Deletion of nuclear factor-E2-related factor-2 leads to rapid onset and progression of nutritional steatohepatitis in mice. *American Journal of*

Physiology-Gastrointestinal and Liver Physiology, 298, G283-G294.

SUGIYAMA, Y. & FUJITA, T. 1985. Stimulation of the respiratory and phosphorylating activities in rat brain mitochondria by idebenone (CV-2619), a new agent improving cerebral metabolism. *FEBS letters*, 184, 48-51.

SUN, C., LI, S. & LI, D. 2016. Sulforaphane mitigates muscle fibrosis in mdx mice via Nrf2-mediated inhibition of TGF- β /Smad signaling. *Journal of Applied Physiology*, 120, 377-390.

SUN, C., YANG, C., XUE, R., LI, S., ZHANG, T., PAN, L., MA, X., WANG, L. & LI, D. 2015. Sulforaphane alleviates muscular dystrophy in mdx mice by activation of Nrf2. *Journal of Applied Physiology*, 118, 224-237.

SUSIN, S. A., LORENZO, H. K., ZAMZAMI, N., MARZO, I., SNOW, B. E., BROTHERS, G. M., MANGION, J., JACOTOT, E., COSTANTINI, P. & LOEFFLER, M. 1999. Molecular characterization of mitochondrial apoptosis-inducing factor. *Nature*, 397, 441-446.

TALBOT, D. A., LAMBERT, A. J. & BRAND, M. D. 2004. Production of endogenous matrix superoxide from mitochondrial complex I leads to activation of uncoupling protein 3. *FEBS letters*, 556, 111-115.

TAMARI, H., OHTANI, Y, HIGASHI, A, MIYOSHINO, S & MATSUDA, I 1982. Xanthine oxidase inhibitor in Duchenne muscular dystrophy. *Brain & Development* 4, 137-143.

TARNOPOLSKY, M., MAHONEY, D., VAJSAR, J., RODRIGUEZ, C., DOHERTY, T., ROY, B. & BIGGAR, D. 2004. Creatine monohydrate enhances strength and body composition in Duchenne muscular dystrophy. *Neurology*, 62,

1771-1777.

- TARNOPOLSKY, M. & MARTIN, J. 1999. Creatine monohydrate increases strength in patients with neuromuscular disease. *Neurology*, 52, 854-854.
- TATSUMI, R., LIU, X., PULIDO, A., MORALES, M., SAKATA, T., DIAL, S., HATTORI, A., IKEUCHI, Y. & ALLEN, R. E. 2006. Satellite cell activation in stretched skeletal muscle and the role of nitric oxide and hepatocyte growth factor. *American Journal of Physiology-Cell Physiology*, 290, C1487-C1494.
- TERRILL, J. R., RADLEY-CRABB, H. G., GROUNDS, M. D. & ARTHUR, P. G. 2012. N-Acetylcysteine treatment of dystrophic mdx mice results in protein thiol modifications and inhibition of exercise induced myofibre necrosis. *Neuromuscular Disorders*, 22, 427-434.
- THIMMULAPPA, R. K., LEE, H., RANGASAMY, T., REDDY, S. P., YAMAMOTO, M., KENSLER, T. W. & BISWAL, S. 2006. Nrf2 is a critical regulator of the innate immune response and survival during experimental sepsis. *The Journal of clinical investigation*, 116, 984-995.
- THOMAS, G. D., SANDER, M., LAU, K. S., HUANG, P. L., STULL, J. T. & VICTOR, R. G. 1998. Impaired metabolic modulation of α -adrenergic vasoconstriction in dystrophin-deficient skeletal muscle. *Proceedings of the National Academy of Sciences*, 95, 15090-15095.
- THOMAS, G. D., YE, J., DE NARDI, C., MONOPOLI, A., ONGINI, E. & VICTOR, R. G. 2012. Treatment with a Nitric Oxide-Donating NSAID Alleviates Functional Muscle Ischemia in the Mouse Model of Duchenne Muscular Dystrophy. *PLoS ONE*, 7, e49350.

- THOMSON, W. 1969. The biochemical identification of the carrier state in X-linked recessive (Duchenne) muscular dystrophy. *Clinica chimica acta; international journal of clinical chemistry*, 26, 207.
- THOMSON, W. & GUEST, K. E. 1963. A trial of therapy by nucleosides and nucleotides in muscular dystrophy. *Journal of neurology, neurosurgery, and psychiatry*, 26, 111.
- THOMSON, W. & SMITH, I. 1978. Allopurinol in Duchenne's muscular dystrophy. *The New England journal of medicine*, 299, 101.
- THOMSON, W. H. S., LEYBURN, P & WALTON, J N 1960. Serum enzyme activity in muscular dystrophy. *British Medical Journal*, 1276-1281.
- THOMSON, W. H. S. & SMITH, I. 1978. X-linked recessive (Duchenne) muscular dystrophy (DMD) and purine metabolism: Effects of oral allopurinol and adenylate. *Metabolism*, 27, 151-163.
- TIDBALL, J. G., ALBRECHT, D. E., LOKENSGARD, B. E. & SPENCER, M. J. 1995. Apoptosis precedes necrosis of dystrophin-deficient muscle. *Journal of cell science*, 108, 2197-2204.
- TIDBALL, J. G. & WEHLING-HENRICKS, M. 2004. Expression of a NOS transgene in dystrophin-deficient muscle reduces muscle membrane damage without increasing the expression of membrane-associated cytoskeletal proteins. *Molecular genetics and metabolism*, 82, 312-320.
- TIDBALL, J. G. & WEHLING-HENRICKS, M. 2007. The role of free radicals in the pathophysiology of muscular dystrophy. *Journal of Applied Physiology*, 102, 1677-1686.

- TIMMONS, J. A., LARSSON, O., JANSSON, E., FISCHER, H., GUSTAFSSON, T., GREENHAFF, P. L., RIDDEN, J., RACHMAN, J., PEYRARD-JANVID, M. & WAHLESTEDT, C. 2005. Human muscle gene expression responses to endurance training provide a novel perspective on Duchenne muscular dystrophy. *The FASEB Journal*, 19, 750-760.
- TIMPANI, C. A., TREWIN, ADAM J, STOJANOVSKA, VANESA, ROBINSON, AINSLEY, GOODMAN, CRAIG A, NURGALI, KULMIRA, BETIK, ANDREW C, STEPTO, NIGEL, HAYES, ALAN, MCCONELL, GLENN K, RYBALKA, EMMA 2016. Attempting to compensate for reduced nNOS protein with nitrate supplementation cannot overcome metabolic dysfunction but rather has detrimental effects in dystrophin-deficient mdx muscle. *Neurotherapeutics*, Accepted
- TIMPANI, C. A., HAYES, A. & RYBALKA, E. 2015. Revisiting the dystrophin-ATP connection: How half a century of research still implicates mitochondrial dysfunction in Duchenne Muscular Dystrophy aetiology. *Medical Hypotheses*, 85, 1021-1033.
- TINSLEY, J., DECONINCK, N., FISHER, R., KAHN, D., PHELPS, S., GILLIS, J.-M. & DAVIES, K. 1998. Expression of full-length utrophin prevents muscular dystrophy in mdx mice. *Nature medicine*, 4, 1441-1444.
- TINSLEY, J. M., POTTER, A. C., PHELPS, S. R., FISHER, R., TRICKETT, J. I. & DAVIES, K. E. 1996. Amelioration of the dystrophic phenotype of mdx mice using a truncated utrophin transgene.
- TORNHEIM, K. & RUDERMAN, N. B. 2011. Intermediary Metabolism of

Carbohydrate, Protein, and Fat. *Metabolic Basis of Obesity*, 25-51.

TRACEY, I., DUNN, J., PARKES, H. & RADDA, G. 1996. An in vivo and in vitro ¹H-magnetic resonance spectroscopy study of mdx mouse brain: Abnormal development or neural necrosis? *Journal of the neurological sciences*, 141, 13-18.

TRACEY, I., DUNN, J. F. & RADDA, G. K. 1996. Brain metabolism is abnormal in the mdx model of Duchenne muscular dystrophy. *Brain*, 119, 1039-1044.

TRACEY, I., SCOTT, R. B., THOMPSON, C. H., DUNN, J. F., BARNES, P. R., STYLES, P., KEMP, G. J., RAE, C. D., PIKE, M. & RADDA, G. K. 1995. Brain abnormalities in Duchenne muscular dystrophy: phosphorus-31 magnetic resonance spectroscopy and neuropsychological study. *Lancet*, 345, 1260-1264.

TREUER, A. V. & GONZALEZ, D. R. 2015. Nitric oxide synthases, S-nitrosylation and cardiovascular health: From molecular mechanisms to therapeutic opportunities (Review). *Molecular medicine reports*, 11, 1555-1565.

TSAI, J. J., DUDAKOV, J. A., TAKAHASHI, K., SHIEH, J.-H., VELARDI, E., HOLLAND, A. M., SINGER, N. V., WEST, M. L., SMITH, O. M. & YOUNG, L. F. 2013. Nrf2 regulates haematopoietic stem cell function. *Nature cell biology*, 15, 309-316.

TUON, L., COMIM, C. M., FRAGA, D. B., SCAINI, G., REZIN, G. T., BAPTISTA, B. R., STRECK, E. L., VAINZOF, M. & QUEVEDO, J. 2010. Mitochondrial respiratory chain and creatine kinase activities in mdx mouse brain. *Muscle & Nerve*, 41, 257-260.

- TURNER, P. R., FONG, P., DENETCLAW, W. F. & STEINHARDT, R. A. 1991. Increased calcium influx in dystrophic muscle. *The Journal of Cell Biology*, 115, 1701-1712.
- TURNER, P. R., WESTWOOD, T., REGEN, C. M. & STEINHARDT, R. A. 1988. Increased protein degradation results from elevated free calcium levels found in muscle from mdx mice.
- TURRENS, J. F. & BOVERIS, A. 1980. Generation of superoxide anion by the NADH dehydrogenase of bovine heart mitochondria. *Biochemical Journal*, 191, 421-427.
- UAESONTRACHOON, K., QUINN, J. L., TATEM, K. S., VAN DER MEULEN, J. H., YU, Q., PHADKE, A., MILLER, B. K., GORDISH-DRESSMAN, H., ONGINI, E. & MIGLIETTA, D. 2014. Long-term treatment with naproxcinod significantly improves skeletal and cardiac disease phenotype in the mdx mouse model of dystrophy. *Human molecular genetics*, ddu033.
- VAGHY, P. L., FANG, J., WU, W. & VAGHY, L. P. 1998. Increased caveolin-3 levels in mdx mouse muscles. *FEBS letters*, 431, 125-127.
- VAN BENNEKOM, C., OERLEMANS, FT, KULAKOWSKI, S & DE BRUYN CH 1984. Enzymes of purine metabolism in muscle specimens from patients with Duchenne-type muscular dystrophy. *Advances In Experimental Medicine And Biology* 165, 447-450.
- VAN PUTTEN, M., DE WINTER, C., VAN ROON-MOM, W., VAN OMMEN, G.-J., AC'T HOEN, P. & AARTSMA-RUS, A. 2010. A 3 months mild functional test regime does not affect disease parameters in young mdx mice.

Neuromuscular Disorders, 20, 273-280.

- VANDEBROUCK, C., MARTIN, D., COLSON-VAN SCHOOR, M., DEBAIX, H. & GAILLY, P. 2002. Involvement of TRPC in the abnormal calcium influx observed in dystrophic (mdx) mouse skeletal muscle fibers. *The Journal of cell biology*, 158, 1089-1096.
- VEERAPANDIYAN, A., SHASHI, V., JIANG, Y. H., GALLENTINE, W. B., SCHOCH, K. & SMITH, E. C. 2010. Pseudometabolic presentation of dystrophinopathy due to a missense mutation. *Muscle & nerve*, 42, 975-979.
- VIANELLO, S., CONSOLARO, F., BICH, C., CANCELA, J.-M., ROULOT, M., LANCHEC, E., TOUBOUL, D., BRUNELLE, A., ISRAËL, M., BENOIT, E. & DE LA PORTE, S. 2014. Low doses of arginine butyrate derivatives improve dystrophic phenotype and restore membrane integrity in DMD models. *The FASEB Journal*, 28, 2603-2619.
- VIANELLO, S., YU, H., VOISIN, V., HADDAD, H., HE, X., FOUTZ, A. S., SEBRIÉ, C., GILLET, B., ROULOT, M., FOUGEROUSSE, F., PERRONNET, C., VAILLEND, C., MATECKI, S., ESCOLAR, D., BOSSI, L., ISRAËL, M. & DE LA PORTE, S. 2013. Arginine butyrate: a therapeutic candidate for Duchenne muscular dystrophy. *The FASEB Journal*, 27, 2256-2269.
- VIEIRA, N. M., ELVERS, I., ALEXANDER, M. S., MOREIRA, Y. B., ERAN, A., GOMES, J. P., MARSHALL, J. L., KARLSSON, E. K., VERJOVSKI-ALMEIDA, S. & LINDBLAD-TOH, K. 2015. Jagged 1 rescues the Duchenne muscular dystrophy phenotype. *Cell*, 163, 1204-1213.
- VIEIRA, N. M., GUO, L. T., ESTRELA, E., KUNKEL, L. M., ZATZ, M. & SHELTON,

- G. D. 2015. Muscular dystrophy in a family of labrador retrievers with no muscle dystrophin and a mild phenotype. *Neuromuscular Disorders*.
- VIGNOS JR, P. & WARNER, J. 1963. Glycogen, creatine and high energy phosphate in human muscle disease. *The Journal of laboratory and clinical medicine*, 62, 579.
- VIGNOS JR, P. J. & LEFKOWITZ, M. 1959. A biochemical study of certain skeletal muscle constituents in human progressive muscular dystrophy. *Journal of Clinical Investigation*, 38, 873.
- VILQUIN, J. T., BRUSSEE, V., ASSELIN, I., KINOSHITA, I., GINGRAS, M. & TREMBLAY, J. P. 1998. Evidence of mdx mouse skeletal muscle fragility in vivo by eccentric running exercise. *Muscle & nerve*, 21, 567-576.
- VIOLA, H. M., DAVIES, S. M., FILIPOVSKA, A. & HOOL, L. C. 2013. The L-type Ca²⁺ channel contributes to alterations in mitochondrial calcium handling in the mdx ventricular myocyte. *American Journal of Physiology-Heart and Circulatory Physiology*, ajpheart. 00700.2012.
- VIOLLET, B., ANDREELLI, F., JORGENSEN, S. B., PERRIN, C., FLAMEZ, D., MU, J., WOJTASZEWSKI, J. F., SCHUIT, F. C., BIRNBAUM, M. & RICHTER, E. 2003. Physiological role of AMP-activated protein kinase (AMPK): insights from knockout mouse models. *Biochemical Society Transactions*, 31, 216-219.
- VOISIN, V., SEBRIE, C., MATECKI, S., YU, H., GILLET, B., RAMONATXO, M., ISRAEL, M. & DE LA PORTE, S. 2005. L-arginine improves dystrophic phenotype in mdx mice. *Neurobiol Dis*, 20, 123-30.

- VOLEK, J. S., DUNCAN, N. D., MAZZETTI, S. A., STARON, R. S., PUTUKIAN, M., GOMEZ, A., PEARSON, D. R., FINK, W. J. & KRAEMER, W. J. 1999. Performance and muscle fiber adaptations to creatine supplementation and heavy resistance training. *Medicine and science in sports and exercise*, 31, 1147-1156.
- VOTYAKOVA, T. V. & REYNOLDS, I. J. 2001. $\Delta\Psi_m$ -Dependent and-independent production of reactive oxygen species by rat brain mitochondria. *Journal of neurochemistry*, 79, 266-277.
- WALLACE, D. C. 1999. Mitochondrial diseases in man and mouse. *Science*, 283, 1482-1488.
- WALLIS, R. M., CORBIN, J. D., FRANCIS, S. H. & ELLIS, P. 1999. Tissue distribution of phosphodiesterase families and the effects of sildenafil on tissue cyclic nucleotides, platelet function, and the contractile responses of trabeculae carneae and aortic rings in vitro. *The American journal of cardiology*, 83, 3-12.
- WANG, G. & LU, Q. 2013. A nitrate ester of sedative alkyl alcohol improves muscle function and structure in a murine model of Duchenne muscular dystrophy. *Molecular pharmaceutics*, 10, 3862-3870.
- WANG, Y., LIANG, Y. & VANHOUTTE, P. M. 2011. SIRT1 and AMPK in regulating mammalian senescence: a critical review and a working model. *FEBS letters*, 585, 986-994.
- WATKINS, S. C. & CULLEN, M. J. 1987. A qualitative and quantitative study of the ultrastructure of regenerating muscle fibres in Duchenne muscular

- dystrophy and polymyositis. *Journal of the Neurological Sciences*, 82, 181-192.
- WATT, M. J. & HOY, A. J. 2012. Lipid metabolism in skeletal muscle: generation of adaptive and maladaptive intracellular signals for cellular function. *American Journal of Physiology-Endocrinology and Metabolism*, 302, E1315-E1328.
- WEBSTER, C., SILBERSTEIN, L., HAYS, A. P. & BLAU, H. M. 1988. Fast muscle fibers are preferentially affected in Duchenne muscular dystrophy. *Cell*, 52, 503-513.
- WEGENER, G. & KRAUSE, U. 2002. Different modes of activating phosphofructokinase, a key regulatory enzyme of glycolysis, in working vertebrate muscle. *Biochemical Society Transactions*, 30, 264-269.
- WEHLING, M., SPENCER, M. J. & TIDBALL, J. G. 2001. A nitric oxide synthase transgene ameliorates muscular dystrophy in mdx mice. *The Journal of Cell Biology*, 155, 123-132.
- WEHLING-HENRICKS, M., JORDAN, M. C., ROOS, K. P., DENG, B. & TIDBALL, J. G. 2005. Cardiomyopathy in dystrophin-deficient hearts is prevented by expression of a neuronal nitric oxide synthase transgene in the myocardium. *Human molecular genetics*, 14, 1921-1933.
- WEHLING-HENRICKS, M., OLTMANN, M., RINALDI, C., MYUNG, K. H. & TIDBALL, J. G. 2009. Loss of positive allosteric interactions between neuronal nitric oxide synthase and phosphofructokinase contributes to defects in glycolysis and increased fatigability in muscular dystrophy. *Human Molecular Genetics*, 18, 3439-3451.

- WEHLING-HENRICKS, M. & TIDBALL, J. G. 2011. Neuronal nitric oxide synthase-rescue of dystrophin/utrophin double knockout mice does not require nNOS localization to the cell membrane. *PLoS One*, 6, e25071.
- WELLS, D. J., WELLS, K. E., ASANTE, E. A., TURNER, G., SUNADA, Y., CAMPBELL, K. P., WALSH, F. S. & DICKSON, G. 1995. Expression of human full-length and minidystrophin in transgenic mdx mice: implications for gene therapy of Duchenne muscular dystrophy. *Human Molecular Genetics*, 4, 1245-1250.
- WHITFIELD, J., LUDZKI, A., HEIGENHAUSER, G., SENDEN, J., VERDIJK, L., LOON, L., SPRIET, L. & HOLLOWAY, G. 2016. Beetroot juice supplementation reduces whole body oxygen consumption but does not improve indices of mitochondrial efficiency in human skeletal muscle. *The Journal of physiology*, 594, 421-435.
- WILLIAMS, I. A. & ALLEN, D. G. 2007. Intracellular calcium handling in ventricular myocytes from mdx mice. *American Journal of Physiology-Heart and Circulatory Physiology*, 292, H846-H855.
- WILLMANN, R., POSSEKEL, S., DUBACH-POWELL, J., MEIER, T. & RUEGG, M. A. 2009. Mammalian animal models for Duchenne muscular dystrophy. *Neuromuscular disorders*, 19, 241-249.
- WINDER, W., HOLMES, B., RUBINK, D., JENSEN, E., CHEN, M. & HOLLOSZY, J. 2000. Activation of AMP-activated protein kinase increases mitochondrial enzymes in skeletal muscle. *Journal of applied physiology*, 88, 2219-2226.
- WINEINGER, M. A., WALSH, S. A. & ABRESCH, R. T. 1998. The effect of age and

- temperature on mdx muscle fatigue. *Muscle & nerve*, 21, 1075-1077.
- WINTERBOURN, C. C. & METODIEWA, D. 1994. The reaction of superoxide with reduced glutathione. *Archives of Biochemistry and Biophysics*, 314, 284-290.
- WITTING, N., KRUUSE, C., NYHUUS, B., PRAHM, K. P., CITIRAK, G., LUNDGAARD, S. J., HUTH, S., VEJLSTRUP, N., LINDBERG, U. & KRAG, T. O. 2014. Effect of sildenafil on skeletal and cardiac muscle in Becker muscular dystrophy. *Annals of neurology*, 76, 550-557.
- WONG, L. C., PERNG, C., HSU, C., BAI, R., SCHELLEY, S., VLADUTIU, G., VOGEL, H. & ENNS, G. 2003. Compensatory amplification of mtDNA in a patient with a novel deletion/duplication and high mutant load. *Journal of medical genetics*, 40, e125-e125.
- WONG, L. J. C., WLADYKA, C. & MARDACH-VERDON, R. 2004. A mitochondrial DNA mutation in a patient with an extensive family history of Duchenne muscular dystrophy. *Muscle & nerve*, 30, 118-122.
- WOZNIAK, A. C. & ANDERSON, J. E. 2007. Nitric oxide-dependence of satellite stem cell activation and quiescence on normal skeletal muscle fibers. *Developmental Dynamics*, 236, 240-250.
- WROGEMANN, K., JACOBSON, B. & BLANCHAER, M. 1973. On the mechanism of a calcium-associated defect of oxidative phosphorylation in progressive muscular dystrophy. *Archives of biochemistry and biophysics*, 159, 267-278.
- WU, M., NEILSON, A., SWIFT, A. L., MORAN, R., TAMAGNINE, J., PARSLOW, D., ARMISTEAD, S., LEMIRE, K., ORRELL, J. & TEICH, J. 2007.

Multiparameter metabolic analysis reveals a close link between attenuated mitochondrial bioenergetic function and enhanced glycolysis dependency in human tumor cells. *American Journal of Physiology-Cell Physiology*, 292, C125-C136.

YAKES, F. M. & VAN HOUTEN, B. 1997. Mitochondrial DNA damage is more extensive and persists longer than nuclear DNA damage in human cells following oxidative stress. *Proceedings of the National Academy of Sciences*, 94, 514-519.

YATES, M. S., TRAN, Q. T., DOLAN, P. M., OSBURN, W. O., SHIN, S., MCCULLOCH, C. C., SILKWORTH, J. B., TAGUCHI, K., YAMAMOTO, M. & WILLIAMS, C. R. 2009. Genetic versus chemoprotective activation of Nrf2 signaling: overlapping yet distinct gene expression profiles between Keap1 knockout and triterpenoid-treated mice. *Carcinogenesis*, 30, 1024-1031.

YIN, H., PRICE, F. & RUDNICKI, M. A. 2013. Satellite cells and the muscle stem cell niche. *Physiological reviews*, 93, 23-67.

YOGEV, O., YOGEV, O., SINGER, E., SHAULIAN, E., GOLDBERG, M., FOX, T. D. & PINES, O. 2010. Fumarase: a mitochondrial metabolic enzyme and a cytosolic/nuclear component of the DNA damage response. *PLoS Biol*, 8, e1000328.

YOUNG, E. M. & LEIGHTON, B. 1998. Evidence for altered sensitivity of the nitric oxide/cGMP signalling cascade in insulin-resistant skeletal muscle. *Biochemical Journal*, 329, 73-79.

YOUNG, M. E. & LEIGHTON, B. 1998. Fuel oxidation in skeletal muscle is

- increased by nitric oxide/cGMP—evidence for involvement of cGMP-dependent protein kinase. *FEBS letters*, 424, 79-83.
- YOUNG, M. E., RADDA, G. K. & LEIGHTON, B. 1997. Nitric oxide stimulates glucose transport and metabolism in rat skeletal muscle in vitro. *Biochemical Journal*, 322, 223-228.
- YOUNKIN, D. P., BERMAN, P., SLADKY, J., CHEE, C., BANK, W. & CHANCE, B. 1987. ³¹P NMR studies in Duchenne muscular dystrophy. *Neurology*, 37, 165.
- YU, Z., LI, P., ZHANG, M., HANNINK, M., STAMLER, J. S. & YAN, Z. 2008. Fiber type-specific nitric oxide protects oxidative myofibers against cachectic stimuli. *PLoS One*, 3, e2086.
- ZATZ, M., PAVANELLO, R., LAZAR, M., YAMAMOTO, G., LOURENÇO, N., CERQUEIRA, A., NOGUEIRA, L. & VAINZOF, M. 2014. Milder course in Duchenne patients with nonsense mutations and no muscle dystrophin. *Neuromuscular Disorders*, 24, 986-989.
- ZATZ, M., RAPAPORT, D., VAINZOF, M., PASSOS-BUENO, M. R., BORTOLINI, E. R., PAVANELLO, R. C. M. & PERES, C. A. 1991. Serum creatine-kinase (CK) and pyruvate-kinase (PK) activities in Duchenne (DMD) as compared with Becker (BMD) muscular dystrophy. *Journal of the Neurological Sciences*, 102, 190-196.
- ZATZ, M., VIEIRA, N. M., ZUCCONI, E., PELATTI, M., GOMES, J., VAINZOF, M., MARTINS-BACH, A. B., GARCIA OTADUY, M. C., BENTO DOS SANTOS, G., AMARO JR, E., LANDINI, V. & ANDRADE, T. 2015. A normal life

- without muscle dystrophin. *Neuromuscular Disorders*.
- ZHANG, W., TEN HOVE, M., SCHNEIDER, J. E., STUCKEY, D. J., SEBAG-MONTEFIORE, L., BIA, B. L., RADDA, G. K., DAVIES, K. E., NEUBAUER, S. & CLARKE, K. 2008. Abnormal cardiac morphology, function and energy metabolism in the dystrophic mdx mouse: an MRI and MRS study. *Journal of molecular and cellular cardiology*, 45, 754-760.
- ZHANG, Y. & DUAN, D. 2011. Novel mini-dystrophin gene dual adeno-associated virus vectors restore neuronal nitric oxide synthase expression at the sarcolemma. *Human gene therapy*, 23, 98-103.
- ZHANG, Y., YUE, Y., LI, L., HAKIM, C. H., ZHANG, K., THOMAS, G. D. & DUAN, D. 2013. Dual AAV therapy ameliorates exercise-induced muscle injury and functional ischemia in murine models of Duchenne muscular dystrophy. *Human molecular genetics*, 22, 3720-3729.
- ZHANG, Y.-K. J., YEAGER, R. L., TANAKA, Y. & KLAASSEN, C. D. 2010. Enhanced expression of Nrf2 in mice attenuates the fatty liver produced by a methionine-and choline-deficient diet. *Toxicology and applied pharmacology*, 245, 326-334.
- ZHAO, G., LIU, Y., FANG, J., CHEN, Y., LI, H. & GAO, K. 2014. Dimethyl fumarate inhibits the expression and function of hypoxia-inducible factor-1 α (HIF-1 α). *Biochemical and biophysical research communications*, 448, 303-307.
- ZHU, M., FAN, Y., XU, X., WANG, G., SHEN, Y., PAN, Y. & DING, S. 1998. Abnormal expression of inducible nitric oxide synthase in Duchenne muscular dystrophy muscles. *Chinese science bulletin*, 43, 860-863.

ZITER, F. A., ALLSOP, K. G. & TYLER, F. H. 1977. Assessment of muscle strength in Duchenne muscular dystrophy. *Neurology*, 27, 981-981.

ZUCCONI, E., VALADARES, M. C., VIEIRA, N. M., BUENO, C. R., SECCO, M., JAZEDJE, T., DA SILVA, H. C. A., VAINZOF, M. & ZATZ, M. 2010. Ringo: discordance between the molecular and clinical manifestation in a golden retriever muscular dystrophy dog. *Neuromuscular Disorders*, 20, 64-70.